

Historic Mortars

@Seismicisolation

RILEM BOOKSERIES

Volume 7

RILEM, The International Union of Laboratories and Experts in Construction Materials, Systems and Structures, founded in 1947, is a non-governmental scientific association whose goal is to contribute to progress in the construction sciences, techniques and industries, essentially by means of the communication it fosters between research and practice. RILEM's focus is on construction materials and their use in building and civil engineering structures, covering all phases of the building process from manufacture to use and recycling of materials. More information on RILEM and its previous publications can be found on www.RILEM.net.



For further volumes:
<http://www.springer.com/series/8781>

@Seismicisolation

Jan Válek • John J. Hughes
Caspar J.W.P. Groot
Editors

Historic Mortars

Characterisation, Assessment and Repair



Springer

@Seismicisolation

Editors

Jan Válek
ARCHISS Department of Diagnostics
of Historic Structures
Institute of Theoretical and Applied
Mechanics, AV ČR, v.v.i.
ARCHISS, Prague
Czech Republic

John J. Hughes
Faculty of Engineering and Science
University of the West of Scotland
Paisley, Scotland, UK

Caspar J.W.P. Groot
Delft University of Technology
Delft, The Netherlands

ISSN 2211-0844
ISBN 978-94-007-4634-3
DOI 10.1007/978-94-007-4635-0
Springer Dordrecht Heidelberg New York London

ISSN 2211-0852 (electronic)
ISBN 978-94-007-4635-0 (eBook)

Library of Congress Control Number: 2012940739

© RILEM 2012

This work is subject to copyright. All rights are reserved by the Publisher, whether the whole or part of the material is concerned, specifically the rights of translation, reprinting, reuse of illustrations, recitation, broadcasting, reproduction on microfilms or in any other physical way, and transmission or information storage and retrieval, electronic adaptation, computer software, or by similar or dissimilar methodology now known or hereafter developed. Exempted from this legal reservation are brief excerpts in connection with reviews or scholarly analysis or material supplied specifically for the purpose of being entered and executed on a computer system, for exclusive use by the purchaser of the work. Duplication of this publication or parts thereof is permitted only under the provisions of the Copyright Law of the Publisher's location, in its current version, and permission for use must always be obtained from Springer. Permissions for use may be obtained through RightsLink at the Copyright Clearance Center. Violations are liable to prosecution under the respective Copyright Law.

The use of general descriptive names, registered names, trademarks, service marks, etc. in this publication does not imply, even in the absence of a specific statement, that such names are exempt from the relevant protective laws and regulations and therefore free for general use.

While the advice and information in this book are believed to be true and accurate at the date of publication, neither the authors nor the editors nor the publisher can accept any legal responsibility for any errors or omissions that may be made. The publisher makes no warranty, express or implied, with respect to the material contained herein.

Printed on acid-free paper

Springer is part of Springer Science+Business Media (www.springer.com)

@Seismicisolation

Preface

The publication of *Historic Mortars: Characterisation, Assessment and Repair* focuses on research and practical issues connected with mortars on historic structures.

The book is divided into four main parts: Characterisation of Historic Mortars, Repair Mortars and Design Issues, Experimental Research into Properties of Repair Mortars, and Assessment and Testing. The parts divide the chapters according to their main focus, but one should not expect this publication to be an explanatory textbook. Instead, it aims to present the latest work of researchers in this field. The individual contributions were selected from the contributions to the *2nd Historic Mortars Conference*, which took place in Prague, September 22–24, 2010. The chapters were reviewed and completed when necessary or possible before presenting them to you. This peer review process by the editors ended up with the 34 individual contributions included in this publication. One extra chapter reviewing and summarising the state-of-the-art knowledge covered by this publication was added as a starting and navigational point for the reader. The editors believe that having these chapters in print is worth the effort and they hope that it may stimulate further research into historic mortars and related subjects.

@Seismicisolation

Acknowledgements

Everybody who contributed and attended the HMC2010 in Prague is acknowledged as it was the cradle of the idea and the source of the knowledge for this publication. The Czech Ministry of Education, Youth and Sport is thanked for its financial contribution towards the publication under the grant No. LA09008. Mr. Tomáš Matas is thanked for his tireless formatting effort. The Institute of Theoretical and Applied Mechanics, Academy of Sciences of the Czech Republic is also acknowledged for its underpinning during the whole process of preparation.

In Prague

Jan Válek

@Seismicisolation

Contents

Historic Mortars: Characterisation, Assessment and Repair.	
A State-of-the-Art Summary	1
Jan Válek, John J. Hughes, and Caspar J.W.P. Groot	
Part I Characterisation of Historic Mortars	
Historic Documents in Understanding and Evaluation	
of Historic Lime Mortars	15
Cornelia Marinowitz, Claudia Neuwald-Burg, and Matthias Pfeifer	
The Earliest Use of Lime and Gypsum Mortars in Cyprus	25
Maria Philokyprou	
Mineralogical and Microstructural Analysis of Mortars	
from Kushite Archaeological Sites	37
Jean-Pierre Letourneau and Serge Feneuille	
Cement Microstructures and Durability in Ancient	
Roman Seawater Concretes	49
Marie D. Jackson, Gabriele Vola, Dalibor Všianský, John P. Oleson, Barry E. Schetzel, Christopher Brandon, and Robert L. Hohlfelder	
Historic Mortars with Burned Alum Shale as an Artificial Pozzolan	77
Sölvé Johansson and Jan Erik Lindqvist	
Nineteenth Century “Novel” Building Materials: Examples	
of Various Historic Mortars Under the Microscope	89
Johannes Weber, Karol Bayer, and Farkas Pintér	
Lime Mortar with Natural Hydraulic Components: Characterisation	
of Reaction Rims with FTIR Imaging in ATR-Mode	105
Anja Diekamp, Roland Stalder, Jürgen Konzett, and Peter W. Mirwald	

Characterisation of Dolomitic Lime Mortars from the Benedictine Monastery in Riesa, Saxony (Germany)	115
Heiner Siedel, Steffen Michalski, and Bernd Ullrich	
Hydraulicity in Historic Lime Mortars: A Review	125
Jan Elsen, Koenraad Van Balen, and Gilles Mertens	
Characterisation of Decorative Portuguese Gypsum Plasters from the Nineteenth and Twentieth Centuries: The Case of the Bolsa Palace in Oporto.....	141
Teresa Freire, António Santos Silva, Maria do Rosário Veiga, and Jorge de Brito	
Repair Mortars Studied for the Conservation of Temple G1 in Mý Son, Vietnam	153
Cristina Tedeschi, Luigia Binda, and Paola Condoleo	
Characteristics of Mortars from Ancient Bridges	165
Dita Frankeová, Zuzana Slížková, and Miloš Drdácký	
Diagnosis, Characterisation and Restoration of the Internal Renders of Santíssimo Sacramento Church in Lisbon.....	175
António Santos Silva, Giovanni Borsoi, Maria do Rosário Veiga, Ana Fragata, Martha Tavares, Fátima Llera, Belany Barreiros, and Telma Teixeira	
Part II Repair Mortars and Design Issues	
Masonry Repair Options and Their Philosophical Ramifications	197
Alan M. Forster	
Conservation of Historic Renders and Plasters: From Laboratory to Site.....	207
Maria do Rosário Veiga	
Comparison Between Traditional, Lime Based, and Industrial, Dry Mortars	227
Albert Jornet, Cristina Mosca, Giovanni Cavallo, and Guido Corredig	
Repair Mortars for the Sandstones of the Cathedral of Berne.....	239
Christine Bläuer, Hermann Häberli, Annette Löffel, and Bénédicte Rousset	
Compatibility of Repair Mortars with Nineteenth Century Natural Cement Cast Stone from the French Rhône-Alpes Region.....	247
Myriam Bouichou, Elisabeth Marie-Victoire, Emmanuel Cailleux, and Denis Sommain	
Two Views on Dealing with Rain Penetration Problems in Historic Fired Clay Brick Masonry	257
Caspar J.W.P. Groot and Jos Gunneweg	

Part III Experimental Research into Properties of Repair Mortars

Experimental Study of Hot Mixed Mortars in Comparison with Lime Putty and Hydrate Mortars	269
Jan Válek and Tomáš Matas	
The Effect of Calcination Time upon the Slaking Properties of Quicklime	283
Dorn Carran, John Hughes, Alick Leslie, and Craig Kennedy	
The Hydration of Modern Roman Cements Used for Current Architectural Conservation	297
Christophe Gosselin, Karen L. Scrivener, Steven B. Feldman, and Wolfgang Schwarz	
The Effect of Relative Humidity on the Performance of Lime-Pozzolan Mortars.....	309
Ioannis Karatasios, Maria Amenta, Maria Tziotziou, and Vassilis Kilikoglou	
Morphological and Chemical Influence of Calcium Hydroxide on the Plasticity of Lime Based Mortars.....	319
Deborah Klein, Sonja Haas, Sven-Olaf Schmidt, and Bernhard Middendorf	
Water Transport Between Mortar and Brick: The Influence of Material Parameters	329
Roel Hendrickx, Staf Roels, and Koenraad Van Balen	
Problems in the Assessment of the Stress-Strain Relationship of Masonry	343
Claudia Neuwald-Burg and Matthias Pfeifer	
Influence of the Mechanical Properties of Lime Mortar on the Strength of Brick Masonry	359
Adrian Costigan and Sara Pavía	
Influence of Interfacial Material Pore Structure on the Strength of the Brick/Lime Mortar Bond	373
Mike Lawrence, Pete Walker, and Zhaoxia Zhou	
Grouts for Injection of Historical Masonries: Influence of the Binding System and Other Additions on the Properties of the Matrix.....	383
Ioanna Papayianni, Maria Stefanidou, and Vasiliki Pachta	
Lime Based Grouts for Strengthening of Historical Masonry Buildings in Slovenia	393
Mojmir Uranjek, Vlatko Bosiljkov, Roko Žarnić, and Violeta Bokan Bosiljkov	

Part IV Assessment and Testing**Characterisation of Mortars Using Drilling Resistance**

- Measurement System (DRMS): Tests on Field Panels Samples** 413
Dória Costa Portugal, Ana Magalhães, and Maria do Rosário Veiga

- In Situ Techniques for the Characterisation of Rendering Mortars.....** 425
Ana Paula Ferreira Pinto, Rita Nogueira, and Augusto Gomes

- Application of ^1H NMR to the Hydration Monitoring
of Lime-Pozzolan Mortars.....** 435

Maria Tziotziou, Eleni Karakosta, Ioannis Karatasios, Michalis Fardis,
Pagona Maravelaki-Kalaitzaki, Georgios Papavassiliou,
and Vassilis Kilikoglou

- Non-standard Testing in Characterisation and Consolidation
Assessment of Historic Mortars.....** 443
Miloš Drdácký

- RILEM Publications.....** 451

- RILEM Publications Published by Springer.....** 461

- Author Index.....** 463

Part I

Characterisation of Historic Mortars

Historic Documents in Understanding and Evaluation of Historic Lime Mortars

Cornelia Marinowitz, Claudia Neuwald-Burg, and Matthias Pfeifer

Abstract Sophisticated analysing proceedings have been used in the past to assess the composition of hardened mortars. Chemical and mechanical tests combined with microscopic investigations seem to provide all the information required for the design of repair mortars which physically and visually are appropriate for restoration purposes. Lime putty and hydrated lime of varying quality meanwhile are currently available. Nevertheless, the results are not always convincing. The limit of the analysing techniques has become evident in conservation practise. Knowledge of how mortars have been fabricated, mixed, stored and applied is as important as the chemical composition. The authors have therefore collected information on the fabrication, compositions and use of mortars revealed by an examination of written historic sources.

1 Introduction

Laboratory tests on new mortars for restoration or repair having the same composition as a historic prototype rarely show neither the same appearance nor the same mechanical behaviour. One reason is a lack of knowledge of the ancient techniques of lime burning, slaking and tooling. Studying the historic documents therefore is not only relevant for historical research but is also of technical interest. Mortar production in pre-industrial time depended on the specific geological situation.

C. Marinowitz
Netzwerk Bau und Forschung, Tengen, Germany
e-mail: Marinowitz@aol.com

C. Neuwald-Burg (✉) • M. Pfeifer
Karlsruhe Institut für Technologie, Karlsruhe, Germany
e-mail: claudia.neuwald@t-online.de; matthias.pfeifer@kit.edu

Lime for the construction of the town hall of Bremen, for example, was obtained by burning shells due to a lack of limestone in northern Germany. The focus of this paper is on documents from the late middle ages from Southern Germany and Zurich where limestone was available.

2 Historic Sources

2.1 Original Mortar Samples – Limits of Technical Analysis

The most important source for historic mortar technology is the monument itself. Laboratory investigations on historic mortar samples provide information on the type of binder and aggregates and the binder aggregate ratio. In some cases the lime slaking process can be determined. More difficult is the identification of the origin of the ingredients. Sometimes hydraulic material is found close to pure lime mortar in the same part of an old building. This may occur when lime of different provenance has been used or when a pozzolanic component has been added. Information on the origin of the limestone would help to interpret the chemical analysis in such a case.

Particle size of the original binder and original water content (water-binder-ratio) of the fresh mortar can not be determined. The various methods of slaking, mixing, tooling the same ingredients produce mortars with different characteristics like bulk density and texture. In conservation practise frequently the question arises of which slaking method should be adopted for a repair mortar to match with the original mortar. Burnt lime could have been slaked with a surplus of water and matured for days, months or years. In other cases it was dry slaked under a layer of sand. A third method consisted in crushing burnt limestone and using it unslaked to prepare the so called *hot mortar*. The applied methods can not always be concluded from laboratory analysis (Figs. 1 and 2).

2.2 Written Documents

Eckert evaluated a multitude of historic texts related to the fabrication and use of lime mortar and traced developments in mortar technology from Roman antiquity to modern times [1]. In Italy a detailed collection of mortar recipes was published by *Archolao* [2]. Mostly, these recipes came from theoretical treatises of architecture from the fifteenth to the nineteenth century. In early middle ages contemporary descriptions of mortar fabrication are rare. The few known texts reveal the symbolic meaning of every human action in that time. The documents are more religious contemplation than technical account. More reliable documents are preserved from the late middle ages. A very precious source is the *Baumeisterbuch* of *Endres Tucher* [3]. *Tucher* was the public master builder of Nuremberg from 1464 to 1475.



Fig. 1 Presumably dry slaked medieval mortar with fine cracks in lime lump (*top left corner*)
(Photography: Neuwald-Burg 2008)

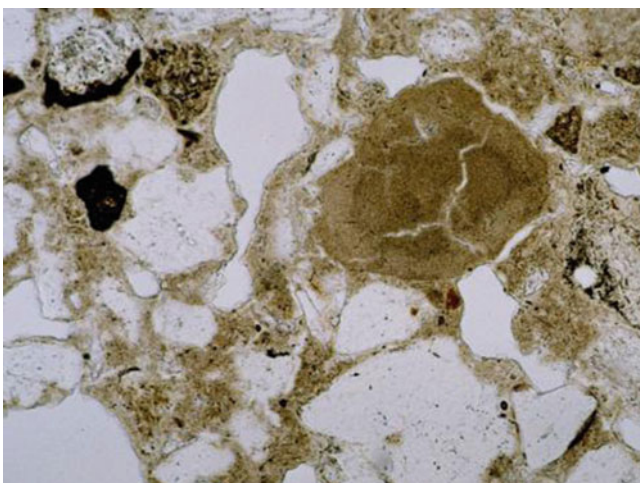


Fig. 2 Thin section of laboratory hot mortar (Photography: IFS-M 2437, Institut für Steinkonservierung e.V. Mainz, Dr. Karin Kraus)

The detailed description of his professional duties gives a very close view on organisation, construction and municipal life in the fifteenth century.

A document of similar importance is the *Zuricher Baumeisterbuch* from 1573 [4]. Both towns, Nuremberg and Zurich, had a high building activity at that time. The availability of building material especially of limestone was similar. Thus it could be expected that fabrication and employ of lime mortar was similar as well.

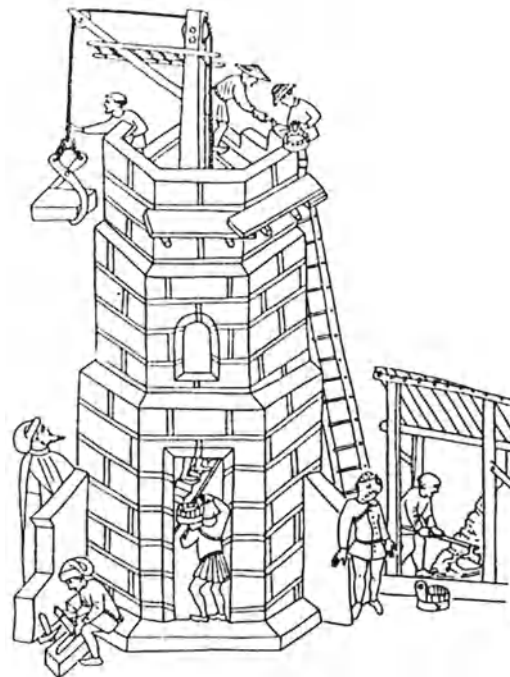


Fig. 3 Mortar prepared in an open hut (Binding (2001) p. 30, Abb. 67 (Berlin, Staatliche Museen zu Berlin, Kupferstichkabinett, MS 78 E1, fol 11, Rudolf von Ems Weltchronik (Toggenburg Bibel) Illumination))

In this paper both books are studied together with about 30 unpublished documents, mostly building accounts from Zurich, in order to get an insight into the local conditions of mortar fabrication at that time [5].

2.3 Depictive Representations

Though they are widely published, representations of building sites and of craftsmen still offer details on the fabrication of mortar which scarcely have been discussed until now.

Eckert investigated the medieval representations on mortar fabrication collected and published by *Binding* [1, 6, 7]. More than 100 pictures from eleventh to fifteenth century are preserved. The largest number of illustrations date from the fifteenth century (79 documents). Most of them show mortar as a pile of material, presumably sand and quicklime which is chopped or turned with a hoe.

Frequently a water bin is shown close to the pile. Sometimes the pile is protected by a roof (Fig. 3). In 17 pictures mortar is prepared in a case or frame of timber which

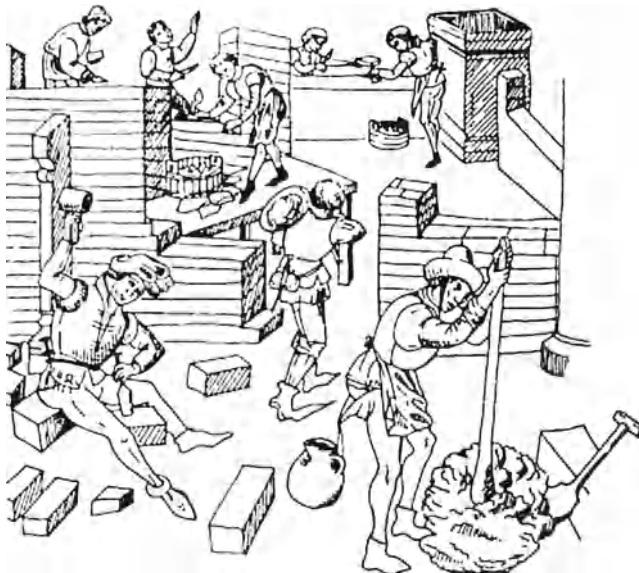


Fig. 4 Ramming mortar with rounded stake (Binding (2001) p. 170, Fig. 534a. (Strasbourg, Bibl. Nationale et Universitaire, Ms. 532, fol. 3, Augustinus, Cité de Dieu, Illumination, Netherlands))

could indicate the preparation and maturing of lime putty. The only picture showing a kiln on the construction site is an early mosaic from Palermo (twelfth century). Lime here is slaked in a closed case and seems rather liquid. An example for ramming an almost dry mixture is seen in Fig. 4. The procedure of ramming or beating can help to crush pieces of unslaked quicklime and to homogenise the lime-sand-mix. Ramming also consolidates the sand and lime putty by extruding surplus of water and air. The binder-sand contact is improved and workability increases compared to mixing by chopping and turning over.

3 Mortar Fabrication in Nuremberg and Zurich Around 1500

3.1 *Provenance of Limestone*

Both towns, Nuremberg and Zurich profited from limestone deposits. *Tucher* enumerates four quarries around Nuremberg which were about 20 km distant [3]. This distance corresponded to 1 day of travelling. A fifth quarry was explored some 40 km away at Deinschwang. Lime from Deinschwang was of better quality according to the master builder and therefore was worth the higher costs and efforts of transportation. *Tucher* commends the good yield and workability of this lime which was equally suitable for masonry mortar, rendering and limewash.

In Zurich the supply of lime was worse. The reason for this was not a lack of natural deposits but neglect by the building master. Quarries around Zurich were situated in distances between 0.8 and 24 km. Additionally the quarries around *Rüti* (43 km distance) could easily be assessed using the lake as way of transportation. The limestone in this case was burnt at or close to the quarry and the burnt material (quicklime) was packed and transported in *Röhrli*, special sealed wooden barrels which protected the hazardous material from air and water. Another source of limestone was the river Sihl. Here pebbles could be collected and burned during the winter, when the quarries were inaccessible [4].

Rights of ways could have presented another impediment to procure limestone. Litigations of this type are documented for both towns.

3.2 Sand

Sand usually is the most important component by volume in mortar. Nevertheless *Tucher* does not mention sand at all. In Zurich every citizen had to procure the sand he needed individually. In spite of that rule, one resolution concerning sand is documented charging the master builder with the provisioning of enough sand in the municipal lime hut to accommodate the demand. In 30 accounts of building materials from the years 1531 to 1752 the purchase of sand occurs only once. This means that suitable sand must have been easily available and presumably free of costs in both cities.

3.3 Fabrication and Storage

3.3.1 Nuremberg

None of the documents referred to in this study treats the process of lime burning itself but it is mentioned where the kilns were situated and how the production was planned in advance.

Two kilns were situated on the territory of Nuremberg. The public master builder was responsible for the provisioning of the town with building material. *Tucher* knew the exact quantities of limestone and the amount of wood one filling of a kiln would need. Providing enough firewood often represented a major problem. The surroundings of Nuremberg had been stubbed out due to the large demand for timber and fuel. Wood had to be ordered a long time in advance. As *Tucher* complains, the firewood sometimes had been stolen. Thus the heat obtained in the kiln was insufficient for lime burning. This could endanger a whole building project.

Lime also was burnt by peasants in the vicinity. This gave them a little secondary income. When needed *Tucher* had one or two supplementary kilns erected directly on the market place. This was necessary when the price for lime increased due to price-fixing agreements of the peasants or in cases of increasing demand.

The burnt lime was stored dry in special huts. No indication of pits for slaking can be found in the *Baumeisterbuch*. The product was sold as quicklime but the order is reported that a building master must have the lime slaked before handing it out. The product then is sold '*melbsweis*'. This unusual German term signifies 'like flour' which would indicate that the pieces of quicklime had been reduced to powder in the slaking process. In fact quicklime breaks into pieces when the amount of water added is less or just exactly sufficient to turn all the oxide of Calcium into hydroxide. Only with excess of water it becomes a paste or liquid lime putty. Thus in Nuremberg in the end of the fifteenth century probably lime was pre-slaked and transported in a dry state to the building site, where it was mixed with sand and water.

3.3.2 Zurich

Most lime kilns in Zurich belonged to the brickyards, but the municipality of Zurich also maintained one kiln [4]. In 1540 lime here was stored in special barrels mainly as quicklime for use in masonry mortar and some as lime putty for limewash. This changed in the following years. Preserved inventories of the lime huts indicate that from 1600 to 1612 lime was mainly stored as lime putty and between 1620 and 1670 the whole municipal stock was lime putty. The reason for this change is not yet understood. Around 1600 there was an increasing demand for stucco on interior walls. This might explain the large storage of lime putty. Before, masonry mortar and plaster had been produced with the same type of binder but using different sands. Stucco needed a fine graded, homogeneous binder. The total absence of quicklime in the stock is nevertheless striking and it would be of interest to investigate whether lime putty has been used for setting mortar at that time. It was not before 1670 that quicklime reappeared in the inventories.

3.4 Mortar Fabrication

Numerous German terms like *mortarrührer* (mortar stirrer) *mortarkocher* (mortar cooker) or the latin *caementarius* describe the profession of a mortar maker. Representations of craftsmen from the fifteenth century in Nuremberg show the mortar maker in an almost stereotype manner (Fig. 5). Only one folio represents a closed mortar case with a pile of sand or dry slaked lime (a sand-lime-paste or powder) and two water bins close beside (Fig. 6). The timber case here is divided into two sections, both filled with mortar. The horizontal surface indicates a rather liquid consistency. This could show the process of slaking burnt lime and maturing lime putty but the absence of pieces of burnt limestone in the otherwise detailed representation makes it more liable that a pre-slaked mixture is diluted for a lime-wash or rendering mortar. The mortar maker was responsible for the fabrication of mortar for the stonemasons, plasterers and the roofers.



Fig. 5 Mortar maker in Nuremberg in 1425 (Hausbuch der Zwölfbrüderstiftungen, Amb. 317.2° Folio 36 recto (Mendel I), Staatsbibliothek Nürnberg)

Even though his wage was inferior to that of a mason, he was not an untrained worker or helper. However, reliable craftsmen were rare in medieval towns and good mortar was not always guaranteed.

Tucher complains about unskilled workers unable to produce reasonable mortar for the roofer and therewith endangering the building project. And in Zurich it was reported that in 1541 the mortar sold of the municipal building yard repeatedly was not properly slaked but *burnt*.

In summer 1541 the lime hut in Zurich was reorganized. The building yard with the lime hut was situated outside the town. Here, mortar was prepared and stored together with the municipal provision of tiles. Regularly the sale of tiles and *mortar* (not *lime* as usually was sold in other towns) was recorded. According to *Guex* mortar was prepared at the lime hut by dry slaking with water and sand [4]. The accounts also refer to the delivered quantities of lime and sand. The given quantities allow a rough estimation of the most common binder aggregate ratio. A ratio of 1:3 is assessed which seems reasonable and typical for masonry mortar in regions with limestone deposits and normal graded sand.



Fig. 6 Preparation of lime mortar in 1522 (Hausbuch der Zwölfbrüderstiftungen, Amb. 279.2° Folio 13 verso (Landauer I), Staatsbibliothek Nürnberg)

4 Conclusions

Whether better lime was obtained by slaking and maturing or by dry slaking depended on the features of the available limestone variety. In pre-industrial times the possibilities of mortar fabrication were determined by the specific local conditions. The practise of burning lime pebbles reported in Zurich could explain larger scatterings in the chemical composition of the binding matrix observed in some analysis, because material transported by the river was more heterogeneous than quarry material. Even today the qualities of burnt limestone are difficult to predict. Recent analytical research in Germany to establish a prediction model revealed the complexity of this issue [8].

Apart from local geological conditions, infrastructure, economic situation and changes in the architectural treatment of surfaces sometimes political realities had an influence on mortar fabrication. Lime burning and slaking was organized by the civil administration. In the fifteenth century mainly dry slaked lime or lime paste were applied. Lime putty apparently became widespread in Zurich in the seventeenth century. No indication for grinding burnt lime could be found for preparation of hot

mortar. Which technology exactly has been applied for different purposes is not yet fully understood. Current analytical research focuses on detecting the characteristics of hot lime, dry slaked or matured putty binders.

Comparing the documents related to mortar fabrication in the late middle ages of Zurich and Nuremberg, this paper shows that mortar composition is too complex to be summarized in a couple of generalised formulas. Collecting and evaluating historic documents can provide a better understanding of regional phenomena. Together with specific analytical investigation of historic specimens as well as on restoration mortars it should become possible to distinguish local findings and avoid inaccurate generalisations.

References

1. Eckert, H.: Altes Mauerwerk nach historischen Quellen. In: Wenzel, F. (ed.) Erhalten historisch bedeutsamer Bauwerke. Jahrbuch 1991 des SFB 315, pp. 19–64. Ernst und Sohn, Berlin (1993)
2. Archolao, C.: La ricette del restauro. Malte, intonachi, stucchi dal XI al XIX secolo, 2nd edn. Venice (2001)
3. Tucher, E.: Baumeisterbuch der Stadt Nürnberg. In: Von Weech, F. (ed.) Bibliothek des Literarischen Vereins (1862), Bd. 64. Reprint, Amsterdam 1968 (1464–1475)
4. Guex, F.: Bruchstein, Kalk und Subventionen – das Zürcher Baumeisterbuch als Quelle zum Bauwesen des 16. Jahrhunderts. Mitteilungen der Antiquarischen Gesellschaft in Zürich, Bd. 53, Zurich (1986)
5. 30 unpublished documents. Staatsarchiv Zurich. For details please contact marinowitz@aol.com
6. Binding, G.: Der mittelalterliche Baubetrieb in zeitgenössischen Abbildungen. Wissenschaftliche Buchgesellschaft, Darmstadt (2001)
7. Binding, G.: Baubetrieb im Mittelalter. Wissenschaftliche Buchgesellschaft, Darmstadt (1993)
8. Hogewoning, S., Marbun, B., Wolter, A.: Forschungsbericht 1/08 der Forschungsgemeinschaft Kalk und Mörtel e.V, Köln (2008)

The Earliest Use of Lime and Gypsum Mortars in Cyprus

Maria Philokyprou

Abstract The microstructural investigation of prehistoric mortars selected from various archaeological sites of Cyprus demonstrated that the discovery of lime and gypsum technology had occurred on the island during the Neolithic period. This technology was already known in the Near East since earlier periods (Epi-Paleolithic period). Lime mortars were widely disseminated during the Chalcolithic period, whereas the use of gypsum mortars was rather limited on the island during all of the prehistoric periods. The discovery of crushed-brick lime mortars during the Late Bronze Age constitutes an innovation and can be associated with the overall prosperity of the era. The use of these mortars seems to have occurred simultaneously with the Mycenaean world. The selection of the raw materials for the preparation of mortars was based on the geology of each area. The absence of volcanic rocks in Cyprus led to the use of bricks as additives in the preparation of hydraulic mortars.

1 Introduction

Lime and gypsum mortars were used extensively in various structures in Cyprus, employed mainly as plaster coatings. This paper presents the results of an extensive research aiming to investigate the chronological evolution of these two main types of mortars during the earliest periods of antiquity in Cyprus. This research also aims to investigate the different methods of their preparation and to identify the pyrotechnology known during these periods. The ultimate aim is for the results to form a database for investigations of mortar from all the different periods of antiquity of the island. It is also hoped that the results will form the basis

M. Philokyprou (✉)
University of Cyprus, Nicosia, Cyprus
e-mail: philokyprou.maria@ucy.ac.cy

for the development of compatible mortars for conservation purposes. Lime and gypsum mortars have been in use without any significant changes in the vernacular architecture of the last two centuries on the island before the introduction of cement, showing the high level of pyrotechnology reached in these early periods of antiquity.

Lime and gypsum, which have been the two main mortar binders since antiquity, are derived from the burning of limestone and gypsum rocks respectively. The discovery of lime and gypsum plasters introduced a revolutionary pyrochemical advance, in which natural rocks underwent chemical change when heated, and when crushed to powder and mixed with water, created a paste that could be easily worked [1]. The chemical composition of lime and gypsum binders is identical to that of the corresponding natural rocks, although their microstructure is different. The technology in the production of pozzolanic or crushed brick-lime mortars is more complex. These can be manufactured by mixing lime with pulverized clay materials called pozzolans (natural or artificial). When finely ground, the pozzolans react with lime at normal temperatures in the presence of water or moisture to form stable calcium silicate/aluminate hydrates. The hydraulic character of such mortars is due to the reactions between the pozzolanic material and the lime binder.

During the prehistoric periods, in most areas, either gypsum or lime was preferred. In the Levant (Syro-Palestine coast), Anatolia and Greece [2, 3], lime plaster was almost exclusively the material of choice. In these areas [4] the use of gypsum plasters in the earliest periods of antiquity is rather limited. According to Gourdin and Kingery [4], the limited use of gypsum can be related to the difficulty in maintaining the low temperatures required for the preparation of gypsum plasters, as well as to the solubility of this material which makes it unsuitable for exterior use. However, gypsum is the material of choice in the area of the Tigris and Euphrates and further to the East [1, 5]. Recent studies have shown that in ancient Egypt, lime was also used: a fact that contradicts the previous beliefs that gypsum was exclusively used in this region [6]. Geographically, Cyprus constitutes an interesting case, as it is located in the lime region between the Levant, Anatolia and Greece [1], but has very notable deposits of gypsum.

2 Experimental

This research was based on the investigation of 120 prehistoric samples of lime and gypsum mortars derived from various archaeological sites of Cyprus (Neolithic, Chalcolithic, Bronze Age – as shown in Fig. 1). Initially, plasters and mortars were studied *in situ* (photographed, measured) and then samples were selected for laboratory analyses. The different layers of plasters were counted, the thickness of each was measured and the bond at each interface was investigated in detail. Special attention was given to the presence of admixtures and additives and their distribution throughout the mortars. Some of the samples constituted rather porous



Fig. 1 Map of Cyprus showing the sites from which samples were collected.

- Neolithic sites: Kalavasos Tenta, Khirokitia
- Chalcolithic site: Kissenerga – Mosphilia
- Late Bronze Age sites: Kition, Hala Sultan Tekke, Kalavasos-Ayios Dhimitrios, Maroni-Vounres, Alassa-Paliotaverna, Maa-Palaiokastro

crushable materials, but most were dense and coherent. The samples also differed in terms of grain size, colour, texture and surface roughness.

2.1 Methodology

All of the samples selected (120) were thoroughly observed in the laboratory under a stereoscopic microscope, followed by the preparation of thin sections of each specimen. These sections were examined using a petrographic microscope for the identification of the binder and the aggregates. The preliminary microscope observations led to a selection of a smaller number of samples (70) for further mineral analyses using X-Ray Diffraction (XRD) as well as for chemical quantitative analyses. From the results of these analyses, the 20 most characteristic and representative examples were subjected to a more detailed investigation. For the examination of the microstructure of these samples in the micron particle size, an SEM (Phillips 515) equipped with EDAX 9900 (Accelerating voltage: 25 kV, Counting time: 1,000 s, Standardless software for quantitative analysis: SUPQ) was employed to determine their composition in different parts through the analysis of the binders, aggregates, and reaction products. Differential thermal analysis (DTA) and thermogravimetry (TG) were employed for some lime plasters so as to determine the nature of the mortar constituents and to investigate the degree of their hydraulicity.

2.2 Results and Discussion

In this paper the cumulative results derived from the analyses of a large number of samples are presented in chronological order. The samples are divided into different categories regarding their period and the settlement from which they were collected as well as their general composition (gypsum, lime, crushed-brick lime mortars).

2.2.1 In Situ Observations

The coating plaster of the Neolithic as well as Bronze Age walls was very often set in thin, successive layers. The placement of successive layers to produce a thicker coating was also observed in the wider area of the Near East [7]. The final external visible thin coating of lime was often applied above a base mud layer. This base layer contributed to better adhesion of the external coating to the structure of the wall. In the lower part of the vertical wall where it meets the horizontal floor, a series of small rounded stones was sometimes laid to ease the curvature of the wall coating [8], which continued as a floor coating. The floor plaster often constituted two or three successive layers. A fine-grained coating was often laid on one or two coarser substrates and sometimes placed on a base layer of flat stones [8]. This technique has also been widely observed in the Middle East since the Neolithic period [9]. These successive layers of different floor plasters during the earliest periods were associated not only with the construction technology but also with the duration of the structures. The thickness of the floors was also affected by social factors and particularly by the Neolithic custom of burial beneath the plaster floors – a practice that resulted in extensive use of plaster. This custom was widespread not only in Cyprus [8] but also in the Near East [7].

2.2.2 Laboratory Data and Results

The mineral (petrographic, XRD) as well as the chemical analyses carried out showed that during the Neolithic period, lime and gypsum – either separately or in combination – were used as plaster coatings for walls and floors. The samples selected were derived from the two most important settlements of this period: Kalavasos-Tenta and Khirokitia (Fig. 1). Floors and walls were usually coated with a thin, whitish plaster layer laid on a base of friable mud plaster. Samples were selected from the hardest and most dense final plaster layers. The XRD and chemical analyses of the samples showed that the plaster samples taken from Kalavasos-Tenta can be divided into separate categories based on their mineral and chemical composition [8]: gypsum plasters, lime plasters, and gypsum-lime or lime-gypsum plasters. Samples having both calcite and gypsum as their main components belong to the last two categories. The samples having a high percentage (more than 10% and less than 40%) of sulphur trioxide (SO_3) are considered gypsum-lime, whereas the samples with a lower percentage of SO_3 (less than 10%) are considered to be lime-gypsum. On the other hand, the samples from Khirokitia are mainly lime plasters.

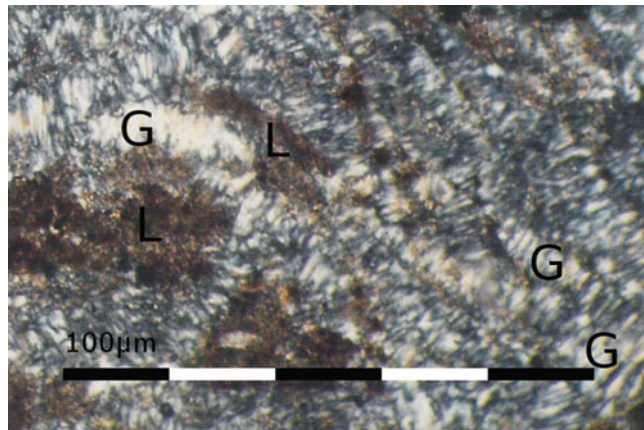


Fig. 2 Thin section (with cross nicols) of a Neolithic gypsum-lime plaster from Kalavasos-Tenta. The grains of calcite (C) are surrounded by the gypsum crystals (G)

The examination with a petrographic microscope and an SEM revealed that gypsum is the binding material in the gypsum and gypsum-lime mortars. Most of these mortars showed more than 20% SO₃. The structure of these Neolithic plasters is very different from the irregular microcrystalline morphology of the natural gypsum rock but also differs from the needle-like structure of the contemporary gypsum plasters. This is possibly due to the non-controlled heating procedure which leads to a different microstructure, but more probably is due to the age of the samples (7000 B.C.). Gourdin and Kingery made similar observations when studying Neolithic mortars from the Near East, recognising gypsum crystals of hard burned material in some samples [4]. According to Kingery et al. [1], the faceted gypsum grains observed in a plaster ball under investigation were formed by metamorphic grain coarsening over time. In the gypsum-lime mortars, gypsum crystals often surround the grains of calcite, giving the impression that the calcite is acting as an aggregate (Fig. 2).

The observation with a petrographic microscope of the samples of Kalavasos-Tenta and Khirokitia, which are mainly of a calcitic composition, revealed that in these cases, lime constitutes the binder. The observation of thin sections of the lime mortars confirmed the existence of siliceous aggregates. There were often pieces of igneous rocks (diabase) and a few silicates (quartz, pyroxenes, feldspars). The observations of the samples in the SEM showed that the crystalline form of the lime is different from the crystalline structure of the raw material used for its manufacture, as the large volume – change during the calcination process creates large strains in the surface layer of the reaction product forming small interconnected particles during the loss of CO₂. When mixed with water, the (expansive) hydration reaction forces it apart firstly into a CaOH powder and then into a putty (colloidal hydroxide). Thus, during recarbonation, extremely fine-grained calcium carbonate is produced with particles less than 1 μm in size [1, 4]. Thus, the crystalline form of the sample (size, uniformity) confirmed the calcination and hydration procedure (Fig. 3).

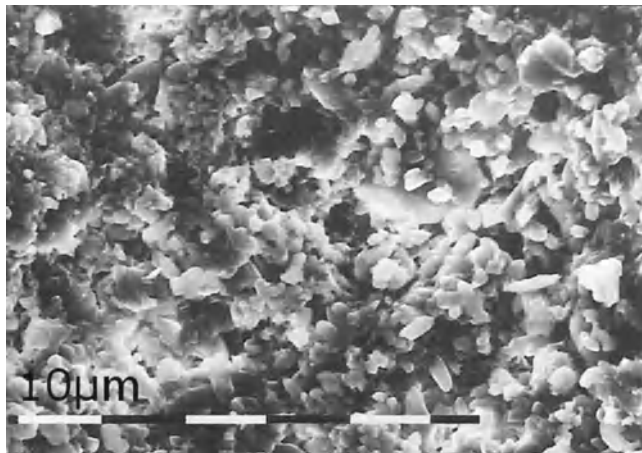


Fig. 3 SEM Photo showing the microstructure of a Neolithic lime mortar from Kalavasos-Tenta. Small rounded lime grains of small size (1–10 µm)

This very early use of lime mortars in Cyprus is not surprising since the invention of lime in the Near East can be dated back to the earliest periods of antiquity. According to Frierman [10], the production of lime originated in Anatolia and then spread to the Levant. More recent studies [1, 11] have shown that the invention of lime in the Near East can be dated back to the Epi-Paleolithic period (12000 B.C.) while the earliest use of lime in architecture took place in the Early Natufian period (10300 B.C.). This plaster production was disseminated in the Aceramic Neolithic period and particularly in the seventh and sixth millennium B.C. when thick plaster floors were widely adopted [1].

The fossils, observed mainly in thin sections of lime and lime-gypsum mortars, suggest the presence of aggregates of calcitic composition. According to Hughes et al. [12], small lime lumps of under-burnt or over-burnt quicklime can often be recognized in the historic lime mortars, showing that the calcination process was not complete. The presence of lime lumps is sometimes interpreted as having been caused by a practice where damp aggregate is deliberately mixed with roughly crushed quicklime [13]. This was a typical ancient and traditional technique [4]. The use of lime and gypsum plasters appears to be associated with the emergence of permanent architecture during the Neolithic period of the island, accompanied by the need for building materials resistant to environmental conditions. This theory is also supported by Kingery et al. [1], who reported that “the appearance of permanent architecture brought with it the desirability of building materials resistant to environmental weathering.” In Cyprus during the Neolithic period, the knowledge of the technology for plaster production, in relation to the rest of the civilization, either suggests a sophisticated culture that was introduced to the island from abroad or constitutes an evolution of an earlier local civilization.

Chalcolithic mortars were mainly collected from Kissonerga-Mosphilia, one of the most important sites of this period (Fig. 1). Their detailed investigation showed

that the lime heating process was widespread on the island during this period, as several plaster floors of considerable thickness were found, all consisting of one or two dense layers of lime, 5–10 cm thick. In his PhD thesis on Prehistoric Cypriot Buildings, Thomas [14] gives some preliminary estimates regarding the Chalcolithic floors of Kissonerga. For the largest circular house of the settlement with a diameter of 15.0 m and a floor thickness of 10 cm, the required lime was calculated to be 2.5 m³. For smaller structures with a diameter of about 9.5 m, approximately 1 m³ lime was probably used. These thick lime floors were quite different from the Neolithic thin final layers of lime. The study of the thin sections showed that the binder is microcrystalline-calcite. The examination of the microstructure of the plasters using the SEM revealed a uniform fine-grained material (calcite grains 1–3 µm). The physical (hardness and thickness) and chemical characteristics, as well as the microstructure of the Chalcolithic floors, suggest that the combustion process of limestone was widespread during this period. It can be deduced that lime plaster floors have existed since the Neolithic period, but in most cases they just constituted one or two very thin upper layers. Thus, the process of heating limestone, although known during the Neolithic period, was widely disseminated during the Chalcolithic period.

The results for the Bronze Age lime plasters were based on analyses of samples selected from six very significant sites of the Late Bronze Age (Kalavasos-Ayios Dhimitrios, Maroni-Vournes, Hala Sultan Tekke, Maa-Palaiokastro, Kition and Alassa-Palaiotaverna – Fig. 1). In the primary rooms of important public buildings, the coatings of the flooring were thick and consisted of hard calcitic material [8] that was recognised under the SEM as lime. The discovery and use of crushed brick-lime mortars for the first time in the Late Bronze Age constitutes the most important evolution in the manufacture of lime mortars during this period. Their main use was in floors, where the capillary rise of water was expected (bath rooms and workshops) and in various water-related structures (water channels). Small reddish particles were observed in all samples during examination under an optical microscope. These particles were recognized as ceramic fragments in thin sections (Fig. 4). The high quantities of aluminium, iron, and silicon oxides are directly related to the addition of clay ceramic material during the preparation of the mortars. The identification by XRD of gehlenite, a mineral that is seldom found in nature but is characteristic of the use of ceramics heated to 800–1,060°C or natural hydraulic lime, is important. The presence of anorthite in some samples also confirms the use of ceramics [15].

The observations under the SEM showed that crushed brick-lime mortars have a compact microstructure of the type formed in hydraulic mortars. The ceramic fragments in the thin sections appeared as reddish clay inclusions (Fig. 4). The ceramic is extremely fine and uniformly distributed, with some grains smaller than 1 mm. The small size of the ceramic grains considerably increases the interaction surface area of the ceramic with the calcium. During the consolidation phase, the grains of the ceramic, particularly their periphery, seem to react with calcium hydroxide to create calcium silicate and aluminate hydrates, which results in the hydraulicity of the mortars. The pozzolanicity of these mortars is attributed to the adhesion reactions occurring at the ceramic matrix interface. It is known that brick powder has a high pozzolanicity when it is heated to low temperatures. Ancient ceramics were

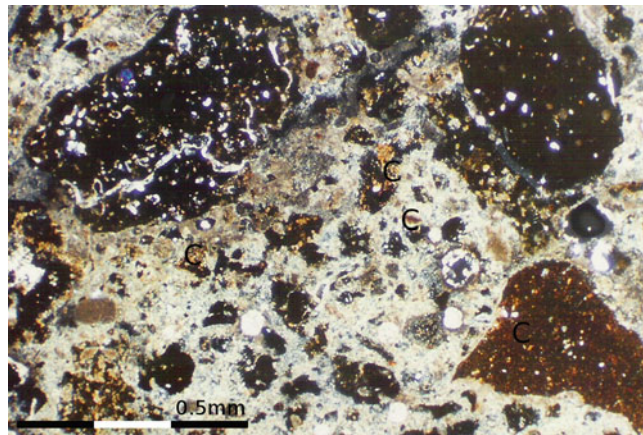


Fig. 4 Thin section (with cross nicols) of a Late Bronze Age crushed-brick lime plaster of a water channel from Kalavasos-Ayios Dhimitrios. Red irregular inclusions of ceramics (K) of different sizes (0.1–1.5 mm) in a lime matrix

often heated to relatively low temperatures, and so they were suitable as pozzolanic additives. The thermal curves confirmed that the examined crushed brick-lime mortars were hydraulic. Weight loss, estimated through thermal analyses, between 200°C and 600°C is attributed to the loss of structurally bound (hydraulic) water, i.e. due to the decomposition of calcium silicate and calcium aluminate hydrates. The Late Bronze Age crushed brick-lime mortars consist of 5–8% structurally bound water, so they present a moderate hydraulic character.

The appearance of the crushed brick-lime plasters in Cyprus during this period can be associated with the overall prosperity of the era and particularly with the emergence of urban centres. The appearance of crushed brick-lime mortars seems to occur simultaneously in the Mycenaean and Minoan world as well [3]. Recent studies have shown the use of natural pozzolanic additives in the later Minoan periods in Crete [16]. On the other hand, in the Levant, the earliest use of lime plasters with hydraulic properties is dated to the Early Bronze Age, and thus appears to precede the use of the similar mortars in Cyprus [8].

With the exception of the widespread use of gypsum plasters in the settlement of Kalavasos-Tenta, gypsum plasters are to be found mainly during the Late Bronze Age for special applications (i.e. as a material for the fastening of wooden elements). The limited use of gypsum is surprising, since the island has very notable deposits of gypsum rocks. Observations by SEM on the Late Bronze Age gypsum plasters revealed the existence of various well-shaped elongated or rather rounded crystals (Fig. 5). The microstructure of these samples is very similar to the structure of other historic gypsum mortars, but differs from contemporary ones [1, 4, 17].

According to Middendorf [17], a long-term weathered gypsum mortar is made up of large rounded crystals due to accumulated crystallization process induced by wet and dry cycles during weathering processes, and thus differs from

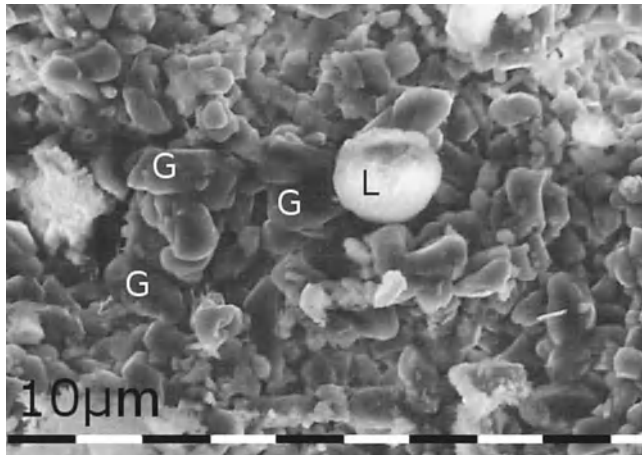


Fig. 5 Thin section of a Late Bronze Age gypsum plaster found near a door frame in Kalavasos-Ayios Dhimitrios. Rounded flat gypsum crystals (G) with a small number of rounded lime grains (L)

contemporary gypsum mortars. The procedure described by Strahan [18] was followed for further verification of the manufacturing method of gypsum mortars. According to this theory, the final gypsum product of calcination can be distinguished from the natural rock by the XRD diagram when samples are mixed with acetone. By using acetone slurry on a quartz plate, the preferred orientation of the crystals is duplicated. The relationship between the three major gypsum XRD peaks was investigated ($7.56, 4.28, 3.06 \text{ \AA}$) and the intensity of the peak of 7.56 \AA (first peak) was compared to the other two samples. According to Strahan, the peak of 7.56 \AA is consistently lower than the other two in the plasters. The prehistoric plasters examined showed the first peak to be lower than the others, confirming this assumption.

The analyses under the SEM indicated that most of the samples have a compact microstructure typical of old historic mortars, with aggregates well-embedded in the matrices [1, 4]. Chemical quantitative analyses showed that in most of the aerial and crushed-brick lime plasters, the relationship between silicon and aluminum oxides is linear (Fig. 6). The same relationship can be observed between silicon and ferric oxides. This leads to the conclusion that these oxides are related to the existence of clay minerals in aerial lime mortars. In crushed brick-lime mortars this can be related either to ceramic additives or to the presence of raw clay mineral composition. The relationship between silicon and calcium oxides appears to be of an inverse nature in all lime mortars. Gypsum mortars constitute a different case with a limited content of aggregates. The diagrams and the analyses showed that the gypsum mortars, especially those of the Bronze Age, were prepared by the calcination of pure gypsum rocks, whereas lime mortars always had other additives, either due to the composition of the raw material or to the addition of aggregates during the manufacturing process.

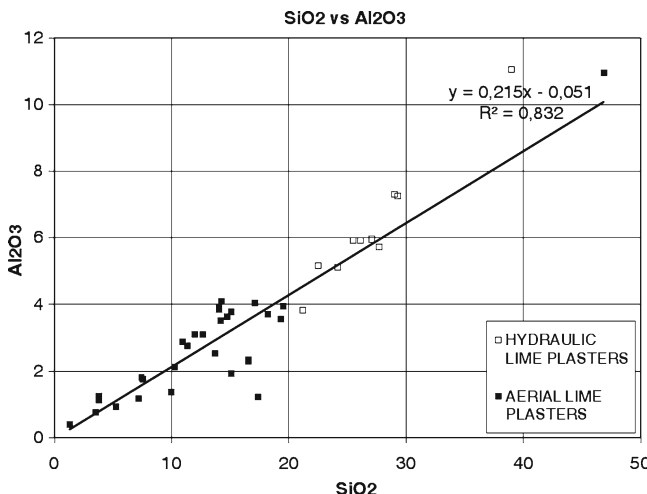


Fig. 6 Diagram showing the relationship between Al_2O_3 and SiO_2 in aerial lime and crushed-brick lime mortars of the Bronze Age (Diagram derived from the results of bulk chemical analyses of the samples)

3 Conclusions

The investigation showed the chronological evolution regarding the use of mortars in Cyprus. Lime and gypsum seem to have been used since the Neolithic period. Lime was the material of choice during all the prehistoric periods, whereas the use of gypsum was rather limited. The use of the different types of plasters, especially during the Neolithic period was related to the environment in the vicinity of the settlements. This explains the wide use of gypsum, lime, gypsum-lime and lime-gypsum mortars in Kalavasos-Tenta, where the neighbouring rocks and soils were of these compositions. The preference for the use of lime mortars in Khirokitia was also connected with the presence of such rocks and soils in the immediate environment. The discovery of crushed-brick lime mortars during the Late Bronze Age constitutes an innovation, and it is associated with a significant evolution in the pyrotechnology of this period. The preference for the use of ceramic as a hydraulic additive instead of natural pozzolans is due to the absence of such physical volcanic minerals on the island.

This research demonstrated the need for the use of a combination of different characterisation techniques for the detailed study of ancient mortars [19]. It is obvious that the investigation of the various types of plasters gives information about the knowledge level of technology, the economy and organization of the production of a region, and the distribution of raw materials and finished products.

Acknowledgement The information for the preparation of this paper is derived from an unpublished PhD thesis, submitted by the author to the University of Cyprus and supervised by Professor Vassos Karageorghis as well as from one multidisciplinary research program on

ancient plaster technology financed by the Research Promotion Foundation of Cyprus (with code RPF 34/99). The laboratory analyses were carried out in the Research Center of Democritos, Athens (SEM with EDAX, qualitative XRD analyses) and in the laboratories of two government departments (Geological Survey Department, Cyprus: Chemical analyses, Institute of Geological and Mineral Exploration, Athens: Quantitative XRD analyses, Petrographic analyses, Thermal analyses).

References

1. Kingery, W.D., Vandiver, P.B., Prickett, M.: The beginnings of pyrotechnology, part II: production and use of lime and gypsum plaster in the pre- pottery Neolithic Near East. *J. Field Archaeol.* **15**, 219–244 (1988)
2. Davey, N.: *A History of Building Materials*. Phoenix House, London (1961)
3. Shaw, J.W.: *Minoan Architecture: Materials and Techniques*. Annuario della Scuola Archeologica di Atene et delle Missioni Italiane in Oriente XLIX. Nuova Serie 33. Rome (1973)
4. Gourdin, W.H., Kingery, W.D.: The beginnings of pyrotechnology: Neolithic and Egyptian lime plaster. *J. Field Archaeol.* **2**, 133–150 (1975)
5. Arnold, D.: *Building in Egypt*. Oxford University Press, New York (1991)
6. Borelli, E., Laurenzi Tabasso, M.: Which binder for the Egyptian plasters of the Pharaohs' monuments? In: *Proceedings of the 8th International Congress on Conservation of Stone*, Berlin, pp. 1447–1456 (1996)
7. Garfinkel, Y.: Burnt lime products and social implications in the pre-pottery Neolithic B villages of the Near East. *Paleorient* **13**, 69–76 (1987)
8. Philokyprou, M.: Building materials and structures of the architecture in Cyprus, from the Neolithic period until the Late Bronze Age. PhD thesis, University of Cyprus (1998)
9. Ronen, A., Bentur, A., Soroka, I.: A plastered floor from the Neolithic village, Yiftahel (Israel). *Paléorient* **17**(2), 149–155 (1991)
10. Frierman, J.D.: Lime burning as the precursor of fired ceramics. *Isr. Explor. J.* **21**, 212–216 (1971)
11. Thusen, I., Gwozdz, R.: Lime plaster in Neolithic Hama, Syria. *Paleorient* **8**, 99–103 (1982)
12. Leslie, A.B., Hughes, J.J.: Binder microstructure in lime mortars: implications for the interpretation of analysis results. *Q. J. Eng. Geol. Hydrogeol.* **35**, 257–263 (2002)
13. Hughes, J.J., Leslie, A.B., Callebaut, K.: The petrography of lime inclusions in historic lime based mortars. In: *Proceedings of the 8th Euroseminar on Microscopy Applied to Building Materials*, Athens, pp. 359–364 (2001)
14. Thomas, G.D.: Prehistoric Cypriot mud buildings and their impact on the formation of archaeological sites. PhD thesis, University of Edinburgh (1995)
15. Péreinet, G., Courtois, L.: Évaluation des températures de cuisson de céramiques et de vaisselles blanches néolithiques de Syrie. *Bulletin de la Société Pr. Française* **80**, 157–160 (1983)
16. Maravelaki-Kalaitzaki, P., Bakolas, A., Moropoulou, A.: Physico-chemical study of Cretan ancient mortars. *Cem. Concr. Res.* **33**, 651–661 (2003)
17. Middendorf, B.: Physico-mechanical and microstructural characteristics of historic and restoration mortars bases on gypsum: current knowledge and perspective. In: Siegesmund, S., Weiss, T., Vollbrecht, A. (eds.) *Natural Stone, Weathering Phenomena, Conservation Strategies and Case Studies*, pp. 165–176. Geological Society, London (2002)
18. Strahan, D.K.: Naturally deposited versus intentionally applied gypsum on archaeological materials from Harappa, Pakistan. *J. Field Archaeol.* **18**, 527–530 (1991)
19. Papayianni, I.: A holistic way of studying mortars and bricks of ancient masonry for manufacturing compatible repair materials. In: *Proceedings of the 4th International Symposium on the Conservation of Monuments in the Mediterranean*, Rhodes, pp. 265–274 (1997)

Mineralogical and Microstructural Analysis of Mortars from Kushite Archaeological Sites

Jean-Pierre Letourneau and Serge Feneuille

Abstract This paper presents the XRD, XRF and porosimetry analyses and SEM-EDX observations of nine mortars: three Egyptian plasters (New Kingdom, fifteenth to eleventh century B.C.) and six Meroitic mortars (first century AD) collected on temples, palaces and pyramids in archaeological sites located between the Third and Fourth Cataract. The two first Egyptian samples were mainly composed of gypsum plaster. The third one and a bedding mortar collected on a Meroitic pyramid were composed of siliceous sand bound by about 30% kaolinite-rich clay. A coating mortar collected on another Meroitic pyramid, probably highly lixiviated, had a similar composition with only 11% clay. The other Meroitic samples appeared as conventional fully carbonated lime-sand mortars. The compositions of the decorative surface layers varied from clay to lime or lime-and-gypsum, in the form of painting or applied as fresco. This extreme diversity of compositions observed is particularly interesting from an archaeological point of view. The knowledge of the various techniques used enables us to have a better understanding of foreign influences on building workers in ancient North Sudan.

1 Introduction

Building materials often contain a lot of archaeological information and reveal the history of techniques. The use of mortars as a facing material is a major feature of Kushite architecture in the Northern Sudan. Knowing the initial composition of

J.-P. Letourneau (✉)
Lafarge Centre de Recherche, Saint-Quentin-Fallavier, France
e-mail: jp.letourneau@cegetel.net

S. Feneuille
French Section of the National Corporation for Antiquities
and Museums, Khartoum, Sudan
e-mail: sfeneuille@wanadoo.fr

these mortars is therefore a matter of importance from an archaeological point of view and for the faithful restoration of the monuments concerned. However, until the year 2000, this issue received very little attention [1, 2].

In a first study presented in HMC08 [3], the analysis of Meroitic mortars (two first centuries AD) coming from Kushite archaeological sites around the ancient city of Meroe led us to propose the hypothesis that these mortars were originally lime-and-gypsum based. This study was recently completed by petrography [4]. Moreover, analyses of a gypsum-rich caliche from Omdurman (200 km upstream of Meroe) and a Sudanese gypsum from the Red Sea, with respectively 0.18% and 0.94% SrO, are compatible with our hypothesis, mainly based on the strontium sulphate as a tracer of a previous presence of gypsum in our mortars.

Two other samples coming from Dukki Gel, located 500 km north from other sites, with a low SrO content, clearly did not belong to the same series. So it was particularly interesting to check if other mortars coming from sites near Dukki Gel had a composition similar to those already studied or were made using different techniques. Thus, this paper presents the chemical, mineralogical and microscopic analyses of these two Dukki Gel mortars, in comparison with seven new samples collected in archaeological sites located at or near Dukki Gel, along the Nile Valley between the Third and Fourth Cataract.

2 Origin of the Samples

The series presented here is made up of four bedding mortars used for laying bricks and five coating mortars having a protective or decorative function.

The oldest samples are three Egyptian plasters or bedding mortars collected in the archaeological site of Dukki Gel, located near the 3rd Cataract (Fig. 1):

- DG1, from Hatshepsut's temple (fifteenth century B.C.),
- DG2, Akhenaton's temple (fourteenth century B.C.),
- DG3, from a Ramesside temple, not precisely dated (thirteenth to eleventh century B.C.).



Fig. 1 Photos of Egyptian plasters

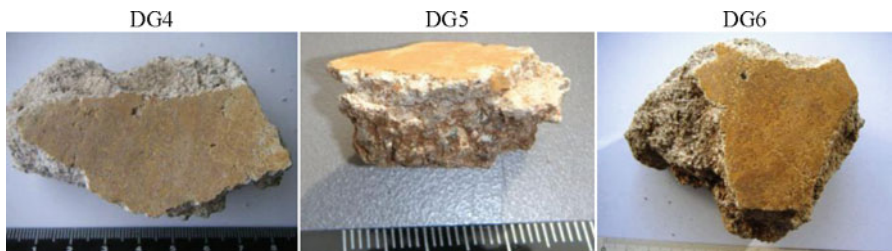


Fig. 2 Photos of Dukki Gel meroitic mortars



Fig. 3 Photos of Gebel Barkal and Kawa mortars

Three facing mortars of the Meroitic period were also collected in Dukki Gel, in the Amun temple of Natakanmani (first century AD): DG4 and DG5 from the previous study [3] and a new mortar DG6 (Fig. 2). These samples appear very similar, the mortar being covered by a thin decorative layer not analysed except by EDX for DG6.

Two other Meroitic facing mortars came from Gebel Barkal, located near the 4th Cataract (Fig. 3):

- GB1, from the palace of Natakanmani (first century AD), is relatively homogeneous, the external layer having a finer structure than the core.
- GB2, collected on a Meroitic pyramid (first to third century AD), is a red and brittle mortar covered by a white and hard crust only analysed by EDX

The ninth sample K1 was a bedding mortar from a late Meroitic pyramid (dated first to third century AD), from the site of Kawa located 50 km south of Dukki Gel (Fig. 3).

3 Analytical Techniques

It is necessary to use complementary analytical techniques for chemical, mineralogical and microstructural characterisations to obtain optimum understanding of these materials [5]. Except for the microscope observations, the external layers of samples

DG4, DG5, DG6, GB1 and GB2 were previously removed for characterizing the mortar alone. The mineralogical and chemical analyses were carried out on the whole series. X-Ray Diffraction (XRD) was used for identifying the nature of crystalline phases, such as binder components, sand or impurities. The elemental quantitative composition was determined by X-Ray Fluorescence (XRF) on fused beads, after measurement of the loss on ignition at 950°C.

The porosity and the pore size distribution were measured by mercury intrusion porosimetry on small pieces of dried mortar. Microscopic observations were performed on polished sections by Scanning Electron Microscope (SEM), associated with EDX for identifying the chemical elements.

Finally, samples with clay binder were analysed by ^{27}Al MAS-NMR in order to determine a possible evolution of aluminium coordination, which would indicate that the clay has been heated and partially transformed into badly crystallized reactive phases such as metakaolinite.

4 Results

4.1 Mineralogy

Table 1 gives the mineralogical composition of each dried mortar determined by X-ray diffraction, with a semi-quantitative evaluation only based on the peak intensities. These results clearly show three families of mortars, with gypsum, clay and lime or calcite binders.

The first two Egyptian mortars are based on calcium sulphate, in the form of gypsum for DG1 and gypsum, hemi-hydrate and anhydrite for DG2. Quartz (siliceous sand) is also present as a secondary or minor phase.

The third Egyptian mortar DG3 and the two Meroitic mortars GB2 and K1 appear composed of siliceous sand only bound by kaolinite, a clay mineral.

The other Meroitic facing mortars from Dukki Gel (DG4 to DG6) and Gebel Barkal GB1 have a similar composition corresponding to a lime-based mortar, with a high content of quartz and calcite. GB1 contains also calcium sulphate as a minor phase.

4.2 Chemical Composition

The results of XRF analysis of the mortars are reported in Table 2. Chemical elements are expressed in their oxide form. The loss on ignition (LOI) gives a good estimation of hydrates and carbonates content when present and helps to estimate the binder content.

The presence of calcium sulphate in the two first Egyptian mortars is confirmed by their large content of sulphur (SO_3) and calcium.

Table 1 Mineralogical composition by XRD

	Gypsum		Clay			Lime			GB1
	DG1	DG2	DG3	GB2	K1	DG4	DG5	DG6	
Quartz	+	++	+++	+++	+++	+++	+++	+++	+++
Calcite	+	-	-	-	-	+++	+++	++	+++
Gypsum	+++	+++	-						(+)
H-hydrate		++	-						+
Anhydrite		+++	-						
Cordierite	+	-	-		(+)				
Feldspars		+	(+)		+	+	(+)	(+)	(+)
Kaolinite	+	+++	+	++	-	-	-	-	

+++ Major phase, ++ Secondary phase, + Minor phase, (+) Traces

Table 2 Chemical composition by XRF (expressed in %)

	Gypsum		Clay			Lime			GB1
	DG1	DG2	DG3	GB2	K1	DG4	DG5	DG6	
SiO ₂	10.03	18.77	80.65	91.97	79.05	30.85	33.99	31.27	38.83
Al ₂ O ₃	1.77	3.42	12.42	4.39	10.84	1.38	1.84	1.61	2.08
Fe ₂ O ₃	0.84	1.84	1.28	1.05	2.34	0.92	1.07	1.01	1.21
CaO	29.67	27.63	0.16	0.08	0.73	23.75	24.13	30.03	26.48
MgO	0.59	0.65	0.12	0.06	0.45	9.92	9.07	5.27	1.11
K ₂ O	0.14	0.28	0.19	0.06	0.71	0.23	0.33	0.13	0.13
Na ₂ O	0.14	0.35	0.04	0.08	0.26	0.53	0.40	0.09	0.57
SO ₃	36.02	36.66	<DL	<DL	<DL	0.33	0.40	0.26	3.61
SrO	0.05	0.04	<DL	<DL	<DL	0.02	0.03	0.04	0.11
LOI	20.45	10.05	5.20	2.01	4.58	32.13	28.29	29.07	25.49
Total	99.87	100.14	100.51	99.91	99.93	100.42	100.09	99.18	99.97

Table 3 Porosity of mortars

Samples	DG5	DG6	GB1	GB2	K1
Porosity (%)	32.8	30.2	27.1	21.9	38.7

The clay mortars DG3, GB2 and K1 are characterized by a very high content of silica and a quasi-absence of calcium.

The other Meroitic mortars present a similar composition, with high calcium content and LOI, those from Dukki Gel having a higher proportion of magnesium. The presence of calcium sulphate in GB1 results in 3.6% SO₃ in the chemical composition.

4.3 Porosity

Table 3 gives the total porosity measured on five mortars. Porosities are quite variable, the extreme values being measured on the mortars from the Gebel Barkal pyramid

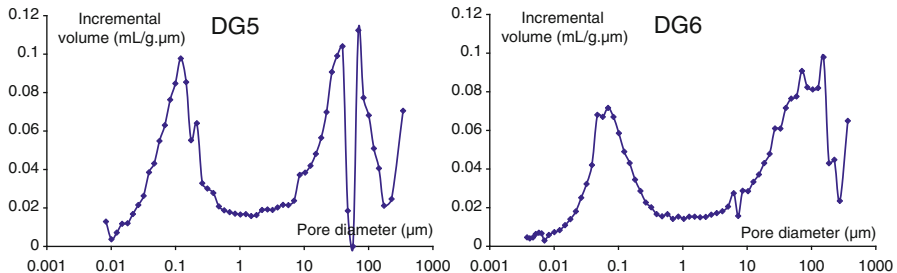


Fig. 4 Pore size distribution of DG5 and DG6

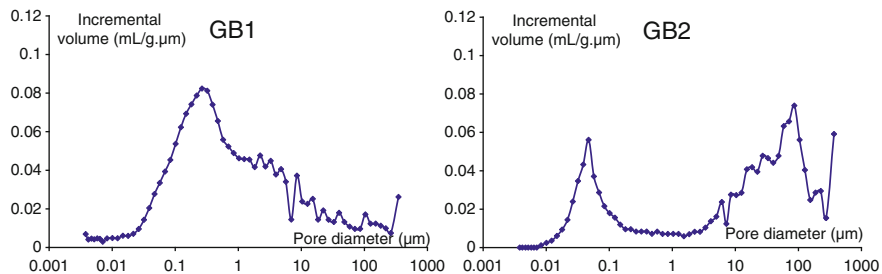
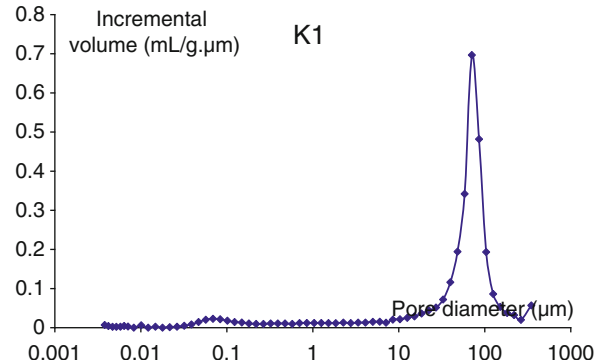


Fig. 5 Pore size distribution of GB1 and GB2

Fig. 6 Pore size distribution of K1



(22%) and the Kawa pyramid (39%). The other facing mortars from Dukki Gel and Gebel Barkal have the same level of porosity, about 30%.

Figures 4, 5, and 6 show the pore size distributions of the mortars. The meroitic mortars DG5 and DG6 (Fig. 4) have a similar bimodal distribution, with maxima at about 0.1 and 70–100 µm.

GB1 has a broad pore distribution with a maximum at 0.25 µm, while GB2 has a bimodal distribution with maxima at 0.05 and 90 µm (Fig. 5).

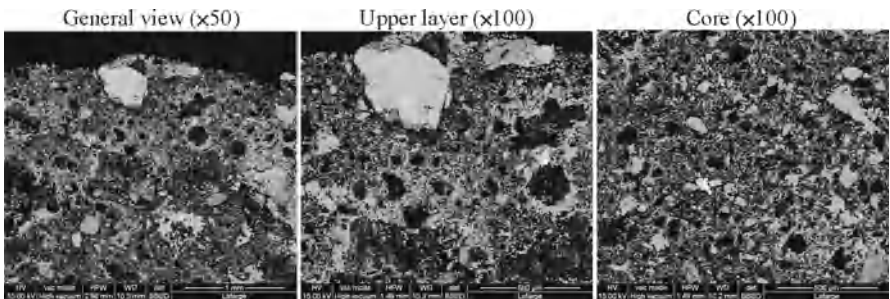


Fig. 7 SEM observation of DG1 (gypsum mortar)

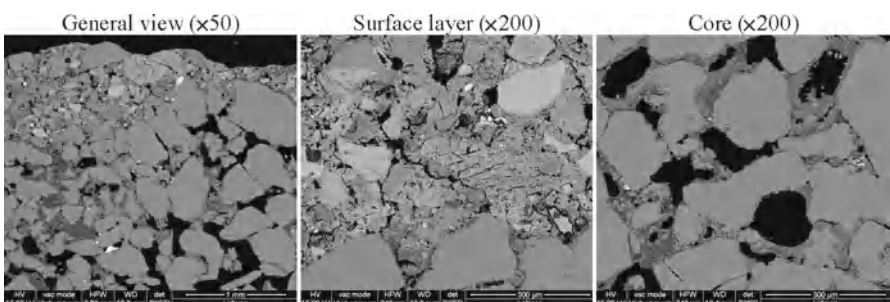


Fig. 8 SEM observation of GB2 (clay mortar)

Finally, the pore size of K1 is practically unidimensional, the distribution curve having only a single narrow peak centred at 70 µm (Fig. 6).

4.4 SEM-EDX Observations

Four samples representative of the different families were observed by SEM on polished sections in order to have a better understanding of their microstructure: the first Egyptian mortar, the new facing mortar from Dukki Gel and the two mortars from Gebel Barkal.

The Egyptian mortar DG1 (Fig. 7) appears with a bi-layer structure. The observation of the core shows a fairly porous structure, with a combination of fine gypsum needles and large grains. Needles typically come from the hydration of hemi-hydrate, while the large grains may be residual gypsum from an incomplete burning. The upper layer (several mm thick), probably due to settling, has a less compact structure than the core and a higher proportion of large grains of gypsum.

The core of the clay mortar GB2 (Fig. 8) is composed of a quite porous and probably very permeable structure, with angular grains of quartz interconnected by a few points of adhesive clay. It may consist of a mixture of sand and clay, or a natural

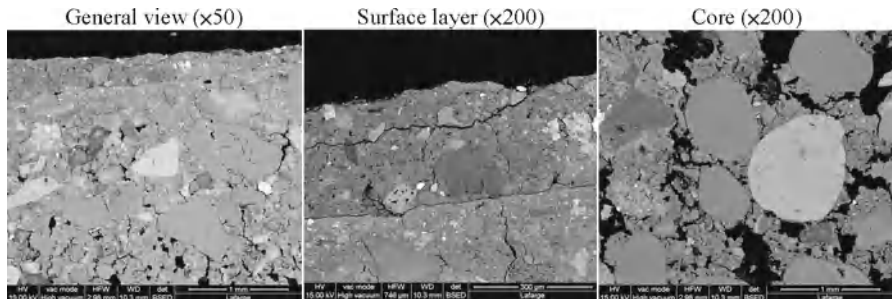


Fig. 9 SEM observation of DG6 (calcite mortar)

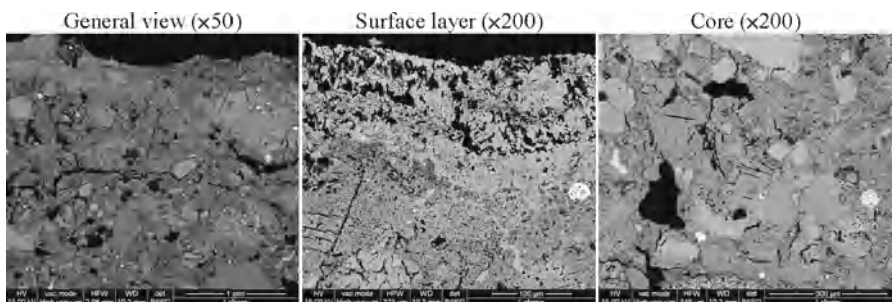


Fig. 10 SEM observation of GB1 (calcite mortar)

quartz-rich sediment. This mortar is covered by a very compact painting layer mainly consisting of calcium carbonate with traces of magnesium, without sand.

SEM observation of the core of the facing mortar DG6 (Fig. 9) shows siliceous sand in a calcium-rich binder. EDX analysis gives a widespread presence of Mg associated with Ca, indicating a magnesian calcite. The decorative surface layer (upper part in central photo) is made of silicon, aluminium and iron, without calcium or magnesium, and could probably consist of clay minerals.

The sample GB1 (Fig. 10) also appears as a mortar of carbonated lime and silica sand. EDX analysis confirms the presence of calcium sulphate. The lighter surface layer also contains calcite and calcium sulphate; its silica content, determined by XRF on a separate specimen, is only three times lower than the core.

4.5 ^{27}Al MAS-NMR Analysis

Two clay mortars DG3 and GB2 were analysed by ^{27}Al MAS-NMR in order to measure the coordination state of Al atoms in the clay structure. For both samples, Al was almost totally in the form Al(VI) with a large peak at 3.4 ppm (Fig. 11),

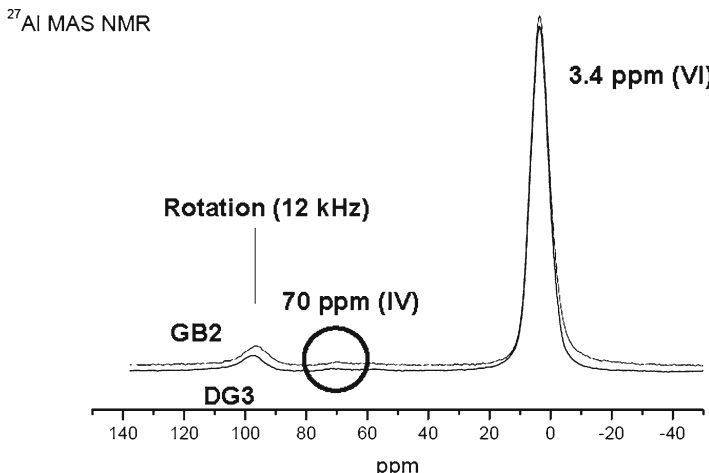


Fig. 11 ^{27}Al MAS-NMR spectra of DG3 and GB2

showing that clay mineral was not modified by any degradation or reaction such as geopolymserisation [6]. Traces of Al (IV) were only identified by very small peaks around 70 ppm, with intensity slightly over the detection limit.

5 Interpretation

All results show that the studied mortars may be classified into three categories. An estimation of their quantitative composition, calculated from the chemical and mineralogical analyses, is reported in Table 4. Calcium sulphate was calculated from SO_3 , taking into account the possible formation of SrSO_4 from SrO . Magnesium and excess calcium not combined as sulphate were considered in the form of carbonates and expressed as “limestone”. Kaolinite was calculated from Al content using the theoretical composition $\text{Al}_2\text{Si}_2\text{O}_5(\text{OH})_4$. Finally, sand was considered as the residual part, corresponding to quartz and minor phases. A good accordance was checked between the theoretical LOI of calculated phases and the experimental values. For gypsum mortars, a possible distribution gypsum-anhydrite was calculated by estimating the water content from the LOI and the calculated content of limestone.

The two Egyptian gypsum mortars are similar and contain approximately 75% calcium sulphate, in the form of gypsum, hemi-hydrate and anhydrite (NB: calculations only based on gypsum and anhydrite). The very low level of strontium in these samples, compared to that of Sudanese gypsum, suggests that the gypsum probably came from Egypt.

The content of kaolinite in clay mortars varies from 11% to 31%. ^{27}Al NMR analysis of DG3 and GB2 shows that kaolinite structure has not been modified by

Table 4 Estimated present composition of mortars (mass %)

		Sand	Limestone	Gypsum	Kaolinite	Anhydrite
Gypsum mortars	DG1	13	9	77	–	0
	DG2	22	5	48	–	24
Clay mortars	DG3	69	–	–	31	–
	GB2	89	–	–	11	–
	K1	73	–	–	27	–
Lime mortars	DG4	37	63	1	–	–
	DG5	38	62	1	–	–
	DG6	35	64	1	–	–
	GB1	47	45	8	–	–

reaction that could explain their durability such as geopolymserisation. This also indicates that clay was used in its raw state, without any burning process. However, it is not possible to say if these mortars consist of an artificial mixture of sand and clay, or a natural quartz-rich clay sediment. The two bedding mortars, positioned between bricks, were protected from leaching, thus explaining their higher kaolinite content. The surface mortar GB2 has probably been more leached and has the lowest kaolinite content. The presence of a hard and compact painting of calcium carbonate has undoubtedly contributed greatly to its durability.

In the series of lime mortars, the composition of the three samples from Dukki Gel is very similar, with about 63% of carbonated lime in the form of magnesian calcite. SEM shows that DG6 is covered by a clay decorative layer. One can reasonably think that the composition of the decorative layers of DG4 and DG5 is identical.

The high magnesium content of these mortars suggests they were made with magnesian lime, which would be consistent with the presence of dolomitic marbles near Dukki Gel. However, the ratio MgO/CaO in mortars (from 0.13 to 0.33) is significantly lower than that of marbles that we have studied elsewhere (up to 0.67).

The difference could be explained by a partial dissolution of magnesium carbonates, some of them such as nesquehonite ($MgCO_3 \cdot 3H_2O$) and hydromagnesite ($3MgCO_3 \cdot Mg(OH)_2 \cdot 3H_2O$) being much more soluble than calcite. This dissolution would also explain the high level of porosity observed in these mortars.

Finally, the mortar from Gebel Barkal GB1 is quite different from other lime mortars, with a lower content of calcite, and better calcium purity. The external layer is also based on calcite and silica. The low, but significant presence of gypsum (or hemi-hydrate) in this mortar cannot be considered only as an impurity and could correspond to the residual amount of a gypsum binder, associated with lime or crushed limestone, as supposed in our previous study [3].

6 Conclusions

The analyses carried out on this new series show three very different types of compositions, with gypsum plasters, clay-sand mortars and more conventional lime-sand mortars. The composition of the decorative surface layers varies from clay to lime or lime-and-gypsum, in the form of painting or applied as fresco.

This extreme diversity of compositions observed in these mortars and their decorative or protective layers is particularly interesting from an archaeological point of view. The knowledge of the various techniques used enables us to have a better understanding of foreign influences on building workers in ancient North Sudan [7].

It thus appears that gypsum mortars, based on techniques and raw materials coming from Egypt, were used only during the Egyptian colonization. Lime mortars were known and used at least since the first century AD. Finally, clay mortars were known as early as the Ramesside time, and were still in use in the first century AD and maybe later.

Acknowledgements We want to thank very sincerely all the colleagues who put the samples studied here at our disposal: the National Corporation for Antiquities and Museums, Vincent Rondot, Head of the French section, Charles Bonnet in Dukki Gel, Murtada Bushara Mohamed in Gebel Barkal and Derek Welsby in Kawa. We want also to thank Jean-Baptiste d'Espinose from ESPCI in Paris for the NMR analyses, the Lafarge Group for its financial and technical support, and particularly the Analysis Department of Lafarge Centre de Recherche that carried out the analyses, and Catherine Bouillon for the SEM observations.

References

1. Hinkel, F.W.: Examination of Meroitic mortar and plaster. *Meroitica* **10**, 827–833 (1984)
2. Errigo, C.: I templi Meroitici di alcuni siti archeologici del Sudan: caratterizzazione dei materiali con proposta di intervento conservativo. Thesis, Università di Roma (1996)
3. Letourneau, J.P., Feneuille, S.: Chemical and physical analyses of meroitic mortars, T_I_21_HMC008. Paper presented in HMC08, 1st Historical Mortars conference, Lisbon, 24–26 Sept 2008
4. Bouchar, M.: Petrographic study of Meroitic mortars from an Amun temple (el-Hassa) In: Válek, J., Groot, C., Hughes, J.J. (eds.): 2nd Historic Mortars Conference HMC2010 and RILEM TC 203-RHM Final Workshop, Prague, Czech Republic, 22–24 Sept 2010, pp. 55–64, RILEM Publications S.A.R.L. France (2010)
5. Frizot, M.: L'analyse des mortiers antiques, problèmes et résultats. In: Symposium ICCROM Mortars, Cements and Grouts Used in the Conservation of Historic Buildings, Rome, pp. 331–339 (1981)
6. Singh, P.S., et al.: Structural studies of geopolymers by ^{29}Si and ^{27}Al MAS-NMR. *J. Mater. Sci.* **40**(15), 3951–3961 (2005)
7. Feneuille, S., Letourneau, J.P., Bouchar, M.: Archaeological information derived from physical and chemical analyses of Kushite mortars. In: 12th International Conference for Nubian Studies, London, 1–6 Aug 2010

Cement Microstructures and Durability in Ancient Roman Seawater Concretes

Marie D. Jackson, Gabriele Vola, Dalibor Všianský, John P. Oleson,
Barry E. Scheetz, Christopher Brandon, and Robert L. Hohlfelder

Abstract Roman hydraulic maritime concretes of the central Italian coast have pumiceous volcanic ash, or *pulvis Puteolanus*, from the Bay of Naples as mortar pozzolan. Petrographic and mineralogical analyses of cement microstructures in relict lime, tuff, and pumice clasts suggest that pozzolanic reaction at high pH produced gel-like calcium-aluminum-silica-hydrate cements. Orthorhombic 11 Å-tobermorite, with unit cell dimensions $a=5.591(1)\text{Å}$, $b=3.695(1)\text{Å}$, $c=22.86(1)\text{Å}$, developed in the residual cores of portlandite clasts and in certain pumiceous clasts, as well.

M.D. Jackson (✉)

Department of Civil and Environmental Engineering, University
of California at Berkeley, Berkeley, CA, USA
e-mail: mdjackson@berkeley.edu

G. Vola

CTG Italcementi, Bergamo, Italy
e-mail: gabriele.vola@gmail.com

D. Všianský

Institute of Geological Sciences, Masaryk University, Brno, Czech Republic
e-mail: daliborv@centrum.cz

J.P. Oleson

Department of Classics, University of Victoria, Victoria, Canada
e-mail: jpoleson@uvic.ca

B.E. Scheetz

Larson Transportation Institute, Pennsylvania State University, University Park, PA, USA
e-mail: bscheetz@engr.psu.edu

C. Brandon

Pringle Brandon Architects, London, UK
e-mail: Chris-Brandon@pringle-brandon.co.uk

R.L. Hohlfelder

Department of History, University of Colorado, Boulder, CO, USA
e-mail: Robert.Hohlfelder@Colorado.edu

Ettringite and calcium-chloroaluminate formed in discrete, perimetral microstructures and in the cementitious matrix. Phillipsite and chabazite cements may reflect later dissolution of alkali-rich volcanic glass at pH 9–10. The cement systems have remained stable for 2,000 years, during partial to full immersion in seawater. Vitruvius' *De architectura* and other ancient texts describe the raw materials of the concretes, preparation of lime, and construction of submerged wooden forms. Information concerning the materials, formulations, and installations of the concretes was apparently spread by movement of central Italian engineers around the Mediterranean but also, perhaps, by the circulation of sub-literary engineering manuals. Further analytical investigations will determine the diverse chemical processes that produced the cement microstructures, and why the harbour constructions have endured for two millennia.

1 Introduction

Hydraulic, pozzolanic concretes, first developed by the Romans in second century BCE, were widely used in important harbour constructions along the Mediterranean seacoast, over several centuries. Between 2002 and 2009, the ROMACONS group drilled Roman maritime concretes in 11 harbours [1–6]. These structures have remained cohesive and intact in the seawater environment for 2,000 years. ROMACONS drilled a first group of concretes between 2001 and 2006 from harbours along the central Italian coast (Fig. 1): the Cosa (PCO.2003), ~60 BCE, and Santa Liberata breakwaters (SLI.2003, SLI.2004), ~50 BCE, in Tuscany, the ports

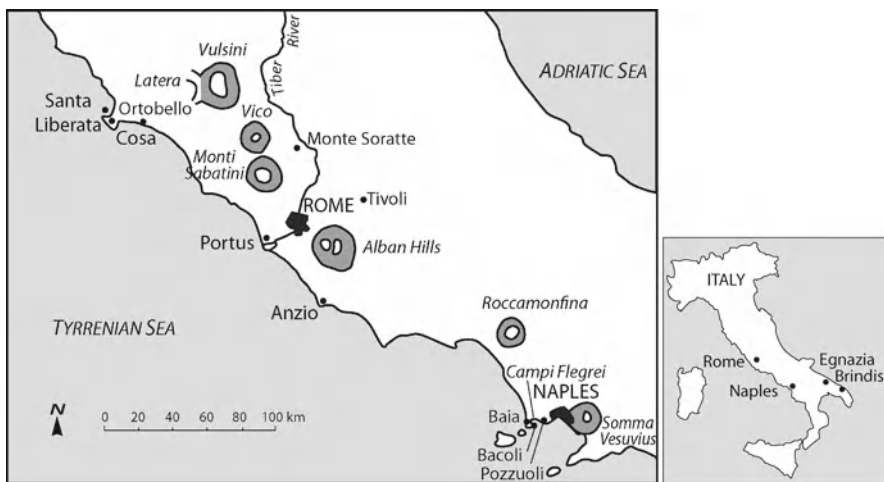


Fig. 1 Ancient Roman harbours and volcanic districts of the central Italian coast

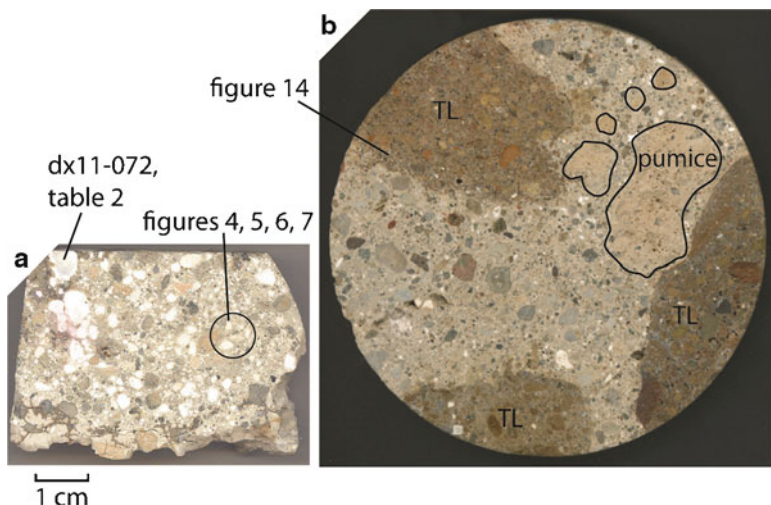


Fig. 2 Photos of mortar fabrics and the locations of analyses of aggregate clasts and cement microstructures (a) Portus Claudius (POR.2002.PO2), (b) Portus Traianus (PTR.2001.01)

of Claudius (POR.2002), ~50 CE, and Trajan (PTR.2002), ~115 CE, at Ostia Antica near Rome, the port of Nero at Anzio (ANZ.2002), ~65 CE, and the port structures at Baiae (BAI.2006), mainly first century BCE, in the Gulf of Naples. Between 2005 and 2009, ROMACONS drilled more distant harbours: Egnazia (EGN.2008) on the Adriatic coast near Brindisi, first century BCE, Caesarea Palestinae (CAE.2005) in Israel and Alexandria (ALE.2007) in Egypt, both first century BCE, Chersonissos (CHR.2007) in Crete, first centuries BCE/CE, and Pompeiopolis (POM.2009) near Mersin in Turkey, of which the visible breakwaters, at least, belong to mid-second century CE [5]. This chapter describes some characteristic cement microstructures in the mortars of concretes from the central Italian coast harbours, to provide a foundation for further investigations into their extraordinary durability and longevity, as well as the expertise of the builders who carried out the underwater constructions. The mortar fabrics are compared to those of a historically accurate *pila* constructed in Brindisi harbour by the ROMACONS group in 2004 and drilled at 6 months (BRI.2005.01), 12 months (BRI.2005.02), and 24 months (BRI.2006) [7, 8], and at 42 months (BRI.2008) and 60 months (BRI.2009) (Table 1). The concretes of the harbours at greater distance from Rome will be described in a future publication.

The ancient concretes are highly complex, composite cementitious materials, with remarkably heterogeneous fabrics (Fig. 2). The fundamental binding substance is a hydraulic pozzolanic mortar, prepared from lime hydrated with seawater and pumiceous volcanic ash, the *pulvis Puteolanus* of Vitruvius [1] (*pulvis*, literally, “powdery earth”), which was sometimes augmented with local sands. *Pulvis Puteolanus*, now popularly called *pozzolana*, is a powdery, incoherent, vitric ash

Table 1 X-ray diffraction analyses of mortar components

Specimen	Predominant cements	Subordinate cements	Pozzolan
PORTUS COSA mid-first century BCE, center of Pier 1 on modern beach ^a			
PCO.03.01A cm	Cal Vat	Etr Str Phi-K	San Qtz Anl
PCO.03.01C wi	Tbm Cal	Str Wo Etr Vat	–
PCO.03.01A p	Phi-K Vat	Tbm Cbz Cal	San Anl
PCO.03.01A p	Phi-K	Vat Tbm	–
PCO.03.01A tuff	Phi-K Cbz-Ca	–	–
SANTA LIBERATA mid-first century BCE; center of <i>pila</i> off northwest <i>piscina</i>			
SLI.04.A mor	Cal	Cbz Clc Vat	Ill San An Anl
SLI.03.01 wi	Etr Tbm	Vat Hyc Cal	–
PORTUS NERONIUS ca. 65 CE; center of <i>pila</i> of southeast breakwater ^a			
ANZ.02.A1 mor	Phi-Na Vat	Tbm Cbz-Ca Cal	San Anl Mus
ANZ.02.A1 wi	Tbm Cal	Wo Etr Vat Brc Hyc Arg–	–
PORTUS CLAUDIUS ca. 50 CE; western mass of north mole ^a			
POR.02.PO2C cm	Cal Vat Arg	Hyc	–
POR.02.PO2A rlc	Tbm Cal	Wo Etr Hyc Gp	–
POR.02.PO2C pum	Cal Vat	Arg Phi Tbm	San
PORTUS TRAIANUS ca. 115 CE; mole and quay at entrance to hexagonal basin ^a			
PTR.02.01 cm	Cal Vat	Etr Hyc Phi	Anl Di San Ill
PTR.02.01 wi	Tbm Cal	Wo Etr Nor Vat Flr Hyc /	–
PTR.02.01 p	Cbz-Ca Cal	Phi-K	Hem Bio Di Mus
BAIAE mid-first century BCE, various structures in Pozzuoli Bay ^a			
BAI.06.01 wi	Cal Tbm	Phi Cbz-Ca Hyt	Sa Anl Ill
BAI.06.02 wi	Cal	Phi Cbz-Ca	Sa Anl Ill
BAI.06.03 wi	Cal Tbm	Phi Cbz-Ca Hyt	Sa Anl Ill
BAI.06.04 wi	Cal	Phi Cbz-Ca Hyt	Sa Anl Ill
BAI.06.05 tuff	/	Phi Cbz-Ca	Sa Anl Ill
BRINDISI HARBOUR , November 2004, 8 m ³ concrete <i>pila</i> ^{b, c, d}			
05.BRI.top mortar, 6 mos	Cal Vat	Hyc Chm	Anl San
05.BRI.bottom mortar	Cal Vat	Hyc Chm Por	Anl San
05-BRI cm	Cal Vat	Hyc	Anl San
05-BRI cm, 12 mos	Cal Vat	Cbz Phi	Anl San
06-BRI cm, 24 mos	Cal Vat	Phi	Anl San
08-BRI cm, 48 mos	Cal Vat Hyc	Cbz Phi	San Anl Ill
08-BRI wi	Cal Por	Vat Hyc Sjg	–
09-BRI cm, 60 mos	Cal Vat	Hyc	Anl Di
09-BRI wi	Cal Por	Ett Hyc	–
08-BRI tuff	Phi-K Cbz-Ca	Cal	Anl Ill San

Mineral abbreviations follow [9]

cm cementitious matrix, wi white inclusion, p pumice, mor mortar, rlc relict lime clast

^aOleson et al. [1]^bOleson et al. [7]^cGotti et al. [8]^dVola et al. [5]

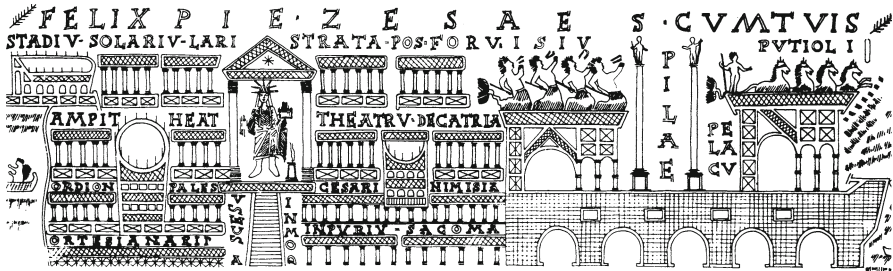


Fig. 3 The arched concrete pier, or *pilae*, at Puteoli harbour, now modern Pozzuoli at Campi Flegrei, about 250 CE. Drawing on glass vessel, Narodny Museum, Prague [20]

pozzolan from the Gulf of Pozzuoli at the northwest sector of the Bay of Naples [1, 7, 8]. A pozzolan is a siliceous, aluminous material that by itself has no cementitious value, but in the presence of moisture chemically reacts with calcium hydroxide ($\text{Ca}(\text{OH})_2$) to form compounds with cementitious properties [10]. Supplemental pozzolanic materials enhance the durability of modern maritime concretes, through various processes [10–14]. The lithologic provenance of *pulvis Puteolanus* seems to be the Neapolitan Yellow Tuff, which erupted from Campi Flegrei caldera about 15 ka, and has both incoherent ash and lithified tuff facies [15]. The decimeter-sized coarse aggregate, or *caementa*, of the Portus Cosa, Santa Liberata, and Baiae concretes is predominantly vitric-crystal tuff, presumably quarried from Campi Flegrei deposits, as well [1, 7]. The Portus structures have vitric-lithic Tufo Lionato tuff from Alban Hills volcano [16]. Builders placed the concrete mixtures in inundated or even completely submerged forms [17, 18], where they set and cured in seawater, out of contact with atmospheric CO_2 . Here, durability corresponds to the capacity of pozzolanic cements to bond the mortar components and coarse aggregate for a very long time.

Harbours were the most important element in the physical infrastructure that supported the Roman imperial economy, and thus made the Roman imperial socio-political system possible. The consistent presence of *pulvis Puteolanus* in the concretes suggests that the experimental formulations may have taken place near the Bay of Naples, but little is known about the spread of this technology, particularly for the immense marine structures built far from central Italy [1, 3, 5]. For example, when was the volcanic ash-hydrated lime formula discovered, and how much did it vary? How was the lime calcined and slaked, the mortar mixed, and the concrete placed in the sea? How did knowledge of the properties of the volcanic ash pozzolan travel to large and small marine construction sites outside of Italy: through the movement of engineers, or by means of technical handbooks on harbour engineering? Analyses of the seawater mortar fabrics and consideration of ancient Roman literary and inscriptional sources [19] provide new insights into Roman builders' expertise and possible applications of their materials and methods to enhancing the durability of modern seawater concretes (Fig. 3).

2 Materials and Methods

The mortar specimens come mainly from discs sliced from 1 to 6 m long, 9 cm diameter drill cores, which are stored in core boxes under ambient, sub-aerial conditions in a warehouse at CTG Italcementi in Bergamo, Italy. Petrographic maps were drawn on digital optical photomicrographs taken with a 2 \times objective on an Olympus BX51 microscope, to describe the characteristic features of the heterogeneous mortar fabrics. Descriptions of tuff fabrics follow [16]. Polished thin sections, often panoramic in size, 6.5 by 4 cm, were prepared from part of the disc; powders for X-Ray diffraction analyses (XRD) were commonly prepared from the rest. The cementitious binding matrix was lightly crushed or scratched out from the mortar, and sieved to pass the #100 sieve, <0.0159 mm. Relict lime inclusions and volcanic particles, mainly pumice and tuff fragments, were carefully scratched out or hand-picked. XRD analyses used a Bruker D8-Advance X-ray powder diffractometer with Cu K α radiation ($\lambda=1.54184$ Å) and fixed divergence slits at the CTG Italcementi labs (Table 1). A Leo Scanning Electron Microscope (SEM), equipped with a Sirius Energy Dispersive X-ray Spectrometer (EDS) at CTG Italcementi and a JEOL 6,700F Field Emission (6/7/Hosler) instrument at Pennsylvania State University were used in the backscatter electron mode (BSE) with EDS spot or area analyses on polished thin sections, to describe the altered aggregate clasts and cement phases. SEM elemental maps of carbon coated, polished thin sections, acquired with a JSM-6480LV instrument at Northern Arizona University at 20 kV voltage in the high vacuum mode, show Ca, Si, Al, S, Cl, and K concentrations in these fabrics. Major element compositions of bulk mortar specimens appear in [1, 5–8]. Refinements of the lattice parameters of tobermorite from the XRD analyses used the Rietveld method, performed using the fundamental parameters approach with background coefficients, cell parameters, zero-shift error, sample absorption and phase fraction, with the unit cell dimensions of the ICDD #191364 orthorombic tobermorite model [21] and Topas 3 software (Table 2). The March-Dollase function was used to determine the preferred orientation of the 11 Å tobermorite.

3 Previous Studies of Mortar Fabrics

The seawater mortars have four predominant components: *pulvis* pozzolan composed of coarse gravel to fine silt-sized grayish orange (10YR 7/8–8/5) to yellow gray (5Y 8/3–7/2) vitric tuff, pumice, palagonite, and crystal fragments; occasional sedimentary and/or volcaniclastic sands; a cementitious binding matrix containing clasts <2 mm with diverse cements; and dull white (N9) opaque inclusions, mainly 0.1–1 cm (Fig. 2). The crystalline cements frequently include rock forming mineral cements of the earth's crust, such as tobermorite, a rare crystalline calcium-silica-hydrate, and phillipsite and chabazite, which are zeolitic alkali-rich aluminosilicates (Table 1) [6]. This mineral assemblage occurs in recent volcanic ash deposits immersed in the

Table 2 11 Å Tobermorite lattice parameters from X-ray diffraction analyses of white inclusions, based on the ICDD number 191364 orthorhombic structural model [21]

Tobermorite specimen	Unit cell dimensions (Å)			Volume (Å ³)
	a	b	c	
PORTUS COSA , relict lime dx2010-0947 (PCO.2003.1C)	5.591(1)	3.697(1)	22.85(1)	472.5(1)
PORTUS COSA , relict lime dx09-077 (PCO.2003.1A)	5.5967(1)	3.6929(1)	22.891(1)	473.1(1)
SANTA LIBERATA , relict lime dx2010-0946 (SLI.2003.03)	5.600(1)	3.6929(1)	22.891(1)	474.4(1)
PORTUS CLAUDIUS , relict lime dx11072 (POR.2002.PO2A)	5.581(1)	3.686(1)	22.736(1)	467.8(1)
PORTUS CLAUDIUS , relict pumice dx03-030 (POR.2002.PO2C)	5.530(1)	3.679(1)	22.57(1)	459(1)
PORTUS NERONIS , relict lime dx11-074 (ANZ.2002.A1)	5.5927(1)	3.6942(1)	22.864(1)	472.4(1)
BAIAE , relict lime dx04-055 (BAIA.2001.01)	5.595(1)	3.6980(1)	22.903(1)	473.8(1)

ocean at Surtsey volcano in Iceland [22]. Zeolites commonly cement volcanic ash in seawater and saline lake brines [23–25], and subaerial pyroclastic deposits of central Italy [15, 16, 26]. Paradoxically, the Roman seawater cement assemblages represent temperature fields that are ordinarily considered incompatible in modern cement pastes [10, 27]. In the ancient mortars, tobermorite is often associated with ettringite microstructures (Table 1) [6], but ettringite ($\text{Ca}_6\text{Al}_2(\text{SO}_4)_3(\text{OH})_{12}\cdot 26\text{H}_2\text{O}$) is typically stable up to 70°C at atmospheric pressures, while tobermorite ($\text{Ca}_5\text{Si}_6\text{O}_{16}(\text{OH})_2\cdot 4\text{H}_2\text{O}$) or Al-tobermorite ($\text{Ca}_5\text{Al}_{0.7}\text{Si}_{5.3}\text{O}_{16}(\text{OH})_{1.3}\cdot 4\text{H}_2\text{O}$) is typically synthesized at 120–180°C, although low-temperature forms may develop at 60°C [27, 28]. Phillipsite and chabazite generally precipitate from fluids with 9.1–10 pH [22–24], higher than the 7.9–8.2 pH of Mediterranean seawater, but lower than the 12.7 pH of portlandite ($\text{Ca}(\text{OH})_2$) present at the initiation of curing [7, 11]. Seawater temperatures along the central Italian coast are about 17.5°C in August to 19.0°C in June, and salinity is about 37.5–37.9 between Rome and Naples [29].

A diagenetic microstructural approach provides insights into the ancient cement microstructures. Diagenesis is the study of the physical and chemical changes undergone by a rock after its deposition, including the development of mineral cements during lithification, which result from chemical adjustments to particular environments. Diagenetic perspectives are useful in describing the evolution of cement precipitation in the seawater mortars, and the development of presumably incompatible crystalline cements as chemical responses to changing pH and seawater infiltration over the 2,000 year lifespans of the maritime structures [6, 11]. Microstructural perspectives are useful in describing discrete mortar components at several scales of analysis. For example, integration of petrographic and scanning electron microscope studies and maps, followed by the extraction of specific mortar

components for XRD, illustrates processes of pozzolanic reaction in relict lime and volcanic clasts, the development of diverse cement phases over time, and the subsequent alteration of these components in the seawater concrete system [6, 11–14]. Bulk analyses of the overall mortar composition are generally avoided, because these give averaged results of the heterogeneous fabrics (Fig. 2) and little insight to processes at the millimeter scale.

The predominant reactive component of the *pulvis* pozzolan seems to be alkali-rich volcanic glass. Neapolitan Yellow Tuff glass contains about 8 wt.% K₂O and 3–4 wt.% Na₂O [15], and the bulk chemistry of the related Bacoli Tuff used in the Brindisi experimental concretes has a similarly alkalic composition [5–8, 15]. Authigenic zeolite cements – phillipsite, chabazite, and analcime – commonly form greater than 50 wt.% of the Neapolitan Yellow Tuff [15]. These minerals have good pozzolanic reactivity with hydrated lime [13]. The Portus Cosanus mortars also contain quartz sands, presumably from beach deposits near the harbour site [1, 7]. The Portus Traianus mortars also contain scoriaceous volcaniclastic sands, from Alban Hills deposits [30].

The lithologic origins and preparation of the lime in the central Italian coast harbour constructions, which span 300 km of the shoreline and about 165 years of construction history, remain unclear. The lime compositions seem to have been rather pure CaO, with little argillaceous or hydraulic component detectable through petrographic studies or XRD analyses. Certain relict lime clasts in the Baiae specimens, however, retain rhombohedral dolomitic pseudomorphs. The material characteristics of lime in European historic mortars typically show large variations, which result from diverse processes of calcination, slaking, and mixing with the mortar aggregate [31–34]. Specifically, temperature variations in the kiln produce underburned particles, with limestone fabrics still partially intact; overburned particles, with dead-burned, refractory fabrics; and viable CaO quicklime particles, which react to form portlandite when slaked [31–34].

Roman archaeologists tend to infer a wet slaking procedure for the mortars of concrete walls and foundations based, in part, on Vitruvius' rather terse recommendations in *De architectura*, completed about 20 BCE [*De arch* 2.5.1]: "We must also be diligent about lime, which is cooked from white stone (*albo saxo*). That [lime] which is from dense and hard [limestone] will be useful in construction. When it will be slaked or quenched (*extincta*), then let it be mixed with sand; if it will be excavated sand (*harenae fossiciae*), three [parts] sand and one [part] lime are mixed together (*infundantur*).” Some archaeologists infer that builders used slaked lime putty (Ca(OH)₂) that was matured, or aged [7, 19]. Before construction, it was remoistened and then mixed with the volcanic pozzolan [7]. Installation of the Brindisi experimental pila followed a similar procedure, with wet slaking of aged slaked lime to form stiff putty, immediately followed by the incorporation of *pulvis puteolanus* in a 2.7:1 pozzolan to lime volume ratio [7]. A great deal of effort was required to laboriously mix the lime putty and incorporate the *pulvis* pozzolan into a wet mix that was lowered by baskets into the wooden form submerged in seawater [7]. The experimental mortar had a markedly lower percentage of white nodules than the ancient mortars [7, 8]. In fact, Vitruvius' instructions for mixing mortars for harbour constructions are somewhat obscure

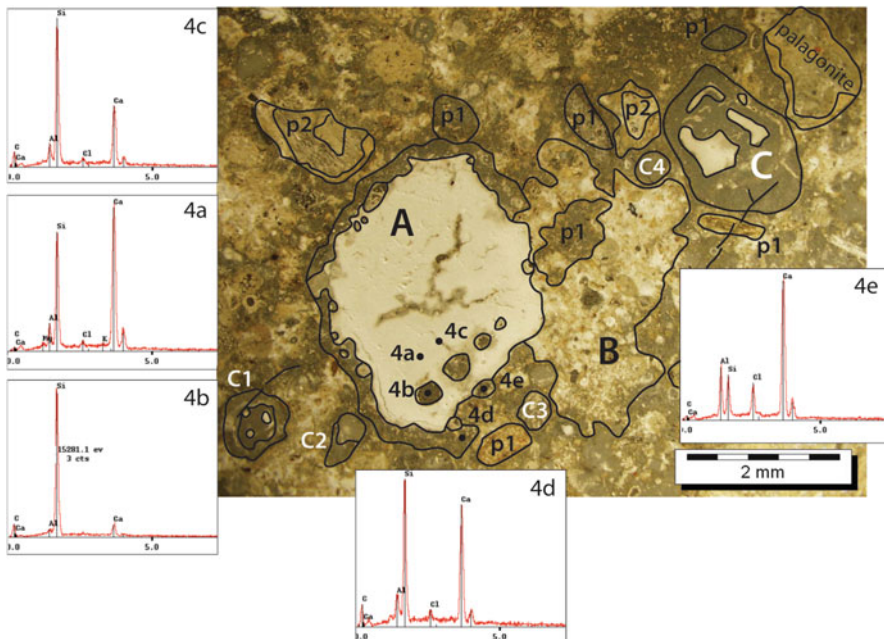


Fig. 4 Optical micrograph (plane polarized light) and SEM-EDS analyses of regions associated with partially dissolved relict lime clasts in a Portus Claudius mortar (POR.2002.PO2)

[*De arch 5.12.2*]: “Earth (*pulvis*) is to be brought from the region extending from Cumae to the promontory of Minerva and mixed (*misceatur*) in the mortar trough (*mortario*) so the [ingredients] correspond two to one.” Here, he implies that *pulvis* was mixed with lime, but he does not clarify the slaking process or mixing method. The presence of white lime nodules in some European historic mortars suggests a “hot mixing” process [31–34]. In some mortars wet aggregate was thoroughly mixed with lime fragments [31]; in others, fine quicklime was dampened with a little water, covered with aggregate to retain the exothermic heat produced by the $\text{CaO} + \text{H}_2\text{O} = \text{Ca}(\text{OH})_2$ reaction, and left for a few days before further mixing and installation [32]; and in still others, lime putty was mixed with aggregate [34]. The ancient concrete fabrics and texts should provide clues to Roman builders’ methods [19].

4 Characteristic Mortar Microstructures

Petrographic and SEM images illustrate microstructures (Figs. 4, 5, 6, 7, 8, 9, 10, 11, and 12) present as white inclusions in the Roman maritime mortars [1, 5–8]. At the time of drilling, the Portus Claudius and Portus Cosa specimens were exposed sub-aerially; the Portus Neronis and Santa Liberata specimens were continuously immersed in seawater for 2,000 years [1].

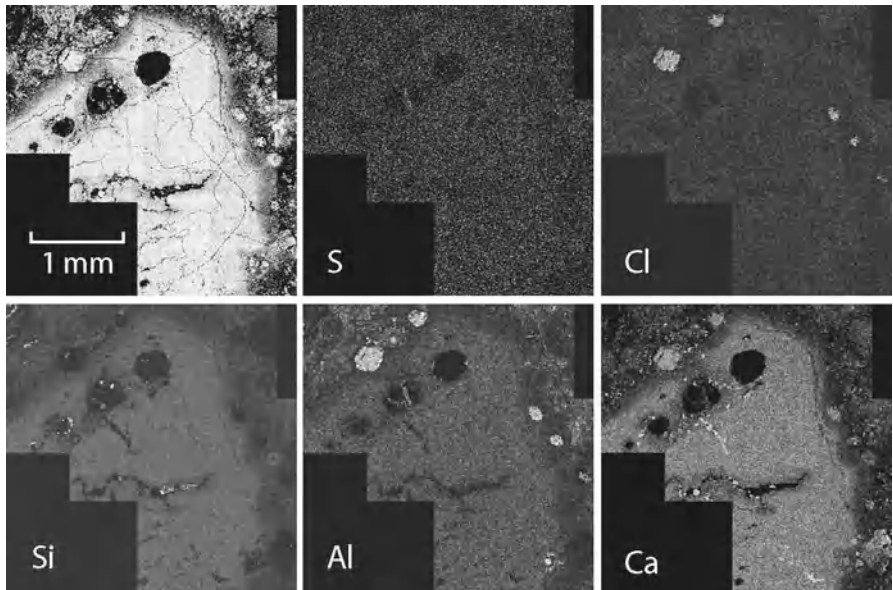


Fig. 5 SEM elemental maps of a subarea of Fig. 4 rotated 180° clockwise, showing a back scattered electron (BSE) image on the *upper left*, and the qualitative distribution of sulfur (S), chlorine (Cl), silica (Si), aluminum (Al), and calcium (Ca) in the partially dissolved relict lime clast. Note the association of Al, Ca and Cl in calcium-chloroaluminate microstructures

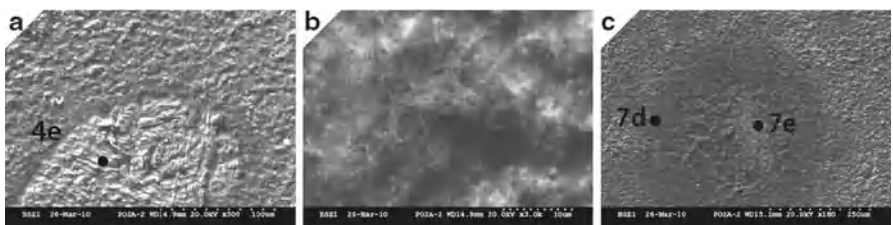


Fig. 6 SEM-BSE images of cement hydrates (a) calcium-chloroaluminate (Fig. 4e), (b) tobermorite (Fig. 7d), (c) silica-calcium-alumina ring and calcium-chloroaluminate core, (Fig. 7d, 3e)

4.1 Portus Claudius, Relict Lime Clast

Figures 4 and 5 shows a dull white, altered lime clast (A) in contact with a tuff fragment (B), whose vitric matrix has mottled zones of white opacity associated with poorly crystalline cement hydrates. A neighboring relict lime clast has isolated opaque areas (C), as well. Smaller lime clasts (C1, C2, C3, C4) are partially to wholly dissolved. Smaller pumices (p1) are mainly dissolved; larger pumices (p2) have opaque cores and partially dissolved perimeters. The opaque mass

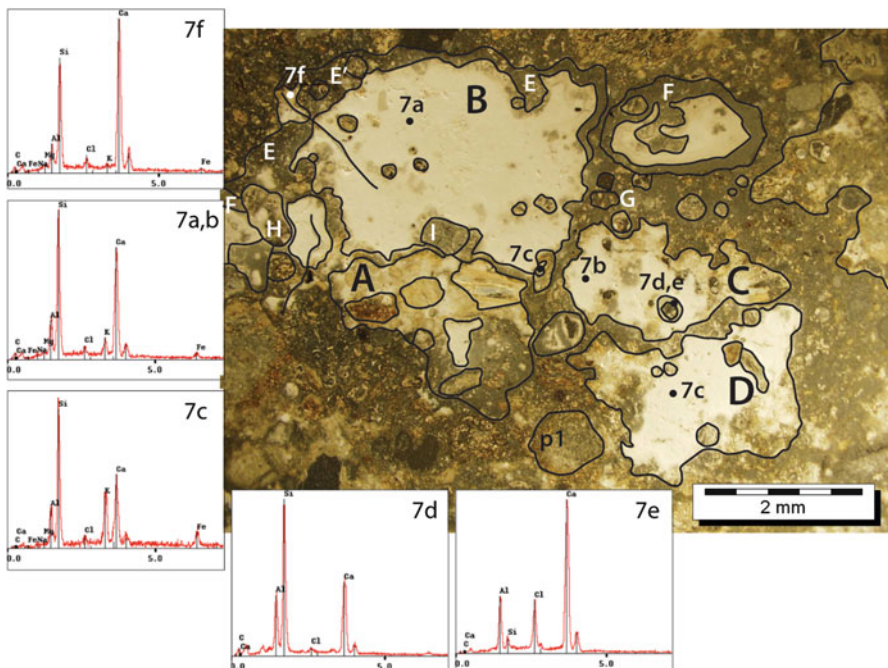


Fig. 7 Optical micrograph (plane polarized light) and SEM-EDS analyses of regions associated with pumiceous tuff clasts of *pulvis Puteolanus* in a Portus Claudius mortar (POR.2002.PO2)

(A) has a cryptocrystalline fabric, dark gray and light brown (5Y 4/2) in plane polarized light (PPL), with a composition compatible with aluminum-bearing tobermorite (Fig. 4a). Four sub-spherical openings have silica-rich points (Fig. 4b), perhaps dissolved *tintinnides* macrofossils. A dissolution fissure and the perimetral rind have calcium-silica-aluminium-hydrate (CASH) compositions (Fig. 4c, d). The rind makes a distinct boundary with the cementitious matrix. It contains quartz crystals shattered during calcining of the host limestone, and bead-like microstructures with calcium-silica-chloroaluminates cores and drying shrinkage (Figs. 4e, 6a). The cementitious matrix has microcrystalline calcite, vaterite, aragonite and hydrocalumite (Table 1). The SEM elemental maps (Fig. 5) show concentrations of silica (Si), aluminum (Al) and calcium (Ca) associated with CASH at the center of the partially dissolved relict lime clast (Fig. 4a) and concentrations of calcium, aluminum and chlorine (Cl) in the interfacial zones. There are no sulfur (S) concentrations or ettringite. The maps suggest a “shrinking core” process [35]: the dissolution at (A) terminated before the entire portlandite clast was consumed, and the residual opaque nucleus records the development of cryptocrystalline CASH, but tobermorite crystals are not well-developed. Gel-like CASH formed in the dissolved rims of lime clasts.

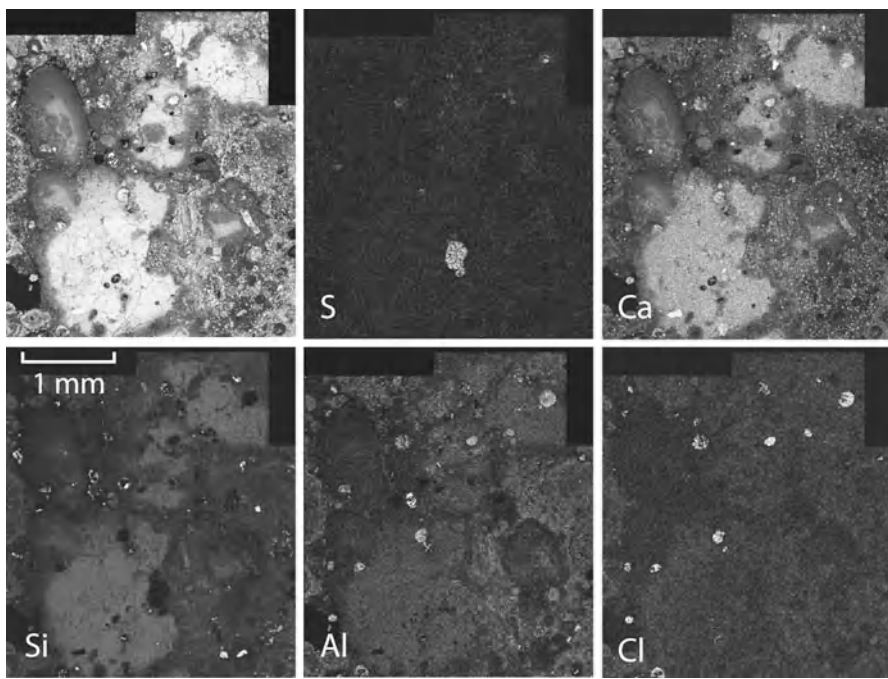


Fig. 8 SEM elemental maps and BSE image (*upper left*), rotated 90° clockwise from Fig. 7, showing the qualitative chemical compositions of the relict vitric tuff regions

4.2 Portus Claudius, Relict Tuff Clast

Figures 7 and 8 show a cluster of dull white, vitric tuff clasts. Pumice and glass fragments are preserved in a patchy yellowish orange (10YR 7/6, PPL) volcaniclastic texture (A) that grades to lightly opaque gray (N4, PPL), similar to Fig. 4b. Traces of volcaniclasts also occur in the deeply opaque, dark gray (5Y 4/2, PPL) masses at B, C, and D. Potassic-magnesium-iron-calcium-aluminum-silica-hydrate cements (KMFCASH) (Fig. 7a, b) reflect altered volcanic ash, as does the opaque core of a pumice with a dissolved perimeter (Fig. 7c). Tobermorite fibers containing aluminum occur in the most densely opaque mass (D) (Figs. 6b, 7b). The rind around the largest tuff clast (B) varies from lightly opaque (E') to colorless (E), similar to the rim of the partially dissolved lime clast nearby (F); lightly opaque CASH patches also occur in this rind (Fig. 7f). An annular microstructure has an opaque calcium-chloroaluminate inner zone and CASH outer zone (Figs. 6c, 7d, e). Sub-spherical microstructures 0.1–1 mm in diameter may contain a similar muddy opacity (G) or ettringite crystals with second order birefringence and low (-) relief (H), or even a complex combination of both materials (I). Overall, the maps record the perimetral dissolution of vitric tuff clasts, and precipitation of a gel-like CASH rind (E, E'); a gradational alteration to white cryptocrystalline opacity in residual tuff cores (A, B, C, D) with locally crystalline tobermorite (D) (Fig. 6b); and peripheral

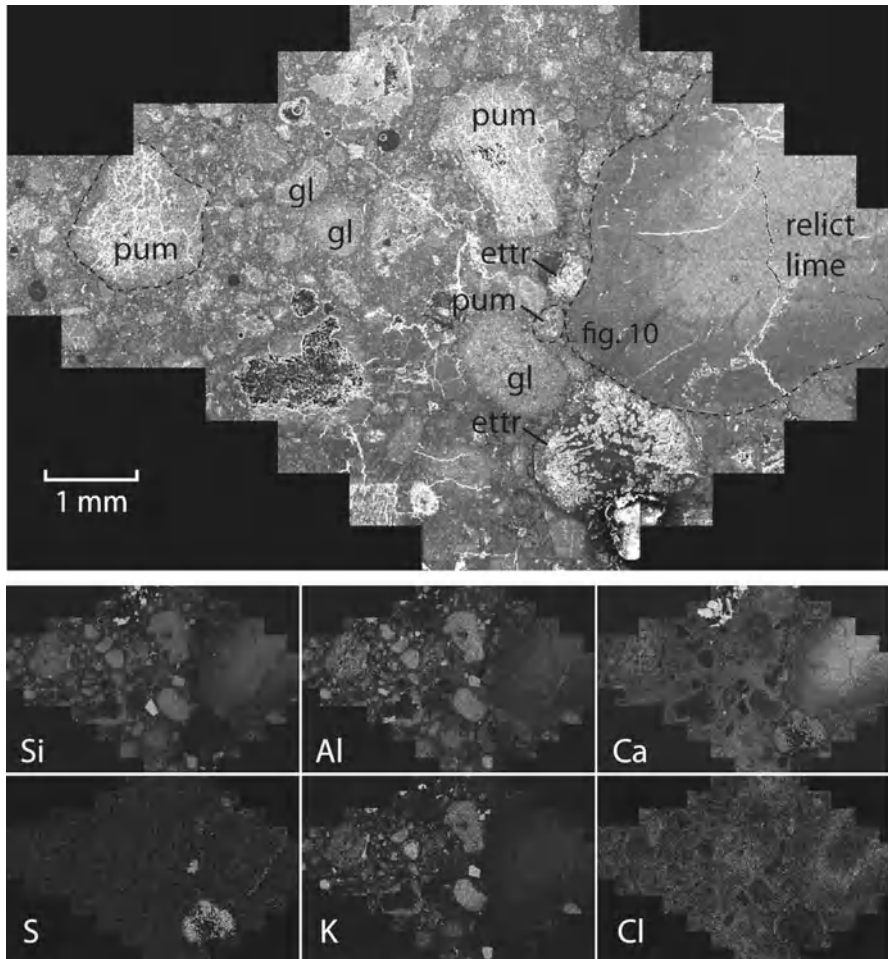


Fig. 9 SEM elemental maps and a BSE image (*top*) of a Portus Neronis (ANZ.2002) relict lime clast tobermorite specimen dx11-074), its interfacial zone, and the surrounding pumiceous cementitious matrix. The chlorine image is enhanced to emphasize its weak but diffuse distribution. *pum* pumice, *gl* glass fragments, *ettr* ettringite

sulphate and chlorine microstructures (G, H, I). The complex but highly discrete chemical concentrations are shown by SEM elemental maps (Fig. 8).

4.3 Portus Neronis, Relict Lime and Pumice Clasts

The SEM elemental map of Fig. 9 shows the pumiceous cementitious matrix of the Anzio harbor mortar, to the left, and a relict lime clast, to the right, with fracture traces as fine white lineations that traverse its partially dissolved perimeter.

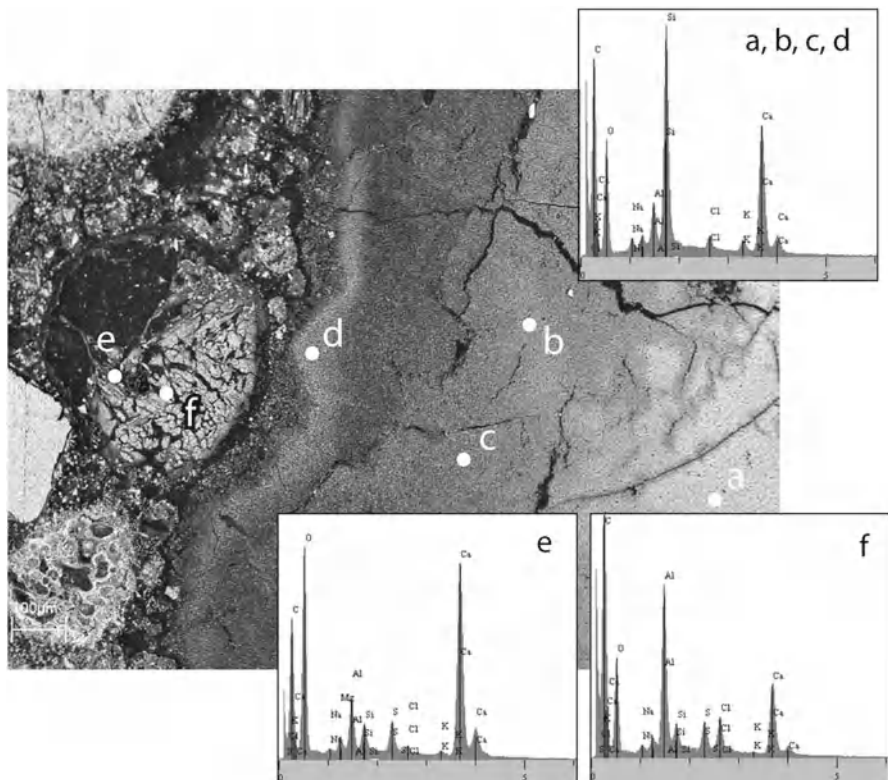


Fig. 10 SEM-BSE images and EDS analyses of CASH (**a**, **b**, **c**, **d**), ettringite (**e**), and altered ettringite (**f**) of the interfacial zone of the relict lime clast of Fig. 9, Portus Neronis

The complex CASH rind (Figs. 9, 10) has a rather uniform composition, going from the petrographically opaque center (Fig. 10a) to the colorless perimeter (Fig. 10b, c, d). The nucleus is tobermorite (Table 2, analysis dx11-074). Ettringite occurs in two sub-spherical microstructures along the interfacial zone, shown by concentrations of calcium, sulfur, and aluminum (Fig. 9). Most of the ettringite is altered (Fig. 10e), and contains a small amount of silica, and it further decomposes to poorly crystalline material enriched in aluminum, calcium, and chlorine (Fig. 10f). In contrast, in a Portus Cosa mortar, relatively fresh ettringite crystals (Fig. 11a) traverse a relict void surrounded by a complex CASH rim (Fig. 11c). The more altered ettringite crystals show decreased aluminum, calcium and sulfur, and enrichment in silica (Fig. 11b). Further examination of these textures will give insights into the processes that sequestered sulfate and chlorine ions in the mortar fabric.

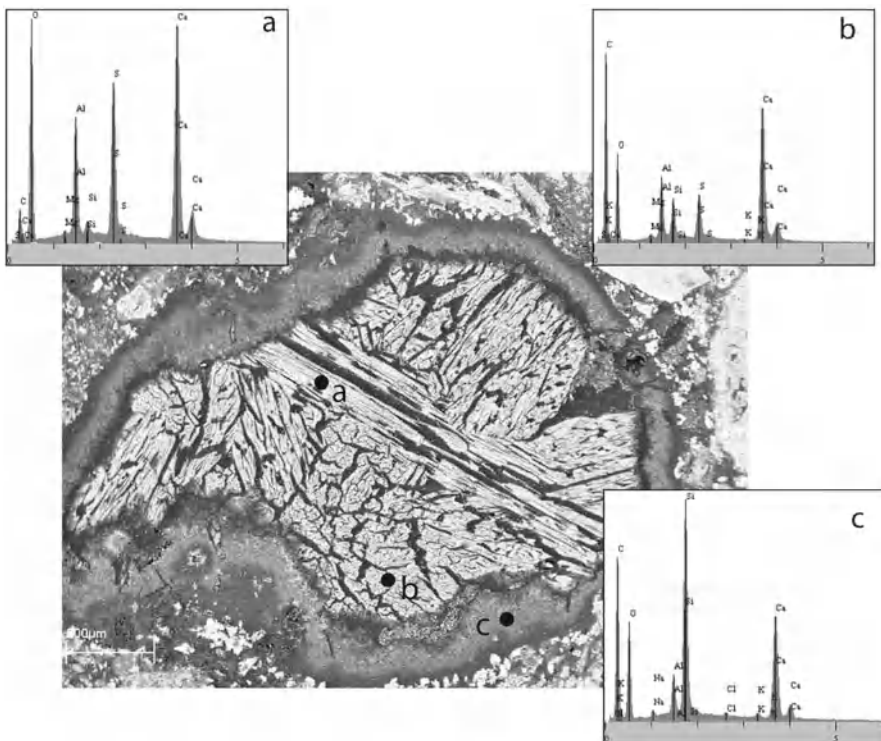


Fig. 11 SEM-BSE images and EDS analyses of ettringite (a), altered ettringite (b), and CASH rind (c) surrounded by the cementitious matrix of a Portus Cosa mortar (PCO.2003.01)

4.4 Variations in the Microstructures of White Inclusions

Petrographic studies of white inclusions in the seawater mortars reveal important textural relationships (Fig. 12). The partially dissolved relict lime clasts of the Portus Cosa mortar retain traces of cracks with opening displacements that protrude about 50–150 μm into the cementitious matrix (Fig. 12a, b). These textures suggest quicklime particles that hydrated to portlandite *in situ* and expanded [31–34]. They then partially dissolved, developing petrographically colorless CASH gel in their perimetral zones and opaque CASH or Al-tobermorite in their relict portlandite cores. In the Santa Liberata mortar (Fig. 12c), the gel-like CASH in the fractured lime clast altered to sparry calcite, but the opaque cryptocrystalline CASH appears relatively unaltered. Relict lime clasts in the Baiae mortar commonly have intact and homogeneous opaque cores (Fig. 12d), surrounded by a less opaque zone, and a dissolution rind with colorless CASH and alteration to calcite. The absence of fracturing suggests that the clast may have entered the seawater system as portlandite, either as a previously matured slaked lime particle, or as a recently hydrated particle,

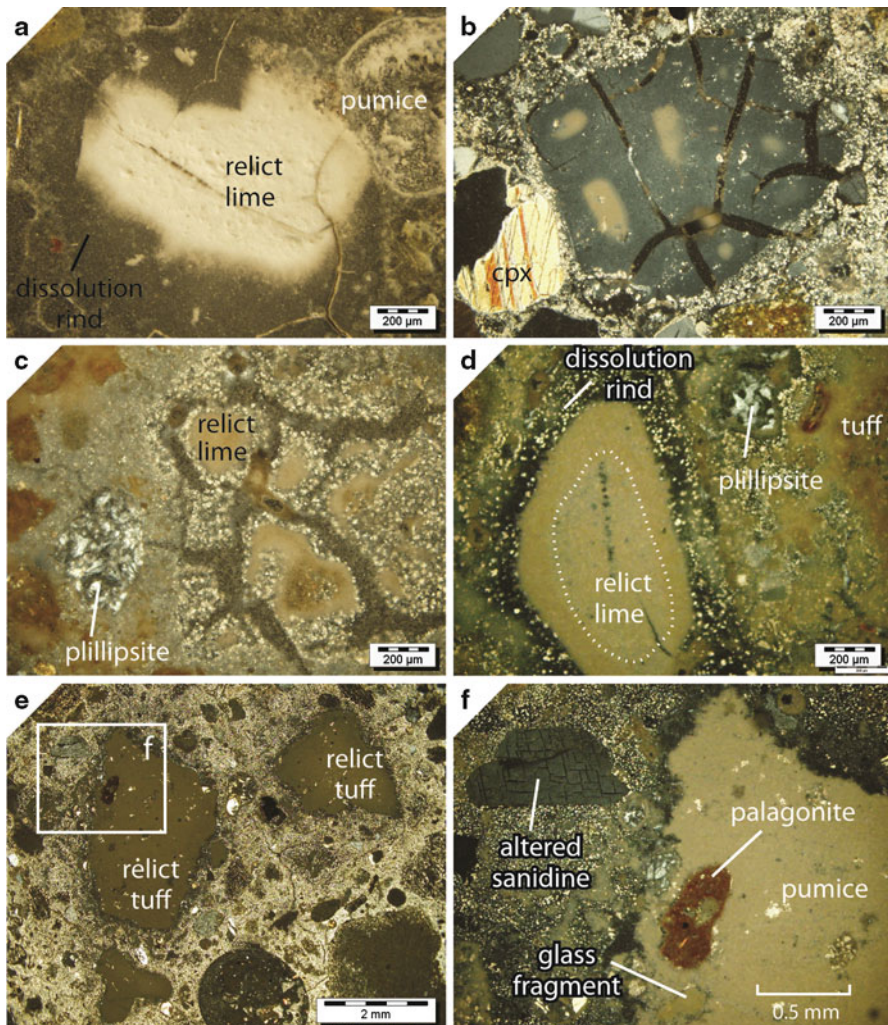


Fig. 12 Optical micrographs of white inclusions, (a) and (b) lime clasts with fractures, Portus Cosa (PCO.2003.01), (c) lime clast with fractures, Santa Liberata (SLI.2003), (d) lime clast with homogeneous texture, Baiae (BAIA.2006.03), (e) and (f) tuff clasts partially altered to opaque cements, Baiae (BAIA.2006.03), (a) and (e) are plane polarized light (PPL), (b, c, d, f) are crossed polarized light (XPL). Note the phillipsite microstructures in the cementitious matrix of (c) and (d)

perhaps damp-slaked with the *pulvis* pozzolan before immersion in seawater. The vitric matrix of a relict tuff particle, which contains palagonite, pumice, and sanidine crystal fragments (Fig. 12e, f), developed a white opacity, similar to the tobermorite in the Portus Claudius mortar (Figs. 6b, 7b, c, d, 8). Another pumice, adjacent to a relict lime clast (Fig. 12a) has similarly opaque cement, presumably CASH. The Santa Liberata and Baiae mortars have localized phillipsite cement microstructures in their cementitious matrix (Fig. 12c, d).

5 Characteristic Zeolite Cement Microstructures

Zeolite cements occur in the vesicles of relict pumice clasts, shown by the phillipsite rosettes in a Santa Liberata partially dissolved pumice fragment (Fig. 13a) as well as in discrete voids in the cementitious binding matrix, shown in a Portus Cosa mortar (Fig. 13b). Discrete chabazite microstructures also occur in pumice clasts and the cementitious matrix (Table 1) [6]. In the Portus Traianus concrete (Fig. 2), the zeolitized palagonitic fabric of the Tufo Lionato coarse aggregate apparently altered *in situ*, so that the fine vitric fraction was almost entirely consumed to produce dense new phillipsite cements that are intergrown with the natural, authigenic phillipsite of the tuff [16]. The *pulvis Puteolanus* that was presumably derived from an incoherent facies of the Neapolitan Yellow Tuff likely contained natural zeolites,

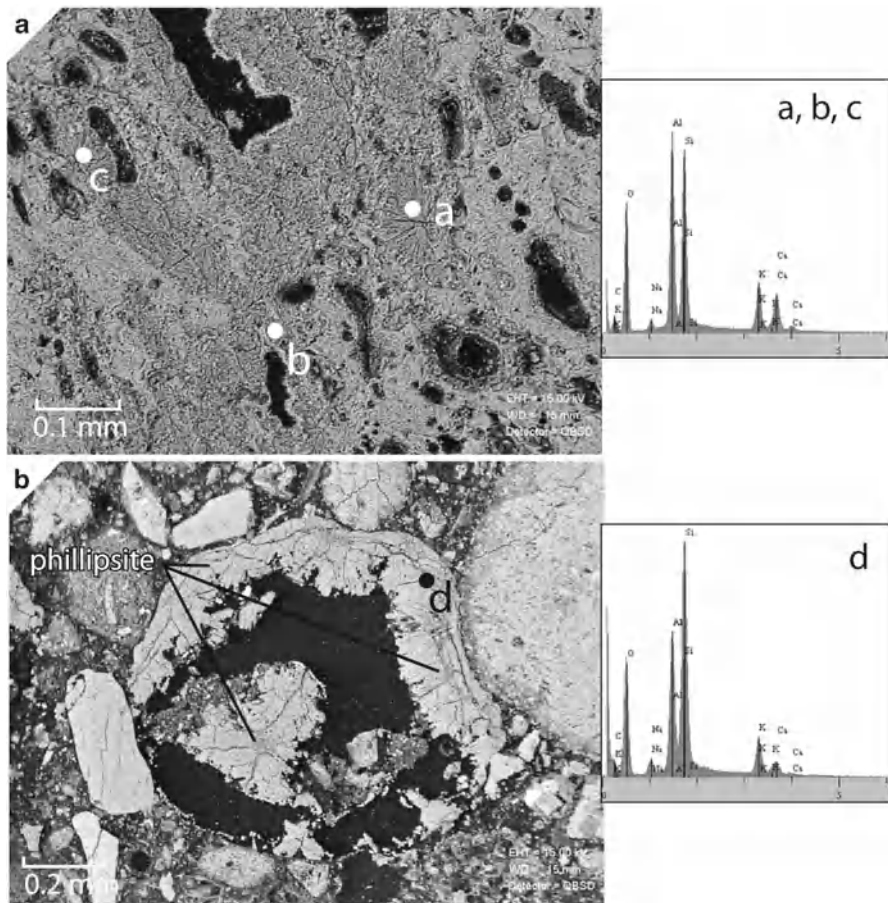


Fig. 13 SEM-BSE images and EDS analyses of phillipsite in (a) pumice vesicles, Santa Liberata (SLI. 2003) and (b) a void in the cementitious matrix, Portus Cosa (PCO.2003 01)

but it is not known if all the zeolite was consumed during pozzolanic reaction. The phillipsite of the Neapolitan Yellow Tuff has Si:Al at about 2.54–2.82 and Na:K at 0.42–0.68 [15]. In comparison, Si:Al in phillipsites of marine and saline lake ash deposits ranges from 2.44–2.79 [24] to 3.12–4.06 [23], while phillipsites in the recent Surtsey basalt tephra deposits have Si:Al at 2.04–2.46 [22]. Further analyses will distinguish more precisely the compositions of phillipsite and chabazite that formed in the mortars, but qualitative, preliminary EDS analyses suggest variable ratios (Fig. 13) with both potassic and sodic phillipsite and calcic chabazite (Table 1). The presence of fresh, euhedral zeolite cements within the binding matrix suggests that (1) the pH of interstitial fluids in the mortar fabric fell significantly from that of the elevated levels of the portlandite-buffered system, and (2) once formed, the zeolite crystals remained stable and did not participate in further pozzolanic reactions. These *in situ* zeolite cements, and those of the harbour concretes at greater distances from Rome [6], may reduce the porosity of the mortar fabrics and tuff coarse aggregates and contribute to the overall durability of the maritime structures through reductions in permeability and seawater ingress at long curing times [10, 11].

6 Brindisi Experimental Mortars

The cementitious binding matrix of the young Brindisi mortar, formulated with matured lime putty hydrated with seawater and then incorporated with *pulvis* pozzolan, has a rather consistent assemblage of microcrystalline calcite, vaterite, and hydrocalumnite, and little or no portlandite [5–8]. Portlandite does, however, persist in occasional coarse white inclusions (Table 1). Similarly, the cementitious matrix of the ancient mortars has a predominantly calcite, vaterite, and/or aragonite, and hydrocalumnite assemblage, with subordinate cement phases having close associations with lime and volcanic clasts (Table 1, Figs. 4, 5, 6, 7, 8, 9, 10, 11, 12, and 13). Although tobermorite is associated with relict lime clasts and certain altered vitric tuff clasts in the ancient mortars (Table 1, Figs. 4, 5, 6, 7, 8, and 9), it is not detected in the experimental mortar. However, ettringite is associated with a portlandite inclusion in the 2009 Brindisi mortar specimen (Table 1). At the petrographic scale, the Brindisi mortar fabric appears quite different from the ancient mortars (Fig. 14). The cementitious matrix of the 2005 mortar, drilled at 12 months curing, is composed of irregular sub-centimetric zones with rather evenly dispersed pumice shards and volcanic crystals, and tiny relict plates of portlandite (Fig. 14a). The narrow opaque selvages that surround these zones incorporate very fine vitric ash shards, and they become progressively more opaque, as in the 2008 mortar, drilled at 48 months curing (Fig. 14b). The cementitious matrix of the 2009 mortar shows low birefringence, and amorphous CASH predominates. Puzzlingly, the 2008 mortar shows a stronger evolution of cements, with two distinctive constituents: a densely opaque brownish matrix (Fig. 14b), probably composed of poorly crystalline cements in altered vitric ash, and a fine grained, first order birefringent microcrystalline cementitious phase. Phillipsite and chabazite in the 2008 mortar are associated with vitric tuff clasts, but it is not clear when these formed (Table 1).

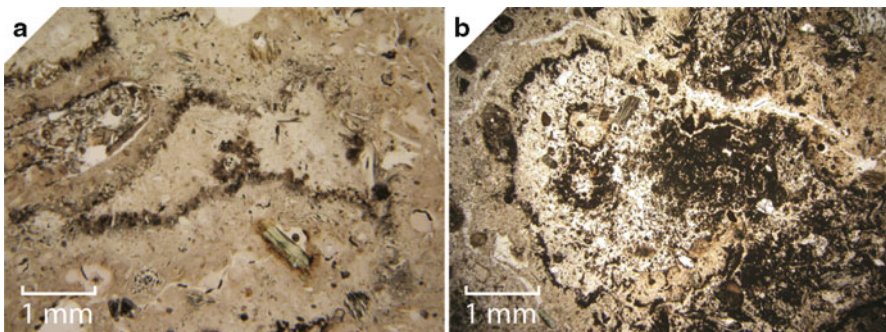


Fig. 14 Optical micrographs, plane polarized light, showing the cementitious matrix of the Brindisi concrete experiment (a) BRI.05, 12 months curing, (b) BRI.08, 48 months curing

7 Tobermorite Compositions and Lattice Parameters

Refinements of the lattice parameters of tobermorite identified through XRD analyses of relict lime clasts and one pumice clast (Table 2) provide a reference for gaining insights into the crystallization processes of calcium-silica-hydrate in the ancient seawater mortars. Although tobermorite is generally considered to form at elevated temperatures, usually through geothermal or autoclave processes at $>120^{\circ}\text{C}$ [21, 27, 28, 36], recent studies have detected tobermorite in historic mortars through XRD analyses [37–39]. However, little is known about the crystalline structure of these cements, which presumably formed in a low temperature environment. Diffractograms of relict lime clasts from Portus Claudius (Fig. 2, dx09-077), Portus Neronis (Figs. 9, 10, dx11-074), and Portus Iulius at Baiae (Fig. 15, dx04-055) show a uniform coincidence of tobermorite peaks.

The ICDD 191364 orthorhombic structural model ($\text{Ca}_{2.25}[\text{Si}_3\text{O}_{7.5}(\text{OH})_{1.5}] \cdot 1\text{H}_2\text{O}$) [21] fits the unit cell dimensions of the ancient tobermorites quite well (Table 2), as shown by the good correspondence with the Portus Neronis specimen (Fig. 16), rather than a monoclinic structure [36]. Calculations of the unit cell dimensions with Al^{3+} in the Roman seawater tobermorite suggest that aluminum substitution may not have a strong effect on the lattice parameters.

8 Inferences from Cement Microstructures

The predominance of alkali-rich vitric tuff in the ancient concretes suggests that geological perspectives can be useful in understanding their puzzling but pervasive cement assemblages. Hydrothermal alteration of basaltic glass tephra at $24\text{--}169^{\circ}\text{C}$ during the 12 years following the 1963–1967 eruption of Surtsey volcano, Iceland, for example, released elements that migrated and combined to form analcite, phillipsite, and tobermorite [22]. The 11 Å tobermorite formed mainly below sea level at $70\text{--}169^{\circ}\text{C}$ [22]. Locally elevated pH, above the typical 7.5–8.4 of seawater, developed

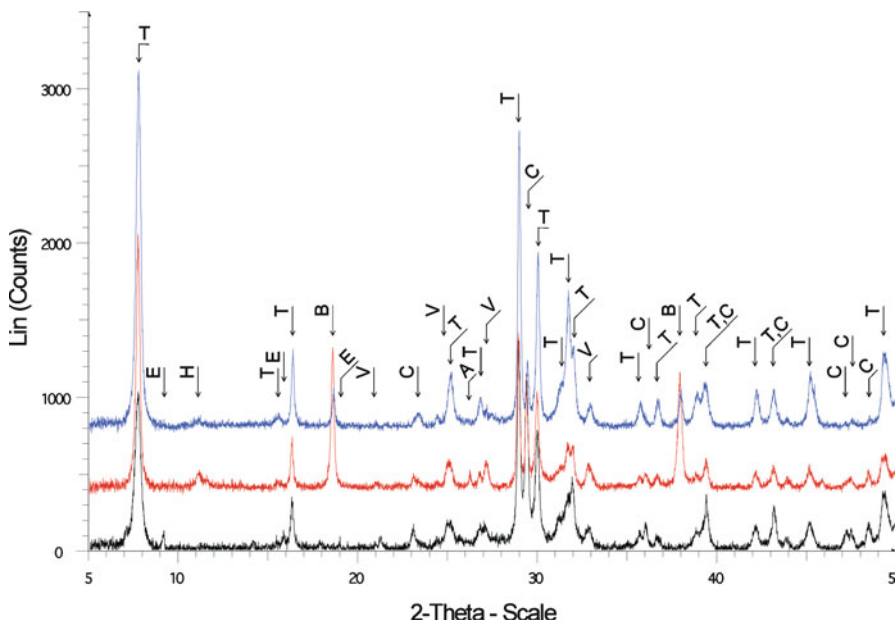


Fig. 15 X-ray diffractograms of tobermorite in relict lime clasts (Table 2) (*Top*) Portus Claudio dx09-077, (*Middle*) Portus Neronis dx11-074, (*Bottom*) Baiae, Portus Iulius dx04-05. $T = 11 \text{ \AA}$ tobermorite, E ettringite, H hydrocalumite, B brucite, V vaterite, A aragonite, C calcite

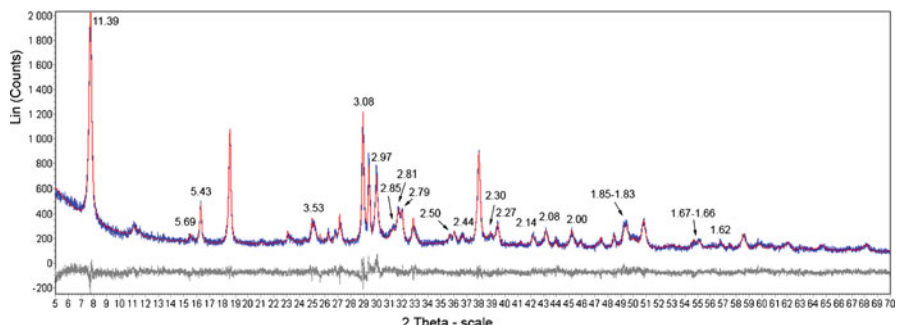


Fig. 16 Rietveld whole profile fitting of Portus Neronis specimen dx11-074, tobermorite d values in \AA , *Upper curves*: measured polyphase diffractogram and results of fitting to orthorhombic 11 \AA tobermorite [21], *Lower curve*: difference between the diffractogram and calculated curve

when hydrolysis of basalt glass formed smectite [22–25]. Phillipsite crystallized in basaltic glass vesicles in variable amounts. In saline lakes, silica-rich rhyolite and silica-poor trachytic volcanic ash sediments alter over a few hundred to a few thousand years, to form phillipsite at pH ~9.1–10 [23, 25]. Their Si:Al and Na:K vary, reflecting the composition of dissolving glass and saline lake brines, and their silica and aluminum activities [23–25].

Pozzolanic reaction is the sum of dissolution and topochemical reactions at particle surfaces at high pH, ≥ 12.7 , and the subsequent precipitation of cements [13]. The perimetral dissolution of the lime and vitric tuff clasts (Figs. 4, 7, 9), and their gel-like, silica-rich CASH rinds, now partially altered to microcrystalline calcium carbonate (Fig. 12b, c), record this process. The maximal amount of $\text{Ca}(\text{OH})_2$ that the volcanic pozzolan could combine was evidently not as great as the total lime in the ancient system. Many hydrated lime clasts were only partially dissolved; yet, after 5 years curing of the Brindisi experimental mortar, portlandite persists only in the coarsest lime particles (Table 1). In the ancient mortars, the release of SiO_2 and $\text{Al}_2\text{O}_3 + \text{Fe}_2\text{O}_3$ into solution by pozzolanic processes [9, 11] may have reacted with the portlandite at elevated pH to form CASH and, eventually, 11 Å tobermorite (Figs. 4, 5, 6, 7, 8, and 9) [6, 35]. The tobermorites have some aluminum substitution, common in most cement hydration systems [28], but this does not seem to affect the lattice parameters. Pozzolanic reactions in tuff clasts produced amorphous KMFCASH (Fig. 7a, b, d), and some tobermorite, as well.

The strong bonding of lime and the lack of free $\text{Ca}(\text{OH})_2$, would have had a favorable effect on concrete durability [10–14]. The lime leaching rate would have been very low, so there was little apparent increase in porosity, which facilitates penetration of aggressive ions and erosion in modern portland cement concretes [6–10]. Because there was little $\text{Ca}(\text{OH})_2$ to react with seawater salts – NaCl , CO_3^- , SO_4^- , Mg^{++} – gypsum and ettringite did not apparently form quantities large enough to produce dangerous expansions [9–14]. Instead, ettringite seems to occur in microstructures along the interfacial zones of relict lime clasts (Figs. 9, 10), in isolated voids (Fig. 11), or adjacent to vitric tuff clasts (Figs. 6, 7, 8) [6]. If, at $\text{pH} > 12$, the high solubility of aluminum caused it to preferentially migrate to voids farther from pozzolan grains [11, 35], precipitation of chloroaluminate (Figs. 4, 5, 6), perhaps as Friedel's salt [40], and sulphoaluminate would have been favored in these discrete microstructures. Phillipsite may be associated with dissolution of alkali-rich volcanic glass [15, 16, 22–24] at lower pH, 9.1–10, and eventual precipitation in relict pumice glass and voids (Figs. 12c, d, 13) [6].

Wollastonite (CaSiO_3) (Table 1) may reflect lime that was over-calcined at $>848^\circ\text{C}$. Indeed, pseudo-calcite indicative of dead-burned lime occurs in both the Portus Claudius and Portus Cosa mortars. If the lime was calcined from the limestone bedrock of the Appennines at Monte Soratte near Rome, then it is ~ 95 wt.% CaO [30]. However, the lithologic origins of the limestones are, as yet, unknown and Roman builders' methods for slaking the lime and hydrating the wet mortar mix remain unclear. The textures of some relict lime clasts suggest that they were emplaced as quicklime particles that hydrated *in situ* (Fig. 12a, b, c), but others may derive from previously slaked and matured lime (Fig. 12d). The elevated temperatures often associated with tobermorite crystallization remain enigmatic. Significantly, Bacoli tuff-lime pastes hydrated in distilled water at ambient temperatures formed crinkly foil tobermorite after 5 years curing [41].

Modern, low permeability concretes generally show good durability in the marine environment, if steel reinforcements remain free of corrosion and expansion from chlorine attack [10–12]. Deterioration occurs when permeability is high, due to inadequate

initial consolidation or subsequent microcracking, for example. Chemical attack then increases the porosity of the cement paste, reduces mechanical strength, and encourages erosion and loss of constituents [10–14]. In submerged structures, surficial CO₂ and magnesium ion attack can produce insoluble reaction products – aragonite, brucite, and ettringite – that reduce permeability and seawater ingress [10]. Although chlorine can penetrate more deeply into the concrete, its chemical interaction with aluminate and ferric phases to form stable Friedel's salt ($3\text{CaO}\cdot\text{Al}_2\text{O}_3\cdot\text{CaCl}_2\cdot10\text{H}_2\text{O}$) can beneficially influence durability by slowing the movement of chlorine ions towards steel reinforcements [10–13, 40]. Concrete mixtures with pozzolanic supplements, such as metakaolin, silica fume, and fly ash, reduce calcium hydroxide and produce dense, stable C-S-H. They limit the formation of abundant gypsum and ettringite and, thus, related expansions and cracking in the interior of structures [10–14]. *Pulvis Puteolanus* pozzolan has similar aluminate and ferric components. Its vitric and zeolitic pozzolanic constituents may be associated with the sequestration of chlorine and sulphate ions in crystalline microstructures (Figs. 7, 8, 9, 10, and 11), and the preservation of the cohesiveness of the ancient unreinforced concretes even in intertidal and splash zones [1], which are most vulnerable to attack [10–12]. Roman technologies for maritime concrete constructions may have applications for enhancing modern concrete durability in the marine environment.

9 Ancient Technologies: Raw Materials and Installation of Roman Maritime Concretes

In *De architectura*, Vitruvius emphasizes that the pozzolanic aggregate of mortars in marine concretes should come from the Bay of Naples and, more specifically, from the area around Baiae with *pulvis Puteolanus* deposits.

There is also a variety of powder (*pulvis*) which naturally effects an admirable result. It originates (*nascitur*) in the Baiae region and in the territory of the municipalities around Mount Vesuvius. When mixed with lime (*calx*) and rubble (*caementa*), it not only furnishes stability in building, but also, when a pier is erected in the sea the [*pulvis*, *calx*, and *caementa*] become solid underwater. (*De arch.* 2.6.1)

In his *Questions about Nature (Quaestiones Naturales)*, the first century CE philosopher Seneca mentions *pulvis* from Puteoli in the context of calcareous waters that naturally cement sedimentary deposits.

The water [of the Hebrus River] is adulterated and throws a sediment (*limus*) of such a nature that it cements and hardens objects. In just the same manner that the powdery earth of Puteoli (*Puteolanus pulvis*) becomes rock if it touches water, so by contrast, if this water touches something solid it clings to it and forms concretions. (*QN* 3.20.3)

There is a similar comment in Pliny's *Natural History*:

But other creations belong to the Earth itself. For who could marvel enough that on the hills of Puteoli there exists a dust (*pulvis*)—so named because it is the most insignificant part of the Earth—that, as soon as it comes into contact with the

waves of the sea and is submerged, becomes a single stone mass, impregnable to the waves and every day stronger, especially if mixed with stones quarried at Cumae. (HN 35.166)

Seneca and Pliny undoubtedly knew that *pulvis* had to be mixed with lime to make a coherent mortar, so they may be glossing over the full pozzolanic formula to make a rhetorical point. On the other hand, these observant natural scientists may be referring to natural concretes, or volcanic tuffs, that form through lithification of ash during alteration by ground and surface waters [16, 24] or, perhaps, even to the indurated ash deposits that occur in seawater and seacliffs along the Bay of Naples, as at Procida and the Parco Virgiliano at Posillipo, for example. Late third century BCE builders or engineers may have noticed this phenomenon and experimented with substitution of *pulvis* for beach or river sands in mortars.

Early experimentation with mortars for maritime construction could have very well taken place at Puteoli, which in the third and second centuries BCE was the only important port in the vicinity of the *pulvis* deposits. Until the completion of the Claudian and Trajanic harbours at Portus (Fig. 1), Puteoli served as the major harbour for the city of Rome, 200 km away, particularly for grain imports [42]. In the early second century BCE, a long breakwater composed of large, closely spaced concrete piers (*pilae*) connected by low concrete vaults (Fig. 3) was constructed to accommodate the growing sea trade serving Rome. In early first century CE Strabo praised the natural suitability of the local “sand-ash” at Puteoli for the construction of concrete breakwaters.

Puteoli has become a very great emporium, since it has an artificially constructed harbour, something made possible by the natural qualities of the local sand (*ámmos*), which is well suited to the lime and takes a firm set and solidity. Therefore, by mixing the sand-ash (*ammokónia*) with the lime, they can run moles out into the sea and in this way make the exposed shore into a protected bay, so that the biggest cargo ships can anchor there safely. (*Geography* 5.4.6)

In second century CE, Dio Cassius also described the properties of the dust (*kónis*) used at Baiae harbour (*History* 48.51.3–4), built by Agrippa in 37 BCE [19].

Lime was the most expensive ingredient in a concrete mix [20]. Pliny (HN 36.176) states that skimping on lime in a mortar mix was the main reason for the collapse of buildings in Rome. Vitruvius emphasizes the need for selectivity (*De arch.* 2.5.1; cf. Pliny HN 36.174): “...one must be careful that, in regard to lime (*calx*), it is burned from white rock, whether [hard] or [softer] limestone (*silex*). The lime from close-grained, harder stone will be the most useful in structural forms, while that made from porous stone will be best in plaster.” He discusses the calcining of limestone (*De arch.* 2.5.2–3); explicitly states that lime should be slaked before it is added to the mortar mix (*De arch.* 2.5.1); and describes the exothermic reaction produced by hydration of quicklime (*De arch.* 2.5.3). Pliny (HN 36.176), however, refers to “old building laws” requiring the ageing of *intrita*, which in context should be slaked lime putty, for 3 years prior to use.

Vitruvius provides the only extant description of how Roman builders constructed concrete structures in the sea, including the method of placement of pozzolanic mortars and coarse aggregate in wooden formwork [1, 4, 6, 17, 18].

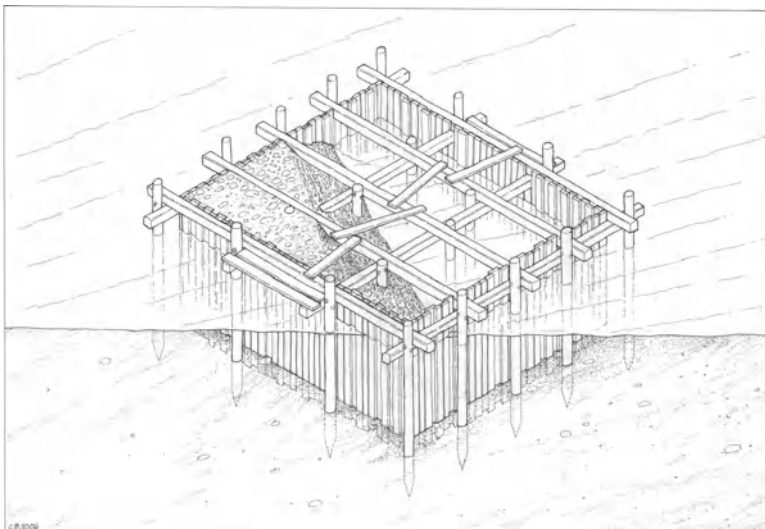


Fig. 17 A inundated timber form, constructed *in situ* on the sea floor, based on Vitruvius' description [*De arch.* 5.12.3], and underwater investigations of Roman maritime structures [17]

If, however, we have no natural harbour situation suitable for protecting ships from storms, we must proceed as follows. If there is an anchorage on one side and no river mouth interferes, then a mole composed of concrete structures (*structurae*) or rubble mounds (*aggeres*) is to be built on the other side and the harbour enclosure constructed in this manner. Those concrete structures that are to be in the water must be made in the following fashion. In the designated spot, formwork (*arcae*) enclosed by stout posts and tie beams (*stipitibus robustis et catenis inclusae*) must be let down into the water and fixed firmly in position. Then the area within it at the bottom, below the water, must be levelled and cleared out, [working] from a platform of small crossbeams (*ex transtris?*). There, the coarse aggregate (*caementa*) and the mortar (*materia*) from the trough mixed as described above (p. 7) must be heaped up (*caementis ex mortario materia mixta...ibi congerendum*), until the space left for the concrete within the form has been filled (*De arch.* 5.12.3).

The impressions of timber formwork on concrete structures indicate that builders drove wood piles into the seabed and framed these with horizontal beams (Fig. 17) [18]. Vertical boards, mainly about 25–30 cm wide and 3–8 cm thick, were placed closely together against the beams, with gaps generally less than 2 cm, and pounded into the seafloor. The impressions of horizontal cross beams on Portus Neronis concrete indicate that these were placed about 1 m above the ancient sea level. Continuous runs of concrete in long moles, as at Baiae (Fig. 3), were laid in sections with the end bulkhead of the formwork removed after each casting. The surviving timber planking at several sites suggests that builders left the formwork in place after the concrete had set, perhaps to protect the structure from erosion in its early stages of curing [18]. Ongoing analyses will further clarify Roman methods for

preparing lime, mixing mortars, and hydrating concretes in seawater; engineers' understanding of the mechanisms of pozzolanic reaction and curing; and the effects of these processes on the durability of the seawater structures.

10 How Did Expertise with These Technologies Spread?

Roman engineers had a nuanced understanding and sophisticated knowledge of the geologic materials and preparation of both terrestrial and submarine lime-volcanic ash mortars, based on empirical experience [1–8, 30] as well as stationary and floating forms for placing concretes in marine environments [1–8, 17, 18]. How did the technical information for these technologies travel around the Mediterranean? The two enormous breakwaters sheltering the outer basin at Caesarea in Israel, for example, were constructed of about 35,000 m³ of hydraulic concrete in first century BCE. The mortars have *pulvis Puteolanus* shipped 2,000 km from Puteoli, about 24,000 m³ weighing 52,000 ton [3]. It seems likely that Herod requested technical assistance from Rome for this colossal project, probably from his friend Agrippa, who built the Portus Iulius harbour near Puteoli. Agrippa would have sent harbour engineers from Italy, military engineers who reflected the same practical expertise as their contemporary, Vitruvius—himself a retired military engineer—who evidently recommended the use of *pulvis Puteo-lanus*, augmented with local sand, coarse aggregate, and lime [1, 5]. Elaborate single-use barge forms identical to those documented at Caesarea were used in the concrete structures in the Alexandria harbour in first century CE [17, 18]. While the movement of military engineers around the Mediterranean is the most likely explanation for the spread of harbour construction technology, it is also possible that sub-literary manuals incorporating technical information in written and graphic form moved with these engineers, or even independently. Traces of manuals of this type (*commentarii*) have been discerned in the archaeological evidence for military and agricultural equipment, and wooden pumps [19, 43]. They could have also existed for concrete construction in the sea. This could help explain the use of *pulvis Puteolanus* in the concrete of small, out-of-the-way harbours such as Chersonisos on Crete, where imperial involvement was unlikely.

11 Conclusions

Mortars of Roman maritime concretes from the central Italian coast have remarkably consistent cement compositions and microstructures, associated with the dissolution of lime and vitric tuff clasts at high pH, precipitation of gel-like CASH in perimetral rinds, and crystallization of orthorhombic 11 Å tobermorite in clast nuclei. Ettringite and calcium-chloroaluminate precipitated in discrete microstructures and voids. Phillipsite and chabazite crystallized at lower pH, possibly from dissolution of volcanic glass. The diverse microstructures in relict lime clasts,

including *in situ* expansive fracturing in some clasts and homogeneous textures in the residual cores of others, indicate that further analyses are needed to clarify methods for slaking lime, mixing mortars, and hydrating the concretes in seawater. Even so, it is clear that engineers developed extraordinarily effective technologies for the selection and transport of lime and *pulvis Puteolanus* to harbour sites, the preparation of hydraulic mortars, the installation of concrete mixes in forms submerged in seawater, and the distribution of this expertise through the Mediterranean. The mortar cements have analogies to durable natural rock cements that develop in volcanic ash submerged in seawater and saline lakes. They display a striking resistance to chemical dissolution and attack.

Acknowledgements We thank U. Costa and F. Massazza at CTG Italcementi, and H.-R. Wenk and P. J. M. Monteiro, at University of California at Berkeley, for discussions regarding cement chemistry. B. Zanga, N. Colombi, M. Segata, C. Kosso, T. Hoisch, and B. Black assisted with this research. The Loeb Foundation at Harvard University and Project No: MSM 0021622427 at Masaryk University provided funding.

References

1. Oleson, J.P., Brandon, C., Cramer, S., et al.: The ROMACONS project: a contribution to the historical and engineering analysis of hydraulic concrete in Roman maritime structure. *Int. J. Naut. Archaeol.* **33**, 199–229 (2004)
2. Brandon, C., Hohlfelder, R.L., Oleson, J.P., et al.: The Roman Maritime Concrete Study (ROMACONS). the roman harbour of chersonisos in crete and its italian connection. *Mediterranée* **1**(2), 25–29 (2005)
3. Hohlfelder, R.L., Brandon, C., Oleson, J.P.: Constructing the harbour of caesarea palaestina. *Int. J. Naut. Archaeol.* **36**, 409–415 (2007)
4. Brandon, C., Hohlfelder, R.L., Oleson, J.P.: The concrete construction of the roman harbours of baiae and portus iulius. *Int. J. Naut. Archaeol.* **37**, 374–379 (2008)
5. Vola, G., Jackson, M., Oleson, J.P., et al.: Mineralogical and petrographic characterisation of ancient Roman maritime concretes from Mediterranean Harbours. In: Valek, J., Groot, C., Hughes, J. (eds.) Proceedings of the 2nd Historic Mortars Conference and RILEM TC 203-RHM Final Workshop, pp. 381–388. Prague, 22–24 September 2010
6. Vola, G., Gotti, E., Brandon, C., et al.: Chemical, mineralogical and petrographic characterisation of ancient Roman hydraulic concrete cores from Santa Liberata, Grosseto, Italy and Cesarea Palestina, Israel. *Period. Miner.* **80**(2), 99–120 (2011)
7. Oleson, J.P., Bottalico, L., Brandon, C., et al.: Reproducing a Roman maritime concrete structure with Vitruvian pozzolanic concrete. *J. Rom. Archaeol.* **19**, 29–52 (2006)
8. Gotti, E., Oleson, J.P., Bottalico, L., et al.: A comparison of the chemical and engineering characteristics of ancient Roman hydraulic concrete with a modern reproduction of Vitruvian hydraulic concrete. *Archaeometry* **50**, 576–590 (2008)
9. Siivola, J., Schmid, R.: List of mineral abbreviations. http://www.bgs.ac.uk/scmr/docs/papers/paper_12.pdf (2007)
10. Mehta, P.K., Monteiro, P.J.M.: Concrete: microstructure, properties, materials. McGraw-Hill, New York (2006)
11. Massazza, F.: Concrete resistance to seawater and marine environment. *Il Cem.* **1**, 3–26 (1985)
12. Mehta, P.K.: Concrete in the marine environment. Elsevier, Oxford (1990)

13. Massazza, F.: Properties and applications of natural pozzolanas. In: Bensted, J., Barnes, P. (eds.) Structure and performance of cements, pp. 326–352. Taylor & Francis, London (2002)
14. Glasser, F.P., Marchand, J., Samson, E.: Durability of concrete-degradation phenomena involving detrimental chemical reactions. *Cem. Concr. Res.* **38**, 226–246 (2008)
15. De'Gennaro, M., Cappelletti, P., Langella, A., et al.: Genesis of zeolites in the neapolitan yellow tuff: geological, volcanological and mineralogical evidence. *Contrib. Mineral. Petrol.* **139**, 17–35 (2000)
16. Jackson, M.D., Marra, F., Hay, R.L., et al.: The judicious selection and preservation of tuffs and travertine building stone in ancient Rome. *Archaeometry* **47**, 485–510 (2005)
17. Brandon, C.: How did the Romans form concrete underwater? In: Valek, J., Groot, C., Hughes, J. (eds.) Proceedings of the 2nd Historic Mortars Conference and RILEM TC 203-RHM Final Workshop, pp. 73–81. Prague, 22–24 September 2010
18. Brandon, C.: The concrete-filled barges of King Herod's harbor of sebastos. In: Swiny, S., Hohlfelder, R.L., Swiny, H.W. (eds.) *Res maritimae, Cyprus and the eastern Mediterranean from prehistory to late antiquity*, pp. 45–58. Scholars Press, Atlanta (1997)
19. Oleson, J., Jackson, M.: How did expertise in maritime hydraulic concrete spread through the Roman empire? In: Valek, J., Groot, C., Hughes, J. (eds.) Proceedings of the 2nd Historic Mortars Conference and RILEM TC 203-RHM Final Workshop, pp. 285–282. Prague, 22–24 September 2010
20. Shaw, J.: Greek and roman harborworks. In: Bass, G. (ed.) *A history of seafaring based on underwater archaeology*, pp. 87–112. Walker, New York (1972)
21. Hamid, S.A.: The crystal structure of 11Å natural tobermorite $\text{Ca}_2.25[\text{Si}_3\text{O}_7.5(\text{OH})1.5]\text{H}_2\text{O}$. *Z Krist.* **154**, 189–198 (1981)
22. Jakobsson, S., Moore, J.G.: Hydrothermal minerals and alteration rates at Surtsey volcano, Iceland. *Geol. Soc. Am. Bull.* **97**, 648–659 (1986)
23. Hay, R.L.: Phillipsite in saline lakes and soils. *Am. Mineral.* **49**, 1366–1387 (1964)
24. Sheppard, R.A., Gude, A.J., Griffin, J.J.: Chemical composition and physical properties of phillipsite from the Pacific and Indian oceans. *Am. Mineral.* **55**, 2053–2062 (1970)
25. Hay, R.L.: Geologic occurrence of zeolites. In: Sand, L.B., Mumpton, F.A. (eds.) *Natural zeolites, occurrence, properties, and use*. Pergamon, Oxford (1978)
26. Passaglia, E., Vezzalini, G.: Crystal chemistry of diagenetic zeolites in volcanoclastic deposits of Italy. *Contrib. Mineral. Petrol.* **90**, 190–198 (1985)
27. Lea, F.M.: *Chemistry of cement and concrete*, 2nd edn. Arnold, London (1970)
28. Barnes, M.W., Scheetz, B.E.: The chemistry of Al-tobermorite and its co-existing phases at 175°C. In: Scheetz, B.E., et al. (eds.) *Specialty cements with advanced properties*. Materials Research Society Symposia Proceedings, vol. 179, pp. 243–271. Materials Research Society, Pittsburgh (1991)
29. Marullo, S., Santoleria, R., Bignami, F.: Seasonal and interannual variability of the western mediterranean sea. *Coast. Estuar. Stud.* **46**, 135–154 (1994)
30. Jackson, M., Deocampo, D., Marra, F., et al.: Mid-pleistocene Pozzolanic volcanic Ash in ancient Roman concretes. *Geoarchaeology* **25**(1), 36–74 (2010)
31. Leslie, A.B., Hughes, J.J.: Binder microstructure in lime mortars: implications for the interpretations of analysis results. *Q. J. Eng. Geol. Hydrogeol.* **35**, 257–263 (2002)
32. Forster, A.: Hot-lime mortars: a current perspective. *J. Archit. Conserv.* **3**, 7–27 (2004)
33. Elsen, J.: Microscopy of historic mortars—a review. *Cem. Concr. Res.* **36**, 1416–1424 (2006)
34. Valek, J., Zeman, A.: Characteristics of lime particles in hot mixed mortars. In: Proceedings of the 12th Euroseminar on Microscopy Applied to Building Materials, Dortmund, 15–19 September 2009
35. Scheetz, B., Loop, C., White, W., et al.: Diagenesis of FBC ash in an acidic pit lake. http://www.dep.state.pa.us/dep/deputate/minres/BMR/beneficial_use/19CHAPT11/Chapter11.pdf (2004)
36. Merlini, S., Bonaccorsi, E., Armbruster, T.: The real structure of tobermorite 11Å: normal and anomalous forms, OD character and polytypic modifications. *Eur. J. Mineral.* **13**, 577–590 (2001)

37. Moroloupo, A., Bakolas, A., Biskibou, K.: Characterization of ancient, byzantine, and later historic mortars by thermal and X-ray diffraction techniques. *Thermochim. Acta* **269/270**, 779–795 (1995)
38. Charola, A.E., Henriques, F.M.A.: Hydraulicity in lime mortars revisited. In: *Historic Mortars: characteristics and tests*, RILEM TC-197COM, Paisley, Scotland (2000)
39. Cantisani, E., Cecchi, A., Chiaverini, I., et al.: The binder of the Roman concrete of the Ponte di Augusto at Narni (Italy). *Period. Mineral.* **71**, 113–123 (2002)
40. Birnin-Yauri, U.A., Glasser, F.P.: Friedel's salt, $\text{Ca}_2\text{Al}(\text{OH})_6(\text{Cl}, \text{OH})_2\text{H}_2\text{O}$: its solid solutions and their role in chloride binding. *Cem. Concr. Res.* **28**, 1713–1723 (1998)
41. Sersale, R., Orsini, P.G.: Hydrated phases after reaction of lime with 'pozzolanic' materials or with blastfurnace slags. In: *Proceedings, Fifth International Symposium on the Chemistry of Cement*, pp. 114–121. Tokyo (1969)
42. Meiggs, R.: *Roman Ostia*, 2nd edn. Oxford University Press, Oxford (1973)
43. Oleson, J.P.: Well-pumps for dummies: was there a Roman tradition of popular, Sub-literary engineering manuals? In: Minonzio, F. (ed.) *Problemi di Macchinismo in Ambito Romano*. Museo Comunale, Como (2004)

Historic Mortars with Burned Alum Shale as an Artificial Pozzolan

Sölvé Johansson and Jan Erik Lindqvist

Abstract From the mid-eighteenth century extensive research in Sweden and in present day Finland focused on the development of mortars with hydraulic properties, the results mainly published by the Royal Swedish Academy of Science. The aim was to replace imported Italian pozzolan and Dutch trass with a pozzolan produced in Sweden. Several products based on burned alum shale were developed. Cambrian alum shales with a high content of bitumen were fired without additional fuel to produce pozzolanic shale ash. The bituminous alum shale was used directly as a fuel in the lime burning process from the late eighteenth century. The alum shale mortars have a red-brown colour due to the high content of iron oxides. The mortars are hard, strong and generally have a good durability, both as masonry mortars and renders. Microscopic analysis shows that often only a skeleton remains of the shale particles and that large parts of the particles are consumed by the pozzolanic reaction. The field of application was initially restricted to structures in contact with water, such as locks in canals and harbours, but conventional building construction was also an early application.

1 Introduction

In the seventeenth century, waterside construction in Sweden was largely managed by Dutch engineers using Dutch techniques and pozzolanic trass mortars. One example is the city of Gothenburg, which was established on the marshy banks near the mouth of the Göta River in 1621. It was built by Dutch engineers using a Dutch city plan.

S. Johansson (✉)
Byggkonsult Sölvé Johansson AB, Trollhättan, Sweden
e-mail: solve@bksjab.se

J.E. Lindqvist
Swedish Cement and Concrete Research Institute, Stockholm, Sweden
e-mail: janerik.lindqvist@cbi.se

Later on, during the eighteenth century, mercantilist ideas grew stronger; these were accompanied by an increasing belief in the need to make knowledge and natural resources useful. According to this economic theory, the wealth of the nation was important. Wealth for the people was not considered a useful target; quite the contrary, poverty for the common people was seen as a necessary motivation for people to work. This focus on the wealth of the nation rather than its population was reflected in many leading-edge building projects at the time in Sweden as well as in other parts of Europe. A number of demanding canal building projects were completed in Sweden during the eighteenth century and the first half of the nineteenth century. These required a suitable building material of which mortars that could harden under water were an important part. The political leadership in Sweden during the mid-eighteenth century was much in favour of research. As a result of this a number of prominent researchers in the field of chemistry and mineralogy were engaged in the development of suitable mortars that could be based on Swedish materials [1–5]. The line that was most favoured was the use of synthetic pozzolans based on shale ash sourced from burned alum shale. As a result, Sweden concentrated on the development of mortars with these properties while other European countries were more focused on the development of hydraulic binders.

2 Limestone and Alum Shales Used for Lime and Pozzolan Production in Sweden

The limestone used for lime production in Sweden is of two main types. One type is a sedimentary limestone from the counties of Skåne, Öland, Gotland Västergötland, Östergötland, Närke and Jämtland. Their chemical composition ranges from a pure limestone at a few sites to those with a high content of silica; the age of these limestones range from Tertiary to Cambrian. The other rock type used is a Pre-Cambrian metamorphic marble of a calcitic and dolomitic composition from southern central Sweden.

Alum shales of Cambrian age are widespread in Scandinavia and on the eastern side of the Baltic Sea. These are characterised by a high content of organic material, commonly about 10% and sometimes as high as 30%. They are also characterised by the high content of elements such as uranium, thorium, vanadium and molybdenum [6]. These shales occur in several areas in Sweden, but it is only the alum shales on the island of Öland and in the counties of Västergötland, Östergötland and Närke that have organic contents high enough for use as a fuel.

3 Development of Mortars with Artificial Pozzolans

There are several early examples of mortars with burned alum shale. Early occurrences include twelfth century lime paintings in Fornåsa [7] and medieval masonry churches in the county of Jämtland in northern central Sweden. In these cases the alum shale was probably burned with the limestone. Alum shale mortars were used in a few

rare cases in the masonry of medieval castles in central Sweden [8]. These examples may sometimes reflect local practices where alum shale mortars were intentionally used as early as the medieval period.

The following description of the early development of hydraulic and pozzolanic materials in Sweden is based mainly on Johansson [9] and to some extent Strömbäck [10].

A large part of the technology used for waterside construction in Sweden during the seventeenth and the first half of the eighteenth century was imported from the Netherlands where the techniques were partly developed during the expansion of Amsterdam in the early seventeenth century. This prompted Sven Rinman to make a visit to the Netherlands in 1746–1747. He was later involved in research on the topic of shale ash production at Garphyttan in 1770–1771. The purpose of this shale ash production plant was the development of a cement that could be used for waterside construction. Rinman studied 23 different mortar mixes based on burned alum shale, brick dust, slag and trass; he showed that the mortars based on hard burned, partly melted, alum shale and lime did harden in water and that these mortars had properties comparable to the trass mortars. The mortars produced had no added aggregate and therefore the burned alum shale served also as an aggregate in these mortars. Production of Garphyttan Cement continued from 1779 to 1828 with an annual production of 50 tons. The cement was delivered to mines and used in the construction of locks, houses and bridges such as the Norrbro Bridge in Stockholm (1788).

Johan Ulfström was responsible for the repair of canal locks in the Hjälmar Canal in 1772. He developed a mortar called “Ulfström Cement” based on a burned alum shale or trass which was mixed to a stiff paste with hydraulic lime and water for two hours. The mortar had to be used within a few hours after mixing.

Another researcher, Bengt Qwist Andersson, was responsible for cement and clinker production at Brinkebergskulle from 1770. He performed tests on different imported natural pozzolans as well as burned alum shale. Assessment of the burned alum shale used here demonstrated that it had properties similar to volcanic pozzolans.

The alum shale mortars were further developed in connection with the building of several canals and locks in Sweden during the late eighteenth and early nineteenth centuries. There was at this time an active programme of research and development in this field. The most important work was probably conducted by Gustaf Erik Pasch, who in 1817 began researching mortars for the construction of the Göta Canal. In his research he investigated the importance of the burning temperature and particle size distribution in alum shale ash. The alum shales could be burned at low temperatures but the important factor was that the particles were finely milled. He also investigated the mix proportions of the mortars. He suggested a number of mortar mixes where the mix proportions of lime, sand and alum shale ash varied with the lime used.

4 Production and Utilisation

Alum shale lime mortar was called “cement”, while “Swedish Cement” was a name used by Sven Rinman. The manufacture of mixed and burned alum shale lime mortar required an industrial process that was initiated just after the first successful attempts



Fig. 1 Gustaf's Locks at Brinkebergskulle in the Göta River, constructed 1772–1778 with an alum shale mortar from the cement factory at Brinkebergskulle (Photo: Sölve Johansson 1989)

at production had been completed. Manufacturing was concentrated at two major cement factories. One of them was at Garphyttan which was commissioned in 1771 as a direct result of Sven Rinman's trials in 1770–1771. Alum shale lime mortar was made here until about 1828, for use in hydraulic engineering projects etc., in Mälardalen and Stockholm, and possibly also for the 1800 Locks at Trollhättan. Another factory was established at Brinkebergskulle. Planning for a "cement and clinker works" was started as early as 1761, but the manufacture of clinker only began in 1770 and the manufacture of cement probably did not start until 1772 when the work on Gustaf's Locks commenced (Fig. 1). Qwist Andersson was responsible for production in both cases.

The mortar was not solely used for infrastructure projects, although its main application was initially the locks in the Hjälmare Canal and Brinkebergskulle (1772 and 1772–1778 respectively), it was also used in housing projects. The Old Town Hall in Skövde (1775–1776) is a very early example and is probably the first of its kind in Sweden.

Alum shale lime mortar from Brinkebergskulle was used for the locks in the Hjälmare Canal and Brinkebergskulle, and also as a cement mortar for joints in the construction of various buildings at the neighbouring Onsjö Manor (1774–1793), as well as joints in the locks that were constructed in the Göta River at the end of the 1700s and possibly also in the 1800 Locks at Trollhättan. All these projects were in the west of Sweden.

Consequently, with the development of two alum shale lime factories, at Garphyttan and Brinkebergskulle, this type of mortar gained a strong position. The mortar was utilised in demanding construction and building projects during the 1800s until the introduction of Portland cement at the beginning of the 1860s, and above all from the start of the 1880s when domestic production of Portland cement was in force in Sweden.

Alum shale lime mortar was used extensively during the 1800s for projects such as the Göta Canal (1810–1832) etc. This mortar was further developed by Gustaf Erik Pasch, who experimented with the choice of lime and mixing ratios. Natural hydraulic lime, both from orthoceratite limestone and strong bituminous antraconite, was preferred following comprehensive trials. Knowledge concerning production and utilisation of alum shale lime mortar was subsequently spread in Sweden through publication in the building handbooks of the 1800s and the early 1900s.

Alum shale lime mortar was also manufactured at Vargön under the name of “Vargö cement” during the period 1840–1888, for projects such as the Locks in Trollhättan (1838–1844), Stockholm Lock (1843–1850), Saima Canal in Finland (1847–1856) and the Dalsland Canal (1864–1868). The initiative for this cement manufacture was taken by colonel engineer Nils Ericson.

In addition, local manufacturing of alum shale lime mortar probably occurred in Västergötland, where a very large number of buildings have been reported as using this type of mortar. This applies not only to the prominent buildings commissioned by the state, such as law courts and church buildings, but also to modest private buildings and housing.

Alum shale lime mortar was utilised above all for bricklaying and jointing, but it has also been used for rendering and broom finishing. The latter was used especially on exposed façades facing south and west. It was also utilised as a set mortar in the mounting of façade ornamentation, for example on Karlstad Town Hall. This type of façade ornamentation consisted of gypsum and natural cement.

Knowledge about the production and use of alum shale lime mortar obviously did not disappear with the rising popularity of Portland cement in construction and hydraulic engineering projects in the 1880s. Its use did however become limited. Alum shale lime mortar – or rather alum shale lime cement mortar – was used in the making of red Örebro render during the 1910s and 1920s (Fig. 2). The burnt alum shale for this production was brought from Lanna and Latorp, from sites such as Garphyttan. This mortar is still produced as a restoration mortar for buildings originally built using the Örebro render.

The usage of alum shale mortar for house building increased during the nineteenth century. In the 1920s the process was adapted for the production of autoclave-aerated concrete. Production continued until the 1970s, when it was abandoned due to the high radon emissions deriving from the uranium content in the shale ash present in these blocks.

5 Microstructural Characteristics

5.1 Methods

The quantitative microscopic analysis was performed according to the methods described by Lindqvist and Sandström [11] and the COM-C1 method [12]. Size distribution was assessed using NT BUILD 486. The chemical analysis of acid-soluble components was performed according to the methods described in Lindqvist et al. [13].



Fig. 2 Örebro render at domestic house in central Örebro. The house was built 1912–1913 with a red render based on burnt alum shale from Latorp near Garphyttan (Photo: Sölve Johansson 2002)

The scanning microscopy was performed using Jeol 5100LV equipped with a Link Inca EDS equipment for micro chemical analysis. The instrument was used in low vacuum mode. XRD was used to identify mineral phases and amorphous hydration products. The instrument used was a Siemens D5000 powder diffractometer, operating with Cu K_α radiation for 20 range between 10° and 70° at 0.5°/min. About 30 samples have been analysed and those presented in the tables have been selected in order to illustrate the variation of properties in a representative way.

5.2 Microstructural Characteristics

The colour of the paste in the shale ash mortars is a relatively dark red, which is mainly due to the presence of iron oxides and hydroxides from the burned shale. In several cases the paste is uncarbonated or not fully carbonated; an uncarbonated paste implies the presence of CSH gel. The cement index, assessed through analysis of acid-soluble components, gives a hydraulicity that ranges from that of a pure lime mortar to a strongly hydraulic mortar (Table 1). There are small remnants of unhydrated cement clinker grains in some of the mortars which probably come from the burning of a lime shale mix, mainly in samples from the eighteenth and nineteenth century mortars – a technique favoured by Sven Rinman in the 1770s. An example is sample SP6 from the masonry of a private house built in 1788. This sample also

Table 1 Results from analysis of acid soluble components given in weight-%

Sample	Mg	Al	Fe	CaO	SiO ₂	CI
SP6	0.34	0.94	0.34	8.6	1.22	0.52
SP4	0.77	1.17	0.23	17	1.66	0.34
SP47	0.084	0.551	0.35	11.19	2.929	0.85
SP48	0.06	0.128	0.111	11.53	0.386	0.12

The cementation index CI according to Eckel [14] is also given in the table. SP6 masonry mortar private house 1788, SP4 military fortress 1779–1782, SP47 and SP48 town hall 1775–1776

Table 2 Examples of grain size distributions given in volume-% based on microscopic assessment

	SP47	SP48	S1 Out	S1 In	SP41	SP40
mm	Vol %	Vol %	Vol %	Vol %	Vol %	Vol %
4	100					
2	87			100		
1	78	100	100	90	100	100
0.5	46	95	96	59	74	74
0.25	20	75	75	32	33	33
0.125	5	19	26	9	8	8
0.063	0.5	1.8	3	1.6	0.9	0.9

contains the calcium silica mineral gismondite. There is also cement clinker in samples from locks built 1788 and 1844. The latter samples are not included in the tables. The main part of the CSH-gel is formed through a pozzolanic reaction which is probably based on the formation of reactive glass during the burning process.

The air content in the mortars shows a large variation. The shape of the air voids varies from irregular and elongated to well-rounded. Fluorescent microscopy shows that there are generally very few cracks; these are mainly in the form of shrinkage cracks and cracks between different layers of renders, and occasionally as open cracks between the different layers in the same layer of render. In some cases the shrinkage cracks can occur around and within shale ash particles.

The aggregate is mostly fine grained with a maximum grain size of 2 or 4 mm with a well graded size distribution (Table 2). Other properties, such as the shape of the aggregate, show no difference when compared to other mortar types from the same region and time.

Preserved shale particles, which are elongated often with an ellipsoid shape, display internal shrinkage cracks and adhesion cracks due to the shrinkage of the shale ash particles. The finer particles have largely reacted, leaving just the larger shale ash particles which have to a large extent also reacted to different degrees. These range from intact or almost intact particles, to mainly fine-grained particles, where only a skeleton of the iron oxides and hydroxides remain (Figs. 3 and 4).

The mix proportions, based on point counting, vary from very binder-rich to those that compare with modern pozzolanic mortars (Table 3).

Detailed analysis using electron microscopy demonstrates that shale ash particles that may seem inert at low magnification show a reaction at higher magnification.

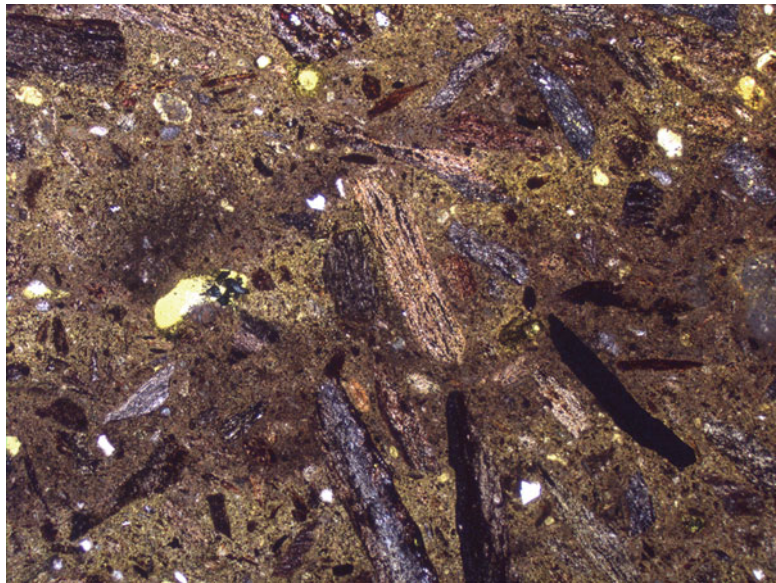


Fig. 3 A sample with a high amount of shale ash particles that is partly or almost fully reacted. Sample SP9 from a private building built in 1788. The image was taken by optical microscope using plain light, the surface measures $2.7 \times 2.0 \text{ mm}^2$

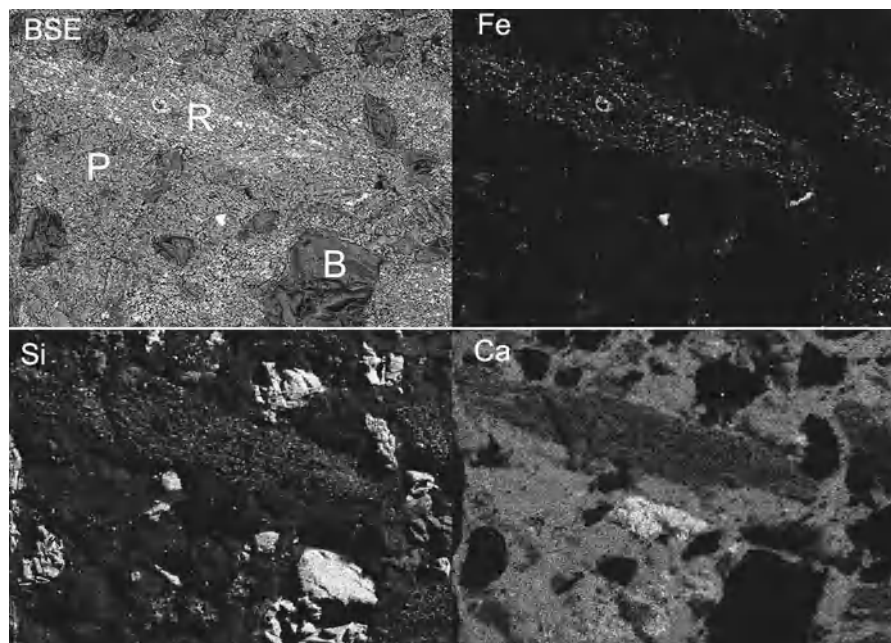


Fig. 4 Shows the back scatter electron image (BSE) combined with EDS maps of the distribution of iron (Fe), silica (Si) and calcium of an almost totally reacted shale ash particle. R burned shale, P lime paste, B aggregate. Repair mortar from a royal castle in south eastern Sweden. Probably nineteenth century. The instrumental magnification is 200 \times

Table 3 Examples of mortar compositions based on microscopic analysis

	SP42	SP4	Näs 2	SP13	S1out	B thin
	Vol %	Vol %	Vol %	Vol %	Vol %	Vol %
Air	5	5	8	3	4	4
Aggregate	43	7	37	37	36	51
Paste	49	69	40	55	59	37
Lime lump	0	0	10	0	1	7
Cement	2.2	0	0	0	1	1
Shale ash	2	18	4	5	2	1
Period	1750	1779	1820	1865–1868	1890	1905
Mortar	Masonry	Masonry	Masonry	Masonry	Rend	Rend
Type	House	Fortress	Church	Lock	House	House
Location	Skåne	West Sweden	Northern central Sweden)	West Sweden	West Sweden	West Sweden

Results are given in volume percentages. The samples come from masonry and renders of houses in Sweden. The samples are ordered by age, with the oldest which are from 1750 to the left and the youngest from 1905 to the right

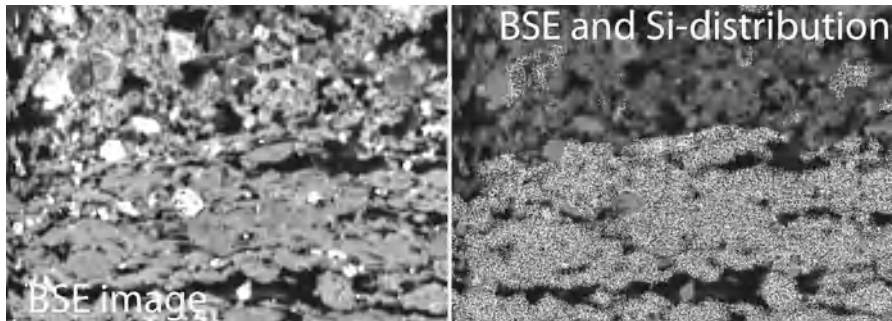


Fig. 5 The right hand image shows as white dots the distribution of Si^{4+} close to the shale ash particle seen in the lower part of the image. The Si-element map were transformed to binary image using adaptive grey value segmentation and then combined with the BSE image. Sample SP51 render on the old town hall in Skövde, 1775–1776. Instrumental magnification 1,500 \times

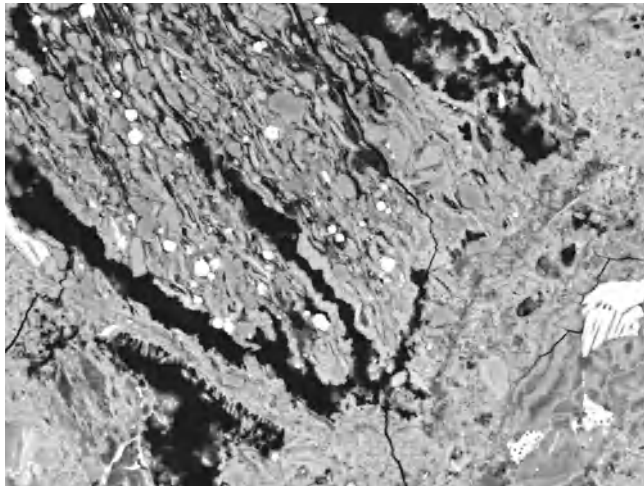


Fig. 6 SEM/BSE image of a shale ash particle rim which is partly decomposed by a pozzolanic reaction. As a result of the reaction there is no sharp contact between the particle and the surrounding paste. The ash particle shows internal shrinkage cracks. Sample SP51 render on the old town hall in Skövde, 1775–1776. Instrumental magnification 750 \times

Shale ash particles may display sharp grain boundaries in the low magnification BSE images as well as in the chemical distribution. At higher magnification it can be seen that there is a zone of paste that is enriched in Si surrounding the shale ash particle (Figs. 5 and 6).

X-ray diffraction shows a broad hump in the range 10°–20° 2 θ and around 30° 2 θ implying that the sample contains amorphous CSH gel (Fig. 7). XRD analysis also shows the presence of the minerals calcite, hematite and the zeolite gismondite [9].

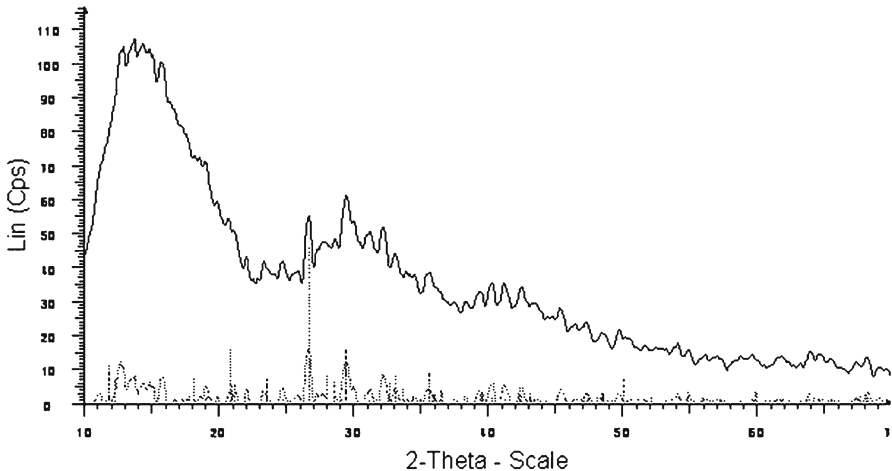


Fig. 7 X-ray diffractograms of the sample SP6. The broad band shows the presence of an amorphous CSH-phase. The diffractogram is shown after smoothing

6 State of Preservation

The old canals and locks that are mentioned in the text are protected as fixed ancient monuments in accordance with Swedish legislation concerning the preservation of historic monuments and the buildings that have been examined in most cases are architectural monuments. This signifies that these constructions and buildings are well protected. It is necessary however, in connection with measures taken on these objects, to ensure that all forms of mortar are protected in practice, e.g. jointing mortar, grout and finishing mortar.

7 Discussion/Conclusion

Alum shale lime mortar, which was called “cement”, emerged in 1770 as a direct result of Swedish research into mortars during the 1700s which had the main objective to find domestic supplies for hydraulic engineering projects. This constituted a breakthrough for the Swedish pozzolana mortars. The brickdust lime mortar that had been introduced a century earlier was only partially pozzolanic. The production and utilisation of both natural cement and alum shale lime mortar required an industrial process that started after the first successful attempts. The utilisation was not only for infrastructure projects, for which the mortar primarily was intended, initially the locks in the Hjälmare Canal and Brinkebergskulle (1772 and 1772–1778 respectively), but also in housing projects. The Old Town Hall at Skövde (1775–1776) is a very early example, probably the first of its kind in Sweden. Its utilisation as mortar,

grout and render was extensive until the 1880s when these types of mortar were replaced by Portland cement. Alum shale lime mortar was used from the 1770s until the 1920s for a variety of purposes, e.g. jointing and render. One type of alum shale lime mortar is the Örebro render from the 1910s and 1920s, which came into use again in the 1990s for restoration objects. The micro structural analysis confirms the pozzolanic properties of the burned alum shale. The analysis furthermore illustrates the variation and development of this type of mortars.

Acknowledgement The XRD analyses were performed by Dr Britt-Marie Stenari, Chalmers, and the analysis of acid soluble components by Peter Nyman, SP, which is kindly acknowledged.

References

1. Gadd, P.A.: Rön och försök med murbruk och cement-arter. Kungliga Svenska Vetenskapsakademiens handlingar **XXXI**, 189–206 (1770)
2. Pash, G.E.: Berättelse om de vid Motala ström anställdde Murbruksförsök, inlämnade till Götha Canals Direction år 1818 och 1822 års Berättelse om de vid Göta Kanal anställda Murbruksförsök. Jernkontorets annaler Stockholm **1824**, 192–296 (1824)
3. Qwist Andersson, B.: Försök anställdt på Trass. Kungliga Svenska Vetenskapsakademiens handlingar **XXXI**, 49–66 (1770)
4. Qwist Andersson, B.: Försök med Terra Puzzolana och cement. Senare stycket. Kungliga Svenska Vetenskapsakademiens handlingar **XXXIII**, 120–132 (1772)
5. Qwist Andersson, B.: Försök med Terra Puzzolana och cement. Kungliga Svenska Vetenskapsakademiens handlingar **XXXIII**, 28–42 (1772)
6. Andersson, A., Dahlman, B., Gee, D.G., Snäll, S.: The Scandinavian Alum Shales, Sveriges Geologiska Undersökning Ca 56, 50 pp (1985)
7. Henningsson, A.: The Romanesque wall painting above the vaults in Fornåsa Church. Examination and developing of a conservation proposal. Documented in GIS. Diploma thesis on CD. University of Applied Science, Cologne (2003)
8. Feldt, A.C., Modén, E.: Murbruk som källmaterial. Östergötlands museum. Rapport 19:2001, Linköping (2001)
9. Johansson, S.: Hydraulic lime mortar Its Production and Utilisation in Sweden in Buildings from the Middle Ages until present Time. Göteborg Stud. Conserv. **20**, 327 (2007) (In Swedish with summary in English)
10. Strömbäck, L.: Gustaf Erik Pasch, Göta kanal och bruket av hydrauliskt cement. In: Polhem. Göteborg: Svenska nationalkommittén för teknikhistoria (SNT), 1983. ISSN 0281-2142; 1993 (11), s. 135–143 (1993)
11. Lindqvist, J.E., Sandström, M.: Quantitative analysis of historical mortars using optical microscopy. Mater. Struct. **33**, 612–617 (2000)
12. COM-C1: Assessment of mix proportions in historical mortars using quantitative optical microscopy. RILEM TC-COM: Characterization of old mortars. Mater. Struct. **34**, 387–388 (2001)
13. Lindqvist, J.E., Nijland, T., von Konow, T., Wester Plessier, T.S., Nyman, P., Larbi, J., van Hees, R.: Analysis of mortars with additives. Nordtest Technical Report 594 (2006)
14. Eckel, E.C.: Cement Limes and Plasters. Wiley, New York (1922)

Nineteenth Century “Novel” Building Materials: Examples of Various Historic Mortars Under the Microscope

Johannes Weber, Karol Bayer, and Farkas Pintér

Abstract Starting in the late eighteenth century, the age of industrialisation brought about a number of new binder systems of hydraulic nature meant to answer the demand for improved mortar strength even at moist conditions. Such mortars form an important part of today’s architectural heritage and are therefore frequently encountered, either as primary materials or as historic restoration mortars, when historic objects are studied in the course of restoration. This paper deals with the basic features of a selection of those cementing materials which were “novel” at their time: Sorel cements, iron hammer scale mortars, and natural Roman as well as early Portland cements. The analytical approach followed is based on light and scanning electron microscopy, believed to provide primary tools to identify the mortars and to understand some of their key properties. Sorel cement mortars were studied at examples of flooring and stone repair mortars, respectively. Both were frequently encountered applications of this binder prepared from a mixture of caustic magnesia and magnesium chloride. In both types of mortar, the binder appears composed mainly of magnesium oxychloride hydrates, whereas the matrix porosity varies from highly porous to dense. The aggregates range in composition from wood fibres to stone fragments, reflecting the capacity of Sorel cement to yield strong mortars with almost any kind of filler. Hammer scale mortars were

J. Weber (✉)

Institute of Art and Technology/Conservation Sciences,
University of Applied Arts Vienna, Vienna, Austria
e-mail: johannes.weber@uni-ak.ac.at

K. Bayer

Faculty of Restoration, University of Pardubice,
Pardubice, Czech Republic
e-mail: karol.bayer@upce.cz

F. Pintér

Scientific Laboratory, Federal Office for the Protection of Monuments,
Vienna, Austria
e-mail: farkas.pinter@bda.at

prepared by adding files of metallic or oxidic iron to lime and sand. They were used for fillings or joints in masonry where they developed significant levels of hardness and strength. The observations by microscopy show that migration of rust products from the iron scales into the surrounding lime matrix is a key factor contribution to the high strength properties of such mortars. Nineteenth century Roman cements were produced from argillaceous limestone at temperatures as low as about 900°C. In their mineralogical composition they differ significantly from NHL and Portland cements. Consequently, Roman cements follow a specific path of hydration, generally yielding highly porous mortars of considerable strength. Whilst light microscopy is a good tool to identify Roman cement mortars by the abundant presence of binder-related particles, the SEM observations help understand their properties, as the calcium silicate hydrates formed in a Roman cement paste are of a coarse nature with card-house-like intergrowth. Early Portland cement mortars produced in the second half of the nineteenth century form the last group of materials addressed in this contribution. By the coarse size of their clinkers they can be easily identified in thin sections, however the lower amount of alite, as compared to modern Portland cements, is obvious. This observation is discussed in terms of lower temperatures of calcination as compared to modern successors.

1 Introduction

The nineteenth century was marked by a rapid industrial development and remarkable construction activities leading to the rapid growth of cities and accompanied by the production and use of new materials and technologies. New types of mineral binders and mortars were employed both for construction and for decorative purposes. These materials have survived in the immovable heritage from that century, and today they represent an important issue in our efforts of preservation. However, their presence evokes a lot of questions. Which are their relevant material properties? How should these materials be treated? Which are the most compatible materials available today for the repair and maintenance? To answer these and other questions, comprehensive research on the historic materials is required. Material characterisation, knowledge of the properties and of the way they were produced have to be assessed, in order to understand their specific and unique properties, their resistance against degradation and their corrosion mechanisms. Only answering these essential questions would enable appropriate restoration, search for compatible conservation materials, and further prevention.

Various methods are used to identify historic mineral materials nowadays. Microscopy, both optical and scanning electron microscopy, is one of the most frequent methods employed to study the composition, characteristics and microstructural properties of these mineral compounds.

This paper presents the use of microscopy for the study and characterisation of several less well-known mineral binders and mortars used in the nineteenth century.

2 Methods

Samples were studied on thin sections and polished sections, by means of polarising microscopy (PM) using transmitted and incident (reflected) light. The same sections were eventually observed by scanning electron microscopy (SEM), using back-scattered electron (BSE) facilities. Several instruments were employed both at high and at low vacuum, thus no apparatus specifications are given. In all cases energy-dispersive X-ray systems (EDX) was used for chemical analyses.

Microstructures of the matrix of a sample were studied preferentially on fresh fracture faces, using both secondary electron (SE) and BSE detectors.

3 Sorel Cement Mortars

Magnesia cement, also called Sorel cement after its inventor Stanislas Sorel, is, in fact, not a cement according to today's terminology, since it is not resistant to water on a long term. The binder was first produced in 1867. In the late nineteenth century and probably until after World War I, Sorel cement was used for a wide range of applications, such as artificial stones, floorings, millstones, repair mortars and even glues for broken stone parts. Today's use is mostly in the field of floor screeds for industrial purposes. More data related to this application are given by Schnell [1].

Sorel cement belongs to the class of acid-base binders, with caustic magnesia, MgO, produced from calcining magnesite, $MgCO_3$, to which magnesium chloride, $MgCl_2$, is added either as solution or in the solid state [1]. The resulting salt is reported to be a magnesium oxychloride hydrate of the formula $3MgO \cdot MgCl_2 \cdot 11H_2O$ [2], probably in intimate mixture with magnesium hydroxide, $Mg(OH)_2$, precipitated in a colloidal form [3]. The binder starts to set after approx. 40 min and should be hard after 9 h at relatively low shrinkage. The final strength of a floor screed is impressive, with tensile strengths from 5 to 20 MPa and compressive strengths from 20 to 100 MPa. The low resistance to the action of moisture has however limited the application of Sorel cements.

Mortars and grouts from Sorel cement may contain considerable amounts of almost any kind of filler, and the use of wooden fibres in that context, increasing the thermal insulation capacity of a floor, has led to the name of *xylolith* [1].

Sorel cement mortars have been identified by the authors in a number of cases ranging from repair mortars and stuccoes for marble sculptures, glues for archaeological stone objects, inlays for structured façade renders, and floors. Some of those findings were related to outdoor applications, where the material was strongly weathered but still in place.

Thin sections under the polarising microscope show a brownish matrix which cannot be identified further, apart from several characteristic phases of residual or secondary nature. These comprise residual carbonates, brucite ($Mg(OH)_2$), in aggregates of tiny crystals, and hydromagnesite ($Mg_5[(OH)_2/(CO_3)_4] \cdot 4H_2O$), as spherical grains of radial-fibrous appearance.

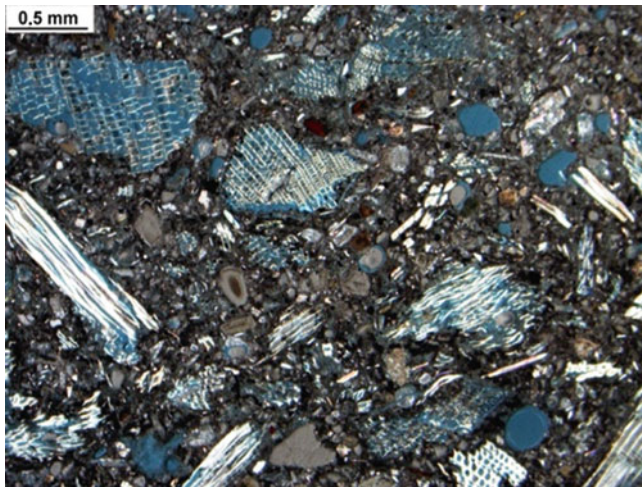


Fig. 1 1930 Sorel cement flooring mortar, filled with wood fibres; abundant air voids; *blue* resin, parallel Nicols

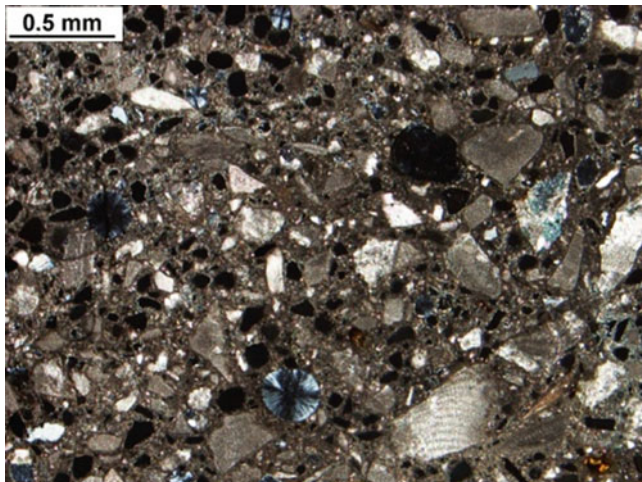


Fig. 2 Nineteenth century Sorel cement mortar; matrix with isotropic periclase, air voids filled with hydromagnesite; crossed Nicols

The mortar structure is largely dependant on the type and amount of filler adjusted to the mode of application. Figure 1 shows a *xylolith*-type flooring mortar with high internal porosity due to the abundant wood fibres and frequent air voids caused by the liquid consistency. Figure 2 illustrates a nineteenth century stone repair mortar applied to a marble sculpture outdoors. Its abundant filler consists of limestone fragments; the lower water:cement ratio is reflected by residual periclase, MgO, and the air voids are filled with secondary hydromagnesite.

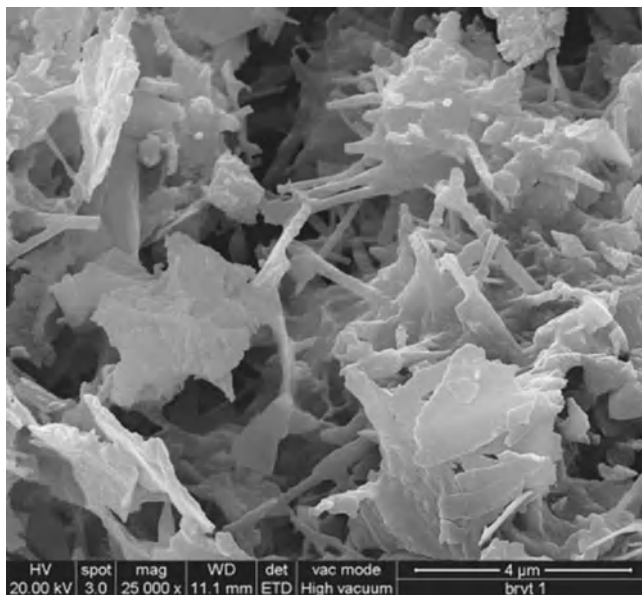


Fig. 3 Porous Sorel cement matrix; magnesium oxychloride hydrate crystals; SEM-SE

The microstructure of the Sorel cement matrix provides additional information to understand the high mechanical strength attributed to these mortars. The crystals of magnesium oxychloride appear in prismatic shapes from tiny acicular to coarser pillared, sometimes intergrown with platy crystals. The porosity within the matrix varies from fairly high, with pore sizes in the range of <5 µm (Fig. 3), to relatively low, with just a few air voids in an otherwise compact structure (Fig. 4).

4 Iron Hammer Scale Mortars

High strength lime mortars of reddish to dark red colour can be found as nineteenth century materials for stone and masonry repair as well as for repointing, for example brick walls. The presence of iron in metallic form or as oxides can be detected by visual inspection or sometimes even by the magnetic properties. A range of historic recipes for mortars or putties usually called Iron Filings or Borings Cements are based on the use of iron scales [4]. Their admixture to lime, however, is rarely documented in written sources [5], even if in the restoration community they are well known as hammer scale mortars. There is a lack of knowledge about their properties and the mechanisms leading to the strength they develop.

Hammer scale is a waste product from ironsmithing or smelting which consists mainly of tiny flakes of iron converted to iron oxides such as magnetite, Fe_3O_4 , or haematite, Fe_2O_3 . According to [5], the scale was ground and admixed to lime to prepare a mortar which was reported to harden considerably, particularly in moist

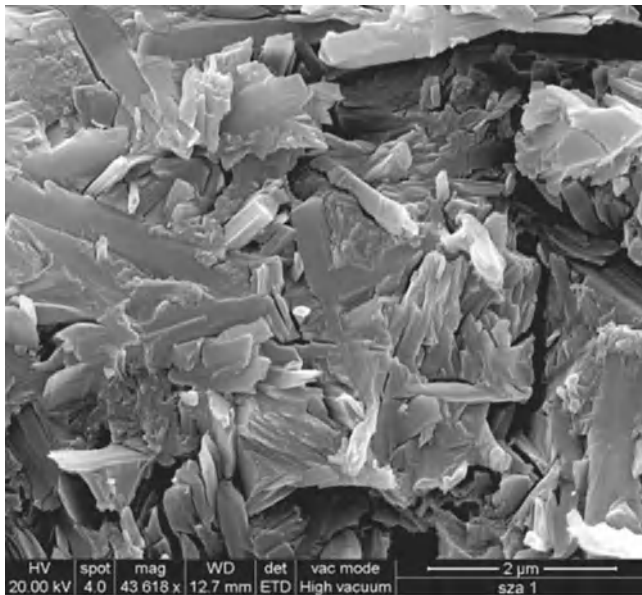


Fig. 4 Dense Sorel cement matrix, magnesium oxychloride hydrate crystals; SEM-SE

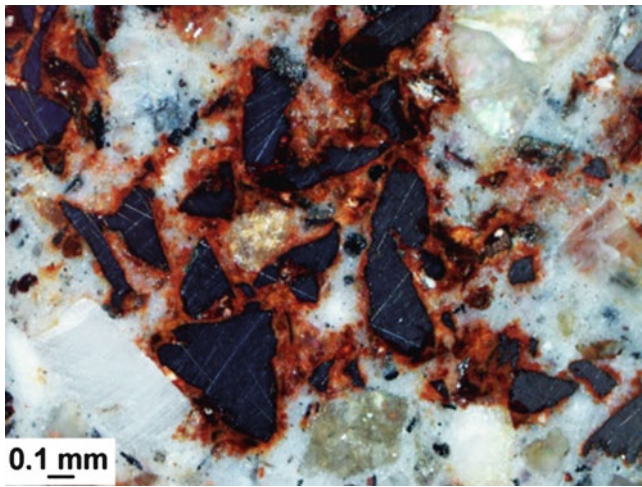


Fig. 5 Iron hammer scales with "rusty" haloes in a nineteenth century pointing mortar; incident light

places. The same article in [5] offers an explanation for the hardening of hammer scale mortars by addressing the well-known fact of rust subjected to volume expansion when forming from iron through the action of moisture and atmospheric acid.

The analysis of hammer scale mortars by means of microscopy and SEM supports the above hypothesis. Figure 5 from a nineteenth century pointing mortar

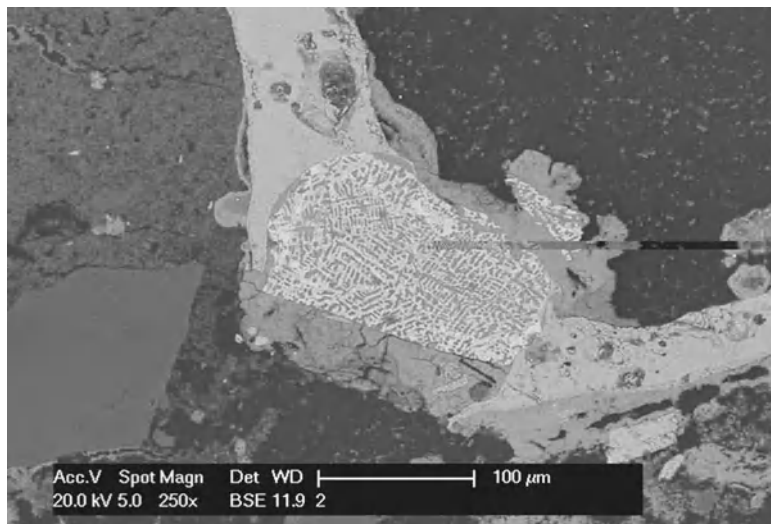


Fig. 6 Iron hammer scale with metal surrounded by iron oxide; SEM-BSE

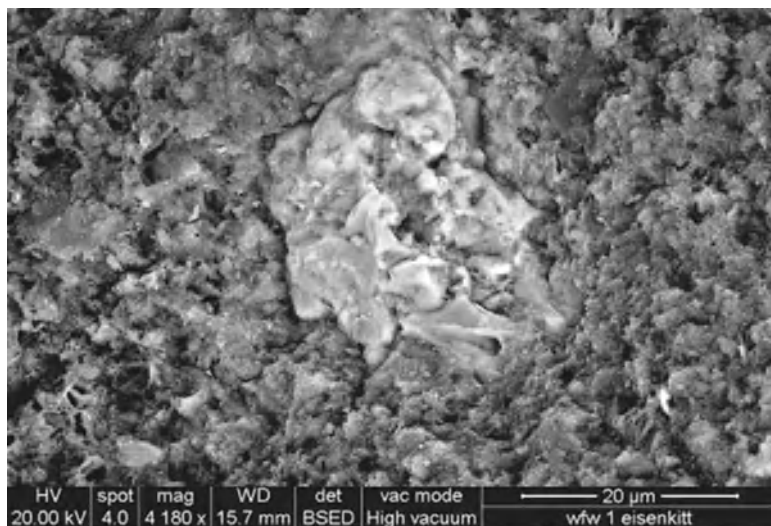


Fig. 7 Lime matrix surrounding hammer scale, densified by iron compounds; SEM-BSE

shows flakes of a dark grey iron phase, either haematite or magnetite. Both oxides have formed at high temperatures. Occasionally, metallic iron is still preserved in the core of such fragments (Fig. 6). Inert fillers such as e.g. quartz are also present.

Most of the iron oxide scales are surrounded by irregular areas of red colour, where iron hydroxides and hydrated oxides were precipitated in the pores of the surrounding calcite matrix (Fig. 7). No evidence for the formation of a calcium ferritic phase could be found, and small needle-shaped crystals growing within the matrix

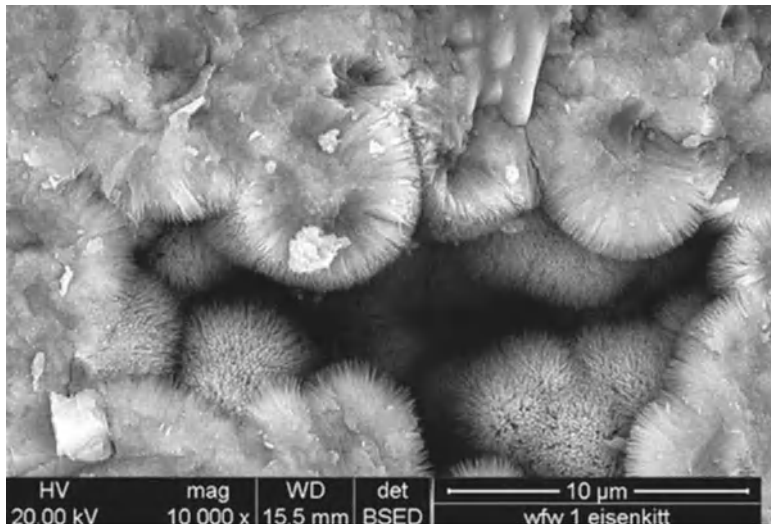


Fig. 8 Needles of iron compound (goethite?) around a binder pore; SEM-BSE

(Fig. 8) contain just iron and no calcium, and are hence likely to represent a mineral of the goethite type, $\text{FeO}(\text{OH}) \cdot \text{H}_2\text{O}$. Even if an exact mineralogical identification of the phases involved has not been performed in the present study, the principles of reaction are clear: the oxidation – rusting – of the scales is accompanied by the migration of colloidal iron hydroxides into the lime matrix where they precipitate and crystallise in the binder pores, causing significant compaction. Similar effects by an analogous process had been described for crystalline marble whose cracks were “healed” by iron hydroxides having migrated from rusting iron rebars [6].

5 Roman Cements

Several papers, e.g. [7–14], have recently dealt with Roman cements (RC) – natural cements produced at temperatures well below sintering, i.e. in the range of about 800–900°C. These hydraulic binders played an important role in building construction and façade decoration, especially in Western and Central Europe.

When analysing historic RC- mortars it should be kept in mind that they differ from Portland cement or NHL-mortars not so much in their chemical composition as in respect to mineral content and appearance of the residual clinker, along with the microstructure of the hydrated cement matrix. The nature of the raw feed, typically argillaceous limestone, and the low temperatures of calcination lead to the formation of characteristic cement compounds and binder microstructures. Their identification must be primarily based on microscopy and SEM. Weber and Gadermayr in [12] have presented the range of residual phases typically present in RC-mortars, as well as their visual appearance under the polarising microscope and

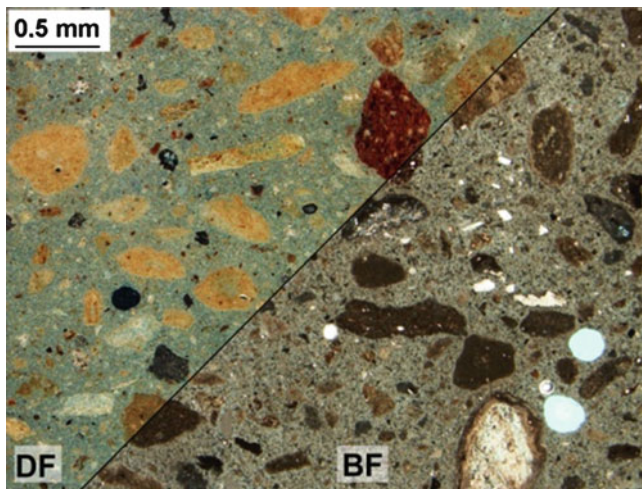


Fig. 9 Nineteenth century RC-mortar with characteristic binder nodules; the red grain is a brick fragment; transmitted light in bright field (BF) and dark field (DF)

SEM. Figure 9 shows a nineteenth century RC-mortar at low magnification, where the brownish colour and the abundant binder nodules form the primary features of distinction. The nodules mark areas of incomplete or non-ideal hydration due to non-reactive phases formed by either sub- or super-optimal calcination, both conditions being inherent to the process of production. The sub-optimal nodules are characterised by incomplete decomposition of carbonate and/or insufficient reactions with the silicates, while the super-optimal grains typically contain coarse belite, C_2S of the β -form, gehlenite, C_2A_2S , and sometimes even products of local melting (Fig. 10). Both nodule types seem to play an essential role as inert fillers.

The reactive portion of a RC “clinker” is known to consist of an amorphous phase and highly reactive α' -belite mixed with less reactive β -belite [8, 9]. Historic Roman cement mortars combine high strength with high porosity in the capillary range. This specific feature is even more pronounced for mortars with very low amounts of aggregate. SEM-studies of the matrix help understand the properties mentioned. As already stated, for example in [9] and [12], the calcium silicate hydrates formed in a Roman cement paste is of an unusually coarse nature with card-house-like intergrowth (Fig. 11). Abundant calcite crystals, formed in most of the historic mortars upon carbonation, yield additional strength.

6 Early Portland Cements

When dealing with early Portland cement (PC) mortars, it should be remembered that their binders differ from today’s OPC. The analyses of early PC (see e.g. [17]) suggest that, before the introduction and technical development of rotary kilns which replaced the shaft kilns in the 1890s, the usual peak kiln temperatures were

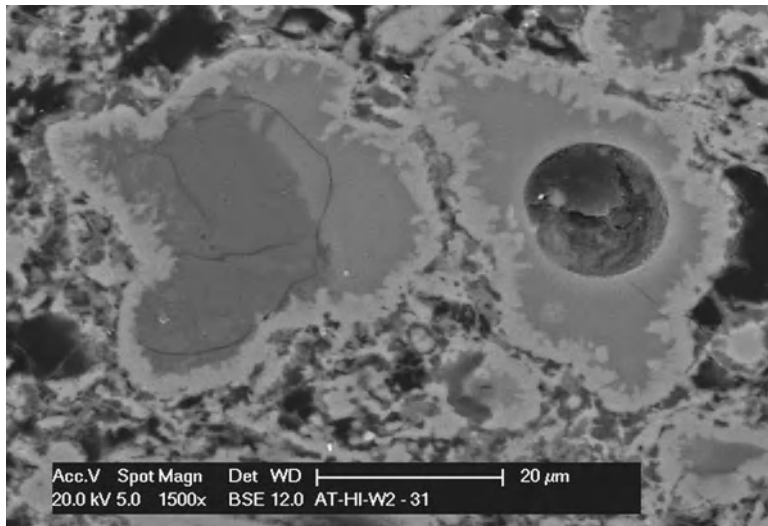


Fig. 10 RC binder residues with silica grains to which diffusion of Ca and alkalis has caused zoning with even local melting (*right*). Matrix with partially hydrated belite, C_2S ; SEM-BSE

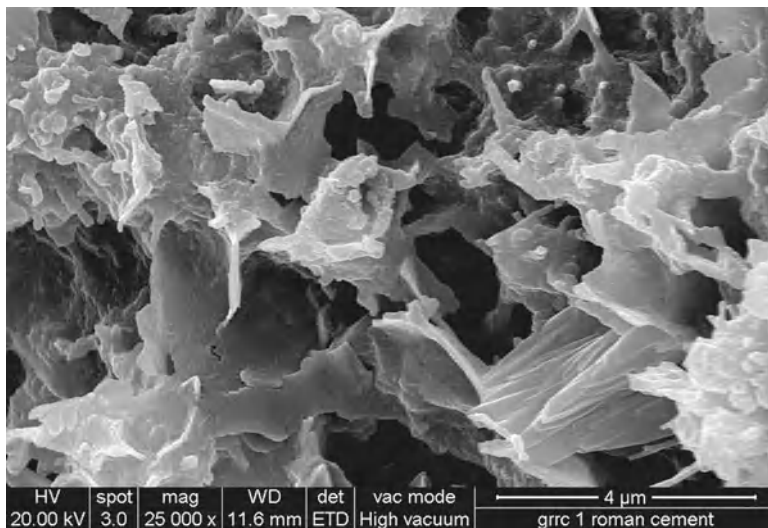


Fig. 11 Matrix of historic RC-mortar with coarse calcium silicate hydrate, C-S-H; SEM-SE

rather in the range of about 1,200–1,300°C – the temperature of sintering for most raw feeds – rather than 1,450°C as for OPC. The main clinker phase of modern PC (see e.g. [15]), alite, C_3S , is therefore rarely found in early cements, while the other phases of significance, such as belite, C_2S , aluminate, C_3A , and ferrite, C_4AF , would form before or as soon as the above point of sintering is reached. Two more important

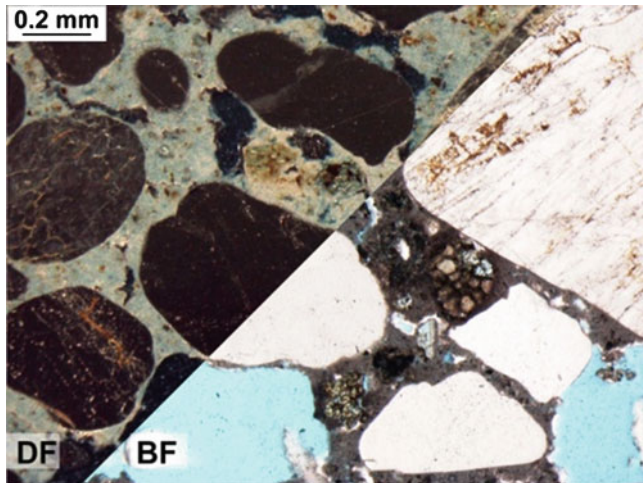


Fig. 12 Early PC-mortar with coarse clinker residues with interstitial ferrite; transmitted light in bright field (BF) and dark field (DF)

developments in the manufacturing process towards modern Portland cements were the addition of gypsum to control setting, and the use of ball mills to grind clinker and raw materials [16].

All historic handbooks make a clear distinction between Roman and Portland cements, pointing to the slower set, more rapid strength gain, and higher final strength of PC (e.g. [15]). From the point of view of the clinker composition, the difference between early PC and RC can be explained by several factors: first, belite present in an early PC was most probably of the β -type in contrary to the α' -polymorph typical for RC; second, not the amorphous phase present in RC, but rather C_3A was the phase responsible for the onset of stiffening and early strength in PC pastes; finally, the higher temperatures of PC calcination would have caused higher rates of reaction within the raw feed, leading to coarser Ca-silicate crystals as well as less solid solutions, and thus less unhydrated binder-related particles in the final product as compared to RC.

A distinctive feature in sections of early PC-mortars viewed under the microscope is therefore the low amount or even lack of brownish binder nodules. As soon as, with temperatures of calcination exceeding about 1,100°C, iron starts to be incorporated in the ferrite phase, the colour of the cement turns from yellowish-reddish to greenish-greyish. Figures 12 and 13 show examples.

From modern PC mortars the early ones can be distinguished by their much coarser clinker residues – in the range of 200 μm or more as compared to 20 μm – and by the lack of C_3S in them.

Viewed by SEM on fracture surfaces, the microstructure of the hydrated matrix of historic Portland cement can be described as more compact than in Roman cements (Fig. 14), with C-S-H forming a dense framework even if some areas remain more open-porous. The hydrates are, however, much coarser than in modern

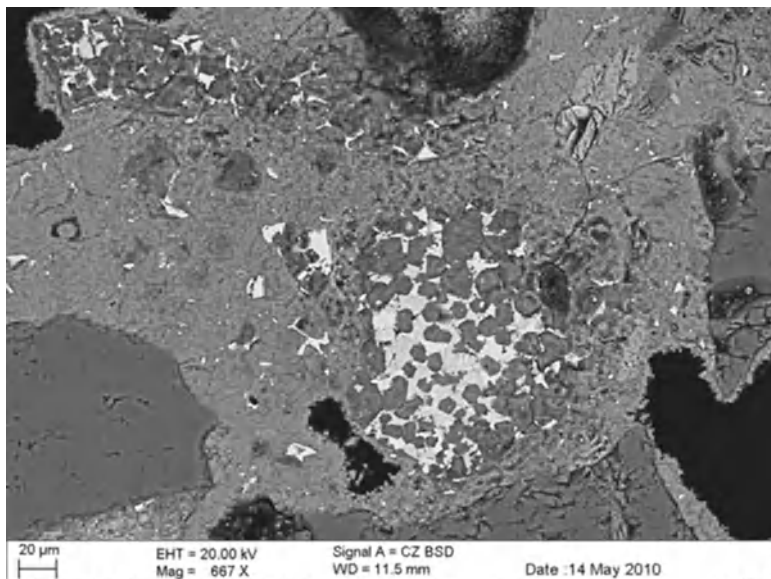


Fig. 13 Early PC binder with small hydrous silica (dark grey) and interstitial ferroaluminate (bright), surrounded by a dense matrix of carbonated C-S-H; SEM-BSE

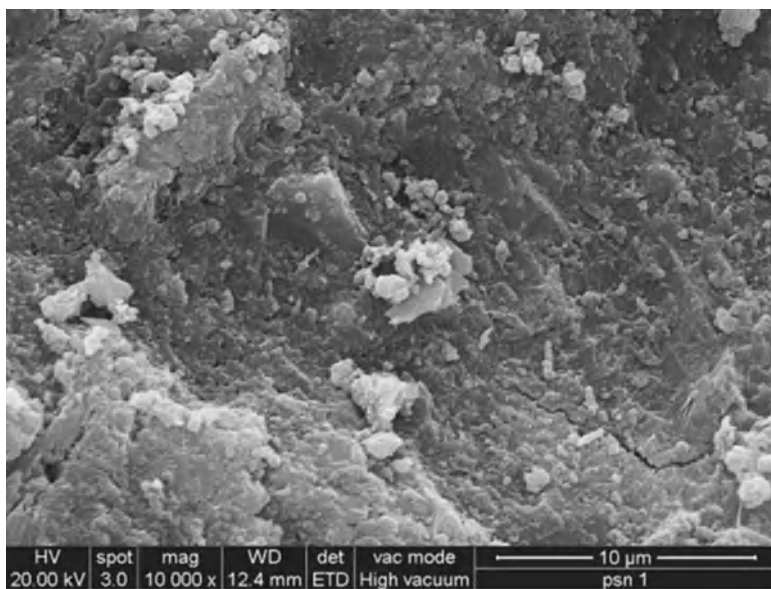


Fig. 14 Dense matrix of a nineteenth century PC-mortar; SEM-SE

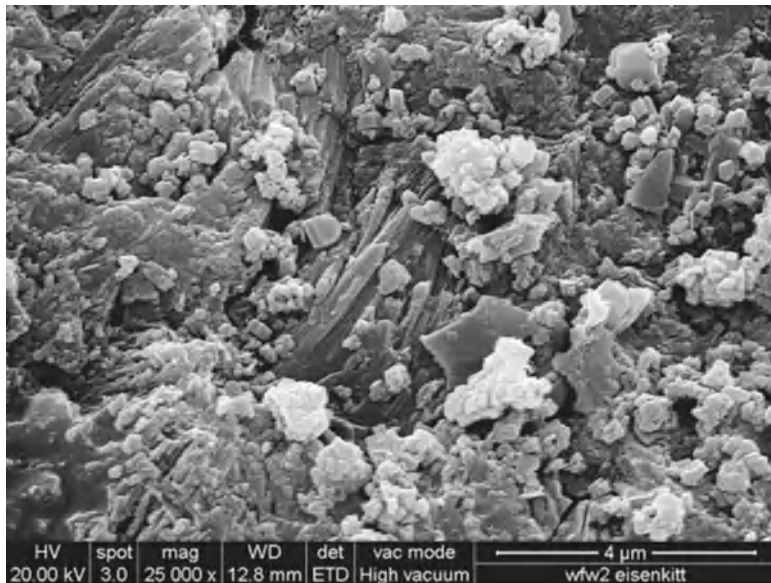


Fig. 15 Dense matrix of nineteenth century PC-mortar with coarse C-S-H and calcite; SEM-SE

cements (Fig. 15); when growing inside larger voids, they tend to develop acicular shapes. Rhombohedral crystals of calcite can be found quite frequently, since all of the samples investigated revealed extended or full carbonation. In such carbonated pastes residual clinker particles, where Ca-silicates have been largely or wholly converted into a highly porous C-S-H of low Ca/Si ratio, approaching hydrous silica [17] (Fig. 13), are found. Historic PC mortars and concretes, however, often reveal some large residual unhydrated clinker particles containing C_3S and C_2S , especially if the w/c ratio was low.

7 Summary and Conclusions

The mortar systems presented herewith have in common that only scarce in-depth knowledge of their exact composition and properties is available to the field of conservation. They belong to significantly different families of binder, hence a common approach to characterise the historic mortars in a way relevant to address some key questions of restoration was found in the microscopic analysis of their main constituents and their microstructures.

Sorel cements play a specific role in that their development was the result of modern industrial chemistry far beyond any traditional technique of production. Formed by magnesium oxychloride hydrates, these binders were meant for specific interior applications rather than for purposes of building construction, even if in practice they were also frequently employed for small works outdoors. It is thanks to their easy working and good mechanical properties that the occasional use of Sorel cements as

binders for floorings survived up until today, despite their sensitivity to the action of moisture due to the chemical nature of the binder minerals. The historic Sorel cement mortars presented in this study indicate their wide range of formulations. The presence of wooden aggregates is characteristic for floorings, while mineral aggregates are typical for stone repair mortars. The differences in the porosity of the binders, evidenced by a more or less dense packing of the prismatic hydrate crystals, as well as the presence of residual periclase, are believed to be due to different w/b ratios according to the consistency needed to obtain good workability for specific applications. More systematic studies are required to establish the effect of mortar formulations on those properties which are important for issues of compatibility.

Iron hammer scale mortars constitute one of the many attempts to improve the strength of lime mortars under most conditions. The admixture of small flakes of iron and iron oxides to lime mortars leads to the development of significant strength and durability. The key mechanism involved could be figured out by the study: colloidal iron compounds migrate into the lime matrix surrounding the scales, where they precipitate in the pores forming compact binder areas. Thus, this process constitutes a controlled method of volume expansion due to the formation of rust in the interior of the structure. The generally good state of preservation of historic hammer scale mortars and the simple way of preparing them would call for their reintroduction for purposes of restoration, however, based on a series of laboratory tests to establish the best source of scales and exact mixing protocols.

As Roman cement mortars were in much wider use than the above systems, their reintroduction in the conservation and restoration of our architectural heritage is of particular importance. The methods of microscopy applied in this study allow assessment of a number of key questions related to the composition of the cements, and help to understand the most significant mortar properties, i.e. high porosity at remarkable strength. The unusually coarse nature and the card-house-like microstructure of the calcium silicate hydrates forming in a Roman cement paste are the factors responsible for the mentioned properties which make this system interesting for many types of application in the fields of restoration and even new construction. Current studies, for example within the EU-project ROCARE, are being performed in order to improve the knowledge of Roman cements and to help them in entering the market of mineral binders.

Early Portland cement mortars have been included in this study to account for the increasing number of PC-based historic structures as objects of conservation. The process of Portland cement production followed a path of industrial development, from shaft to rotary kilns and from coarse grinding to fine milling of the clinker, to name just the most important factors which changed since these cements were first produced in the nineteenth century. The key conclusion, i.e. the scarce occurrence of alite and the reduced reactivity of early PC-clinker as compared to modern cements, is briefly discussed and shown through a few examples under the microscope. Despite the differences from modern PCs, the relatively compact microstructure formed by the binder hydrates of the historic mortars places them close to modern OPC-mortars. It can be expected for the near future that more research results will be produced by conservation scientists dealing with historic structures of Portland cement.

Acknowledgements Studies on historic cements were partially funded by the EU: ROCEM (FP5 – contract EVK4-CT-2002-00084) and ROCARE (FP7 – project No. 226898).

References

1. Schnell, W.: Magnesiaestrichs – Stand der Technik und Anwendungsgebiete. In: Seidler, P. (ed.) Handbuch Industrieboeden Planung, Ausfuehrung, Instandhaltung, Sanierung. expert-Verlag, Renningen-Malmsheim (1994)
2. Otto, W., Seeger, M., Flick, W., Hermann, G.: Magnesium-Verbindungen, anorganische. In: Ullmanns Enzyklopaedie der Technischen Chemie, vol. 16, 4th edn. Verlag Chemie, Weinheim/New York (1978)
3. Foerst, W. (ed.): Ullmanns Enzyklopaedie der Technischen Chemie, vol. 4, 3rd edn. Urban & Schwarzenberg, München/Berlin (1953)
4. Spon, E.: American Library Edition of Workshop Receipts, vol. 2. Spon & Chamberlain, New York (1903)
5. Flörke, H.G., In: Krünitz J.G. (eds.): Oekonomisch-technologische Encyklopädie, vol. 94, pp. 1773–1858. Pauli, Berlin (1803) (digital edition online by Seifert, H.U., Reinstein, H., University of Trier. www.kruenitz1.uni-trier.de)
6. Weber, J., Beseler, S.: Marble decay under the microscope: a phenomenological case study on Sterzing marble sculptures from the gardens of Schoenbrunn, Vienna. In: Proceedings of the 11th International Congress on Deterioration and Conservation of Stone, Torun, pp. 547–554, 15–20 Sept 2008
7. Weber, J., Gadermayr, N., Bayer, K., Hughes, D., Kozlowski, R., Stillhammerova, M., Ullrich, D., Vyskocilova, R.: Roman cement mortars in Europe’s architectural heritage of the 19th century. *J. ASTM Int.* **4**(8), Paper ID JAI100667 (2007). Available online at www.astm.org
8. Tišlová, R.: Hydration of natural cements. PhD thesis Institute of Catalysis and Surface Chemistry, Polish Academy of Sciences, Krakow (2008)
9. Tišlová, R., Kozlowska, A., Kozlowski, R., Hughes, D.C.: Porosity and specific surface area of Roman cement pastes. *Cem. Concr. Res.* **39**, 950–956 (2009)
10. Weber, J., Kozlowski, R., Hughes, D., Gadermayr, N., Mucha, D., Jaglin, D.: Microstructure and mineral composition of Roman cement clinkers produced at defined calcination conditions. *Mater. Charact.* **58**, 1217–1228 (2007)
11. Adamski, G., Bratasz, L., Mayr, N., Mucha, D., Kozlowski, R., Stillhammerova, M., Weber, J.: Roman cement – key historic material to cover exteriors of buildings. In: Repair Mortars for Historic Masonry, Proc pro067 RILEM TC 203-RHM, pp. 2–11, January, 2005 (2009)
12. Weber, J., Gadermayr, N.: Materialwissenschaftliche Charakterisierung von Romanzementen des 19. Jahrhunderts. In: Diekamp, A. (ed.) Naturwissenschaft & Denkmalpflege, pp. 157–165. Innsbruck University Press, Innsbruck (2007)
13. Cailleux, E., Marie-Victoire, E., Sommain, D., Brouard, E.: Microstructure and weathering mechanisms of natural cements used in the 19th century in the French Rhône-Alpes region. In: Repair Mortars for Historic Masonry, Proc pro067 RILEM TC 203-RHM, pp. 82–93, January, 2005 (2009)
14. Gosselin, C., Vergès-Belmin, V., Royer, A., Martinet, G.: Natural cement and monumental restoration. *Mater. Struct.* **42**, 749–763 (2009)
15. Stark, J., Wicht, B.: Zement und Kalk. Baupraxis Birkhäuser, Basel (2000)
16. Tarnawski, A.: Kalk, Gyps, Cementkalk und Portland-Cement in Oesterreich-Ungarn. Selbstverlag, Wien (1887)
17. Hewlett, P.C.: Lea’s Chemistry of Cement and Concrete. Elsevier, Burlington (2006)

Lime Mortar with Natural Hydraulic Components: Characterisation of Reaction Rims with FTIR Imaging in ATR-Mode

Anja Diekamp, Roland Stalder, Jürgen Konzett, and Peter W. Mirwald

Abstract Reaction rims of natural hydraulic relicts in historic mortars were investigated using a novel technology; a FTIR-spectrometer equipped with a focal plane array detector enabling in ATR-mode IR imaging with a spatial resolution of $1.0\text{ }\mu\text{m}$. IR spectra show two regions with main absorption bands at $1,280\text{--}1,580\text{ cm}^{-1}$ and $900\text{--}1,120\text{ cm}^{-1}$. Bands at $1,450$ and $1,396\text{ cm}^{-1}$ correspond to the asymmetric stretching of CO_3^{2-} , indicating two different forms of CaCO_3 ; the $900\text{--}1,120\text{ cm}^{-1}$ group of bands is assigned to Si-O stretching vibrations indicating C-S-H phases. The ratio of the integral absorbance of these two main regions of absorption bands shows an inhomogeneous spatial distribution in the reaction rim. From this variation we conclude that the reaction rims consist of areas containing both calcite and aragonite in addition to C-S-H phases and areas containing aragonite and C-S-H phases, the latter with a lower Ca/Si ratio and a higher degree of polymerization. SiO_2 gel is present in both areas.

1 Introduction

The major mineral phase of limestone that is used for the production of lime mortar is calcite [CaCO_3]. If silicate phases, in particular clay minerals and quartz, are present in addition, then hydraulic or latent hydraulic/pozzolanic components may form during firing of the limestone, provided that the temperatures are sufficiently high. In contact with water they will hydrate to form calcium silicate hydrate [C-S-H] phases. In case of the latent hydraulic/pozzolanic components activation by $\text{Ca}(\text{OH})_2$ is required.

A. Diekamp (✉) • R. Stalder • J. Konzett • P.W. Mirwald

Institute of Mineralogy and Petrography, University of Innsbruck, Innsbruck, Austria

e-mail: anja.diekamp@uibk.ac.at

The degree of hydraulicity of the binder has an important effect on the properties of the mortar. C–S–H phases are the main hydration products in Portland cement and are mainly responsible for its physical, chemical, and mechanical properties. Although the amount of hydraulic components may be very small in natural hydraulic lime binder (so-called sub-hydraulic binders), their effect on final strength and porosity cannot be excluded [1].

In Portland cement, C–S–H appear as extremely variable, poorly crystalline or amorphous phases [2]. The detection of the hydraulicity of a natural hydraulic lime binder, especially in sub-hydraulic binders, with common methods such as wet chemical analyses, differential thermal analysis (DTA) or X-ray diffraction (XRD) is difficult. Virtually nothing is known about the nature of the hydration products in sub-hydraulic lime binders.

The degree of hydraulicity of any binder can be quantified with wet chemical methods by determination of the amount of acid-soluble silica [3, 4]. This is considered a proxy for the hydraulic components. Nevertheless, there are limitations imposed on the determination of the exact amount of the acid-soluble silica-content and its interpretation. This is the case (1) when carbonate-bound aggregate is used [4], (2) when very fine grain size fractions of the aggregates (e.g. quartz sand) act as pozzolanic components [5] or (3) dolomitic lime is part of the binder [6].

Alternatively the degree of hydraulicity can be evaluated by differential thermal analysis (DTA), where the weight loss of the binder fraction in the temperature range 200–600°C (representing the loss of water chemically bound to C–S–H or calcium aluminate hydrates) is set in relation to the weight loss at temperatures >600°C (loss of CO₂ due to decarbonation) [7, 8]. However, to make use of this method, the presence of organic substances, clay minerals, hydrated salts, hydrous magnesium phases (e.g. in dolomitic lime mortars [9]) and relics of carbonate-bound aggregates whose decomposition would interfere with the release pattern of H₂O or CO₂ must be excluded.

In many cases XRD is not an option for the determination of hydraulicity due to the low modal amount and/or poorly crystalline character of the hydraulic phases.

Even more difficult is the characterisation of hydraulic products in their spatial context. SEM investigations on fracture surfaces only reveal the textures along an internal zone of weakness. In polished thin sections C–S–H phases are not detectable by microscopy. Nevertheless, diffuse cloudy structures [5, 10] and reaction rims around hydraulic particles [6, 11] are taken as indication for the presence of hydraulic phases. While elemental mapping of Si with electron microprobe (EMPA) is able to detect the spatial distribution of C–S–H phases in reaction rims, the detection of C–S–H phases in binder areas is very difficult or even impossible because of the additional presence of very fine grained siliceous aggregates [12].

An alternative method to observe the spatial distribution and the structural character of solids is high resolution Fourier transform infrared (FTIR) microspectroscopy mapping or raster scanning [13].

In this study we characterize the distribution and nature of C–S–H phases in reaction rims with FTIR imaging.

2 Analytical Methods

2.1 Microscopy and Electron Microprobe Analysis

More than 300 samples representing the periods from Romanesque to Baroque were collected from Western Austria (Tyrol) and Northern Italy (South Tyrol). Approximately 60% of the samples are dolomitic or magnesian lime mortars and 40% are lime mortars with natural hydraulic or sub-hydraulic binder.

For this study Gothic plasters (~1,500 AD) from the Finstermünz-Fortress in the upper Inn-Valley, Austria, were selected because of the high concentration of latent hydraulic components in binder and in lime lumps. In a first step their mineralogy and textures were studied using polished thin sections.

Identification and quantitative analysis of the mineral phases were then carried out by electron microprobe analysis (EMPA, JEOL JXA 8100) in both energy and wavelength dispersive analytical modes. Analytical conditions of 15 kV accelerating voltage and 10 or 5 nA beam current were used with spot sizes between 3 and 50 µm to minimize beam damage of the analyzed phases. To study element distributions wavelength dispersive X-ray mapping was performed. In addition to quantitative and mapping analysis, the backscattered electron (BSE) imaging mode was used to study textures and assemblages on a micrometer scale.

2.2 FTIR Spectroscopy

IR absorption spectra were recorded at room temperature using a Bruker Vertex 70 FTIR spectrometer combined with a Hyperion 3000 microscope equipped with a Ge-ATR-objective, a focal plane array (FPA) detector, a globar light source and a KBr beamsplitter. The FPA detector consists of 64×64 mercury-cadmium-telluride (MCT) detectors, enabling in combination with the ATR-objective FTIR imaging of an area measuring 32×32 µm with a spatial pixel resolution of 0.5 µm. Using a FPA-detector, the locus of the measured point is determined by the position of the detector itself and no optical aperture is necessary. Thus, the spatial resolution of the mid-IR-signal is only limited by the wavelength of the IR-radiation (i.e., approximately 1 µm at $2,000\text{ cm}^{-1}$ when an ATR-crystal with an index of refraction of five is applied). For each spectrum, 64 scans in the $850\text{--}3,950\text{ cm}^{-1}$ range were performed with a spectral resolution of 8 cm^{-1} . Thus, an area of 32×32 µm could be imaged within less than 1 min, and by sequential analysis larger areas could be mapped in a few minutes.

Data reduction was performed by defining the high and low wave number margin of an absorption band. In between these two points a linear background was subtracted and the area of the absorption band was calculated. The ratio of the integral absorbance of the most characteristic absorption bands (i.e., the absorption band between $1,280$ and $1,580\text{ cm}^{-1}$, characteristic to carbonate, and the absorption band

between 900 and 1,120 cm⁻¹, characteristic to C–S–H) was calculated, and the obtained value was colour-coded and graphically displayed as map.

3 Results and Discussion

3.1 Microscopy and Electron Microprobe Analyses

Optical microscopic images of the investigated mortars often show diffuse cloudy structures in the binder and in binder related particles (lime lumps sensu stricto [10]). In some instances transparent glass patches of up to several hundred µm in size (Fig. 1) surrounded by these cloudy structures may also be present.

In a Gothic plaster (~1,500 AD) from the Finstermünz-Fortress in the upper Inn-Valley, Austria, the glasses are rich in K and Si (average composition: 67.3 wt.% SiO₂; 15.1 wt.% K₂O; 7.4 wt.% CaO; 6.7 wt.% Na₂O; 1.1 wt.% MgO and 0.9 wt.% Al₂O₃) and frequently contain idiomorphic needles of wollastonite [CaSiO₃]. They formed during partial melting of silicates in the firing process of impure limestone. The most likely source of K is mica (biotite or muscovite), which is a very common constituent of siliceous carbonates (marls).

Even though individual phases within the cloudy rims cannot be identified due to their extremely small grain size, the inhomogeneous grey scale distribution of the BSE images (Fig. 2) clearly indicates a mixture of phases. The BSE images also show that the reaction rims are significantly less porous than the matrix. Elemental mapping reveals these cloudy rims to be enriched in Si and Mg compared to the matrix (Fig. 2). Large area EMPA with a rastered beam of the Ca- and Si-rich reaction rims yield a wide range in Ca/Si-ratios and very low absolute magnesium concentration of ~1 wt.%. [12]

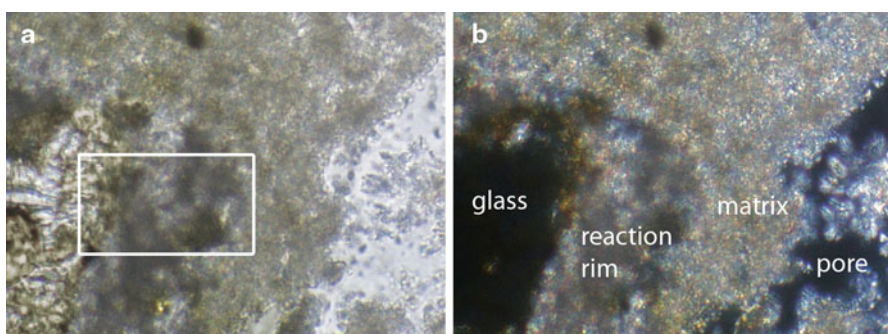


Fig. 1 Thin section photomicrograph with (a) plane polaris, (b) crossed polars of an area in a lime lump (Gothic plaster from Finstermünz-Fortress/Austria). A glassy, hydraulic relict (located at the left image edge) is in contact with a cloudy reaction rim and surrounded by a fine grained matrix. Parts of a pore structure are visible on the right hand side (Field of view 0.18 mm, the frame in (a) marks the region for the FTIR-imaging)

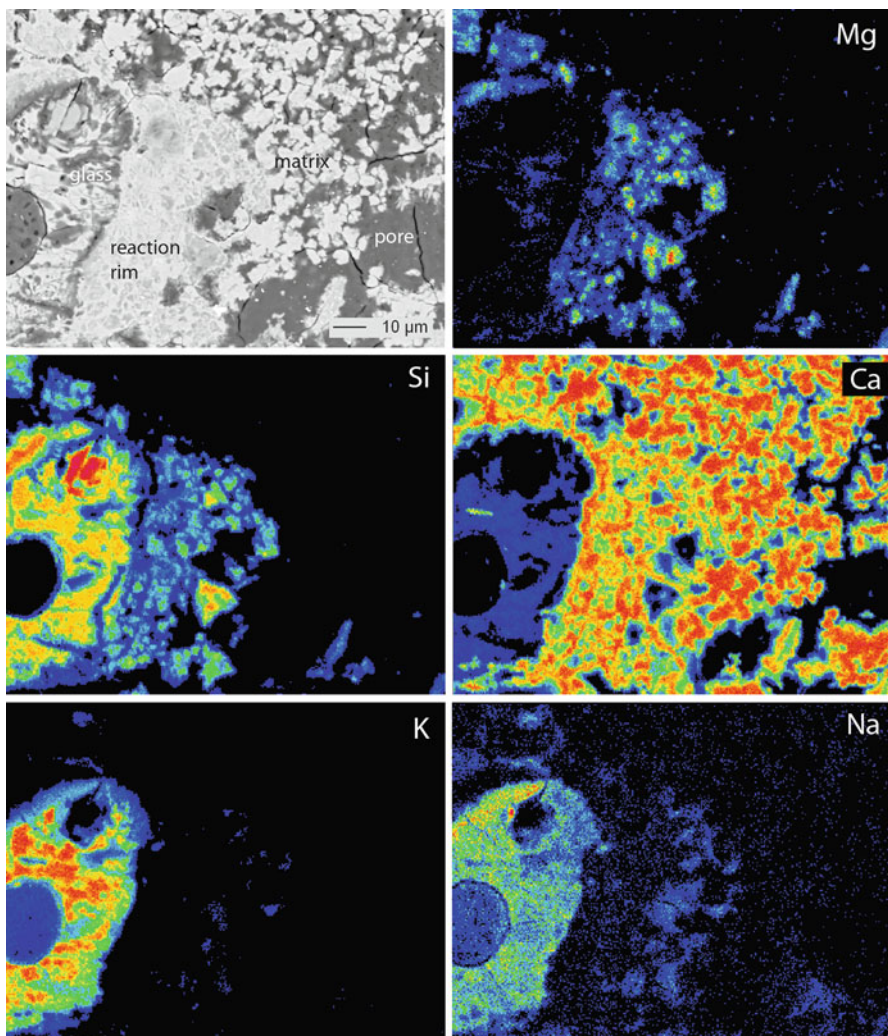


Fig. 2 EMPA-BSE image and elemental mapping of magnesium, silicon, calcium, potassium and sodium of an area in a lime lump (compare Fig. 1, Gothic plaster from Finstermünz-Fortress, Austria). Elemental concentration is proportional to colour temperature

3.2 FTIR Spectroscopy

For FTIR analyses two groups of bands were selected: group I in the range of 1,280–1,580 cm⁻¹ is assigned to carbonate phases, group II in the range of 900–1,120 cm⁻¹ is assigned to C–S–H phases. To detect the relative proportion of carbonates and C–S–H phases in the cloudy reaction rim (marked area in Fig. 1), the modal amount of these phases is then deduced from the area ratios of these groups of bands and are graphically displayed as map in Fig. 3. The map shows an inhomogeneous

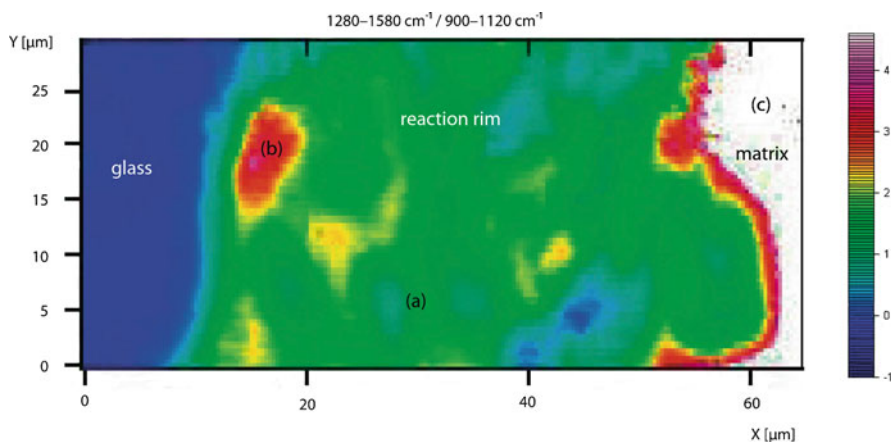


Fig. 3 FTIR-ATR image of the reaction rim (marked area in Fig. 1a): colours (scale bar on the right hand side) represent the ratio of the integral absorbances of the absorption bands in the region 1,280–1,580 cm⁻¹ to the absorption bands in the region 900–1,120 cm⁻¹

spatial distribution of the areas intensity ratios, whereby cold colours represent high II/I-ratios and warm colours (including pink and white) represent high I/II-ratios, respectively. Representative ATR spectra from the reaction rim and from the surrounding matrix were extracted and are shown in Fig. 4a–c.

All ATR spectra show bands at 1,450 cm⁻¹ and/or 1,396 cm⁻¹. These bands can be attributed to the asymmetric stretching (v^3) of CO₃²⁻ in carbonates: the band at 1,396 cm⁻¹ to calcite; the bands at 1,450 and 1,080 cm⁻¹ to aragonite. This assignment is consistent with results from X-ray diffraction, where both polymorphs of CaCO₃ were detected in corresponding powder probes. The main bands at 1,450 cm⁻¹ and 1,396 cm⁻¹ are shifted towards lower wave numbers compared to literature data obtained by KBr-technique [14, 15], but compare well to ATR spectra from the RRUFF database [16].

Both spectra Fig. 4a, b in the cloudy reaction rim show bands in the region of 950–1,100 cm⁻¹ and a shoulder at ~1,200 cm⁻¹. These bands are related to the presence of silica compounds. The bands at 950–1,100 cm⁻¹ correspond to the asymmetric and symmetric stretching vibrations of Si–O bonds. C–S–H phases contain a characteristic set of bands centered at ~970 cm⁻¹ which are assigned to Si–O stretching vibrations of the Q² tetrahedra [15]. Yu et al. [15] show that this group of bands is shifted systematically towards higher wave numbers with decreasing Ca/Si ratios. They further show that in a mixture of C–S–H phases and SiO₂ gel the Si–O band broadens, and the main position is shifted towards higher wave numbers. The shift of the Si–O band reflects a higher Si content and a higher degree of polymerization due to the presence of Q³ and Q⁴ sites in the SiO₂ gel. The occurrence of Q³ sites is also specifically related to a broad shoulder at 1,200 cm⁻¹ [15]. Based on BSE imaging and elemental mapping [12], which reveal that the rim consists of newly formed Ca- and Si-phases, the 1,041 cm⁻¹ band in spectrum (a) and the bands at 964 and 1,026 cm⁻¹, respectively, in spectrum (b) are attributed to C–S–H phases. This interpretation is in agreement with Yu et al. (*op. cit.*).

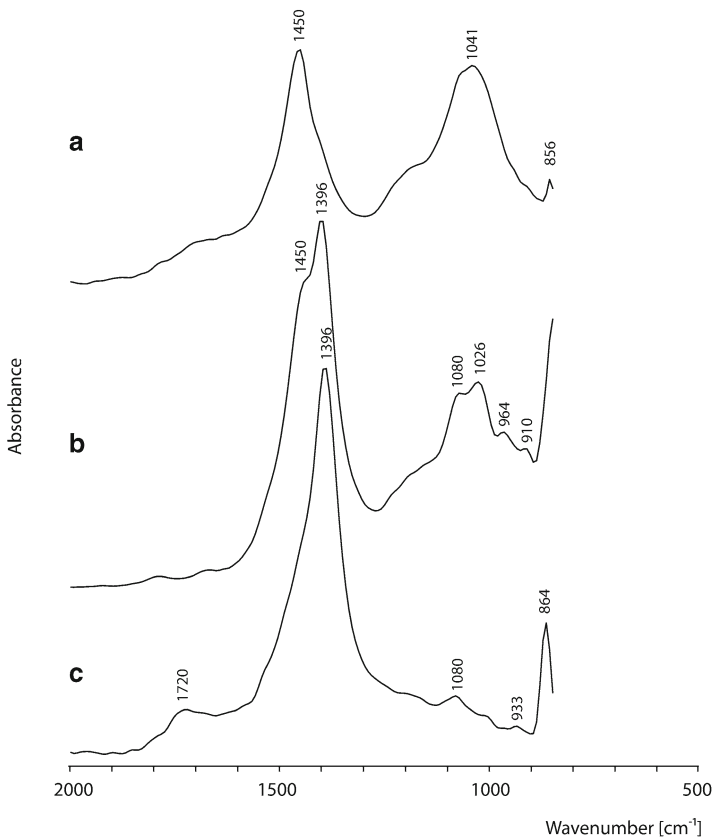


Fig. 4 ATR spectra obtained from areas (a), (b) and (c) in Fig. 3: (a) area consisting of aragonite, C–S–H phases and SiO₂ gel; (b) area consisting of calcite, aragonite, C–S–H phases and SiO₂ gel; (c) area next to the reaction rim (within the white area in Fig. 3), dominated by calcite

In spectrum Fig. 4a the main band in the 950–1,100 cm⁻¹ region is centered at 1,041 cm⁻¹ and is very broad. This indicates a high Si content of the C–S–H phases and, in addition, the occurrence of polymerized SiO₂ gel. The presence of SiO₂ gel is also consistent with the broad shoulder at 1,200 cm⁻¹.

In spectrum Fig. 4b bands at 910, 964, and 1,026 cm⁻¹ are assigned to Si–O stretching vibrations at Q² sites of the C–S–H phase. The band at 1,080 cm⁻¹ is attributed to aragonite. Again, the shoulder at 1,200 cm⁻¹ is assigned to Si–O stretching vibrations in Q³ sites of SiO₂ gel. The group of bands at 964–1,026 cm⁻¹ is shifted towards lower wave numbers, which might be due to a lower Si content of the C–S–H phases and a lower degree of polymerisation. In both areas (a) and (b) of the reaction rim, the presence of SiO₂ gel and aragonite indicate carbonation of C–S–H phases as observed in carbonated cement pastes [17].

Spectrum Fig. 4c obtained from matrix (Fig. 1b) is largely dominated by calcite.

4 Summary and Conclusion

K- and Si-rich glasses are present in the binder of ~500 year old mortars and plasters. The glasses formed during partial melting of silicates in the firing process of impure limestone. The reaction rims around the glass patches indicate that they act as latent hydraulic components, forming C–S–H phases.

With FTIR-ATR imaging the spatial distribution of different phases in a reaction rim was determined on a micrometer scale.

Our investigation shows that the reaction rims consist of CaCO₃, C–S–H phases and SiO₂ gel in variable proportions. In areas with low carbonate to C–S–H phase ratios, carbonate is mainly present as metastable aragonite. The associated C–S–H phases show a comparatively low Ca/Si ratio and a high degree of polymerization. In areas with high carbonate-to-C–S–H phase ratios, both, aragonite and calcite are present. The C–S–H phases show a comparatively higher Ca/Si ratio combined with a lower degree of polymerization. The presence of SiO₂ gel and aragonite indicate carbonation of C–S–H phases. The matrix outside of the cloudy reaction rim consists mainly of calcite.

FTIR imaging measured in ATR-mode is a promising new method to gain information on the hydraulicity of natural hydraulic mortars in its spatial distribution on a micrometer scale and to characterize the hydration and carbonation products as well.

Acknowledgement This study was carried out within the framework an EU-Interreg project entitled “Interdisciplinary investigations of selected monuments as key examples for optimized planning of conservation measures” and a national project entitled “Historic building materials in Tyrol”. The funding for these projects, provided by the EU, the Austrian Federal Ministry for Education, Arts and Culture, the state of Tyrol and the Autonomous Province of Bolzano – South Tyrol is gratefully acknowledged.

References

1. Lindqvist, J.E., Johansson, S.: Sub-hydraulic binders in historic mortars. In: Groot, C. (ed.) Repairs Mortars for Historic Masonry. RILEM Proceedings pro067, pp. 224–230, RILEM Publications S.A.R.L. France (2009)
2. Richardson, I.G.: The calcium silicate hydrates. Cement Concr. Res. **38**, 137–158 (2008)
3. Rilem TC 203-RHM: Repair mortars for historic masonry. Testing of hardened mortars, a process of questioning and interpreting. Mater. Struct. **42**, 853–865 (2009)
4. Middendorf, B., Hughes, J.J., Callebaut, K., Baronio, G., Papayanni, I.: Investigative methods for the characterisation of historic mortars – Part 2: Chemical characterisation. Mater. Struct. **38**, 771–780 (2005)
5. Middendorf, B., Kraus, K., Ott, Chr.: Influence of the fines of natural sands as pozzolanic components on the interpretation of the acid soluble silica content of historic lime mortars. In: Jaffe, R.C. (ed.) Proceedings of the International Building Lime Symposium, Orlando, FL, 9–11 March 2005, p. 11. http://www.nationallime.org/IBLS05Papers/Middendorf_Influence.pdf (2005). Accessed 1 June 2010
6. Blaeuer, C., Kueng, A.: Examples of microscopic analysis of historic mortars by means of polarising light microscopy of dispersions and thin sections. Mater. Charact. **58**, 1199–1207 (2007)

7. Maravelaki-Kalaitzaki, P., Bakolas, A., Moropoulou, A.: Physico-chemical study of Cretan ancient mortars. *Cement Concr. Res.* **33**(5), 651–661 (2003)
8. Bakolas, A., Biscontin, G., Contardi, V., Franceschi, E., Moropoulou, A., Palazzi, D., Zendri, E.: Thermoanalytical research on traditional mortars in Venice. *Thermochim. Acta* **269**(270), 817–828 (1995)
9. Diekamp, A., Konzett, J., Wertl, W., Tessadri, R., Mirwald, P.W.: Dolomitic lime mortar – a commonly used building material for medieval buildings in Western Austria and Northern Italy. In: Lukaszewicz, J.W., Niemcewicz, P. (eds.) *Proceedings of the 11th International Congress on Deterioration and Conservation of Stone*, vol. I, pp. 597–604, 15–20 September 2008, Torun, Poland (2008)
10. Elsen, J.: Microscopy of historic mortars – a review. *Cement Concr. Res.* **36**, 1416–1424 (2006)
11. Elsen, J., Brutsaert, A., Deckers, M., Brulet, R.: Microscopical study of ancient mortars from Tournai (Belgium). *Mater. Charact.* **53**, 289–294 (2004)
12. Diekamp, A., Konzett, J., Bidner, T., Mirwald, P.W.: Kalkmörtel und Kalkputz in Tirol. In: Bläuer-Böhm, C., Zehnder, K. (eds.) *Eurolime Newsletter No. 4; Proceedings of the 4th International Eurolime Meeting*, 4–6 August 2005, Freilichtmuseum Ballenberg, Schweiz (2005)
13. Joseph, E., Prati, S., Sciuotto, G., Ioele, M., Santopadre, P., Mazzeo, R.: Performance evaluation of mapping and linear imaging FTIR microspectroscopy for the characterisation of paint cross sections. *Anal. Bioanal. Chem.* **396**, 899–910 (2010)
14. Andersen, F.A., Brecevic, L.: Infrared spectra of amorphous and crystalline calcium carbonate. *Acta. Chem. Scand.* **45**, 1018–1024 (1991)
15. Yu, P., Kirkpatrick, R.J., Poe, B., McMillan, P.F., Cong, X.: Structure of Calcium Silicate Hydrate (C–S–H): near-, mid-, and far-infrared spectroscopy. *J. Am. Ceram. Soc.* **82**, 742–748 (1999)
16. Downs, R.T.: The RRUFF Project: an integrated study of the chemistry, crystallography, Raman and infrared spectroscopy of minerals. Program and Abstracts of the 19th General Meeting of the International Mineralogical Association in Kobe, Japan, pp. 3–13. <http://rruff.info> (2006). Accessed 1 June 2010
17. Black, L., Breen, C., Yarwood, J., Garbev, K., Stemmermann, P., Gasharova, B.: Structural features of C–S–H(I) and its carbonation in air – a Raman spectroscopic study. Part II: carbonated phases. *J. Am. Ceram. Soc.* **90**, 908–917 (2007)

Characterisation of Dolomitic Lime Mortars from the Benedictine Monastery in Riesa, Saxony (Germany)

Heiner Siedel, Steffen Michalski, and Bernd Ullrich

Abstract The binders of joint mortars, renders and plasters used during several construction phases in the history of the Benedictine monastery in Riesa have been identified as dolomitic lime. Magnesite and/or hydromagnesite could be determined as the magnesium bearing carbonate phases beside calcite in the binder. Most of the mortars contain carbonate lumps, partially with altered silicate mineral inclusions, that represent remnants of the original structure of the late Palaeozoic dolomites which were used as the local raw material for lime production over the centuries. Low contents of aluminous silicates in the limestone might have contributed to the formation of hydraulic components. Hydrotalcite has been determined by XRD in some of the samples investigated.

1 Introduction

The Benedictine monastery in Riesa, a city situated about 40 km north-west of Dresden at the river Elbe, was founded in the year 1119 and is one of the oldest buildings of its kind in Saxony. Several times in history it was destroyed and reconstructed. Most of the buildings were converted after secularization in the sixteenth century and the last restoration intervention dated from 1909. Large parts of the façade were in a bad condition after another 80 years of exposure. The eastern wing, the dormitory of the former monastery complex, was thoroughly restored from the late 1990s onward. In the framework of restoration measures, investigations into the building's history made evident several construction periods dating from the Romanesque (thirteenth century) until the early twentieth century.

H. Siedel (✉) • S. Michalski • B. Ullrich

Institute of Geotechnical Engineering, Dresden University of Technology, Dresden, Germany
e-mail: Heiner.Siedel@tu-dresden.de

Mortar samples from historical renders, plasters and joint mortars, assigned to different construction periods by the restorer, were taken at the eastern façade for mineralogical characterisation (Table 1, Figs. 1 and 2). The aim of this study was to derive information about the types of mortar used in different construction periods.

Due to intensive physical and chemical weathering, large parts of the façade showed only remnants of historical renders at the time of sampling (Fig. 1). Salt efflorescence was frequently detected on the surface of renders and building stones. Samples of the efflorescing salts were taken at several points for X-ray diffraction analysis to get information about chemical weathering.

2 Analytical Methods

All mortar samples were first examined under the stereo microscope. Part of every sample was used for a polished thin section, another for phase analysis of the binder using X-ray diffraction (XRD) and thermal analysis with combined Differential Thermal Analysis (DTA) and Thermogravimetry (TG). The pieces used for XRD and DTA/TG were carefully ground in an agate mortar; coarse aggregate grains were separated by sieving to get a concentrate enriched in binder. The binder concentrate was ground <63 µm for XRD and thermal analysis. XRD was performed with Siemens D5000 equipment ($\text{Co}_{\text{K}\alpha}$, 40 kV, 30 mA, 5–80°, step 0.02°, step time 2 s), DTA/TG was performed with a Netzsch STA 409 PG (in static air, temperature range 25–1,000°C, heating rate 10 K/min). Some of the thin sections were coated with carbon and additionally investigated under a Zeiss EVO 50 scanning electron microscope (SEM) coupled with a ROENTEC detector XFlash 3001 for standardless elemental analysis by energy-dispersive spectroscopy (EDS). Results of chemical analyses were calculated as oxides. Due to artificial side effects resulting from the coating and impregnation of materials with organic resin during preparation, CO_2 contents were not determined. The presence of carbonate, however, is indicated by an excess of oxygen in the analyses concerned.

3 Results

3.1 Aggregate

Analysis of aggregates under the petrographic microscope allowed a survey of the aggregate used within the mortars during various construction periods. Grains with diameters below 2 mm (95–99%) dominate the aggregate of nearly all mortar samples investigated. Remarkable amounts of bigger grains (up to 10%) were only found in samples RIE-FM 3, RIE-PU 10, and RIE-PU 11. Most of the grains are sub-rounded to well-rounded, indicating an origin from natural sands. Quartz and

Table 1 Samples from the east façade of the eastern wing of the Benedictine monastery in Riesa

Sample number	Position	Construction period	Peculiarities
RIE-FM 1 (E)	Joint mortar from deep inside the base (gap in the stonework)	Early Gothic	Brownish mortar, no lumps visible in the binder.
RIE-FM 2 (E)	Joint mortar from the window jamb of the third window right of the main entrance, top floor	Romanesque	Light mortar, rich in binder; no lumps visible in the binder; crushed ceramics in the aggregate.
RIE-FM 3 (E)	Joint mortar, above first window to the north, top floor	Romanesque	Reddish mortar, rich in binder; occasionally white lumps.
RIE-PU 1 (E)	Render from the northern part, between ground floor and top floor	Romanesque	Beige mortar, rich in binder; no lumps visible in the binder.
RIE-PU 2 (E)	Render from the northern part, between ground floor and top floor	Romanesque	Light pink mortar, rich in binder; occasionally white lumps.
RIE-PU 3 (E)	Render from the ground floor, northern part	Early Gothic	Beige mortar, rich in binder, no lumps visible in the binder.
RIE-PU 4 (E)	Render from the top floor, right of the main entrance	Renaissance/Baroque (?)	Beige mortar with quartz aggregate up to 5 mm, occasionally white lumps in the binder.
RIE-PU 5 (E)	Render from the top floor, right of the main entrance	Late nineteenth century	Beige-grey mortar with quartz aggregate up to 5 mm; occasionally light beige lumps in the binder.
RIE-PU 6 (E)	Render on bricked up Romanesque portal	1909	Light mortar, no lumps visible in the binder.
RIE-PU 7 (E)	Render from the top floor, right of the sixth window from north	Gothic	Light brownish mortar, rich in binder, without visible lumps.
RIE-PU 8 (I)	Plaster on window jamb, top floor, third window from south	Romanesque	Light mortar, rich in binder; occasionally white lumps.
RIE-PU 9 (I)	Plaster on window jamb, top floor, second window from south	Romanesque	Light beige mortar, rich in binder; no lumps visible in the binder.
RIE-PU 10 (I)	Plaster layer right below RIE-PU 9	Romanesque	Brownish mortar, rich in binder; occasionally lumps in the binder.
RIE-PU 11 (I)	Transition layer between joint mortar and plaster, right below RIE-PU 10	Romanesque	Light mortar, rich in binder, with quartz and rock aggregate up to 10 mm; occasionally lumps.
RIE-PU 12 (I)	Plaster from the top floor, right of the fourth window from north	Renaissance/Baroque (?)	Light mortar, rich in binder; no lumps visible in the binder.

E from the exterior, I from the interior



Fig. 1 State of the façade with remnants of historic renders at the time of sampling

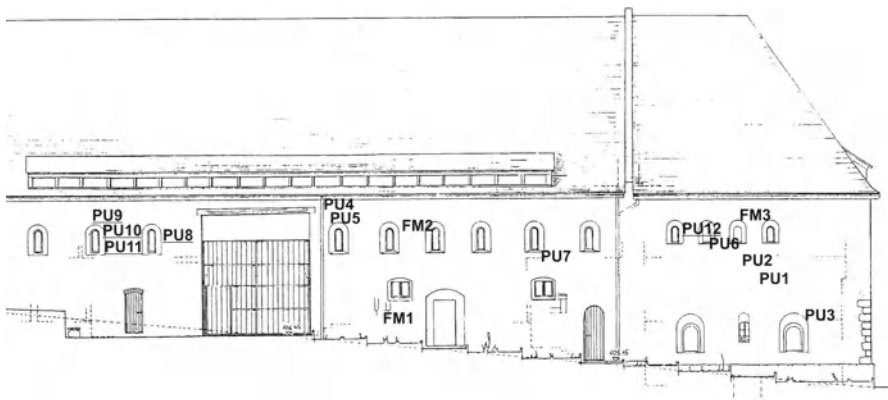


Fig. 2 East façade of the eastern wing of the former Riesa Monastery with sample positions (*underlined*: plaster samples from the interior)

fragments of polycrystalline quartz, porphyry, and occasionally volcanic tuff are dominant. Samples RIE-FM 2 and RIE-PU 8 additionally contain crushed ceramics. Slag particles were found in samples RIE-PU 5 and RIE-PU 6. The pink and reddish colours of some mortars are a result of the high amounts of red quartz in the aggregate (RIE-FM 3, RIE-PU 2).

3.2 Binder

The binders of the mortars were characterised by combined XRD and DTA/TG analysis (Table 2). XRD can identify crystalline phases but not amorphous compounds. Randomly ordered phases with low crystallinity and/or very small crystalline particles ($<0.1\text{ }\mu\text{m}$) cannot be detected very accurately, especially when their content in the sample is small [1]; as a result some phases could be found by DTA, but not by XRD analysis.

As can be seen from Table 2, all mortars contain both calcium carbonate phases and magnesium carbonate phases. Differentiation between the hydrous magnesium carbonates nesquehonite ($\text{MgCO}_3\cdot3\text{H}_2\text{O}$) and hydromagnesite ($(\text{Mg}_5[(\text{OH})_2/(\text{CO}_3)_4]\cdot4\text{H}_2\text{O}$) can be problematic in thermal analysis, especially in the presence of gypsum [1].

Therefore, thermal effects between 200°C and 550°C were generally assigned to “hydrous magnesium carbonate”. Traces of crystalline hydromagnesite were detected in two samples by XRD (RIE-PU 7 and 12), but no nesquehonite was found. Patterns of a hydrotalcite-like phase ($\text{Mg}_6\text{Al}_2[(\text{OH})_{16}/\text{CO}_3]\cdot4\text{H}_2\text{O}$) (?) could be clearly detected in the XRD diagrams of some of the samples. Thermal effects of hydrotalcite are superimposed by those of other compounds. Remarkable contents of gypsum were found in most of those mortars which have been exposed to rain on exterior walls and on the interior side of window jambs. The only salts detected in efflorescence were magnesium sulphates (epsomite $\text{MgSO}_4\cdot7\text{H}_2\text{O}$ and hexahydrite $\text{MgSO}_4\cdot6\text{H}_2\text{O}$) beside some gypsum. This pattern is well-known from many other case studies on historic buildings with dolomitic lime mortars in Saxony [e.g. 2–4], and must be attributed to intensive chemical weathering due to environmental influences.

Microscopic identification of single phases within the binder is impossible due to the very fine grain size. In most of the samples, however, the binder matrix contains carbonate lumps in the dimension of some $100\text{ }\mu\text{m}$ to some mm which appear darker and denser than the matrix with a fine-grained structure. Sometimes they show internal structures with darker patches or small inclusions. Aggregate is not present within these lumps. Some of the lumps are criss-crossed by cracks which do not continue in the matrix.

A typical example is shown in the photomicrographs in Fig. 3. As can be seen from the element mapping images and from point analyses with EDS, the lumps contain calcium and magnesium carbonates and very small inclusions ($<100\text{ }\mu\text{m}$) rich in silicon and aluminium. Figure 3d, f clearly demonstrate the spatial distribution of separate magnesium and calcium carbonate phases in the lumps as well as in the binder matrix. Some of the inclusions were investigated in more detail by SEM/EDS analyses. Examples are given in Figs. 4 and 5. Inclusions show a core with high silicon and/or aluminium contents, respectively.

According to EDS analysis, the inclusion in Fig. 4a consists of 97 wt.% SiO_2 in the core and 40 wt.% MgO and 51 wt.% SiO_2 within the inner rim. The inclusion in Fig. 4b (cf. Fig. 5) contains SiO_2 (41 wt.%), Al_2O_3 (28 wt.%) and K_2O (27 wt.%) within the core and high contents of MgO (28 wt.%) and SiO_2 (58 wt.%) and additionally Al_2O_3 (7 wt.%) within the inner rim. The amount of CaO is low ($<1.7\text{ wt. \%}$)

Table 2 Phases in the binder enriched fraction of mortars from the east facade of the eastern wing of the Benedictine monastery in Riesa

Sample number	Calcite		Aragonite		Magnesite		Hydromagnesium carbonate		Hydrocalcite		Gypsum	
	XRD		DTA		XRD		DTA		XRD		DTA	
	XRD	DTA	XRD	DTA	XRD	DTA	XRD	DTA	XRD	DTA	XRD	DTA
RIE-FM 1 (E)	++	++	+	(+) ^a	-	-	++	+	(+) ^a	-	-	-
RIE-FM 2 (E)	++	++	+	(+) ^a	++	-	+	(+)	(+) ^a	-	-	-
RIE-FM 3 (E)	++	++	-	(+)	++	-	-	-	-	++	++	++
RIE-PU 1 (E)	++	++	-	-	(+)	-	+	-	-	++	++	++
RIE-PU 2 (E)	++	++	-	-	+	++	-	-	-	++	++	++
RIE-PU 3 (E)	++	++	-	-	+	-	-	-	-	++	++	++
RIE-PU 4 (E)	++	++	-	-	+	-	-	-	-	++	++	++
RIE-PU 5 (E)	++	++	+	(+) ^a	-	++	-	-	-	++	++	++
RIE-PU 6 (E)	++	++	-	-	-	++	-	-	-	++	++	++
RIE-PU 7 (E)	++	++	++	(+) ^a	-	++	(+) ^b	++	-	-	-	-
RIE-PU 8 (I)	++	++	-	-	++	-	-	-	-	-	-	-
RIE-PU 9 (I)	++	++	-	-	++	-	-	-	-	++	++	++
RIE-PU 10 (I)	++	++	-	-	(+)	-	++	-	-	(+)	(+)	(+)
RIE-PU 11 (I)	++	++	-	-	(+)	-	++	+	(+) ^a	-	-	-
RIE-PU 12(I)	++	++	-	-	++	(+) ^b	++	-	-	-	-	-

E from the exterior, *I* from the interior

++ = dominantly present, + = present, (+) = possibly present, - = not detected, as indicated by the intensity of XRD/DTA peaks. Components from aggregate (quartz, feldspar, mica) are neglected

^aThermal effects superimposed by those of other more dominant phases
^bHydromagnesite

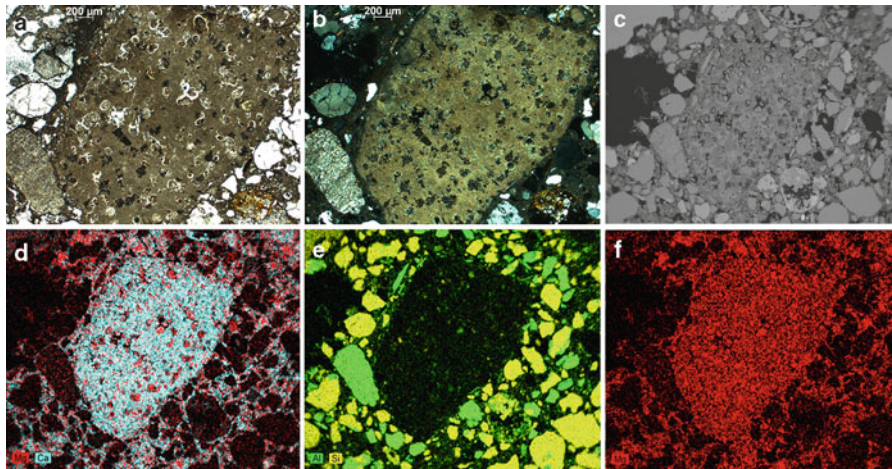


Fig. 3 Lump in the binder matrix of sample RIE-PU 3 (diameter > 3 mm) in photomicrographs from petrographic microscope (**a** Nicols parallel, **b** Nicols crossed) and SEM (**c** back scattered electron (BSE) image, **d–f** mapping of element distribution by EDS: Mg red, Ca blue, Si yellow, Al green)

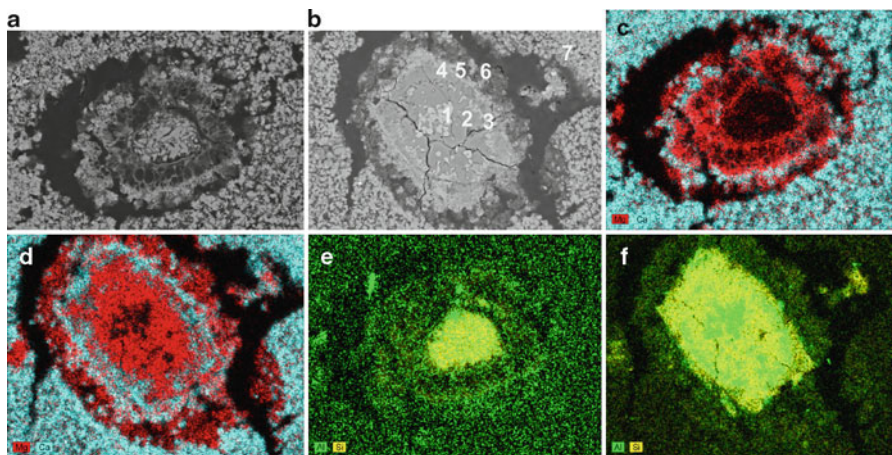


Fig. 4 Inclusions in the lump displayed in Fig. 3 (RIE-PU 3) at higher magnitude in SEM (**a, b**) back scattered electron (BSE) image, **c–f** mapping of element distribution by EDS

in both the core and the inner rims. The adjoining outer rims show an alternating dominance of Ca and Mg phases, converting from silicates/alumino-silicates near the core to carbonates in the outer zones. The inclusions could be interpreted as silicate minerals (such as K-feldspar in Fig. 4b) from the raw limestone that have been affected by the burning process. The lumps may therefore be remnants of small dolomite pieces which, although calcined and slaked, i.e. chemically altered, still show patterns of the original petrographic structure of the raw material (fine-grained, with

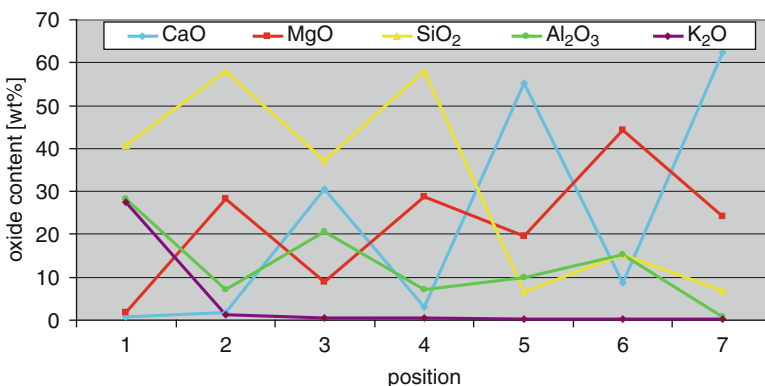


Fig. 5 Results of standardless EDS point analyses on a thin section, representing a profile across the inclusion in Fig. 4b. The numbers in Fig. 4b mark the spot positions for analyses 1–6 (7 = binder matrix, analysed area ca. 1,500 μm^2). Oxygen excess was only detected in 5, 6 and 7

silicate inclusions). EDS analyses, however, must be discussed with some care, because they are semi-quantitative and do not allow a calculation of mineral phases.

4 Discussion and Conclusions

Investigations into the binders of the thirteenth – early twentieth century joint mortars, renders and plasters from the eastern wing of the Riesa monastery have demonstrated the permanent use of dolomite or dolostone in local lime production over the centuries. It is thought that the dolomite was sourced from deposits of late Palaeozoic origin (Upper Permian, Zechstein) located about 15 km south-west of Riesa.

The occurrence of magnesite and/or hydromagnesite phases beside calcite in the binder are in good accordance with the results obtained from historical dolomitic lime mortars studied by other authors [2, 3, 5–7]. Brucite was not detected in Riesa although it is also known to be present in historical binders [6, 7]

The samples investigated in this study can be divided into three groups according to the type of magnesium phases in the binder:

1. Samples with only hydromagnesite beside calcite (FM 1) or very small contents of magnesite (questionable) beside calcite and hydromagnesite (PU 10, PU 11). They come from the interior wall (PU 10, PU 11) or from inside the wall (FM 1).
2. Samples with both magnesite and hydromagnesite beside calcite (FM 2, PU 1, PU 7, PU 12). PU 12 comes from the interior, the others come from the exterior; PU 1 and PU 7 contain gypsum.
3. Samples with magnesite as the only magnesium phase beside calcite (FM 3, PU 2 – PU 6, PU 8, PU 9). Most of these samples come from the exterior of the building. Samples PU 8 and PU 9 from the interior were taken from the window jamb that has been affected by external influences like rain. Seven of these eight

samples additionally contain gypsum as an indicator of chemical weathering due to environmental influences.

There is no relation between construction age of the mortars and the phase content of their binders.

As known from other investigations [8], behaviour of the magnesium phases during burning, slaking and setting of the lime is somewhat different from that of the calcium phases. After the de-carbonation of dolomite during burning, Ca and Mg form new spatially separate phases, i.e. hydroxides from slaking and carbonates from setting. The size and spatial distribution of the coexisting calcium and magnesium carbonates in the binder and in enclosed lumps are displayed in Fig. 3. Although the thermodynamically stable magnesium carbonate phase is magnesite [9], the occurrence of hydrous magnesium carbonates (hydromagnesite, nesquehonite) has often been reported from field studies as well as from laboratory investigations of dolomitic binders [2, 3, 5–8]. Samples in this study with only hydromagnesite (group 1) come from sheltered positions and might represent the first stage of carbonation of the magnesium phase by the formation of amorphous, hydrous magnesium carbonate (brucite is absent). Samples from the exterior, which are exposed to long-term, intensive contact with the air and rain water, frequently contain only magnesite beside calcite.

The occurrence of magnesite might indicate a “mature” stage of the development of the magnesium carbonate phase towards the stable state. This is in good accordance with the investigations of micro-scale profiles on Baroque dolomitic lime renders at a façade in Altenburg (Germany) by Zier and Seifert [10]. These authors found differences in the phase content of the surface layer of the plaster (0–1 mm depth, with calcite, very small amounts of magnesite, and gypsum) and the adjacent deeper layers (2–5 mm depth: calcite and magnesite; 5–10 mm depth: calcite and hydromagnesite/magnesite; > 10 mm depth: calcite and hydromagnesite).

Gypsum, formed by chemical weathering of the mortars due to air pollution, is present within the majority of samples from the exterior and is also evident as salt efflorescence together with magnesium sulphate on the building’s surface. The presence of magnesium and calcium sulphates in salt efflorescence is typical for monuments with dolomitic lime mortars [2–4] and indicates chemical reactions of acid rain with the binder and the migration of newly formed sulphates to the surface. Due to their better solubility compared with calcium sulphate, magnesium sulphates are preferably dissolved and transported to the surface by advection with water in the structure of dolomitic lime mortars. This was demonstrated in laboratory tests for magnesium and calcium sulphates [11] as well as on buildings [12] and is also reflected in efflorescence samples from Riesa by the dominance of magnesium sulphate over gypsum. As a consequence, the binders of the mortars are depleted in MgO and do not represent the original CaO/MgO ratio of the raw dolomite any more. Further investigations are needed to elucidate possible interactions of magnesium carbonate and sulphate formation in polluted environments.

Hydrotalcite, which was determined in three of the samples by XRD, might have formed by the reaction of magnesium with aluminous silicate compounds

from the raw dolomite or from the aggregate. More detailed investigations into the spatial distribution, size and shape of the hydrotalcite phase are necessary to understand its formation.

Acknowledgements Financial support for parts of this study from the German Federal Foundation for the Environment (DBU Az 15678) is gratefully acknowledged. Thanks are due to Mechthild Noll-Minor for her help during sampling and for providing information about construction history.

References

1. Siedel, H., Michalski, S., Ullrich, B., Zier, H.W.: Zur Identifikation von Magnesiumverbindungen im Kalkmörtel. Berichte Institut für Steinkonservierung Mainz **16**, 13–20 (2003)
2. Siedel, H.: Dolomitische Kalkmörtel als Quelle für steinschädigende Salze an der Tulpentreppe im Dom zu Freiberg/Sachsen. Jahresberichte Steinzerfall – Steinkonservierung **4**, 173–180 (1992)
3. Siedel, H.: Effects of salts on wall paintings and rendering in Augustusburg Castle. In: Rammlmair, D., et al. (eds.) Applied Mineralogy in Research, Economy, Technology, Ecology and Culture, vol. 2, pp. 1035–1038. A.A. Balkema, Rotterdam/Brookfield (2000)
4. Siedel, H.: Alveolar weathering of Cretaceous building sandstones on monuments in Saxony, Germany. In: Příkryl, R., Török, A. (eds.) Natural Stone Resources for Historical Monuments. Geol. Soc. London Spec. Publ. 333, pp. 11–24. Geological Society, London (2010)
5. Bruni, S., Cariati, F., Fermo, P., et al.: Characterization of ancient magnesian mortars coming from northern Italy. Thermochim. Acta **321**, 161–165 (1998)
6. Paama, L., Pitkänen, I., Rönkkölä, H., Perämäki, P.: Thermal and infrared spectroscopic characterization of historical mortars. Thermochim. Acta **320**, 127–133 (1998)
7. Diekamp, A., Konzett, J., Mirwald, P.W.: The occurrence of magnesite and hydromagnesite in medieval dolomitic lime mortars. Mitt Österr Miner Ges **155**, 49 (2009)
8. Niesel, K., Schimmelwitz, P.: Zur Kenntnis der Vorgänge bei der Erhärtung und Verwitterung von Dolomitkalkmörteln. Tonindustrie-Zeitung **95**, 153–161 (1971)
9. Königsberger, E., Königsberger, L.C., Gamsjäger, H.: Low-temperature thermodynamic model for the system $\text{Na}_2\text{O}\text{-MgCO}_3\text{-CaCO}_3\text{-H}_2\text{O}$. Geochim. Cosmochim. Acta **63**, 3105–3119 (1999)
10. Zier, H.W., Seifert, F.: Schäden an Dolomitkalkputzen bei Einwirkung von Luftschaadstoffen. Berichte Institut für Steinkonservierung Mainz **16**, 39–46 (2003)
11. Hoffmann, D., Rooß, H.: Wechselwirkung zwischen Schwefeldioxid und Kalkmörteln. Materialprüfung **19**(8), 300–304 (1977)
12. Klemm, W., Siedel, H.: Sources of sulphate salt efflorescences at historical monuments – a geochemical study from Freiberg, Saxony. In: Riederer, J. (ed.) Proceedings of the 8th International Congress on Deterioration and Conservation of Stone, vol. 1, pp. 489–495, Berlin (1996)

Hydraulicity in Historic Lime Mortars: A Review

Jan Elsen, Koenraad Van Balen, and Gilles Mertens

Abstract Natural hydraulic limes were used in ancient times and are still produced today. A comparison of the chemistry and mineralogy of currently available NHL2 and NHL5 limes indicate that there are no clear differences except for the amount of ‘undefined material’, mainly comprising an amorphous phase. The chemical composition of these different limes is nearly identical. However, the classification of ancient hydraulic limes is mainly based on their chemistry, obtained from the analysis of ancient mortar binders. Moreover, it is shown that the phase composition of these limes evolves with time, making their classification uncertain and difficult.

1 Introduction

A variety of binders have been used in the past [1]. The oldest types; clays and bitumen, were readily available (Fig. 1). Materials needing heating and subsequent mixing with water before application were used subsequently. The use of gypsum-based plaster (hemi-hydrate: $\text{CaSO}_4 \cdot 0.5\text{H}_2\text{O}$) probably dates back earlier than the use of lime since its production from gypsum requires lower temperatures compared to the production of lime from limestone and was therefore easier to obtain. Both binders harden in air.

A next step in the development was the manufacture of ‘hydraulic’ binders obtained by mixing lime with pozzolans. ‘Hydraulic’ refers to the ability of the binder to harden under water [2]. More recently, other types of hydraulic binders are

J. Elsen (✉) • G. Mertens

Department of Earth and Environmental Sciences, KULeuven, Leuven, Belgium
e-mail: jan.elsen@ees.kuleuven.be

K. Van Balen

Department of Civil Engineering, KULeuven, Leuven, Belgium
e-mail: koenraad.vanbalen@bwk.kuleuven.be

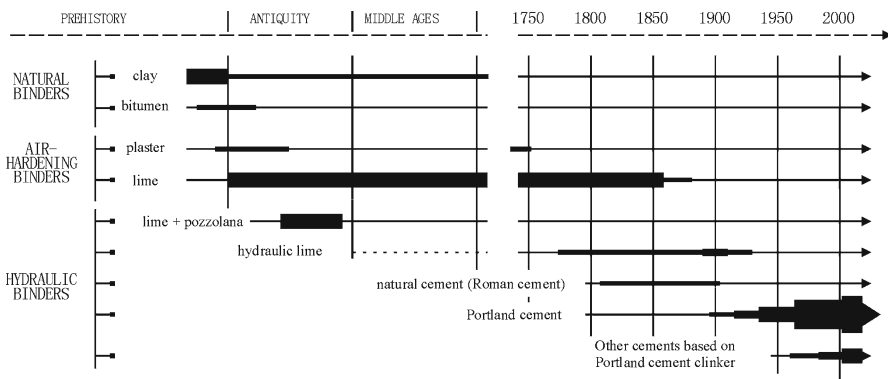


Fig. 1 Use of binders during history (Adapted from Furlan and Bissegger [1])

obtained; either by burning an impure limestone or by mixing Si- and Al- bearing materials with a pure limestone and burning them together.

Although the hydraulicity of ancient mortars provides us with technological information, or with information useful for their restoration, it appears to be very difficult to measure. This article starts with a tentative definition of hydraulicity and then discusses the chemistry and mineralogy of some commercial hydraulic limes that are presently available on the market. Afterwards, a survey will be provided on the current knowledge about ancient hydraulic mortar technology and finally an overview of the methods that have been used to identify and measure this hydraulicity in ancient mortars will be given. The last part of the paper shows, with an example, that the hydraulicity of ancient mortars cannot always be determined unambiguously. Less attention will be paid to the addition of pozzolanic materials to lime. This subject was treated in more detail, for example by Charola and Henriques [3].

2 Definitions

Hydraulic limes are limes containing enough free CaO to be slaked with water and capable of setting under water. A minimum amount of free CaO must be present in the calcined product to reduce the entire mass to a powder when it is slaked [4]. The combination of the free CaO with water induces an expansion that leads to the disintegration of the freshly burnt limestone. The maximum amount of free CaO is determined by the second condition; which is, if too much free CaO is present, the product will not be able to harden under water. There are a large range of products that comply with this definition. They are commonly classified according their chemical composition and more specifically to their Cementation Index ‘CI’ (Eq. 1) or Hydraulicity Index ‘HI’ (Eq. 2) [4, 5]. Boynton [6] proposed a classification into ‘feeble’, ‘moderately’ and ‘eminently hydraulic’ limes based on their Cementation Index. In the

European norm (EN459-1:2001), the following classes of natural hydraulic limes with pozzolanic additives are defined; NHL2, NHL3.5 and NHL5. However, they do not correspond to Boynton's classes and tend to neglect the 'feeble hydraulic limes'. As the strength of the binders is tested at 28 days, according to the norm, 'feeble hydraulic' limes tend to be omitted because their final strength is only attained at longer curing times. The main reason is that carbonation plays a major role in their hardening. Carbonation is generally a much slower process than the hydration reactions that are dominant in the more hydraulic binders. This has important implications for restoration where 'feeble' or even more feeble hydraulic binders have been used. Lindqvist [7] defined a class of sub-hydraulic mortars as having a hydraulic character between that of the pure air limes and the 'feeble hydraulic limes' defined by Boynton [6].

$$CI = \frac{2.8SiO_2 + 1.1Al_2O_3 + 0.7Fe_2O_3}{CaO + 1.4MgO} \quad (1)$$

$$HI = \frac{SiO_2 + Al_2O_3}{CaO} \quad (2)$$

The term 'hydraulic lime' was first suggested by Vicat. 'Lean lime' and 'water lime' were terms used previously.

Hydraulic limes can also be produced by adding pozzolans to non-hydraulic limes. This technique was known since ancient times and was re-evaluated during the Renaissance. However, since the eighteenth and mainly during the nineteenth century, the use of pozzolans in lime for water-related structures or foundations became common practice. Pozzolans react with the $Ca(OH)_2$ in the lime to form reaction products similar to those formed in the previously defined natural hydraulic limes (NHL2, NHL3.5 and NHL5).

3 Present-Day Natural Hydraulic Limes

At the time of writing, natural hydraulic limes (NHL's) are produced in a relatively small number of places in Western Europe; for example by Otterbein and Hessler-Kalkwerke in Germany, by CIMPOR in Portugal, by Singleton Birch and Roundtower in the UK, by the SOCLI-group, Lafarge, Boehm and St. Astier in France and by Tassullo in Italy. Some of these, as well as others such as Unilite, sell pre-mixed mortars and concretes based on natural hydraulic lime. The mineralogical composition of some of these limes is presented in Fig. 2. Part of the data in this figure was obtained from Rietveld refinement of the X-Ray Powder Diffraction (XRPD) patterns of the natural hydraulic limes after mixing them with an appropriate crystalline standard (10 wt.% ZnO). The other part of the data was obtained from Kraus et al. [8]. Their quantitative phase analyses were determined by the combination of chemical and XRPD data.

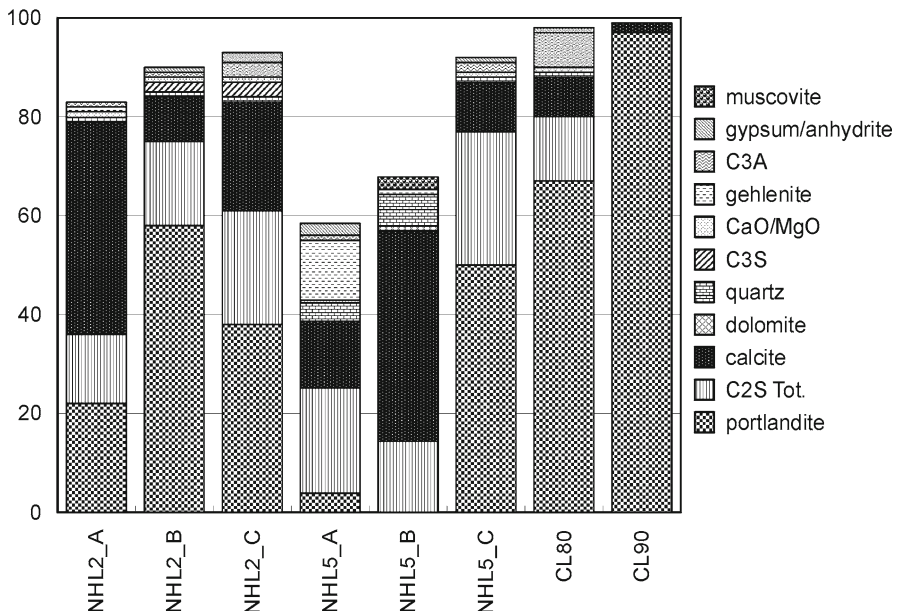


Fig. 2 Mineralogical composition of the non-amorphous fraction of the studied limes: NHL2 and NHL5 samples are classified as hydraulic, CL80 and CL90 as non-hydraulic

The chemical composition of the NHL's can be found in Fig. 3. For comparison, the composition of two non-hydraulic limes ('CL80' and 'CL90') is plotted in the same figures.

From these data it appears that there is no clear correlation between the mineralogy and the type of lime. However, the portlandite content in the non-hydraulic limes is higher than that in the hydraulic limes. Although 'CL80' is classified as non-hydraulic, Kraus et al. [8] identified considerable amounts of C_2S and C_3A . These minerals are mostly characteristic for hydraulic binders. Nevertheless, the concentration of C_2S and C_3S in the non-hydraulic limes is lower than in the hydraulic ones. In accordance with this, higher SiO_2 contents are observed in the hydraulic limes compared to the non-hydraulic limes.

The only clear difference between the NHL2 and the NHL5 samples lies in the amount of 'undefined material'. Most of it consists of amorphous material, although it possibly includes a small amount of undefined minerals that could be overlooked in the XRD spectra. Nevertheless, the amount of 'undefined material' appears to be generally higher in the more hydraulic NHL5 samples compared to the NHL2 samples. No clear difference could be observed between the chemistry of the NHL2 and NHL5 samples. The content of the main elements in NHL5_C for instance is similar to that in NHL2_B and NHL2_C. This is an indication that the chemistry alone is probably insufficient to give a clear indication about the hydraulicity of the sample.

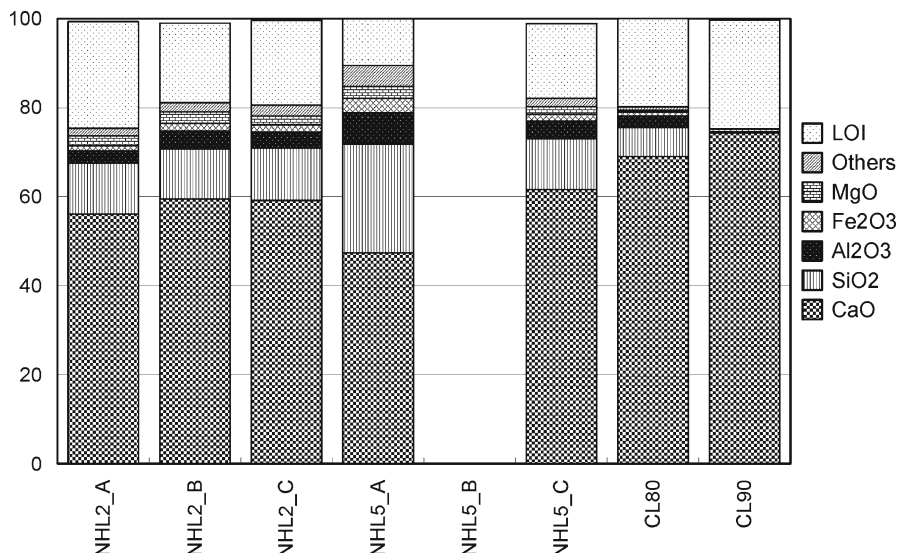


Fig. 3 Chemical composition of the studied limes: NHL2 and NHL5 samples are classified as hydraulic, CL80 and CL90 as non-hydraulic (no analysis result for NHL_5)

4 Historical Development of Hydraulic Lime Mortars

The Greek knowledge of the use of highly siliceous, volcanic Santorin Earth (a pozzolan) goes back to 500–300 B.C. [9]. The use of pozzolanic materials in mortars used in the construction of draining canals dated 400 B.C., has also been noticed in Olynthos, on the mainland to the north [10]. In Eastern civilizations, rice husk ash was used as a pozzolan [11]. Other Greek mortars, in which no pozzolans were used, were found to be extremely hard. This is perhaps due to the quality of the limestone, which was of lower purity compared to that used by the Romans [12]. For the Romans, the best lime was that produced from pure limestone.

Around the third century B.C., Roman builders discovered how to make hydraulic mortars [13]. A natural deposit of reactive ‘sand’, similar to that found by the Greeks on the Island of Santorin, was discovered near Mount Vesuvius. This ‘pulvis puteolanus’ (‘earthy material from Puteoli’) survived in many languages as ‘pozzolana’.

Hydraulic mortar and concrete was used on land by the later third century B.C. [14]. Whenever pozzolanic materials were not available and a mortar insoluble in water was needed, the Romans used a mixture of hydrated lime and crushed ceramics. Many names have been used to designate these crushed ceramics over the world; Horasan in Turkey, Surkhi in India, Homra in Arabic countries and Cocciopesto in Italy [15, 16]. The most common name for this type of mortar is ‘opus testaceum’ [17, 18].

In a few areas, ‘sands’ resembling those found near Mount Vesuvius, for example Trass from the Eifel region in Germany, were used to produce hydraulic mortars.

During Roman dominion, little seems to have changed in preparation techniques and mortar composition [19]. After Roman times, a clear uniform mortar and lime composition is lacking.

Even though studies about medieval mortars are scarcer than those that deal with mortars and mortar technology from classical antiquity, it appears that great differences exist in their composition. Whereas medieval mortars from Pamplona (Spain) appear to be non-hydraulic [20], others from Crete (Greece), for instance, show a clear hydraulic character [21]. Even in the same area, for example in the city of Pisa, mortars with a hydraulic character and non-hydraulic mortars were used interchangeably without any *apparent* reason [22].

However, studies of a sixteenth century dockyard in Venice, Italy, indicate the deliberate use of hydraulic lime for foundations and air-lime for indoor masonry [23]. Mortars made with hydraulic lime also seem to be used deliberately in Ottoman baths in Budapest during the same period [24]. Whereas the only hydraulic mortars known from the Roman era are those made from pure lime mixed with pozzolans, medieval hydraulic mortars appear to be prepared either from the addition of pozzolans or from burnt and slaked clay-bearing limestone [25]. Moreover, there are indications of the use of a variety of pozzolanic additions, ranging from classical crushed ceramics [23, 26], volcanic ash [26, 27] or metamorphosed soils (agghiara; see [28]) to the addition of fine opal-A ($\text{SiO}_2 \cdot \text{nH}_2\text{O}$) from unclear origin [29]. The use of specific deposits with pozzolanic properties, known from Roman times, such as for instance Trass – was revived during the Middle Ages [30, 31].

Bleazard [32] identifies a gradual decline in the quality of the mortar after Roman times, throughout the Middle Ages and notes that mortars in Saxon and Norman buildings often show evidence of bad mixing and the use of imperfectly burnt lime. By contrast, some authors [27] claim that the use of particular sands, rich in volcanic ashes, in south-Italian mortars from the tenth to eleventh century reveal a deep knowledge of the properties of raw materials and a deliberate selection of building materials.

During the Renaissance, ancient techniques of mortar manufacture and raw material choice were re-evaluated [18, 32]. Contemporaneous writings testify to the deliberate use of hydraulic limes prepared from impure limestone. Beside ‘white lime’ (pure lime), ‘dark lime’ (hydraulic lime) was obtained from the calcination of grey and dark limestones (Palladio, 1570 and Scamozzi, 1615 in [33]).

From this, it appears that conflicting ideas and perceptions about the technological knowledge and practices in the Middle Ages exist.

The first detailed investigations carried out in the field of hydraulic limes made from impure limestone were those of John Smeaton. His investigations in 1756 led to the discovery that mortars with limes made from impure limestone gave the best results [32] for the ability to harden under water (cold-water test). By dissolving the limestones in nitric acid he obtained an insoluble residue of quartz SiO_2 and clayey material to which he attributed the hydraulicity. At about the same time in Sweden, Bergmann (1735–1784) attempted to discover why some limes harden when immersed in water [34]. The hydraulic limes he analysed, all contained manganese. Therefore he attributed their hydraulicity to the presence of this element. In France, at the beginning of the nineteenth century, Guyton de Morveau analysed the properties of an artificial mixture with the same composition as the natural limes studied by Bergmann.

He calcined it and found that the lime obtained was an excellent ‘water lime’. He also attributed this property to the manganese (4%) and not to the clay, which had been added in a proportion of 6% to the lime carbonate [35]. In Switzerland, Saussure (1740–1799) also dissolved ‘meagre limes’ in acid and found that the residue was composed of quartz and clay. However, he adds that “the manganese would appear to have greater influence than the siliceous content”. Vitalis (in 1807), among others, found that some good quality hydraulic limes contained no manganese, and stated that “clay was the chief source of their water setting properties” [35].

The French engineer Collet Descotils (in 1813) was the first to relate clearly the properties of the meagre limes to the presence of silica. He stated that an intimate combination of silica with lime is produced when these limes are slaked. He found that the silica in the limestones that were used was insoluble in acid, whereas it became soluble in the lime derived from it. His conclusions were correct in that a high quality meagre lime must contain a high quantity of finely disseminated siliceous matter. A more detailed discussion on the origin of modern hydraulic binders and their classification can be found in [36].

The hydraulicity of binders is highly variable. The first attempt to classify hydraulic binders was made by Louis Vicat [5], who introduced the Hydraulicity Index (see Eq. 2). In this formula, Vicat compiled all the knowledge then available and was able to directly relate hydraulicity to the SiO_2 and Al_2O_3 contents. However, equal importance was incorrectly attributed to the two constituents. Gradually it was found that Fe_2O_3 and MgO also had an influence on the hydraulicity. An adapted formula was therefore developed about a century later by E.C. Eckel [4]. The formulation of this Cementation Index is shown in Eq. 1. It was conceived to be a direct expression of the quantity of CaO combined with the other constituents to form hydraulic minerals. The use of this cementation index is based on a number of assumptions. Firstly, it is assumed that all available SiO_2 combines with CaO to form C_3S (Ca_3SiO_5) and that all Al_2O_3 combines to form C_3A ($\text{Ca}_3\text{Al}_2\text{O}_6$). MgO is considered equivalent to CaO and Fe_2O_3 to Al_2O_3 . This is clearly an oversimplification, since the mineralogy of hydraulic binders is more complex than assumed here. Eckel emphasized that the properties of hydraulic binders not only depend on their composition (‘CI’), but also on the conditions of their manufacture. The hydraulic properties are indeed indirectly related to the burning temperature and time, since these influences the mineralogy of the final product [37].

5 Determining the Hydraulicity of Ancient Mortars

5.1 Remaining Hydraulicity in Ancient Mortars

Some calcareous binders in ancient mortars are hydraulic. To determine this hydraulicity, which can be deduced from microscopic observations only in some rare cases, a chemical analysis is useful. However, the main difficulty resides in separating the binder from the other mortar constituents. Generally, this is achieved by dissolving

a part of the mortar, or a previously disaggregated fraction of the mortar, in a dilute acid [21, 27, 38–42]. Other studies [17, 43, 44] mention the analyses of the entire mortar or a smaller grain size fraction after disaggregation and sieving. However, the results of such analyses are not helpful to obtain any information on the binder, because a significant contribution of the aggregate can never be ruled out.

A wide range of analyses methods to determine the chemistry of mortars, or more particularly the binder fraction have been used. Difficulties arise when trying to compare the results of these analyses. In an attempt to obtain uniformity in the procedure for the chemical analysis of binders, Middendorf et al. [45] introduced a standardised methodology.

However, difficulties were previously observed during the implementation of the method. Hofkens [46] made an evaluation of different analysis procedures and concluded that the treatment of the sample with HCl (10%) appears most straightforward. Many other authors [20, 39, 47–49] have adopted the determination of the soluble silicic acid content. Specifically, 1g of sample is dissolved in 50 ml HCl (10%) and the suspension is filtered after 5 min of reaction. The filtrate is used for the determination of Si by ICP-OES or AAS.

From the amounts of the main elements, the hydraulicity (Eq. 1) and cementation indices (Eq. 2) can be calculated. However, high acid-soluble silicic acid contents, resulting in a high ‘HI’ and ‘CI’, might not provide clear evidence for the use of hydraulic lime as binder material [45]. The silica might as well originate from pozzolanic additives that reacted with a more or less pure lime binder.

In general, the contribution of acid soluble SiO_2 from the aggregates is considered to be limited [50]. However, the use of hot HCl in mortar analyses revealed that part of the aggregate fraction may dissolve, especially clays such as smectites and kaolinites [40].

If the methodology previously described is considered to be suitable to assess the bulk chemistry of the binder, microprobe analyses are useful to provide more detailed information about points or areas in polished thin sections including information about individual mineral phases. The main restriction is that no volatile components like CO_2 and H_2O can be measured. In spite of this limitation, electron microprobe methods have previously proven useful for the analyses of ancient mortars [22, 26, 39].

Additional information on the mineralogy of the mortars can be obtained by X-ray diffraction; the data complement the results of the petrographical and chemical analyses. The identification of the nature of the binder is easily made with X-ray diffraction by the identification of hydrated calcium silicates or aluminates that point towards the use of hydraulic binders. Some authors [47] state that a mineralogical analysis can make a distinction between different types of hydraulic binders possible. X-ray diffraction also makes possible the identification of pozzolanic admixtures, which are sometimes too fine to be recognisable in thin sections.

The patterns produced from thermo-gravimetric (TG) analysis of ancient mortars are often subdivided into temperature ranges that show characteristic mineral transformation during heating. For calcareous binders, most authors [15, 19, 21, 51–53] make a distinction between hygroscopic water (in the temperature range from 30°C

to 120°C), water from hydrated salts (120–200°C), the loss of water bound to hydraulic compounds (200–600°C) and the loss of CO₂ (>600°C).

In particular, TG appears to be useful for the differentiation of hydraulic and non-hydraulic mortars [51]. Most often [21, 26, 51–55] a plot is made of the weight loss >600°C and of the ratio of the weight losses >600°C and from 200°C to 600°C. Samples with high amounts of water bound to hydraulic compounds and proportionally low amounts of CO₂ are considered to be hydraulic.

Many studies reveal the presence of crushed ceramics in Roman mortars [44, 56–59] but also in younger mortar samples from the medieval period [15, 60, 61]. In addition to these fired clay-based materials, other types of pozzolans have been found in ancient mortar samples, both natural and artificial. Some authors make mention of slag fragments [62], charcoal [56] and flint [9, 63] particles. However, in many cases it is difficult to distinguish between the deliberate use of these mineral admixtures and their accidental addition.

It is however difficult to determine whether the hydraulicity of a mortar is induced by the addition of the supplementary materials or by the use of natural hydraulic lime. An analysis of the Binder Related Particles can be therefore be useful [64, 65]. The chemistry of the binder related particles is expected to be identical to that of the limestone used to prepare the lime.

5.2 Vanishing Hydraulicity of Ancient Mortars

We previously suggested that making a chemical analysis of the binder alone and as a whole is probably impossible, because it is closely intermixed with the aggregate. Moreover, different dissolution techniques are likely to yield distinct results. Therefore, the authors [66] analysed the binder fraction in a selected set of thin sections from mortars excavated at the Cathedral of Tournai [39] with an electron microprobe (CAMECA SX 50 at 15 kV and 6 nA). Small areas of approximately 15 µm × 12 µm (depth of a few µm) were quantitatively analysed (the results are presented in Table 1).

A first important observation is that the binder can be very heterogeneous within one mortar sample. If some analysis reveals compositions near to that of pure C-S-H, other analyses within the same mortar reveal areas that are much poorer in SiO₂ and with a Cementation Index of only 0.09.

Secondly, the results reveal that the Cementation Indices of the binder calculated from the microprobe results are systematically higher (with one exception out of 12 samples) than those calculated from the chemical analyses obtained by acid dissolution used for the determination of the bulk chemistry. Looking at a smaller scale, it appears that the binder in many samples does not consist of a single phase, but appears to be composed of at least two distinct components that are intimately intermixed (Fig. 4). In several samples, a lightly coloured zone (in BSE mode) with a composition close to that of pure Ca-carbonate is intermixed with darker material rich in Si and having an average composition of 8 wt.% CaO, 16 wt.% SiO₂,

Table 1 Microprobe analyses of the binder for a selection of mortar samples from Tournai

Sample name	Number of analyses		SiO_2	Al_2O_3	Fe_2O_3	MgO	CaO	Cl
D03B	4	Average	4.2	0.6	0.0	0.1	47.6	0.26
		Stdev.	1.3	0.3	0.0	0.1	2.8	0.09
D06B (z1)	3	Average	16.6	3.0	0.1	0.2	24.6	2.03
		Stdev.	2.3	0.3	0.1	0.0	1.2	0.38
D06B (z2)	4	Average	8.6	1.3	0.3	1.4	39.1	0.63
		Stdev.	1.7	0.3	0.2	0.7	2.4	0.15
D07B (z1)	2	Average	12.3	1.4	0.7	0.2	39.5	0.92
		Stdev.	0.2	0.4	0.7	0.2	0.7	0.02
D07B (z2)	3	Average	0.1	0.1	0.1	0.1	0.1	0.11
		Stdev.	0.1	0.1	0.1	0.1	0.1	0.05
D08B	3	Average	3.1	0.4	0.4	0.2	50.6	0.18
		Stdev.	0.8	0.1	0.0	0.1	1.2	0.05
D09B	4	Average	5.7	0.7	0.1	0.1	47.2	0.36
		Stdev.	0.9	0.2	0.1	0.0	1.1	0.07
D19B	6	Average	5.4	1.3	0.6	0.3	41.9	0.40
		Stdev.	2.1	0.7	0.8	0.3	2.9	0.16
D20B	5	Average	6.7	1.0	0.5	0.2	44.3	0.46
		Stdev.	1.5	0.2	0.3	0.0	1.7	0.12
D22B	3	Average	3.4	0.3	0.1	0.1	45.0	0.22
		Stdev.	0.5	0.1	0.2	0.0	1.7	0.03
D23B	5	Average	5.7	0.8	0.6	0.3	47.4	0.36
		Stdev.	2.4	0.4	0.4	0.2	2.1	0.15
D36B (z1)	5	Average	23.4	3.7	1.0	0.7	19.0	3.57
		Stdev.	1.7	1.1	0.8	0.3	3.1	0.46
D36B (z2)	2	Average	1.6	0.3	0.0	0.4	53.7	0.09
		Stdev.	0.0	0.1	0.0	0.1	0.5	0.00
D41B	6	Average	2.9	0.4	0.4	0.2	50.5	0.18
		Stdev.	1.6	0.2	0.2	0.3	4.0	0.11
D48B	6	Average	6.0	0.8	0.4	0.2	40.3	0.47
		Stdev.	2.1	0.4	0.2	0.0	5.9	0.20

Analyses inside one zone (z) are made at a distance of less than approximately 1 mm from each other. The distance between two zones in one thin section is at least 1 cm

and 2 wt.% Al_2O_3 at these specific location. The composition of the latter phase is however variable and ranges between CaO contents of 0–10 wt.% and SiO_2 contents of 15–70 wt.%. These specific point analyses (volume of approximately 5–10 μm^3) reveal the heterogeneous nature of the binder that has an average composition of 18 wt.% CaO , 14 wt.% SiO_2 , 2 wt.% Al_2O_3 as determined by the analyses of larger areas ($15 \mu\text{m} \times 12 \mu\text{m}$ and a depth of a few μm). Because of the porous nature of the binder, these analyses are only suitable to establish the concentration ratios between different oxides. The ratios of $\text{Ca/Si}=1.3$ and $\text{Si/Al}=7.5$ are similar to those found in C-S-H [66]. It is therefore suggested that segregation has occurred in the C-S-H phase, whereby Ca and Si are moving into separate phases. The lightly coloured zones correspond to that of nearly pure Ca-carbonate and are an indication

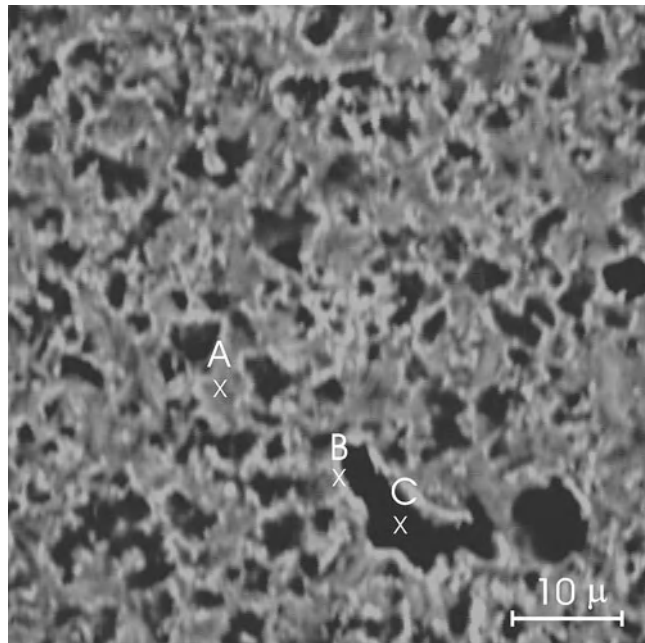


Fig. 4 BSE micrograph of the hydraulic binder in a mortar sample from Tournai with a *lightly coloured zone* (B) rich in Ca (CaO: 49.3 wt.%; SiO₂: 1.4 wt.%; Al₂O₃: 0.2 wt.%), a *darker zone* rich in Si (A) (CaO: 8.3 wt.%; SiO₂: 15.5 wt.%; Al₂O₃: 1.6 wt.%) and a *black zone* (C) corresponding to the porosity. These are average analyses results of points (volume of approximately 5–10 μm^3) obtained at 15 kV and 6 nA

that a carbonation reaction of the C-S-H has occurred resulting in a carbonate phase and a silica-rich phase. The spatial distribution of the two phases confirms these results as the lightly coloured material in Fig. 3 is consistently located on the outside, adjacent to the pores and enclosing the darker zones that are richer in silica. This carbonate phase could also be a secondary phase, but often vaterite was identified for this carbonate phase which is a typical carbonation reaction product of C-S-H phase [67].

Microprobe analyses can only reflect the chemical composition at specific locations in the binder, but does not necessarily reveal the exact mineralogy of the different components. Ca-carbonates are observed in each X-ray diffraction pattern of the binder-enriched fraction (<63 μm fraction of the gently disaggregated mortar sample). Calcite, one of the Ca-carbonate polymorphs, is indeed present in each sample. However, vaterite (CaCO_3) and aragonite (CaCO_3), other Ca-carbonate polymorphs, are also present in many samples. Remarkably, their occurrence and abundance appears to be related to the hydraulicity (read CI) of the samples determined from their chemical analyses by acid dissolution. Vaterite and aragonite are generally considered to be less stable compared to calcite at atmospheric pressures and near-room temperatures. Therefore, they do not occur upon carbonation

of pure lime (portlandite). However, these two polymorphs were proven to form upon carbonation of C-S-H [67].

This phase evolution might have consequences for the bulk chemical analyses, since the dissolution of these neo-formed phases might differ significantly from that of the phases initially present.

6 Conclusions

Knowledge about the physical, chemical and mineralogical evolution is important for the design of durable mortars that are not only required for restoration purposes but also for modern technological applications. From a chemical and mineralogical viewpoint, the composition of the currently available natural hydraulic limes is different from that of the non-hydraulic limes. However, the differences between samples of NHL2 and NHL5 limes are less obvious and mainly based on the amount of amorphous material. In ancient times, hydraulic limes were used in mortars. Although hydraulic binders made from the addition of pozzolans to lime are identified in many mortar samples since Antiquity, the natural hydraulic limes made from impure limestone seem to be used less frequently. Many questions remain about their deliberate use, because the theoretical knowledge of hydraulicity only dates from the end of the eighteenth century. Moreover, the analysis of ancient lime binders is not straightforward because it is difficult to separate from aggregate in ancient mortars. In addition, the identification and classification of hydraulic binders is complicated by their physico-chemical evolution through time.

References

1. Furlan, V., Bissegger, P.: Les mortiers anciens. Histoire et essai d'analyse scientifique. *Revue Suisse d'art et d'Archéologie* **32**, 2–14 (1975)
2. Deloye, F.-X.: Hydraulicité et pouzzolanité. *Bulletin de liaison des Laboratoires des ponts et chaussées* **184**, 94–95 (1993)
3. Charola, X.A.E., Henriques, F.M.A.: Hydraulicity in lime mortars revisited. In: Bartos, P.J.M., Groot, C.J.W.P., Hughes, J.J. (eds.) *Proceedings of the RILEM International Workshop ‘Historic Mortars: Characteristics and Tests’*, Paisley, Scotland, pp. 95–104, RILEM, France (1999)
4. Eckel, E.: *Cements, Limes and Plasters* (A facsimile of the 3rd edn.). Donhead publishing, Shaftesbury (2005) (3rd edn published in 1928)
5. Vicat, L.J.: Recherches expérimentales sur les chaux de construction, les bétons et les mortiers ordinaires, 49 p. Goujon, Paris (1818)
6. Boynton, R.S.: *Chemistry and Technology of Lime and Limestone*, 2nd edn. Wiley, New York (1980)
7. Lindqvist, J.E.: Sub-hydraulic binders in historic mortars. Conference on ‘repair mortars for historic masonry’, pp. 1–7. Delft University of Technology, Delft (2005)
8. Kraus, K., Qu, A., Strübel, G.: Eigenschaften von mörteln aus kalken mit natürlichen und zugemischten hydraulischen anteilen. Institut für steinconservierung, Bericht Nr. 12 (2001)
9. Idorn, M.G.: *Concrete Progress from Antiquity to the Third Millennium*. Telford, London (1997). ISBN 0-7277-2631-5
10. Papayianni, I., Stefanidou, M.: Durability aspects of ancient mortars of the archeoloigcal site of Olynthos. *J. Cult. Herit.* **8**, 193–196 (2007)

11. Malinowski, R.: Durable ancient mortars and concretes. *Nord. Concr. Res.* **1**, 1–22 (1981)
12. Klemm, W.A.: Cementitious materials: historical notes. In: Skalny, J.P. (ed.) *Materials Science of Concrete*, pp. 1–26. American Ceramic Society, Westerville (1989)
13. Oleson, J.P., Brandon, Ch., Cramer, S.M., Cucitore, R., Gotti, E., Hohlfelder, R.L.: The ROMACONS project: a contribution to the historical and engineering analysis of hydraulic concrete in Roman maritime structures. *Int. J. Naut. Archaeol.* **33**(2), 199–229 (2004)
14. Adam, J.P.: *Roman Building, Materials and Techniques*. B.T. Blatsford Ltd., London (1994). 155 p
15. Böke, H., Akkurt, S., İpekoğlu, U.E.: Characteristics of brick used as aggregate in historic brick-lime mortars and plasters. *Cem. Concr. Res.* **36**, 1115–1122 (2006)
16. Shi, C., Day, R.L.: Chemical activation of blended cements made with lime and natural pozzolans. *Cem. Concr. Res.* **23**, 1389–1396 (1993)
17. Yücel, K.T., Gülmez, S.: Chemical, mineralogical and petrographical analyzes of historical building materials of Hellenistic, Roman, Byzantine and Seljuk's period in Anatolia. In: Hughes, J.J., Leslie A.B., Walsh, J.A. (eds.) *Proceedings of the 10th Euroseminar on Microscopy Applied to Building Materials*, Paisley, pp. 1–21, 21–25 June. University of Paisley, Paisley (2005)
18. Baronio, G., Bindu, L., Lombardini, N.: The role of brick pebbles and dust in conglomerates based on hydrated lime and crushed bricks. *Construct. Build. Mater.* **11**(1), 33–40 (1997)
19. Genestar, C., Palou, J., Pons, C.: Thermal study of historic mortars from Mallorca. In: 1st historical mortars conference, Lisbon, Portugal, pp. 1–12, 24–27 September 2008
20. Alvarez, J.I., Navarro, I., Martín, A., García Casado, P.J.: A study of the ancient mortars in the north tower of Pamplona's San Cernin church. *Cem. Concr. Res.* **30**, 1413–1419 (2000)
21. Maravelaki-Kalaitzaki, P., Bakolas, A., Karatasios, I., Kilikoglou, V.: Hydraulic lime mortars for the restoration of historic masonry in Crete. *Cem. Concr. Res.* **35**, 1577–1586 (2005)
22. Franzini, M., Leoni, L., Lezzerini, M.: A procedure for determining the chemical composition of binder and aggregate in ancient mortars: its application to mortars from some medieval buildings in Pisa. *J. Cult. Herit.* **1**, 365–373 (2000)
23. Biscontin, G., Birelli, M.P., Zendri, E.: Characterization of binders employed in the manufacture of Venetian historical mortars. *J. Cult. Herit.* **3**, 31–37 (2002)
24. Pintér, F., Csányi, S., Weber, J., Bajnóczki, B., Tóth, M.: 16th century hydraulic mortars from the Ottoman Rác bath in Budapest, Hungary. In: Middendorf, B., Just, A., Klein, D., Glaubitt, A., Simon, J. (eds.) *Extended Abstracts (and CD-Rom with full papers) of the 12th Euroseminar on Microscopy Applied to Building Materials (EMABM)*, Dortmund, Germany (2009)
25. Luxán, M.P., Dorrego, F.: Ancient XVI century mortar from the Dominican republic: its characteristics, microstructure and additives. *Cem. Concr. Res.* **26**(6), 841–849 (1996)
26. Bultrini, G., Fragaia, I., Ingo, G.M., Lanza, G.: Minero-petrographic, thermal and microchemical investigation of historical mortars used in Catania (Sicily) during the XVII century AD. *Appl. Phys. A* **83**, 529–536 (2006)
27. Bruno, P., Calabrese, D., Di Pierro, M., Genga, A., Laganara, C., Manigrassi, D.A.P., Traini, A., Ubbrìaco, D.: Chemical-physical and mineralogical investigation on ancient mortars from the archaeological site of Monte Sannace (Bari-Southern Italy). *Thermochim. Acta* **418**, 131–141 (2004)
28. Belfiore, C.M., La Russa, M.F., Mazzoleni, P., Pezzino, A., Russo, L.G., Viccaro, M.: Technological study of “ghiara” mortars from the historical city centre of Catania (Eastern Sicily, Italy) and petro-chemical characterisation of raw materials. *Environ. Earth Sci.* (2010). doi:10.1007/s12665-009-0418-5
29. Tunçoku, S.S., Caner-Saltik, E.N.: Opal-A rich additives used in ancient lime mortars. *Cem. Concr. Res.* **36**, 1886–1893 (2006)
30. Nijland, T.G., Larbi, J.A., de Rooij, M.R., Polder, R.B.: Use of Rhenish trass in marine concrete: a microscopic and durability perspective. *Heron* **52**(4), 269–286 (2007)
31. van Hees, R.P.J., Brendle, S., Nijland, T.G., de Haas, G.J.L.M., Tolboom, H.J.: Decay of Rhenish tuffs in Dutch monuments. Part 2: laboratory experiments as a basis for the choice of restoration stone. *Heron* **48**(3), 167–177 (2003)
32. Bleazard, G.: The history of calcareous cements. In: Hewlett, P.C. (ed.) *Lea's Chemistry of Cement and Concrete*, 4th edn, pp. 1–23. Butterworth Heinemann, Oxford (1998)

33. Moropoulou, A., Bakolas, A., Anagnostopoulou, A.: Composite materials in ancient structures. *Cem. Concr. Res.* **27**, 295–300 (2005)
34. Mary: 1817 Louis Invents Artificial Cement, 190 p. Normandie Roto Impression s.a., Lonrai (2000)
35. Pasley, C.W.: In: Wingate, M. (ed.) *Observations on Lime*, 160 p. Donhead publishing, Lower Coombe (First published in 1838) (1997)
36. Mertens, G., Lindqvist, J.E., Sommain, D., Elsen, J.: Calcareous hydraulic binders from a historical perspective. In: *Proceedings of the Historical Mortar Conference HMC08*, Lisbon, Portugal (2008)
37. Mertens, G., Elsen, J., Laduron, D., Brulet, R.: Minéralogie des silicates de calcium présents dans des mortiers anciens à Tournai. *ArcheoSciences – Revue d'Archéométrie* **30**, 61–65 (2006)
38. Miranda, J., Pires, J., Carvalho, A.P.: Assessment of the binder amount of mortars by various techniques. In: *1st Historical Mortars Conference*, Lisbon, Portugal, pp. 1–12, 24th–27th September 2008
39. Elsen, J., Brutsaert, A., Deckers, M., Brulet, R.: Microscopical study of ancient mortars from Tournai. *Mater. Charact.* **53**, 289–294 (2004)
40. Alvarez, J.I., Martín, A., García Casado, P.J., Navarro, I., Zornoza, A.: Methodology and validation of a hot hydrochloric acid attack for the characterization of ancient mortars. *Cem. Concr. Res.* **29**, 1061–1065 (1999)
41. Adriano, P., Santos Silva, A., Veiga, R., Mirão, J., Candeias, A.: Unravelling the secrets of traditional lime mortars. In: *1st Historical Mortars Conference*, Lisbon, Portugal, pp. 1–18, 24th–27th September 2008
42. Santos Silva, A., Veiga, R., Adriano, P., Magalhães, A., Pires, J., Carvalho, A., Cruz, A.J., Mirão, J., Candeias, A.: Characterization of historical mortars from Alentejo's religious buildings. In: *1st Historical Mortars Conference*, Lisbon, Portugal, pp. 1–17, 24th–27th September 2008
43. Bonilla, T., Almeida, H., Carneiro, A.: Physical-chemical characterization of mortars in the church and Sacred Heart of Jesus Sanctuary, Igarassu, Pernambuco, Brazil. In: *1st Historical Mortars Conference*, Lisbon, Portugal, pp. 1–14, 24th–27th September 2008
44. Starinieri, V., Papayianni, I., Stefanidou, M.: Study of materials and technology of ancient floor mosaics' substrate. In: *1st Historical Mortars Conference*, Lisbon, Portugal, pp. 1–9, 24th–27th September 2008
45. Middendorf, B., Hughes, J.J., Callebaut, K., Baronio, G., Papayianni, I.: Chemical characterisation of historic mortars In: Groot, C., Ashall, G., Hughes, J. (eds.) *Characterisation of Old Mortars with Respect to Their Repair – Final Report of RILEM TC 167-COM*, pp. 39–56. RILEM, Bagneux (2004)
46. Hofkens, T.: *Chemisch-mineralogische karakterisering van de mortels van de domestic area te Sagalassos (Turkije)*. Master-thesis, unpublished, KULeuven, Leuven (2003)
47. Callebaut, K., Elsen, J., Van Balen, K., Viaene, W.: Nineteenth century hydraulic restoration mortars in the Saint Michael's Church (Leuven, Belgium). Natural hydraulic or cement? *Cem. Concr. Res.* **31**, 397–403 (2001)
48. Callebaut, K.: Characterisation of historical lime mortars in Belgium: implications for restoration mortars. PhD thesis, KULeuven, Belgium, unpublished (2000)
49. Degryse, P.: Mineral resources and their use on the territory of Sagalassos (SW Turkey). PhD thesis, KULeuven, Belgium, unpublished (2001)
50. Schouenborg, B., Lindqvist, J.E., Sandström, H., Sandström, M., Sandin, K., Sidmar, E.: Analysis of old lime plaster and mortar from southern Sweden – a contribution to the Nordic seminar on building limes. SP Report 1993-34, 34p (1993)
51. Moropoulou, A., Bakolas, A., Bisbikou, K.: Characterization of ancient, byzantine and later historic mortars by thermal and X-ray diffraction techniques. *Thermochim. Acta* **269**(270), 779–795 (1995)
52. Bakolas, A., Biscontini, G., Contardi, V., Franceschi, E., Moropoulou, A., Palazzi, D., Zendri, E.: Thermoanalytical research on traditional mortars in Venice. *Thermochim. Acta* **269**(270), 817–828 (1995)
53. Bakolas, A., Biscontini, G., Moropoulou, A., Zendri, E.: Characterization of the lumps in the mortars of historic masonry. *Thermochim. Acta* **269**(270), 809–816 (1995)

54. Silva, D.A., Wenk, H.R., Monteiro, P.J.M.: Comparative investigation of mortars from Roman Colosseum and cistern. *Thermochim. Acta* **438**, 35–40 (2005)
55. Moropoulou, A., Polikreti, K., Bakolas, A., Michailidis, P.: Correlation of physicochemical and mechanical properties of historical mortars and classification by multivariate statistics. *Cem. Concr. Res.* **33**, 891–898 (2003)
56. Pavía, S., Caro, S.: An investigation of Roman mortar technology through the petrographic analysis of archaeological material. *Construct. Build. Mater.* **22**, 1807–1811 (2008)
57. Baronio, G., Binda, L.: Study of the pozzolanicity of some bricks and clays. *Construct. Build. Mater.* **11**(1), 41–46 (1997)
58. Kramar, S., Lux, J., Mirtič, B.: Characterization of mortars from the roman archaeological site near Mošnje (Slovenia). In: 1st Historical Mortars Conference, Lisbon, Portugal, pp. 1–10, 24th–27th September 2008
59. Benedetti, D., Valetti, S., Bentempi, E., Piccioli, C., Depero, L.E.: Study of ancient mortars from the Roman Villa od Pollio Felice in Sorrento (Naples). *Appl. Phys. A* **79**, 341–345 (2004)
60. Degryse, P., Elsen, J., Waelkens, M.: Study of ancient mortars from Sagalassos (Turkey) in view of their conservation. *Cem. Concr. Res.* **32**, 1457–1463 (2002)
61. Güleç, A., Tulun, T.: Physico-chemical and petrographical studies of old mortars and plasters of Anatolia. *Cem. Concr. Res.* **27**(2), 227–234 (1997)
62. Diekamp, A., Konzett, J., Mirwald, P.W.: Mineralogical characterization of historical mortars from Tyrol, Austria and South-Tyrol, Italy. In: 1st Historical Mortars Conference, Lisbon, Portugal, pp. 1–11, 24th–27th September 2008
63. Fratini, F., Pecchioni, E., Cantisani, E.: The petrographic study in the ancient mortars characterization. In: 1st Historical Mortars Conference, Lisbon, Portugal, pp. 1–10, 24th–27th September 2008
64. Elsen, J.: Microscopy of historic mortars – a review. *Cem. Concr. Res.* **36**, 1416–1424 (2006)
65. Mertens, G., Van Balen, K., Elsen, J.: Microscopy as a tool for the provenance determination of raw materials and production technology used in ancient mortars from Tournai (Belgium). In: 12th Euroseminar on Microscopy Applied to Building Materials, University of Dortmund, Dortmund, Germany (2009)
66. Mertens, G.: Characterisation of historical mortars and mineralogical study of the physico-chemical reactions on the pozzolan-lime binder interface. PhD thesis, KULeuven, Belgium (2009). ISBN 978-90-8649-285-5
67. Stepkowska, E.T., Pérez-Rodríguez, J.L., Sayagués, M.J., Martínez-Blanes, J.M.: Calcite, vaterite and aragonite forming on cement hydration from liquid and gaseous phase. *J. Therm. Anal. Calorim.* **73**, 247–269 (2003)

Characterisation of Decorative Portuguese Gypsum Plasters from the Nineteenth and Twentieth Centuries: The Case of the Bolsa Palace in Oporto

**Teresa Freire, António Santos Silva, Maria do Rosário Veiga,
and Jorge de Brito**

Abstract The use of gypsum plaster for the interior coating of walls and ceilings in the Portuguese architecture was particularly expressive in the period between the eighteenth and the twentieth century. However, information about this important heritage is almost nonexistent, which is leading to a rapid loss of important patrimony. In this paper the results of the characterisation of five gypsum plaster samples from the second half of the nineteenth century belonging to the *Arabian Room* of the *Bolsa Palace*, located in Oporto, North of Portugal, are presented and discussed. XRD and TGA-DTA techniques were used to establish the mineralogical composition, and the relative proportions of the binders. Optical microscopy and FESEM-EDS observations were performed both in fractured and polished surfaces in order to determine the stratigraphy and the composition of individual layers. The results of this characterisation work showed that the plasters used were mainly composed of gypsum and hydrated lime in different proportions – a feature that was correlated with the application techniques of the decorative elements analysed – and allowed the determining of the restoration interventions they had already been submitted to. Some physical properties like the dynamic modulus of elasticity and capillary absorption were also determined, and a correlation between the results obtained was established with previous studies performed by the authors.

T. Freire (✉) • A.S. Silva • M. do Rosário Veiga
Laboratório Nacional de Engenharia Civil, Lisbon, Portugal
e-mail: mtlfreire@gmail.com; ssilva@lnec.pt; rveiga@lnec.pt

J. de Brito
Instituto Superior Técnico, Lisbon, Portugal
e-mail: jb@civil.ist.utl.pt

1 Introduction

The preservation of building construction cultural heritage is considered of major importance to understand human History.

In fact, the knowledge of the materials and techniques used and their evolution throughout the different historical periods and geographical regions worldwide are a precious source of information, not only from the architectural and construction point of view, but also from the human and social sciences' [1, 2].

In the twentieth century the preservation of the world's cultural heritage began to be highlighted, particularly in Europe, with the elaboration of various international documents, aiming at establishing directives and rules to be followed on the patrimony interventions, namely the Athens Charter (1931), the Venice Charter (1964) and, more recently, the Krakow Charter (2000) [3]. In this last document the preservation of the original materials is strongly recommended.

The historical evolution of their use in the construction of buildings is thus of extreme importance, as it helps the researchers on the establishment of new methodologies of intervention.

The use of gypsum plasters in European architecture is thought to have been introduced by the Greeks, who received the knowledge of how to manufacture and use this material from the Egyptians and the Minoans [4].

Via the Romans, this knowledge also reached Central and Northern Europe. Throughout the centuries it became part of the traditional European way of building, alone or mixed with other materials, like lime, sand and several organic additives.

Contrary to what is thought, it had very distinct applications, such as masonry mortars, floor screeds and relieved decorations of walls, architectural elements or a base for decorative frescoes [4]. The medieval technology of gypsum mortars and floor screeds, for example, has been rediscovered and used in restoration and reconstruction works only in the last decade of the twentieth century [5].

However, gypsum plasters had their heyday, without a doubt, in the Baroque and Rococo periods with the possibility of imitating noble materials, like marble, often even more rich in colour and veining than the original materials [6].

In Portugal, the use of gypsum plasters was also thought to have been likely since the Roman period, especially for the manufacture of elaborate decorations or as a base of wall paintings [7, 8]. However, recent studies of characterisation of the materials used for the plastering of walls and ceilings did not confirm it so far [9].

In fact, these analytical studies showed that the use of gypsum plasters in Portugal was only particularly expressive between the eighteenth century and the early twentieth century.

The quality and variety of decorations in Portuguese monumental and domestic architecture from that period contrasts with the lack of information on the materials and the techniques of application used to produce them [7, 10, 11]. Therefore, the study of this subject is significant for the restoration and conservation of such an important heritage and should provide a decisive contribution for the reduction of its rapid loss [10–13].



Fig. 1 General view of the *Arabian Room* (*left*) and detail of some stucco decorations (*right*)

The present research occurs in this context, where the microstructural, chemical and physical characterisation of the decorative historical gypsum plasters from the nineteenth and twentieth centuries is the first step to reach the final purpose: the development of new compatible gypsum products for the repair of the ancient plasters.

Besides the lack of knowledge about the materials used, there are usually no records about their techniques of preparation and application, even from subsequent interventions on existing mortars [10]. The case study presented in this paper follows that trend. The aim of this research is to study the materials used and also the methodology adopted by the plasterers for their application.

2 Experimental Programme

2.1 Case Study – The Arabian Room of the Bolsa Palace

The samples studied in this paper belong to the *Arabian Room* of the *Bolsa Palace*, a building located in the city of Oporto, in the North of Portugal. Considered an architectural icon of the nineteenth century and also one of the greatest examples of the neoclassical style, it is classified as a national monument.

The *Arabian Room* (Fig. 1) is the most emblematic of all the palace's rooms and the only one of its kind in the country as it embodies the clearest expression of the neo-Moorish art in Portugal. Its construction began in 1862 and was finished only in 1880. The coloured stucco decorations were inspired by the Palace of the Alhambra, in Granada, Spain, and cover practically the whole ceilings and walls, constituting one of the richest and most original decorative Portuguese gypsum plasters of this period [14].

Unfortunately there are no historical records about the decoration of this room, neither about the materials, nor about the techniques of application used. Thus the characterisation work became an essential basis for the restoration works performed there in 2010.

Table 1 Identification and description of samples

Identification	Sample description
PB1	Frame from the ceiling (gilded) (Fig. 2)
PB2	Ornaments from the breathing holes of the ceiling (gilded) (Fig. 2)
PB3	Octagonal base of PB2 (gilded) (Fig. 2)
PB4	White ornaments from the ceiling
PB6	Preparation layers and ornament of a wall of the gallery (with polychromes)

**Fig. 2** Sample PB1 (left) and PB2 plus PB3 (right)

2.2 Sampling

A total of six samples were collected by the authors in two different ways: indirectly, meaning they had been previously detached due to some anomaly in the building (five samples) and directly on site (sample PB6). They all belong to elements of the decorative program.

After the first visual observation, sample PB5 was rejected due to strong evidence of not being original: the golden layer is painted and the interior metal frame is not rusted like the others, showing a superficial blue colour (possibly copper reacting to copper sulphate).

The identification and description of the samples studied is summarized in Table 1; Fig. 2 shows two of these samples.

2.3 Analytical Methods

The mineralogical and chemical properties of the samples were determined using the analytical methodology developed by Santos Silva et al. [15]. After a detailed visual observation of the samples and photographic recording, they were dried at 40°C for approximately 12 h. To enable the detection of the possible presence of hygroscopic compounds or soluble salts that can lose their crystallinity, the samples were not dried to mass constancy. Each specimen was split into several fractions to be used for different techniques.

Polished surfaces of the gypsum samples were prepared by impregnation under vacuum with an epoxy resin. They were observed with an Olympus stereo-zoom microscope in order to study the textural properties of the layers in the samples (to define the stratigraphy) and to identify the mineralogy and morphology of the aggregates and possible pigments. Images were recorded digitally.

The stereo-zoom microscope was also used to observe the fractured surfaces of some of the samples, giving an invaluable contribution to the clarification of their techniques of application.

X-ray diffraction was performed to allow a further insight into the mineralogy of the binder and other constituents such as the aggregates. A Philips X'Pert diffractometer with cobalt K α radiation, a step equal to 0.05°/s, and between 3° and 74° 20, was used.

The thermo-analytical techniques provided additional data on the quantitative composition of the samples, namely the relationship between the gypsum and calcite content. A Setaram TG-DTA analyser was operated in an argon atmosphere and with a uniform heating rate of 10°C/min from room temperature to 1,000°C.

Scanning electron microscopy observations on polished surfaces were performed in backscattered electron image mode (BSE) on a field emission scanning electron microscope (FESEM) JEOL JSM7001F coupled with an OXFORD energy dispersive spectrometer X-RAY detector (EDS). The polished surfaces were sputtered with a gold palladium film in a BALTEC sputter coater.

Some physical properties were also determined using a methodology developed by Veiga et al. [16]. The samples collected were irregular; they were cleaned of any powder and biological colonisation before being maintained within a controlled environment (23°C and 50% RH). Water absorption tests were performed using the capillary absorption by contact technique [16]. The dynamic modulus of elasticity was determined using ultrasounds, based on the emission of high frequency sound waves and the measurement of their velocity through building materials, allowing the calculation of elastic parameters (BS 1881-Part 203). Special exponential electrodes were used with sharp ends that provide good contact with the samples surface (Fig. 3).

3 Results and Discussion

The data obtained by visual observation of the samples, both directly and with the stereo-zoom microscope, is summarized in Table 2 (Fig. 4). It was difficult to determine how many layers composed samples PB1 and PB6, and only after observation under the stereo-zoom microscope was it decided which of them would be able to be separated and analysed by XRD and TGA-DTA.

In the case of PB1 a polished surface was prepared for stratigraphic analyses (Fig. 5).

Due to the large number of layers and low thickness of most, their composition was first determined by FESEM-EDS (Table 3, Fig. 6).



Fig. 3 Determination of the dynamic modulus of elasticity

Table 2 Visual observation of the samples

Sample	No. of layers	Identification	Description
PB1	Min.10	PB1/1 + PB1/2	White plaster layers from within the moulded frame ^a
		PB1/3	Very thin yellowish plaster layer, immediately above PB1/1 + PB1/2 that seemed to display some flexibility
		PB1/4	Very thin layers (at least 7), consisting of the preparation for the 1st gold leaf application and subsequent restoration operations, till the 2nd gold leaf (the last layer, already decayed)
PB2	1	PB2	Fragments from a breathing hole ornament of the ceiling. This ornament showed traces of Armenian bole, gold leaf and restoration plaster(s)
PB3	1	PB3	Octagonal base of PB2. It presented restoration plaster(s) and traces of Armenian bole and gold leaf
PB4	1	PB4	Fragments of white ornaments from the ceiling. These fragments had traces of a blue paint in the base of the side faces that had a different colour in one of them
PB6	3	PB6/1	White preparation layer of a wall of the gallery (Fig. 4, left)
		PB6/2	Thin layer that is the finishing layer in the surfaces where there are no ornaments applied (with polychromes) and works as “glue mortar” between the preparation layer (PB6/1) and the ornaments (PB6/3)
		PB6/3	Ornaments moulded directly on the wall, applied with the PB6/2 layer still fresh (with polychromes) (Fig. 4)

^aAnalysed together by XRD and TGA-DTA as it was very difficult to have a physical separation with 100% certainty



Fig. 4 Sample PB6: preparation layer, PB6/1 (*left*) and ornament, PB6/3 (*right*)

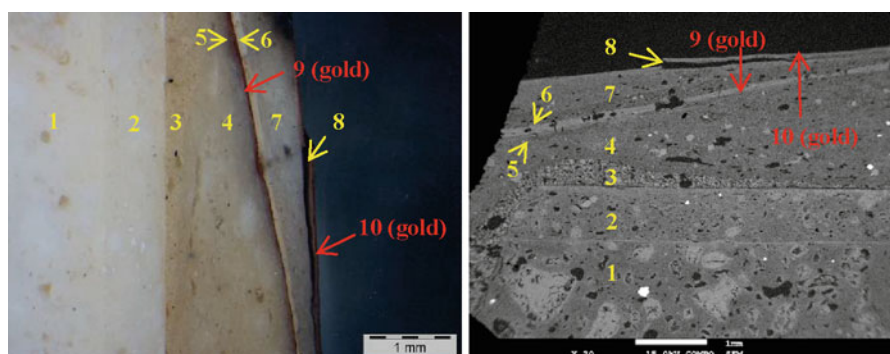


Fig. 5 Polished surface of PB1: stereo-zoom microscope (*left*) and SEM-BSE image (*right*)

Table 3 FESEM-EDS results for sample PB1 stratigraphic analysis

Sample	Layers				
PB1	1+2	3, 6	4, 7	5, 8	9, 10
EDS	Ca, S, C, O (gypsum, calcite)	Ca, C, O (calcite)	Ca, S, O (gypsum)	Si, Al, Mg, Ca, Fe (Armenian bole)	Au, traces of Ag

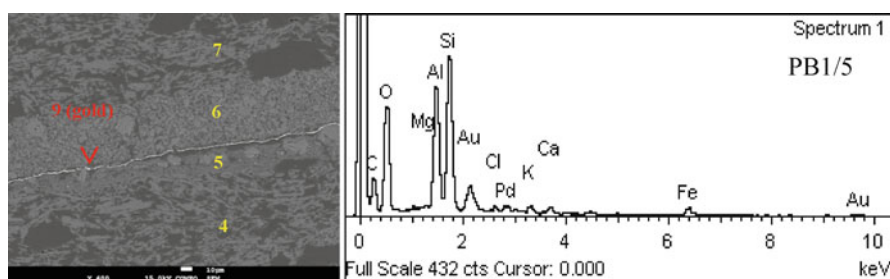


Fig. 6 Polished surface of PB1: FESEM image (*left*) and EDS of layer 5 (*right*)

Table 4 XRD results and calculated gypsum/calcite content through TGA results

Sample	Identified crystalline compounds					Calculated gypsum and calcite contents (%)	
	Gypsum	Calcite	Quartz	Celestine	Halite	$\text{CaSO}_4 \cdot 2\text{H}_2\text{O}$	CaCO_3
PB1/1 PB1/2	+++	++/+++	?	—	—	63	32
PB1/3	++	+++	trc	—	trc	26	69
PB2	++++	—	trc	—	—	97	3
PB3	++++	+	?	—	—	90	6
PB4	+++	+++	?	—	—	51	45
PB6/1	++++/++++	++	trc	trc	—	77	18
PB6/2	++++/++++	+	trc	trc	—	83	9
PB6/3	++++	trc	trc	trc	—	93	1

Notation used in XRDPeak intensity:

++++ very high proportion (predominant compound)

+ weak proportion

+++ high proportion

trc traces

++ medium proportion

— not detected

The first restoration layer is the 6th. Its morphology and composition is similar to the 3rd layer and differs from all the others. In fact, calcite is the main constituent of these two layers which also have a common function: to promote good binding with the precedent layer in order to be strongly attached to it.

This pattern in similarity of composition / morphology / function can also be observed between the other original *versus* restoration layers (3, 4, 5 and 9 similar to 6, 7, 8 and 10, respectively).

XRD and TGA-DTA analyses were then applied to the first two layers together (it was not possible to separate them) and to the third layer (Table 4).

For the mix of the first two layers, XRD and TGA-DTA results are in agreement with those obtained by FESEM-EDS, indicating that they are mainly composed of gypsum, with calcite being the second constituent. However, for the third layer EDS analyses detected only calcite, while XRD and TGA-DTA clearly indicated the presence of gypsum, probably due to sample contamination during its separation.

Another feature that was noticed in the observation of the polished surface of PB1 is the change in the design of the frame due to the restoration; the lines of the original piece have been slightly straightened as a result of this procedure.

Sample PB6 was also observed under the stereo-zoom microscope in order to clarify some uncertainties: (a) PB6/1 seemed to have 2 distinct layers, as it showed a preferential fracture pattern and (b) the way the PB6/3 had been moulded (directly on site or pre-cast) was an enigma. These observations gave the answers to the previous questions: (a) a very discrete interface exists in part of the polished surface of PB6/1 (Fig. 7), which means that the plaster was in fact applied in two parts; however each part must have been applied immediately after the other, as the intergrowth of the crystals between them seems to be very high indicating the lack of two distinct layers; (b) the interface between PB6/2 and PB6/3 has small empty

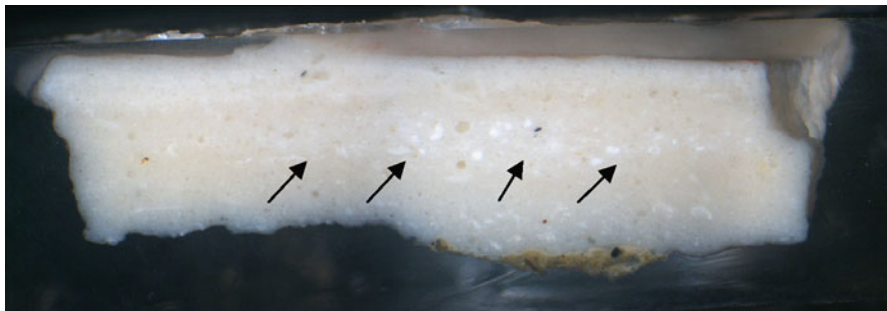


Fig. 7 Very discreet interface between two “layers” on sample PB6/1

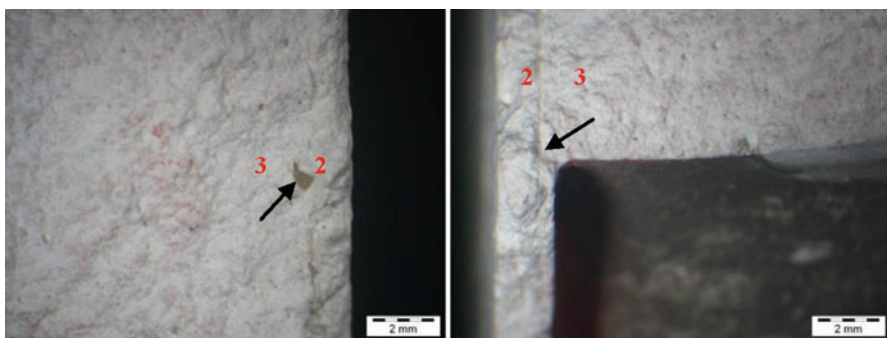


Fig. 8 Interface between layers 2 and 3 on sample PB6

Table 5 Results of the physical properties determined and comparison with the calculated chemical content

Sample	DME (MPa)	Ccc – 5 min (kg/m ² /h ^{1/2})	Bulk density ^(a) (kg/m ³)	Calculated gypsum and calcite content (%)	
				CaSO ₄ ·2H ₂ O	CaCO ₃
PB4	970	24.38	995	51	45
PB6/3	2,590	–	1,045	93	1

^aCalculated: weight/(area of the base × height)

holes that are present in both (Fig. 8, left) which means they were applied one after the other or, in other words, the ornament PB6/3 has been moulded directly on site, when PB6/2 was still fresh. In fact, an accurate observation of other areas of this interface confirms this information, like the evidence that PB6/3 was pressed against PB6/2 (Fig. 8, right).

Physical properties were only determined in the samples where the quantity and shape were appropriate to perform the corresponding experimental techniques. The dynamic modulus of elasticity (DME) was determined in samples PB4 and PB6/3 and the coefficient of capillary absorption by contact (Ccc) only in sample PB4 (Table 5).

The low DME of sample PB4 is in agreement with its high Ccc after 5 min and follows the usual inverse relationship between these two parameters; however, it is lower than usually found in samples with the same gypsum/calcite composition and density [17]. The use of air entraining admixtures is a possible explanation but is very difficult to prove.

On the other hand, for sample PB6/3 the DME result is in total agreement with those already found in previous studies for samples of pre-cast elements with high gypsum content [17].

4 Conclusions

All the samples analysed showed evidence of having already undergone some restoration which, in the case of PB1, introduced a slight change in the design of the respective element.

The samples belonging to decorative gypsum plasters can be divided into two groups: (1) those prepared with a mixture of gypsum and hydrated lime that has carbonated and appears now as calcite (PB1/1 + PB1/2 and PB4); (2) those prepared mainly with gypsum (PB2 and PB3 were pre-cast and PB6/2 and PB6/3 were applied directly on site, one immediately after the other).

The use of a mixture of gypsum and lime in PB1/1 and PB1/2 can be explained by the fact that they form the inner structure of a frame which seems to have been moulded on a bench, a technique that requires a longer time to mould a piece. In fact, it is similar to moulding a frame *in situ*, for example, where the need for a thicker consistency and a longer setting time of the paste is also fulfilled by the use of a mixture of gypsum and hydrated lime [17, 18].

On the contrary, the paste for precast has to be poured onto a mother mould in a quite liquid consistency and it is desirable to set quickly after that, a situation where the use of gypsum without hydrated lime is advantageous. In the case of sample PB4 the reason for not using this procedure must have been different as one can clearly see that the constituent elements were pre-cast before being applied to the ceiling.

The preparation layer PB6/1 was applied directly on the mortar as is usual in these situations. It has an average thickness of 6 mm and presents a textured pattern in the outer face, in order to improve adhesion of the subsequent layer PB6/2. The volumetric proportion of gypsum to hydrated lime used to prepare it is above 2:1, i.e. is much higher than the 1:1 proportion usually used in similar cases [17, 18]. Maybe the experimental data from other case studies of the north of Portugal will help to find out whether this was due to a regional influence or just a coincidence.

The materials used in the manufacture of the decorative gypsum plasters of the *Arabian Room* of the *Bolsa Palace*, in Oporto, were carefully chosen according to the purpose and techniques of application, even in some of the later interventions (the case of the frame from the ceiling, corresponding to sample PB1). The stucco decoration of this room's walls and ceilings is undoubtedly one of the most precious works of art of its kind in Portugal.

Acknowledgements Teresa Freire's PhD research is being supported by the scholarship SFRH/BD/40128/2007 from Fundação para a Ciência e Tecnologia (FCT). The authors would like to thank technicians Susana Couto and Paula Menezes from the Materials Department and Ana Maria Francisco from the Buildings Department of LNEC, for their support in the execution of the experimental work.

References

1. Gourdin, W.H., Kingery, W.D.: The beginnings of pyrotechnology: Neolithic and Egyptian lime plaster. *J. Field Archaeol.* **2**(1–2), 133–150 (1975)
2. Kingery, W.D., Vandiver, P.B., Prickett, M.: The beginnings of pyrotechnology, part II: production and use of lime and gypsum plaster in the pre-pottery Neolithic near East. *J. Field Archaeol.* **15**(2), 219–244 (1988)
3. http://www.igespar.pt/pt/patrimonio/legislacao_sobre_patrimonio/. Accessed 9 June 2011
4. Starck, J., Wicht, B.: Zur historie des gipses. *ZKG Int.* **52**(10), 527–533 (1999)
5. Middendorf, B., Knöfel, D.: Characterization of historic mortars from buildings in Germany and the Netherlands. In: Baer, N.S., Fitz, S., Livingston, R.A. (eds.) *Conservation of Historic Brick Structures: Case Studies and Reports of Research*. Donhead Publishing, Dorset (1998)
6. Gárate Rojas, I.: Artes de los yesos, yeserías y estucos, 381 p. Instituto Español de Arquitectura. Editorial Munilla-Lería, Madrid (1999). ISBN 84-89150-25-7
7. Vieira, E.: Traditional techniques of plasterwork and simulated plasterwork decorations in the north of Portugal. A contribution to their study and conservation. Master thesis, University of Évora, Évora, Portugal (in Portuguese) (2002)
8. Silva, H.: Giovani Grossi and the evolution of decorative plasterwork in Portugal in the 18th century. Master thesis, Lusíada University, Lisbon, Portugal (in Portuguese) (2005)
9. Freire, T., Santos Silva, A., Veiga, R., de Brito, J.: Characterisation of Old Portuguese plasters from walls and ceilings. In: *Proceedings of the 3rd Portuguese Congress of Construction Mortars*, Paper 11, 14 p. (in Portuguese) (2010)
10. Cotrim, H., Veiga, R., de Brito, J.: Freixo palace: rehabilitation of decorative gypsum plasters. *Constr. Build. Mater.* **22**(1), 41–49 (2008)
11. Cotrim, H., Veiga, R., de Brito, J.: Methodology for the rehabilitation of ancient gypsum plasterwork. *J. Build. Apprais.* **3**(3), 195–212 (2007)
12. Silveira, P., Veiga, R., de Brito, J.: Gypsum coatings in ancient buildings. *Constr. Build. Mater.* **21**(1), 126–131 (2007)
13. Silveira, P., Veiga, R., de Brito, J.: Cracking of ancient gypsum plasters. In: *Proceedings of the XXX IAHS World Congress on Housing*, Coimbra, pp. 1779–1785, September 2002
14. The Palácio da Bolsa. ArtEditores, Porto (2009)
15. Santos Silva, A., Paiva, M., Ricardo, J., et al.: Characterization of Roman mortars from the archaeological site of Tróia (Portugal). *Mater. Sci. Forum* **516**, 1643–1647 (2005)
16. Veiga, M.R., Magalhães, A., Bosiljkov, V: Capillarity tests on historic mortar samples extracted from site. Methodology and compared results. In: *Proceedings of the 13th International Brick and Block Masonry Conference*, Lisbon (2004)
17. Freire, T., Santos Silva, A., Veiga, M.R., de Brito, J.: Characterization of Portuguese historical gypsum mortars: a comparison between two case studies. *Mater. Sci. Forum* **636–637**, 1258–1265 (2010). Online since 2010/Jan/12 <http://www.scientific.net>
18. Freire, T., Santos Silva, A., Veiga, M.R., de Brito, J.: Characterization of Portuguese historical gypsum mortars. In: *Proceedings of the 1st Historical Mortars Conference*, Lisbon (2008). T_I_54_HMC008 (available in CD)

Repair Mortars Studied for the Conservation of Temple G1 in Mŷ Son, Vietnam

Cristina Tedeschi, Luigia Binda, and Paola Condoleo

Abstract Since 2001 the authors have been involved with the archaeologists of the Fondazioni Lerici, Politecnico di Milano, in the preservation of some Hindu temples in Mŷ Son, Vietnam. The characterisation of the brick-masonry materials was carried out at the Politecnico di Milano. Especially interesting was the successful study of the natural resin used to bond externally the bricks in the masonry; this allowed the formulation of a new compatible resin to be used for the conservation project. In the masonry internal leaf, the joint material, based on clay, was substituted by a new hydrated lime and powdered bricks mortar. The results of the research presented here allowed the direct application of the new materials in the conservation project of G1, G3, and G5 of group G.

1 Introduction

When the contemporary principles and theories of conservation that have been developed mainly in the Western world are applied to Asian monuments, it is a difficult task to compromise with the position of the experts in that part of the world. Furthermore, when the monuments are at the state of ruin in archaeological sites it becomes more difficult to apply these principles. Conservation in countries that have suffered wars and consequent poverty is even more difficult, also due to lack of advanced techniques and materials.

The authors have been working since 2001 on the conservation of a group of buildings in Mŷ Son, Vietnam (called group G by H. Parmentier). The groups of temples in Mŷ Son were called by alphabetic letters from A to N by Parmentier,

C. Tedeschi (✉) • L. Binda • P. Condoleo
DIS, Politecnico di Milano, Milan, Italy
e-mail: tedeschi@stru.polimi.it

who discovered them in the jungle near DaNang at the end of the nineteenth century. Conservation works on group G began in 2004, followed by the Politecnico di Milano, within the framework of a tripartite contract between Politecnico, Institute for Conservation in Hanoi, and UNESCO, supported by the Italian Ministry of Foreign Affairs. The group G was built, as all the others, in brick masonry with some peculiarities.

Principles were applied to the preservation of the buildings, especially for the use of new materials, mortars, resins, and bricks. The choice of the new materials was made according to some important criteria: (i) the possibility of finding local materials and production techniques, (ii) control of the parameters defining the quality and compatibility of the new materials, and (iii) execution of the works on site by non-specialized workers.

The climate in Mŷ Son, typical of the tropical areas, has deeply influenced the choice of the mortar to be used to consolidate the internal part of the wall, which was two- or three-leaf masonry; the original material between the pieces of bricks constituting the internal leaf was simply clay and brick powder. In the meantime, the external joints were found to be made with a resin coming from a local tree. Therefore, when the works on the G group started, an investigation was carried out in the Northern and Central part of Vietnam in order to find a hydraulic binder. On the basis of the experimental research based on chemical, physical, petrographical, and mechanical tests, different compositions – from hydrated to hydraulic lime-based mortars – were examined. Unfortunately no suitable hydraulic lime was found in Vietnam, so the only possibility was to prepare a mortar based on hydrated lime and brick powder, which testing indicated was the best fit due to the proven pozzolanicity of the brick powder.

The paper will describe the results of the experimental tests in laboratory and on-site, where some specimens were prepared following the special conditions of temperature and humidity of the site. The difficulties of preparing the brick powder following the imposed grain size distribution and of realizing on-site the mortar composition and the quality control with available rough tools will also be described.

The chosen mortar composition gave acceptable properties in the short- and long-term, and some samples from the site examined in thin section and at SEM after 2 years gave evidence that very good pozzolanic reactions had taken place. Even at visual inspection, the top joints exposed to humid and rainy climate are still showing compactness.

2 Description of the Mŷ Son Hindu Temples

The archaeological area of Mŷ Son is situated in Central Vietnam, 30 km southwest from Da Nang; it is located in a valley surrounded by low mountains dominated by the Rang Meo mountain, and it is crossed by the Thu- Bôn river. The Mŷ Son area (Figs. 1 and 2) is 15 ha wide and composed of several groups of buildings made with brick masonry, each organized around a main temple (*Kalan*). Mŷ Son is the most

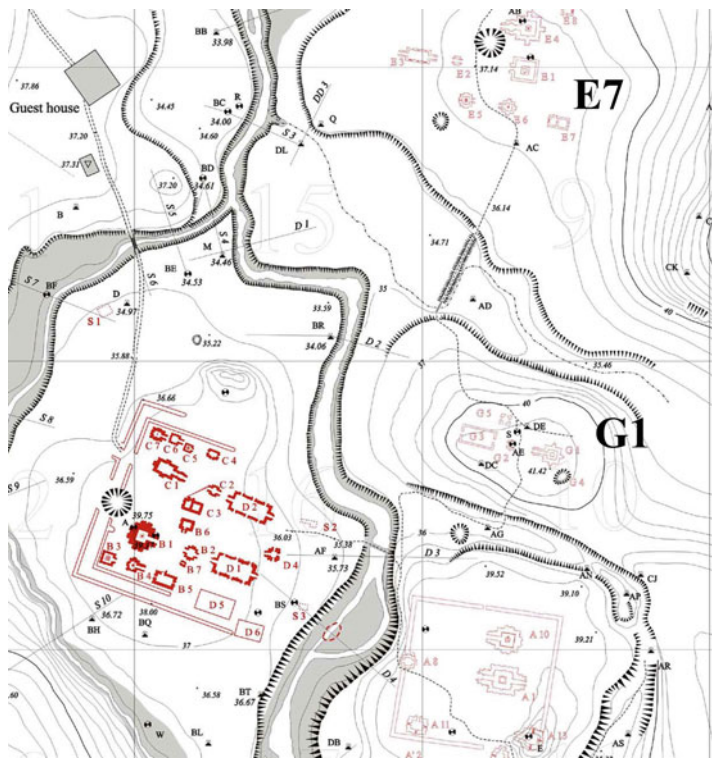


Fig. 1 The archaeological area of Mý Son

important holy place of the Champa kingdom. The Cham people built over 70 buildings here, from the sixth to the fourteenth century AD, but now only 30 with at least 1 m in elevation are still recognizable. The site was rediscovered after centuries of abandonment in 1898 and studied at the beginning of the twentieth century by French architect H. Parmentier, from the École Française d'Extrême Orient (EFEO) [1]. A Vietnamese-Polish expedition (led from 1982 until 1986 by K. Kwiatkowski and K. Hoang Dao) carried out restoration works on some group of buildings damaged during the war at the end of the 1960s [2].

The buildings in Mý Son are made of fired bricks thinly joined by natural resin. The wall section is made of two leaves with small connections or three leaves, with brick rubble in the middle and faced externally with bricks (Fig. 3). The most peculiar characteristic of the brick masonry was the special construction technique which created a bond between bricks so tight they practically did not show real joints (Fig. 4). The special building technique protects the walls from the attack of the vegetation; where the thin joint is not damaged, there are only very low biological attacks [3].

In order to realize a more tight physical bond, the technique of *rub-joining* was used during wall construction before applying the resin. Scratches can be seen on



Fig. 2 Mỹ Sơn: view of the groups C and D of temples



Fig. 3 Section of the wall



Fig. 4 The thin mortar joints masonry in prospect



Fig. 5 Scratches due to the rub-joining procedure

the horizontal and vertical surfaces of the bricks in contact with other bricks. The scratch can be clearly observed by a magnifier and even by naked eye (Fig. 5) [4].

Following some hypotheses that organic natural materials could have been used as binder between the bricks as in historic buildings in other parts of Vietnam and Southeast Asia, a careful study was carried out on materials sampled from the Mỹ Son masonry walls. Furthermore, it was decided for the safety and durability of the masonry in the future to use a new mortar based on hydrated lime and brick powder in the locally reconstructed parts and, when possible, to connect the three or two leaves.

3 Characterisation of the Existing Materials

In order to carry out laboratory research on the masonry materials, samples were taken during several visits to the site, starting from 2000. The samples were collected from the groups A, D, E, and G, which was a group of interest for the Italian pilot project. At DIS, Politecnico di Milano, the authors carried out several tests on the sampled materials in order to detect the properties of: bricks, brick assemblages, and joint material.

3.1 Material Sampling

Due to the difficulty of sampling without damaging the walls, the number of samples was rather small to be statistically representative of the materials used. Nevertheless the experimental research gave rather good results, as will be shown below. All the brick samples were taken from the material available on the ground (buildings A1, A13, B9, D4, and G1) or in the ruins (E4, E5, and E7) in order to avoid spoiling the standing parts of the buildings. In 2001, a special glue of vegetal origin, used for caulking of boats, was bought at the local market in Hoi An (RES1); in 2004 another resin coming from local trees (called Daù Rai) and sold as glue was bought close to the Mŷ Son site (RES2).

3.2 Chemical, Physical, and Mechanical Tests on Bricks, Joints, and Rubble Filling

The analyses concerned the bricks and the binder in the external joints and in the inner leaf of the walls. Chemical analyses according to [5] were carried out on the sampled materials [6].

The results showed that the composition of all sampled brick is the same, despite apparent visual differences. The composition of the bricks and of the so-called joint is also the same, but contains an organic resin. The presence of a very low CaO content in the joint (from 2.33% to 4.48%) showed that no lime was used in the external joints. Chemical analyses were also carried out on the material sampled from the internal leaf of the walls. They show that the composition of this material does not differ from that of the bricks [7].

Physical tests were performed on four to six small brick cubes (40 mm side) cut from the bricks; the tests were carried out according to the European standard (UNI EN 2001). The results show a certain in-homogeneity; nevertheless, some orientation values can be given as an average: (i) bulk density = 1,630 kg/m³, (ii) I.R.S from 0.41 to 1.92 kg/m²/min, (iii) water absorption coefficient = 160.09 g/cm² × s^{0.5}, and (iv) water absorption by total immersion between 18.18% and 23.99%.

Some XRD tests carried out on a specimen from A1 show that the bricks were fired at a temperature below 900°C, [7].

Compression tests were carried out on cubes (40 mm × 40 mm × 40 mm). Once again, all of the values were very much scattered, between 8 and 14 N/mm². The modulus of elasticity E and the Poisson coefficient were also calculated, and the values are typical of a rather soft material [7].

4 The Natural Resin Used for the External Joints

The “Giulio Natta” Department of Chemistry, Materials and Industrial Chemistry of the Politecnico di Milano (G. Zerbi), and the Institute of Biology of the Faculty of Science of the University of Milan (F. Tomé) have performed the chemical characterisation of the resin found in the joint [8]. The identification of the main components of the organic materials was carried out mostly by means of infrared spectroscopy with FT-interferometers. To help in the analysis, a few procedures of separation of the components have been followed, such as evaporation *in vacuo* and extraction with suitable solvents.

The idea behind these analyses was that the materials used in the building of the Mŷ Son temples should be fully related to what nature offers in the area and what people can manufacture locally from the resins of the trees that grow in the surrounding area. These trees belong to the species of the *dispterocarpaceae*.

The results of the analyses are as follows:

1. Identification of the chemical nature of sample of resin found in the area of Mŷ Son, RES1 (a special resin, liquid at room temperature, used for caulking boats) and RES2 (extracted as viscous fluid from a local tree called “Daù Raì”). The infrared spectrum of RES1 shows that Dammarenediol seems to have the highest relative concentration with respect to many other possible substances in much lower concentration. Difference spectroscopy provides the infrared spectrum of the volatile component of RES 1, which can be identified as alloaromadendrene. The two materials RES1 and RES2 are practically identical, thus indicating that the local people obtained the glue from local trees.
2. Analysis of the material scratched away from the joint (JRES1). Figure 6 shows the great similarity of the organic component extracted from JRES1 with the solid residue of RES1. The spectrum shows, however, that some chemical modifications have occurred from RES1 to JRES1. It is likely that the resin taken from the brick originally could have been just the resin from the trees; self-oxidation processes that possibly occurred over the many years could justify the spectral changes observed.

In conclusion, the new resins have a similar composition to the old ones and can be used for joint repair.

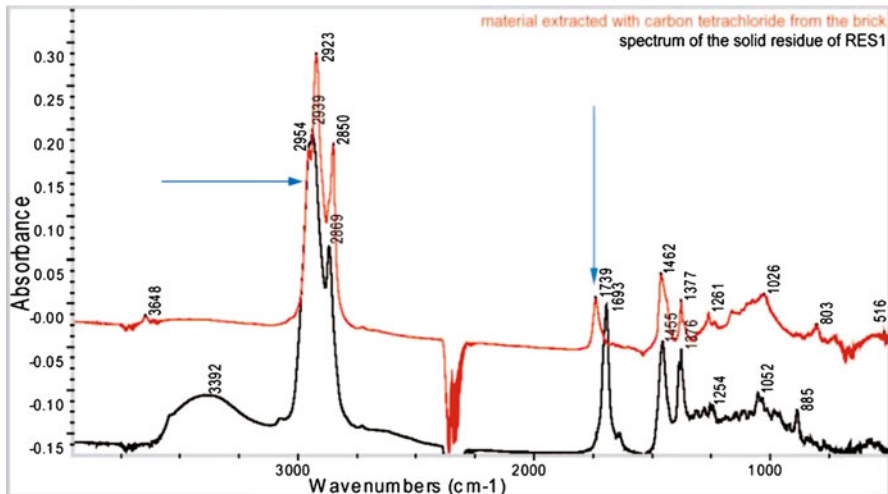


Fig. 6 Comparison of the FT-IR spectra of the material extracted with carbon tetrachloride from the brick (red) and the FT-IR spectrum of the solid residue of RES1

5 The Repair Mortar Composition

It was decided to use a lime based mortar for the repair or reconstruction of the internal leaf of the walls; the resin could not be used because the internal joints between rubble bricks were rather thick and the original joints were simply filled by clay. This mortar should be a hydraulic one, but as said above, it was practically impossible to find a hydraulic lime in the Mŷ Son area. Therefore, it was decided to choose a mortar made with hydrated lime and brick powder and/or pebbles if it could be detected that the Mŷ Son bricks were pozzolanic. Tests were carried out on powdered bricks from the site. The bricks were ground very fine and the powder showed a positive behaviour at the pozzolanicity test carried out at the Politecnico di Milano (Fig. 7). The pozzolanicity test was performed according to the European Standard [10] used for cement, adapted to the special case. The bricks showed pozzolanicity after 30 days.

In the meantime, the research of the lime was started in the area around Mŷ Son in order to minimize the price of transportation. Since it was impossible to find a lime from stones, as the existing quarries had been closed in order to avoid the continuous spoiling, only natural lime coming from the sea shells could be found. Lime samples from the nearby village of Lang Co, from the village of Kiem Lam, and from Hoi An were collected along with a putty lime from Ha Noi. The third lime from Hoi An was finally chosen after comparison by chemical and physical tests was carried out in Milan at DIS, Politecnico [9]. It was the best mortar available in the Mŷ Son area, and therefore it was chosen.

It was then decided to produce two types of mortars: (a) with fine aggregates for thin joints, and (b) with coarser aggregates for thicker joints. The maximum diameter size varies according to the thickness of the joint from 2 to 16 mm (Figs. 8 and 9).

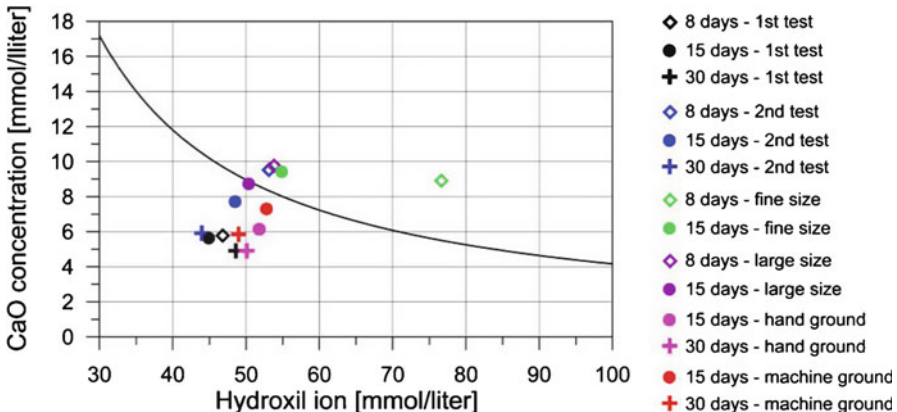


Fig. 7 Pozzolanicity tests on sampled bricks

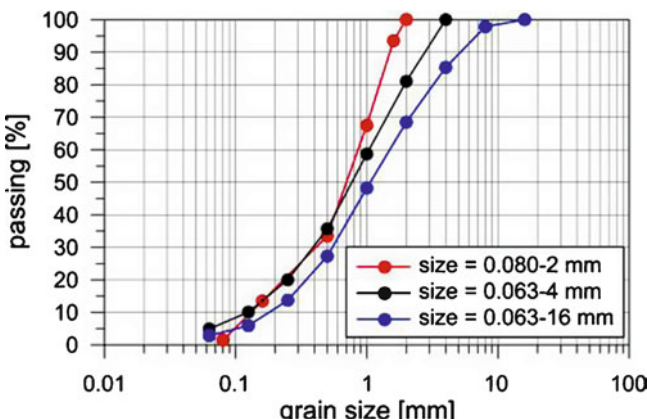


Fig. 8 Grain size distribution of aggregate for new mortars

During the intervention, specimens were prepared on-site, cured at the site environment, and sent to Milan for testing (Fig. 9). Flexural and compressive tests were carried out in Milan according to the European Standard [11].

The results are given in Table 1, where σ_f is the flexural strength and σ_c is the compressive strength. As seen in Table 1, the mortars were tested at different ages of curing, but the number of days did not follow the same increase as is normally done in laboratory. This was due to the fact that some mortars were prepared on-site and tested in Milan whenever possible. Nevertheless, both the scattering in the data and the values of the tensile strength were rather acceptable for a low strength hydraulic mortar.

The chosen mortar was first used for the repair of the two remains of the buildings G3 and G5, which only emerged from the ground from 50 to 100 cm, in order to check the compatibility of the new materials used in external and internal joints.



Fig. 9 Specimens realized on site

Table 1 Flexural and compressive tests

Specimen	Age of curing days	σ_f [N/mm ²]	σ_c [N/mm ²]	Age of curing, days	σ_f [N/mm ²]	σ_c [N/mm ²]
MT.04.1	90	0.79	2.15	480	1.25	4.77
MT.04.2	90	0.66	2.85	480	0.82	3.05
MT.04.3	270	1.37	4.40	270	1.37	4.40
MV.06.1	28	0.85	2.12	90		2.64
MI.06.1	28	0.96	3.19	90		2.35
MS.05.1	240	0.53	1.36	240	0.53	1.36
MS.05.2	160	0.67	1.40	160	0.67	1.40

The works ended in 2005, and up to now they have shown a very good behaviour. In 2009 the works started on the most important building of group G, the Kalan G1.

The results found by the observation of new mortars in thin section and with the SEM-EDS were very interesting. Three specimens were observed, two sampled on-site from G3 (MS.05.1 and MS.05.2) and one in the laboratory at DIS-Politecnico (MS.06.1). The results of analysis of the thin sections of MS.05.1 on a polarised microscope are shown in Figs. 10a, b. It can be easily seen that in all the sections, reaction rims between binder and brick pebbles are present, also showing a pozzolanic reaction which is still ongoing in MS.05.1. The SEM-EDS observations of MS.05.1 (Figs. 11a–c) show the presence of reaction rims composed of calcium and aluminium, calcium and silica, silica, and calcium and aluminium.

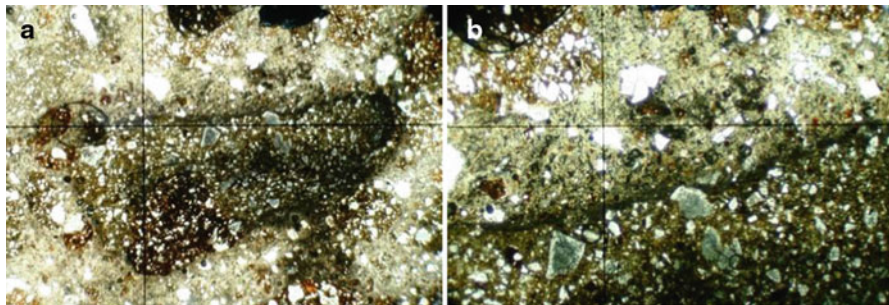


Fig. 10 Specimen MS.05.1: (a) photomicrograph in transmitted light ($3.5\times$); (b) photomicrograph in transmitted light ($10\times$)

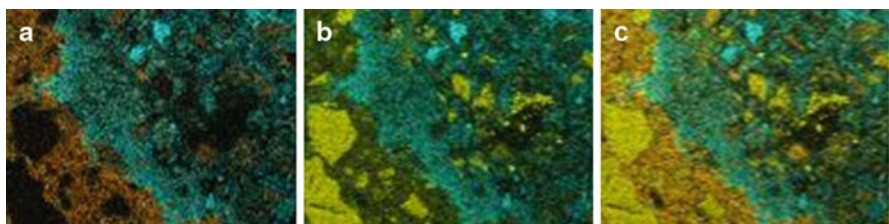


Fig. 11 Reaction rims composed: (a) calcium and aluminium; (b) calcium and silica; (c) silica, calcium and aluminium

6 Conclusions

After the application of the new materials on G3 and G5 ended in 2005, the observation of their durability and the optical tests on the sampled mortars some conclusions can be made: (i) the resin and mortar used in Mŷ Son show a good durability after 5 years, (ii) the optical observations of the new mortar made after 2 years show good pozzolanic reaction of the brick powder with the lime, and (iii) the new materials can be adopted in the conservation of the main kalan G1.

References

1. Parmentier, H.: Inventaire descriptif des monuments čams de l'Annam. E. Leroux, Paris (1909-1918)
2. Kwiatkowski, K.: Recherches sur les monuments du Champa, Rapport de la Mission Polono-Vietnamienne 1981-1986. Wydawnictwa PKZ, Warszawa (1990)
3. Condoleo, P.: I templi di Mŷ Son: indagini e progetto di conservazione del Gruppo G. PhD thesis in Preservation of Culture Heritage of Architecture Politecnico di Milano (2007)
4. Bo Xay Dung.: Report on building techniques of Champa Towers, Hanoi (1996)

5. ASTM Designation: C114-69.: Standard Method for Chemical Analysis of Hydraulic Cement. ASTM, Conshohocken (1996)
6. Ballio, G., Baronio, G., Binda, L.: First results on the characterisation of bricks and mortars from My Son Monuments. Conserving the past – an Asian perspective of authenticity in the consolidation, Int. Workshop: Hoi An and Mỹ Sơn, Vietnam, pp. 204–213, 25 February–3 March 2001
7. Binda, L., Tedeschi, C., Condoleo, P.: Characterisation of materials sampled from some Mỹ Sơn Temples. In: 7th Conference of ICCE, Tehran, Iran, 8–10 May 2006, CD-ROM (2006)
8. Binda, L., Zerbi, G., Condoleo, P., Mannucci, E., Tedeschi, C.: Study of a natural resin used as joint for the brick masonry of Hindu temples in Mỹ Sơn (Vietnam). In: 14th International Brick Block Masonry Conference (14IBMAC), Manly Pacific Sydney, Australia, CD-ROM
9. CEN: Methods of testing cement. Pozzolanicity test for pozzolanic cements. EN 196–5 (2008)
10. Binda, L., Condoleo, P., Tedeschi, C.: Materials characterization. In: Champa and the Archaeology of My Son (Vietnam), pp. 283–311. NUS, Singapore (2009)
11. CEN: Methods of test for mortar for masonry. Part 11: Determination of flexural and compressive strength of hardened mortar. EN 1015–11:1999 (1999)

Characteristics of Mortars from Ancient Bridges

Dita Frankeová, Zuzana Slížková, and Miloš Drdácký

Abstract Mortars from two medieval bridges (Charles Bridge in Prague and a bridge in Roudnice) and two Roman bridges (Ponte di Augusto in Narni and a bridge in Sardinia) were analysed using various techniques to obtain their chemical and physical characteristics. The analysis of binder quality was based on thermogravimetric analysis, using a methodology which enables the hydraulicity of the mortar to be expressed by the $\text{CO}_2/\text{H}_2\text{O}$ ratio. The mechanical tests were performed on non-standard mortar specimens. The ratio binder/aggregate was determined dissolving the binder by an acid, and a sieving analysis was applied to the separated aggregate. The material characteristics of mortars from historic bridges were compared with each other, taking into account the requirements for mortar strength according to construction function and degree of exposure.

1 Introduction

Bridges are fascinating engineering works which in many places have survived in service for thousands of years not only due to their excellent structural concepts and features but also owing to the quality of the materials and the excellent technological skills of their builders. The mortars of ancient bridges were analysed in the past from the point of view of the aggregate and binder characteristics, but there are few references concerning the relation between chemical composition and the mechanical characteristics.

D. Frankeová (✉) • Z. Slížková • M. Drdácký
Institute of Theoretical and Applied Mechanics (ITAM), Academy of Science
of Czech Republic, Prague, Czech Republic
e-mail: frankeova@itam.cas.cz; slizkova@itam.cas.cz; drdacky@itam.cas.cz

This paper presents data from a more complex analytical approach applied to a study of the mortars from four ancient bridges – two Roman and two medieval built in different environments. The medieval bridges did not introduce remarkable innovations into bridge engineering and were based on the proven Roman design and construction. However, some material development is apparent.

The scope of the paper does not allow for a very detailed analysis and description of the results, or for repetition of data already published elsewhere. Therefore, the methodology for non-standard testing is not included, and reference is made to other papers [1–4].

2 Experimental

2.1 Sampling

2.1.1 Charles Bridge in Prague

During the preparations for recent repairs to Charles Bridge in Prague, a probe was dug and several samples of the medieval mortar and stone were extracted for testing in the ITAM laboratories.

2.1.2 Gothic Bridge in Roudnice

One of the oldest bridges in Bohemia (in the Czech Republic) did not survive the Thirty Years War in the seventeenth century, when it was blasted and almost totally destroyed. Some remains of the bridge were recently taken from the river bed, and they were made available for testing the mortar characteristics.

2.1.3 Roman Bridge in Narni

A core drilled into a pier of a Roman bridge at Narni delivered samples of a lime concrete of varying composition and with varying chemical and physical characteristics [5]. The question was raised whether the varying composition, which corresponds with various levels of the pier, might have been intentionally designed to take into account the variable loading or other functional conditions. The mechanical characteristics of the lime concrete from the Roman bridge at Narni were therefore tested on non-standard specimens, using the ITAM methodology for tests of this kind.



Fig. 1 Investigated bridges: Charles Bridge in Prague (*above*), Gothic bridge in Roudnice (*left*), Roman bridge in Narni (*right*)

2.1.4 Roman Bridge in Sardinia

A small sample of lime mortar extracted from a Roman bridge in Sardinia was tested in bending and compression.

Figure 1 shows photos of investigated bridges, while a list of the sampling sites and a description of the mortars samples are given in Table 1.

2.2 Analytical Methods

The following analytical methods were applied to the mortar samples:

Optical microscopy – polished thin sections of the mortar samples were examined by an optical polarising microscope

Wet chemical analysis – about 10 g of powdered sample was dissolved in 2 M HCl according to the RILEM methodology [6]. Dissolving binder by acid attack enabled

Table 1 Sampling sites

Site	Century of construction	Symbol of sample	Functional type of mortar
Charles Bridge, Prague, CR	Fourteenth	KM 1A, KM 1B	Joint mortar of an inner hammer-dressed stone arch
		KM 1C	Cast infill mortar above the stone arch
Gothic bridge, Roudnice, CR	Fourteenth	R 3	Fine-grained joint mortar of ashlar stone arch
		R 4	Coarse-grained joint mortar of ashlar stone arch
		R 8	Cast infill mortar on the top of ashlar stone arch
Ponte di Augusto, Narni, I	First BC	N 1	Cast infill mortar in pier core
		N 2	Cast infill mortar in pier core
		N 3	Mortar in footings
		N 4	Mortar from the foundations
Roman bridge, Sardinia, I	Third BC	Sa 1	Bridge rail joint mortar

its separation from aggregate and so allowed an estimation of the binder/aggregate ratio. Subsequent element analysis of dissolved binder by gravimetric and volumetric methods was performed and cementation index *CI* of mortar binder was calculated according to [7] as

$$CI = \frac{2.8xSiO_2 + 1.1xAl_2O_3 + 0.7xFe_2O_3}{CaO + 1.4xMgO}$$

Granulometry of the aggregate – aggregate was after separation from the binder sieved and the granulometric distribution was expressed as the fineness modulus $F.M. = \frac{\sum x_i}{100}$

where x_i is cumulative percentage retained on sieves 0.125, 0.25, 0.5, 1, 2, 4 mm from ISO 3310-1 sieves series;

Thermal analyses (thermogravimetry/differential scanning calorimetry) – TG/DSC analysis was performed in order to determine the composition of the binder. The experiments were carried out over a temperature range of 30–1,000°C with a heating rate of 10°C/min in a nitrogen atmosphere on a fraction <0.063 mm;

Porosity accessible to water – according to RILEM I. 1 [8];

Bulk density – determined by means of hydrostatic balance weighing;

Water uptake coefficient – according to DIN EN ISO 15148;

Mechanical tests – a three-point bending and compression test was performed on a non-standard mortar specimen according to ITAM methodology [1, 2].

3 Results and Discussion

3.1 Microscopic Observations

The results from a microscopic analysis of the samples from Charles Bridge indicate that the dominant component of mortars aggregate is river quartz sand. K-feldspar, plagioclase and mica can be determined among the other lithic grains.

The aggregate in the bridge at Roudnice is very similar to the aggregate used for Charles Bridge, where the main component is quartz. Orthoclase, plagioclase and mica are present in smaller amounts.

The mortars from Narni Bridge have a rather different microscopic appearance – there are aggregate grains of various colours and shapes, some of them were 2–3 cm in size. The binder colour of N1 and N2 is whitish, while for samples N3 and N4 the colour is light grey and dark grey. Microscopic analysis determined that the aggregate is mainly made up of rounded fragments of micritic limestone and secondarily of chert and travertine fragments, quartz, feldspars and pyroxene. Samples N3 and N4 contain tuff fragments, which make the material strongly porous [5].

3.2 Chemical Composition

Thermal analysis and wet chemical analysis were carried out in order to characterize the quality of the binder. The comparative hydraulic character of the lime was expressed by the $\text{CO}_2/\text{H}_2\text{O}$ ratio, which is the ratio between the mass loss above 600°C due to the CO_2 released by decomposition of the carbonates, and the mass loss in the range 200–600°C, due to the loss of the water bound to the hydraulic compounds [7, 9]. By comparing the loss due to CO_2 release and the $\text{CO}_2/\text{H}_2\text{O}$ ratio we can sort the mortars into two groups, as follows:

- hydraulic lime mortars with 3–6% of bound water and 18–34% of CO_2 , $\text{CO}_2/\text{H}_2\text{O}$ ratio reaches values between 4.5 and 9.5
- natural pozzolanic mortars with more than 5% of hydraulic water and less than 20% of CO_2 , while $\text{CO}_2/\text{H}_2\text{O}$ ratio is less than 3.

Results of the wet chemical analysis provided data for characterisation of aggregate, expressed as fineness modulus, and for classification of binder hydraulicity according to its cementation index.

The data obtained from the thermal and wet chemical analysis are reported in Table 2. In the case of the Narni Bridge samples, the wet analysis described above could not be applied, because the aggregate consists mainly of carbonates so it would dissolve during an acid attack together with the binder.

From the results of both analyses it is obvious that all tested samples were of hydraulic nature. According to the recommended thermogram interpretation [7, 9], the samples from Charles Bridge and N3 and N4 from Narni Bridge were classified

Table 2 Chemical analysis of mortars

Sample	TG analysis			Wet analysis				Hydraul. grade
	Struct. bound water % w	CO ₂ % w	CO ₂ /H ₂ O ratio	Binder nature	B/A weight ratio	Aggr. nature	Fineness modulus aggregate	
KM 1A	5.9	8.7	1.4	Natur.pozz.	1:2.7	Silic.	3.0	1.3
KM 1B	8.5	7.8	0.9	Natur.pozz.	1:3	Silic.	2.9	1.1
KM 1C	10.0	9.2	0.9	Natur.pozz.	1:2.4	Silic.	2.5	0.9
R 3	4.6	23.2	5.0	Hydr. lime	1:0.8	Silic.	1.7	0.6
R 4	4.1	18.3	4.4	Hydr. lime	1:2.4	Silic.	2.6	0.3
R 8	4.1	12.3	3.0	Hydr. lime	1:3.3	Silic.	3.9	+
N 1	4.2	22.2	5.3	Hydr. lime	1:3 ^a	Carb.	+	+
N 2	6.2	19.4	3.1	Hydr. lime	1:2 ^a	Carb.	+	+
N 3	6.1	11.7	1.9	Natur.pozz.	1:2 ^a	Carb.	+	+
N 4	6.5	12.9	1.9	Natur.pozz.	1:2 ^a	Carb.	+	+
Sa 1	4.5	35.9	7.9	Hydr. lime	1:1	Silic.	+	+

+ Not analysed

^aWeight ratio was obtained by recalculation of the volume ratio determined by optical microscopy analysis of thin section of mortar

as natural pozzolanic mortars because their content of CaCO_3 is lower than 20%, while the content of structurally bound water is higher than 5%. In the case of Charles Bridge fine-grained clayey-calcareous silicate is present [10], and it probably played the role of a pozzolanic material. Cantasani et al. [5] made a detailed analysis of the sample N2 of Narni Bridge and they suppose that the high hydraulicity of the mortar may be due to the fact, that the lime was produced from local sources of cherty limestone. This might explain the high Si content, and consequently the weight loss higher than 5% (6.2%) in the range of 200–600°C. In samples N3 and N4 the presence of pozzolanic material – tuff – was microscopically confirmed.

The mortars from Roudnice Bridge were probably prepared using moderately hydraulic lime as a binder. The values for the structurally bound water released during heating of the samples did not exceed 5%, which indicates the use of natural hydraulic lime without the addition of pozzolana.

3.3 Physical Characteristics

The compression strength values of the Charles Bridge mortars are quite high (except the sample 1B) and correspond with the determined chemical composition of the binder (lime with natural pozzolanic material). The compression strength values in the Roudnice Bridge mortars, which consist of river sand and hydraulic lime, are slightly lower (from 3.7 to 5.4 MPa) but the bending strength of this type of mortar is higher, as shown in table 3.

The attained values of bending (flexural tension) strength of mortars from the Ponte di Augusto Bridge at Narni and the mostly significantly plastic behaviour correspond with typical lime mortar characteristics. It can be concluded that the bending strength (modulus of rupture) reaches values from 0.3 to 1.3 (1.5) MPa. The measured values are influenced by quite gross aggregate grains. This is especially apparent when small specimens are tested. We can therefore expect the tension strength measured on standard specimens to exhibit higher figures.

The compression strengths measured on non-standard mortar specimens of slenderness inferior to 1 exhibit higher values than those from the standard tests. These were estimated using empirical correction coefficients dependent on the slenderness, the strength of the mortar and the length of the base. The compression strength values in the Narni Bridge samples N1, N3 a N4 are quite low in the ranges between 1 and 2 MPa, corresponding to a high ratio of gross aggregate grains. In the investigated Roman mortar, the aggregates and their packing and compacting play an important role. The strength measured on sample N2 mortar was strongly influenced by the very large size of the aggregate grains in the test specimens. A pessimistic value of the strength may be estimated from the stress/displacement diagram around the moment when the material started to stiffen significantly. This happened at about one-fourth or one-fifth of the total force. Under such an assumption the strength of the sample N2 mortar would be about 2.8–3.5 MPa, which would be in better accordance with the rather low bending strength.

Table 3 Physical characteristics of the mortars

Sample	Bulk density, kg/m ³	Porosity, % vol.	Compressive strength, MPa	Bending strength, MPa	Water upt. coef., kg/m ² h ^{-0.5}
KM 1A	1,690	39.1	5.2	1.4	5.2
KM 1B	1,564	39.6	2.8	2.4	1.5
KM 1C	1,599	38.2	8.9	2.3	6.3
R 3	1,500	38.6	5.1	2.6	6.7
R 4	1,711	32.7	3.7	3.2	3.5
R8	1,855	28.7	5.4	2.4	+
N 1	1,690	36.0	1.9	0.9	+
N 2	1,790	31.0	14.5	0.4	+
N 3	1,300	50.0	1.6	1.2	+
N 4	1,160	54.0	1.0	0.3	+
Sa 1	1,486	43.2	1.5	1.2	+

+ Not analysed

The measured mechanical characteristics (strength and stiffness) vary in a rather large range of values, which may indicate that the cast lime concrete parts did not attract a high level of technological care.

It does not seem likely that the different composition of the Narni pier lime concrete was designed intentionally and for the purposes of changing load carrying capacity from the point of view of the statistics of the structure. However, it might be interesting to evaluate the dynamic characteristics of a structure made of such a material and its earthquake resistance.

The results of tests of mortar from Sardinia were 1.53 MPa for compression and 1.22 MPa for bending. These test results correspond very well with the Narni Bridge results.

4 Conclusions

The production technology and especially the raw material composition of mortars differ from locality to locality, and also from culture to culture. The analysed samples show the use of a binder of high hydraulicity, which was probably achieved in different ways. While the mortars from the bridge at Roudnice (R3, R4, R8) and from Narni Bridge (N1, N2) seem to be made from hydraulic lime obtained from local impure limestone, the mortars from Charles Bridge and from the footings of Narni Bridge (N3, N4) appear to be pozzolanic. In historic mortars, pozzolanic materials were commonly added. These contain high amounts of hydraulic oxides, which can react with lime and form water-resistant hydrated calcium and aluminium silicates. Such manufacturing technologies were often kept secret, so that no kind of documentation is left.

The nature of the pozzolana and aggregate mixed in the mortar was dependent on local resources. In the Czech lands, for example, quartz sand with feldspar and mica

admixtures (as observed in the Charles Bridge and Roudnice samples) is typically used as aggregate in historic mortars, in contrast to the analysed ancient mortars from areas where various limestones and other lithotypes were available for aggregate.

The results of the thermal analysis indicate that samples of mortars used as cast infill, or mortars for foundation masonry (KM 1C, R8, N3, N4) have the highest hydraulicity values. Samples of joint mortars (R3, R4, Sa1) are richer in calcium carbonate, what improves the workability of original mortars, so the workable time could be intentionally modified by changing of mortar composition.

Earlier research indicated that there are apparent tendencies toward simple and direct interdependencies among some parameters [2]. Naturally, there is a strong linearly reciprocal relation between density and porosity, and therefore also other apparently dependent parameters, e.g., water absorption. That is, a reduction in porosity implies a rise in density. Further, a rise in density correlates with an increase in both compressive strength and bending strength, and consequently a rise in porosity correlates with a decrease in strength. When assessing the results, we should have in mind how heterogeneous our sample of historic mortars is.

The other parameters influence the mechanical characteristics in a more complex way and cannot be simply revealed from a limited number of samples. It seems that a rise in the binder-to-sand ratio does not simply cause a corresponding rise in the strength parameters.

Acknowledgement The authors gratefully acknowledge support from the grant GAČR 103/09/2067 from the Czech Science Foundation.

References

1. Drdácký, M., Slížková, Z.: Mechanical characteristics of historic mortars from tests on small-sample non-standard specimens. *Mater. Sci. Appl. Chem.* **17**(1), 20–29 (2008)
2. Drdácký, M., Mašín, D., Mekonone, D.M., Slížková, Z.: Compression tests on non-standard historic mortar specimens. In: Proceedings HMC 08 (Historic Mortars Conference), Lisbon (2008)
3. Drdácký, M., Slížková, Z., Frankeová, D.: Identification of historic materials by small sample testing. In: Proceedings Zkoušení a jakost ve stavebnictví, pp. 283–294 (2009)
4. Drdácký, M.: Non-standard testing of mechanical characteristics of historic mortars. *Int. J. Archit. Herit.* **5**, 1–12 (2011)
5. Cantisani, E., Cecchi, A., Chiaverini, I., Fratini, F., Manganelli Del Fá, C., Pecchioni, E., Rescic, S.: The binder of the Roman concrete of the Ponte di Augusto at Narni (Italy). *Per. Mineral.* **71**, 113–123 (2002)
6. Middendorf, B., Hughes, J.J., Callebaut, K., Baronio, G., Papayiani, I.: RILEM TC 167-COM: characterisation of old mortars with respect to their repair. *Mater. Struct.* **38**, 761–780 (2005)
7. Moroupolou, A., Bakolas, A., Anagnostopoulou, E.: Composite materials in ancient structures. *Cem. Concr. Compos.* **27**, 295–300 (2005)
8. RILEM: Recommended tests to measure the deterioration of stone and to assess the effectiveness of treatment methods / Tentative Recommendations, RILEM Commission 25-PEM. *Matériaux et Constructions* **13**(75), 175–253 (1980)

9. Moroupolou, A., Bakolas, A., Bisbikou, K.: Characterization of ancient, Byzantine and later historic mortars by thermal and X-ray diffraction techniques. *Termochim. Acta* **269**(270), 779–795 (1995)
10. Příkryl, R., Novotná, M., Weishauptová, Z., Šťastná, A.: Materials of original masonry infill of Charles Bridge and its composition. *Průzkumy památek* **16**(1), 107–123 (2009)

Diagnosis, Characterisation and Restoration of the Internal Renders of Santíssimo Sacramento Church in Lisbon

António Santos Silva, Giovanni Borsoi, Maria do Rosário Veiga, Ana Fragata, Martha Tavares, Fátima Llera, Belany Barreiros, and Telma Teixeira

Abstract The *Santíssimo Sacramento* Convent in the Alcântara quarter of Lisbon is one of the most important ecclesiastical structures of the *Filipino Period* (1580–1640), showing an innovative architectural layout. An intervention aiming at the repair and restoration of the interior plasters of the *Santíssimo Sacramento* Church was performed in 2009 and 2010. To support the restoration plan, a physical, mechanical and chemical-mineralogical characterisation of the internal plasters of the church was carried out. In this paper the main results are presented, such as various types of plasters, mortars, stuccos and pigments; and also the nature of the main anomalies were identified and characterized. The results obtained contributed to the identification of the main decorative programs characterized by the use of different materials and techniques. The mortars are in very good condition, being composed of aerial calcitic lime with quartzitic and basaltic aggregates. The stuccos are comprised by gypsum and non-hydraulic lime, while the decorative layers features lime with some precious pigments, such as ultramarine (*lapislazzuli*) and gold-foil gildings. The plaster conservation and restoration works were performed with compatible repair materials selected according to the physical-chemical characterisation and on the evaluation of the conservation state.

A.S. Silva (✉) • G. Borsoi • M. do Rosário Veiga • A. Fragata • M. Tavares
Laboratório Nacional de Engenharia Civil, Lisbon, Portugal
e-mail: ssilva@lnec.pt; gborsoi@lnec.pt; rveiga@lnec.pt; afragata@lnec.pt; marthal@lnec.pt

F. Llera • B. Barreiros • T. Teixeira
In Situ – Conservação de bens Culturais, Lda, Estoril, Portugal
e-mail: fatimallera@insitu.pt; belanybarreiros@insitu.pt; telmateix@gmail.com

1 Introduction

The *Santíssimo Sacramento* Church of Lisbon (Fig. 1), located in the ancient Convent of Santíssimo Sacramento, is an excellent example of Lisbon's seventeenth century rich architecture and one of the most important constructions built during the Spanish dynasty (1580–1640). Having been founded on the 20th of October 1605, the Convent became occupied by nuns in 1616. In 1620 the church was demolished, perhaps for its lack of size and magnitude, being rebuilt in 1635 under the third and last reign of Filipe III of Portugal (IV of Spain). The convent's construction characterises the *Filipino* period in Portugal; a period during which religious power was dominant [2].

The church exhibits a unique architectural style (due to its resemblance in plan to a Greek cross), when compared to other convents on the Iberian Peninsula. It is attributed to Master Frei João de Vasconcellos, the architect of another Dominican Church in Lisbon (*São Domingos de Benfica*); although it is not known for sure who the real author of the architectural plan was. However, the *Santíssimo Sacramento*'s church does share similar traits to the *Convento das Bernardas Recoletas de Alcalá de Henares* in Spain [2], highlighting the possibility that a Spanish architect may have had an influence in the project.

The church features a single nave and three altars facing east, and was constructed using vaulted supports. These supports were followed by a floor plan in the shape of a Greek cross contained within a square, which was lit by six lateral windows.

The chapel, situated in the eastern arm of the Greek cross, was built upon a polygonal crypt or sacristy. This chapel housed an altar of gilded carved wood where the Blessed Sacrament's tabernacle and monstrance were placed for reverence.

The church underwent several transformations, initially reflecting the church's influence of Juan de Herrera and his work in El Escorial. This marked the trends of a new taste for austerity and pragmatism in Mannerist architecture during the Spanish reign of Portugal, in which we designate as the first program (seventeenth century).

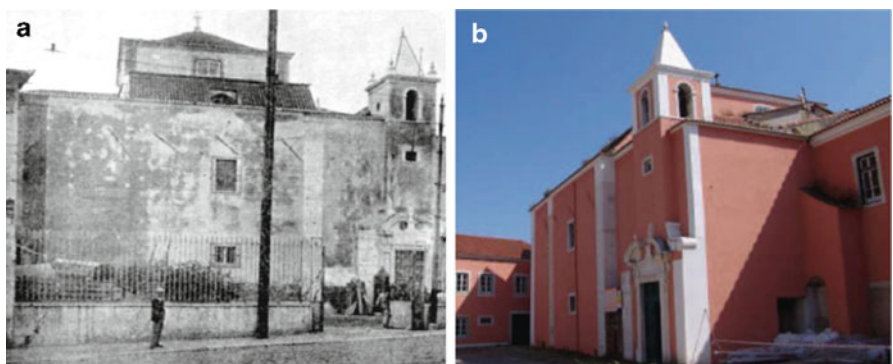


Fig. 1 Pictures of the *Santíssimo Sacramento* Church in (a) 1929 [1] and (b) 2010

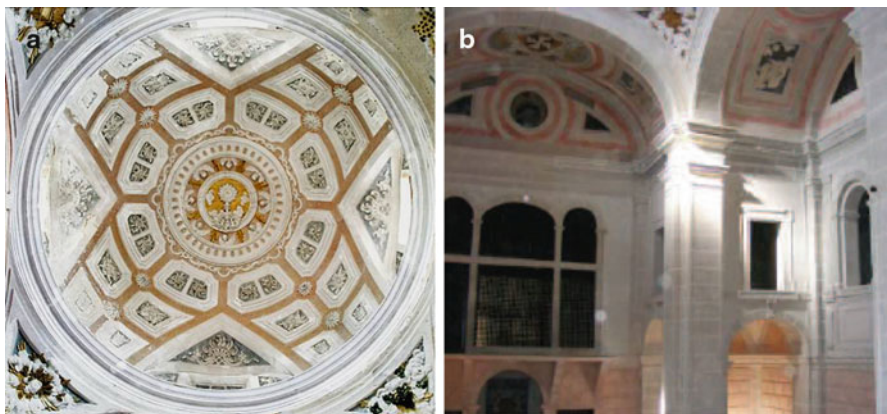


Fig. 2 Pictures of the interior of the Church of Sacramento: (a) View of the polychrome stucco within the Dome; (b) view of the vertical projections in ornamental plaster

This included features such as simple, classic and pragmatic embellishments; the use of monumental structure; suppression of the choir; approximation of the high altar; and a unique nave. In this church, fake stone techniques still feature in vertical projections, namely lime mortar renderings with fake joints imitating grey and off-white granite stone, a feature very common in Madrid as in El Escorial.

During the reign of D. João V (1689–1750), constructor of the famous Portuguese Mafra's Convent, this church underwent a massive re-decoration campaign, which we designate as the second program (end of eighteenth – beginning of the nineteenth century). Here, decorative renderings made with Stucco and plaster-work, still presented in the domes and vaults, simulate various types of ornamental Portuguese stones, like rose marble, embellishing the architecture, colour and scenic impact, much in the style of the French influence of Louis XIV (Fig. 2).

The constructive history of the church points out that the plasters and stuccos found could belong to different periods, between the seventeenth and the nineteenth centuries. The stratigraphy of the layers and the composition of the mortars, paintings and pigments will reveal the chronology and period identification.

The church survived the terrible earthquake of 1755, however its decline started in 1834 with the suppression of the religious orders in Portugal. At the beginning of the twentieth century the convent passed into the control of the Army and suffered several alterations. At the end of the 1990s the convent was acquired by the Foreign Affairs Office, which decided to refurbish the entire complex.

This paper presents the main detected anomalies, the chemical, mineralogical, microstructural and physico-mechanical characterisation of the internal renders (mortars, stuccos and mural paintings) as well as the restoration works carried out in the *Santíssimo Sacramento*'s Church in Lisbon.

2 State of Conservation

The interior renders and stuccoes were in a very bad condition; being their state of conservation poor, and the supporting structure beneath plainly visible in many areas, urgent restoration measures are required to be undertaken.

The principal cause of deterioration was an excessive accumulation of water coming from various sources and in various forms, most notably as rain-water infiltration, high interior moisture and condensations.

Over several years, the building's abandonment and its usage as a warehouse and storage for military equipment largely contributed to its degradation, allowing for the accumulation of debris as well as rat and pigeon guano. The roof has been damaged for a long period before recent works started, allowing rain-water infiltrations to the ceiling (Fig. 3).

In addition, a number of other problems were identified, the greatest among them being the presence of oxidized metallic elements used for fixing the decorative elements in plaster (Fig. 4a); as a result, cracks and detachment of the plasters took place. The presence of early restoration mortars containing Portland cement was detected in various regions of the church, as well as multiple paint-coats covering most of the decorative renderings, thus hiding the beauty and form of the original decorative work and contributing to its aesthetic degradation and deterioration.

The main problems observed in the renderings were: saline efflorescence (Fig. 4b), loss of cohesion, loss of adherence, detachment (Fig. 5a), open gaps, generalized dirtiness, repainting and previous interventions (Fig. 5b).



Fig. 3 View of the south vault, with different degradation phenomena such as detachment, efflorescence, loss of cohesion and adherence

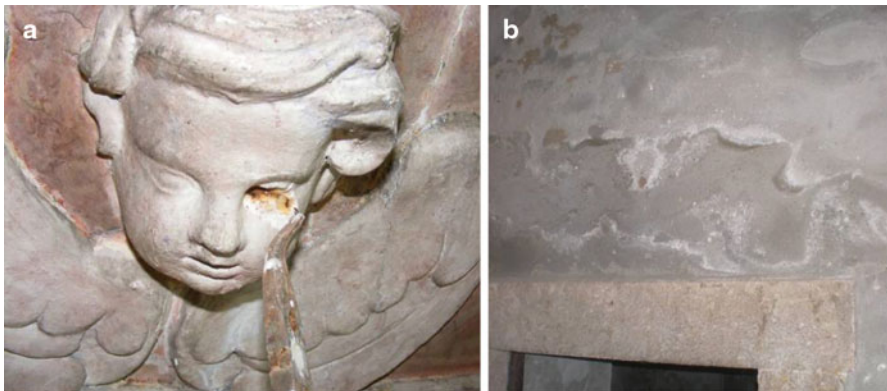


Fig. 4 (a) Oxidation of the metallic structural elements (b) presence of salt and concretions

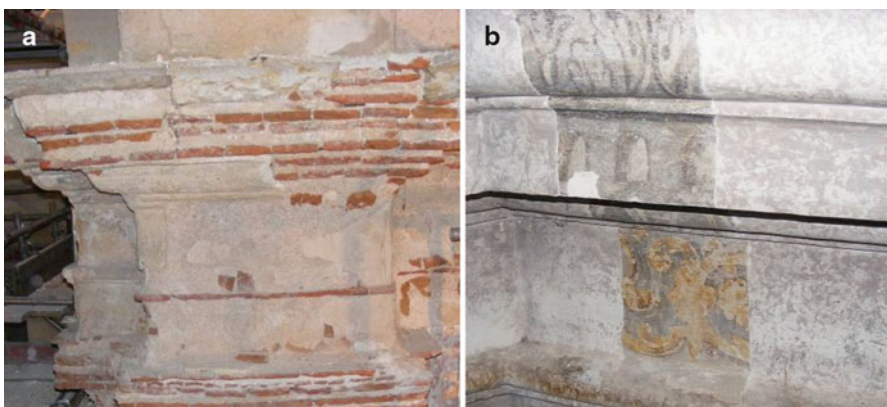


Fig. 5 (a) Detachment of the mortars, showing the brick structure (b) Juxtaposition of finishing, mural painting and whitewash over the original render

3 Chemical, Mineralogical, Microstructural, Physical and Mechanical Characterisation of the Renders

3.1 Sampling and Characterisation Methodology

The selection of the sampling sites was carried out according to LNEC's methodology for the characterisation of renders in ancient buildings [3, 4], and following the information previously collected from archaeological and historical research on the Sacramento's complex [2, 5]. The aim was to identify the different materials used in the two main programs, to study their compositions and their state of conservation. No samples were collected from highly deteriorated zones, since their bad conservation state induced its removal and substitution with new compatible repair mortars.

Table 1 Identification of the samples, type and their localization

Samples identification	Layers identification	Constitution	Location
1	M1	Mortar	West wall, South part
	P1A	Mural painting	
	S1	Stucco	
	P1B	Mural painting	
2	M2	Mortar	Dome vault
	S2	Stucco	
	P2	Mural painting	
3	M3	Mortar	North wall, West part
	S3	Stucco	
	P3	Mural painting	
4	M4	Mortar	Dome's moulding
	S4 -1st layer	Stucco	
	S4 -2nd layer	Plaster	
	P4	Mural painting	
5	M5	Mortar	South wall , East part
6	S6	Stucco	Dome – South vault, East part
7	S7	Stucco	Dome – South vault, West part
8	P8	Mural painting	Dome – red painting, marble imitation
9	P9	Mural painting	Dome – blue painting
10	P10	Mural painting	Dome vault – grapes
11	P11	Mural painting	Dome vault – leaf
12	P12	Mural painting	Dome vault – grapevine leaf
13	P13	Mural painting	Dome vault – golden sunbeam

Thirteen mortars, plasters and mural paintings samples were collected from different zones, as shown in Fig. 6 and described in Table 1.

The physical and chemical characterisation methodology developed by the authors [3, 4] comprises a wide range of techniques that complement each other; XRD analysis was performed with a Philips PW3710 X-ray diffractometer with 35 kV and 45 mA, using Fe-filtered Co K α radiation ($\lambda = 1.7903 \text{ \AA}$). Diffractograms were recorded in the range 3–74°20, at increment of 0.05° with a count time of 1 s for each step.

For thermal analysis a Setaram TGA-DTA analyser was used; samples were analysed in an argon atmosphere, with a uniform heating rate of 10°C/min, from room temperature to 1,000°C.

Thin sections and polished surfaces of the plasters were prepared by vacuum impregnation with an epoxy resin. These specimens were dried over 12 h in an oven at 60°C, and then vacuum impregnated with an epoxy resin; the impregnated cross sections were finally polished with abrasive Al₂O₃ solutions (15 and 9 μm), and then with three diamond abrasive solutions (6, 3 and 1 μm).

The selected samples were observed with an Olympus SZH stereoscopical microscope and an Olympus PMG3 metallurgical microscope, while petrographical

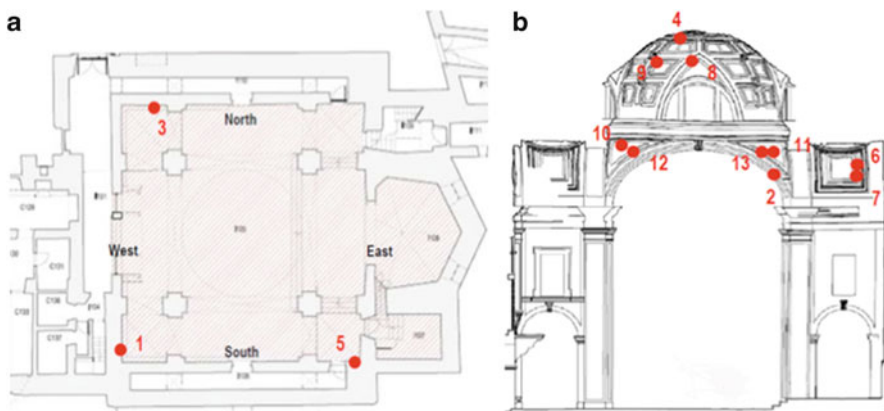


Fig. 6 (a, b) Plan and section of *Santíssimo Sacramento* Church showing the sample sites selected [2]

observations were performed using an Olympus BX60 polarized microscope and images were recorded digitally.

Micro FT-IR analysis was performed by a Nexus FT-IR 5700 spectrophotometer, coupled with a Nicolet Continuum MCT microscopy; the spectrum were done in the range 4,000–700 cm⁻¹, with resolution of 4 cm⁻¹ and 128 scans for each sample.

For the chemical analysis, small portions of the plasters were carefully disaggregated and all types of impurities and limestone grains were separated. Samples were afterwards attacked with warm diluted hydrochloric acid (1:3) to separate the siliceous aggregates from the binder. For the soluble fraction, the amounts of potassium and sodium (expressed in terms of their oxides) were determined by Atomic Absorption Spectrometry (AAS) in a Shimadzu AA-6300 spectrometer, chloride ion was determined by potentiometry, the sulphate ion was determined by infra-red analysis of SO₂ content obtained after calcination of the sample in a Leco CS244 and the soluble silica by the polyethylene oxide method. The insoluble residue was weighed and sieved to determine the particle size distribution of the aggregate fraction i.e. the siliceous sand.

Scanning electron microscopy observations were performed on a scanning electron microscope (SEM) Jeol JSM-6400 coupled with an Oxford energy dispersive spectrometer (EDS) x-ray detector.

Absorption capillarity coefficient was measured considering the capillarity coefficient by contact (Ccc) [6, 7], weighing the samples first and after being kept in contact with water for 5 min.

Compression and flexural strength tests were performed using testing methods adapted to irregular samples and validated in previous works [8, 9], based on the EN1015-11; a ETI HM-S machine was used for the tests, with a load cell of 200 kN. The characterisation concentrates on the walls, roof and dome renders, and includes mortars, stuccos and mural paintings. The main objectives of the characterisation of these materials were the determination of their stratigraphy, composition and the renders conservation/degradation state.

Table 2 Mineralogical composition of the mortars assessed by XRD

Crystalline phases	M1			M2			M3		M4	M5
	1st L		2nd L	3 rd L			G	G	F	G
	G	G	F	G	G	F	G	G	G	G
Quartz	+++	+++	T/+	+++	++/+++	+/++	+++	+++	+++	+++/++++
Feldspars	+/++	+/++	T	++	++	T/+	++	+/++	+/++	++
Mica	?	?	-	?	-	-	-	-	-	-
Pyroxene	T	T	-	T	-	-	T	-	-	T
Calcite	+++	+++	+++/++++	+++	++	+++	+++	++/+++	++/+++	++/+++
Gypsum	-	-	-	-	+	++	-	+/++	-	-
Halite	T	T/+	T/+	T	T/+	+	T	T	T	T
Hematite	T	T	T	T	-	-	T	-	-	T

Peak intensity: +++ high, ++ medium, + low, T traces, ? doubtful presence, - undetected
L Layer, G Bulk sample, F Binder rich fraction

Table 3 Mineralogical composition of the stuccos assessed by XRD

Crystalline phases	S1	S2	S3	S4		S6	S7
				1st L	2nd L		
Quartz	-	+	-	-	-	+	+
Feldspars	T	+	?/T	-	-	-	-
Calcite	+++	+++/++++	+++	+++	+++	+++	+++
Gypsum	+++	++	+++	+++	+++	-	-
Anhydrite	T	-	?	T	T	-	-
Halite	-	-	-	-	-	T	T

Peak intensity: +++ high, ++ medium, + low, T traces, ? doubtful presence, - undetected
L Layer, G Bulk sample, F Binder rich fraction

3.2 Characterisation Results

Tables 2 and 3 present the mineralogical composition of the mortars and stuccos, respectively, obtained by XRD analysis. The results show that mortars of *Santíssimo Sacramento*'s Church are essentially of two types: a first group (M1, M3, M5) composed of calcitic lime binder with quartzitic and basaltic aggregates. This group, which corresponds to the first program, shows contamination by chlorides, which may come from marine aerosols and/or by the use of unwashed sea sand. The second group of mortars (M2, M4), collected from the dome and vault (second program), present a lower quantity of calcitic lime binder and a notable quantity of gypsum. These mortars are made with only quartzitic aggregates, being also contaminated by chlorides, even more than the first mortars group.

The stuccos, with exception of the S6 and S7 samples, are essentially made of mixtures of calcite with gypsum; the samples S1, S2 and S4 present a calcite:gypsum ratio of approximately 1:1.

The TGA-DTA analysis confirmed the XRD results. Lime mortar samples (Fig. 7a) reveal an important weight loss in the range between 550°C and 900°C,

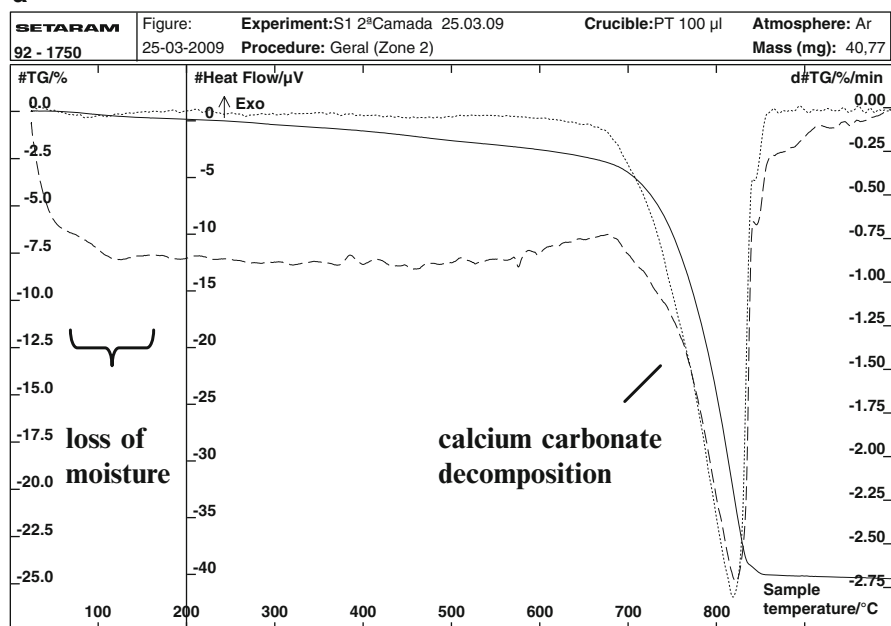
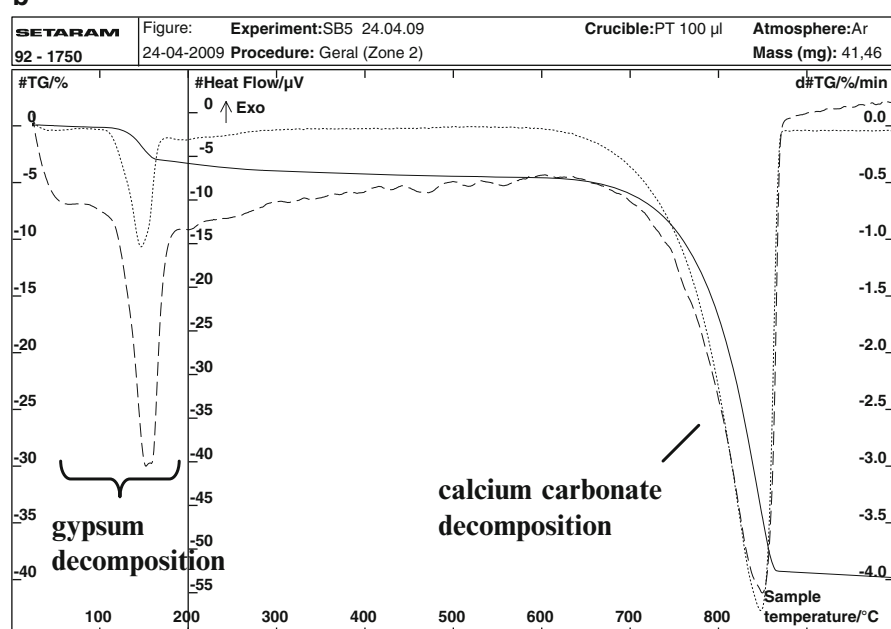
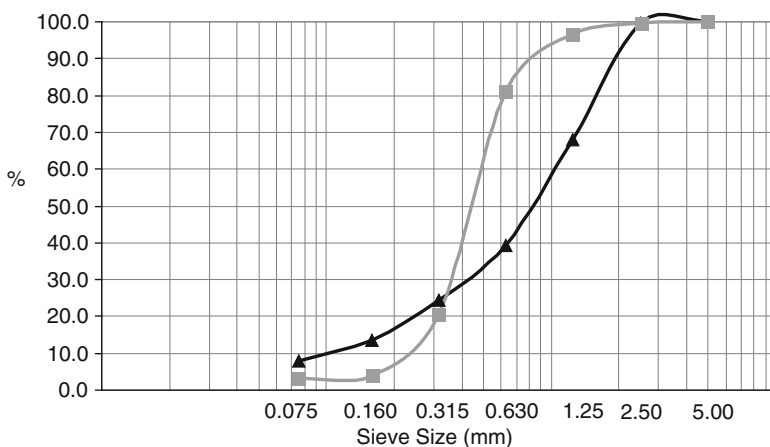
a**b**

Fig. 7 (a) TGA-DTA curve of mortar M1-2nd Layer. (b) TGA-DTA curve of mortar S1

Table 4 Mortars M1 and M2 chemical data (wt.%)

Sample identification	Insoluble residue				Soluble silica	
	Sodium (Na^+)	Potassium (K^+)	Sulphate (SO_4^{2-})	Chloride (Cl^-)		
M1	43.75	0.38	0.09	0.05	1.73	0.21
M2	58.48	0.57	0.14	2.67	2.99	0.17

**Fig. 8** Mortars sand grain-size distribution of (a) M1 (▲) and (b) M2 (■)

corresponding to the decarbonation of calcium carbonate, while gypsum-rich stucco samples (Fig. 7b) show a typical weight loss between 25°C and 200°C corresponding to the gypsum decomposition.

Table 4 presents the chemical results of M1 and M2 mortar samples. They represent two groups of analysed mortars (first programme – calcitic lime mortars and second programme – lime-gypsum mortars), confirming the XRD and TGA/DTA results. This highlights that mortar M1, compared to M2, has a larger binder quantity. Besides, mortar M2 is much richer in soluble salts, namely in chlorides and sulphates (gypsum as binder according XRD).

The grain size distribution of the insoluble residues (siliceous sand), presented in Fig. 8, is very important in the production of compatible mortars for restoration works. These results revealed that mortar M2 has aggregates mainly with diameters between 0.315 and 1.25 mm, while sample M1 shows a more evenly graded, well-sorted grain-size distribution, which is related to its different composition and functionality.

Impregnated polished sections were observed under a stereomicroscope and shows that all mortars contain rounded lime lumps (Fig. 9), which could indicate that lime was slaked with a minimum amount of water to convert CaO into $\text{Ca}(\text{OH})_2$ [10, 11]. The use of both basaltic and quartzitic aggregates in mortar M1 is evident, while M2 mortar presents only quartzitic aggregates. Shell fragments were shown for all mortars, suggesting aggregates of marine origin.

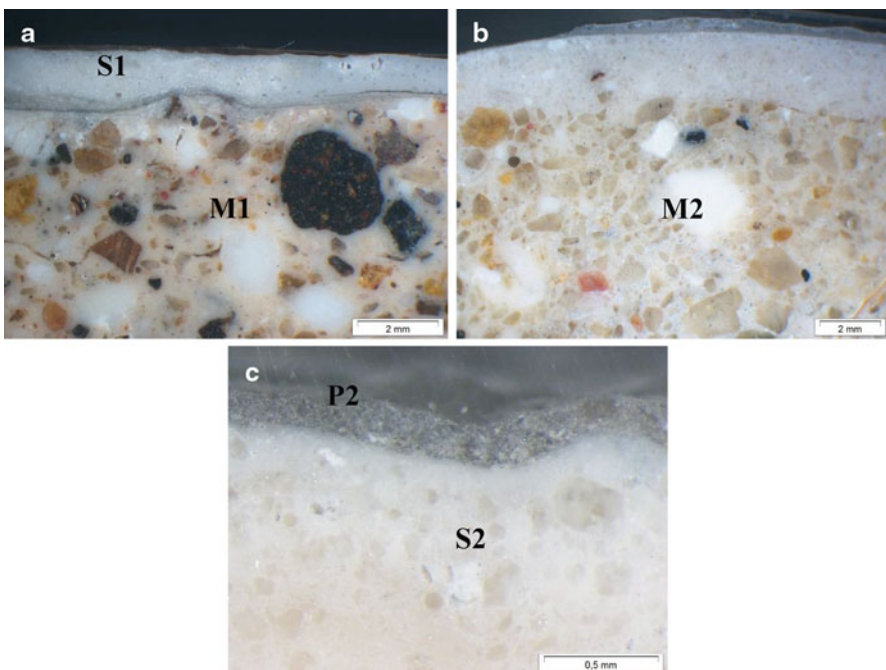


Fig. 9 Polished cross sections of renders observed using a stereoscopic microscope: (a) M1 mortar and its stucco S1; (b) M2 mortar and (c) detail of its painting layer (P2) and stucco (S2)

All renders are covered by white stucco, decorated with layer painting or with *fresco* mural painting. The observation of render 1 shows the existence of an older layer painting (P1A), probably from the seventeenth century, covered by white stucco (S1) and a new layer painting (P1B). This latter layer structure seems to be an indication of a previous intervention, probably between the end of eighteenth century and the beginning of the nineteenth century, since some artificial pigments (e.g. ultramarine), identified in the dome and applied in the same period, were synthesized only since the beginning of nineteenth century.

The microscopic analysis of the mural painting samples reveal the use of a great number of inorganic pigments, such as ultramarine, azurite, iron ochres, red and green earths, gold leaf, as can be seen in Fig. 10 and afterwards confirmed by EDS analysis. Traces of natural ultramarine were identified in older layers of some samples (Fig. 10a).

Moreover, different preparation materials were identified, including barite, white lead, gypsum and calcite – Fig. 10. Evidences of natural ultramarine (*lapislazuli*) [12] were found, onward replaced by other decorative solutions. This is probably due to the degradation causes described in Sect. 2.

The observation under the petrographic microscope underlines that the quartzitic and basaltic grains present a subrounded morphology, suggesting an alluvial origin for the aggregates. Moreover, traces of reaction rims are evident around the basaltic

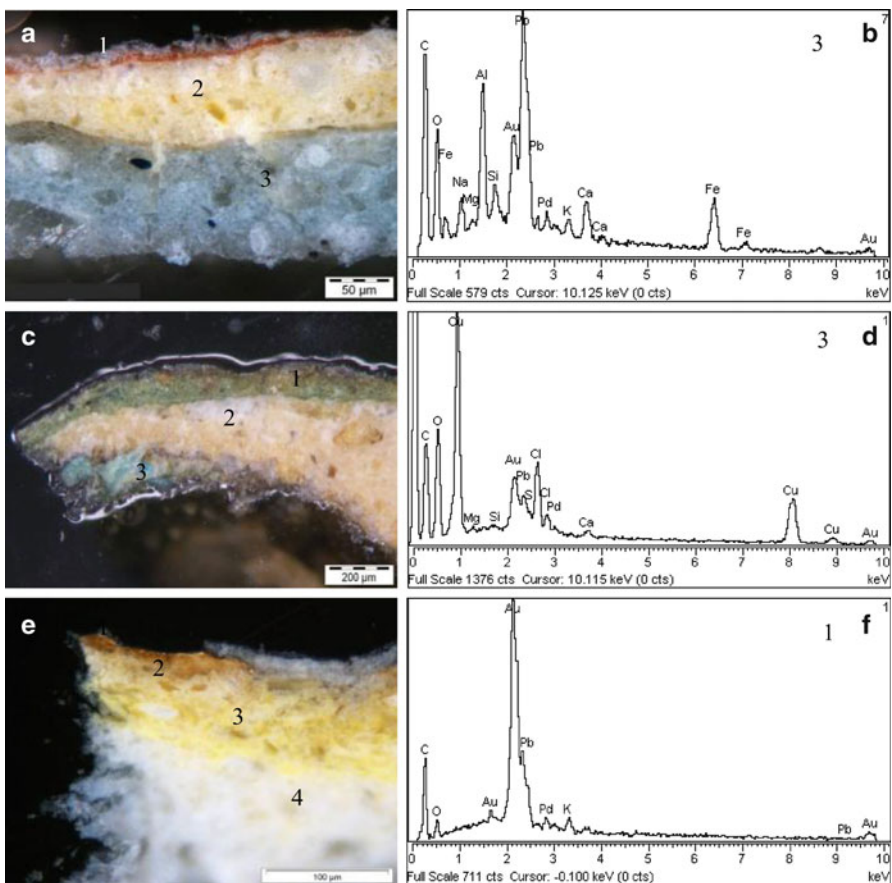


Fig. 10 Observation of polished sections of the mural paintings using a stereoscopic microscope: (a) P8 with the superficial *red* earth layer (1), its preparation (2) and the oldest layer (3) which shows particles of natural ultramarine (*lapislazuli*); (b) EDS spectrum of layer (3); (c) P12 with the superficial layer (1) of *green* earth pigment, its *yellowish* preparation (2) and the oldest layer of azurite (3); (d) EDS spectrum of layer (3); (e) P13 with the superficial *thin* gold foil (1), its adhesive (2), the *yellow* preparation (*bolo*) and the *white* preparation coating (4, usually made of gypsum) for the *gold-foil*; (f) EDS spectrum of layer (1)

aggregates (Fig. 11b), suggesting a probable occurrence of pozzolanic reactions between these aggregates and the calcitic lime. These reactions create neoformation products, such as calcium-silico-aluminates, normally responsible for the mechanical resistance improvement of these old mortars.

Mortars SEM analysis showed that all mortars have a compact matrix, typical of old lime mortars, with aggregates firmly incorporated in the calcitic binder (Fig. 12b). Besides, this allowed the confirmation of the aggregates nature and of halite (Fig. 12a) [13]. Moreover, it was possible to observe the presence of biological colonization.

Stuccos SEM analysis show that they are composed of gypsum and calcite.

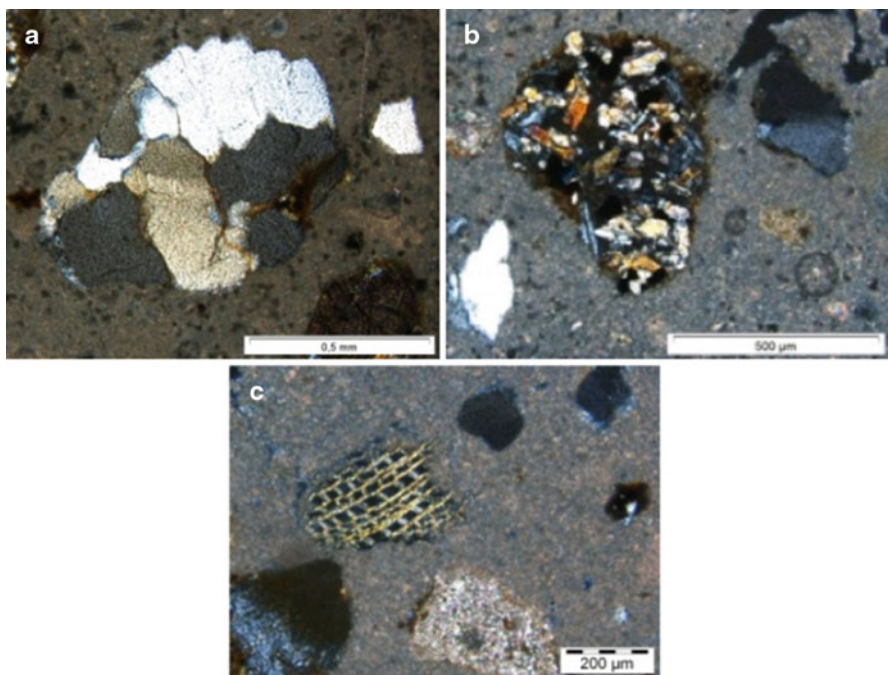


Fig. 11 Thin-section M1 mortar observation: (a) Quartzitic sand grain; (b) Basaltic sand grain; (c) Wood particle

In order to identify the possible presence of organic compounds, namely natural additives or recent restoration products, micro-FTIR analysis were performed in mortars M1 and M4, which have presented the highest weight losses by TGA-DTA in the range of 220–400°C. The results obtained (Figs. 13 and 14) from the residue of the samples after extraction in ether underline the presence, in remarkable quantity, of Paraloid B-72, an acrylic resin commonly used as consolidant and protective since the 1960s.

Besides the Paraloid B-72, mortar M4 presents a small quantity of a polyamide, not well identified. These results show a restoration intervention, in the internal renders of the church, which was probably executed during the Convent's last occupation (second half of the twentieth century).

After preliminary *in-situ* analysis, some other physical and mechanical tests were performed in the most representative mortar samples. Table 5 presents absorption capillarity coefficient and of the compressive strength results of mortars M1 and M2, including the assessment of the stucco layer (S1) on the M1 render's performance.

As can be seen in Table 5, the lime-gypsum mortar M2 presents the highest absorption capillarity coefficient, compared with the lime-based mortar M1 tested with its stucco and painting layers.

However, the compressive strength of mortar M2 is higher than in mortar M1's. The presence of the stucco does not induce a variation in the mechanical resistance of plaster M1.

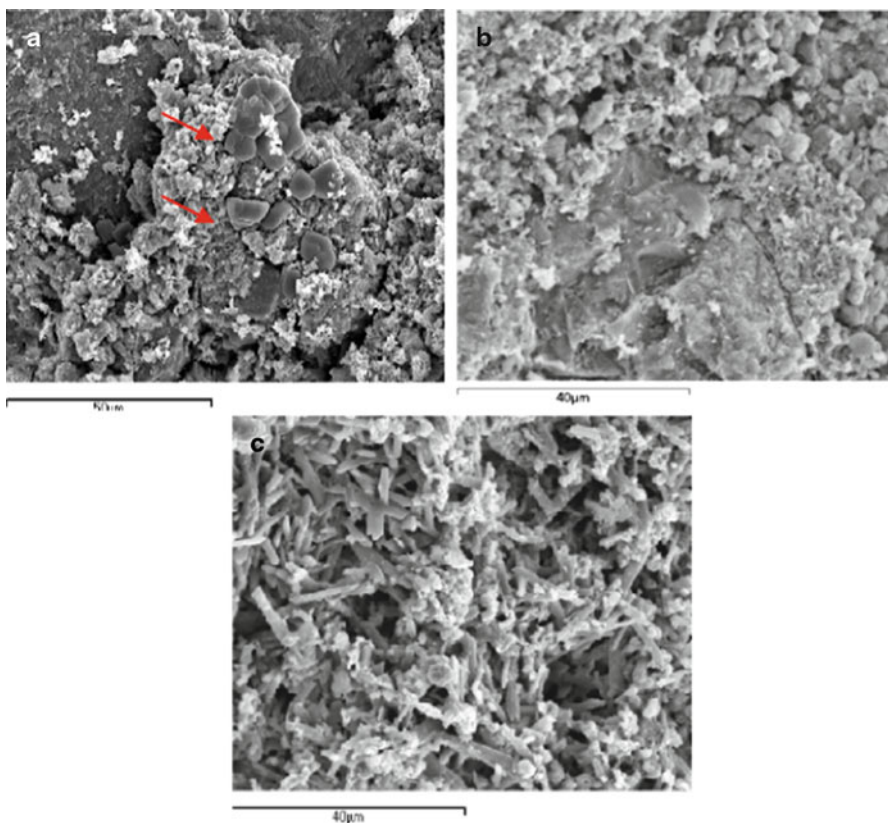


Fig. 12 M1 render SEM micrographs; (a) Mortar halite crystals; (b) Mortar paste matrix; (c) Stucco S1 paste detail presenting a gypsum and calcitic binder nature

These values were compared with a reference mortar, prepared with a 1:3 calcitic lime:aggregate ratio, using calibrated sands with mean particle sizes <2 mm; these mortars were stored for 90 days at $T=20\pm2^{\circ}\text{C}$ and $\text{HR}=50\%$. The comparison confirmed that the mechanical resistance of M1 and M2 mortars is good; confirming the recommendation regarding the preservation and restoration of existing plasters [14].

4 Restoration Tasks

All restoration tasks were undertaken by specialized professionals in various areas of conservation and restoration (mural painting, decorative painting, sculpture, wood-work, stained glass and stone-work), and supervised by IGESPAR (The Portuguese Institute for the Management of Architectural and Archaeological Heritage). Figures 15, 16, 17, and 18 resume the main restoration stages.

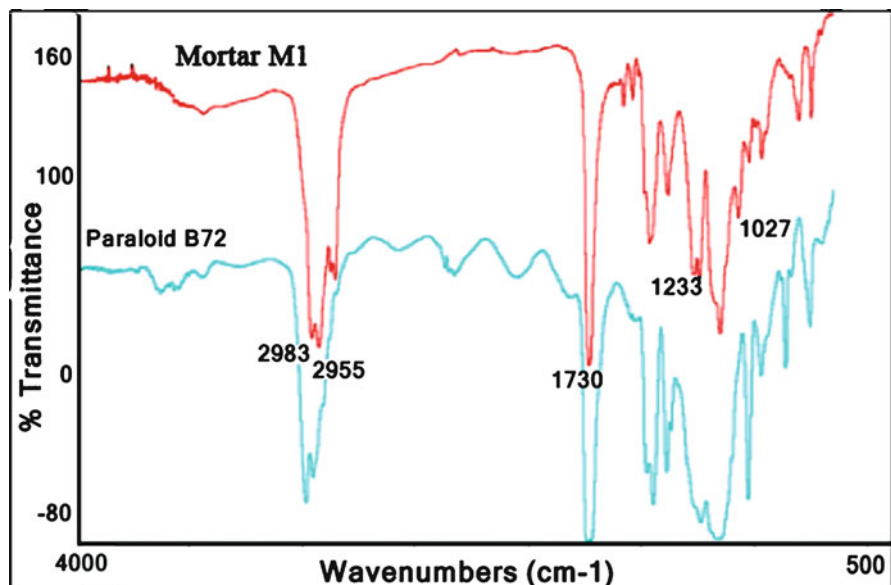


Fig. 13 M1 mortar micro-FTIR spectrums

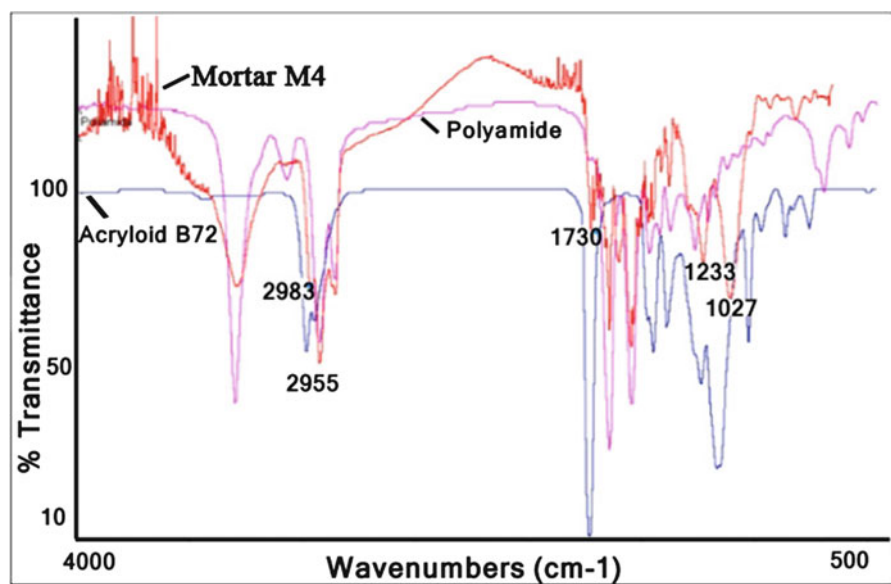


Fig. 14 M4 mortar micro-FTIR spectrums

Table 5 Physical-mechanical results of analysed samples

Samples	Capillarity coefficient by contact at 5 min (Cc5) ($\text{kg}/\text{m}^2 \cdot \text{min}^{1/2}$)	Maximum absorption value(kg/m^2) (saturation time)	Compressive strength (N/mm 2)
1 (M1+P1A+S1+P1B)	0.11	2.2 (>24 h)	2.40
M1	0.89	0.3 (24 h)	2.45
M2	1.54	0.3 (30 min)	3.20
Reference mortar ^a	1.1–1.6	0.3 (>24 h)	0.6–1.6

^aCalcitic mortar prepared in laboratory (90 days)

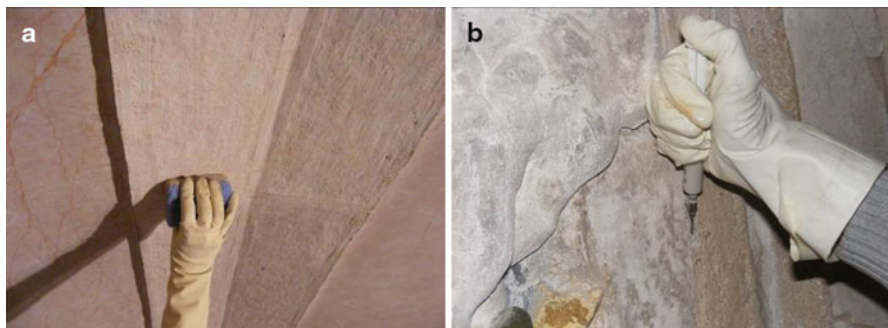


Fig. 15 (a) Surface cleaning – dry cleaning with latex rubbers and soft brushes; wet cleaning with gel – carboxilmethylcelulose and sodium bicarbonate; (b) consolidating over loss of adherence – Grouting with industrial lime mixture (PLM – I®)



Fig. 16 (a) Treatment of oxidized elements – elements destined to be restored were treated with a rust converter; elements that could not perform their function were removed (excessive deterioration), and those that retained a function were replaced with fibreglass; (b) Fixation of the pictorial layer – located with an acrylic copolymer – Acryl 33® and Klucel G according to needs

The plaster conservation and restoration works were performed with compatible repair materials selected based on the physical-chemical characterisation, after being tested in order to verify that their porosity and mechanical strength were close to the pre-existent [15].

Figures 15, 16, 17, and 18 describe the different stages of restoration.

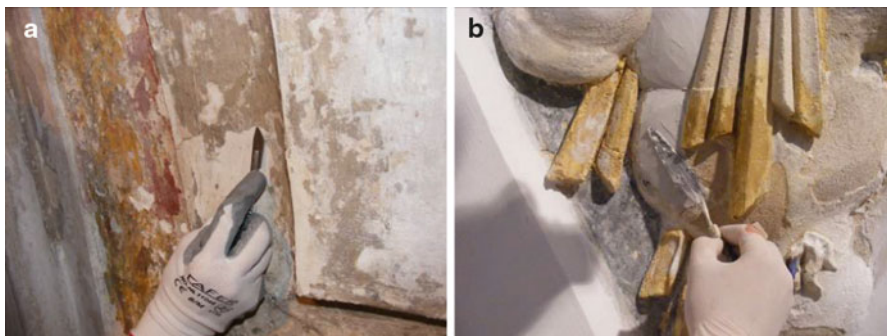


Fig. 17 (a) Removal of the juxtaposition of inadequate layers of whitewash and mortar – through mechanical means (chisels and mallets, scalpels, fibreglass pens and precision equipment such as micro drills and vibrating pens); (b) Filling the gaps and restitution of the decorative elements with a new mortar composed of slaked lime, silica sand, with similar colour and texture to the original, according to previous tests

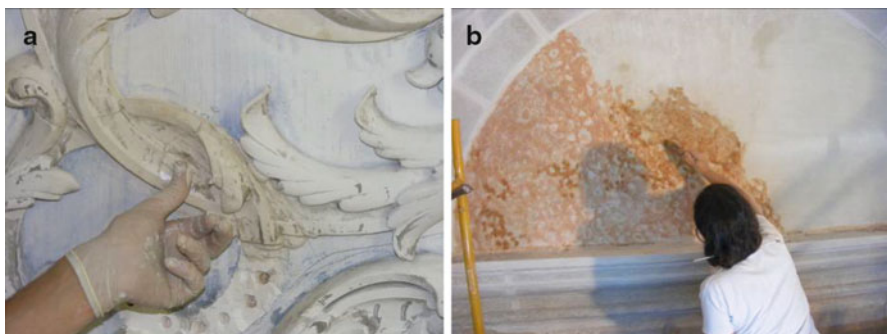


Fig. 18 (a) Reconstruction and restitution of missing decorative gypsum plaster elements within the chapel; (b) Pictorial reintegration – by an ‘illusionist’ approach or special techniques such as *rigattino* using inorganic pigments with limewash

5 Conclusions

Santíssimo Sacramento’s Church is an excellent example of the diverse stylistic and decorative solutions used in Portuguese architecture over the course of time. The church shows a multiplicity of different technical possibilities for decorative renderings, including fake stone renderings.

The diagnosis campaign has shown that the interior renders were in a very bad condition, requiring urgent restoration. The main deterioration causes were related to accumulation of water, mainly due to rain-water infiltration, excessive humidity and condensation. The water infiltrations were found to be related to roof damage over a long period. This was solved by the restoration works. The presence of early restoration mortar containing Portland cement was detected in various parts of the church.

The main problems observed were saline efflorescence, loss of cohesion and adherence, detachments, open gaps, general dirtiness, re-painting and previous conservation interventions.

The chemical, mineralogical, microstructural, physical and mechanical characterisation have shown that the renders are composed of several layers of a calcitic lime based mortar, a stucco and a lime-based mural painting.

The mortars present some differences in the composition: a first group (mortars M1, M3, M5) having calcitic lime binder, with aggregates composed of quartzitic and basaltic grains; a second group (mortars M2 and M4) composed of calcitic lime and gypsum binder and siliceous sand. Moreover the physical analysis underlines that the first group of samples have lower mechanical resistance and also lower capillary absorption coefficient compared with the second. The gypsum content of M2 explains the differences.

The presence of basaltic aggregates in the first group have probably induced the occurrence of pozzolanic reactions, improves the mechanical strength of these mortars. The lime-gypsum mortars of the second group are consistent with the spread of gypsum plasters in the interior, decoration during the Portuguese baroque and neoclassic periods [16]. All mortars present shell fragments, which, associated with sand grains sub-rounded morphology, indicates aggregate marine origin. This feature can also explain the contamination by chlorides, probably due to the unwashed marine aggregates.

The stuccos are composed of gypsum and/or calcitic lime. In S1 and S4 stuccos, the presence of anhydrite was also detected, probably introduced to increase the mechanical resistance and workability of the stuccos.

The mural paintings are constituted by many different pigments, such as ultramarine (both natural and artificial), yellow, red and green earth, azurite and gold leaf, with different preparation materials, such as barite, lead white, gypsum and calcite as binder media. Moreover, two different painting phases were identified: the first with more precious pigments (including the natural blue ultramarine – *lapislazuli*), dated from the complex's second construction program (seventeenth century); the second with stronger colours, but with poorer materials (ex. natural earths), probably dating back to the nineteenth century.

The results obtained lead to the conclusion that the mortars tested are in very good condition, only presenting superficial degradation. Although no samples were collected from the deteriorated zones, it was possible to verify the cohesion and capacity of the selected zones. Gypsum based plasters appeared to be in rather good condition, despite the water leakage through the Church's roof over a long period.

Concerning the composition of the stuccos, the seventeenth century stuccos were produced using mainly lime mortars, whereas in the eighteenth century gypsum was used as an addition with a 4:1 lime:gypsum ratio. However, the ratio between gypsum and lime had evolved to a 1:1 ratio in nineteenth century restoration campaigns. These conclusions are consistent with previous studies regarding Portuguese lime-gypsum stuccos composition [17].

During the restoration process of the church's renders, various distinct decorative solutions were discovered hidden beneath many coatings of gypsum layers and limewash.

This kind of fake stone-work undoubtedly marks, with eloquence, a spatial, formal, technical and monument decorative transformation. These renderings are architectural and artistic documents that span over various eras, constituting a historic record of both decorative values and technical solutions, due to the diversity of materials and techniques found in restoration processes. This conservation and restoration methodology creates a new language in monuments art history.

Acknowledgements The work presented is a part of the study for the restoration of Santíssimo Sacramento Convent, developed for the MNE (Ministry of Foreign Affairs) and for the IGESPAR (Institute for the Management of the Architectural and Archaeological Patrimony).

The authors acknowledge the support of the National Laboratory of Civil Engineering (LNEC), where the characterisation work was carried out. They also wish to thank the technical support of Prof. José Mirão from the University of Evora in the petrographic analysis, Dr. Isabel Ribeiro and Dr. Sara Valadas from *Instituto dos Museus e da Conservação* (IMC) for the micro-FTIR analysis, and Dr. Dora Soares from LNEC in the chemical analysis. And finally, the authors would like to show their gratitude to IGESPAR and the architects Irene Frazão and João Seabra, both responsible for the restoration works project.

References

1. Freire, J.P.: Alcântara: apontamentos para uma monografia, Coimbra (1929)
2. Silva Matos, R.M.: Do Observantíssimo Mosteiro Chamado do Sacramento de Religiosas de Sam Domingos – Monografia Histórica e Artística do Convento e Igreja do Santíssimo Sacramento, Rua do Sacramento a Alcântara, 43–51 (Lisboa). Ministério dos Negócios Estrangeiros, p. 95 (2008)
3. Santos Silva, A.: Caracterização de Argamassas Antigas – Casos Paradigmático. Cadernos de Edifícios Nº 2 – Revestimentos de paredes em edifícios antigos, LNEC, pp. 87–101 (2002)
4. Veiga, M.R., Aguiar, J., Santos Silva, A., Carvalho, F.: Methodologies for characterization and repair of mortars of ancient buildings. In: Proceedings of the 3rd International Seminar Historical Constructions, Guimarães, pp. 353–362. Universidade do Minho, Braga, November 2001
5. Magalhães, M.B.R.: Convento do Santíssimo Sacramento de Alcântara (Lisboa): análise preliminar dos espaços arquitectónicos, p. 61. IGESPAR IP, Divisão de Arqueologia Preventiva e de Acompanhamento, Lisboa (2008)
6. Veiga, M.R., Magalhães, A., Bosilikov, V.: Capillarity tests on historic mortar samples extracted from site. Methodology and compared results. In: 13th International Masonry Conference, Amsterdam (2004)
7. Magalhães, A., Veiga, M.R.: Physical and mechanical characterization of ancient mortars – application to the evaluation of the state of conservation. Mater. Constr. **59**(295), 61–77 (2009)
8. Valek, J., Veiga, M.R.: Characterization of mechanical properties of historic mortars – testing of irregular samples. Adv. Archit. Ser. **20**, 365–374 (2005)
9. CEN, EN 1015-11.: Methods of test for mortar for masonry – Part 11: determination of flexural and compressive strength of hardened mortar, Brussels (1999)
10. Schouenborg, B., Lindqvist, J.-E., Sandström, M., Sandim, K., Sidmar, E.: Analysis of old lime plaster and mortar from southern Sweden. Swedish National, Testing and Research Institute, SP Report 34 (1993)
11. Elsen, J., Brutsaert, A., Deckers, M., Brulet, R.: Microscopical study of ancient mortars from Tournai (Belgium). Mater. Charact. **53**, 289–294 (2004)
12. Eastaugh, N., Walsh, V.: The Pigment Compendium – Optical Microscopy of Historic Pigments, pp. 40–46. Elsevier Butterworth-Heinemann, Oxford (2004)

13. Adriano, P., Santos Silva, A., Veiga, M.R., Mirão, J., Candeias, A.E.: Microscopic characterisation of old mortars from the Santa Maria Church in Évora. In: Proceedings of the 11th Euroseminar on Microscopy Applied to Building Materials, p. 14. Faculdade de Ciências da Universidade do Porto, Porto, Junho (2007)
14. Veiga, M.R., Fragata, A., Velosa, A.L., Magalhães, A.C., Margalha, M.G.: Lime-based mortars: viability for use as substitution renders in historical buildings. *Int. J. Archit. Herit.* **4**(2):177–195 April–June 2010. Lourenço, P.B., Roca P. (eds.) Special Issue: Select Papers from HMC 2008 – The First Historical Mortars Conference. Taylor & Francis, Philadelphia. ISSN 1558-3058
15. Veiga, M.R., Fragata, A.: Study of Internal Renders of Santíssimo Sacramento Church, in Alcântara, Lisbon (in Portuguese), LNEC Report, Lisbon (2009)
16. Freire, T., Santos Silva, A., Veiga, M.R., Brito, J.: Characterization of Portuguese historical gypsum mortars: a comparison between two case studies. *Mater. Sci. Forum* **636–637**, 1258–1265 (2010)
17. Freire, T., Santos Silva, A., Veiga, M.R., Brito, J.: Characterization of Portuguese Historical Gypsum Mortars. In: HMC08 – 1st Historical Mortars Conference 2008: Characterization, Diagnosis, Conservation, Repair and Compatibility, Lisbon, LNEC, 24–26 Sept 2008. ISBN 978-972-49-2156-3

Part II

Repair Mortars and Design Issues

Masonry Repair Options and Their Philosophical Ramifications

Alan M. Forster

Abstract It would be assumed that a survey of a masonry structure would result in the production of an objective report. This situation cannot necessarily be guaranteed as the experience and understanding of masonry deteriorology and repair will vary from practitioner to practitioner. The difference in reporting will clearly determine alternative starting positions for the repair works, with divergence in the project potentially occurring when philosophical tenets are applied. The selection of repairs can be significantly influenced by the different professional's philosophical perspectives that can be broadly categorised as, purist, pragmatist and cynic. These perspectives may direct the approach to repair, placing emphasis of the intervention towards what is of greatest perceived value to the practitioner; for example, honesty over aesthetic integrity and vice versa. This paper investigates how and why projects may start at a subjective point (although perceived as being relatively objective) and be prone to further divergence when building conservation philosophies are applied. This situation would go some way in explaining why two professionals would be confronted with the same structure, yet the outcome of the finished repair project could be significantly different.

1 Introduction

The assessment of a deteriorating masonry structure should lead to an objective evaluation of condition. Whilst traditional visual approaches to survey may have a degree of subjectivity, they are still one of the most commonly adopted methods of inspection. This is ostensibly due to their ease of undertaking, relative low cost and

A.M. Forster (✉)

School of the Built Environment, Heriot-Watt University, Edinburgh, Scotland, UK
e-mail: a.m.forster@hw.ac.uk

they do not rely upon specialist technical survey equipment. Whatever the method of survey, an objective set of requirements must be established for the building to enable a repair strategy, or more simply an agreed method of work to be established. The repair options available must also be subjected to the application of building conservation philosophy that may result in project divergence.

2 Evaluation of Condition and Condition Surveys

Building survey has been defined as '*a comprehensive, critical, detailed and formal inspection of a building to determine its condition and value*' [1]. Condition surveys are one widely adopted form of survey [2], that are assumed to be objective however, they are inevitably subjective in nature, due in part to different surveyor's education and experience in investigating and reporting diagnostics. Straub [3] highlights this situation stating '*the practice of condition assessment by building inspectors yields variable results due to subjective perceptions of inspectors. Surveyor variability is defined as the situation where two or more surveyors, surveying the same building, arrive at very different survey decisions. This variability is caused by a variety of factors such as previous experience, attitude to risk and, heuristics – the use of “rules of thumb” – a leaning towards a particular opinion regardless of the available evidence.*' Exacerbating this situation, the evaluation and understanding of stone decay mechanisms is a specialist area and could be surmised to be out-with 'average' professional training. It may therefore be unrealistic to expect the non specialising professionals to evaluate complex masonry projects [2].

Whatever the skill base of the lead professional it has been recognised that tacit investigative protocol is initiated in the formulation of any survey. Douglas and Ransom [4] discuss what they call the 'hierarchy of investigating diagnostics', indicating that this area can be subdivided into, protocols (key defects risk areas and principles for building [5]), testing techniques (destructive and non-destructive) and cognitive branches (critical thinking, problem solving and decision making processes). These cognitive branches can be considered as being the most subjective. Additionally, Ruston [6] has proposed the 'HEIR' (History, Examination, Investigation and Report) method of diagnostics that formalises the survey process, but this still does not reconcile the subjectivity of examination and reporting. In addition to this tacit knowledge, applied university education and aspects of specific professional training are also utilised [2, 7] to form decisions relating to condition. Both the author and Ashurst [2] agree with some of the primary education requirements for surveying such structures (such as an understanding of building pathology, inspection and materials science), however, objectivity is still arguable. The combination of the objective and subjective aspects of diagnostics are reflected by Hollis [8] who states that '*Surveying buildings is an art; verifying the cause of the failure is a science. The surveyor's work involves a combination of both art and science*'. As with any 'art' its subjectivity makes commonality in reporting difficult to achieve.

Exacerbating this situation, no standard approach exists for survey work of this nature and as Ashurst [2] indicates; '*Architects and surveyors will create their own approach*'. It is the authors' view that an individual approach is acceptable as long as it is logical, well considered, rigorous, and encapsulates the majority of aspects of the hierarchy of building diagnostics and other specific practice based guides. General best practice has been established within the United Kingdom and many Common Wealth Countries by the Royal Institution of Chartered Surveyors [9] and although the guidance appears relatively comprehensive, it does not include specific, somewhat specialised stone decay mechanisms [10]. An objective initial starting point for any buildings' requirements cannot therefore be guaranteed. This situation may be especially pronounced if the surveyor is not experienced; with significant divergence potentially occurring from other reporters.

3 Philosophical Tenets

The way in which we approach any repair project should be underpinned by building conservation philosophy. It is important to realise that almost every technical repair intervention should be assessed against the 'guiding lights' [11, 12] or 'ethics' (those forming the broader issues or key concepts to be considered) and 'principles' (specific criteria upon which conservation works should be based) of building conservation philosophy. These ethics and principles have been summarised by Bell [13];

Ethics include; Authenticity, integrity, avoidance of conjecture, respect for age and historic patina, respect for the contribution of all periods, inseparable bond with setting and rights of the indigenous community.

Principles include; Minimal (Least) intervention, legibility (honesty and distinguishability), materials and techniques (like for like materials), reversibility, meticulous recording and documentation and sustainability.

It could be assumed that the importance associated with each of the ethics and principles will vary from person to person, depending on their perspective and what they perceive to be of greater value. It is obviously best to consider them as holistically as possible, whilst comparing and contrasting the individual concepts. A skewed focus, or over reliance on any one of the ethics or principles will lead to a selected repair that may be eminently suitable in one respect, but clearly fails in other aspects. Stirling [14], believes that conservation professionals can be broadly categorised as having one of three philosophical viewpoints, namely,

Purists' view: '*the idea that there can be alternative philosophical approaches to the preservation of buildings is seriously misleading. Correctness cannot be watered down*'.

Pragmatists' view: '*a sound philosophy is one which points in the right general direction – that of truthfulness. Its precise application must depend on the building and its circumstances. If I am in command of all the facts, then the building itself will tell me what to do.*'

Cynics' view: '*conservation is a completely artificial procedure, interfering with natural processes of decay of absolution. Conservation philosophies are therefore necessarily artificial.*'

The application of ethics and principles are therefore viewed through the professionals' personal philosophical view point, creating the potential for further divergence. It is however also important to understand that there are no absolutes in conservative repair, only greater levels of defence for selected repairs [15, 16]. The first rule of conservation is that there should be '*no dogmatic rules... each case must be considered on its own merits*' [17].

4 Masonry Repair Options and Their Philosophical Ramifications

Although a client may be specific about initiating repair works to fabric they may not be aware of the need to conform to building conservation philosophy. These issues must be raised by the lead professional who should highlight the implications of repair works set within the context of philosophical ethics and principles [11]. It is obvious that the experience of the practitioner is critical to project success; but it should also be recognised that the inclusion of advice from specialist masonry contractors is also extremely beneficial [2]. Additionally, it is also critical that the lead professional has sufficient knowledge of the range of alternative repair options available for the treatment of deteriorating masonry substrates. Some of these are outlined in the following section, however, it must be emphasised that it is not to be viewed as a comprehensive list of all available techniques.

4.1 Do Nothing

Doing nothing can in many cases be a reasonable approach, that has lead to the retention of much historic material. Although a masonry substrate may appear to be in a condition that would warrant intervention this may not be necessarily be the case as many projects may be undertaken to simply restore the aesthetics and integrity of a building [17]. These types of intervention are clearly a deviation from the minimal intervention philosophical tenet and can have a negative influence on the authenticity of the structure. That being said, work that requires a higher degree of intervention could in theory be substantiated if they protect the underlying masonry. Decisions to do nothing must be undertaken by assessing holistic building performance, and understanding the importance and relationship of each associated element and component.

4.2 *De-scale*

In cases where the removal of friable and loose masonry material is expedient for safety reasons it may be necessary to opt for de-scaling. This process can be a temporary emergency measure or part of a longer term minimal intervention strategy. Descaling entails the simple removal of loose masonry and in excessive cases cutting back decaying stone. This approach, although relatively cheap to execute, is irreversible and clearly leaves a variable aesthetic appearance that can debase the integrity of the building. De-scaling could however be argued to be a reasonable course of action, due to it being relatively minimal intervention in nature. This approach may be considered by many to be insensitive as in many situations the loose and friable surfaces can be saved by using high quality masonry repair techniques, such as pinning, dowelling and consolidation.

4.3 *Pinning, Dowelling and Flaunching*

Pinning, dowelling and flaunching techniques are utilised for the consolidation of delaminating masonry surfaces. They require selective holes to be drilled along the affected delaminating surfaces and roughened nylon or high grade stainless steel threaded bars to be inserted into the holes. These are subsequently encased in modified lime grouts, with pigmented lime mortars used to cap the holes. The delaminating layers are also grouted along the failure planes and can also be flaunching with a lime mortar ‘skew’ along the treated edge. Pinning delaminated stone is least intervention in nature and retains the maximum amount of fabric, but is costly and time consuming to execute. In addition, it is vital that great consideration is given to the selection of any consolidant or grout prior to use as they are difficult to reverse.

4.4 *Stone Replacement*

Stone replacement entails the removal of decaying masonry and replacing with a suitable matching stone. The replacement stone type should be derived from a host of analytical techniques and not simply visual matching [18, 19]. Purists may argue that replacing stone with well matched material does however raise issues of distinguishability of new from existing fabric. This poses the question is well matched stone replacement ultimately dishonest? It is obvious that a ‘trade off’ occurs with honesty and distinguishability being set against the principle tenets of integrity and like for like materials. Slight variation in tooling effects could go some way to distinguish the repair from existing fabric, but as the finish erodes this would be lost. A professional that places greater emphasis upon honesty over integrity may wish to specify plastic, tile or other distinguishable alternative repairs.



Fig. 1 Overzealous masonry replacement, Newcastle upon Tyne

Stones that have eroded to the point that the structural integrity is questionable could warrant replacement. That being said, wholesale replacement of masonry (Fig. 1) should be avoided as this is not minimal intervention, resulting in unnecessary loss of historic material and debasement of authenticity. Conversely, the replacement of isolated stones leads to the retention of a higher degree of original fabric with additional benefits for the authenticity of the fabric.

Critics of stone replacement may however, argue that if the structural integrity of the masonry is not in question then lime based plastic repairs may be philosophically more sensitive in nature, owing to a greater potential for reversibility, and retention of more fabric.

4.5 Stone Indenting

Indenting masonry is the process of replacing an isolated section of stone and piecing it into the existing (Fig. 2). A good indent should be almost seamless and attached using a suitable mortar. These repairs can be undertaken to carved stone sections or flat faces, and can be considered as being relatively minimal intervention in nature as they are localised. They do however require the removal of a certain amount of stone forming a pocket to house the new material. Stone indenting would initially be honest as the existing and new works would be distinguishable. However, as the stone weathers, and soiling occurs the ability to do so is diminished. The reversibility of stone indenting interventions are questionable as the only real approach is to ‘cut out’ the repair. Clearly, if a minimal intervention approach was paramount, then plastic (mortar) repairs may achieve better results.



Fig. 2 Stone indent to *column*, Brandenburgh Gate, Berlin

4.6 Tile Repair

Tile repairs are undertaken using clay plain tiles (Fig. 3) or natural stone slips. These are built up in bonded layers and accommodate voids left behind by deteriorated masonry.

These forms of repair are visually obtrusive and are highly distinguishable and therefore honest. Stone slip repairs can be more subtle and harmonising in the context of stone substrates. Critics [20] of the repairs indicate that they only indicate the philosophical stance that the lead professional has taken, and ultimately debase the integrity of the structure. The ability to reverse the repairs once executed is high if they are built in relatively soft lime mortars.

4.7 Lime Mortar Plastic Repair

Plastic repair is the process of removing friable and decaying masonry material and utilising mortar to form new flat or profiled surfaces. The term ‘plastic’ relates to the plasticity of the materials and not that it contains polymers [21]. These can be attached via suction bonds or armatures depending upon their location and substrate type.



Fig. 3 Honest repair in plain clay tiles to limestone and flint substrate

Suction bond plastic repairs are relatively reversible as they can be cut out with little damage to the substrate. These repairs can be considered to be minimal intervention when set in a context of replacement stone, but they have a lower life expectancy than other intervention types. The degree of honesty of these repairs is a function of the mortar specification, with a high degree of indistinguishability being achieved if pigments and careful aggregate selection are utilised. Profiled plastic repairs have many advantages over replacement stone in so much as they enable the maximum amount of fabric to be retained whilst being relatively reversible.

4.8 Repair Mortars

The starting point for any mortar for repair should be analysis of the existing material. It could however, be argued that those mortars that best replicate the existing materials are indistinguishable and could be considered as being dishonest. Conversely, those that match the mortar on a performance may tend to be honest, but deviate from the philosophical concept of ‘real’ like for like materials replacement.

Materials that attempt to replicate historic aged mortars can never be fully achieved, when assessed on a microstructure level. This is due to the texture of a mortar modifying over the life of material. In addition, the complexity of historic mortars is considerably greater than their modern counterparts [22]. The aggregates within these historic mortars can also be more varied than those aggregates available for modern conservation works [23]. The philosophical paradox is that the better the replicating specification, the greater the potential dishonesty. One potential practical answer could be to encourage different surface finish effects on pointing, but this still does not reconcile the problem of honesty once the finish has deteriorated. This situation could therefore be negated by matching the materials properties, whilst using clearly different aggregate.

5 Conclusions: Divergence of Project

A lack of uniformity in the reporting of masonry condition could be argued to create a variable starting position for the selection of masonry repairs. The experience of the professional in masonry repair will have a direct relationship on what strategy is selected. Additional deviation in repair strategies occur when the subjective application of building conservation philosophy is undertaken. It is clear that alternative surveyors looking at the same building could determine different needs for the structure; one estimating minimal intervention, whilst the others favouring a greater degree of work. It must however be emphasised that these differences are out-with philosophical perspectives with a purist and cynical practitioner determining the same requirements for the substrate.

Upon determination of the requirements the surveyors would then be expected to select suitable repairs of which there are numerous. One of the surveyors may have a better understanding of philosophy and the ramifications of the different interventions, whilst the others may not take this into consideration. The philosophical stance or viewpoint of the lead professional is clearly pivotal as a purist and cynic could lead to significantly different repair types being selected. Purists may favour repairs that direct the observer to their presence and that are to greater or lesser degrees obtrusive (such as tile repairs), whilst pragmatists would place less emphasis upon this and tend towards holistic integrity of the repaired structure. Cynics of building conservation philosophy would in theory pay no attention to the tenets. This would not automatically mean that cynics would undertake poor quality, indefensible repairs as they should still be bound by best practice and an understanding of building performance. The aesthetic appearance of the building has the potential for significant difference and highlights the importance of engaging an experienced practitioner, ascertaining their philosophical perspective prior to project commencement.

References

1. Watt, D.: Building Pathology: Principles and Practice. Blackwell, London (1999)
2. Ashurst, J.: Conservation of Ruins. Butterworth-Heinemann, Oxford (2007)
3. Straub, A.: Dutch standard for condition assessment of buildings. *J. Struct. Surv.* **27**(1), 23–35 (2009)
4. Douglas, J., Ransom, W.: Understanding Building Failures, 3rd edn. Taylor & Francis, Oxford (2005)
5. Addleson, L., Rice, C.: Performance of Materials in Building. Butterworth-Heinemann, Oxford (1992)
6. Ruston, T.: Understanding why buildings fail and using ‘Heir’ methodology in practice’, latest thinking on building defects in commercial buildings: their diagnosis, causes and consequences, one-day conference, London, 15 July 1992
7. RICS.: Assessment of professional competence: RICS Education and Qualification Standards. RICS <http://www.RICS.org> (2009). Accessed Apr 2010
8. Hollis, M.: Surveying Buildings, 5th edn. RICS Books, London (2005)
9. RICS.: Guide to Building Surveys and Inspections of Commercial and Industrial Property. RICS guidance note, 3rd edn. RICS, London (2005)
10. Webster, R.: Stone Cleaning and the Nature, Soiling and Decay Mechanisms of Stone. Donhead, London (1992)
11. Earl, J.: Building Conservation Philosophy, 3rd edn. Donhead, Somerset (2003)
12. BS 7913.: The principles of the conservation of historic buildings. BSI (1998)
13. Bell, D.: Technical Advice Note 8: The Historic Scotland Guide to International Charters. HMSO, Edinburgh (1997)
14. Stirling, J.S.: Building Conservation Philosophy. Unpublished lecture notes, Heriot-Watt University, Edinburgh (1997)
15. Forster, A.M.: Building conservation philosophy for masonry repair: part 1 ‘Ethics’. *J. Struct. Surv.* **28**(2), 91–107 (2010)
16. Forster, A.M.: Building conservation philosophy for masonry repair: part 2 ‘Principles’. *J. Struct. Surv.* **28**(3), 165–188 (2010)
17. Powys, A.R.: Repair of Ancient Buildings. Society for the Protection of Ancient Buildings, Kings Lynn (1995)
18. BRE.: Building Research establishment (BRE), stone list. <http://projects.bre.co.uk/condiv/stonelist/corsehill.html> (2010). Accessed Mar 2010
19. Scottish Executive: Building with Scottish Stone. Crown Copyright, Arcamedia, Edinburgh (2005)
20. Hill, P.: Conservation and the stonemason. *J. Archit. Conserv.* **1**(Part 2), 7–20 (1995)
21. Ashurst, J., Ashurst, N.: Practical Building Conservation: stone masonry: English Heritage Technical Handbook, vol. 1. Gower Technical Press, Avon (1988)
22. Hughes, J.J., Banfill, P.F.G., Forster, A.M., Livesey, P., Nisbet, S., Sagar, J., Swift, D.S., Taylor, A.: Small-scale traditional lime binder and traditional mortar production for conservation of historic masonry buildings. In: Proceedings of International Building Lime Symposium, Orlando, FL, pp. 1–13 (2005)
23. Scotland, H.: Tan 19: Scottish Aggregates for Building Conservation. Crown Copyright, Edinburgh (1999)

Conservation of Historic Renders and Plasters: From Laboratory to Site

Maria do Rosário Veiga

Abstract In interventions on historic renders and plasters, the first step is to decide upon the strategy: repair or substitution, based on an evaluation of the cultural value of the render or plaster, of the building itself and on a careful diagnosis of the typology of defects, their quantity and reparability. New renders or repaired renders should fulfil the main functions they are required to, especially protection and aesthetic functions. Compatible materials should always be used. Compatibility is needed for durability, not of the render, but of the wall as a whole, and also for preserving the documentary and symbolic value of the building as well as its image. Compatibility is defined in relation to the substrate and the existing mortars. Therefore tests need to be carried out on the old materials and on possible solutions, to compare characteristics and assist in the selection of the best. It is acceptable to begin using non-destructive or slightly destructive *in-situ* tests, because with them it is possible to collect useful information quickly and without destruction of the historic renders. Simple mechanical and physical tests can be carried out on the old mortars and a few chemical tests can also be performed, with portable equipment. If rigorous and complete tests are needed, some samples can be collected and tested in the laboratory, using methods adapted to non-regular, possibly friable specimens. The characteristics of the mortars to use can be established, based on the results obtained, in order to fulfil both functionality and compatibility. However, sometimes it is not possible to obtain enough data about old materials, especially concerning masonry as a whole, which is more difficult to test than mortars. For this situation, some general requirements have been established, based on previous work carried out on Portuguese historic masonry buildings, which can be used without risk of damaging existing materials. Decisions concerning the materials to use, especially binder materials, should also take into account the climatic and environmental conditions. Appropriate application techniques, workmanship and curing conditions are indispensable in

M.do Rosário Veiga (✉)

Laboratório Nacional de Engenharia Civil (LNEC), Lisbon, Portugal

e-mail: rveiga@lnec.pt

achieving good aesthetic, physical and mechanical results. Therefore it is important to know what conditions are available for the application phase. An effective knowledge of the historic materials and of the possible compatible solutions, of their characteristics and problems, is essential; tests are an important tool but the interpretation of their results in order to take useful decisions is a complex task, requiring a multidisciplinary team efficiently coordinated.

1 Conservation Strategy Decision Making

1.1 *Strategy and Factors*

When facing an intervention on old renders, the first step – and probably the most important one – is deciding upon the strategy to implement. Two basic alternatives are possible:

- Preservation and repair with compatible materials
- Substitution by compatible new renders

Many factors should be taken into account, some of them of a subjective nature, others more technical and quantifiable:

1. Cultural value (for example combinations of historic value, artistic value, technical value and value associated with rarity).
2. State of conservation of the background and its capacity to be repaired (reparability).
3. State of conservation of the render: severity and intensity of anomalies and their reparability.
4. Compatibility of the render with its current (or foreseen) use and the environmental conditions.
5. Available workmanship.

Factor 1 dominates. However, most cases fall in the category of “medium cultural value”. The technical team has essentially to deal with factors 2, 3 and 4, although an opinion on 1 and 5 is usually required. This decision requires a diagnosis and quantification of the wall’s anomalies (both masonry and render), as well as an evaluation of the future actions on the rendered surface that are foreseen.

1.2 *Diagnostics*

In many cases of planning interventions on renders and plasters quite simple and quick investigations and observations are enough to establish a diagnosis [1]:

1. Observation by a trained person:

- 1.1. Presence of moisture.

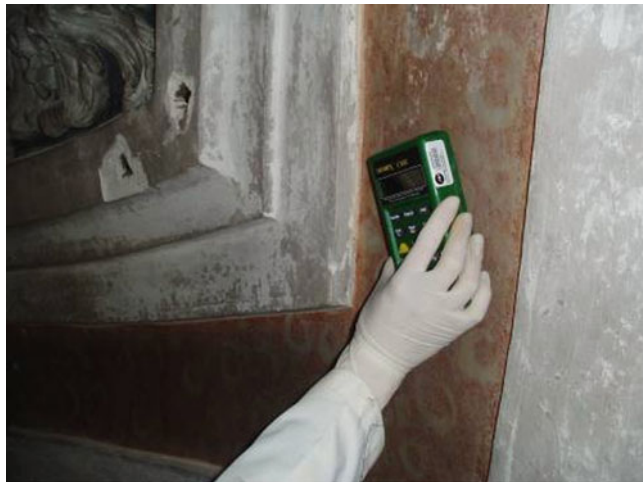


Fig. 1 Moisture measurements with a portable humidimeter



Fig. 2 Modulus of elasticity by ultra-sound measurements

- 1.2. Type of defects: fungus, black crusts, detachments, lack of cohesion, cracks and micro-cracks, brown stains of corrosion products.
- 1.3. Quantity and localisation of defects.
2. Moisture measurements: localisation and intensity of moisture, map of moisture distribution (Fig. 1), using comparative, indicative measurements.
3. Mechanical and physical *in-situ* and laboratory tests (Figs. 2, 3, and 4).



Fig. 3 Water absorption by capillarity of irregular samples



Fig. 4 Compressive strength of irregular samples

These actions allow important questions to be addressed:

- Is moisture a problem? Observations 1.1, 1.2, 1.3 and action 2 should provide an answer. Where does the moisture come from? Actions 1.3 and 2 will help to discover it.
- Apart from moisture, what other causes of defects are there? 1.1, 1.2, 1.3, 2 and possibly 3 will furnish the appropriate information. Structural problems – deformation? Salty fog? Pollution? Corrosion of metallic elements (Fig. 5)? Poor interventions with incompatible materials?



Fig. 5 Corrosion of metallic elements may require partial removing of the plaster



Fig. 6 Repair of render detachment using grouts is a delicate, complex technique

- Are there defects with a low degree of reparability (Fig. 6)? Detachment and lack of cohesion are usually the most difficult defects to repair [2–4]. Observations 1.2 and 1.3 will generally allow the identification of these types of anomalies and action 3 will permit some quantification.
- Are renders and plasters globally affected, in a significant degree? Namely, are they globally too weak and permeable? Action 3 will help to get this answer [5–7].

The results of these simple diagnostic actions and their careful interpretation should provide significant information including: the identification of the main causes of defects and the way to control them; the identification of the defects of masonry and the possibility of evaluating the need to remove the render or plaster locally or globally; the classification of the state of conservation of the render or plaster itself, considering the intensity of defects and their reparability classed as high, medium or low levels of degradation.

1.3 Foreseen Actions

Old buildings today can be subjected to different loads, due to change in use or diverse environmental conditions. It is necessary to verify if the current or future conditions of the building may suggest changes or enhancements to particular characteristics of renders and plasters. For example, for renders, higher pollution or traffic vibrations may now occur or for plasters, different uses such as museums, music or theatre rooms may require different physical characteristics.

1.4 Decision Making

Based on the actions and observations mentioned above a decision about preservation and repair or substitution is possible. Table 1 gives an idea of the systematisation of decision processes for the case of “medium cultural value”.

2 Choice of Materials

2.1 Fulfilment of Main Functions

The main functions of renders and plasters are:

- Protection of masonry (against external actions such as impact, abrasion, weather, pollution).
- Regularisation (making look smooth or consistent) of the walls.
- Finishing and decoration.

The repair or renewal of renders and plasters is intended to fulfil these main functions. They have no structural functions, but they have a significant role in the protection of structural old masonry and hence on its durability and general good performance. The mortars to use don't need high strength, but some resistance to friction and impact, some deformability to follow masonry displacements without cracking and some ability to delay rain water penetration and to allow the easy evaporation of water from inside old porous walls.

Table 1 Support for intervention strategy decision making

Cultural value	State of conservation of the substrate	State of conservation of the render/plaster	Compatibility with use and actions	Recommended strategy
Medium	Good	Good	Bad	Protect or reinforce the render/plaster in a compatible way (ex. silicate based painting)
	Good	Bad	Good	Repair and consolidation of the render/plaster
	Bad	Good	Good	Repair the substrate with techniques of low intrusivity;
	Bad	Bad	Good	Keep the render/plaster filling lacunae and reintegrating aesthetically
	Bad	Good	Bad	Repair the substrate with techniques of low intrusivity;
	Bad	Good	Bad	Partial substitution of render/plaster
	Good	Bad	Bad	Repair the substrate with techniques of low intrusivity;
	Bad	Bad	Bad	Reinforce the render/plaster in a compatible way
High	Good	Bad	Bad	Analyse the viability of repair and consolidation of the render/plaster against partial substitution with compatible techniques and materials
	Bad	Bad	Bad	Repair of the substrate and substitution of the render/plaster with compatible materials

2.2 Compatibility

Renders and plasters are a part of the walls. Materials both for their repair and for their renewal should be compatible with the existing mortars and substrates [8–11].

This means essentially:

- there should be no new damage as a result of the intervention;
- they should be consistent with the overall appearance, now and after ageing

How can repair and substitution materials be harmful to existing materials? Some properties of new mortars can produce damaging actions:

- The introduction of stress due to higher stiffness and different thermal dilation coefficients, producing differential deformations in relation to the old materials in contact. Shrinkage of the new mortar, thermal variations and deformations of the masonry will produce stresses at the interface between old and new materials, damaging the weakest material (Fig. 7). The stresses are higher when differences between characteristics are larger [12]. As the extant material should be preserved, it must not be the weakest.



Fig. 7 Mechanical damage due to incompatible new render



Fig. 8 Damage due to reduction of water permeability of the walls

- The reduction of the drying ability of the wall through the application of renders with lower capillarity and lower water vapour permeability than the existing ones may result in the retention of water inside the masonry and higher capillary rise on the wall. This could become a problem in historic buildings, especially when there is water coming from under the foundation level or when the masonry is water saturated due to roof deterioration. Any soluble salts present in the walls will be transported by capillary rise and spread into larger areas of the masonry. Eventually they will crystallise at the new drying surface, often the interface between masonry and render, producing damage of the masonry and detachment of the render (Fig. 8).

- Driving the water through older mortars or stones, due to lower capillarity compared to new materials. In fact, when more impermeable materials are used, the water transport through the capillary net is diverted to the most permeable old materials in contact, accelerating their degradation.
- Introduction of new salts due to the presence of cement or other constituents containing soluble salts [13].

How can new products affect aesthetics?

- Different texture or colour due to different aggregates, different binder nature or different pigments.
- Differential ageing due to the different nature of constituents (resins, organic pigments, etc.).

A set of compatibility requirements can be established considering these issues. In Table 2 a correspondence is established between compatibility requirements and material characteristics.

2.3 Environmental Considerations

The choice of materials is also limited by some environmental conditions: weather, the proximity of the sea and pollution. Rainy weather, salty fog and spray of salty water and high pollution are factors that may militate against the use of pure air lime mortars. In Portugal, air lime mortars were used in the past in misty, salty environments [14, 15], but today it is difficult to guarantee appropriate conditions of application and curing, so some hydraulicity is advisable. In moderately dry climates (like the South of Portugal), away from the sea, air lime mortars can be a good solution, except when high levels of pollution exist and create the danger of damage by acid attack.

2.4 Site Testing

Compatibility is defined in relation to the background and the existing mortars. Thus, it is important to determine the main characteristics of the masonry and the old renders, in order to design new mortars with similar characteristics. *In-situ* testing, especially using non-destructive methods, is a first approach to evaluate significant characteristics (Figs. 1, 2, 9, 10, 11, and 12). Generally they have to be used in a comparative basis, as there are currently no sufficient correlations with laboratory tests.

In Table 3 some simple tests, non-destructive or slightly destructive, are considered, and related (qualitatively) with performance.

It is also now possible to perform *in-situ* some mineralogical tests with portable equipment. One of the most used is X Ray Fluorescence, with portable equipment, permitting for example the discrimination of the type of binder, or other compounds

Table 2 Compatibility requirements and new mortars characteristics

Requirements	Rc and Rf	E	C	Wvp	S	α	Materials (direct influence)
Main functions	Protection against impact and abrasion	Medium (indicative)	Medium (indicative)	—	—	Low-medium	—
	Protection against rain penetration	—	—	Medium	—	Low	—
	Protection against pollution attack	—	—	Medium	—	Low	Air lime (CaCO_3) is vulnerable to acid rain and pollutant gases in general (SO_2 , CO_2 and NO_2)
	No introduction of stress	Low	Low	—	—	Low	No high proportion of cement
	No retention of water inside walls	—	—	Medium	High	—	Similar to old mortars and substrate
	No driving water through old materials	—	—	Similar or higher than old mortars	High	—	No water repellents, no resins
	No introduction of new salts	—	—	—	—	—	No water repellents, no resins
	No aesthetic effect	—	Low	Similar or higher than old mortars	High	Low	No cement
	Global analysis	Low-medium	Low-medium	Medium – similar to old mortars and/or substrates	High	Low	Similar to old mortars and substrate
							Similar aggregates, similar binder Similar pigments No cement, no resins Similar aggregates, similar binder Similar pigments No cement, no resins, no water repellent, similar aggregates, similar binder, similar pigments

Rc compressive strength, Rf flexural strength, E modulus of elasticity, C Capillary coefficient, Wvp water vapour permeability, S shrinkage, α coefficient of thermal dilation



Fig. 9 Evaluation of water permeability with Karsten tubes



Fig. 10 Evaluation of mechanical strength with Pendular Schmidt Hammer

present, such as salts. The “Hercules Center”, of Évora University, in Portugal, makes this equipment available to the scientific community. X Ray Diffraction with a portable apparatus is also possible.

For current situations *in-situ* tests may give enough information for decision making concerning the choice of repair materials.



Fig. 11 Evaluation of surface hardness with a durometer



Fig. 12 Identification of presence of some salts with colorimetric strips

Table 3 Relation of *in situ* tests with performance characteristics

	Moisture measurement	Pendular Schmidt hammer	Durometer	Ultrasound	Karsten tubes	Salt colorimetric stripes or salt kits
Mechanical strength	—	X	X	X	—	—
Dynamic modulus of elasticity	—	X	—	X	—	—
Water permeability	—	—	—	—	X	—
Presence of salts on the surface	—	—	—	—	—	X

Table 4 Relation of laboratory tests with performance characteristics

Main laboratory tests on samples removed from site	Chemical mineralogical and microstructural characterisation [10, 16]	Compressive strength [17]	Capillary water absorption [18]	Porous structure by MIP [19]
Objective	Composition; microstructure; products of alteration	Resistance against mechanical loads	Protection from water penetration and promotion of drying	Hygric behaviour and behaviour to salts

2.5 *Laboratory Testing*

More specific tests are carried out in the laboratory, whenever needed (Figs. 3 and 4). Laboratory tests require the collection of samples, so in this sense they are always destructive. For this reason and also for economic and time constraints, they must be complementary to site testing and usually be limited to those that are unavoidable. Due to limitations of dimensions, shape and cohesiveness of plaster samples collected from buildings, not every laboratory technique can be used and the number of possible tests is smaller than for laboratory produced specimens. In Table 4 the most useful groups of complementary laboratory tests are presented and related to characteristics and performance.

2.6 *Requirements*

The characteristics of the mortars to use can be established based on the sets of results obtained, in order to fulfil both functionality and compatibility, as summarised in Table 2. However, sometimes it is not possible to get enough data concerning the old materials, especially about the masonry, which is rather more difficult to test than mortars. For that situation, some general requirements have been established, based on previous work carried out on Portuguese historic masonry buildings, which can be used without risk of damaging existing materials [10]. These requirements, summarised in Table 5, consider medium to low strength masonry of irregular stone, agglomerated with lime mortars, which are very common in old buildings in the south of Portugal.

2.7 *Global Analysis and Decision Making for Repair and Substitution Solutions*

Subsequently a global analysis of all the data – observations, tests and available conditions – is needed to choose a mortar for repair or substitution.

Table 5 General requirements concerning some characteristics for rendering and plastering repair mortars for historic buildings

Type of render	Mechanical characteristics at 90 days (N/mm ²)				Hygric behaviour at 90 days	
	R _f	R _c	E	A	W _{vap}	S _d
Exterior render	0.2–0.7	0.4–2.5	2,000–5,000	0.1–0.3 or cohesive rupture	<0.08	<1.5; > 1.0
Interior render	0.2–0.7	0.4–2.5	2,000–5,000	0.1–0.3 or cohesive rupture	<0.10	–

R_f flexural strength, R_c compressive strength, E modulus of elasticity, A bond strength, W_{vap} water vapour permeability, S_d thickness of air with equivalent diffusion, C Capillary coefficient

What are the choices for possible compositions of the binder(s) to use? The most compatible binders are: air lime, hydraulic lime free of salts, and air lime plus pozzolans (either natural or artificial). Although cement should be avoided as a single binder for the repair of historic lime mortars, lime-cement mixes can also be acceptable binders for that purpose, in some circumstances [20, 21].

The volumetric ratio 1:3 (binder:aggregate), or near this proportion, is currently adopted. This is the proportion that theoretically assures the highest compaction of the mortar, when the aggregate has a well-balanced grain size distribution. It has also been verified in practice that contemporary renders with a higher proportion of binder have a strong tendency to crack, although there is much evidence of their successful use in the past.

The groups of mixes considered as possibly compatible, and their basic average range of characteristics, are compiled in Table 6. The range of results presented is based in previous work [20–24].

The characteristics of all these types of mixes may be adjusted and improved by manipulating the aggregate type and grain size distribution, the type of lime, when two binders are mixed, variation of their relative proportions, considering the method of application and the curing conditions and, possibly, the use of some additives or admixtures.

3 Application

After decisions about materials are made, it is important to guarantee the appropriate conditions of application, concerning technique, workmanship and curing.

For lime mortars, the application technique is particularly important: the exact quantity of mixing water (enough for good workability but not too much, for good compaction); long mixing; several thin coats; careful curing, avoiding quick drying and closing cracks when they occur during the early stage of application etc. [25, 26].

Table 6 Average range of characteristics of some types of mortars

Mix and volumetric proportion binder:aggregate	Range of values (indicative)			Basic application field (indicative)
	Compressive strength (MPa)	Dynamic modulus of elasticity (by frequency of resonance) (MPa)	Water capillary absorption coefficient ($\text{kg}/\text{m}^2 \cdot \text{min}^{1/2}$)	
Lime:sand (1:3)	0.2–0.8	2,300–4,100	1.1–1.6	Mild weather (not too humid or very dry); non-aggressive conditions; interior surfaces (plasters)
Lime + pozzolan: sand (1:2–1:3)	0.5–2.3	2,500–4,500	1.3–2.3	Frequent presence of moisture, due to rainy weather or to capillary rising water (because the pozzolanic reaction needs moisture for long time)
Lime + some hydraulic lime: sand (1:2–1:3)	0.4–1.0	1,600–5,600	1.2–1.9	Variation between dry and humid weather
Hydraulic lime ^a : sand (1:2–1:3)	0.6–3.1	1,100–7,500	1.0–2.4	Variation between dry and humid weather and some aggressive conditions
Lime + some cement: sand (1:3)	0.9–5.1	3,000–6,500	1.0–2.0	Aggressive conditions: for example exposed to sea spray and high pollution

^aUse hydraulic lime free of salts and of low hydraulicity (NHL 3.5 or HL 3.5)

The application of air lime renders, or air lime and pozzolan renders, requires careful and rigorous workmanship. Plasterers normally working with modern materials and not used to the application of this kind of mortars on large surfaces, will probably not achieve good results (appropriate physical and aesthetic characteristics), except if constant supervision is provided.

Appropriate curing is one of the main secrets of ensuring the success of lime renders. The carbonation of calcium hydroxide requires some humidity for the dissolution of the carbon dioxide but not too much, to allow its reaction with calcium hydroxide. This reaction is slow, so it is necessary to provide special conditions for several days, maybe some weeks. On the other hand, most of the mixing water of lime mortars is not used up in hydration reactions as happens in hydraulic binders, so it leaves the mortar, through evaporation or due to absorption by the substrate, causing high shrinkage. This can produce cracks, which must be closed while the mortar is still in a plastic state [22].

4 Examples

Some case studies of historic buildings' renders and plasters repaired with compatible mortars are represented in Figs. 13, 14, 15, and 16 [1, 6, 7, 14].



Fig. 13 Main LNEC building: repair with air lime mortar



Fig. 14 Inglesinhos Convent: substitution air lime render



Fig. 15 Sacramento church: repair and partial substitution of plasters using air lime, hydraulic lime mortars, gypsum and air lime mixes



Fig. 16 S. Bruno Fortress: substitution air lime plus cement render

5 Conclusions

Decisions about conservation strategy and about the materials to use for the conservation of historic renders and plasters are based on several factors, both of a subjective and an objective nature. Tests play an important role, for an evaluation of the severity of anomalies and for an assessment of compatibility by a comparison of the characteristics of existing materials and proposed solutions. However, they are only a part of the methodology. They should come after a careful expert observation and they must be adequately interpreted. The type of tests and their localisation are to be

chosen in order to obtain the maximum information with the minimum intrusion and disruption to the original fabric, and without taking more time than is necessary to fulfil the objectives. Hence, *in-situ* tests must be used first followed by complementary laboratory tests. Previous results in similar buildings and materials must be taken into account. Functionality, compatibility and adaptation to the prevailing environment and foreseen actions must be considered. Considering all of these factors carefully, creates a new perspective that aims to ensure the improvement of the durability of the whole building, respecting its characteristics.

To plan adequate interventions on historic buildings is a complex task, requiring many skills; therefore a multidisciplinary team must be chosen to do it and given a reasonable amount of time.

References

1. Veiga, M.R., Fragata, A., Tavares, M., Magalhães, A., Ferreira, N.: Inglesinhos convent: compatible renders and other measures to mitigate water capillary rising problems. *Int. J. Build. Apprais.* **5**(2), 171–185 (2009). doi:[10.1057/jba.28](https://doi.org/10.1057/jba.28). ISSN:17428262
2. Tavares, M., Veiga, M.R., Fragata, A.: Conservation of old renderings – the consolidation of renderings with loss of cohesion. *Conserver Património* **8**, 13–19, December 2008
3. Tavares, M., Fragata, A., Veiga, M.R.: A consolidação da falta de aderência de rebocos antigos – um estudo com diferentes argamassas para grouting. In: *2º Congresso Nacional de Argamassas de Construção*, APFAC, Lisbon, November 2007
4. Tavares, M., Magalhães, A., Veiga, M.R., Aguiar, J.: Métodos de diagnóstico para revestimientos de edificios antiguos. Importancia y aplicabilidad de los ensaios in situ. *Boletín del Instituto Andaluz del Patrimonio Histórico*, nº 53 – Especial criterios, pp. 11–17, April 2005
5. Magalhães, A., Matias, L., Vilhena, A., Veiga, M.R., Pina dos Santos, C.: Non-destructive testing for the assessment of moisture defects on ancient walls. Some case studies. In: *8th international conference on non-destructive investigations and microanalysis for the diagnostics and conservation of the cultural and environmental heritage*, Lecce, Italy, May 2005
6. Magalhães, A., Veiga, M.R.: Physical and mechanical characterisation of ancient mortars. Application to the evaluation of the state of conservation. *Materiales de Construcción* **59**(295), 61–77 (2009). doi:[10.3989/mc.41907](https://doi.org/10.3989/mc.41907)
7. Santos Silva, A., Borsoi, G., Veiga, R., Fragata, A., Tavares, M., Llera, F.: Physico-chemical characterization of the plasters from the church of “Santíssimo Sacramento” in Alcântara, Lisbon. In: *HMC2010*, Prague, September 2010
8. Papayianni, I.: Criteria and methodology for manufacturing compatible repair mortars and bricks. In: *Compatible Materials Recommendations for the Preservation of European Cultural Heritage*. National Technical University, Athens (1998)
9. Moropoulou, A., Bakolas, A.: Range of acceptability limits of physical, chemical and mechanical characteristics deriving from the evaluation of historic mortars. In: *Compatible Materials Recommendations for the Preservation of European Cultural Heritage*. National Technical University, Athens (1998)
10. Veiga, M.R., Santos Silva, A., Aguiar, J., Carvalho, F.: Methodologies for characterisation and repair of mortars of ancient buildings. In: *International Seminar on Historical Constructions 2001*. Guimarães, Universidade do Minho, pp. 353–362, November 2001
11. Lanas, J., Alvarez, J.J.: Masonry repair lime-based mortars: factors affecting the mechanical behaviour. *Cem. Concr. Res.* **33**, 1867–1876 (2003)
12. Veiga, M.R., Velosa, A., Magalhães, A.: Evaluation of mechanical compatibility of renders to apply on old walls based on a restrained shrinkage test. *Mater. Struct.* **40**(10), 1115–1126 (2006)

13. Gonçalves, T., Rodrigues, J., Abreu, M., Esteves, A., Santos Silva, A.: Causes of salt decay and repair of plasters and renders of five historic buildings in Portugal. In: Conference Heritage, Weathering and Conservation, vol. 1, pp. 273–284. Balkema, Madrid (2006). ISBN 0-415-41272-2
14. Santos Silva, A., Veiga, M.R.: Degradation and repair of renders in ancient fortresses close to the sea. In: MEDACHS 08 – 1st international conference construction heritage in coastal and marine environment, Lisbon, LNEC, 8 p (2008)
15. Borges, C., Santos Silva, A., Veiga, M.R.: Ancient mortars under action of marine environment: a physico-chemical characterization. In: HMC2010, Prague, September 2010
16. Candeias, A.E., Nogueira, P., Mirão, J., Santos Silva, A., Veiga, M.R., Casal, M.G., Seruya, A.I.: Characterization of ancient mortars: present methodology and future perspectives. In: International Workshop Chemistry for the Conservation of Cultural Heritage: Present and Future Perspectives, EU-ARTECH, Perugia, Italy, 4 p (2006)
17. Válek, J., Veiga, R.: Characterisation of mechanical properties of historic mortars – testing of irregular samples. *Adv. Archit. Ser.* **20**, 365–374 (2005)
18. Veiga, M.R., Magalhães, A., Bosiljkov, V.: Capillarity tests on Historic mortar samples extracted from site. Methodology and compared results. In: 13th International Masonry Conference, Amsterdam, July 2004
19. Magalhães, A., Moragues, A., Veiga, M.R.: Application of some methods on evaluation of porous systems of wall renderings. In: VII Congreso Internacional de rehabilitación del patrimonio y edificación, Lanzarote, July 2004
20. Veiga, M.R., Fragata, A., Velosa, A., Magalhães, A., Margalha, G.: Substitution mortars for application in historical buildings close to the sea environment. Analysis of the viability of several types of compositions. In: MEDACHS – Construction Heritage in Coastal and Marine Environments, Lisbon, LNEC, January 2008
21. Veiga, R., Fragata, A., Velosa, A., Magalhães, A., Margalha, G.: Lime-based mortars: viability for use as substitution renders in historical buildings. *Int. J. Archit. Herit.* **4**(2):177–195 (2008), April–June 2010. Lourenço, P.B., Roca, P. (eds.) Special Issue: Select papers from HMC 2008 – The first historical mortars conference. Taylor & Francis, Philadelphia. ISSN 1558-3058
22. Penas, F., Veiga, M.R., Gomes, A.: Hydraulic lime mortars to use in old buildings: advantages and drawbacks. In: HMC08 – 1st historical mortars conference 2008: characterization, diagnosis, conservation, repair and compatibility, Lisbon, LNEC, 24–26 Sept 2008
23. Fragata, A., Veiga, M.R.: Air lime mortars: the influence of calcareous aggregate and filler addition. *Mater. Sci. Forum* **636–637**, 1280–1285 (2010). doi:10.4028/www.scientific.net/MSF.636-637.1280
24. Margalha, G.: Mineral air binders. Hydration processes and the time factor in their quality (in Portuguese). Ph.D thesis by Instituto Superior Técnico (IST) of Technical University of Lisbon, January 2009
25. Cavaco, L., Veiga, M.R., Gomes, A.: Render application techniques for ancient buildings. In: 2nd International Symposium on Building Pathology, Durability and Rehabilitation, Lisbon, LNEC, CIB, November 2003
26. Balksten, K., Klasén, K.: The influence of craftsmanship on the inner structures of lime plasters. In: RILEM Workshop, Delft, January 2005

Comparison Between Traditional, Lime Based, and Industrial, Dry Mortars

Albert Jornet, Cristina Mosca, Giovanni Cavallo, and Guido Corredig

Abstract This contribution faces the problem of choosing, preparing and applying render mortars to be used in restoration and repair of historic buildings. The results obtained in this work clearly show that some industrial “dry mortar” products, even if they are not based on slaked lime binders, can be compatible with traditional, lime based ones, with regard to mechanical and physical properties and, therefore, should have a comparable behaviour.

1 Introduction

Lime based mortars have successfully been used in historic constructions in many different functions: as bedding mortar of masonry, for internal and external coating, as a component of ancient structural concrete or of watertight linings in cisterns and aqueducts, as substrate material for pavements, etc. Malinowsky [1]. Vitruvius in his *The Ten Books on Architecture* recommends the use of particular mixes with addition of sieved crushed brick in damp situations, or the addition of pozzolan for the constructions under water level, Vitruvius [2]. The fall of the Roman Empire was followed by a long period of decline in which important technological knowledge and experience went lost. Only with the translation and new lecture of Vitruvius’ work, the lime mortars technology was rediscovered and newly applied. At the beginning of the nineteenth century new binders, hydraulic lime but specially Portland cement, were discovered and, since considered to be better, stronger and more durable, gradually replaced lime. The use of hydraulic binders in conservation practice has been connected to a large number of failures, Newsom et al. [3],

A. Jornet (✉) • C. Mosca • G. Cavallo • G. Corredig
DACP-SUPSI, Institute of Materials and Constructions, Lugano, Switzerland
e-mail: albert.jornet@supsi.ch

Holmström [4]. This fact, along with the general acceptance of the principles of compatibility and “like for like” philosophy in the conservation practice, have produced a regain of interest for the lime technology and the gradual reintroduction of the lime based mortars in the field of historic building conservation, [4], Gibbons [5], IFS-Bericht [6], Peroni et al. [7], Elert et al. [8]. Despite the fact that a basic understanding of the lime technology has newly been developed, the reintroduction of lime based mortars has been, and still is, accompanied by disappointing failures. This contribution faces the problem of choosing, preparing and applying external coatings to be used in the restoration and repair of historic buildings. The results reported here correspond to an on-going research project conducted in collaboration with the Cultural Heritage authorities, Jornet and Romer [9], Jornet et al. [10]. The final goal is to reach a better knowledge about composition and behaviour of some industrial, dry mortar products, available in the Swiss or in the Italian market (five products) and to gather useful information regarding site practices for the traditional, lime based mortars (four mixes), in order to be able to make the right choice in every situation.

2 Materials and Experimental

2.1 Materials

Two traditional mixes T1 and T3 were prepared using a commercially available dry hydrate lime (powder) produced in Switzerland, corresponding to the class, CL 90, according to the norm EN 459-1, 2002 [11]. The mix T2 was prepared using an approximately 2 year old lime putty, obtained by slaking at the laboratory the same quick lime used to produce the hydrate lime powder employed in mixes T1 and T3, and the mix T4 was prepared using a commercially available lime putty. Also a commercially available, well graded sand having a maximum grain size of 4 mm and composed by metamorphic quartz, both as individual crystals and as polycrystalline aggregates, micaschists, feldspars, micas and amphibolites, was used in all the traditional mixes (Fig. 1a). In the mix T3, brick dust obtained from an illitic clay fired at about 800°C was added.

Five different industrial dry mortar products, produced for the conservation and restoration field to be used as external coatings, were selected (P1 to P5). According to the technical data available, the product P1 is composed by “special hydraulic binders” with pozzolanic reactivity, natural sands with a maximum \varnothing of 2.4 mm, special chemical admixtures and synthetic fibres. The product P2 is cement free, and composed by natural hydraulic lime NHL 3.5, hydrated lime, siliceous sand with a maximum \varnothing of 4 mm, and is free of synthetic additions. The product P3 is composed by a natural hydraulic lime NHL 3.5, natural pozzolan, siliceous fine sand, washed sand from a pit and dolomitic limestone with a maximum \varnothing of 2.5 mm. The product P4 is composed by natural hydraulic lime NHL 5 and calcareous sand with a maximum \varnothing of 3 mm. Finally, the product P5 is composed by

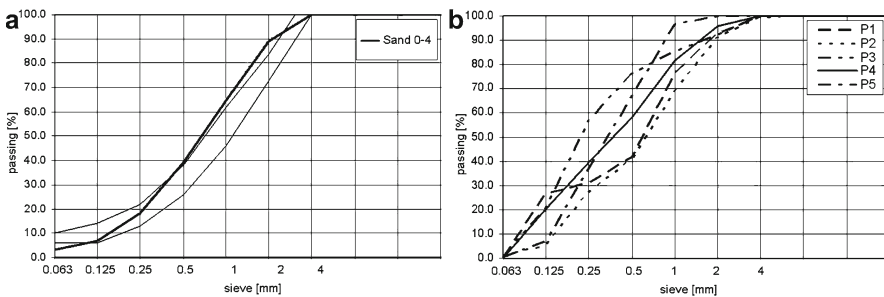


Fig. 1 (a) Grading curve of the sand used in the traditional, lime based, mixes, *left side* (b) grading curves of the dry ready mixed industrial products, *right side*

natural hydraulic lime NHL 3.5, calcareous sand and marble powder with maximum \varnothing of 1.5 mm. The grain size distribution curves of these five products were determined and the results are shown in Fig. 1b.

2.2 Mixes

The mixes T1 and T2 are considered basic mortars and were prepared using respectively, hydrate lime powder or lime putty as binder and a binder/aggregate proportion of 1:2 by volume. The first one was prepared using a paddle mixer, matured for 2 weeks and then thoroughly knocked up before it was applied. The second one, mixed with a hand held mortar whisk, was matured for 1 week. The third mix (T3) was prepared adding half a volume of brick dust, related to the binder, to the basic mix T1. The fourth mix (T4) was prepared by an experienced restorer using a hand held mortar whisk and a binder/aggregate proportion of 1:3 by volume. This mix was also matured for 2 weeks and knocked up thoroughly before it was applied. Water was added to all the mixes in order to reach a suitable workability corresponding to a plastic consistency.

The mixes corresponding to the industrial products were prepared using a hand held mortar whisk, adding the amount of water indicated by the producer and, in general, following the indications given by the producers.

Table 1 contains the available data regarding the composition of the different mixes used.

At the laboratory the mixes were prepared following the procedures indicated in the Norm UNI EN 1015/2:2000 [12].

2.3 Fresh Mortar

Consistency, UNI EN 1015-3, 2000 [13], porosity, UNI EN 1015-7, 2000 [14], and bulk density, UNI EN 1015-6, 2000 [15], were measured on fresh mortar. The results obtained have been summarized in Table 2.

Table 1 Composition of the different traditional mixes (indicated by volume), dosages as dry mass of the dry mortar products, and water content in % of all the mixes except T4

Mixes	T1	T2	T3	T4	P1	P2	P3	P4	P5
Sand 0–4 [mm]	2	2	2	3	25 kg	40 kg	25 kg	25 kg	30 kg
Binder	1	1	1	1					
Addition	–	–	0.5	–					
Water [%]	24	19	17	–	15.2	20.0	20.4	22.0	20.0
Water/binder	2.3	1.6	1.7	–	–	–	–	–	–

Table 2 Fresh mortar properties of all the mixes

Mixes	T1	T2	T3	T4	P1	P2	P3	P4	P5
Ø Spread [mm]	147	172	173	162	168	198	150	178	170
Porosity [vol.%]	2.5	2.9	1.5	3.8	16	15	30	10.5	26
Unit weight [kg/m ³]	1,865	1,922	1,994	1,933	1,880	1,847	1,485	1,955	1,610

All the mixes show spread values within the range of the plastic consistency (140–200 mm). Larger variations can be observed by the mixes corresponding to the industrial products. Significant differences can be observed looking at the porosity as well. While the traditional, lime based, mixes show values comprised between 1.5 and 3.8 vol.%, the values measured by the industrial ones go from 10.5 to 30 vol.%. Roughly, the higher porosity values are related to the lower unit weight ones although the different amounts of water used modify the theoretical relationship.

2.4 Test Specimens and Curing

From each mix following testing specimens were prepared: 9 standard prisms 40×40×160 [mm], 3 discs with a Ø of 100 mm and other 3 with a Ø of 50 mm, both sets 20 mm thick. Compaction was achieved using a vibrating table. All the testing specimens were stored for 90 days in the laboratory at 20±2°C and 65±5% of r.h. In addition, every mix was applied with a thickness of about 20 mm to a substrate of brick which was stored in a rain protected area out side.

An external masonry brick wall, 12 m long, 2 m high and about 0.43 m large, with a little roof, was constructed on top of one the buildings of the campus (Fig. 2). The nine mixes were applied by casting with the trowel, covering a surface of 2 m² facing south and the same surface facing north. After dampening down the wall, a thin first coat of about 5 mm, and two other coats of about 6–8 mm each were applied either after 1 or 2 weeks or after the “right” maturing time. The surface was



Fig. 2 External masonry brick wall showing the protective covering (*left side*) and the different coatings (*right side*)

finished by floating on and pressing back the coating, using a wood float, when the mortar starts to stiffen up. Half of the surface was finished as mentioned before and, on the other half, a final, thin (1–2 mm), finishing coat composed by half volume of lime putty and half volume of marble dust was applied with a steel float and finished up with a sponge float. Only in the case of mix T1, a third area of $2 \times 0.5 \text{ m}^2$, on both sides of the wall, was finished applying three layers of lime wash. A protective enclosure with roof covering and frames covered with fine debris netting and hessian sheeting (dampened when required by the environmental conditions) was provided before the coating application began in September, and was maintained during winter time till the end of March.

2.5 Testing Programme

Compressive and flexural strength were determined respectively on 28, 56 and 90 days old prisms of $40 \times 40 \times 160$ [mm] UNI EN 1015-11, 2001 [16]. The carbonation depth was determined spraying a freshly broken surface with phenolphthalein. From the 90 days old prisms, about 10 mm thick slices were cut and used for the preparation of thin sections on which, observations using optical and fluorescence microscopy were performed. After 90 days of curing, the water absorption coefficient was determined on 50 mm Ø discs, DIN 52617, 1993 [17], while the porosity parameters were determined on small prisms of $40 \times 40 \times 50$ [mm] prepared from the standard prisms, SIA 262/1, Annex A, 2003 [18]. The 100 mm Ø discs were used for the determination of the water vapour transmission properties UNI EN 12572, 2006 [19].

The specimens prepared casting a 20 mm thick layer of render on a substrate of brick will be used to perform accelerated artificial weathering. The renders applied on the external wall will be monitored by visual inspection and by means of non destructive tests. The results obtained should allow the evaluation of the mixes used, in terms of performance and of compatibility.

Table 3 Compressive (f_{cp}) and flexural strength (f_n) on standard prisms at 28, 56 and 90 days

Mixes	T1	T2	T3	T4	P1	P2	P3	P4	P5
Properties [N/mm ²]									
f_{cp28}	0.5	0.8	1.1	0.9	9.5	0.8	4.6	1.9	3.7
f_{fp28}	0.2	0.6	0.4	0.6	1.9	1.0	1.8	1.0	1.8
f_{cp56}	0.6	1.0	1.2	1.0	9.7	0.8	7.3	2.2	4.0
f_{fp56}	0.3	0.6	0.6	0.6	1.9	0.5	3.0	1.2	1.7
f_{cp90}	0.6	1.4	1.2	1.2	9.5	1.5	8.1	2.5	4.5
f_{fp90}	0.3	0.8	0.4	0.7	1.8	0.7	3.2	1.2	1.7

3 Results

3.1 Mechanical Properties

The compressive and flexural strength values obtained have been summarized in Table 3. In this table it can be observed that, if we consider 2.5 N/mm² as upper limit, according to the norm UNI EN 998-1, 2004 [20], the traditional, lime based, mixes (T1 to T4) and the mixes P2 and P4 belong to the same group (class CSI), while mixes P1, and P3 belong to the class CSIV and mix P5 belongs to class CSIII. The comparison between the mix prepared using lime powder (T1) and those prepared using lime putty (T2 and T4) shows clearly higher values by the latter ones. Mix T3, with brick dust addition, shows values similar to those of the mixes prepared with lime putty. The industrial dry mortar mixes show quite variable values going from 1.5 to 9.5 N/mm² at 90 days.

3.2 Physical Properties

Porosity parameters, water absorption coefficient and water vapour transmission values have been summarized in Table 4.

If we consider the air void porosity, which corresponds to the volume of non-saturable pores, (LP) and we compare it with the porosity values measured on fresh mortar, it can be observed that the traditional mixes show clearly higher values, while by the mixes corresponding to the industrial, dry mortar products the opposite is true. This is probably due to the development of shrinkage cracks by the former mixes and to the loss of some air by the latter ones. If we consider the capillary porosity values, pores saturable by capillarity (U_E), the larger variations can be observed by the traditional mixes which have also mostly higher values. The total porosity values (n), sum of air void and capillary porosity, do not vary that much among the different mixes except by the mixes with very high amounts of air voids (P3 and P5).

Table 4 Porosity parameters

Mixes	T1	T2	T3	T4	P1	P2	P3	P4	P5
Properties									
ρ_{110} [kg/m ³]	1,688	1,691	1,743	1,716	1,787	1,687	1,532	1,736	1,483
ρ_{R110} [kg/m ³]	2,694	2,680	2,695	2,717	2,677	2,719	2,680	2,705	2,699
U_B [vol.%]	0.5	0.7	0.5	0.6	1.1	0.6	0.8	0.7	1.0
U_E [vol.%]	29.2	27.6	32.1	24.2	22.0	24.7	20.3	25.7	25.9
n [vol.%]	37.2	36.9	35.3	36.9	33.3	38.0	42.84	35.8	45.0
LP [vol.%]	7.9	9.3	3.2	12.6	11.3	13.3	22.57	10.1	19.1
w_{24} [kg/m ² h]	1.2	1.2	1.4	1.1	0.9	1.2	0.6	1.1	0.9
w_{10} [kg/m ² h]	14.3	12.7	16.5	13.4	5.6 ⁽¹⁾	13.9	0.9 ⁽²⁾	12.3	4.2 ⁽³⁾
μ [-]	13	15	15	12	26	13	20	15	13
S_d [m]	0.35	0.31	0.34	0.28	0.57	0.31	0.47	0.34	0.28

Initial humidity = U_B , capillary porosity = U_E , air avoid porosity = LP, apparent density = ρ_{110} , density at 110°C = ρ_{R110} , water absorption coefficient (w_{24}), and water absorption coefficient after n minutes (w_{10} – value), ⁽¹⁾ w_{30} , ⁽²⁾ w_{360} , ⁽³⁾ w_{60} , water vapour resistance factor = (μ), water vapour diffusion-equivalent air layer thickness = S_d

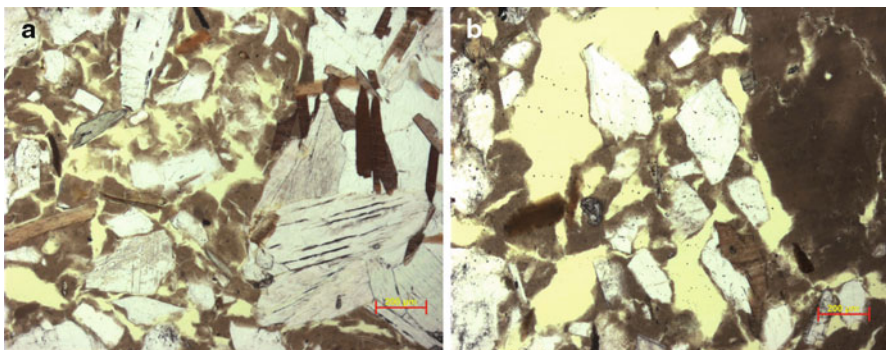


Fig. 3 Photomicrograph with // Nichols of mix T1 showing shrinkage cracks (*left side*) and of mix T2 showing irregularly shaped air voids with lime lumps (*right side*)

Regarding the water absorption it can be said that rather than the coefficient measured at 24 h, w_{24} , (very much dependent on the thickness of the testing specimens), the one measured at shorter times (mostly already at 10 min) gives a much reliable information related to the speed at which water is absorbed by capillarity.

Considering the values at these shorter times (w_{10}) it can be said that, as it happened with compressive strength, the traditional, lime based, mixes along with mixes P2 and P4, form a group characterized by high absorption values, varying from 12.3 to 16.5 $\text{kg}/\text{m}^2\sqrt{\text{h}}$. Mixes P1 and P5 show values around 5 $\text{kg}/\text{m}^2\sqrt{\text{h}}$, while mix P3 shows the lowest value with 0.9 $\text{kg}/\text{m}^2\sqrt{\text{h}}$. The traditional mixes along with mixes P2, P4 and P5, show water vapour transmission values comprised between 13 and 15, which are rather higher than expected as far as the traditional mixes are concerned. Mixes P1 and P3 show a higher water vapour diffusion resistance with clearly higher values.

3.3 Microstructure

The observation of the thin sections of the traditional, lime based, mortars shows that they are characterized by a mostly angular and sub-angular siliceous sand, with 4 mm maximum grain size, quite uniformly distributed in a homogeneous lime matrix with microcrystalline texture. Shrinkage cracks and irregularly shaped air-voids are also frequent. Lime lumps are clearly visible in the mixes prepared with lime putty as well (Fig. 3a, b).

The presence of hydraulic lime characterizes the industrial mortars which are composed by a mainly siliceous sand (P1, P2 and P3) or by a mainly calcareous one (P4 and P5) in a homogeneous microcrystalline matrix. The maximum grain size in most mixes is smaller than that of the traditional ones. Synthetic fibres

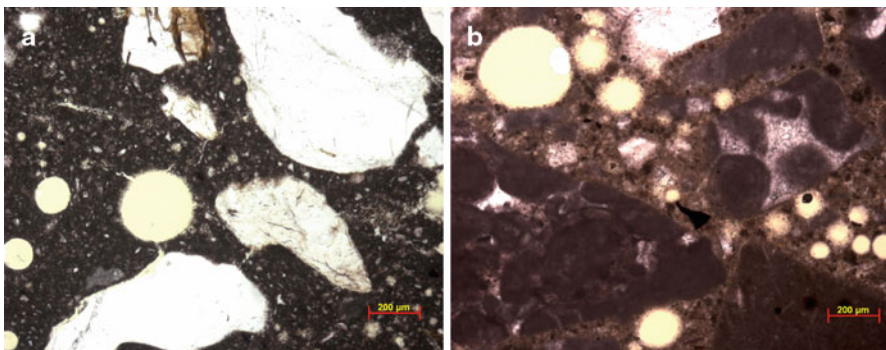


Fig. 4 Photomicrograph with // Nichols of mix P1 showing a dense matrix with some air voids (*left side*) and of mix P4 showing several rounded air voids and calcareous sand grains (*right side*)

are visible in the mix P1. Another characteristic feature of the microstructure is the presence of rounded air-voids indicating the use of an air entraining agent in the composition of the mixes (Fig. 4a, b).

4 Discussion

The results obtained relating to the traditional, lime based, mortars can be summarized as follows: lime based mortars are mainly characterized by low compressive and flexural strength values, by high capillary porosity and water absorption, and by a low resistance to water vapour transmission. The mixes prepared with lime putty (T2 and T4) clearly show higher strength and lower capillary porosity values if compared to the mix prepared with lime powder (T1). The addition of brick dust can significantly increase the strength of the mixes. In addition, the main features related to the microstructure of the matrix, showing a microcrystalline lime texture, are the frequent presence of lime lumps in the mixes made using lime putty and the presence of shrinkage cracks in the mix prepared using lime powder. It is generally accepted that lime mortars are rather weak and vulnerable mainly to frost action and salt crystallisation, in particular at a young age. However, due to their characteristics, they are able to accommodate minor structural and seasonal movements and they allow a quick re-evaporation of moisture absorbed by a porous masonry, Newsom et al. [3].

On the other side, the industrial, dry mortar, products included in this work show basically higher compressive and flexural strength values, lower capillary porosity and water absorption and a higher resistance to water vapour transmission. Two of them (mixes P2 and P4) show clearly lower strength values than the other three, corresponding to class CSI. In this regard, they are very similar to the traditional lime based mortars. The microstructures of the dry mortar products are mainly characterized by an important air-void content and by the presence of hydraulic

lime as binder. The mix-design used is based on a concept which aims at the development of higher mechanical strength employing a hydraulic binder, and at the introduction of air voids as space available to counteract frost action and salt crystallisation. Due to their specific properties and to the frequent use of upper coatings with low water vapour transmission capacities they tend to trap moisture inside the masonry, which finally leads to the failure of the external coating and damage to the whole structure.

Where conservation work involves the repair or replacement of an external lime coating, a detailed investigation in order to establish the nature and the condition of existing coatings and their masonry should be performed. It is assumed, that the compatibility principle and the “like for like” philosophy should be established and applied. However, the principle of compatibility can be apprehended from different points of view as discussed by Hughes and Válek [21]. From a practical point of view, Groot et al. [22] distinguish two approaches to specify new mortars, a “traditional” one, based on the use of traditional materials, and a “modern” one, based on reaching compatible requirements, using if necessary modern materials. Which approach should be followed?

The results obtained in this work clearly show that industrial dry mortar products, even if they are not based on slaked lime as binder, can be compatible with traditional ones with regard to mechanical and physical properties and, therefore, it can be assumed that they should have a similar behaviour. The selection of the right product for external coating in historic buildings has to be performed with the awareness that, in addition to the knowledge required to produce a lime based mortar of good quality, skilled craftsmanship and good site practices are fundamental to the success of the conservation project. If these requirements for one reason or another could not be met, industrial performance compatible products could be an acceptable alternative.

Acknowledgements We would like to thank the technical staff of the Institute of Materials and Constructions and in particular R. Bucellari who has been the driving force for laboratory and practical work. Thanks are also due to the direction of our department which has facilitated the construction of the testing wall. We kindly acknowledge the Swiss National Science Foundation for the funding of our 3 year research project within the framework of DORE (13DPD3-116016/1).

References

1. Malinowsky, R.: Durable Ancient Mortars and Concretes. Nordic Concrete Research, Publication No. 1, pp. 1–22, Nordic Concrete Federation (1982)
2. Vitruvius, P.: The Ten Books on Architecture (trans. Morgan, M.H.). Dover Publications, New York (1969)
3. Newsom, S., Gibbons, P., Brown, S.: External Lime Coatings on Traditional Buildings, TAN 15. Historic Scotland, Edinburgh (2001)
4. Holmström, I.: The use of lime. In: Ward, J.D.D., Maxwell, I. (eds.) Proceedings of the Historic Scotland Lime Conference, Lime News, vol. 4, pp. 48–63, Edinburgh (1995)
5. Gibbons, P.: Preparation and Use of Lime Mortars, Historic Scotland Technical Advice Note 1, revised edn. Historic Scotland, Edinburgh (2003)

6. IFS-Bericht.: Kalkmörtel und Kalkfarbe – Gestern, Heute und Morgen?, IFS Tagung, Bericht Nr. 19, 2. erweiterte Auflage, Mainz (2004)
7. Peroni, S., Tersigni, C., Torracca, G., Cerea, S., Forti, M., Guidobaldi, F., Rossi-Doria, P., De Rege, A., Picchi, D., Pietrafitta, F.J., Benedetti, G.: Lime based mortars for the repair of ancient masonry and possible substitutes. In: Proceedings of Mortars, Cements and Grouts in the Conservation of Historic Buildings. ICCROM, Rome (1982)
8. Elert, K., Rodriguez-Navarro, C., Sebastian-Pardo, E., Hansen, E., Cazalla, O.: Lime mortars for the conservation of historic buildings. Stud. Conserv. **47**(1), 62–75 (2002)
9. Jornet, A., Romer, A.: Lime mortars: relationship between composition and properties, CD. In: Proceedings of the Historical Mortars Conference, Lisbon (2008)
10. Jornet, A., Cavallo, G., Mosca, C.: Lime mortars with mineral additions: properties, CD. In: Proceedings of the 12th Euroseminar on Microscopy Applied to Building Materials, Dortmund (2009)
11. UNI EN 459-1: Calci da costruzione – Definizioni, specifiche e criteri di conformità, Milano (2002)
12. UNI EN 1015-2: Methods of Test for Mortar for Masonry – Part 2, Bulk Sampling of Mortars and Preparation of Test Mortars, Milano (2000)
13. UNI EN 1015-3: Methods of Test for Mortar for Masonry – Part 3, Determination of Consistence of Fresh Mortar (by Flow Table), Milano (2000)
14. UNI EN 1015-7: Methods of Test for Mortar for Masonry – Part 7, Determination of Air Content of Fresh Mortar, Milano (2000)
15. UNI EN 1015-6: Methods of Test for Mortar for Masonry – Part 6, Determination of Bulk Density of Fresh Mortar, Milano (2000)
16. UNI EN 1015-11: Methods of Test for Mortar for Masonry – Part 11, Determination of Flexural and Compressive Strength of Hardened Mortar, Milano (1999)
17. DIN 52617: Bestimmung des Wasseraufnahmekoeffizienten von Baustoffen, Beuth Verlag GmbH, Berlin (1987)
18. SIA 262/1 Annexe A: Perméabilité à l'eau, Construction en Béton – Spécifications complémentaires, Société suisse des ingénieurs et des architectes, Zurich (2003)
19. UNI EN 12572: Hygrothermal Performance of Building Materials and Products – Determination of Water Vapour Transmission Properties, Milano (2006)
20. UNI EN 998-1: Specification for Mortar for Masonry – Rendering and Plastering Mortar, Milano (2004)
21. Hughes, J., Válek, J.: Mortars in Historic Buildings – Literature Review. Historic Scotland, Edinburgh (2003)
22. Groot, C.J.W., Bartos, P.J.M., Hughes, J.J.: Historic mortars: characteristics and tests – concluding summary and state-of-the-art. In: Proceedings of RILEM International Workshop, Paisley, pp. 443–454, (2000)

Repair Mortars for the Sandstones of the Cathedral of Berne

Christine Bläuer, Hermann Häberli, Annette Löffel, and Bénédicte Rousset

Abstract Stone repair mortars used on the cathedral of Berne (Switzerland) have been refined from existing recipes. These hydraulic mortars without any organic additions are prepared on the building site. They are applied as two different layers, a coarser ground layer (KMtl) and a finer surface layer (DMtl) which imitates the stone material. The investigations were undertaken to understand the overall good practical experiences with these materials, and to anticipate the long term performance of this mortar system under the rough exposure conditions on the cathedral. Laboratory investigations included, petrophysical measurements and thin section analysis, of the individual materials but also on the system of DMtl-KMtl-stone. The investigations suggest that the mortars used are in many ways well adapted to the sandstones on the monument, and that the diverse application methods only provoke small differences in the resulting mortars at an early stage. But only in-situ observations will be able to show whether these small differences will lead to problems after long exposure to the elements.

1 Introduction

The repair mortars used for stone repair on the Bernese cathedral on two different Molasse sandstones are hydraulic mortars without any organic additions which are prepared on the building site. They are applied as two layers, a more coarse grained ground layer (KMtl) and a fine grained surface layer (DMtl), the latter imitating the stone material the mortar is used on.

C. Bläuer (✉) • B. Rousset
CSC Sàrl, Fribourg, Switzerland
e-mail: csc@conservation-science.ch

H. Häberli • A. Löffel
Berner Münster-Stiftung, Bern, Switzerland
e-mail: info@haeberli-architekten.ch

These mortars have been refined from recipes of mortars that have already been applied for several decades on diverse Swiss monuments. The investigations reported here were undertaken to understand the overall good practical experiences with these mortars, and to anticipate their long term performance on the rough exposure conditions occurring on the cathedral's tower.

2 Why Repair the Sandstones of the Cathedral with Mortars

The approach to conservation and repair at the Bernese cathedral until 1998 was mainly based on stone exchange. Accordingly, until then the cathedral workshop did not have much experience in stone consolidation, use of repair mortars for stone or any other remedial conservation treatment. Such works were not executed or only for very special cases sourced out to specialised enterprises. By 1998 it became clear that this kind of approach had to be changed drastically, not only it was very destructive towards the heritage materials but also it neglected to a certain extent the general maintenance of the building, was rather costly and not sustainable.

In 1998, on the common initiative of the Berner Münsterstiftung and the new architect in charge, Hermann Häberli, the general approach to the maintenance of the building was changed. Nevertheless, from the beginning it was clear that the cathedral workshop remained the backbone of functioning maintenance and regular care of the building. But this workshop not having the necessary experience in conservation works, external instructors were sought after and, for what concerns the stone conservation, found in the conservators Andreas Walser and Katrin Durheim, who kindly agreed to transfer their very long experience to the collaborators of the workshop by means of practical instructions on-site. They also revealed their recipes of repair mortars, which they had applied for several decades on Zug sandstones on diverse Swiss monuments.

Before applying these mortars on the cathedral of Berne, some of these buildings were visited to inspect the long term performance of the proposed mortars. The result of these inspections was generally satisfying and no records of failures of these mortars have been heard of so far. Nevertheless, in close cooperation with Andreas Walser and Katrin Durheim, it was decided to adapt the recipes a little, to somewhat reduce the strength of the KMtl for the use on the much weaker Bernese compared to the Zug sandstone and to adapt the appearance of the DMtl types to the sandstones at the cathedral of Berne.

3 Mortar Materials and Sample Preparation

The apparent advantage of industrial ready-made products over on-site mixed mortars seems to be their constant recipe, and therefore their constant quality. But usually these recipes are not revealed in detail and they are frequently improved, which

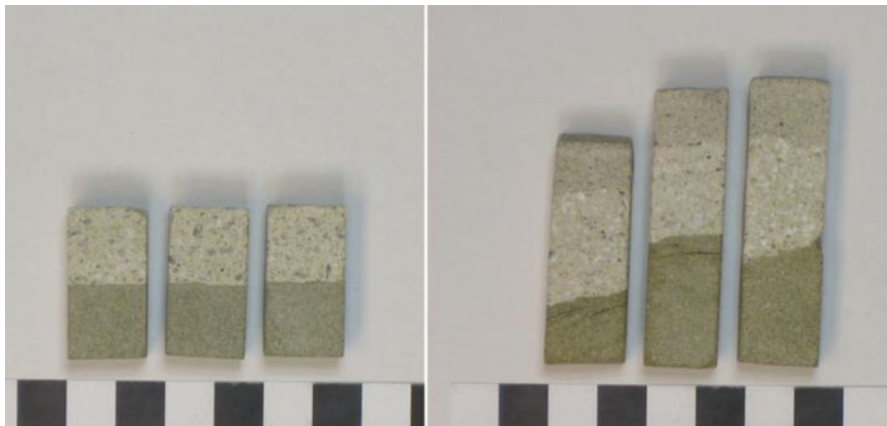


Fig. 1 Left series of two layered samples (so called bicouche = BiC) of KMtl on sandstone and right series of three layered samples (tricouche = TriC) with sandstone, KMtl and DMtl, enumeration of layers from bottom to top

means that the properties of these mortars change with time. The disadvantages of the use of mortars that are mixed on site from binders, sands and water, is that they need to be very carefully mixed, to make sure that their properties do not change from one portion to the next. But on the other hand it can be suspected that the same or very similar raw materials will still be available in decades, and hence it will also in the future be possible to produce the same mortars. These reflections led to the decision to renounce the use of ready-made mortars on the Bernese cathedral, especially so as constancy in workmanship is guaranteed by the cathedral workshop. Nevertheless, it was decided that the mortars should be tested for constancy in their petrophysical properties as well as for their theoretical suitability to be used on the Bernese and Zug sandstones of the cathedral.

All samples were prepared by the collaborators of the cathedral workshop. The mortars were applied as used on-site, i.e. in layers of between about 1 and 4 cm for the KMtl (ground layer) and 0.5–1 cm for the DMtl (finishing layer) on weathered sandstone blocks that had usually been consolidated at least 4 weeks beforehand with silicic acid ethyl esters. To estimate the influence of the application method, the mortars were applied on horizontal as well as vertical surfaces and some of the samples were taken from repair mortars that had been applied on site in the course of the regular restoration works. Further, to test the influence of the time interval between the application of KMtl and DMtl, series of samples with intervals of 0, 3 or 28 days were produced.

From these multilayered materials, consisting in DMtl, KMtl and sandstone, sample prisms were cut, consisting in three, two or one material layers (Fig. 1). The chosen sample preparation has the advantage of well-reflecting the application on-site and allows the extracting of very similar samples on the monument, but it produces samples with layers of varying thickness (Fig. 1) and therefore the laboratory

Table 1 Repair mortar compositions in volume parts

Mortar	Sand	Additions	Binder total	Binder proportions		
				PC	WC	HL
KMtl	12	0	5	2	1	2
DMtl-Zug	16	2	5	3	1	1
DMtl-BE	5	2	2	1	0.5	0.5

KMtl mortar for ground layer, *DMtl-BE* surface layer for Bernese sandstone, *DMtl-Zug* surface layer for Zug sandstone. Binders: *PC* Portland cement, CEM II 42.5, *WC* white cement CEM I 52.5, *HL* hydraulic lime NHL 5

results are not always easy to interpret [1]. When tested in the laboratory the mortar samples were usually between one and a few months old.

The general composition of the mortar materials is given in Table 1. The binders are various mixtures of cement, hydraulic lime and air lime. The additions are a mixture of Trass powder (a German pozzolan) and diatomaceous earth. The sands are mixtures of mainly crushed limestone and quartz sand in the case of the KMtl and diverse coloured sands in the case of the DMtl, with green sand dominating the ones for the Bernese sandstone (DMtl-BE) and rather grey sands in the case of Zug sandstone (DMtl-Zug).

4 Laboratory Analysis

Mortar repairs will to a large extent be executed at the tower of the Bernese cathedral, where these materials will be exposed to quite rough weathering conditions. It nevertheless can be expected that the weathering processes will mainly attack from the outer surfaces towards the core of the mortars and the stones. Water infiltrations from behind can largely be excluded, due to regular checks and permanent, rigorous maintenance of the building. Therefore the tests selected to examine the appropriateness of the repair mortars are such that they characterise mainly the water uptake and drying of the materials through the outer surface.

Total porosity [2] and hygric dilatation after 72 h of water immersion [3] were tested on single materials, i.e. sandstones, KMtl and DMtl. Capillary water uptake [4] and drying rate [4], both determined according to [2], were measured on single materials as well as BiC of DMtl-sandstone, KMtl-sandstone and DMtl-KMtl and TriC DMtl-KMtl-sandstone. For the multilayer samples water uptake was measured with the water suction through the outermost layer contained in the sample, e.g. DMtl or KMtl, and accordingly drying was tested by wrapping up the samples and leaving only the outer most surface open for evaporation.

Finally thin sections were prepared to observe the transitions between DMtl and sandstone, KMtl and sandstone and DMtl and KMtl by means of polarizing light microscopy.

No mechanical properties were tested in a first step because, wherever the repair needs to be rather big, the mortars are applied with reinforcements and plugs out of non corrosive materials as recommended elsewhere [5]. Moreover, as the same

repair mortars have been used for many years on diverse monuments and have never shown mechanical problems of any sort, this was considered not to be the main issue here.

5 Results

The measured laboratory values are given in Tables 2 and 3 as mean values, with the standard deviation and number of measured samples in brackets.

The hygric dilatation (Table 3) of all tested materials is rather similar with the exception of the sandstone of Berne.

The total porosity of the KMtl lies between the values of the sandstones and the two kinds of DMtl (Table 2). Its capillary porosity (water uptake at the end of the capillary suction) is rather high compared with its total porosity. For all other tested materials a much bigger difference between capillary and total porosity was observed.

The speed of capillary suction is, with the exception of the surface layer for repair of Bernese sandstone (DMtl-BE), rather similar for sandstones, mortars for ground layers (KMtl) and surface layers (DMtl). When the capillarity is measured

Table 2 Values for total (Pt) and capillary (Kpt) porosity, specific (A) and linear (B) capillary water uptake, given as: value (standard deviation; number of samples)

Material	Pt (vol-%)	Kpt(vol-%)	A (mg/cm ² min ^{1/2})	B (cm/min ^{1/2})
Sst-BE +/-w	17.7 (0.6; 16)	12.6 (1.2; 11)	36 (12; 12)	0.32 (0.13; 12)
Sst-Zug +/-w	11.3 (2.2; 9)	7.4 (1.2; 9)	26 (16; 9)	0.36 (0.17; 9)
KMtl	20.1 (2.5; 7)	17.2 (0.2; 4)	31 (9; 9)	0.18 (0.05; 9)
DMtl-BE	36.4 (0.3; 3)	21.3 (0.1; 3)	96 (22; 10)	0.45 (0.06; 10)
DMtl-Zug	31.7 (0.2; 3)	16.5 (0.5; 3)	48 (8; 7)	0.28 (0.07; 7)

Sst-BE Bernese sandstone, *Sst-Zug* Zug sandstone, +/-w more or less weathered and consolidated, *KMtl* mortar for ground layer, *DMtl-BE* surface layer for Bernese sandstone, *DMtl-Zug* surface layer for Zug sandstone

Table 3 Hygric dilatation (ϵ_{72h}) and drying at 75% relative humidity and 20°C expressed as weight loss in % of capillary water uptake after 200 and 400 h respectively

Material	ϵ_{72h} (mm/m)	Drying 200 ± 10 h (wt. %)	Drying 400 ± 15 h (wt. %)
Sst-BE +/-w	3.17 (0.40; 8)	82 (8; 11)	86 (5; 10)
Sst-Zug +/-w	1.40 (0.20; 6)	77 (4; 9)	82 (3; 9)
KMtl	1.00 (0.14; 6)	43 (3; 5)	50 (3; 5)
DMtl-BE	1.59 (0.08; 3)	83 (0; 3)	89 (0; 3)
DMtl-Zug	1.40 (0.03; 3)	79 (1; 3)	84 (1; 3)

Values given as: value (standard deviation; number of samples)

Sst-BE Bernese sandstone, *Sst-Zug* Zug sandstone, +/-w more or less weathered and consolidated, *KMtl* mortar for ground layer, *DMtl-BE* surface layer for Bernese sandstone, *DMtl-Zug* surface layer for Zug sandstone

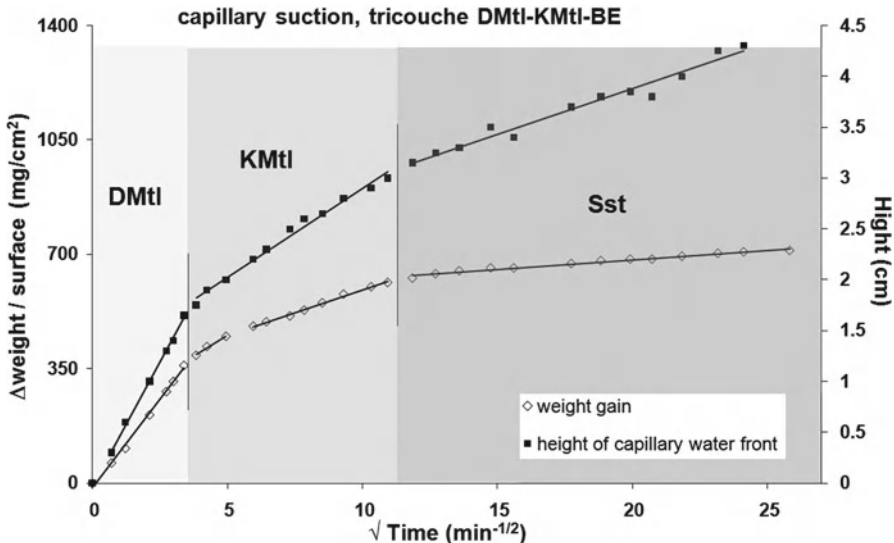


Fig. 2 Typical example of capillary suction curve, through a sample with three layers (surface layer *DMtl*, ground layer *KMtl*, Bernese sandstone *Sst*), with linear regressions on individual parts of the curve

on the TriC-Samples (three layered samples) it can be seen that the water uptake slows down at the material boundaries, but it does not stop (Fig. 2).

In the thin section of the *DMtl* applied on a 3 day old *KMtl*, a very thin but nevertheless clearly distinguishable sinter layer could be observed at the transition between *KMtl* and *DMtl* (Fig. 3). Apart from this the analytical results obtained for mortars applied horizontally or vertically, on specimen in the cathedral workshop or at the building as well as with intervals of 0, 3 or 28 days between *KMtl* and *DMtl* application were very similar.

6 Interpretation

Capillary suction experiments seem to show that no water accumulation can be expected within the boundary layers of the individual materials, but that the water transfer from one material to the other is rather good. This seems especially important if, for one reason or the other, water could penetrate from behind in spite of the measures taken to prevent this.

The big water uptake of the *KMtl* in comparison to its total porosity and in combination to its very slow drying, led to the conclusion that this material might be susceptible to considerable frost damage. On the other hand this material never forms the outer most layer of the building surface, because it is always covered with the *DMtl*. Therefore one of the practical results was that *DMtl* layers should always

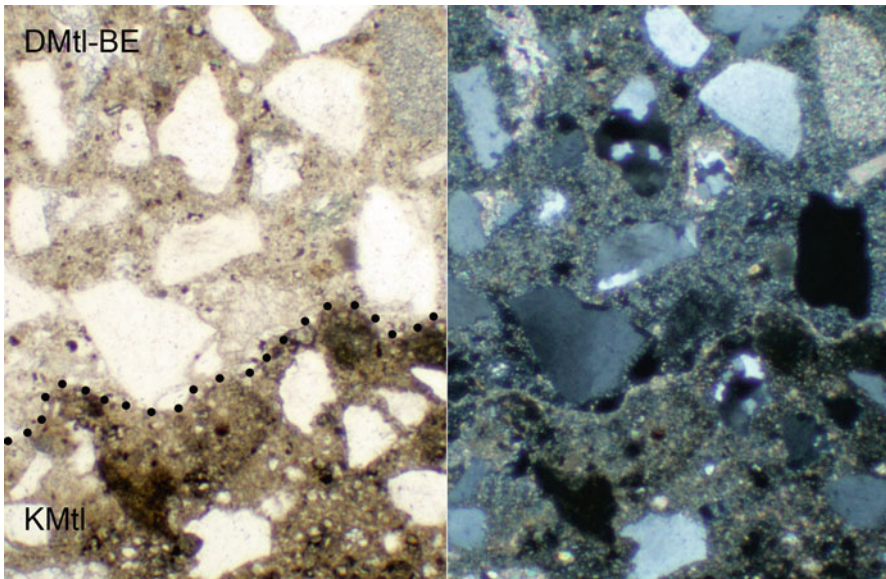


Fig. 3 Transition between *DMtl-BE* and the 3 day old *KMtl* in thin section. The boundary between the two mortars is indicated by a *dotted line* in the *left* picture. *Left* polarized light, *right* crossed polarisers, image height 1.3 mm

have a certain minimal thickness. Further, on the building the mortars will hardly ever, and only at very few places, be exposed to as much water and over such a long period of time as in the capillary suction test. And last but not least, during the regular controls no frost problems have been observed until now on any mortars applied on the cathedral itself.

7 Conclusions

The investigations suggest that the mortars used are in many ways well adapted to the sandstones on hand and that the diverse application methods only provoke small differences in the mortars at an early stage.

Regarding the KMtl it was decided to try to find a replacement material that should have a smaller capillary water uptake and a faster drying behaviour but as good working properties as the original KMtl. The work on this is still in progress, however first results using a different grain size distribution according to the suggestions by Konow [6] and rather hydraulic lime than cement, seem promising.

At the Bernese cathedral much emphasis is put on the consistent documentation of the works, and regular in-situ observations of the treated surfaces are an important part of the maintenance plan that is actually in force. Only in that way will we and the people in charge after us be able to learn from experience.

Acknowledgements We thank Andreas Walser and Katrin Durheim, for sharing their great knowledge and experience with us. Also we thank Fred Burri and Peter Völkle of the cathedral workshop for many discussions and careful preparation of the laboratory samples. Last but not least we would like to thank the Berner Münsterstiftung for financial support and constant encouragement.

References

1. Bläuer, C., Rousset, B.: Testing the mechanical and the petrophysical behaviour of repair mortars. In: Proceedings of the 11th International Congress on Deterioration and Conservation of Stone, Torun, Poland, pp. 795–802, 15–20 September 2008
2. R.I.L.E.M: Altération et protection des monuments en pierre, méthodes expérimentales conseillées. Colloque international, Paris, 5-9 juin 1978
3. Félix, C., Furlan, V.: Mesures automatiques sur des facies gréseux de la dilatation linéaire isotherme par absorption d'eau dans différentes conditions. In: 4th International Congress on the Deterioration and Preservation of Stone Objects, Louisville, pp. 127–134, 1982
4. Rousset Tournier, B.: Transferts par capillarité et évaporation dans des roches – rôle des structures de porosité. Dissertation Université Louis Pasteur, Strasbourg, Sciences de la Terre et de l'Univers, spécialité: pétrophysique (2001)
5. RILEM TC 203RHM: Performance requirements for mortar mixes for surface repairs. Unpublished discussion document 8.3.2010 RILEM TC Repair mortars for historic masonry – Task Group 3 (2010)
6. von Konow, T.: Theory transformed in practice and the results from practice distorting theories. Experiences from masonry restoration at the fortress of Suomenlinna in Finland. In: Proceedings of Workshop RILEM Technical Committee ‘Repair Mortars for Historic Masonry’, January 2005

Compatibility of Repair Mortars with Nineteenth Century Natural Cement Cast Stone from the French Rhône-Alpes Region

**Myriam Bouichou, Elisabeth Marie-Victoire, Emmanuel Cailleux,
and Denis Sommain**

Abstract In the French Alps, near Grenoble, in the middle of the nineteenth century, natural cements were massively used to produce “cast stone” (concrete block) and to simulate natural yellowish to reddish cut stone. In a first project, several historic concrete buildings were studied, and a major decay mechanism was identified: erosion, leading to the loss of the original fake stone appearance. Today, due to a lack of appropriate repair materials, grey Portland cement-based mortars and paintings are used, leading to a complete loss of the original aspect. Therefore, the aim of this second study was to develop and test compatible repair materials to conserve the cultural heritage of this region. Based on the results of the first project, specifications concerning the composition and main properties of compatible repair materials were established. Then, four mortars were selected, two of them being specifically formulated. In a second step, the intrinsic properties of those mortars were characterised, and finally, their mortar/concrete compatibility was assessed.

M. Bouichou (✉)
Cercle des partenaires du patrimoine,
Champs sur Marne, France
e-mail: myriam.bouichou@culture.gouv.fr

E. Marie-Victoire
Laboratoire de Recherche des Monuments Historiques,
Champs sur Marne, France
e-mail: elisabeth.marie-victoire@culture.gouv.fr

E. Cailleux
Centre Scientifique et Technique de la Construction,
Bruxelles, Belgium
e-mail: emmanuel.cailleux@bbri.be

D. Sommain
Centre Technique Louis Vicat,
L'Isle d'Abeau, France
e-mail: d.sommain@vicat.fr

1 Introduction

The oldest concretes encountered in France date back to the middle of the nineteenth century and were made with natural cements. These cements were produced in the Rhône-Alpes region and notably used to cast concrete blocks or quite complex ornaments, which were intended to imitate the colour and the texture of natural stone. One of these is an ochre colour, varying from light brown to red.

In a previous project [1, 2], a preliminary survey revealed that this cultural heritage was, on the whole, quite well-preserved. However, an erosion phenomenon was affecting the majority of the surfaces leading to a gradual disappearance of the concrete skin, which is detrimental to the initial “natural stone aspect.” The current rehabilitation techniques consist of the use of grey Portland cement-based mortars combined with a yellow or brownish paint finish. In fact, as the colours and composition of these concretes are very specific, there is a lack of suitable repairing mortars. Therefore, based on the analysis of the composition and properties of several historic concretes in this region, the aim of this study was to formulate and test natural cement-based repair mortars to restore eroded surfaces and to compare their performances to that of the Portland cement-based mortar currently used.

2 Protocol

The protocol of the study was divided into three steps. The first step consisted of the selection of four repair mortars, two of which were specifically formulated from the specifications established in the first project, based on the analysis of historic concrete.

In a second step, the mortars were characterised in terms of moisture transport, physical and mechanical properties, microstructure, and performance. The intrinsic properties of the four selected mortars were characterized in terms of shrinkage, water porosity, water vapour permeability, capillary suction, dynamic modulus of elasticity, bending, and compressive strength measurements. The microstructure was characterised by optical microscopy (on polished section) and scanning electron microscopy. The performance evaluation was conducted with visual analysis observations.

The third step of the project was dedicated to the evaluation of the compatibility of the selected mortars with historic concrete and to the assessment of the durability of the repair mortar/concrete system. Therefore, natural cement-based slabs were cast using a nineteenth century concrete formula and were artificially eroded. After applying the four mortars to the slabs, visual observations and pull-out tests were carried out on (A) and after three sorts of artificial ageing on (B, C, and D): 10 heating and stormy shower cycles (B), 10 freeze-thaw cycles (C), 10 heating and stormy shower cycles followed by 10 freeze-thaw cycles (D).

3 Requirements and Mortars Selection

The requirements for mortar selection took into account the main characteristics of the historic concrete, the repair type (fine mortar for erosion) and the monument type [3]. The concrete monuments to be repaired are among the first buildings made of concrete in France, with a specific architecture and in a cultural heritage context. As a consequence, criteria such as the preservation of the historic support and the need to use repair material with a colour and a texture close to those of the historic concrete had to be considered.

As quite high alkali contents were measured in the historic concretes to be restored, the use of alkali reactive (even potentially reactive) aggregates had to be avoided. The aggregate size also had to be adapted to the quite small thickness of eroded concrete to be repaired. As a consequence of the high sulphate contents observed in the binder of the historic concrete to be restored, the cement to be used had to show a good sulphate resistance in order to be compatible. To assess the durability of the restoration and to avoid further decay of the historic concrete, the properties of the repair mortars had to be adapted to those of the historic support, in terms of transfer properties (water vapour permeability higher than that of the support) or mechanical performances (modulus of elasticity comparable to that of the support). However, the mortars also had to present a good durability and be able to resist the main stresses that repair mortars usually face (low shrinkage, high tensile strength) [4–7]. Finally, to fit with the aesthetic requirements, cements had to be used that exhibited an ochre colour, either combined with mineral pigments or not.

Based on these requirements, two mortars were specifically designed and two others were selected among repair mortars available on the market (Table 1). It is to be noted that in the Alps region of France, there is a natural cement (so-called Prompt cement) that is still produced using the nineteenth century industrial process and whose composition is very close to that of the cements encountered in preliminary characterisation of the historic concrete. Therefore, this Prompt cement was used in the composition of the two specific designs and in one of the ready-to-use mortars. Furthermore, this cement has a good sulphate resistance. The fourth mortar selected was a Portland cement-based product containing fibres, which is currently used for rehabilitation operations.

Table 1 Repairing mortars selected

Mortar	Cement type	Mortar type	Comments
1	Prompt cement	Ready-to-use	Available on the market
2	Prompt cement	Ready-to-use	Specially formulated
3	Prompt cement	“On site” mortar	Specially formulated, for skilled operator
4	Portland cement	Ready-to-use	Available on the market

4 Mortars Characterisation

4.1 Moisture Transport, Mechanical and Physical Properties

The evaluation of the intrinsic properties of the four selected mortars was presented in a previous paper [8]. The main conclusions are as follows:

- concerning the *moisture transport properties*, the results of porosity measurements were quite scattered, mortar 4 being less porous (less than 15%) and mortar 1 being excessively porous (more than 40%). Water vapour permeability was quite high for mortar 2 and, on the contrary, very low for mortar 4. Finally, the water capillary absorption tests showed that mortar 2 presented a capillary coefficient that was too high.
- regarding shrinkage after 1 year, mortar 1 exhibited the highest values (0.2%). The best results were obtained with mortars 2 and 3, in which shrinkage was quite low and stable with time. Surprisingly, mortar 4, which contains fibres meant to limit the shrinkage phenomenon, showed values higher than mortars 2 and 3.
- the results of bending and compressive strength indicated very low performances of mortar 2 (even though they were increasing with time). On the contrary, the Portland cement-based mortar (mortar 4) presented much higher bending and compressive strength than the three Prompt cement-based mortars. Finally, the dynamic modulus of elasticity were lower than 27 GPa in all mortars, which is the lowest value measured on the historic concretes. No incompatibility was therefore evidenced.

4.2 Microstructure

Optical microscopy observations performed on polished section after borax attack revealed differences in non-hydrated phases. In mortar 4, which is Portland cement-based, clinker grains presented well-crystallised alite and belite, with no clear separation between C4AF and C3A. In mortars 1, 2, and 3, anhydrous residual grains were poorly crystallised, with small alite and belite crystals and well-separated C4AF and C3A phases.

The hydrated phases observed by scanning electron microscopy also varied depending on the binder:

- mainly calcium silicates hydrates (CSH) and ettringite with fresh portlandite for Prompt cement-based mortar
- and mainly CSH, portlandite, and fresh ettringite for Portland cement-based mortar (mortar 4).

These observations indicated that the microstructure of the Prompt-cement based mortars was quite close to that of the historic concretes; on the other hand, mortar 4 had a clearly different microstructure.

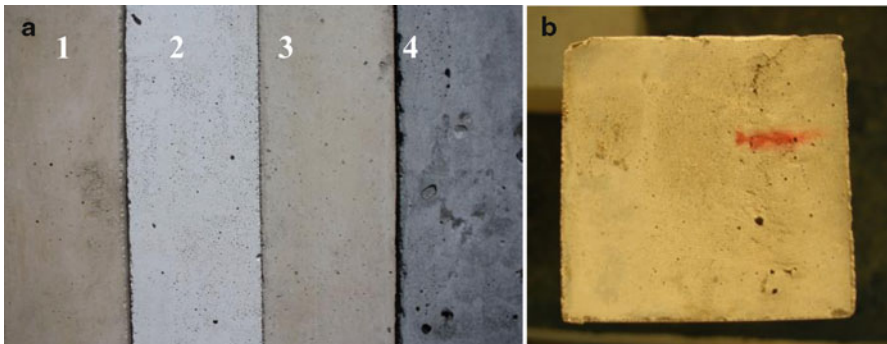


Fig. 1 (a) Colours of the mortars and (b) pigment trace on mortar 1

4.3 *Aestheticism*

The colours of the four mortars can be seen in Fig. 1a. Mortars 1 and 3 have an adapted colour but mortar 1 presents pigments traces (Fig. 1b). Mortar 2 is too white, but it is easy to tint. Mortar 4, whose colour is too grey and difficult to tint, is clearly not suitable.

4.4 *Slabs Manufacture*

Twenty slabs ($50\text{ cm} \times 50\text{ cm} \times 8\text{ cm}$) were cast for the purpose of mortar/concrete compatibility characterisation. The slabs' manufacture has been presented in a previous paper [8]. A composition extracted from documents dating back to the end of nineteenth century was used, using Prompt-cement as a binder. To reproduce a surface similar to the most commonly encountered erosion facials, deactivation products were pulverised on the 20 slabs surfaces just after their casting. After manufacture, the slabs were kept in a room at 20°C and 95% RH and dried in the open air for 28 days.

4.5 *Mortars Application*

The four selected mortars were applied to the slabs (four slabs per mortar). In terms of workability, mortar 1 was very fluid, mortars 2 and 3 were easy to apply, and mortar 4 was sticking to the tools and therefore was quite hard to apply (Fig. 2).

After its application, mortar 1 showed immediate shrinkage cracks (Fig. 3a). After setting, white efflorescence appeared on mortar 4 (Fig. 3b).



Fig. 2 Application of mortars 1 (a) and 4 (b)

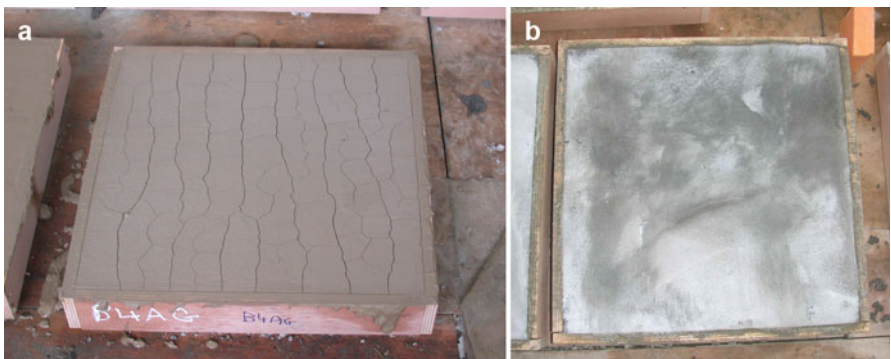


Fig. 3 Shrinkage cracks on mortar 1 (a) and white efflorescence on mortar 4 (b)

After the application of mortars and before the artificial ageing, the slabs were kept for 28 days in a room at 20°C and 65% RH.

4.6 Artificial Ageing

The artificial ageing cycles are presented in Fig. 4.

After artificial ageing, visual analysis was conducted, and then the slabs were kept for 7 days in a room at 20°C and 65% RH before the pullout tests. For each type of artificial ageing one slab per mortar was tested, and five pullout tests were performed per slab. The pullout tests were performed according to the French standard NF EN 1015-12, which consists of sampling a core through the entire thickness of the mortar and up to 3 mm in the concrete support with a core drill (5 cm inside diameter). Then, circular metal pellets (5 cm diameter) are glued to the mortar surface, and the pullout tests are performed using a 500 daN capacity dynamometer. The load is applied

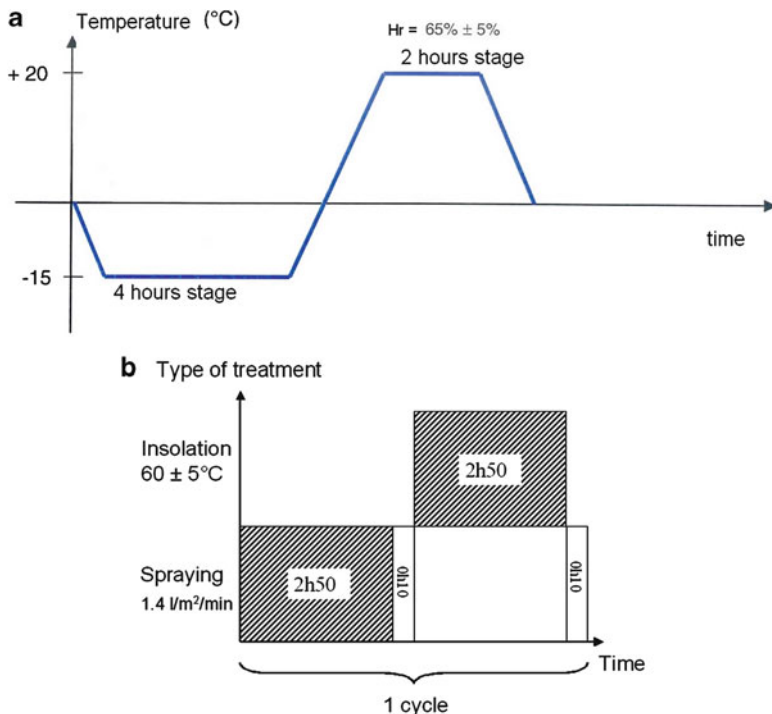


Fig. 4 Artificial aging: (a) freeze-thaw cycles, (b) heating and stormy shower cycles

monotonically, increasing to the fracture point. For each test, the fracture load and the fracture site are noted. Finally, the adhesion strength is calculated as ratio between the fracture average load and the pellet surface (the result is expressed in MPa).

In Fig. 5 the adhesion strengths obtained for each mortar before and after the different artificial ageing are presented. The fracture sites for each mortar before and after the different artificial ageing are given in Table 2.

With a simple cure without artificial ageing (A), the adhesion strength was similar for mortars 2 (0.8 MPa) and 3 (0.6 MPa), while the adhesion strength for mortar 4 was much higher (2 MPa). After the freeze-thaw cycles (B), no important adhesion evolution was noticed. After the heating and stormy shower cycles (C), the adhesion values of mortars 2, 3, and 4 increased (respectively 1.2, 1.6 and 2.9 MPa). After the D cycles, the adhesion strengths for mortar 2 (from 1.2 to 1.3 MPa) were similar to the results obtained from the C cycles, although they decreased for mortar 3 (from 1.6 to 0.4 MPa) and increased for mortar 4 (from 2.9 to 3.7 MPa).

Figure 6 illustrates interface and support fracture sites. With a simple cure (A) and after the freeze-thaw cycles (B), mortars 2 and 3 presented an interface fracture location, whereas mortar 4 presented a support fracture location. After the C cycles, only mortar 2 presented a mortar fracture location, and mortars 3 and 4 presented a break both in the

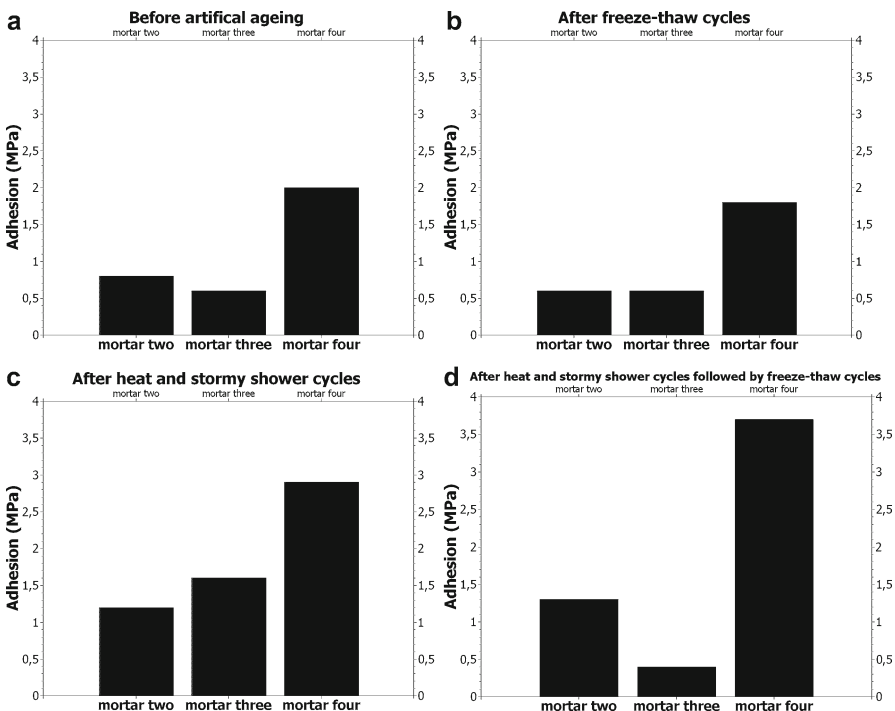


Fig. 5 Adhesion values before and after artificial ageing

Table 2 Fracture sites for each mortar before and after the different artificial ageing

Mortar	A	B	C	D
2	Interface fracture	Interface fracture	Mortar fracture	Mortar fracture
3	Interface fracture	Interface fracture	Support fracture 60% mortar fracture 40%	Mortar fracture
4	Support fracture	Support fracture	Support fracture 60% mortar fracture 40%	Support fracture 60% mortar fracture 40%

support and in the mortar. After the D cycles, mortars 2 and 3 presented a mortar fracture location, whereas mortar 4 presented a support/mortar fracture location.

To summarise, mortar 4 was too adhesive (with cracking in the support), mortars 2 and 3 showed suitable adhesion properties (adhesion strength higher than the 0.4 MPa threshold of the initial specifications); mortar 1, which shrank immediately after its application to the slabs, could not be tested.

After the freeze-thaw cycles (B), no apparent damage was noted for mortars 2, 3, and 4. After the heating and stormy shower cycles (C), cracking was observed for mortars 3 (Fig. 7) and 4, and no damage was noticed for mortar 2. After the heating and stormy shower cycles, followed by the freeze-thaw cycles (D), cracking was

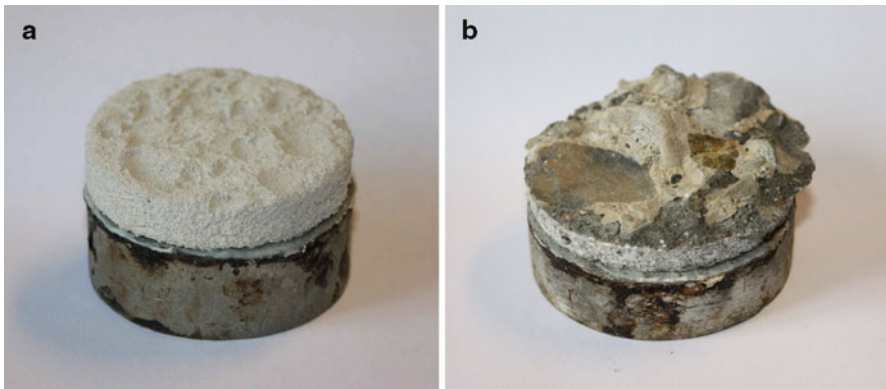


Fig. 6 Interface fracture site (**a**) and support fracture site (**b**)

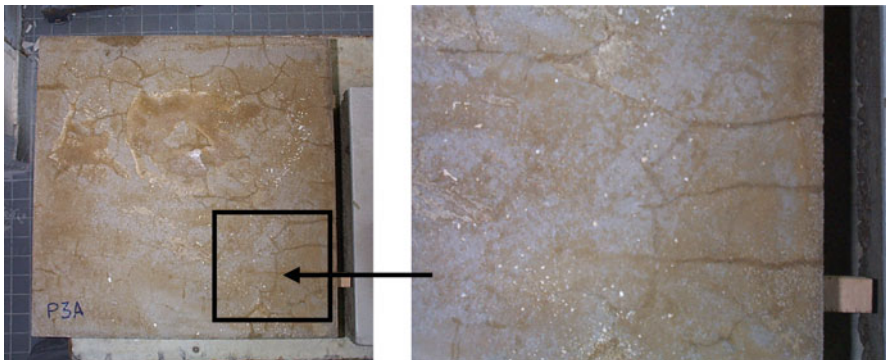


Fig. 7 Cracking observed on mortar 3 after heating and stormy cycles

observed for mortars 3 and 4 and no damage was noticed for mortar 2. Therefore, no additional damage was noted after the (D) cycles.

Mortar 2 showed a good durability whatever the artificial ageing, while mortars 3 and 4 suffered degradations after the heating and stormy shower cycles (C), which may be linked to a deformability deficiency.

5 Conclusions

The aim of this study was to develop and test repair mortar for historic concrete of the nineteenth century encountered in the French Alps area, which is affected by serious erosion. After a first study focused on these historic concretes analysis [1, 2], a list of specifications was established. Based on these specifications, four mortars were selected, their intrinsic properties were characterised, and the compatibility of the system mortars/concrete was tested.

Firstly, the intrinsic properties tests revealed that some mortars were unable to match the specifications. Actually, shrinkage was clearly too high in mortar 1. Mortar 4, which is Portland cement-based, was clearly too impermeable to water vapour. Its mechanical performances also were much higher than the three Prompt cement-based mortars. Only mortars 2 and 3 (specially designed) presented moisture transfer and mechanical adaptations. In terms of microstructure, the use of Prompt-cement in the mortars leads to a microstructure close to those of the historic concrete. Only mortar 3 (on site mortar) presented an adapted colour.

Secondly, the tests performed on slabs presented some incompatibilities. Mortars 1 and 4 were difficult to apply on the slabs simulating the historic concrete. The adhesion strength for mortar 4 was too high, with fracture sites in the support, which is incompatible with the problem of the support conservation. For mortars 2 and 3, the adhesion strengths were sufficient, with cracking position principally at the mortar/concrete interface or in the mortar.

Finally, in terms of resistance to the artificial ageing, only mortar 2 (ready-to-use and specially formulated) showed no degradation for all the cycles types, while the heating and stormy cycles caused cracking in mortars 3 and 4.

To conclude, mortars 1 and 4 are incompatible for the repair of the eroded historic concrete of the nineteenth century of the French Alps area. Mortar 2 corresponds to all the specifications except the colour, but it can be easily tinted. Mortar 3, the “on site” mortar, presents only a deficiency of durability for the heating and stormy cycles. The final step of this study will consist of testing the two best mortars (mortars 2 and 3) on-site in cooperation with skilled operators and with a follow-up in time.

References

1. Cailleux, E., Marie-Victoire, E., Sommain, D.: Microstructural and weathering mechanisms of natural cements used in the 19th century in the French Rhône-Alpes region. In: Proceedings on the International Workshop on: Repair Mortars for Historic Masonry, Delft, 26th–28th January 2005
2. Cailleux, E., Marie-Victoire, E., Sommain, D.: Study of natural cements from the French Rhône-Alpes region. In: Proceedings of the International Conference on Heritage, Weathering and Conservation, Madrid, vol. I, pp. 77–84, 21–24 June 2006
3. Daubresse, A., Caractérisation des mortiers pour le bâti ancien.: Exposé de la journée enduits, bétons et patrimoine, 28 October 1998
4. Thomasson, F.: Les enduits monocouches à base de liants hydrauliques. Unitecta France, Paris La Défense (1982). 129
5. Enduits Monocouches d'imperméabilisation: Certifications et classements des produits du bâtiment, Cahiers du CSTB n°2669. Juillet-Août, Paris (1993)
6. Emmons, P.H., Vaysburd, A.M.: Factors affecting the durability of concrete repair: the contractor's viewpoint. Constr. Build. Mater. **8**(1), 5–16 (1994)
7. Vaysburd, A.M., McDonald, J.E., Emmons, P.H., Poston, R.W.: Performance criteria for selection of repairs materials. In: Malhotra, V.M. (ed.) Fifth International Conference CANMET/ACI, Barcelona, vol. 2, pp. 931–947, 4–9 June 2000, American Concrete Inst. (2001)
8. Bouichou, M., Cailleux, E., Marie-Victoire, E., Sommain, D.: Evaluation of compatible mortars to repair 19th century natural cement cast stone from the French Rhône-Alpes region. Conservar Patrimonio (8):59–66 (2008)

Two Views on Dealing with Rain Penetration Problems in Historic Fired Clay Brick Masonry

Caspar J.W.P. Groot and Jos Gunneweg

Abstract In this paper a comparison is made between two views on solving rain penetration problems in solid historic fired clay brick masonry. The first one aims at protecting the masonry against rain penetration (“rain coat” concept). In the second approach the penetration of rain in the masonry is accepted and the measures taken are focused on improving the *capillary* moisture transport in the masonry and on the application of materials with favourable drying characteristics and/or the enhancement of the drying conditions (“breathing” concept). It is shown that the often preferred protection approach may result into deterioration of the rain penetration problem instead of diminishing it. Also is shown that the second approach generally leads to a significant drying of the walls, thus providing a sound solution for rain penetration problems in solid historic fired clay brick masonry.

1 Introduction

Water leakage in historic solid masonry walls regularly occurs and is a major source of damage; in masonry it causes frost and salt damage; in timber it may lead to rot. Moreover, humidity may have negative effects on the living conditions in historic buildings.

From practical experience and from the literature [1–3] various causes for moisture problems like leaking can be deduced:

- Inadequate material properties of the applied fired clay brick and masonry mortar; incompatibility between brick and mortar properties
- Cracks in masonry

C.J.W.P. Groot (✉) • J. Gunneweg

Delft University of Technology, Stevinlab IV/Stevinweg 4 2628 CN/Delft/ NL

e-mail: mailto:c.j.w.p.groot@tudelft.nl; c.j.w.p.groot@tudelft.nl; j.gunneweg@hetnet.nl

- Inadequate design
- Poor ventilation
- Negative effects of a number of inadequate restoration measures
- Poor workmanship of the builders during construction and/or restoration

This paper is based on a study of rain leakage problems studied in particular in historic masonry of windmills in the west of the Netherlands. These are ideal objects for such a study as wind mills are intentionally exposed to wind and rain (to optimize their functionality) and often show leakage problems. The problems observed in this study are also applicable to historic solid masonry of towers, churches, castles etc.

Before discussing the different measures that may be taken to solve leakage problems some further thought is given to different types of moisture transport in solid masonry.

2 Rain Penetration and Porosity

Brick and mortar are porous media. The moisture absorption in these materials is mostly governed by capillary action and drying by evaporation. For the separate materials moisture transport is relatively easy to understand, for the composite material *masonry* this is more complicated.

2.1 Capillary Water Transport

Optimal contact between mortar and brick is the result of (i) the correct choice of brick and mortar (compatibility) allowing the formation of a dense mortar-brick interface, and (ii) the skill of the mason: the brick should be fully surrounded by mortar (no cavities). Under these conditions, the two capillary systems of brick and mortar are smoothly connected.

Moisture transport from mortar to brick and vice versa are dependent on differences in pore dimensions and pore distributions of the two separate materials. The transport of moisture from brick to mortar may be hindered if the porosity of the mortar is much finer than that of the brick: in that case the mortar acts as a barrier and slows down or even stops moisture transport through the masonry.

Liquid moisture transport may take place in the case of connected capillary pore systems as a result of pressure differences (e.g. wind pressure, drying, ventilation) if the moisture content in brick and mortar is higher than the critical moisture content (at the critical moisture content the capillaries are covered by a thin layer of water). This may lead to leakage and moisture ingress into masonry.

2.2 “Free Water Transport”

Apart from capillary action (in fact moisture transport through capillary pores of porous materials) moisture transport can as well occur as a form of “free” water transport. With this is meant water that travels through a wall along “canals” formed by interconnected fissures, hollows, cavities, cracks etc. (“canal” porosity more than 100 µm in diameter distinguishing it from the capillary action, as the influence of gravity is significant) [4]. Pressure differences, especially wind pressure do have a significant effect on the moisture transport velocity for this type of porosity: water may pour out of the wall as a jet of water.

This is a far more unfavorable condition for leakage than capillary moisture transport, as the capillary water transport velocity is much slower than the “free” water transport velocity

It seems obvious that creating or reinstating conditions of capillary water transport (by filling up the cavities) may significantly improve the water tightness behavior of the wall,

Grout injection may be the proper way to realize this change in water transport behavior in a wall.

3 Two Views on Solving Water Leakage Problems

Basically to solve leakage problems in solid masonry two different methods may be applied [5]. The first one aims at protecting the masonry against rain penetration (“rain coat” concept). In the second approach the penetration of rain in the masonry is accepted and the measures taken are focused on (i) if necessary, improving the *capillary* moisture transport in the masonry (ii) the application of materials with favourable drying characteristics and/or (iii) the enhancement of the drying conditions, e.g. improvement ventilation (“breathing” concept).

The potential and limitations of both views are discussed hereafter.

3.1 Protection Against Rain Penetration

In case of leakage the most logical and promising way to solve this problem seems to be the protection of the masonry from the penetration of rain (rain coat solution). In practice a number of solutions are applied in which this approach is chosen, such as the application of (Fig. 1):

- Render
- Tar
- Thatch on masonry

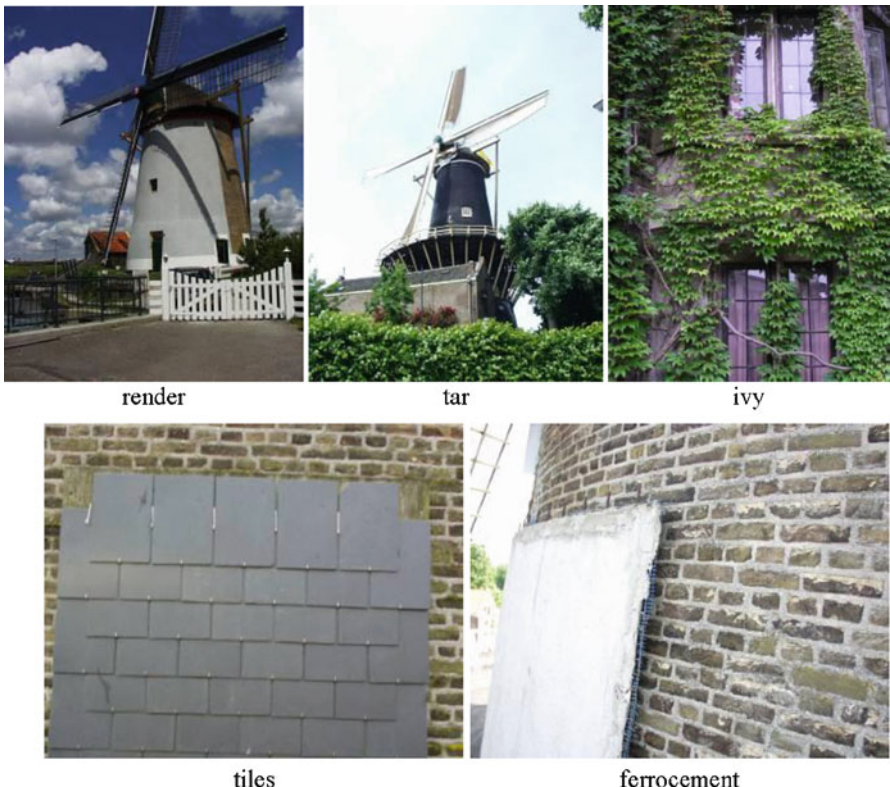


Fig. 1 Examples of protection measures against rain water leakage

- Tiles
- Ivy
- Paints, coatings etc.

Apart from protecting the underlying masonry against rain penetration these solutions have the disadvantage that they significantly alter the visual appearance of the object. This is often unacceptable if the structure has a cultural heritage value.

3.1.1 Water Repellent

In that case, protection against rain penetration is often sought with the application of water repellents, as they are transparent. The assumption then is that the application of water repellent causes (i) rain water to be averted and (ii) the wall to become drier and drier over the course of time.

The water repellent coats the pores and penetrates for some mm's in the wall and allows vapor transport after application of the water repellent: a reason often given

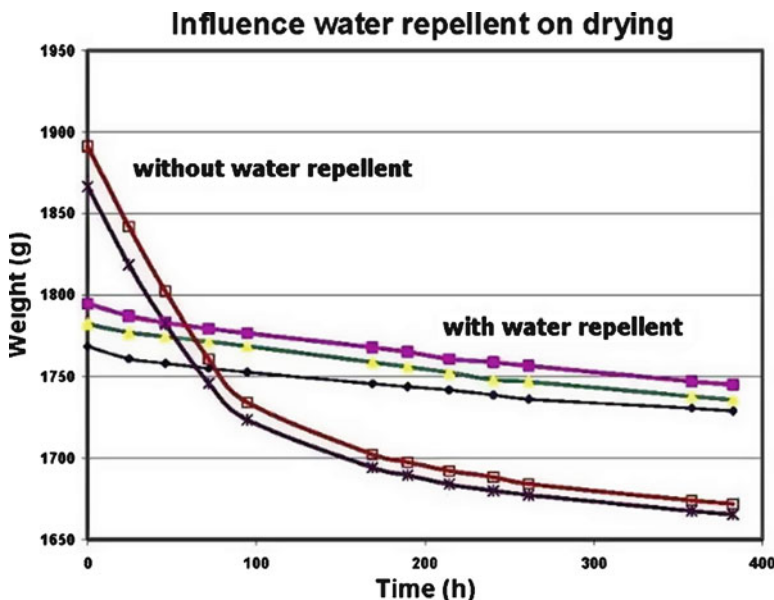


Fig. 2 The application of a water repellent significantly slows down the drying of a wall

by producers of water repellents as a recommendation to use their products. However, drying is not only a function of vapor transport; in most cases also liquid transport plays a role. In fact drying is slowed down as water is stopped by the water repellent layer in the outer face and only can evaporate from the pores some mm's within the wall: a slow process (see Fig. 2).

Inspection of more than 25 masonry wind mills, where water repellents were applied, showed that the leaking problems, instead of diminishing, always increased. A possible reason is that wind mills may develop micro-cracks in the masonry as a result of the heavy dynamic oscillations of the sails.

So rain water may enter through these micro-cracks in the wall instead of being warded off. Also other moisture sources like occasional flooding, continuous rising damp, recurrent inside condensation and hygroscopic moisture uptake may be causes of moisture absorption into the wall. With moisture inside the wall the applied water repellent turns out to be a disadvantage as already shown in Fig. 2: drying is significantly slowed down.

There is also another strong motive to refrain from the application of water repellents in the case of historic masonry. The reason is that very often historic masonry contains salts. Drying leading to salt crystallization just under the repellent layer may cause substantial damage (see Fig. 3).

It can be concluded that protection against rain penetration ("rain coat" concept) may be rather tricky: one should be well aware of possible other moisture sources (which may be unavoidable) and as well take into account possible side effects.



Fig. 3 Salt damage as a result of the application of a water repellent

3.2 Accept Rain Penetration and Focus on the Realisation of Capillary Moisture Transport in the Masonry and Enhance Drying

Intuitively this view (“breathing” concept) seems to be less promising, as the promotion of drying is normally aimed at through materials which also significantly absorb moisture.

However, the following should also be considered:

If the water leakage is caused by “free water transport” measures taken (e.g. injection) to create or reinstate *capillary* moisture transport have the effect that the moisture transport significantly slows down. Experience has learned that well-made solid masonry, having capillary moisture transport only, is generally water tight.

In sound masonry the mortar acts as a barrier; and as been shown in [6], the penetration of rain water in the wall during a shower is limited to a depth of 1.5 brick length (as within this depth moisture always will meet a mortar layer); more water will drain from the outer face of the wall; so, the amount of absorbed water is limited.

Experience from practice shows that in the Netherlands 1 h of rain shower is counterbalanced by 15 h of drying.

3.2.1 Case: Rain Penetration Problems in the Windmill at Maassluis (NL)

In a number of consulting projects this view has been chosen as a guide in solving rain penetration problems; this turned out to be successful. One of the cases, the windmill at Maassluis (NL) showing serious rain penetration problems, will be elaborated.

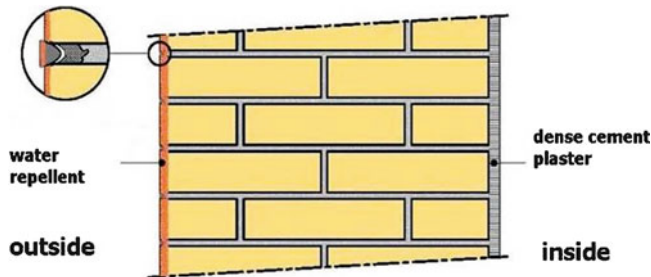


Fig. 4 Cross section of the windmill wall before intervention: at the outer face a water repellent was applied, on the inside a dense cement plaster, the pointing consisted of a dense cement mortar

3.2.2 Starting Conditions

The starting conditions of the masonry were as indicated in Fig. 4. From this figure it can be deduced that an attempt was made to protect the wall against moisture penetration; at the outside face of the windmill a water repellent was applied; the repointing consisted of a dense cement mortar, showing interface micro-cracks as a result of shrinkage, at the inner face a dense cement plaster.

It is clear that if the wall absorbs rain water through e.g. micro-cracks, this moisture is more or less entrapped as drying is hindered at the inside face and is very slow at the outside face.

In order to obtain data on the moisture content situation in the wall, moisture profiles were determined at two places in the windmill wall, using powder samples.

Figure 5 shows that the moisture content in the wall, in spite of the protecting measures (water repellent, dense plaster layer) is very high.

3.2.3 Drying Measures

In a process lasting over 2 years, measures were taken to change the situation from moisture absorbing to drying; to this end the following was done:

- Removal of the plaster
- Two years of drying
- Meanwhile,
 - Application of a simple ventilation system inside the wind mill
 - Removal of pointing mortar and replacement by an open good drying mortar, compatible to the substrate
- After 2 years: application of a new restoration plaster with high porosity and good drying properties.

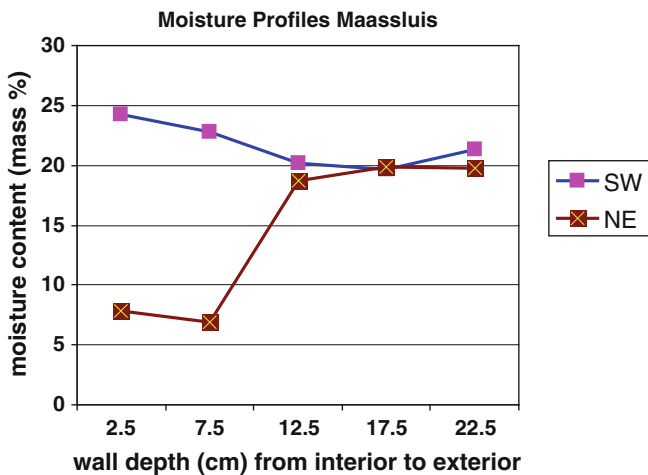


Fig. 5 Moisture content profiles at the south-west side (rain side) and the north-east of the windmill wall [7] (very high moisture content values not exceptional in very highly porous Dutch fired clay bricks)



Fig. 6 TRIME sensor

3.2.4 Monitoring Moisture Content over the Years in Wall of Windmill at Maassluis

In order to verify the effectiveness of the measures taken, moisture content measurements were performed over the years. To this end a TRIME sensor was used [8].

The TRIME technique (Time Domain Reflectometry with Intelligent Micromodule Elements) enables the measurement of a reflection of a pulse that travels through a material. Instrumental to the introduction of the pulse into the material are two antennas at the side of the probe (Fig. 6). These antennas are by means of expansion springs in contact with a tube that is glued to the material.

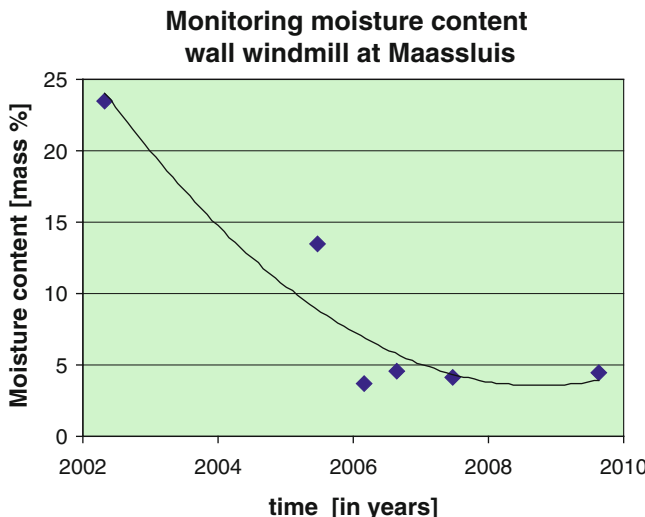


Fig. 7 Drying over the period 2002–2010, monitored using a TRIME sensor

The travelling time of the pulse up and down the conduction rods and into the material provides information about the presence of water in the material, as the travelling time is a function of dielectric properties of the material.

The tube remains in the wall; the moisture content in the wall is monitored by taking measurements from time to time over the course of the years.

The measurements showed that a significant drying of the wall took place over the course of a period of several years.

4 Conclusions

From the study of field cases and the execution of several test cases the following could be concluded:

4.1 Protection Against Rain Penetration (“Rain Coat” Concept)

Many measures (render, tar, thatch, tiles, ivy etc) to realise the “rain coat” concept are not suitable in cases of historic masonry where change of visual appearance is not acceptable.

Protection of the outside face of the masonry by a transparent water repellent and a dense plaster on the inside has often unexpectedly resulted in a significant *increase* of moisture in the wall.

Specifically in historic masonry possible salt damage as a result of the application of water repellent should be considered.

4.2 Accepting Rain Penetration, Promoting Drying (“Breathing” Concept)

In the “breathing” concept rain penetration is accepted and drying is aimed at through the skilful application of materials with good drying characteristics and improving drying conditions (ventilation). A basic condition is that there is capillary moisture transport (preliminary injection may be needed).

It was proven in test cases that this approach resulted in a significant drying of walls; even in case the outside face of the wall still contained water repellent and only the pointing was replaced by adequate good drying repointing material, and on the inside of the wall the dense plaster was replaced by highly porous restoration plaster.

References

1. Grimm, C.T.: Water permeance of Masonry Walls: a review of the literature. In: Borchelt, J.G. (ed.) *Masonry: Materials, Properties and Performance*, ASTM STP 778, pp. 178–199. American Society for Testing and Materials, Philadelphia (1982)
2. Ramamurthy, K., Anand, K.B.: Classification of water permeation studies on masonry. *Masonry Int.* **14**(3), 74–79 (2001)
3. Thomas, K.: Chapter: Rain penetration, dampness and remedial measures. In: *Masonry Walls*, pp. 144–159. Butterworth-Heinemann Ltd., Oxford (1996)
4. Thomson, M., Lindqvist, J.E., Elsen, J., Groot, C.J.W.P.: Chapter 2.5 Porosity of Mortars. In: Groot, C.J.W.P., Ashall, G., Hughes, J. (eds.), RILEM Report 28: Characterisation of Old Mortars with Respect to Their Repair, RILEM, Bagneux (2007)
5. Sass, O., Viles, H.A.: Wetting and drying of Masonry walls. *J. Appl. Geophys.* **70**(1), 72–83 (2010)
6. Groot, C., Gunneweg, J.: The influence of materials characteristics and workmanship on rain penetration in historic fired clay brick masonry. *Heron* **55**, 141–153 (2010)
7. Groot, C., Gunneweg, J.: Vochtproblematiek stenen molens. TU Delft faculteit CiTG, Delft (2002)
8. Groot, C.J.W.P., van Gaanderen, H.J., Heruc, S.: Potential of the TRIME Probe for the determination of moisture content changes in monuments. In: Proceedings International Millennium Congress, vol. 1-1b, no. 18, Icomos, UNESCO (2001)

Part III

**Experimental Research into Properties
of Repair Mortars**

Experimental Study of Hot Mixed Mortars in Comparison with Lime Putty and Hydrate Mortars

Jan Válek and Tomáš Matas

Abstract An experiment was carried out in order to understand the influence of hot mixing on the properties of hardened mortars in comparison with mortars made of lime hydrate and lime putty. Lime from the same quarry and producer was used in the form of lime hydrate, lime putty and quicklime. Two types of quicklime were used, varying in their calcination conditions and also their reactivity. Standard specimens of 40×40×160 mm were cast and evaluated after curing. Mechanical (compressive and flexural strength) and physical properties (open porosity, bulk density, capillary absorption) were determined on the specimens of hardened mortars. Thin sections of the mortars were prepared and evaluated using polarising microscopy in order to describe the structure of mortar including the presence of binder related particles. The produced hot mixed mortars had hardened properties comparable with the lime putty and lime hydrate mortars. Due to the micro-cracks in the binding matrix the hot mixed mortars showed higher porosity and capillary absorption. The heterogeneity of the hot mixed mortars was a result of the preparation technology.

1 Introduction

Characterisation of historic mortars has recently become quite a common activity of workplaces specialising in historic buildings and materials. Many research laboratories are well equipped and existing publications about characterisation methods (e.g. RILEM [1]) provide examples which can be followed. Compositional, physical and even mechanical properties of historic mortars can be determined by established

J. Válek (✉) • T. Matas
Institute of Theoretical and Applied Mechanics, Academy of Sciences
of the Czech Republic, Prague, Czech Republic
e-mail: valek@itam.cas.cz

analytical procedures and tests. However, the interpretation and application of the results can be quite difficult. Results of characterisation of historic mortars could contribute to the design of repair mortars and could also provide information about construction history and mortar production and preparation technologies. The latter point is quite important for a proper characterisation. Lack of knowledge about the production technologies and their effects on the hardened mortar properties and performance could lead to incorrect conclusions from the characterisation of the historic mortars and misleading interpretations of results. Therefore, some basic research on the fresh and hardened properties of lime based mortars made using a variety of historic production technologies is needed.

When appropriate knowledge is lacking, historic lime mortars are assumed to be the same (in performance and properties) as modern lime based mortars or even cement-based concretes. However this assumption may not always be correct. Historic mortars are specific because of their manner of lime burning and their technology of production.

A typical example of a historically widespread mortar preparation method, which is currently not well known, is hot mixing. Mortars prepared directly from quicklime, wet sand and water are called hot mixed mortars. This preparation of mortars has certain benefits as it allows a relatively fast mortar production on site, quicklime can be used soon after its production, which minimises demands on storage of this reactive material, no storage of lime putty is needed and it is applicable for a variety of lime binder compositions. These points were considerably important for builders of historic buildings in the past. On the other hand, the mixing proportions are more difficult to control which leads to a high variability in the mortar produced. Moreover, the hot mixing also provides only limited control over the slaking process and thus historic hot mixed mortars often contain various binder related particles. Historic hot mixed mortars are typically rich in binder and can theoretically be distinguished from mortars made of lime putty or lime hydrate by employing light microscopy on thin sections [2], however more research is needed to identify their characteristic features. Similarly, the knowledge about the effects of hot mixing on the properties of hardened mortars is limited [3].

Many researchers described the existence of binder related particles in historic mortars e.g. [4–6]. These binder-related particles are usually defined as particles of binder which contain no aggregate [7]. Elsen [8] in his review on microscopy of historic mortars distinguishes three types of the binder-related particles: under-burned fragments, over-burned fragments and lime lumps *sensu stricto*, and summarises the possible information which can be gained from their analysis: type of limestone and its composition (under-burned particles), maximum burning temperature (over-burned particles), the manner of mortar preparation (particles *sensu stricto*). Although several researchers have described historic hot mixed mortars containing lime particles, no general identification features exist for their characterisation in terms of the mortar technology production. Experimental production of replicas of historic mortars by traditional technologies can lead to a further distinction among them which could consequently be used for identification of their production technologies [9].

2 Experimental

The objective of the experimental work was an evaluation of the physical and mechanical properties of hardened non-hydraulic lime based mortars. It focused on the comparison of mortars prepared directly from quicklime by a hot mixing method with mortars prepared from lime putty and dry lime hydrate that were commonly used forms of binder. A series of three specimens per mix type were produced from lime hydrate, lime putty and two types of quicklime. Historic mortars are often rich in binder. Therefore, the specimens were prepared from two different binder/filler proportions representing the contemporarily recommended 1:3 and a more historic binder rich 1:0.9 mix proportion (by volume).

2.1 Materials and Specimens

Mortar specimens $40 \times 40 \times 160$ mm were prepared from lime (CL90) and quartz sand. The lime binder used was in three different forms, lime hydrate, lime putty and quicklime, and was from the same quarry and the same lime production factory. The overview of the used binders is presented in Table 1. The lime used contained over 95% calcium (according to the analysis of the producer). The quicklime used in the HB mix was more reactive when slaked with water than the one used in the HA mix. The filler was a standard masonry siliceous river sand with particles ranging between 0 and 4 mm and clay and dust content around 2.9%.

Two mixing ratios 1:3 and 1:0.9 by volume were used based on lime hydrate to sand proportion. The gauging was carried out by weight calculated from the bulk densities of the lime hydrate and (dry) sand. The lime putty was dried out to estimate the amount of water it contained. The dry residue was assumed to be Ca(OH)_2 , i.e. having the same molecular weight as the lime hydrate. Both quicklimes were assumed to be composed only of CaO (5% of the other compounds were neglected for the gauging purposes). The amount of the quicklime added proportionally corresponded (by molecular weight) to the same mass of Ca(OH)_2 gauged in the lime hydrate mix. Water was added to produce similar workability for lime hydrate and

Table 1 Summary of the lime binders and their forms used in the experiment

Code	Form of lime	Additional information
HY	Lime hydrate	Standard, commercially available lime hydrate CL90
LP	Lime putty	Commercially available 2 year old lime putty. The putty was produced by soaking and mixing lime hydrate CL90. Water content 32.6 wt.%
HA	Quick lime	Quick lime $T_{\max} = 73^\circ\text{C}$, $t_{\max} = 33$ min
HB	Quick lime	Quick lime $T_{\max} = 77^\circ\text{C}$, $t_{\max} = 6.4$ min

Table 2 Gauging and mixing procedure

Mix	Lime [g]	Sand [g]	Water [g]	L:S vol.	wt.	Mixing details
HY	152	1,465	250	1:3	1:9.6	Mixed for 5 min
HYII	399	1,100	380	1:0.9	1:2.8	Mixed for 5 min
LP	226 ^a	1,465	180	n.m.	1:9.6 ^b	Mixed for 5 min
LPII	592 ^a	1,100	190	n.m.	1:2.8 ^b	Mixed for 5 min
HA	115	1,465	~700	n.m.	1:9.6 ^b	Mixing with breaks, total time was 30 min.
HAI	302	1,100	~700	n.m.	1:2.8 ^b	Four hundred gram of water was added initially; the rest was added several times in small amounts to compensate for the evaporation and at the end of mixing to adjust the workability
HB	115	1,465	~700	n.m.	1:9.6 ^b	
HBII	302	1,100	~700	n.m.	1:2.8 ^b	

^aadditional water contained in putty $226\text{ g} \times 32.6\% = 74\text{ g}$, $592\text{ g} \times 32.6\% = 193\text{ g}$

^bL lime, assuming by the weight of dry Ca(OH)_2 ; S sand

lime putty mortars. The workability was judged based on experience and the mortar flow was evaluated on a flow table (to EN1015-3) where it reached values comparable to $150 \pm 5\text{ mm}$. More water was needed in the hot mixes to provide water for slaking during the mixing and also to compensate for evaporation. The mortar was mixed in a standard laboratory mixer. The appropriate workability of hot mixed mortars was estimated by experience. Gauging and mixing procedures for the specimens are given in Table 2.

Three prisms $40 \times 40 \times 160\text{ mm}$ were cast per mix type according to EN 1015-11 (Determination of flexural and compressive strength of hardened mortars) and stored at 20°C , 65% RH. The cast specimens in moulds were covered with a flat, saw-cut sandstone block simulating the masonry suction and providing a sufficient weight which would keep the hot mixed mortars compacted inside the mould in case the slaking process continued in the moulds for 7 days. All specimens were exposed to accelerated curing conditions simulating 21 wetting and drying cycles for the last 70 days before their testing. Wetting was done by misting the specimens up to the point when the surface stopped absorbing water and started to be glossy. Non-hydraulic lime binders harden by carbonation, i.e. reaction of calcium hydroxide with carbon oxide [10] forming calcium carbonate. This reaction is a slow process and changes the porosity and pore structure of the binding matrix, mainly pores around $0.1\text{ }\mu\text{m}$ [11]. Carbonation speed depends on CO_2 concentration in the ambient air, pore structure and gas diffusion resistance of mortar (binding matrix), presence of moisture and temperature. Curing by the repetitive wetting and drying was selected as it is a dynamic process when a variety of conditions favourable for carbonation can occur, rather than keeping one stable condition in the laboratory.

Table 3 presents a depth of totally carbonated areas of mortars (identified by Phenolphthalein pH indicator) and the age of the specimens when tested. The carbonated depth divided by the age of specimens represents the carbonation rate (speed) for a comparative purpose. It should be noted that the carbonation depth was

Table 3 Age of specimens and depth of carbonation at the time of testing

	HY	HYII	LP	LPII	HA	HAI	HB	HBII
Age [days]	202	101	195	160	160	77	139	98
Carbonation depth [mm]	17	6	10	3	8	3	8	4
Carbonate rate [mm/day]	0.08	0.06	0.05	0.02	0.05	0.04	0.06	0.04

only an indication of the totally carbonated zone, where pH is lower than 9.0, i.e. CaCO_3 . The carbonation front was in fact deeper and the inner parts of the specimens were partially carbonated. This fact was confirmed by a thermal analysis which was carried out on the specimen made of lime putty. For the mortars LP and LPII the proportion of CaCO_3 of the total binder in the centre (pink, high pH) part is 48% and 10% respectively. The depth of carbonation and its speed was lower for the specimens richer in binder. The specimens HY were almost fully carbonated.

2.2 Testing Methods

The flexural strength of the mortar specimens was determined by the three point bending test according to EN 1015–11. The compressive strength was determined according to the same standard on the halves of the specimens left after the bending test. Bulk density and open porosity of the hardened mortars were determined according to vacuum saturation method (EN 772–4 Determination of real and bulk density and of total and open porosity of natural stone masonry units). Capillary coefficient was determined according to EN 1015–18 (Determination of water absorption coefficient due to capillarity action of hardened mortar). The mortar structure was described on polished thin sections using a transmitted light polarising microscope.

3 Results

The hot mixed mortars were prepared from two types of quicklime and compared to the mortars made of standard lime putty and lime hydrate. Two effects were observed in the test results; firstly, the influence of the form of binder and secondly, the influence of the amount of binder.

3.1 Strength

The mechanical performance of the mortars is summarised by the charts in Fig. 1. The highest compressive strength (1.4–1.6 MPa) was obtained for both lime hydrate mixes and also for the 1:3 (vol.) hot mixed mortars. Both lime putty mortars had

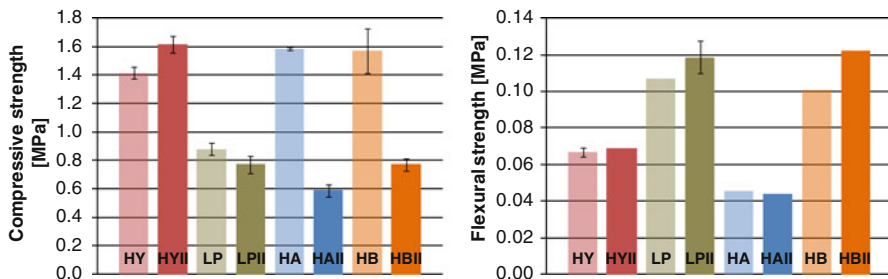


Fig. 1 Compressive and flexural strength of lime mortar specimens

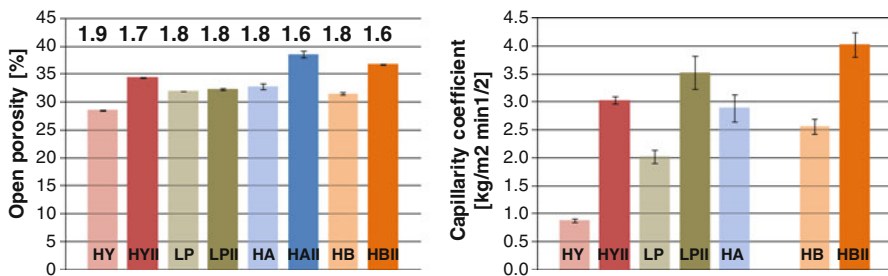


Fig. 2 Open porosity and coefficient of capillary absorption of lime mortar specimens. Bulk density of the specimens is given for comparison above the porosity values in g.cm⁻³

lower compressive strength around (0.8 MPa). The higher amount of binder (mixes 1:0.9 by vol.) caused lower compressive strength (apart from the lime hydrate mix). This reduction of strength in compression was very significant (half of the value) in the case of the hot mortar mixes and was probably connected not only with their increased porosity. The effect of the increased porosity connected to the increased amount of binder can be observed on the specimens HY and HYII in Fig. 2.

The comparison of the influence of the different forms of binder shows that the lime hydrate binder produced mortars with a higher compressive strength than the lime putty mortar but in the case of the flexural strength it was the opposite.

The effect of the form of binder on the flexural strength was dual. In some cases (mainly LPII, HAI, HBII) a high shrinkage caused significant cracking and since the bending test is sensitive to imperfections like this, the specimens broke at significantly lower values. These measurements were disregarded and the error bars are not presented in such cases in the chart. For the specimens which were relatively sound it seems that the higher amount of the binder provided quite a good bond between individual sand grains, which was comparable to, if not better than the 1:3 (vol.) mixes. However, there were some micro-cracks within the binding matrix observed by the microscopic analysis.

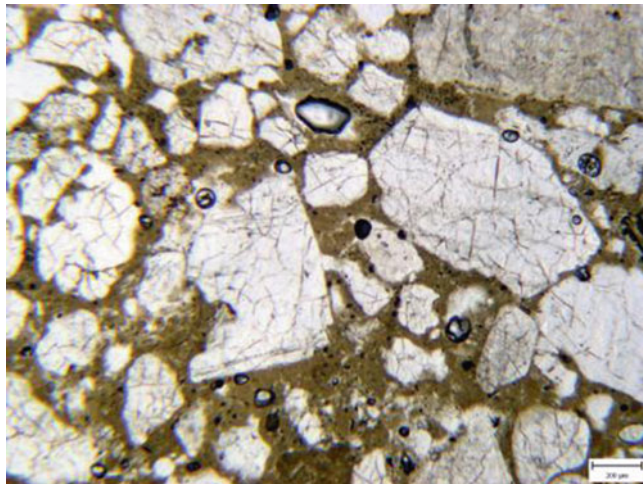


Fig. 3 HY (1:3) in PPL, scale bar 200 μm

In cement and concrete technology, porosity and compressive strength correlates quite well [12]. Therefore, the open porosity of the specimens was determined along with the capillary absorption rate (see Fig. 2). The larger amount of the binder produced in all cases a higher open porosity (pores, voids, micro-cracks) and also quite clearly increased the capillary absorption rate. However, the correlation of the open porosity and compressive strength was not so clear in the case of the tested specimens. Specimens HYII, HAII and HBII had the highest open porosity. This was reflected by the relatively lower compressive strength of the HAII and HBII specimens. However, the comparison of open porosity and compressive strength of HY and HYII specimens shows that even as the porosity increased with the binder content the compressive strength also increased. The correlation of compressive strength and open porosity is, for non-hydraulic lime mortars, strongly affected by other factors which may be of the same magnitude [13, 14].

The structure of the specimens was described using polished thin sections under plane polarised light. The photomicrographs of the individual mortars are presented in Figs. 3, 4, 5, 6, 7, 8, 9, and 10. The higher amount of binder in the mortars is clearly visible in all four cases. The mortar specimens made of lime hydrate were well compacted without shrinkage micro-cracks or large voids. Occasionally rounded air voids were identified. The lime putty mortars (LP) showed a large number of irregular voids and the binding matrix was full of shrinkage micro-cracks, mainly in the mortar LPII where the areas of lime binder concentration between the filler grains were larger. The quality of the hot mixed mortars HA, AHII, HB and HBII was variable for all specimens. In some cases there was quite a large concentration of air voids (see Fig. 9). The hot mixed mortars with the higher amount of the binder (HAII and HBII) also contained a net of shrinkage micro-cracks in the binding matrix (Figs. 8 and 10). The hot mixed mortars also contained binder related particles

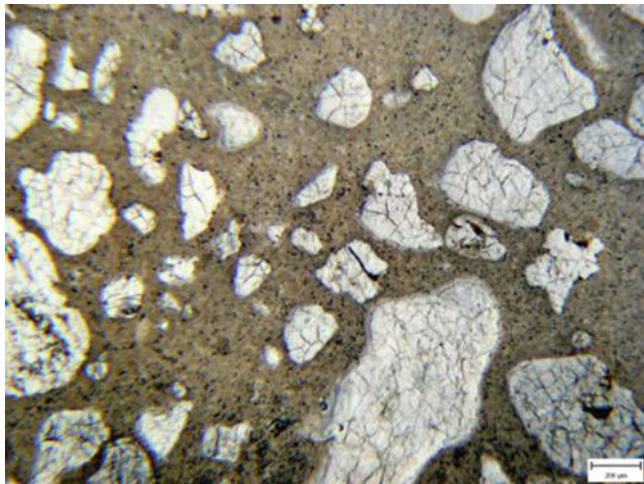


Fig. 4 HYII (1:0.9) in PPL, scale bar 200 μm

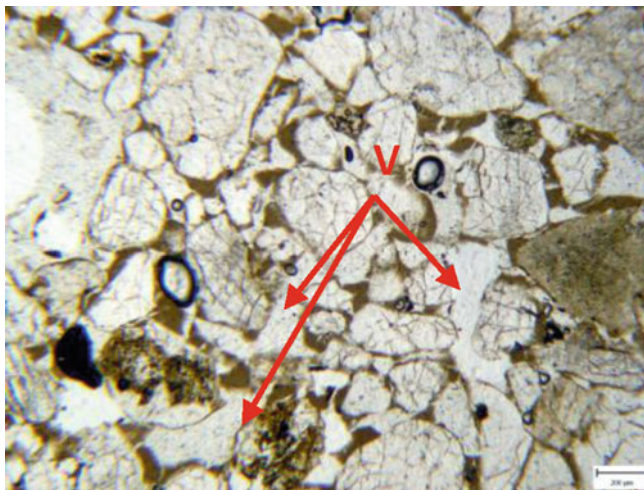


Fig. 5 LP (1:3) in PPL, scale bar 200 μm . V void, LL binder related particle

(in the figures marked as LL). These binder related particles were considered to be produced by the method of slaking and mixing. When the quicklime was slaked separately it slaked well into lime putty and there were no larger particles left. Also the quicklime was from a commercial production which would suggest quite a high efficiency of calcination.

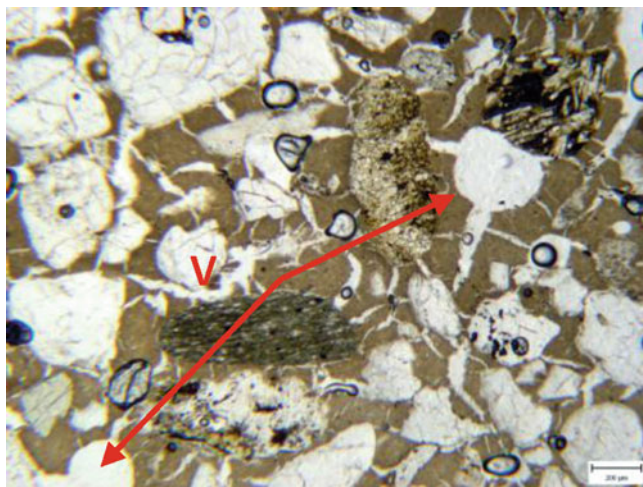


Fig. 6 LPII (1:0.9) in PPL, scale bar 200 μm

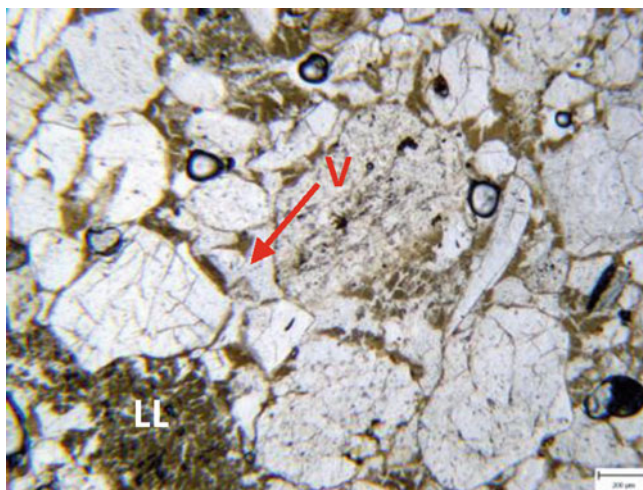


Fig. 7 HA (1:3) in PPL, scale bar 200 μm

4 Discussion

The main point of the experimental work was the description of the hardened properties of the hot mixed mortars in comparison with the mortars made of lime hydrate and lime putty. All four types of mortars were made of non-hydraulic lime of the same origin and very similar composition. The results presented above show that

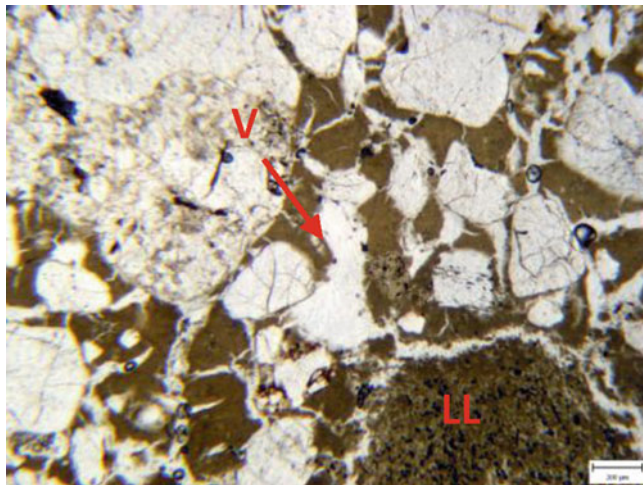


Fig. 8 HAII (1:0.9) in PPL, scale bar 200 μm

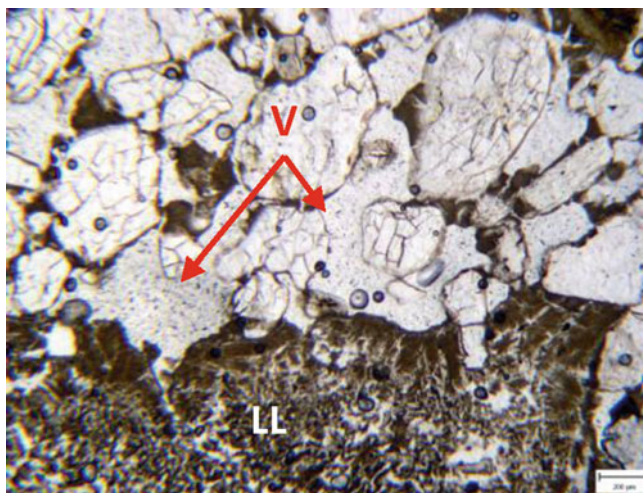


Fig. 9 HB (1:3) in PPL, scale bar 200 μm . V void, LL binder related particle

the form of lime binder along with the method of preparation can significantly influence the hardened mortar properties.

The optical microscopy showed that consistent and well compacted specimens without any clear internal defects were produced only from the dry lime hydrate. The other specimens had some imperfections, like larger voids, shrinkage cracks and micro-cracks in the binding matrix, uneven distribution of binder, and in the case of hot mixed mortars also the presence of larger particles of binder. These imperfections

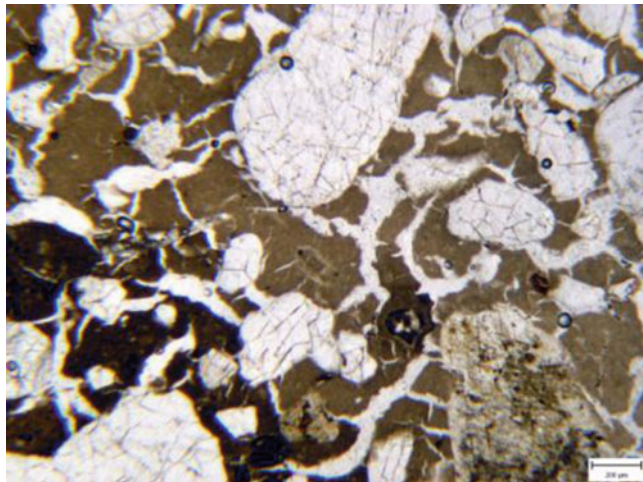


Fig. 10 HBII (1:0.9) in PPL, scale bar 200 μm

influenced the hardened mortar properties and added to their heterogeneity. Some of these imperfections, like the presence of binder related particles, are characteristic features of the way of mortar preparation. However, the shrinkage cracks, micro-cracks and presence of larger voids indicate some technological deficiency during the preparation. Micro-cracks in the binding matrix, similar to those found in the putty and hot mixes, are not so often found in historic mortars which are even richer in binder. One possible explanation could be in the test set-up which may have not sufficiently simulated the moisture transport situation comparing to normal masonry when being built. Under normal conditions the water absorption by the adjacent bricks/stone may be much higher, resulting in much lower moisture content levels in the mortars during hardening.

Nevertheless, some interesting points resulting from the testing could be pointed out:

- The hot mixed mortars had in principle comparable hardened properties as lime hydrate and lime putty mortars. Although, there was no clear evidence of continuation of slaking after casting (like popping out), there were differences in properties which suggested that the lime slaking process was not completely finished when the specimens were cast. This affected the homogeneity of the specimens and thus also the results.
- The compressive strength of the hot mixed mortars was probably mainly affected by the internal integrity of the mortars (amount of micro-cracks). The larger amount of binder led to their significant reduction of strength in compression. Degree of carbonation, mixing proportions and amount of binder seemed to be less relevant, at least for the lime hydrate and lime putty mortars.
- The flexural strength was higher for the lime putty mortars. The higher amount of binder (1:0.9 vol.) has not affected significantly the flexural strength but it

seems that if the binder is sound a higher binder proportion can even increase the flexural strength. All grains are well surrounded by the binder. Although the lime putty mortars had a comparatively lower compressive strength their flexural strength was one the highest. This was despite the fact that the higher amount of lime in the LPII mix caused the micro-cracks in the binding matrix.

- Binder related particles were found in the hot mixed mortars. They were unmixed, not well slaked lime lumps – *sensu stricto*. Their shape was rather irregular and the lumps did not contain any texture of the original limestone. Their presence was rather limited in comparison to some hot mixed mortars prepared from lime calcined by a traditional way at a low temperature (around 900°C) in a wood fired kiln [2]. The irregularity of their shape can be one of the recognisable features when there is a need to distinguish among the binder related particles and their connections to mortar production technology.
- The higher amount of lime binder slowed down the propagation of carbonation through mortar; i.e. there was more lime binder to carbonate per mm of depth. The higher amount of lime binder increased porosity and significantly increased the capillary absorption.
- Micro-cracks in the binding matrix identified by microscopy in the LPII, HAI and HBII were not found in the HYII mortar specimen. Even though the HYII specimen contained areas of binder larger than 0.2×0.2 mm, i.e. those which were typically cracked in the other mortars.

5 Conclusions

Hot mixed mortars are known to have been produced in the past. The experimental study compared the hot mixed mortars with mortars prepared from more standard lime putty and lime hydrate binders. The hot mixing of quicklime with sand affected the properties of hardened mortar specimens on a comparable level to lime putty or lime hydrate. A large number of imperfections in the structure of the hot mixed mortars pointed out on the deficiency of the mixing and production technology. The main problem was the drying shrinkage which caused significant cracks in all specimens apart from the lime hydrate mixture. The drying shrinkage was also probably the cause of small micro-cracks in the binding matrix. It was interesting to note, that the higher amount of the binder caused more micro-cracking but at the same time its effect on the flexural strength was not negative. Future studies on bonding properties of different limes to the aggregate grains could be interesting. Also the hardened characteristics of the hot mixed mortars should be better understood in order to improve our ability to characterise them. Hot mixed mortars will always be quite heterogeneous due to the nature of their production. However, analyses of historic mortars in the literature show that they used to be produced well-compacted and without any significant micro-cracking of binding matrix. Further research could also help to re-develop this traditional technique for the purposes of cultural heritage repairs.

Acknowledgement The research has been carried out with the support of the Institutional Research Plan AV0Z20710524 and LA 09008.

References

1. Groot, C., Ashall, G., Hughes, J.J. (eds.): Characterisation of Old Mortars with Respect to their Repair – RILEM Report 28, RILEM Baguenox (2007)
2. Valek, J., Zeman, A.: Lime particles in hot mixed mortars: characterisation and technological links. In: Proceedings of the 12th Euroseminar on Microscope Applied to Building Materials, TU Dortmund, pp. 341–350 (2009)
3. Malinowski, E., Hansen, T.: Hot lime mortar in conservation – repair and replastering of the Façades of Läckö Castle. In: Proceedings of the 1st Historical Mortars Conference, Lisbon. LNEC (2008)
4. Bakolas, A., Biscontin, G., Moropoulou, A., Zendri, E.: Characterisation of the lumps in the mortars of historic masonry. Thermochim. Acta **269/270**, 809–816 (1995)
5. Bruni, S., Cariati, F., Fermo, P.: White lumps in fifth-to seventeenth-century AD mortars from northern Italy. Archaeometry **39**, 1–7 (1997)
6. Hughes, J.J., Leslie, A., Callebaut, K.: The petrography of lime inclusions in historic lime based mortars. In: Proceedings of the 8th Euroseminar on Microscope Applied to Building Materials, Athens, pp. 359–364 (2001)
7. Leslie, A., Hughes, J.J.: Binder microstructure in lime mortars: implications for the interpretation of analysis results. Quart. J. Eng. Geol. Hydrogeol. **35**. Geological Society of London, London, pp. 257–263 (2002)
8. Elsen, J.: Microscopy of historic mortars – a review. Cem. Concr. Res. **36**, 1416–1424 (2006)
9. Valek, J., Zeman, A.: Properties of historic mortars in relation to technology of their production. In: Proceedings of 11th International Congress on Deterioration and Conservation of Stone, Torun, Poland, pp. 775–783 (2008)
10. Van Balen, K.: Modelling lime mortar carbonation. Mater. Struct. **27**, 393–398 (1994)
11. Lawrence, R.M., Mays, T.J., Rigby, S.P., Walker, P., D'Ayala, D.: Effects of carbonation on the pore structure of non-hydraulic lime mortars. Cem. Concr. Res. **37**, 1059–1069 (2007)
12. Neville, A.M.: Properties of Concrete. Sir Isaac Pitman & Sons, London (1963)
13. Valek, J., Bartos, P.J.M.: Influences affecting compressive strength of modern non-hydraulic lime mortars used in masonry conservation. In: Proceedings of the STREMAH VII, Wessex Institute of Technology, WIT press Southampton, pp. 571–580 (2001)
14. Lanas, J., Alvarez, J.I.: Masonry repair lime-based mortars: factors affecting the mechanical behaviour. Cem. Concr. Res. **33**, 1867–1876 (2003)

The Effect of Calcination Time upon the Slaking Properties of Quicklime

Dorn Carran, John Hughes, Alick Leslie, and Craig Kennedy

Abstract An experiment was conducted to determine how the slaking characteristics of quicklime produced from the calcination of selected limestones relates to calcination time. The experiment also permitted the determination of the optimum calcination time by determining when each limestone was under or over burnt (as indicated by minimum water reactivity values). Four limestones, three from Scotland Dornie, Parkmore, Trearne and one from England- Ham Hill, were calcined at 900°C for a range of times between 2 and 5 h. The limestones used include both granoblastic metamorphic and bioclastic-micritic limestones with variable silicate contents. The resulting quicklimes were tested for reactivity by recording temperature rise and rate of temperature rise during slaking. Sieve analysis of the residue after slaking was performed on some samples. The Dornie limestone was the most reactive with an optimum calcination time of 4 h, Ham Hill was the second most reactive with an optimum calcination time of 3.5 h, Trearne followed at 4 h and the least reactive was the Parkmore sample with an optimum calcination time of 4.5 h. Dornie, Ham Hill and Trearne limestones underwent complete calcination with a weight loss greater than 40%. The experiment showed that the determination of the optimum calcination time through the examination of water reactivity was possible.

D. Carran (✉) • J. Hughes

School of Engineering, University of the West of Scotland, Paisley, Scotland, UK

e-mail: Dorn.Carran@uws.ac.uk; John.Hughes@uws.ac.uk

A. Leslie

British Geological Survey, Murchison House, Edinburgh, Scotland, UK

e-mail: aleslie@bgs.ac.uk

C. Kennedy

Historic Scotland, Edinburgh, Scotland, UK

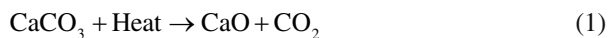
e-mail: craig.kennedy@scotland.gsi.gov.uk

1 Introduction

This article presents the results of an experiment conducted to determine how length of calcination of selected limestones affects the slaking characteristics of quicklime, allowing optimum burning times to be established. The work presented here is an initial stage in a programme where further studies using the selected limestones are conducted to understand better the formation of lime lumps, or lime inclusions, that are commonly encountered in historic mortars. A full understanding of the raw material is required to allow the identification of related processes in the later experimental stages.

When compared to the study of concrete, the research into historic mortar is still in its infancy. The recent emphasis upon sustainability and the authentic and accordant preservation of the past has led to an increased interest into the study and development of traditional materials such as lime mortar. In attempting to better understand historic mortar materials it is elemental to understand the basic behaviours of the core components and how their properties translate into a lime based product. The understanding of limestone calcination is well developed in industry, though a general theory of limestone behaviour is elusive (e.g. [1]), and its relationship to understanding the composition and texture of historic lime mortars is unexplored. The following discussion of the main factors in limestone calcination and quicklime hydration is derived from the texts of Boynton [2] and Oates [3] unless otherwise referenced.

Calcination is the thermal decomposition of calcium carbonate represented by the Eq. 1;



Decomposition is initiated on the exterior of a sample, and the calcination front moves through to the interior of the sample as a result of conduction [4]. To maintain the process of calcination, CO_2 must diffuse through the pores of the rock; therefore the dissociation temperature must be maintained for all the material to be calcined. If burning is halted before decomposition of the carbonate reaches the centre of the lump, then the core becomes underburned. For the centre to decompose and for CO_2 to escape, the surface temperature must exceed the disassociation temperature of the carbonate. The rate of carbonation is controlled primarily by the rate of heat transfer through the calcined layer, the thickness of which increases with calcination time. Dissociation proceeds within an atmosphere of pure CO_2 that exerts an increased pressure (up to 6.8 atm, 6.9 bar, 100 psi) as it attempts to escape. The increase in pressure further increases the temperature which causes the already calcined surface of the lump to become over-burned; this causes shrinkage of the lump and the closure of pores and fissures.

The heat of the kiln can cause the expansion of the crystal matrix which can lead to the decrepitation of crystals into dust. The smaller the crystals the more resistant they are to the heat.

The purer the carbonate, the higher the temperate required for calcination. Also the denser and more crystalline the limestone used, the slower the rate of calcination,

because a dense crystal structure does not allow CO₂ to exit readily. If the limestone contains organic matter, then this can burn away in the kiln and increase the porosity of the rock, which increases gas flow and therefore aids calcination. Each source rock varies in their crystallinity, tendency to decrepitate, impurities, stone size, chemical reactivity, shrinkage rate, density, porosity, surface area and spacing of crystals, all of which can impact upon the rate of calcination and the temperature and duration required for disassociation.

Hydration also referred to as slaking and is represented by;



Quicklime is very reactive with water; the reaction is strongly exothermic. Water migrates into the pores of the quicklime; the heat of hydration once activated produces an internal expansive force; the particles then shatter and disintegrate into crystalline dust or colloidal suspension exposing a fresh surface into which further water can migrate; the particles then dissolve and chemically combine to produce a super saturation of calcium hydroxide. Less reactive particles (such as those that have become over-burned), dissolve more slowly resulting in the formation of crystals around the primary nuclei.

On hydration, weight gain occurs. For pure quicklime this weight gain is usually in the region of 24–27%. Often there will always be a degree of free-water remaining within the hydrate; if this is to be removed heat is required. Generally for the full hydration of high calcium quicklime, 52% of the lime's solid weight in water is required. An increase in surface area can also occur if slaked well.

Slower hydration contributes to crystal growth and the flocculation of particles. Rapid hydration results in smaller particle sizes as they have little time to agglomerate. The rate of hydration can be affected by;

- Purity – The purer the quicklime, the faster the rate of hydration. If there are a large amount of impurities, pores can be blocked and the product will be less impervious.
- MgO content – MgO has a retarding effect on the process.
- Size of quicklime – The smaller the size of the quicklime lumps, the more rapid the rate of hydration.
- Specific surface area of the quicklime [5].

2 Materials

The four limestones (see Fig. 1) used in the experiment were:

Dornie: From the Ballachulish subgroup of the Dalradian rocks of the Highlands of Scotland, near Fort William. It is a medium to coarsely crystalline metamorphosed limestone (a marble) which forms beds of dark grey, fine to medium crystalline limestone interbedded with thinner dark grey pelites [2, 6]. It comprises of coarse equigranular calcite in a granoblastic texture, with finely disseminated accessory



Fig. 1 The four sample limestones. The samples were wetted before the photographs were taken to highlight their textural characteristics (Note scale given by the ruler at the top of each image)

minerals in quantities of a few percent; quartz, sheet silicates, pyrite and some oxides. Bulk analysis results vary, with Robertson et al. [7] suggesting a CaCO_3 content of 95.09% and Holmes [8] proposing a CaCO_3 of 92.12% on average. XRF analysis performed on the same sample set used here in 2006 showed a CaO content of 53.7% and a LOI of 42%. The stone sampled has an average bulk density of 2.68 g/ml and an average open porosity of 2.6%.

Parkmore: This limestone is also from the Dalradian supergroup, from an outcrop of the Blair Atholl subgroup from Dufftown in NE Scotland. A metamorphosed limestone, it appears to be lithologically similar to the Dornie limestone but contains veins of coarse white twinned calcite [9–11]. It has a CaO content of 52.5%, SiO_2 of 2.14% a LOI of 42.6%, contains accessory quartz and muscovite, traces of MgO, Al_2O_3 and Fe_2O_3 have also been found during analysis [10]. The average bulk density of the limestone is 2.69 g/ml and an average open porosity of 2.5%.

Trearne: A biomicritic packstone from the Brigantian sedimentary succession of the Midland Valley of Scotland, about 25 km SW of Glasgow. It is a sedimentary limestone containing abundant crinoid, coral and mollusc fragments and typically 50% micrite (fine calcareous material <63 μm , [12]) with variable amounts of quartz, kaolinite and minor pyrite. Robertson et al. [7] suggest that most quarries in the area were producing limestones with over 90% CaCO_3 content, although more

Table 1 Sample set data for each type of limestone

Limestone	Number of fragments per batch	Size of each fragment (cm)	Weight of each batch (g)
Dornie	12–13	3–7	208
Parkmore	25	3–7	600
Trearn	30	3–7	400
Ham Hill	30	3–7	600

recent figures Trearne were placed at 80.66% [8], and a 2006 analysis on the same sample set utilised here revealed a CaO of 40.4%, SiO₂ of 20.3% (comprised of quartz and kaolinite) and a LOI of 33.9%. The average bulk density is 2.56 g/ml and the average open porosity is 4.6%.

Ham Hill: This limestone is found as a lense within the Upper Yeovil Sands of Somerset. It is a shelly bioclastic sedimentary limestone, with a high average open porosity of 22.5% (our measurements). It is famed for its honey brown colour which is caused by the presence of Goethite, an iron hydroxide; accessory minerals include limonite and quartz [13]. Ham hill has a reported CaO content of 42.9%, SiO₂ of 13.8% and a LOI of 32.1% [14]. It has a bulk density of 2.41 g/ml.

3 The Experiment

The four limestones were calcined in batches at 900°C for times lasting between 2 and 5 h at 30 min intervals, a total of seven residence times at the calcination temperature for each limestone, except for the stone from Trearne quarry that was sampled and tested for calcination times over 3 h. The time selection is based on typical minimum residence time for a traditional batch process lime kiln. The resulting quicklime was cooled and its slaking reactivity determined according to an adaptation of the method given in EN459-2 [15].

Each limestone was crushed into fragments 3–7 cm in size and sample sets each weighing up to 600 g were created consisting of either 25 or 30 fragments (dependant of the specific limestone sample, Table 1). Each sample set consisted of a single batch of one type of limestone.

A programmable ventilated laboratory furnace (Fig. 2) with a volume of 10.3 l was used to heat each sample set from room temperature (~20°C to avoid shock calcination) at a rate of 40°C/min to 450°C. This temperature was maintained for 1 h before the temperature was further increased at the same rate to 900°C (the disassociation temperature of calcite being 898°C [2]). Figure 3 graphically depicts the heating regime.

After calcination, the samples were removed from the furnace and placed on a cold hard surface to cool and weighed to enable the percentage weight loss that occurred during each burning to be calculated. Once the samples had cooled,

Fig. 2 The laboratory furnace (Ney Vulcan 3–550) used in the calcination experiments

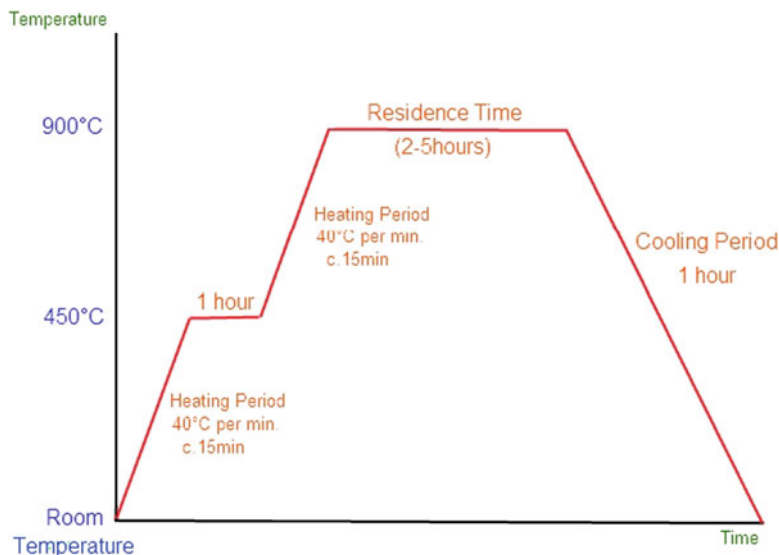


Fig. 3 The heating profile used in the calcination experiments

they were crushed and sieved through a 3.35 mm sieve and 150 g of this sample was selected for testing. Following this the samples were tested for reactivity using the wet slaking test described in BS EN 459-2: 1994 [15] combined with ASTM C110 – 04 [16], where 150 g of quicklime is added to 600 g of distilled water with

a starting temperature of 26–28°C and a pH of 4.2–4.8. The temperature rise was recorded every 30 s for a period of 15 min, whilst the sample was stirred mechanically.

The results of temperature change versus time were recorded and plotted on a series of graphs., The rate of temperature rise in the first 30 s and the temperature (T_u) at which the reaction is 80% complete, was determined for each sample set. T_u was calculated according to the following formula [15].

$$T_u = (0.8 \times T_{max}) + (0.2 \times T_0) \quad (3)$$

Where T_{max} =maximum temperature achieved during slaking, and T_0 is the start temperature.

Sieve analysis of the quicklime residue remaining after the water reactivity experiment was carried out for the Parkmore and Ham Hill limestone sample sets. Once the water reactivity experiment was complete, the residue left in the Dewar vessel was flushed into a set of sieves between 3.35 mm and 500 µm. Each grade of residue was weighed and the weights recorded. These were then plotted on graphs to see how the amount of residue related to the calcination time. This analysis is intended to provide information about the relative consumption of quicklime during slaking and the ‘formation’ of lime-inclusions. Very roughly the more residue after the slaking experiment that is present the more inclusion rich a mortar hot-mixed from that quicklime may be in practice.

4 Results and Discussion

4.1 Weight Loss

Figure 4 displays the percentage weight loss for each limestone for each residence time within the furnace. The Dornie, Trearne and Ham Hill limestones achieved apparently complete calcination, considering their previously recorded LOIs of 42%, 33% and 32% respectively. The weight loss for Ham Hill stone presented here (37–40%) is greater than previously available figures for LOI, suggesting a natural variability in carbonate content depending on the specifics of supply from the quarry. The Parkmore stone shows a slower progress of weight loss culminating at 30–35%. This compares with the previously determined LOI of 42%. It is evident that some property of the stone is preventing calcination similar to the petrographically homologous Dornie stone. One possibility is the presence of coarsely crystalline calcite veins in some, but not all, of the fragments of Parkmore limestone reducing the rate of calcination. In addition, the sample tested may be impure which in turn affects the degree of weight lost [17]; 35% weight loss may be the maximum for this sample of the stone. The percentage weight loss across the sample sets is quite consistent for the times of calcination, and suggests that 2 h of calcination at 900°C for fragments of this size is sufficient for complete calcination, except for the Parkmore stone. The variation in weight loss seen across the graph for Dornie, Ham Hill and Trearne

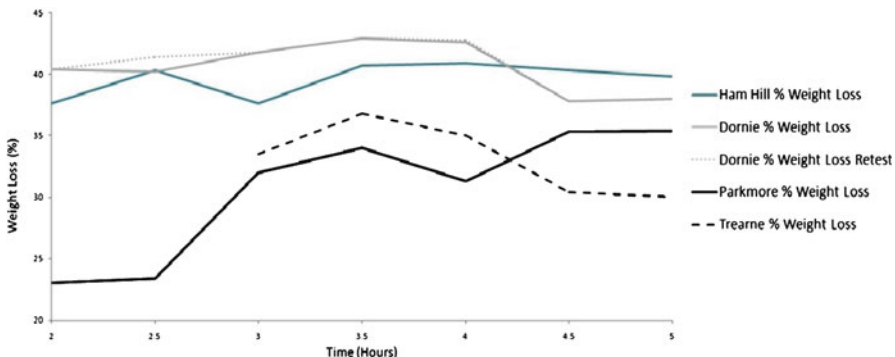


Fig. 4 A comparison of the percentage weight loss for each stone, against residence time at 900°C

perhaps represents the normal variability, and shows the limits of reproducibility for these samples.

Alternatively, it could be suggested that between residence times of 2–3.5 h the samples show a small rise in the percentage of weight lost, hinting that before this point the samples may be under burnt (i.e. not fully burnt), and that at 3.5–4 h, the samples may show their maximum percentage weight loss. Beyond this time, the percentage begins to drop in the Trearne and Dornie limestones. However, as each inflection point in Fig. 4 represents a single burn, it is not possible to argue for patterns of weight development that are significant compared to the variation seen here. For most of the limestones, except for Parkmore, 2–3 h of furnace time achieves full calcination.

Increased residence time does appear to correlate roughly with an increased amount of non-slaked residue that remains in the Dewar vessel after the reactivity test was completed (see below and Fig. 8). This may indicate a progressive indicates over-burning as over burning is accompanied by the densification of the quicklime [18]. The densification can be encouraged by the presence of impurities such as silicon oxide, aluminium oxide and ferric oxide [18], all of which are present within the Parkmore, Trearne and Dornie samples.

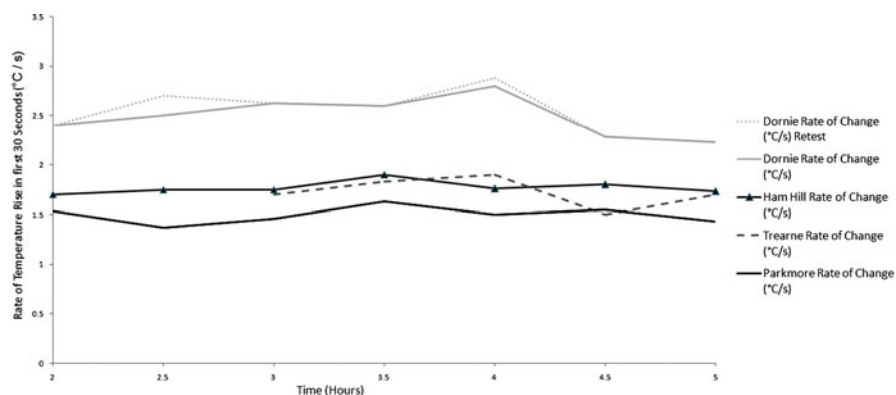
4.2 Reactivity

The rate of temperature rise in the first 30 s of the slaking reaction is generally similar amongst three of the quicklimes produced (Table 2 and Fig. 5). Each of the results in Fig. 5 presents a low variability and an insensitivity to calcination time, in particular for the quicklime derived from the Ham Hill, Trearne and Parkmore limestones. This is consistent with the argument suggesting that the stones had achieved full or nearly full calcination by 2 h of residence time.

Table 2 A comparison of the optimum slaking characteristics for each stone type

Stone type	Parkmore	Dornie	Ham Hill	Trearne
Residence time which produced the most reactive quicklime (hours)	4.5	4	3.5	4
Maximum rate of change in first 30 s ($^{\circ}\text{C}/\text{s}$)	1.63	2.8	1.9	1.9
Tu ($^{\circ}\text{C}$)	52.3	72.8	64.7	57
Maximum weight loss at optimum residence time (%)	35.4	42.9	40.9	36.8
Maximum temperature reached ($^{\circ}\text{C}$)	58.5	84	74	65
Time for reaction to complete (s)	750	30	300	360

The optimum is taken to mean the maximum reaction parameters; slaking temperature maximum rate of temperature rise

**Fig. 5** A comparison of the rate of temperature rise during the slaking test in the first 30 s versus calcination time for each limestone

From the individual time/temperature curves for each stone type in Fig. 6, it is relatively easy to pick out the residence time that produces the most reactive quicklime, and how residence time, even if beyond the point of full calcination is related to this reactivity related temperature evolution.

Dornie quicklime, displays a higher rate of temperature rise than the others (Fig. 5). As seen in Fig. 6b, the Dornie quicklime also exhibits the highest maximum temperature reached and Tu. The “optimum” residence time for Dornie is 4 h; as is indicated by the attainment of the highest maximum temperature during this period as well as the fastest rate of temperature increase (Figs. 5 and 6). For calcination longer than 4 h Dornie shows a slight reduction in the rate of initial reaction, perhaps due to reduction of available surface area, indicating the beginnings of overburning.

The Ham Hill limestone is the second most reactive limestone, and differs from the other limestones by having a lower optimum residence time of 3½ h. Ham Hill quicklime is relatively reactive perhaps due to its high porosity resulting from an

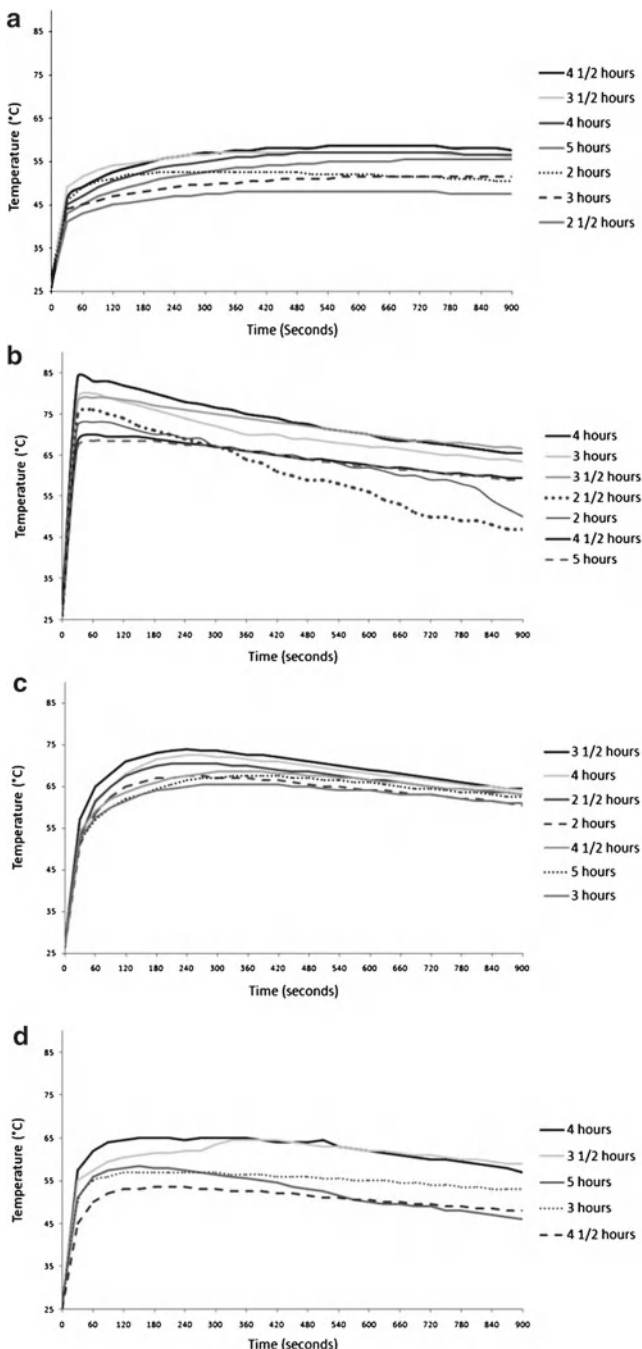


Fig. 6 Temperature versus time plots for slaking reactivity test for each quicklime, for each calcination time. **(a)** Parkmore **(b)** Dornie **(c)** Ham Hill **(d)** Trearne

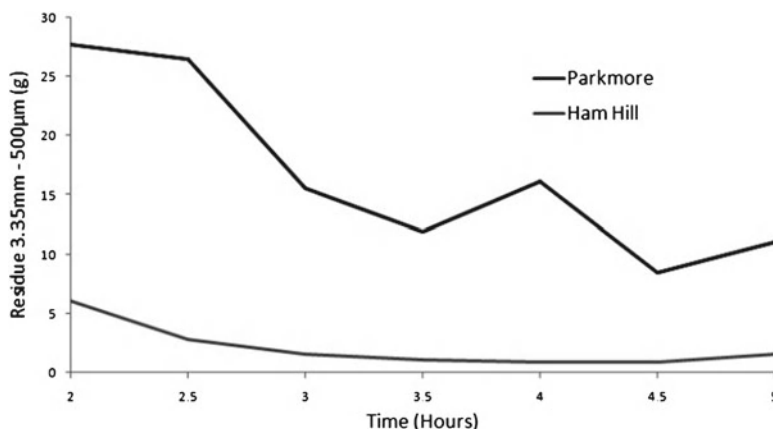


Fig. 7 The results of a residue analysis for the Parkmore and Ham Hill limestones. The residue is expressed as a weight (g) of material retained on a 500 μm sieve after the slaking test was complete at 15 min. The starting weight of quicklime was 150 g

abundance of bioclasts in the stone. The lower rate of reaction and maximum temperature would result from the impurities within this limestone that the previously determined composition and low LOI figure would suggest.

The Trearne limestone, the third most reactive, has a relatively high clay content that could impede the porosity as the fibrous clay particles tend to seal and existing pore spaces within the limestone [19]. This denser limestone is harder to calcine and is therefore less reactive, in addition to producing a quicklime with a lower available lime content.

The Parkmore limestone is the least reactive limestone tested. The low total weight loss even at prolonged calcination times suggests that these samples are not as high in available CaCO_3 as expected, or that calcination resulting in quicklime available to react is impeded by some textural or compositional feature of the limestone. The optimum residence time for the Parkmore limestone was 4½ h, the highest of all the limestones. This is consistent with a ‘slow’ calcination of this stone, as the reactivity and weight loss were still approaching the maximum possible at the longest residence time.

Figure 7 shows the amount of residue following slaking of the Ham Hill and Parkmore quicklimes. The result for Ham Hill suggests that the stone was very well calcined at all temperatures, but less fully reactive when calcined for the minimum time in this experiment. The quicklime produced by the 2 and 2.5 h residence times results in more unreacted (not consumed by hydration in the test) material that survives as residue. The Parkmore result approximately inversely reflects the weight loss with time of calcination and the increase in reactivity with calcination time. Clearly with longer residence time in the furnace the Parkmore stone produces more quicklime available to react. Parkmore if used to produce a traditionally burnt lime would perhaps produce a high content of lime inclusions in any mortar, of course depending on the temperature and time conditions of production.

5 Conclusion

The slaking reactivity test according to EN459 is a suitable method for understanding how calcination residence times affect the reactivity of quicklime. For the limestones tested here the most reactive quicklime is produced from residence times of between 3 and 4 h at 900°C (this agrees with a study by Afridi [20] though for higher (1,100°C) burning temperatures). Three of the limestones tested achieve predicted or greater degrees of calcination by 2 h of furnace residence, meaning that the main conclusions reached here concern the burning time that produces the most reactive quicklime. The slaking-temperature plots (Fig. 6) are the most discriminating for determining the ‘optimum’ calcination time for these quicklimes. The solid lime-residue from the slaking experiments on two of the quicklimes indicates the possibility for lime inclusion production, which varies considerably between the two quicklimes tested. However, it appears that, unsurprisingly, the most reactive quicklime as suggested by the slaking test produce the lowest residue, suggesting that not only is the quicklime more reactive but this correlates with the highest amount of limestone conversion to quicklime (as given by weight loss during calcination). Considering that this simple experiment was conducted at the lowest practical temperature for lime burning, it remains unresolved as to how the optimum time of calcination is related to, or may change with, increasing temperature, and how a mixed temperature regime within a traditional kiln, combined with slaking to make a real mortar relates to the formation of lime inclusions in a mortar.

Acknowledgements Mike Lawrence (Univ. of Bath) is thanked for sending samples of Ham Hill stone. Jan Válek and anonymous reviewers are thanked for their positive comments.

References

1. Hogewoning, S.: The relation between limestone properties and quicklime reactivity. In: 11th ILA Congress 16th–19th May, Prague (2006)
2. Boynton, R.S.: Chemistry and Technology of Lime and Limestone, 2nd edn, p. 578. Wiley Interscience/Wiley, New York/Chichester/Brisbane/Toronto (1980)
3. Oates, J.A.H.: Lime and Limestone: Chemistry and Technology, Production and Uses, p. 455. Wiley, Weinheim/New York/Chichester/Brisbane/Singapore/Toronto (1998)
4. Turkdogan, E.T.: Physical Chemistry of High Temperature Technology. Academic, New York/London/Toronto/Sydney/San Francisco (1980)
5. Moropoulou, A., Bakolas, A., Aggelakopoulou, E.: The effects of limestone characteristics and calcination temperature on the reactivity of the quicklime. *Cem. Concr. Res.* **31**, 633–639 (2001)
6. Prave, A.R., et al.: A composite C-isotope profile for the Neoproterozoic Dalradian Supergroup in Scotland and Ireland. *J. Geol. Soc.* **166**(5), 845–857 (2009)
7. Robertson, T., Simpson, J.B., Anderson, J.G.C.: The Limestones of Scotland, vol. XXXV, p. 221. HMSO – Her Majesty’s Stationery Office, Edinburgh (1976)
8. Holmes, S.: Evaluation of Limestone and Building Limes in Scotland. Historic Scotland Research Report, p. 140. Research and Education Division, Historic Scotland, Edinburgh (2003)

9. Grout, A., Smith, C.G.: Limestone and dolomite resources. Scottish Highlands and Southern Uplands Mineral Portfolio: Technical Report WF/89/5. In: British Geological Survey Mineral Resources Series. BGS, Edinburgh (1989)
10. Muir, A., Hardie, H.G.M.: The limestones of Scotland. Chemical Analyses and Petrography. Special Reports on the Mineral Resources of Great Britain The Limestones of Scotland, vol. XXXVII, p. 156. Her Majesty's Stationery Office Department of Scientific and Industrial Research Geological Survey of Great Britain, Edinburgh (1956)
11. Trewin, N.H.: The Geology of Scotland, 4th edn. The Geological Society of London, Bath (2002)
12. Pickard, N.A.H.: Depositional controls on lower carboniferous microbial buildups, Eastern Midland Valley of Scotland. *Sedimentology* **39**(6), 1081–1100 (2006)
13. Geological-Society: British Regional Geology Survey for Bristol and Gloucester Area, 2nd edn. The Geological Society, London (1975)
14. Lawrence, R.M.H.: A Study of Carbonation in Non-Hydraulic Lime Mortars. University of Bath, Bath (2006)
15. British Standards Institute: BS EN 459-2: 2001 Building Lime: Test Methods, British Standards Institute (2001)
16. ASTM: ASTM C110-10 Standard Test Methods for Physical Testing of Quicklime, Hydrated Lime, and Limestone (2010)
17. Beruto, D.T., et al.: A consecutive decomposition-sintering dilatometer method to study the effect of limestone impurities on lime microstructure and its water reactivity. *J. Eur. Ceram. Soc.* **30**, 1277–1286 (2010)
18. Cunningham, W.A.: Fundamentals of lime burning. *Ind. Eng. Chem.* **43**(3), 635–638 (1951)
19. Gallala, W., et al.: Factors influencing the reactivity of quicklime. *Constr. Mater.* **161**, 25–30 (2008)
20. Afredi, S.K., et al.: Experimental study of calcination-carbonation process for the production of precipitated calcium carbonate. *J. Chem. Soc. Pak.* **30**(4), 559–562 (2008)

The Hydration of Modern Roman Cements Used for Current Architectural Conservation

Christophe Gosselin, Karen L. Scrivener, Steven B. Feldman,
and Wolfgang Schwarz

Abstract Roman cement was extensively used to decorate façades during the nineteenth and at the beginning of the twentieth century. Interest in this material has revived recently for the conservation of architectural Cultural Heritage, using new production sources. This article gives preliminary results on the characterisation of the raw materials and the main reactive phases (using XRD, SEM, selective dissolution and isothermal calorimetry) of a Roman cement recently produced from the Lilienfeld marlstone (Austria), compared with a commercial Roman cement (Vicat, France). The mineralogical composition of the two cements differs strongly due to the presence of sulphate minerals in the marlstone and on the temperature of calcination. Isothermal calorimetry and *in-situ* XRD carried out on cement pastes allow the identification of the AFm and AFt type phases as early age hydration products responsible for the flash setting typical to Roman cements. The alumina rich composition and the polymorphs of dicalcium silicates is strongly different in the Lilienfeld cement. This influences their reactivity at the later ages.

1 Introduction

Patented in England by James Parker in 1796, Roman cement was extensively used in civil engineering structures [1–3] before the invention and development of Portland cement. From the first half of the nineteenth century, Roman cement was

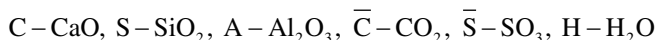
C. Gosselin (✉) • K.L. Scrivener • S.B. Feldman
Laboratory of Construction Materials, Swiss Federal
Technological Institute (EPFL), Lausanne, Switzerland
e-mail: christophe.gosselin@epfl.ch

W. Schwarz
Composite Anode Systems, Vienna, Austria
e-mail: schwarz@cas-composite.com

also used as binder for stone repair mortars and façade decoration of historical buildings all over Europe [4–6]. In the last decade, the properties and durability of historical Roman cement mortars and their compatibility with stone substrates have been demonstrated by many studies [4, 7–9]. The main advantages of Roman cements for stone restoration can be summarised as follows:

- Relative low energy consumption for production, compared to other cements, resulting from low calcination temperatures (800–1,100°C),
- Durability, even in highly polluted environments (urban exposure and aggressive solutions),
- Compatibility with historical building materials (aesthetical, chemical and moisture transfers properties),
- The versatility of mortar formulations and applications techniques.

Roman cement is produced from raw marlstone rather than from a mixture of different source materials, as for traditional cements (ordinary Portland cements, calcium aluminate cements, calcium sulfo-aluminate cements, belites cements etc.). Furthermore, no gypsum is added during the grinding process to regulate the workability of fresh Roman cement mortars. The raw marlstones have a wide range of chemical composition and are calcined at temperatures where sintering and melting would not occur (800–1,100°C). The “clinker” is then finely ground and usually no additional product was added. However, it was difficult to control the composition of Roman cements due to the various compositions of marlstone using a heterogeneous process in shaft kilns [8]. The French company Vicat was a major producer of Roman cement during the last two centuries and the Prompt cement provides technical solutions for masonry repair [10, 11]. The use of Roman cement has been recently revisited by the Rocem project [5] which investigated historic Roman cement mortars to provide compatibility criteria for repair mortars [4], to select appropriate raw materials and optimize the calcination process in laboratory and pilot scale kilns [12–14]. Following on from the Rocem project, the new Rocare project aims at making Roman cement as a compatible and sustainable product, as an alternative solution to available products (lime, hydraulic lime and commercial Roman cements), adapted to local restoration market needs in Europe. This necessitates the fundamental understanding of the mineralogical development during the calcination process and the subsequent hydration reactions once mixed with water, aggregates and chemical admixtures. This article presents new results on the characterisation of two different Roman cements. Throughout, the conventional cement chemistry notation is utilised:



2 Materials and Methods

Two Roman cements were studied. The first cement is the commercial Vicat prompt, obtained by calcination of marlstone from the Chartreuse massif in France with a wide temperature range from 600°C to 1,200°C. The second cement studied here is a

Table 1 Oxide composition of the Lilienfeld and Vicat cements

	SiO ₂	Al ₂ O ₃	CaO	Fe ₂ O ₃	MgO	SO ₃	K ₂ O	Na ₂ O	TiO ₂	LOI
Lilienfeld	30.08	8.97	44.42	3.81	2.44	0.13	1.81	0.54	0.38	7.79
Vicat	18.70	7.51	54.8	3.35	3.90	3.36	1.08	0.30	0.29	6.97

Roman cement produced as part of the Rocem project resulting from the calcination of the Lilienfeld marlstone from Austria in a pilot scale rotary kiln (at 920°C for 300 min), as reported in [15]. The oxide composition of the Lilienfeld and Vicat cements was obtained by XRF and given in Table 1.

The main challenge of this study is the characterisation of the reactive amorphous phases resulting from the calcination of marlstone at low temperatures. Combined techniques for anhydrous cement characterisation (selective dissolution, XRD, EDS mapping) allow the discrimination of intermixed and non crystalline phases responsible for the workability and long term performances specific to these cements.

The characterisation of the anhydrous cements used selective dissolution methods according to the works of Stutzman et al. [16]. The Salicylic Acid/Methanol Extraction (SAM) dissolves alite C₃S, belite C₂S, and free lime. The KOH/sugar solution dissolves the interstitial phases of aluminate and ferrite leaving a residue of silicates and minor phases. Then XRD and SEM were used to characterize the anhydrous cements. XRD powder analysis was carried out with an X'Pert Pro PANalytical diffractometer (Cu tube, $\lambda=1.54$ Å). Scanning Electron Microscopy (SEM, Philips Quanta 200) was used to study the microstructure of the anhydrous cement powders. Pelletised raw cements were impregnated with epoxy resin and polished to obtain cross sections. The microanalysis of phases was done with Energy Dispersive Spectroscopy (EDS, Bruker AXS Quantax). Quantitative elemental mapping was performed using ultra-fast spectral imaging acquisition for 15 min. The Esprit software (from Bruker) allows the acquisition of images with a simultaneous spectral accumulation in a database for each pixel. The set of acquired images were then treated to normalise the intensity of each chemical element with respect to its quantity determined by accumulated EDS spectra. Finally the atomic Ca/Si and Al/Si ratios were calculated from the intensity of quantitative images (using routines developed with Matlab) and mapped inside the most representative grains of the respective cements.

The hydration of cement paste was studied from the first minutes up to 3 months, using isothermal calorimetry and XRD.

Isothermal calorimetry is a technique used to study the kinetics (heat flow is expressed in J.h⁻¹.g⁻¹ of cement) and the total heat (J.g⁻¹ of cement) generated by exothermic reactions occurring in controlled conditions. Five to ten grams of fresh cement paste were cast in a glass vial placed in the calorimeter (TAM Air calorimeter and thermostat 3114/3236 from Thermometric). *In-situ* mixing experiments were done using a specific device equipped with paddle, allowing the measurement of heat flow from the very start of the reaction [17].

The phase assemblage in the hydrated cement pastes was measured by XRD. The hydrated cement paste was prepared by adding water to cement (mass ratio W/C of 0.65) and mixed with a paddle mixer for 1 min at 1,100 rpm. The fresh cement paste

was cast in a plastic vial, de-moulded after 24 h and cured in de-ionized water. A slice of specimen was cut for each test time. The hydration of the cement pastes was stopped by solvent exchange. The paste slices were cut and immersed in isopropyl alcohol for 6 days and then dried in desiccators. The dried slices were ground and sieved at 100 µm before XRD analysis.

3 Results

3.1 Characterisation of the Anhydrous Roman Cements

3.1.1 XRD and Selective Dissolution

Figure 1 shows the XRD patterns of the Lilienfeld and Vicat cements before and after selective dissolution. The main crystalline phases present in the Lilienfeld cement originate from the incompletely calcined marlstone, e.g. quartz and calcite in relatively high amounts and albite and muscovite as secondary phases from the clay fraction. Other crystalline phases result from the calcination of the minerals in the temperature range 800–900°C. Among these phases, the diffraction peaks in the 31–34°20 range have a relatively low intensity and show that the calcium silicates β or α' - C_2S are not well crystalline and discriminated, compared to the β - C_2S present in Vicat cement (Fig. 1). Secondary phases are identified as Portlandite, CH, presumably from pre-hydration of free lime. After extraction of the silicates phases by the SAM method, the XRD pattern reveals small amounts of gehlenite (C_2AS) and a calcium silicate carbonate, tilleyite ($C_3S_2 \cdot 2\bar{C}\bar{C}$), occurring as a natural mineral whose formation has not been reported during the manufacture of cements [18], in contrast to spurrite ($(C_2S)_2 \cdot \bar{C}\bar{C}$, a carbonated form of C_2S [19] identified as traces in the Lilienfeld cement but in greater amounts in Vicat cement. One interesting result is in the strong similarity of the XRD patterns before and after the KOH/sucrose dissolution. The overlap of these two patterns indicates that the Lilienfeld cement contains no significant crystalline aluminate reactants. These results were already reported in [20].

The mineralogy of Vicat cement differs strongly from that of the Lilienfeld one and is composed of a wider range of silicate and aluminate reactants. Due to higher temperature of calcination (up to 1,200°C), the crystallisation of β or α' - C_2S is enhanced, as illustrated by the diffraction peaks in the 31–34°20 range and much less quartz remains compared to the Lilienfeld cement. The selective dissolution methods seem more suitable to the Vicat cement to discriminate the different phases. The main aluminates phases, identified after SAM dissolution, are $C_{12}A_7$, C_3A , C_4AF and $C_4A_3\bar{S}$ and the main silicates phases β or α' - C_2S and spurrite ($(C_2S)_2 \cdot \bar{C}\bar{C}$) are better identified after KOH/sucrose dissolution.

Traces of calcium sulphate $C\bar{S}$ were also identified in the XRD pattern of the raw Vicat cement. Compared to the Lilienfeld cement, the Vicat cement contains higher amounts of sulphur (Table 1) crystallised under the form of anhydrite $C\bar{S}$ and

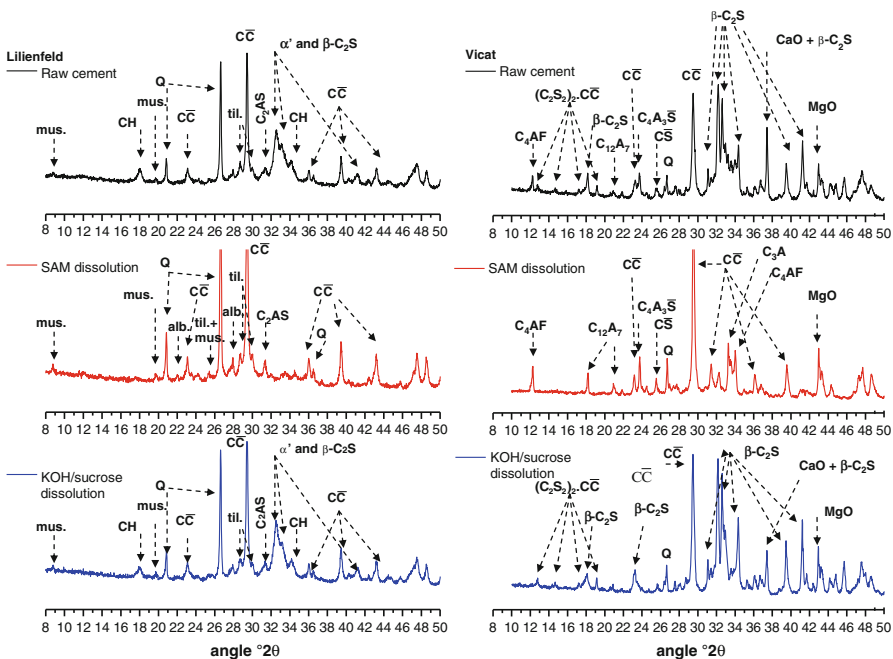


Fig. 1 XRD patterns after SAM and KOH/sucrose selective dissolutions of the Lilienfeld and the Vicat cements (CC calcite, Q quartz, mus muscovite, alb albite, til tilleyite)

ye'elmitte $\text{C}_4\text{A}_3\bar{\text{S}}$ which both contribute to significant changes in the hydration products (Fig. 8). The presence of calcium sulphate $\text{C}\bar{\text{S}}$ can be explained by the release of sulphur from the weathered sedimentary pyrites included in the limestone grains, as illustrated in Fig. 5. Another source of sulphur is seldom observed in the cement grains is calcium monosulphide CaS . This phase could plausibly originate from the reaction between free lime or calcite and gaseous sulphide (from the fuel or anhydrite) under local reducing conditions of calcination (deficient of oxygen in the kiln gas).

3.1.2 SEM and EDS-Mapping Analyses of the Lilienfeld Cement

Polished cross-sections of pelletised Lilienfeld cement powder were prepared prior to SEM examinations, images from which are shown in Fig. 2. The morphology and composition of the nodules appear to be uneven in the sample, but some general features can be identified. As already suggested by XRD, many quartz and calcite grains remain in the nodules, surrounded by a reactive phase appearing brighter grey in BSE mode. This phase presumably results from the diffusion of calcium and silicate ions during the calcination process. However, the EDS mapping (Fig. 3)

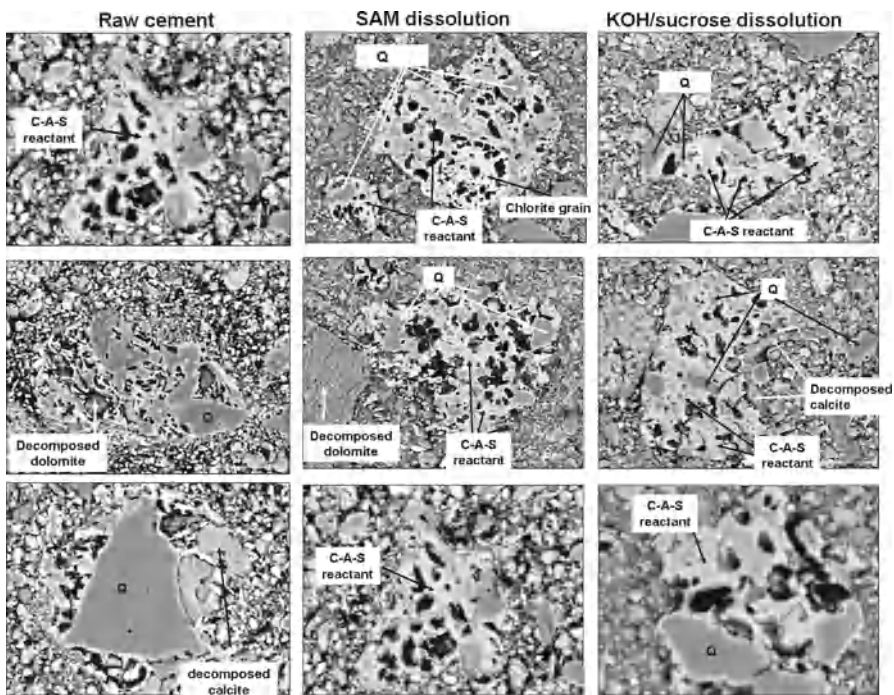


Fig. 2 Microstructure of the Lilienfeld cement grains (*left*: raw cement, *middle*: after SAM dissolution, *right*: after KOH/sucrose dissolution)

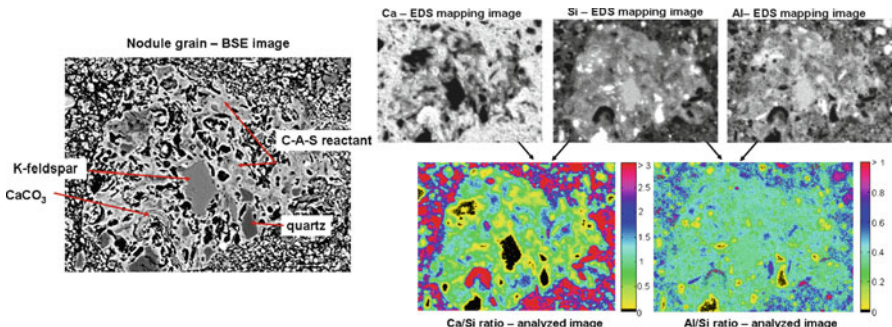


Fig. 3 EDS mapping of the raw Lilienfeld cement

suggests that alumina is systematically present in significant amounts in this phase, which is consequently referred to as C-A-S reactant in this paper. Figure 3 shows the EDS mapping on a nodule containing quartz, calcite and K-feldspar (KAIS_3O_8 as end member) grains surrounded by the C-A-S reactant. The elemental analysis of the cement grain composition gives a Ca/Si ratio unevenly distributed in the grain

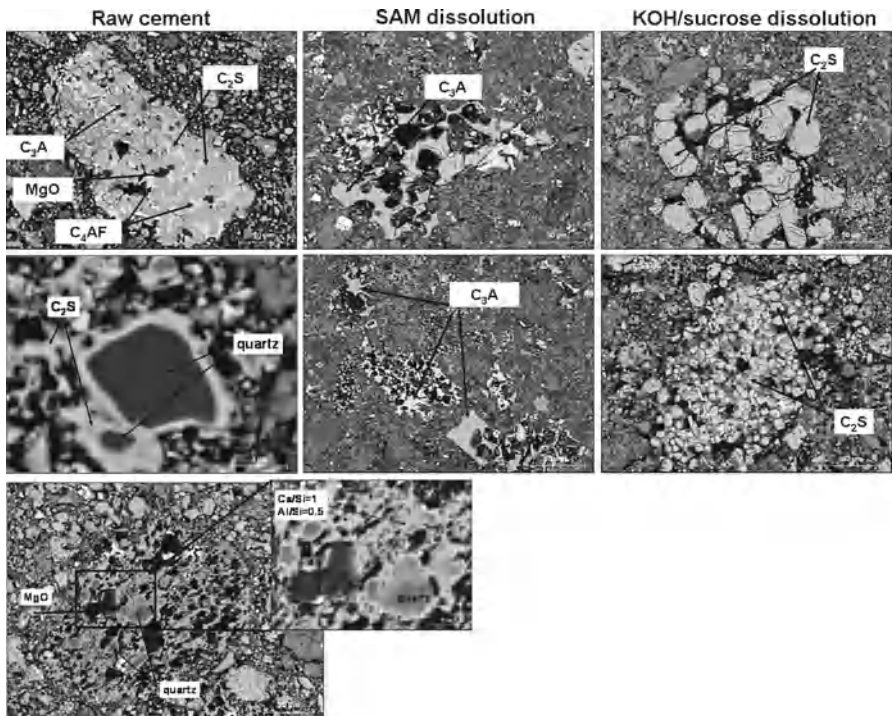


Fig. 4 Microstructure of the Vicat cement grains (*left*: raw cement, *middle*: after SAM dissolution, *right*: after KOH/sucrose dissolution)

and close to 1. The K-feldspar and quartz grains appear in black according to the Ca/Si scale, due to the absence of Ca and the predominance of Si respectively. The calcite grain appears in red due to the high Ca/Si ratio. The composition of the C-A-S phase, appearing in brighter grey in the BSE image, is given by a Ca/Si between 0.5 and 1 and a Al/Si ratio ranging 0.2–0.4. The non stoichiometric composition of this phase can explain the difficulty to relate the diffraction peaks in the 31–34°20 range to actual β or α' - C_2S .

From Fig. 2, it is noteworthy that the morphology of cement grains does not change after selective dissolution methods. First, the intragranular porosity, already observed in the raw cement, does not increase significantly after dissolution. Furthermore, SAM and KOH/sucrose dissolution do not affect the C-A-S phase surrounding quartz and calcite.

3.1.3 SEM and EDS-Mapping Analyses of the Vicat Cement

In contrast with the Lilienfeld cement, the Vicat cement is manufactured at a higher temperature and consequently it is better crystallised. The phases that can be discriminated phases are observed in Fig. 4. A typical grain is composed of C_2S

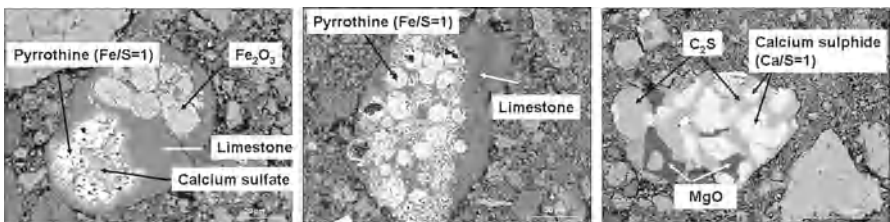


Fig. 5 Specific sulphate phases in the raw Vicat cement grains

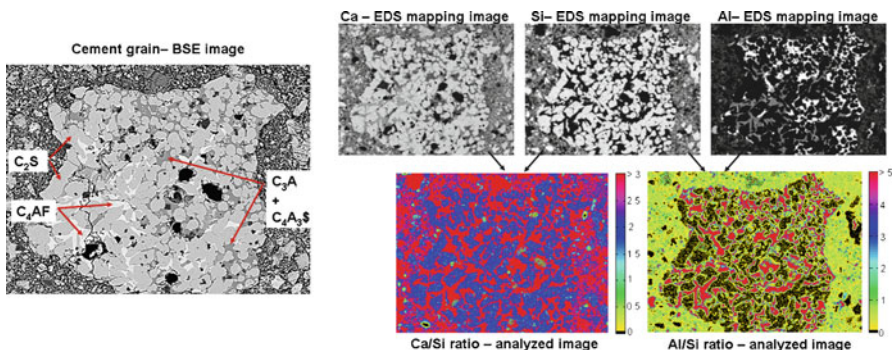


Fig. 6 EDS mapping of the raw Vicat cement grains

grains surrounded by a solid solution of C_3A , $C_4A_3\bar{S}$ and C_4AF . Some clusters of periclase MgO , resulting from the decomposition of dolomitic materials, usually appear as dark areas in BSE images. Figure 5 shows specific phases containing sulphur (anhydrite, pyrrhotine and calcium sulphide).

As already mentioned in the XRD results, little quartz remains in the cement and some porous nodules resulting from incomplete calcination are seldom seen. The morphology and composition of these porous nodules (bottom left image in Fig. 4) are comparable to those present in the Lilienfeld cement (Fig. 2). The XRD results on samples after selective dissolution are confirmed by BSE images (Fig. 4) in which the rounded C_2S grains are removed by SAM solution and C_3A and C_4AF are dissolved after KOH/sucrose dissolution.

The EDS images for the Vicat cement (Fig. 6) show the suitability of the technique to map the silicate and the aluminite phases inside the most representative grains. Contrary to the Lilienfeld cement (Fig. 3), the C_2S grains (blue in Fig. 6) have a stoichiometric Ca/Si ratio of 2 and are well differentiated from the aluminite phases (C_3A , $C_4A_3\bar{S}$ and C_4AF) illustrated in red according to the arbitrary scale bars related to both Ca/Si and Al/Si ratios.

3.2 Hydration of Roman Cements

3.2.1 20°C Isothermal Calorimetry

Figure 7 shows the heat generation during the hydration of the Vicat and the Lilienfeld cements at very early age (with *in-situ* and *ex-situ* mixing). The rapid hydration of both cements is characterised by a single heat flow peak with comparable acceleration rate and intensity. For both systems, the initial heat flow peak corresponds to the dissolution of reactive phases and both the precipitation of hydration products.

The identification of crystalline hydration products was studied by *in-situ* XRD analysis for the first 15 h. From the beginning of hydration, there are very different phase assemblages in the two cements. While ettringite $C_6A\bar{S}_3H_{32}$ and hemicarboaluminate $C_4AC_{0.5}H_{12}$ both precipitate from the first minutes of hydration in the Vicat cement, the first phase identified in the Lilienfeld cement is $C_4AC_{0.5}H_{12}$. This phase dissolves after 5 h hydration, and reacts with carbonate ions from the pore solution to precipitate monocarboaluminate $C_4A\bar{C}H_{11}$, which predominates after 24 h (Fig. 8).

Regardless of the nature of hydration products, the reaction levels off after 8–10 min of hydration for the two systems. This age also corresponds to the end of the workable time of the cement pastes. At later ages, the right graph (low Y-axis scale) shows significant discrepancies in the calorimetric response between the systems.

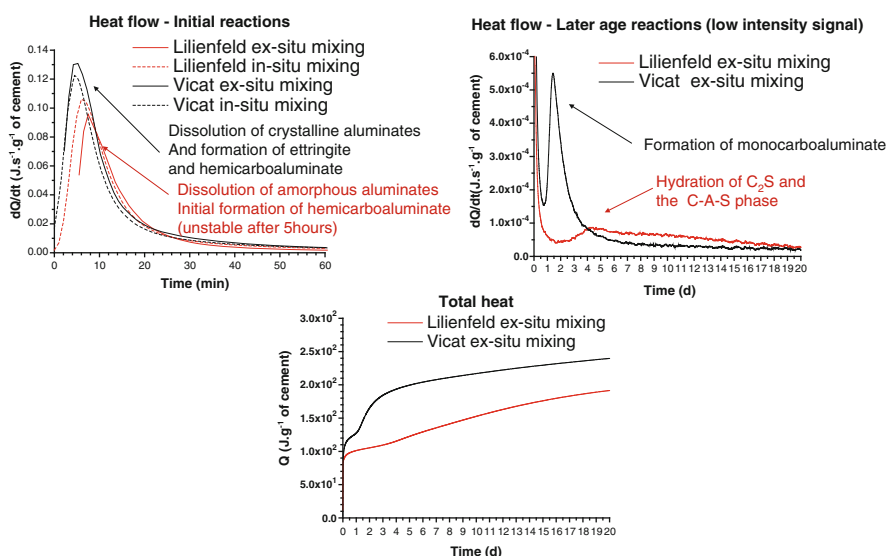


Fig. 7 Heat flow and total heat during early age and long term hydration of the Lilienfeld and the Vicat cements

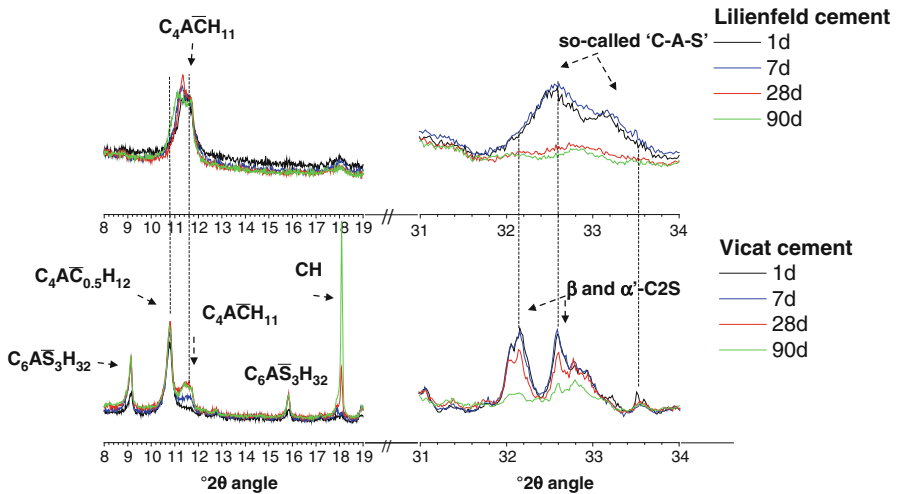


Fig. 8 XRD patterns of hydrated Lilienfeld and Vicat cement pastes

In the Vicat cement, a very sharp peak is observed from 18 h with a maximum after 36 h. According to XRD (Fig. 8), this peak would correspond to the precipitation of monocarboaluminate $C_4A\bar{C}H_{11}$. In the Lilienfeld cement, a much smaller and broader peak is seen from 2 to 3 days of hydration which extends over several days, and would match with the hydration of C-A-S phase as suggested by XRD (Fig. 8). The total heat curves show that the rapid formation of $C_4A\bar{C}H_{11}$ contributes to the higher heat generated by the Vicat cement. However the hydration rate of the C-A-S phase is greater in the Lilienfeld cement in comparison to the slow hydration of well crystallised C_2S in the Vicat cement.

3.2.2 XRD Analysis of Hydrated Cement Pastes

Figure 8 shows the XRD patterns of cement paste cured up to 90 days under water. In the Lilienfeld cement, $C_4A\bar{C}H_{11}$ predominates after 24 h but with a relatively broad diffraction peak which could indicate a solid solution with initial hemicarboaluminate $C_4A\bar{C}_{0.5}H_{12}$, as already suggested by [20]. After 90 days, the hydration of the C_2S and the C-A-S phase seems well advanced, but no crystalline hydration products were identified. In the Vicat cement, the ettringite originally formed and hemicarboaluminate $C_4A\bar{C}_{0.5}H_{12}$ remain stable for 90 days. The precipitation of monocarboaluminate $C_4A\bar{C}H_{11}$ is initiated after 24 h and levels off after 28 days of curing under water. Compared to the C-A-S reactant in the Lilienfeld cement, very little C_2S reacts before 28 days. The hydration of C_2S is well advanced after 90 days and leads to the precipitation of calcium hydroxide CH co-precipitating with amorphous calcium silicate hydrates C-S-H.

4 Conclusions

This paper compares the mineralogy and hydration of two types of Roman cements used for historical masonry. Due to the differences in the raw materials and the calcination process, the Lilienfeld and Vicat cements have different mineralogy and hydration mechanisms. These two cements rapidly hydrate and require retardation admixture for practical applications. The higher calcination temperature in the Vicat cement leads to the formation of crystallized belites, partly carbonated to form spurrite at high CO₂ partial pressure in the shaft kiln, which are relatively low reactivity phases. The presence of sulphates (pyrites) in the raw marlstone leads to formation of calcium sulphate and ye'elimit which rapidly hydrate to ettringite. After a few minutes, the sulphate concentration rapidly becomes undersaturated with respect to ettringite precipitation and the calcium aluminates hydrate to hemicarboaluminate. This phase is unstable in presence of calcite, and monocarboaluminate slowly precipitates during curing under water.

During the calcination of the Lilienfeld marlstone, incomplete crystallisation of calcium silicates occurs within nodules containing significant amounts of calcite and quartz. Clay materials provide aluminate ions leading to the formation of a non stoichiometric C-A-S phase. The XRD and SEM results after selective dissolution indicate that silicate and aluminate are intimately linked in this poorly crystalline C-A-S phase, with a composition $0.5 < \text{Ca/Si} < 1$ and $0.2 < \text{Al/Si} < 0.4$ given by EDS elemental mapping. The diffusion of ions seems to be incomplete under these conditions of calcination to form pure crystallised C₂S. The XRD pattern of this C-A-S phase would suggest a disordered structure for which the reactivity is enhanced compared to the crystallised β and α' -C₂S. However crystalline hydrates as calcium hydroxide, which is the usual product of C₂S hydration, were not detected after 90 days of curing.

Acknowledgements This study was initiated in the frame of the Rocare project (EU 226898) and financially supported by the European Commission (FP7-ENV-2008-1 program).

References

1. Royer, A.: Le "ciment romain" en France: un matériau du XIXe siècle méconnu. *Monumental Semester* **2**, 90–95 (2006)
2. Hughes, D.C., Swann, S., Gardner, A.: Roman cement: part one: its origins and properties. *J. Archit. Conserv.* **13**(1), 21–36 (2007)
3. Bleazard, R.G.: History of calcareous cement, Chapter 1. In: Hewlett, P.C. (ed.) *Lea's Chemistry of Cement and Concrete*, 4th edn. Edward Arnold, London (1998)
4. Weber, J., Gadermayr, N., Bayer, K., et al.: Roman cement mortars in Europe's architectural heritage of the 19th century. *ASTM Spec. Tech. Publ.* **1494**, 69–83 (2008)
5. Weber, J., Gadermayr, N., Kozlowski, R., et al.: Microstructure and mineral composition of Roman cements produced at defined calcination conditions. *Mater. Charact.* **58**(11–12), 1217–1228 (2007)

6. Hughes, D.C., Swann, S., Gardner, A.: Roman cement – Part Two: stucco and decorative elements, a conservation strategy. *J. Archit. Conserv.* **13**(3), 41–58 (2007)
7. Adamski, G., Bratasz, L., Kozlowski, R., et al.: Roman cement – key historic material to cover the exteriors of buildings. In: Groot, C. (ed.) *Workshop Repair Mortars for Historic Masonry*, pp. 2–11. RILEM, Delft (2006)
8. Gosselin, C., Verges-Belmin, V., Royer, A., et al.: Natural cement and monumental restoration. *Mater. Struct./Materiaux et Constructions* **42**(6), 749–763 (2009)
9. Cailleux, E., Marie-Victoire, E., Sommain, D.: Study of natural cements from the French Rhône-Alpes region. In: *Proceedings of the International Conference on Heritage, Weathering and Conservation, HWC 2006*, pp. 77–84 (2006)
10. Sommain, D.: La durabilité des bétons de ciment prompt naturel, Chapitre 15. In: ENPC (ed.) *La durabilité des bétons*, 2nd edn Presses de l'école nationale des Ponts et Chaussées (ENPC) (2008)
11. Avenier, C., Rosier, B., Sommain, D.: Ciment naturel. Glénat, Grenoble (2007)
12. Hughes, D.C., Jaglin, D., Kozlowski, R., et al.: Calcination of marls to produce Roman cement. *J. ASTM Int.* **4**(1) (2007)
13. Hughes, D.C., Jaglin, D., Kozlowski, R., et al.: Roman cements – belite cements calcined at low temperature. *Cem. Concr. Res.* **39**(2), 77–89 (2009)
14. Hughes, D.C., Sugden, D.B., Jaglin, D., et al.: Calcination of Roman cement: a pilot study using cement-stones from Whitby. *Construct. Build Mater.* **22**(7), 1446–1455 (2008)
15. Tislova, R., Kozlowska, A., Kozlowski, R., et al.: Porosity and specific surface area of Roman cement pastes. *Cem. Concr. Res.* **39**(10), 950–956 (2009)
16. Stutzman, P.E., Leigh, S.: Phase Composition Analysis of the NIST Reference Clinkers by Optical Microscopy and X-ray Powder Diffraction. NIST Technical Note 1441 (2002)
17. Costoya, M.M.: Effect of particle size on the hydration kinetics and microstructural development of tricalcium silicate. PhD, Ecole Polytechnique Fédérale de Lausanne (2008)
18. Taylor, H.F.W.: Cement Chemistry. Thomas Telford Publishing, London (1997)
19. Bolio-Arceo, H., Glasser, F.P.: Formation of spurrite, $\text{Ca}_3(\text{SiO}_4)_2\text{CO}_3$. *Cem. Concr. Res.* **20**(2), 301–307 (1990)
20. Vyskocilova, R., Schwarz, W., Mucha, D., et al.: Hydration processes in pastes of Roman and American natural cements. *ASTM Spec. Tech. Publ.* **1494**, 96–104 (2008)

The Effect of Relative Humidity on the Performance of Lime-Pozzolan Mortars

Ioannis Karatasios, Maria Amenta, Maria Tziotziou,
and Vassilis Kilikoglou

Abstract The development of strength in conservation mortars is of particular significance for new synthesized lime-based mixtures in terms of practical application, performance requirements and renovation cost of built monuments. In this work, the effect of relative humidity (RH%) on the strength characteristics of lime-natural pozzolan mortars was studied in three groups of specimens cured at different humidity conditions (45, 65 and 95 RH%). The development of compressive strength of the specimens was determined at preset time periods, from 7 days to 1 year. At the same time periods, the setting products and the microstructure of the mortars were monitored by thermal analysis (DTA/TG) and scanning electron microscopy (SEM/EDX). The results highlight the beneficial effect of elevated humidity on the strength of lime-pozzolan mortars and at the same time some issues related to the reliability and reproducibility of laboratory work in the field are addressed.

1 Introduction

The study of lime-pozzolan systems is of particular significance for modern conservation mortars, since the addition of either natural or artificial pozzolans in lime putty enhances the strength and durability of the produced mixtures. This is achieved through the formation of calcium silicate hydrates (CSH), calcium aluminate hydrates (CAH) and calcium aluminate silicate hydrates (CASH) [1, 2]. The study

I. Karatasios (✉) • M. Amenta • M. Tziotziou • V. Kilikoglou
Laboratory of Archaeological Materials, Institute of Materials Science,
National Centre for Scientific Research “Demokritos”, Athens, Greece
e-mail: ikarat@ims.demokritos.gr; mariaparkaran@yahoo.com; mtzio@ims.demokritos.gr;
kilikog@ims.demokritos.gr

of the above systems contributes towards the improvement of traditional building techniques, and in addition, towards the optimisation of the performance characteristics and durability of the produced mixtures. To this end, it is necessary to understand the effect of the different parameters that affect the performance characteristics of lime-pozzolan mortars, to determine the optimum conditions for laboratory tests (in order to ensure reliability and reproducibility of the results in field) and finally, to highlight any parameters that may affect the performance of such mortars in field applications. The latter poses both structural and economic impacts, since it affects the structural and decorative integrity of architectural monuments, as well as the total conservation/renovation cost.

In this paper, the effect of curing conditions of lime-pozzolan mixtures on the setting process and the mechanism of strength development at an early stage are studied in three groups of mortars each cured at a different relative humidity. The development of their mechanical properties was determined at preset time periods, along with the formation of setting products and the resultant changes in microstructure. The understanding of the influence of relative humidity on the above parameters (setting mechanism, microstructure and strength) is essential for enhancing the durability and field performance of lime-pozzolan mixtures. Finally, this work contributes to the identification of weaknesses in the comparison and interpretation of the laboratory and field performance of lime-pozzolan mixtures.

2 Experimental

2.1 Preparation and Curing of Test Specimens

The binary pastes were prepared by mixing equal parts (w/w) of 1 year matured lime putty, made of laboratory grade calcium hydroxide powder, and a commercial ultra-fine (0–35 µm) natural pozzolan of volcanic origin. By mixing equal parts of calcium hydroxide powder and water (w/w) the real density of lime putty was set to 1,400 kg/m³, while the real and apparent density of pozzolan were 2,400 and 430 kg/m³ respectively. Diffraction analysis of the pozzolanic material revealed that it consisted of an amorphous, glass-like material, accompanied by some secondary crystalline phases such as quartz, illite/muscovite, kaolinite and Na-feldspars (albite, anorthoclase).

The pastes were prepared by mixing all the constituents with de-ionised water up to a standard consistency [3] for 5 min [4]. The water to solid constituents' ratio for all pastes was set at 0.28. In addition, mortar mixtures were prepared by mixing lime, pozzolan, standardised sand (EN 196-1) and water in the ratio described in EN 196-1 [4]. Both the pastes and the mortar mixtures were initially cured for 7 days at 98–100% RH. Then, they were divided into three groups (A, B and C) and stored at 20°C±2°C, at three different RH% levels, namely 95%±3% for group A, 65%±5% for group B and, 45%±5% for group C.

2.2 Monitoring of Setting Process

The setting process of the binary mixtures was studied at preset intervals (1, 3, 7, 14, 28 days) after applying a hydration – stop procedure [5] by immersing the samples in acetone and then, in di-ethyl-ether solutions. This was followed by the drying of the specimens in a ventilated oven at 70°C for 22 h. The phases formed during setting were determined by X-ray powder diffraction (XRD) and differential thermal analysis (DTA/TG). XRD was carried out in a Siemens D500 diffractometer, with a beam step of 0.03°/5 s. Thermal analysis was performed in a Perkin-Elmer Diamond Pyris thermal analyser, in static air conditions from room temperature up to 1,000°C, using a heating rate of 10°C/min. The development of the hydration process and its effect on the microstructure of the specimens was examined in a FEI-Quanta Inspect scanning electron microscope, coupled with energy dispersive X-ray analyser (SEM/EDX). Finally, the compressive strength was measured in three cubic specimens from each group of mortar mixtures [6]. The specimens were tested in an Instron 1195 testing machine, using a displacement rate of 109 µm/s.

3 Results and Discussion

3.1 Microstructure and Setting Products

3.1.1 XRD Analysis

Soon after the mixing of the pozzolan with lime, the formation of different hydrated phases, such as calcium aluminate hydrate (11-203), calcium mono-carboaluminate hydrate (41-219) and calcium aluminate hydroxide hydrate (33-255), is initiated (Fig. 1). Other phases detected in the binder fraction include calcite (CaCO_3) and portlandite ($\text{Ca}(\text{OH})_2$) coming from carbonated and unreacted lime, respectively. The above hydrated phases were formed through the reaction of lime with pozzolan into the pore-solution, and were identified in the diffraction patterns at different curing periods. Their formation is evident after the first 24 h and their peaks are more intense in specimens cured at high humidity levels (groups A and B), while there is a delay in specimens of group C. For the same time period, the ratio of the relative intensity peaks of the hydrated phases over the intensity of the portlandite main peak, increases as the humidity levels of curing conditions becomes higher (Fig. 2).

Although calcium silicate hydrates (C-S-H) are very poorly crystallised materials of varying stoichiometry, their formation was also evidenced in the diffraction patterns by the presence of two faint peaks in the area of $32^\circ 2\theta$ and $50^\circ 2\theta$, along with a third one in the area of $29^\circ 2\theta$ (Fig. 1), which is obscured by the shoulder of calcite [7]. Similarly to the aluminate hydrates, their relative amount increases with the relative humidity levels during curing.

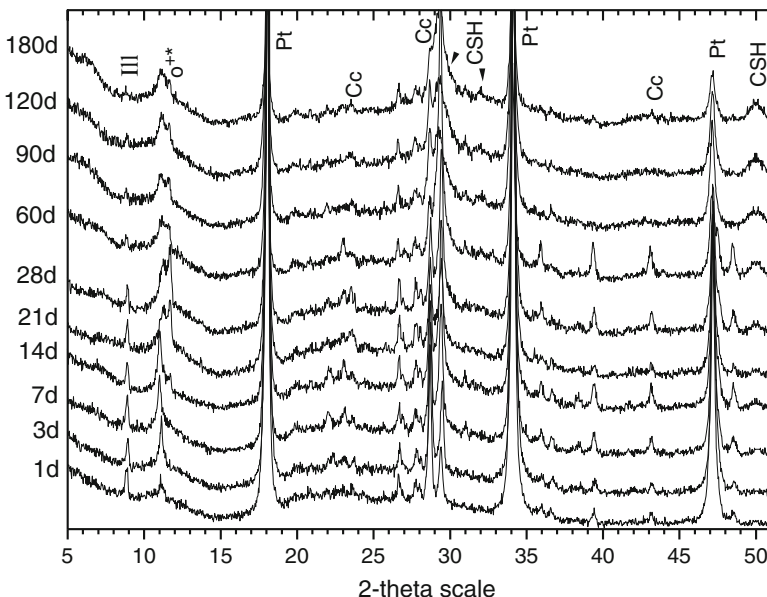


Fig. 1 Diffraction patterns of group A specimens, exhibiting the development of different phases during setting. Calcite reflections are marked by (*Cc*), portlandite by (*Pt*), illite (*III*), calcium aluminate hydrate by (*), calcium mono-carboaluminate hydrate by (+), calcium hydroxide hydrate by (**o**) and calcium silicate hydrate by (*CSH*)

3.1.2 Thermal Analysis

Aiming to further quantify the total amount of the hydrates formed during the setting, thermal analysis was carried out. The evaluation of the DTA/TG plots was based on the interpretation of the first derivative TG plots (DTG). Based on the DTG curves (Fig. 3), the formation of the hydrated phases can be monitored in the range of 100–200°C, where dehydration of poorly crystallized calcium-silicon and calcium-aluminate hydrates (C-S-H, C-A-H) takes place during heating. Peaks in the region of 100–120°C are usually taken to indicate the presence of C-S-H, while those around 140–180°C are indicative for C-A-H and mixed hydrates [8, 9]. Other areas of interest are in the range of 450–550°C and 700–800°C, where dehydration of calcium hydroxide and decarbonation of calcium carbonate are taking place respectively [8]. Thermal transformations up to 90–100°C are also indicative for the evaporation of physically absorbed water, while in the range of 200–600°C chemically bound water of hydraulic compounds (and of other hydroxides) is lost, and in the range of 550–830°C that of clay minerals participating in the pozzolan [10, 11]. The data obtained from DTA/TG measurements were normalised based on the weight loss of the pozzolanic material in the same temperature range, as obtained from comparative measurements on raw pozzolan samples. The results indicated that there is no significant difference in the amount of hydrates formed in mixtures cured

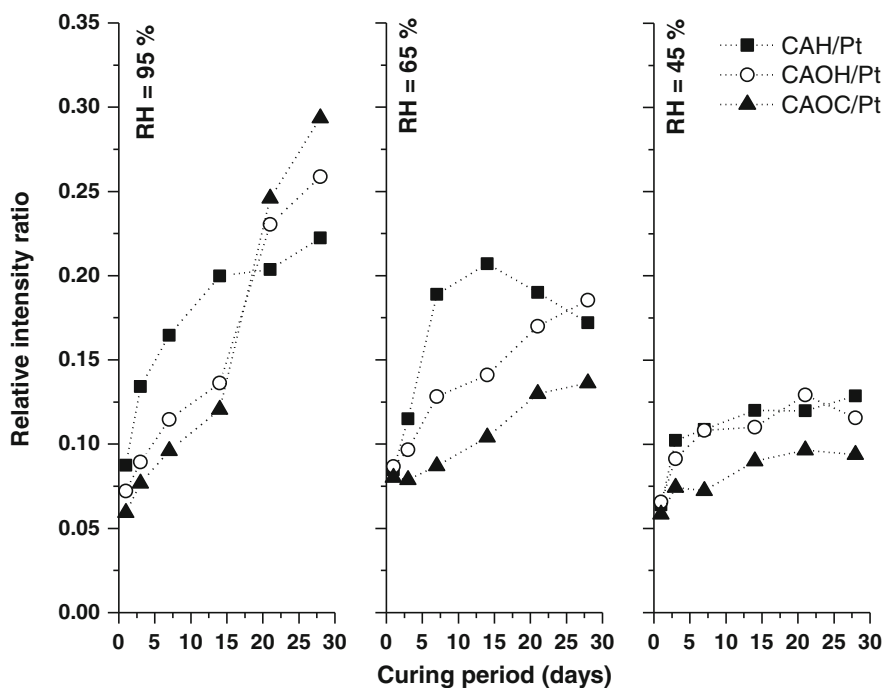


Fig. 2 Relative intensity ratios of calcium aluminate hydrate (CAH), calcium mono-carboaluminate hydrate (CAOC) and calcium aluminate hydroxide hydrate (CAOH), over portlandite (*Pt*) for mixtures cured at different humidity conditions

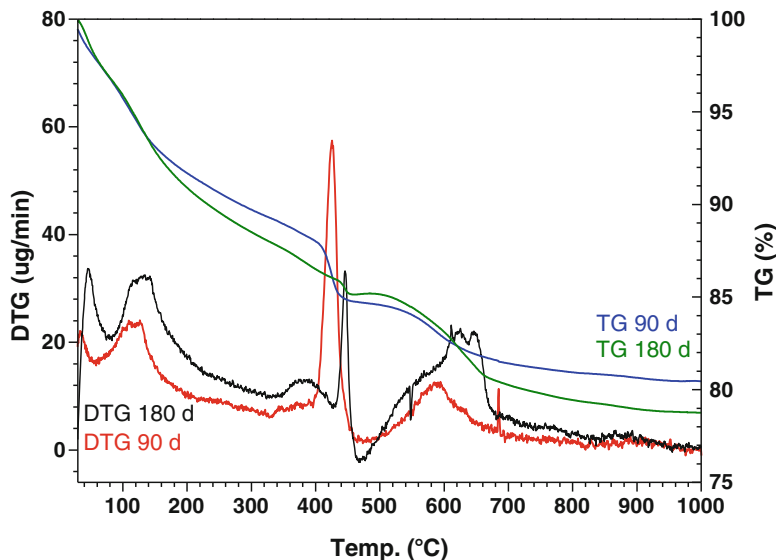


Fig. 3 Evolution of hydrated phases in lime-pozzolan mixtures cured at different humidity conditions, based on DTA/TG analysis

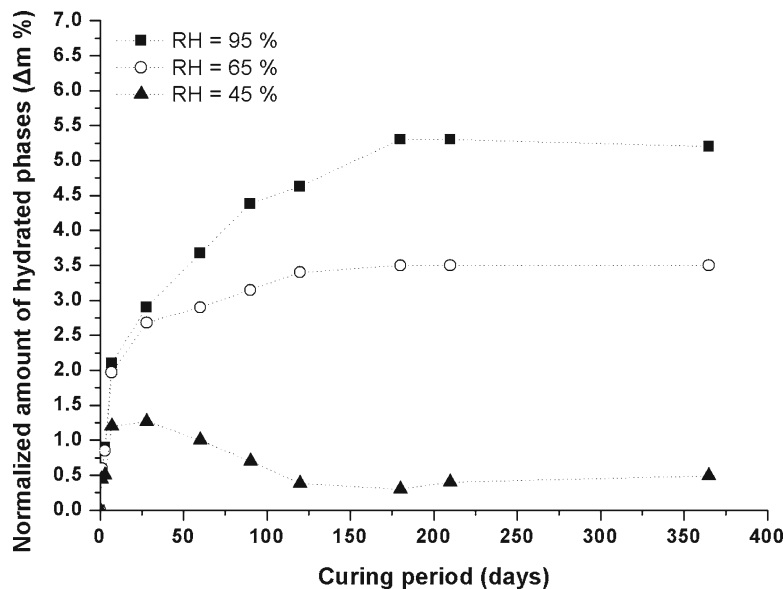


Fig. 4 Evolution of hydrated phases in lime-pozzolan mixtures cured at different humidity conditions, based on DTA/TG analysis

at 65% and 95% RH. However, the mixtures cured at high RH levels exhibited a clear trend towards an increase in the amount of hydrates, compared to those cured at medium RH conditions. In contrast, the pastes cured at C conditions presented no further development of the hydrated products after an initial period of 7 days (Fig. 4).

3.1.3 Microstructure Examination

The examination of the mixtures in the SEM proved that the formation rate and evolution of the above-described hydrated products strongly influenced the development of microstructure of lime-pozzolan pastes. The initial mixing of the solid constituents with water, created a uniform microstructure for all pastes, which was characterised by the presence of inter-granular macro-pores (Fig. 5a), filled with water. During the evolution of setting and curing, the new setting products were formed on the surface of the pore channels and started to fill up the available empty space (Fig. 5). SEM examination of fractured surfaces revealed that during the initial setting period (1–3 days), both pozzolan and calcium hydroxide (lime) particles can be easily distinguished, while the hydration products formed can be hardly detected. After this period, the amount of hydrated phases was considerably increased for groups A and B (Fig. 2), reaching an upper limit at 180, 120 and 28 days for groups A, B and C respectively.

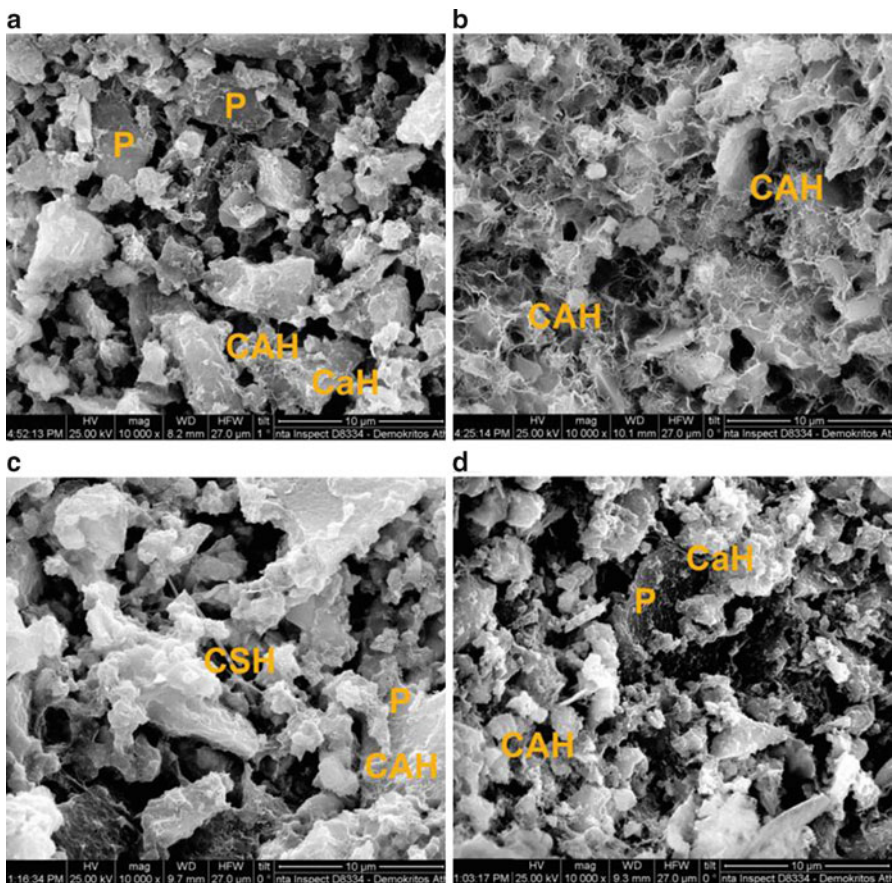


Fig. 5 Microstructure of mortar specimens from group A, after 7 (a) and 28 (b) days of setting, along with groups B (c) and C (d) after 28 days setting period. (P pozzolan, CaH calcium hydroxide, CAH calcium aluminate hydrates, CSH calcium silicon hydrates)

After this period, the evolution of hydrates, and consequently the modification of the microstructure, was strongly influenced by the curing conditions and the available water participating in the hydration reactions. As a result, after 28 days it was easy to distinguish between the three groups on the basis of the developed microstructure (Fig. 5): Group A seems to have a denser microstructure, while its macro-porosity (large capillaries) diminishes due to the enhanced formation of hydrated products. Group B also shows a decrease in the amount of large capillary pores, but it still contains a considerable amount of macro-pores and therefore presents a coarser texture. On the contrary, Group C after 28 days curing exhibits the same microstructure to that of 7 days, with pozzolan particles still visible and a large amount of macro-pores. This, along with X-ray diffraction and thermal analysis results, indicates that hydration is much slower in group C, where the carbonation process dominates.

3.2 Strength Development

The interpretation of the compressive strength values of all specimens (Fig. 6) indicates that the development of mechanical properties is closely related to the curing conditions of the mixtures. After the first 7 days of setting, the mixtures develop only part of their potential total strength, while all specimens present very similar compression values.

Consequently, up to 28 days (which is the setting period proposed by standards [3, 4, 12] for assessing in laboratory the mechanical properties of mortars) the obtained strength values greatly depend on the curing conditions. For humidity levels $\geq 65\%$ RH (standard conditions) a considerable strength development is observed (groups A and B), which increases further by increasing the humidity up to 95% RH. In contrast, samples of Group C present strength values considerably lower, reaching a decrease between 50% and 60%. The monitoring of the compressive strength values for a setting period of 1 year shows that the mixtures cured at an elevated humidity (groups A and B) continuously increase their strength; at this time-scale the differences between the two groups become significant. In contrast, the specimens of group C present no further evolution of their mechanical properties. This pattern (group C) fits better with the field conditions in the majority of conservation projects in the Mediterranean basin and explains the gap between the laboratory and field application performance of lime-pozzolan mortars.

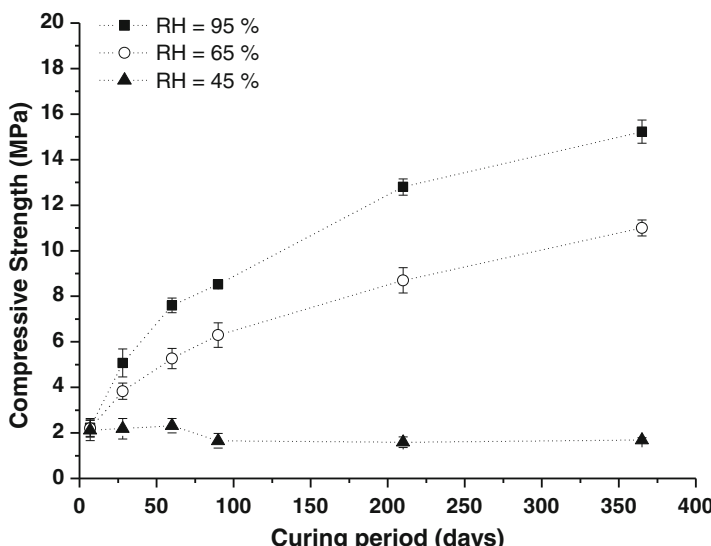


Fig. 6 Development of strength in mortar specimens cured at different humidity conditions

4 Conclusions and Recommendations

The laboratory monitoring of the setting process and strength development indicates that the initial 28 day period is very critical to the formation of microstructure and the future performance of lime-pozzolan mixtures. Thus, it is important to avoid the introduction of any microstructure defects in this period, ensuring the acceleration of the hydration process [13].

At the early stage, after the consumption and/or evaporation of the initially added water, the hydration process is controlled by the hygric properties of the mixtures, their water retention capacity and therefore, the humidity levels of the surrounding environment.

The humidity conditions during setting have a major impact to the process that will dominate. At high RH% levels, when capillary condensation takes place inside the pore network, carbonation is inhibited and hydration processes dominate. The increased humidity results in the solubility of lime, which creates a highly alkaline environment and favours the lime-pozzolan reactions towards the formation of hydrated products. Moreover, capillary condensation blocks the diffusion of CO₂ inside the pores and carbonation is avoided.

The optimum humidity conditions for capillary condensation depend each time on the type, granular distribution and mix proportions of raw materials.

From the elaboration of the results it is indicated that the amount of hydrated products are limited in mixtures cured below 65% RH, while in contrast, the amount of calcium carbonate is increased bellow this limit.

Finally, although the different groups of specimens present a similar strength during the first 7 days, the extension of curing period at humidity levels above 65% RH, multiply the compression strength values of mixtures up to three times in contrast to those that are left to set in open air conditions.

In the above context, the following parameters could contribute towards better practice and performance of lime-pozzolan mortars, especially in field applications:

- The use of a standardised quality matured lime putty instead of dry hydrated lime powder [14],
- The use of an optimum amount of pozzolan, in order to achieve maximum lime consumption within the first few days [15].
- The fineness of the pozzolan should be set below 63 µm, to accelerate the hydration rate [16].
- The use of water retaining agents, in an attempt to ensure that a water supply is retained within the mortar mass for a prolonged period [17].

References

1. Cerny, R., Kunca, A., Vr, T., et al.: Effect of pozzolanic admixtures on mechanical, thermal and hygric properties of lime plasters. Constr. Build. Mater. **20**, 849–857 (2006)

2. Baronio, G., Binda, L.: Study of the pozzolanicity of some bricks and clays. *Constr. Build. Mater.* **11**, 41–46 (1997)
3. EN 1015-3.: Methods of test for mortar for masonry – Part 3: Determination of consistence of fresh mortar (by flow table), European Committee for Standardization (1999)
4. EN 169-1.: Methods of testing cement – Part 1: Determination of strength, European Committee for Standardization (1995)
5. Antiohos, S., Tsimas, S.: Activation of fly ash cementitious systems in the presence of quicklime. Part I: Compressive strength and pozzolanic reaction rate. *Cem. Concr. Res.* **34**, 769–779 (2004)
6. Fortes-Revilla, C., Martinez-Ramirez, S., Blanco-Varela, M.T.: Modelling of slaked lime-metakaolin mortar engineering characteristics in terms of process variables. *Cem. Concr. Compos.* **28**, 458–467 (2006)
7. Chen, J.J., Thomas, J.J., Taylor, H.F.W., et al.: Solubility and structure of calcium silicate hydrate. *Cem. Concr. Res.* **34**, 1499–1519 (2004)
8. Ramachandran, V.S.: Thermal analyses of cement components hydrated in the presence of calcium carbonate. *Thermochim. Acta* **127**, 385–394 (1988)
9. Moropoulou, A., Bakolas, A., Aggelakopoulou, E.: Evaluation of pozzolanic activity of natural and artificial pozzolans by thermal analysis. *Thermochim. Acta* **420**, 135–140 (2004)
10. He, C., Osbæck, B., Makovicky, E.: Pozzolanic reactions of six principal clay minerals: activation, reactivity assessments and technological effects. *Cem. Concr. Res.* **25**, 1691–1702 (1995)
11. Bakolas, A., Biscontin, G., Moropoulou, A., Zendri, E.: Characterization of structural拜占庭 mortars by thermogravimetric analysis. *Thermochim. Acta* **321**, 151–160 (1998)
12. EN 1015-18.: Methods of test for mortar for masonry – Part 18: Determination of water absorption coefficient due to capillary action of hardened mortar. European Committee for Standardization (2002)
13. Ambroise, J., Maximilien, S., Pera, J.: Properties of metakaolin blended cements. *Adv. Cem. Based Mater.* **4**, 161–168 (1994)
14. Cazalla, O., Rodriguez-Navarro, C., Sebastian, E., Cultrone, G., De la Torre, M.J.: Aging of lime putty: effects on traditional lime mortar carbonation. *J. Am. Ceram. Soc.* **83**, 1070–1076 (2000)
15. Basumajumdar, A., Das, A.K., Bandyopadhyay, N., et al.: Some studies on the reaction between fly ash and lime. *Bull. Mater. Sci.* **28**, 131–136 (2005)
16. Day, R.L., Shi, C.: Influence of the fineness of pozzolan on the strength of lime natural-pozzolan cement pastes. *Cem. Concr. Res.* **24**, 1485–1491 (1994)
17. Paiva, H., Esteves, L.P., Cachim, P.B., et al.: Rheology and hardened properties of single-coat render mortars with different types of water retaining agents. *Constr. Build. Mater.* **23**, 1141–1146 (2009)

Morphological and Chemical Influence of Calcium Hydroxide on the Plasticity of Lime Based Mortars

Deborah Klein, Sonja Haas, Sven-Olaf Schmidt,
and Bernhard Middendorf

Abstract The influence of slaked limes (calcium hydroxide) on the fresh mortar properties varies according to morphological and chemical characteristics of the raw material. Until now there have been no sufficient scientific results to describe the parameters of calcium hydroxide that modify the plasticity in mortar systems. The aim of the investigations carried out here is to determine these plasticity regulating parameters. Therefore, several calcium hydroxides from different manufacturers have been analysed. The analyses included characterisation of raw materials and detailed investigations of differently slaked lime and lime putty at different times. Chemical and morphological principles of plasticity have been identified. Furthermore, these results have been evaluated by correlation of pilot plant experiments with defined lime mortars regarding their workability. The resulting material parameters responsible for plasticity are pointed out and distinguished between parameters relevant for plasticity values and those for plasticity development after extended soaking time.

1 Introduction

The method to determine plasticity of lime putties has been developed by W. E. Emley [1] in 1920. After the method was established, broad studies were carried out and primarily combined with analyses about the hydration mechanism of calcium oxides [2–4].

D. Klein (✉) • B. Middendorf

Technische Universität Dortmund, Dortmund, Germany
e-mail: deborah.klein@tu-dortmund.de; bernhard.middendorf@tu-dortmund.de

S. Haas • S.-O. Schmidt

Forschungsgemeinschaft Kalk und Mörtel e.V., Cologne, Germany
e-mail: sonja.haas@kalk.de; sven-olaf.schmidt@kalk.de

Subsequently, comparative studies approved the Emley-Plasticimeter's general suitability to determine plasticity and to differentiate between different hydrates [5]. The Emley-test provides reproducible figures and reflects the differences known in praxis between putties made of wet slaked lime (400 - Emley-units) and putties made of dry slaked lime (100-170 Emley-units). Basic studies regarding plasticity of lime putties have been carried out since about 1960. Then in 2001, rheological properties were reviewed in a literature study [6]. The long period without publications can be attributed to the increasing substitution of hydrated lime by cements and chemical substitutes.

The usage of lime mortars for maintenance and conservation of historical monuments recently attracted scientific interest to the rheology of lime putties. The main advantages of lime based mortars are the high plasticity, the water retention, an open porosity, the high water vapour diffusion and its crack healing function due to resolution processes and recrystallization [7–9].

2 Materials and Methods

In this paper, results from the analysis of ten calcium limes (CL) from ten different regions and manufacturers are presented. The value for CaO + MgO is between 75% (CL 70 acc. EN 459) and 98% (CL 90 acc. EN 459) [10]. Each lime has been chemically and physically analysed.

Regarding comparability for the plasticity measurements all putties had to have a standard consistency verified by a Vicat apparatus [11]. According to ASTM C110-03 [11] lime putties were prepared 24 h before testing. Thus, the water/binder ratios were chosen to reach the required consistency at time of measuring (see Table 1). Additionally the influence of extended soaking time was investigated. Therefore, the material was soaked in a surplus of water with different water/binder ratios (Table 1) and was stored for 28 days. Before the measurement the long-time soaked putties were dried at 40°C to a standard consistency. Table 1 shows the water/binder ratios for each calcium lime while soaking and at the time of measuring with the corresponding plasticity values.

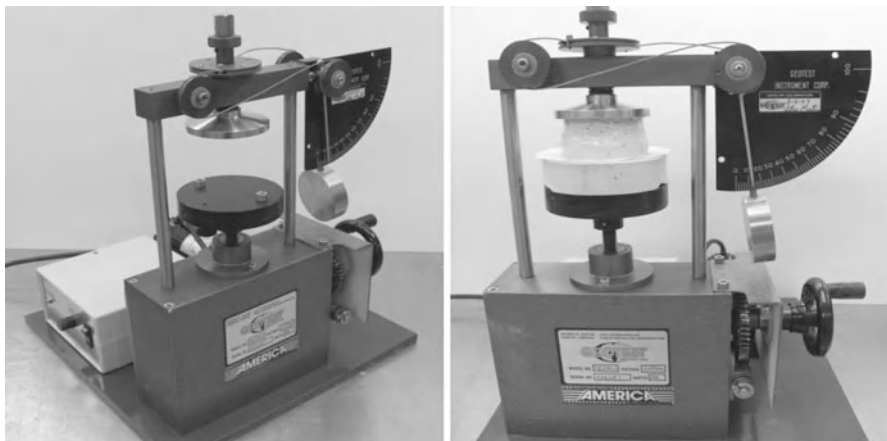
The micrographs of the scanning electron microscope were taken of the dry raw material and of the long-time soaked putties. In order to dry the putties they were rinsed with isopropanol and shortly treated with ultrasonic waves before dried at 40°C. According to the micrographs by an environmental scanning electron microscope for selected samples the treatment of the putties has no influence.

Due to the complexity of the topic this article is focused on lime putties produced from dry hydrated lime.

The determination of plasticity was carried out according to the technique by W. E. Emley [1] using a plasticimeter shown in Fig. 1. The Emley Test method for plasticity takes into account the force required to lift a weight due to friction of the lime putty against a platen. At the same time water is being sucked into a gypsum base plate. The time taken to reach failure is recorded. The starting materials used

Table 1 Overview of analysed materials and their plasticity values

Sample	CL 90-1	CL 90-2	CL 90-3	CL 90-4	CL 90-5	CL 80-6	CL 70-7	CL 90-8	CL 80-9	CL 90-10
Water/binder at measuring	0.8	0.8	0.8	0.8	0.8	0.8	0.8	0.8	0.8	0.8
Plasticity 24 h	206	189	364	162	206	131	117	176	237	166
Water/binder while soaking	1.5	1.5	1.5	1.5	1.5	1.5	1.5	1.5	1.5	1.5
Water/binder at measuring	0.67	0.72	0.72	1.14	0.56	0.81	0.90	0.63	0.68	0.95
Plasticity 28 days	326	202	307	321	251	135	—	219	206	260
Water/binder while soaking	0.9	0.9	0.9	0.9	0.9	0.9	0.9	0.9	0.9	0.9
Water/binder at measuring	0.84	0.82	0.86	0.87	0.74	0.61	0.75	0.70	0.88	0.93
Plasticity 28 days	321	189	423	355	206	125	119	180	189	210

**Fig. 1** Emley plasticimeter

in our experiment to determine Emley plasticity measurement on are lime putties of the same consistency made from dry hydrated lime [1, 11].

The higher the plasticity figure calculated according to the following formula, the higher is the plasticity of the lime putty [11]:

$$P = \sqrt{F^2 + (10T)^2} \quad (1)$$

P plasticity figure

F scale reading at the end of the test

T time in minutes from the time when the first portion of paste was put in the mould to the end of the test

The specific surface of the dry (unsoaked) calcium hydroxide samples was determined via gas adsorption as single-point method according to Brunauer et al. [12]. The samples have been dried at 110°C and rinsed with dried N₂ gas at 120°C for 2 h. The sample weight has been determined after desorption.

The analysis of particle sizes at different times was carried out using He/Ne-Laser granulometry. The samples have been measured as slurry in isopropanol at 50 mm focal width, 30 s ultrasonic exposure and 60 s ultrasonic pause.

3 Analysis

In addition to the physical-mechanical properties of hardened mortar such as density, porosity or durability that hydrated lime provides to mortar, it also provides plasticity to the fresh mortar. This parameter contributes to flexibility, yield, ease of mixing and water retention of the mortar.

The factors responsible for the development of plasticity in hydrated lime are investigated using several calcium hydroxides from different manufacturers. The results are evaluated by correlating objective plasticity values with subjective workability data by judging of an experienced craftsman in pilot plant experiments with defined lime mortars. The resulting material parameters responsible for plasticity are pointed out.

Experience and comparison of the rheological properties of other mineral systems indicate that particle size distribution and particle shape as well as formation of the surface are of primary importance [2]. It is known that the rheology of lime-water suspensions (lime putty) is affected by the amount and the form of available fines of calcium hydroxide [2]. The plasticity also results from the interaction of the liquid phase with the particles of calcium hydroxide and therefore depends on the specific surface. The specific surface of the dry (unsoaked) calcium hydroxide samples was determined according to Brunauer et al. [12]. An increasing plasticity value shows some correlation with increasing specific surface area (SSA) (Fig. 2).

The pore size distribution is also linked to the specific surface area. The higher the amount of small pore diameters, the higher the specific surface area is. Additionally, the pore structure influences the structural changes due to soaking. The pore size distribution of the raw material showed an influence on the development of plasticity after extended soaking time. Thus, the raw material with smaller pore diameters reached higher plasticity values after extended soaking.

The correlation of pore size distribution and increasing plasticity becomes visible in the comparison of maximum pore size distribution and the plasticity values at different times of soaking in Fig. 3. No correlation can be identified for the plasticity values after 24 h, whereas the correlation coefficient after 28 days is 0.68. Taking into account only those samples that increase plasticity with extended soaking time the correlation coefficient is even 0.96.

Coarse particles ($>1\text{ }\mu\text{m}$) of calcium hydroxide, which consist of agglomerates, time-dependently form fines of calcium hydroxide and decisively influence the

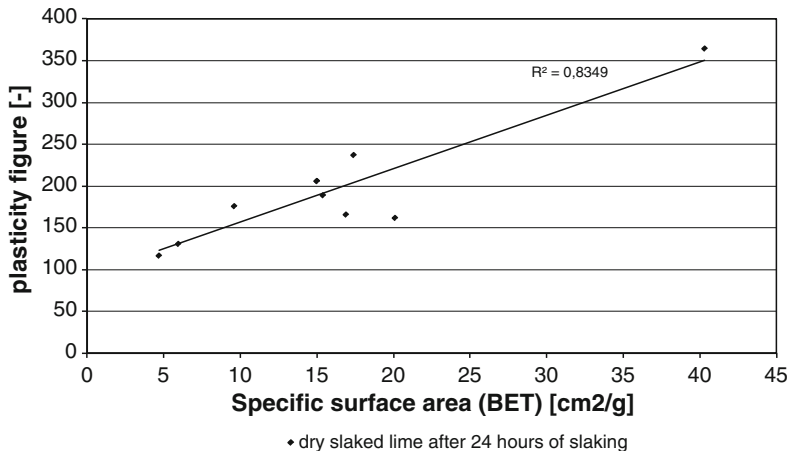


Fig. 2 Scattergram of SSA versus Emley plasticity value

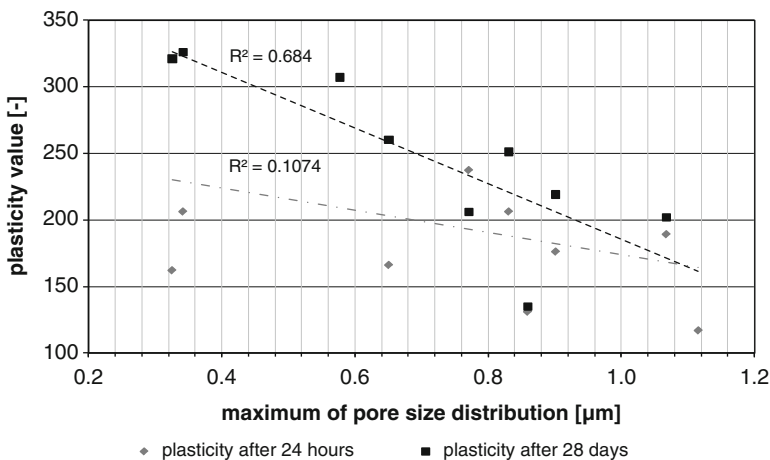


Fig. 3 Maximum of pore size distribution in correlation with plasticity

plasticity. This process is dependent on the crystal habit and morphology of the lime particles. The SEM micrographs (Figs. 4 and 5) illustrate the result of the process of “refinement” [2].

The degree of “refinement” is different with each hydrate and, as is suggested, related to the development of plasticity. The available foreign ions such as Al [13] and structural defects in the $\text{Ca}(\text{OH})_2$ crystal can be divided into those appearing as “notches” that lead to division and refinement causing increased plasticity, and others appearing as “stick points” that avoid such a division, or even lead to a coarsening (see Figs. 4, 5, 6, 7, 8, and 9) [2].

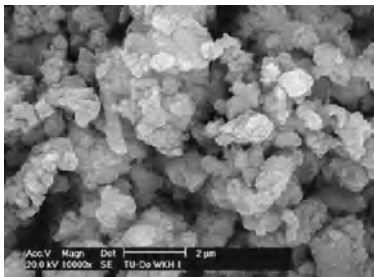


Fig. 4 Calcium hydroxide – sample CL 90-1

extended soaking-time
→
in excess of water

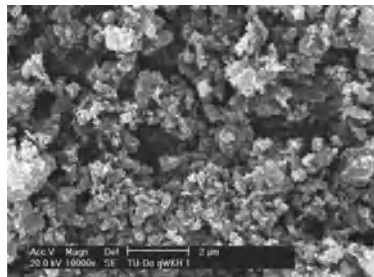


Fig. 5 Calcium hydroxide after 28 days of soaking – sample CL 90-1

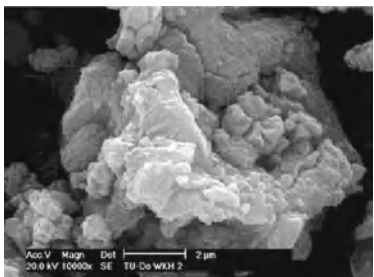


Fig. 6 Calcium hydroxide – sample CL 90-2

extended soaking-time
→
in excess of water

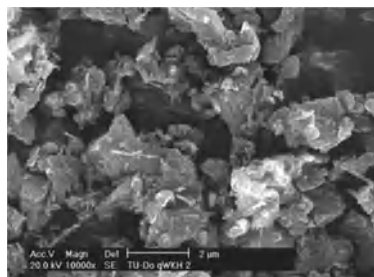


Fig. 7 Calcium hydroxide after 28 days of soaking – sample CL 90-2

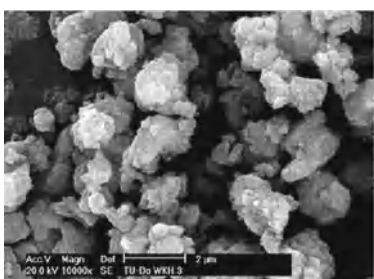


Fig. 8 Calcium hydroxide – sample CL 90-3

extended soaking-time
→
in excess of water

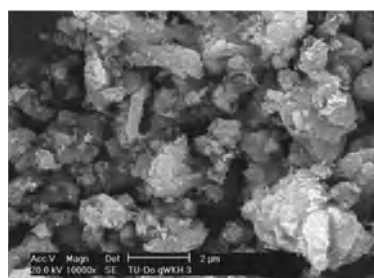


Fig. 9 Calcium hydroxide after 28 days of soaking – sample CL 90-3

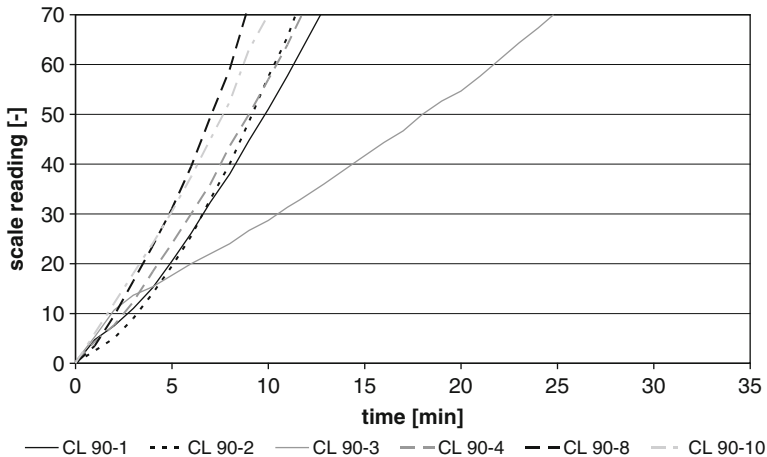


Fig. 10 Development of plasticity in correlation with time – after 24 h of soaking

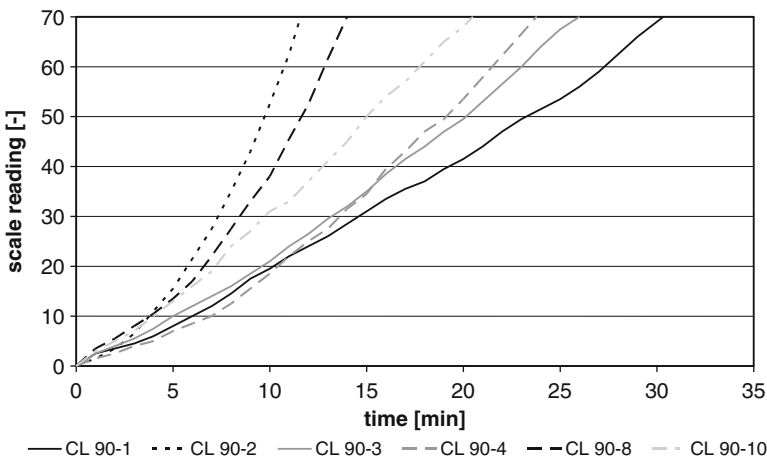


Fig. 11 Development of plasticity in correlation with time – after 28 days of soaking

Based on the Figs. 10 and 11 the temporal influence of soaking time and the process of refinement are apparently visible. The duration of workability and thus the plasticity figure of different samples of slaked lime increase after 28 days of soaking. Especially sample CL 90-1, which shows a distinctive refinement (Figs. 4 and 5) also shows a clear increase in the plasticity. Other samples, such as sample CL 90-3 (see Figs. 8 and 9) remain virtually unchanged.

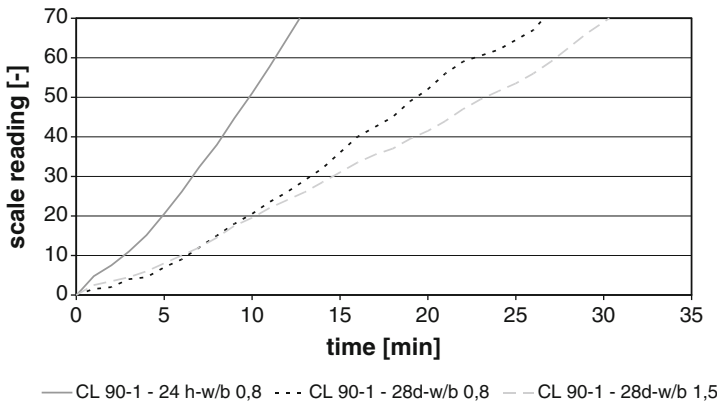


Fig. 12 Plasticity figures after 28 days of soaking in different lime-water proportions compared to the measurement after 24 h

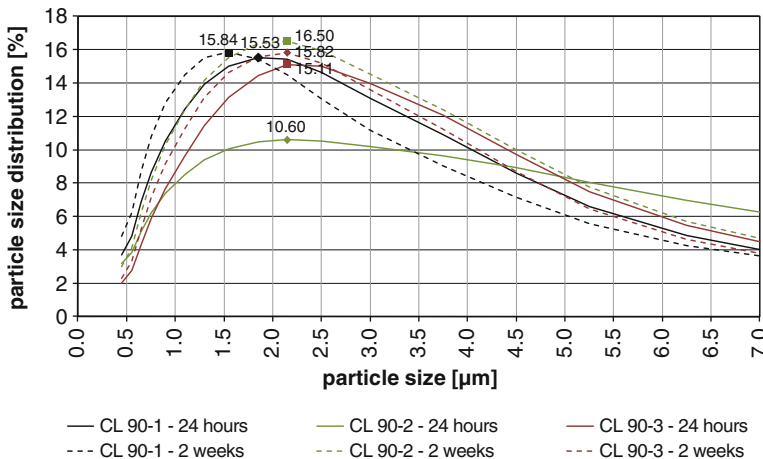


Fig. 13 Particle size distribution at different times of soaking

The 28 day soaked hydrated limes are in a surplus of water with different water/binder ratios (w/b 0.8 and w/b 1.5). Before the measurement all putties were dried at 40°C to a standard consistency. In many cases, the samples that initially soaked in a larger amount of water possess higher plasticity values (see Fig. 12). This observation leads to the conclusion that the amount of available water affects the development and refinement of the hydrated lime particles.

The process of refinement is also indicated with analysis of particle sizes at different times using He/Ne-Laser granulometry. The mode of the particle size distribution of those samples that increase their plasticity with time of soaking moves to finer particle sizes (Fig. 13 – sample CL90-1). Samples which show slightly increased plasticity figures also only show small changes in the curves (see Fig. 13 – sample CL90-3). Several curves become significantly steeper, which

indicates an accumulation of particles of similar size. For sample CL90-2 the amount of particle sizes around 2 µm increases, whereas the amount of coarser particles decreases. For these samples increasing plasticity figures cannot be recorded (see Fig. 13 – sample CL90-2).

Since the curves of three samples with different plasticity development and different plasticity figures look similar after soaking, conclusions about the plasticity cannot be drawn just according to particle size and size distribution, whereas changes due to soaking within one sample can be identified.

4 Conclusion

Plasticity development relies on different parameters. In general it can be said that plasticity values increase with increasing soaking time. Due to crystal habit and morphology coarse particles ($>1\text{ }\mu\text{m}$) of calcium hydroxide consisting of agglomerates time-dependently decrease in particle size when left in water.

The tests in this work have shown the correlation between increasing plasticity values and increasing specific surface area as an interaction of the liquid phase with the particles of calcium hydroxide. Furthermore, the pore size distribution of the raw material showed an influence on the development of plasticity after extended soaking time. Thus, the raw material with smaller pore diameters reached higher plasticity values after extended soaking.

Plasticity is influenced by the particle size distribution of the lime, i.e. plasticity increases with decreasing particle sizes. Since a decisive refinement could not be detected for all samples, conclusions about the plasticity cannot be drawn just regarding particle size and size distribution. Moreover, different behaviours of plasticity development due to extended soaking were identified.

Calcium hydroxides that increase their plasticity over time show a closer connection with the physical properties of the raw material than other samples. Considering only the plasticity values after 24 h the chemical-mineralogical characteristics of the raw material seem to have more importance.

In mortar systems the plasticity is also mainly influenced by the particle size distribution, the particle shape and the amount of used aggregates. Nevertheless, it is obvious that the higher the amount of aggregates the lower the influence of the lime.

The test method developed by Emley for measuring plasticity appears to be an adequate test method for measuring the workability of lime putties. It provides objective data and reveals the evolution of plasticity over time. The objective plasticity values obtained by this testing method have been verified by pilot plant experiments. The results and the rating of experienced craftsmen were in accordance with the results of the laboratory tests.

Acknowledgements This research project AiF-No. 15.650 N “Influence of the morphology of hydrated lime on the plasticity properties of mortar systems” is promoted by the Federal Ministry for Economic Affairs and the Federation of Industrial Research Associations (AiF) and performed by the Association for the Research Foundation of lime and mortar, Cologne, and the Department of Building Materials at TU Dortmund University.

References

1. Emley, W.E.: Measurement of plasticity of mortars and plasters. Technologic papers of the Bureau of standards, No. 169, 27 S (1920)
2. Ney, P.: Physikochemische Grundlagen der Bildsamkeit von Kalken unter Einbeziehung des Begriffs der aktiven Oberfläche. Forschungsberichte des Wirtschafts- und Verkehrministerium NRW, **528**, 80 S, Köln (1958)
3. Wuhrer, J., Radermacher, G., Zager, L.: Hydratationsmechanismus des Calciumoxyds und plastische Eigenschaften der Kalkhydratbreie. Zement-Kalk-Gips **10**, 456–466 (1959). Wiesbaden
4. Kreutz, M., Schimmel, G.: Löschversuche an Branntkalk mit Wasserdampf. Zement-Kalk-Gips **10**, 471–477 (1959). Wiesbaden
5. Zander, H. et al.: Arbeitsergebnisse und Probleme auf dem Gebiet des Löschens. Interner Bericht liegt vor. Bericht über die Tätigkeit des Löschausschusses der deutschen Kalkindustrie 15 Nov 1960
6. Krumnacher, P.J.: Lime and cement technology: Transition from traditional to standardized treatment methods. Master of Science thesis paper, Faculty of the Virginia Polytechnic Institute, 90 S, Blacksburg (2001)
7. Thomson, M.: Properties of lime mortar. Structure Magazine, pp. 26–29. Reedsburg (2005)
8. Pavia, S., Treacy, E.: A comparative study of the durability and behaviour of fat lime and feebly-hydraulic lime mortars. Mater. Struct. **39**, 391–398 (2006)
9. Mira, P., Papadakis, V.G., Tsimas, S.: Effect of lime putty addition on structural and durability properties of concrete. Cem. Concr. Res. **32**, 683–689 (2002)
10. Deutsches Institut für Normung: DIN EN 459-1 – Baukalk – Teil 1: Definitionen, Anforderungen und Konformitätskriterien. Beuth-Verlag, Berlin (2010)
11. American Society for Testing and Materials: Standard test methods for physical testing of quicklime, hydrated lime, and limestone – ASTM C110-02a (2002)
12. Deutsches Institut für Normung: Determination of the specific surface area of solids by gas adsorption using the BET method. Beuth Verlag, Berlin (2003)
13. Gmelin-Institut (Hrsg.): Gmelins Handbuch der anorganischen Chemie – System-Nummer 28. Verlag Chemie, Weinheim (1957)

Water Transport Between Mortar and Brick: The Influence of Material Parameters

Roel Hendrickx, Staf Roels, and Koenraad Van Balen

Abstract This article deals with the phenomenon of the early water transport between fresh mortar and a dry brick. Two bricks with different transport parameters were considered in combination with two different mortars: a lime hydrate mortar and a cement mortar. Water transport was monitored during the first hour after contact using X-ray imaging and simulated using a commercial control volume (CVM) software tool. Such simulations are made possible by a newly developed method to measure transport parameters of fresh mortars. The amount of water leaving the mortar in 1 h depends mostly on two parameters of the mortar: initial and residual water content. The rate of flow across the interface shows a complex behaviour and is larger for cement mortar and for strongly absorbing brick. The accuracy of simulations is somewhat limited by the importance of over-capillary effects in the bricks near the interface. It appears that this over-capillary water is partly distributed over the brick, and partly reabsorbed by the mortar.

1 Introduction

The importance of early water transport from mortar to brick for the workability during bricklaying and the mortar-brick bond of the hardened masonry has been reviewed and discussed by Groot [1]. A mortar should release some water in order to be compacted and gain stiffness, but at the same time this desorption shouldn't go

R. Hendrickx (✉) • S. Roels

Laboratory of Building Physics, Katholieke Universiteit Leuven, Leuven, Belgium
e-mail: roel.hendrickx@bwk.kuleuven.be; staf.roels@bwk.kuleuven.be

K. Van Balen

Division of Building Materials and Building Techniques,
Katholieke Universiteit Leuven, Leuven, Belgium
e-mail: koenraad.vanbalen@bwk.kuleuven.be

too fast because in that case the correct placement of the brick may become difficult. If too much water is desorbed at the end of the process, the left-over quantity may be too low to provide for complete hydration of the binder [2].

Recent research has focused on water transport across interfaces in hardened masonry [3, 4] as well as in the fresh state of the mortar [1, 5–7]. Moisture profiles have been recorded either by neutron transmission [1], NMR [3, 6], or X-ray radiography [2, 4]. X-ray radiography was demonstrated to give reliable results with a sufficient moisture content resolution and spatial resolution [8].

The numerical solution of the problem can be done using discretised transport equations in a FEM or CVM solver, or by simplifying the problem to a sharp-front analysis. The latter is successful when capillary uptake from a liquid surface is studied [4], but it cannot predict cases where the water supply is limited and more smooth moisture contents gradients can be expected. Discrepancies between observations and model results are often observed in the interfacial zone.

Up to day the lack of a reliable experimental method to measure the water retention curve and permeability of fresh mortar has limited the possibilities for model calculations [6]. This has lead to rather speculative analyses based on observations on the hardened material. It has been demonstrated recently that a combination of pressure plate tests, suction tests and permeameter tests can provide the required data [9]. These techniques and the possibilities they offer will be briefly presented. The obtained parameters are used to extend the discussion of the transport over interfaces to the fresh state of the mortar, in observations as well as simulations.

2 Materials: Mortars and Bricks

Two types of mortar were combined with two types of brick. The mortars are a lime hydrate mortar (Tradical 98, CL 90S, EN 459-1) and an ordinary Portland cement mortar (Schwenk, CEM I 42.5R, EN 169-1). The sand is a rather fine and fairly rounded siliceous sand of grading 0/0.5(0/1) according to EN 13139 (sieving procedure EN 933-1). The mortar compositions were derived from practical experiments with experienced masons. Mix ratios and initial water content are listed in Table 1. The procedures used for fixing these data are documented in [2].

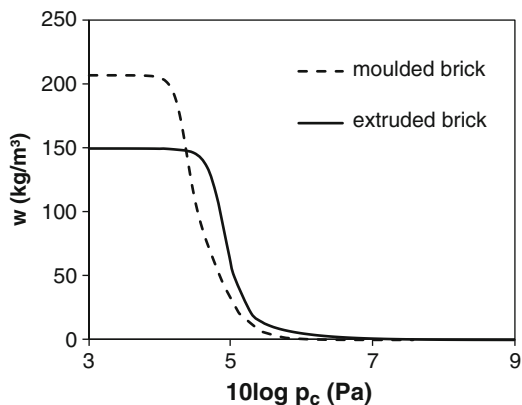
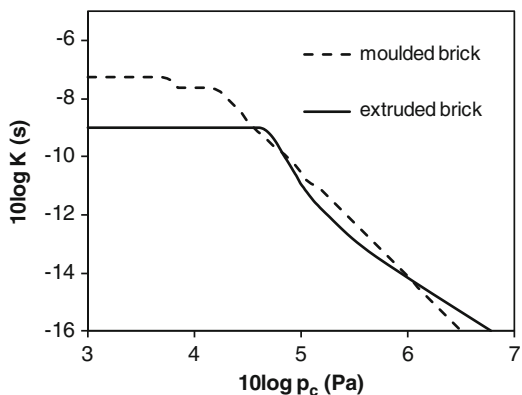
The bricks are one extruded and one moulded fired clay brick. The extruded brick is custom made by Wienerberger. It is the least porous and medium absorbing (Table 2). The moulded brick is of type ‘Spaans rood’ by Wienerberger and has

Table 1 Properties of the mortars

Composition parameters	Lime mortar	Cement mortar
Binder to sand mass ratio (kg/kg)	0.112	0.218
Initial water to binder mass ratio (kg/kg)	2.016	0.907
Initial water content (kg/m ³)	334	313
Residual water content (kg/m ³)	124	54

Table 2 Properties of the bricks

	Extruded brick	Moulded brick
Vacuum saturated water content w_{sat} (kg/m ³)	209	323
Capillary saturated water content w_{cap} (kg/m ³)	150	207
Capillary absorption coefficient (kg/m ² s ^{0.5})	0.19	0.53

Fig. 1 Water retention curves of bricks**Fig. 2** Permeability curves of bricks

higher porosity and faster absorption. Determination of the hygric properties was done by vacuum saturation, mercury intrusion porosimetry (water retention curve) and X-ray radiography (diffusivity, recalculated to permeability). These experimental techniques are documented elsewhere and will not be treated here [10, 11]. The water retention curves and liquid permeabilities are plotted in Figs. 1 and 2. The extruded brick has lower porosity but exerts higher capillary suction than the moulded brick due to its finer pores. The permeabilities are comparable over a certain range of capillary pressure, but the capillary saturated (i.e. low suction) permeability of the moulded

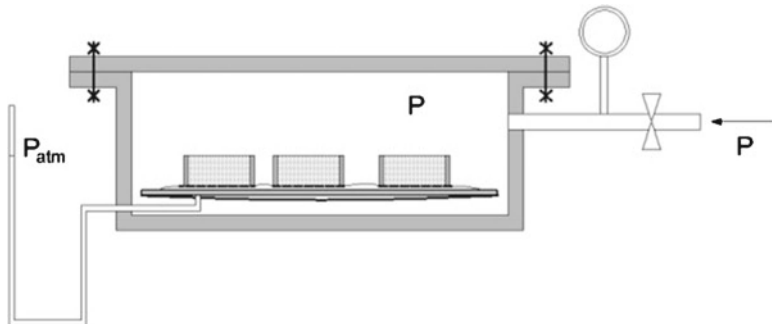
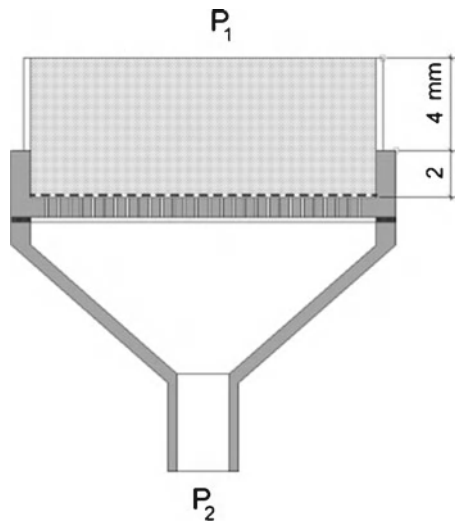


Fig. 3 Section through the pressure plate apparatus with mortar samples in plastic cylinders

Fig. 4 Adapted ASTM suction apparatus



brick is considerably higher. This causes the higher absorption coefficient of the moulded brick. Permeability of the moulded brick was calibrated with a moisture uptake experiment and a drying experiment.

3 Measurement of the Mortars' Transport Parameters

The water transport of a fresh mortar can be characterised by two functions: water content as a function of applied suction (the water retention curve) and permeability as a function of water content or applied suction (permeability curve). Extensive background information and procedures are published in [9]. The experimental methods used to determine water content as a function of suction are the pressure plate method (Fig. 3) and the adapted ASTM suction apparatus (Fig. 4). The first

method consists of applying high air pressure in a closed chamber, to which the mortar specimens are exposed. On the other side of the specimens, the pore water of the mortar is hydraulically connected to the atmosphere via an opening where water can be evacuated. After some time – typically a couple of hours – the mortar reaches an equilibrium water content corresponding to the applied pressure in the chamber. Capillary pressure is the difference between the pressure in the chamber and the water pressure in the mortar, i.e. atmospheric pressure.

The second method, the adapted ASTM suction test, is complementary to the previous method and creates capillary pressure (suction) by applying a vacuum (P_2 in Fig. 4) to the bottom of the sample through a perforated dish. This method is suited to work with relatively low capillary suction, the theoretical maximum being 1 atm. In practice the workable limit is around 0.5 atm (5·10⁴ Pa).

The result of the pressure plate and the suction tests is a series of data couples (w, p_c): water content in [kg/m³] and capillary pressure in [Pa]. These are fitted to an equation as presented by Van Genuchten [12]:

$$w(p_c) = \sum_i l_i \left(1 + (a_i p_c)^{n_i}\right)^{m_i}; m_i = 1/n_i - 1 \quad (1)$$

The resulting curves and the data points are plotted in Fig. 5. The important difference between both mortars is that lime mortar retains more water, which is reflected in the smaller slope of the curve and higher residual water content. The existence of this residual water content in itself is an important notion in the context of this article and is clearly demonstrated by the experimental data. It means that from a certain amount of applied suction, a mortar will not release any more water. This is explained by the infiltration of air in the porous system, which prevents further liquid transport through a continuous liquid film network. As will be demonstrated below, the available amount of water which a mortar can lose to a brick, is the difference between its initial water content and its residual water content.

The permeability of the mortars is determined in the original, i.e. saturated state. This was done in a setup where a classical soil permeameter element is placed in a water bath to create a pressure head h over a cylindrical specimen (Fig. 6). The constant water flow through the mortar is measured by weighing the emerging water, which is removed from the top surface with a pipette. Permeability K_{sat} [s] follows from Darcy's law for saturated flow. The non-saturated permeability $K(p_c)$ follows from an equation for relative permeability by Mualem – Van Genuchten [12]:

$$K_r(p_c) = \frac{\left[1 - (ap_c)^{n-1} \left(1 + (ap_c)^n\right)^{-m}\right]^2}{\left(1 + (ap_c)^n\right)^{m/2}} \quad (2)$$

This equation uses the expression for the water retention curve cited above, and is derived from the concept that the water retention curve gives information on the

Fig. 5 Water retention curves of fresh mortars

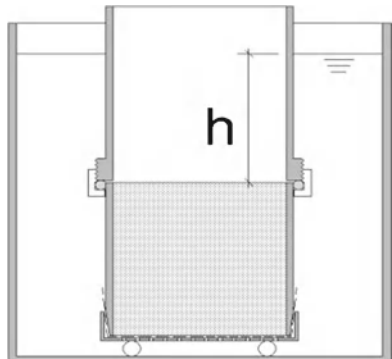
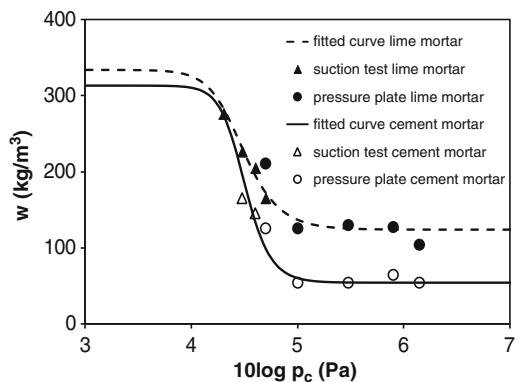


Fig. 6 Permeameter test setup



pore size distribution, and that the pores can be considered a bundle of parallel tubes. The final curves, plotted in Fig. 7, are found as:

$$K(p_c) = K_r(p_c) \cdot K_{sat}. \quad (3)$$

4 X-ray Observations

The test principle consists of placing a specimen between an X-ray source and a detector, which records the intensity of the transmitted radiation first in dry state (reference image, I_{dry}) and then in wet state (I_{wet}) (Fig. 8). The difference between the actual water content at time t and the initial water content in the reference image is calculated from the difference in intensities according to [13]:

$$w = -\frac{\ln(I_{wet} / I_{dry})}{\mu_w d} = -\frac{\ln I_{wet} - \ln I_{dry}}{\mu_w d} \quad (4)$$

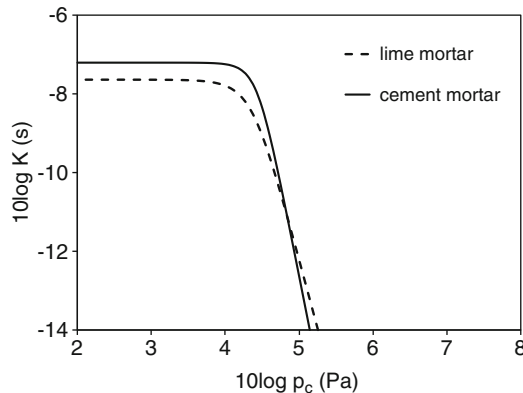


Fig. 7 Permeability curves of fresh mortars

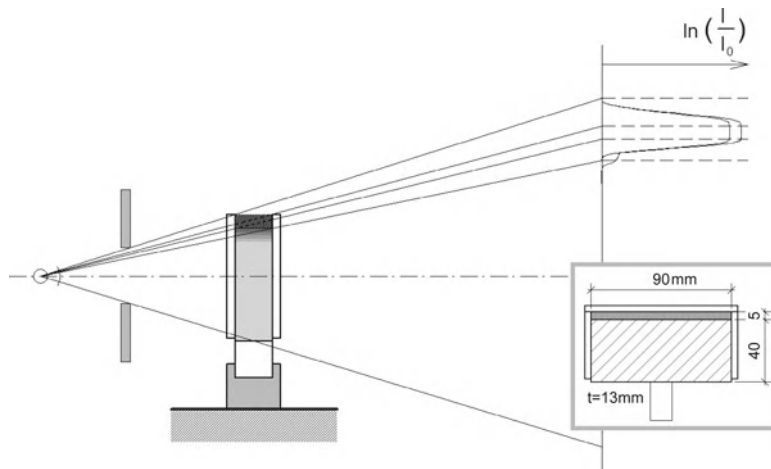


Fig. 8 Schematic setup for X-ray imaging of water transport from mortar to brick. Inset on the right bottom: geometry of the brick slices

with μ_w [1/m] the attenuation coefficient of water, which was measured separately for cement water and lime water for these experiments, and d the thickness of the specimen.

The specimen consists of a brick slice wrapped in tape and in a glued plexi container, which sticks out over a height of 5 mm on the top face (Fig. 8, inset). The assembly is fixed to a base, which is fixed on the sample holder in the X-ray chamber. First an image is taken of the dry specimen. Next a quantity of fresh mortar is brought in the 5 mm high space on top of the brick and sealed against evaporation with tape. From then on, images are taken at 1.5, 3, 6, 15, 30 and 60 min.

Each of the images is recalculated to a 2D array $w(x, y)$, using the equation above. This 2D array of moisture content points was converted to moisture fronts $w(x)$ in the brick or the mortar by averaging over a band of not less than 100 pixels.

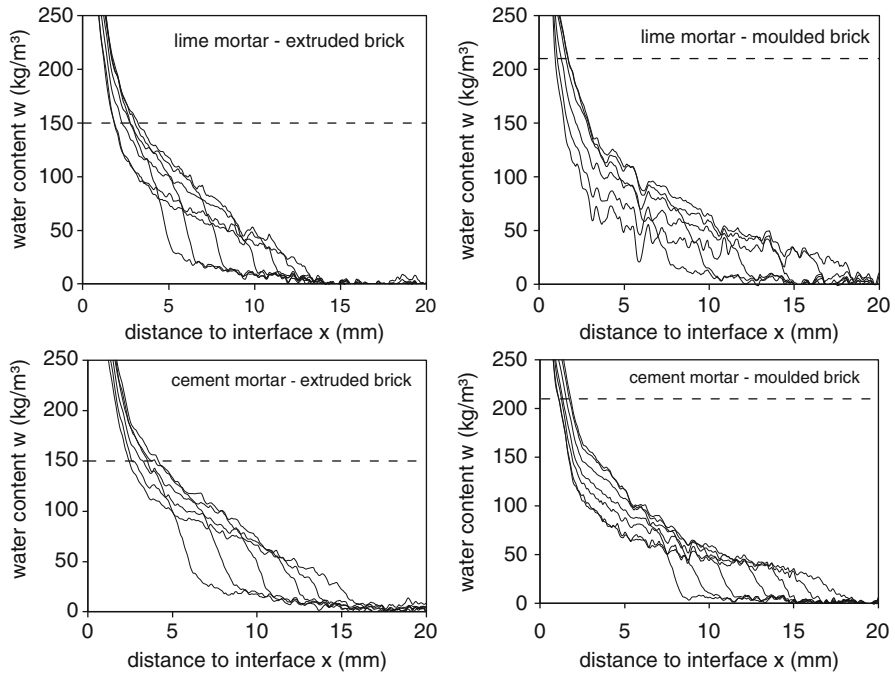


Fig. 9 Moisture fronts in the brick for all combinations of mortar and brick. The capillary water content is indicated with a dotted line. The curves are taken at $t = 1.5, 3, 6, 15, 30$ and 60 min

The results of one out of two tests for each combination were selected and are plotted in Fig. 9. The image is limited to the brick; treatment of the mortar data is more complex and beyond the scope of this article. It can be observed that the moisture content near the interface is larger than the capillary saturated water content, whereas in the bulk of the brick, the moving moisture front does not reach this level. The movement of the front as a function of time is qualitatively similar for all cases, but it can be observed that the early fronts for the moulded brick are slightly ahead of those for the extruded brick, and that those of cement mortar are ahead of those of lime mortar. The transferred water amount is slightly larger for the cement mortar. This points however at large difference between both mortars, because the lime mortar has much higher initial water content: it retains relatively more water. The zone of high water content near the interface decreases over time: this is partly due to diffusion inside the brick, but possibly also to reverse water flow back towards the joint.

5 Numerical Simulations

Capillary liquid water transport was modelled using the FEM software Hamfem [14]. This software is used in building physics applications for combined heat and moisture transport in porous materials. In this case vapour transport can be neglected and

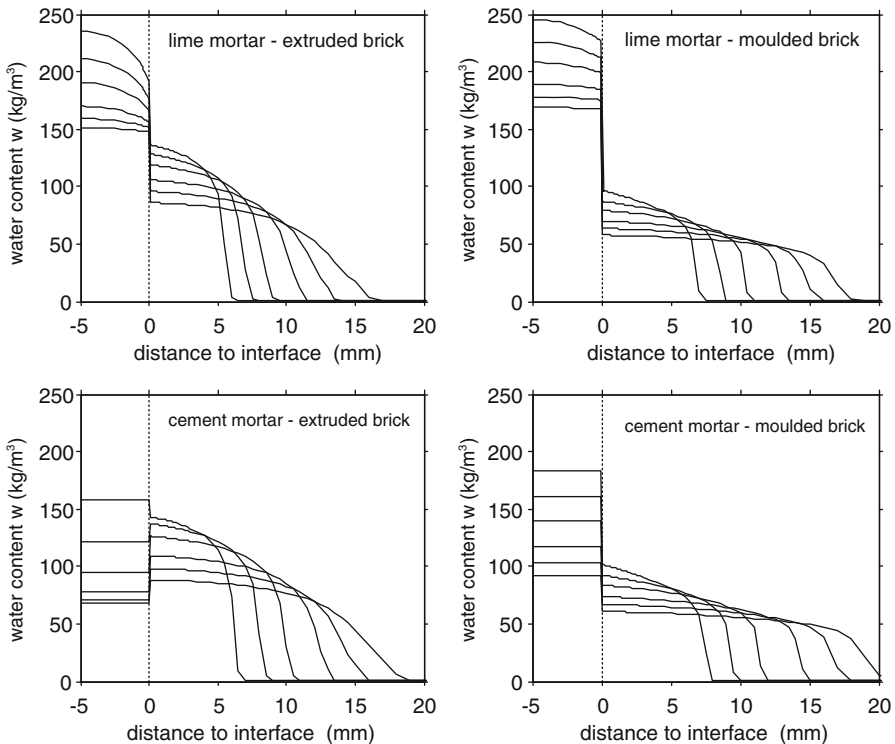


Fig. 10 Numerical calculations (using Delphin 6) of moisture content in mortar and brick at times 1.5, 3, 6, 15, 30 and 60 min. The dotted line indicates the position of the brick-mortar interface

the problem of capillary water transport is solved isothermally. The transport equation solved for each element is:

$$\frac{\partial w}{\partial t} = \frac{\partial}{\partial x} \left(K(p_c) \frac{\partial p_c}{\partial x} \right) \quad (5)$$

A free capillary absorption test and a drying test were simulated to validate and calibrate the material parameters of both bricks. Initial boundary conditions were: dry state for the brick and initial water content of the fresh mix for the mortar.

The results of the simulations are plotted for all four combinations in Fig. 10. They give a full view of the evolution in the mortar, which is difficult to derive from the measured images. The water content in the mortar decreases, while the desorbed water is absorbed by the brick, where it is slowly distributed over the depth. Clearly visible water content gradients develop within the lime mortar, but not within the cement mortar, which has a too high permeability to sustain such gradients. In the initial stage the extruded brick gets loaded with water almost up to capillary saturation (150 kg/m^3), but already after 1.5 min a decrease starts. The moulded brick does

not reach capillary saturation (206.7 kg/m^3), because of its higher permeability (or rather diffusivity), which leads to the faster redistribution of the water. The moisture front proceeds faster, the maximum is lower and the shape of the profile is more flat. The amount of water released by the cement mortar is slightly higher than by the lime mortar, despite its lower initial water content.

The trends of the differences between the four combinations in the simulations (Fig. 10) can be recognised in the measurements in Fig. 9:

- faster redistribution in the moulded brick than in the extruded brick;
- relatively higher liquid content (with respect to saturation) in the extruded brick than in the moulded brick;
- comparable quantity of released water for both mortars, which means relatively much higher water loss for the cement mortar (with respect to initial water content);
- slightly steeper fronts and more horizontal profiles in the moulded brick than in the extruded brick.

The important difference between observations and simulations lies in the observed over-capillary behaviour in the brick near the interface. This phenomenon is not covered by the simulation tool. In most natural and practically relevant situations of water uptake, the entrapment of air hinders full saturation, but in this case, where a mortar layer is in direct contact with the brick and some pressure is exerted on it, higher water content can easily be reached, at least for a short time. It is exactly this over-capillary water which in the early observations leads to an overshoot, and in the later phase to an apparent reversed flow. Indeed it seems that, when the mortar develops an increasing capillary suction e.g. through the formation of hydration products, this over-capillary water (at very low suction potential) is available for backward flow.

Figure 11 displays the calculated cumulative fluxes over the interface for all measurements and model calculations. Experimental fluxes were calculated as the integral of the moisture content curve in the brick, truncated at capillary water content. Here again it can be noted that the overshoot due to over-capillary water in the brick is the main aspect that is not captured by the model. In general however the correspondence to the measurements is satisfactory and the observed trends are reproduced. It can be noted that the initial overshoot is stronger in the moulded brick than in the extruded brick because of the higher permeability near liquid saturation.

Another interesting possibility of the simulation is the information about the flow velocity of the liquid. Especially in the beginning of the process this velocity can be quite high and have an influence on the structure of the interfacial zone. This early flow is very difficult to measure experimentally: in our setup there are no data prior to 1990s. They are calculated here by dividing the flux [kg/m^2] by the time step [s] and the capillary porosity [kg/m^3] of the brick. This means that the result gives an idea of the real velocity in the pores, and not of the macroscopic velocity over the representative volume element. The initial time step for calculation was set on $1.0 \cdot 10^{-3}$ s to obtain the values below 1 s. Figure 12 shows the outcome during the first 25 s after brick-mortar contact. It appears that the predicted initial velocity can be up to 50 mm/min. During the very first stage of approximately 0.25 s the water

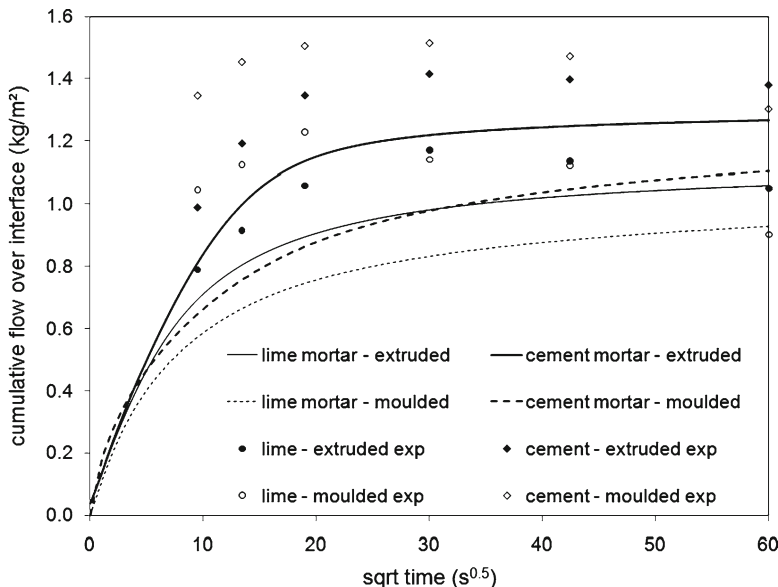


Fig. 11 Overview of water mass fluxes over the mortar-brick interface for all combinations, measured and simulated with the HAM-model (postfix 'exp' for measurements and 'mod' for simulations)

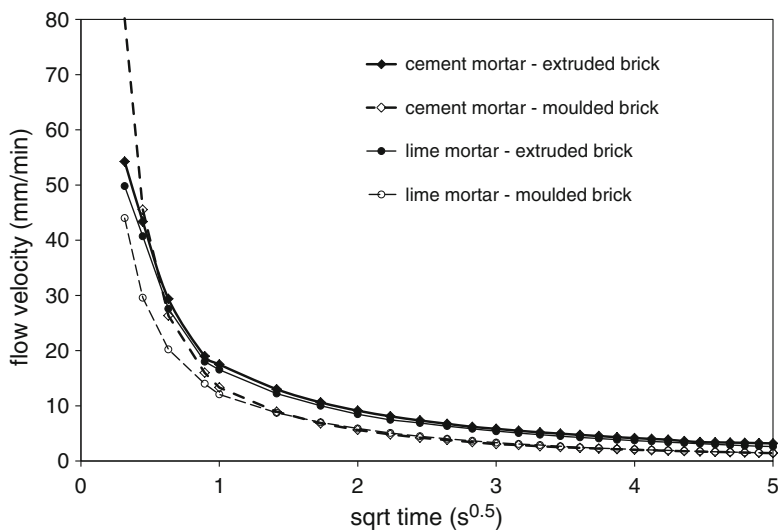


Fig. 12 Flow velocities of the water at the interface, calculated from simulated data

retention of the mortar is dominant: cement mortar loses water faster than lime mortar. But very soon the transport properties of the brick starts to play and the extruded brick leads to a higher velocity in the pores than the moulded brick. This means that the larger suction of the extruded brick dominates the difference in permeability at

that moment. It is useful to consider this result in combination with the profiles in Fig. 10: the extruded brick draws more water out of the mortar, but this water remains longer in the zone near the interface, because redistribution is slower than in the moulded brick.

It is possible that the results in Fig. 12 are a slight overestimation: such would be the case if inertia has a non-negligible effect. In the simulation software inertia effects are neglected. If water passes binder and sand particles at a relative velocity of 60 mm/min or 1 mm/s, the viscous drag on a 1 μm radius sphere would be in the order of magnitude of 10^{-10} N . This is much larger than inertial forces, which are around 10^{-13} N . Considering that viscous drag scales with velocity, it can be assumed that all submicron particles can easily be dragged by the water flow during the first phase of desorption. Probably the blockage of moving particles due to clogging in pores is the major factor to prevent their free movement. Only after 7 min or more the liquid velocity has decreased too much to be able to overcome gravity.

6 Discussion and Conclusions

This paper presents recent developments in both experimental and numerical assessment of the desorption process between a wet mortar and a dry porous brick. A methodology was presented to measure both water retention and permeability of fresh mortars. First a combination of adapted measuring devices and setups was applied. Secondly a set of semi-empirical model-equations was proposed for the analysis of data and the expression of water retention curve and permeability curve.

The obtained data for two mortars (lime mortar and cement mortar) were used together with the transport parameters of two bricks (one extruded, one moulded) for the numerical simulation of early water transport between both. The results were verified with observations by X-ray radiography. The most important conclusions are:

- The model and the measurements agree fairly well on the shape and position of the moisture profiles and on the final water content after 60 min. This can be considered as a validation for the use of the selected material parameters, measuring procedures and model code.
- A discrepancy between model and observations is related to over-capillary behaviour: such behaviour is not modelled in state-of-the-art HAM simulation software, but it is demonstrated that it is rather important in masonry practice.
- The left-over water content in the mortar joint after 60 min depends mostly on the water retention properties of the mortar: the lime mortar retains some 60% of its initial water amount, the cement mortar only 30%. The influence of the type of brick is smaller.
- Within a lime mortar gradients of water content can develop, which is not the case in a normal cement mortar. This is explained by the higher water retention and lower permeability of the lime mortar.
- The modelled and measured fluxes across the interface are comparable in magnitude: it can be assumed that the interface resistance is small.

- The modelled liquid velocity in the pores is about 1 mm/s during the first 0.1 s but it decreases with a factor 10 in less than 4 s. The magnitude of the velocity during the first 7 min or more is high enough to drag along the smallest binder particles.

Acknowledgement Hans Janssen is kindly acknowledged for providing the parameters of the extruded brick and for his advice in using HAMFEM software.

References

1. Groot, C.: Effects of water on mortar-brick bond. Technische universiteit Delft (1993)
2. Hendrickx, R.: The adequate measurement of the workability of masonry mortar. Katholieke universiteit Leuven (2009)
3. Holm, A., Krus, M., Künzel, H.M.: Moisture transport through interfaces in masonry (in German). Int. Z. Bauinstandsetz. **2**, 375–396 (1996)
4. Derluyn, H., Janssen, H., Carmeliet, J.: Influence of the nature of interfaces on the capillary transport in layered materials. Construct. Build Mater. **25**, 3685–3693 (2011)
5. Brocken, H.J.P.: Moisture transport in brick masonry: the grey area between the bricks. Technische universiteit Eindhoven (1998)
6. Brocken, H.J.P., Spiekman, M.E., Pel, L., Kopringa, K., Larbi, J.A.: Water extraction out of mortar during brick laying: a NMR study. Mater. Struct. **31**, 49–57 (1998)
7. Groot, C., Larbi, J.: The influence of water flow (reversal) on bond strength development in young masonry. Heron **44**, 63–78 (1999)
8. Roels, S.: A comparison of different techniques to quantify moisture content profiles in porous building materials. J. Build. Phys. **27**, 261 (2004)
9. Hendrickx, R., Roels, S., Van Balen, K.: Measuring the water capacity and transfer properties of fresh mortar. Cem. Concr. Res. **40**, 1650–1655 (2010)
10. Carmeliet, J.: Determination of the moisture capacity of porous building materials. J. Build. Phys. **25**, 209 (2002)
11. Roels, S., Carmeliet, J., Hens, H.: HAMSTAD WP final report. Moisture transfer properties and material characterisation (2003)
12. Van Genuchten, T.: A closed-form equation for predicting the hydraulic conductivity of unsaturated soils. Soil Sci. Soc. Am. J. **44**, 892–898 (1980)
13. Roels, S., Carmeliet, J.: Analysis of moisture flow in porous materials using microfocus X-ray radiography. Int. J. Heat Mass Transf. **49**, 4762–4772 (2006)
14. Janssen, H.: Conservative modelling of the moisture and heat transfer in building components under atmospheric excitation. Int. J. Heat Mass Transf. **50**, 1128 (2007)

Problems in the Assessment of the Stress-Strain Relationship of Masonry

Claudia Neuwald-Burg and Matthias Pfeifer

Abstract In the restoration or repair of old buildings, the correct estimation of the stress-strain-relationship of the existing structure is an important task. Masonry stiffness is crucial to the load bearing behaviour of a structure. When detailed investigations are lacking, it is common practise to evaluate the masonry stiffness from the compressive strength by standardised empirical relations established for various types of modern masonry. This paper illustrates the danger of this approach in two case studies. The first example is a stone bridge upon the Main at Ochsenfurt. The thickness of the mortar joints in this construction allowed the sampling of mortars suitable for the direct testing of the stress-strain relationship under uniaxial compression. Thus it was possible to calculate the masonry stiffness from the measured elastic modulus of stone and mortar. It became evident that a first rough estimation according to the building standard would not have been safe. In a second case study dealing with masonry pillars it is shown that the quality of mortar samples are influenced by the position of mortar in the masonry section.

1 Introduction

Refurbishment often implies the occurrence of a change of load. Constructions built with slim pillars and old stone bridges subjected to dynamic loads are very susceptible to modifications of this kind. Stiffer parts of the building attract stresses and therefore underestimation of stiffness can be harmful. Medieval or baroque masonry with small units of different types of stone is often too heterogeneous for *in-situ* tests by flat jacks or by sonic tests [1]. The elastic modulus is then evaluated from the moduli of stone and mortar prisms. The modulus of mortar can be derived either from the ultrasonic pulse velocity or from cube strength if suitable mortar prisms for

C. Neuwald-Burg (✉) • M. Pfeifer
Karlsruher Institut für Technologie, MAI, Karlsruhe, Germany
e-mail: claudia.neuwald@t-online.de; matthias.pfeifer@kit.edu

direct determination of stress-strain curves cannot be obtained in sufficient number. Another reliable method for the indirect testing of masonry strength is the method of bed joint drill cores. The ratio of the splitting tensile strength of bed joint drill cores and homogeneous stone cores is approximately equal to the ratio of stone crushing strength and masonry strength [2]. Thus the influence of the mortar joint is taken into account.

By combining these methods the elastic modulus of historic masonry can be assessed with sufficient accuracy for most cases of restoration work, provided that the correlations between the investigated parameters are clearly understood.

2 Case Study: Stone Bridge

The remaining piers and vaults of the medieval stone bridge upon the Main at Ochsenfurt (Southern Germany) date from three different building periods; the Middle Ages, Baroque and nineteenth century (see Fig. 1). The span of arches is between 13 and 16 m. Although the parts in the waterway are missing today, this bridge preserves important information for building history and therefore is protected as a historic monument. Plans to reuse the old structure and rebuild a carriageway raised the question of the strength and deformation properties of the historic remains. Due to the heterogeneity of this masonry and the multitude of stone varieties used, investigations by non-destructive testing methods appeared not to be promising. It was decided to refer to mechanical tests on stone and mortar. These investigations were carried out at the Institute of load bearing structures at the Karlsruhe Institute of Technology (KIT).



Fig. 1 Old bridge upon the Main. Baroque and nineteenth century masonry vaults on the northern bank. The vaults on the southern side of the river (*left*) date from the twelfth to fifteenth century



Fig. 2 Baroque masonry bond

2.1 Sampling

Samples were taken as drill cores with diameters of 93 mm. The relatively large size was chosen in order to obtain bed joint drill cores.

The sampling locations were chosen after diligent visual examination from places which from their exposure were most suspected of being damaged [3]. Reference samples from “healthy” masonry served to understand and calibrate the results.

The oldest parts of the bridge, three vaults on the southern side of the river, date back to the twelfth and fifteenth centuries. Various sizes of roughly carved or chopped stone (average $30 \times 25 \times 50$ cm 3) are still assembled in a good and regular rubble bond. The mortar and limestone has suffered from freeze/thaw and salt degradation due to a dense cement rendering. Endoscope investigation of boreholes however proved that the bed joints were thoroughly filled and that the mortar in the interior of the vaults was well preserved. The drill cores contained large pieces of mortar with a good bond to the limestone and surprising strength. The thickness of the mortar joints (between 2 and 4 cm) permitted sampling of mortar for direct mechanical tests.

On the northern side of the river two vaults from the baroque period and three arches from the nineteenth century are preserved. The baroque arches were built with small rubble material ($25 \times 15 \times 30$ cm 3) and were in a poor condition (Fig. 2). Similar to the medieval vaults, mortar was severely damaged at the surface and large parts of the vault had been repaired with brick masonry fillings (Fig. 3). Behind the deteriorated or repaired surfaces the masonry was in much better condition. Drill cores from the inner section or the baroque vaults contained pieces of mortar that



Fig. 3 Destroyed surfaces and brick masonry fillings



Fig. 4 Nineteenth century masonry composed of large ashlar

were extremely hard. Most of these samples could not be cut into cubes or prisms for mechanical tests due to their irregular shape. Strength and modulus values were therefore assessed using ultrasonic pulse velocity.

The vaults erected in the nineteenth century consist of massive limestone ashlar ($30 \times 48 \times 60\text{--}80 \text{ cm}^3$) with thin bed joints (Fig. 4). Some of the cores presented a very hard mortar up to a depth of 5–10 cm while the material behind was deteriorated from freeze thaw actions (Fig. 5). The loose mortar material was washed out



Fig. 5 Friable mortar behind dense repair

during drilling. Mortar deterioration here was induced by a dense repointing mortar (twentieth century repair) which retained water in the inner section. Cutting mortar prisms or cubes was not possible in this case. The regular shape of the ashlar allowed the assessment of masonry strength by the bed joint drill core method. Cautious drilling with controlled water cooling permitted the sampling of bed joint drill cores, in spite of the friability of the mortar.

The amount of mortar, its state of conservation and the composition varied not only with the construction phases but also within the same section. A repair mortar that could chemically and mechanically match with the original mortar still preserved inside the pillars was needed; as was the identification of the mechanical properties of the existing mortar in order to determine masonry stiffness.

2.2 Mechanical Tests

The mortars from the drill cores were cut into regular cubes and prisms (thickness between 3 and 4 cm) whenever possible (Fig. 6). Although the mortars were of good quality, many of the specimens cracked during cutting. A total of 9 prisms and 30 cubes were obtained. The samples were denominated according to the number of the vault, the location in the arch and a current number. M9.3.4 for instance is the fourth sample from sampling point 3 in vault 9.

After drying, the prisms were tested under uniaxial compression. Load was applied displacement controlled with a speed of 0.1 mm/min (Fig. 7). Figure 8 shows characteristic stress strain curves of mortars from each building period of the bridge.

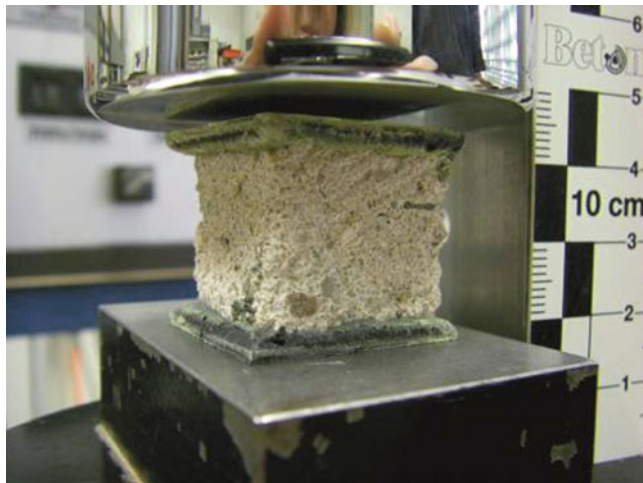
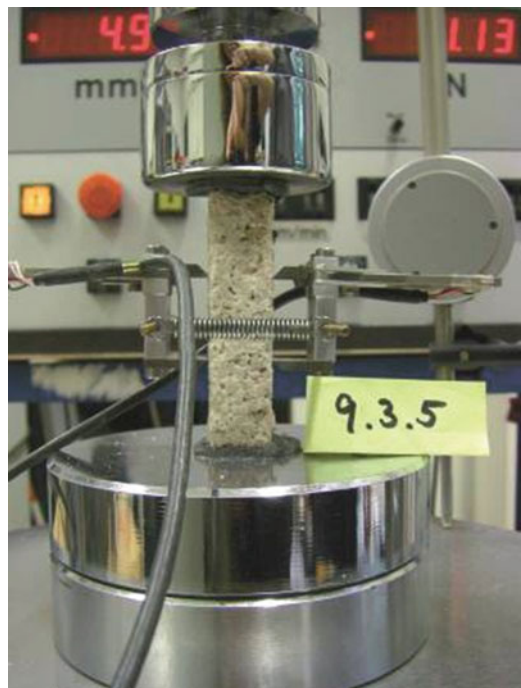


Fig. 6 Mortar cube for compressive test cut from bed joint. A total of 30 samples were tested

Fig. 7 Mortar prism with displacement transducers at mid height on opposite faces. Sample size approximately 20 by 20 by 80 mm



Typical for the old lime mortars, examples M1.1.2 and M3.2.7, is the concave shape of the rising branch and a long yielding plateau after reaching the crushing strength. Compared to line M3 (repair), which was a brittle cement repair mortar, the old lime mortars are significantly more ductile. In spite of the low modulus, they present an astonishing uniaxial compressive strength of more than 5 N/mm².

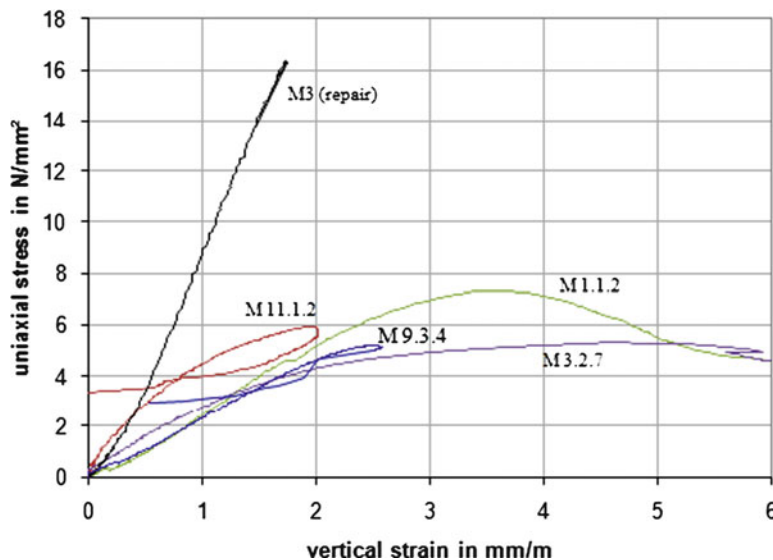


Fig. 8 Stress-strain relationship of medieval (M1, M3) and nineteenth century mortars (M9, M11) compared to a pure cement twentieth century repair mortar

Table 1 Relation between dynamic and static modulus $E_{\text{dyn}}/E_{\text{stat}}$

Sample building period	E_{dyn} [N/mm ²]	E_{stat} [N/mm ²]	$E_{\text{dyn}}/E_{\text{stat}}$ [N/mm ²]
M1.1.2	4,640	2,443	1.90
M3.2.7 middle ages	6,698	3,225	2.08
M3.5.1 – baroque period	9,924	8,021	1.24
M9.3.3	4,694	3,548	1.32
M9.3.4	5,705	2,260	2.52
M9.3.5 nineteenth century	6,577	5,768	1.14
M9.3.6	7,492	5,785	1.30
M9.3.7	8,026	6,819	1.18
M11.1.2	5,678	6,819	0.83
Average			1.50
Standard deviation			0.51
Coefficient of variation [%]			34

The nineteenth century mortars (example M9.3.4 and M11.1.2) equally showed a concave rise of strain, but once they reached the crushing strength there was complete rupture. This behaviour was observed on all of the five specimens from the nineteenth century parts of the bridge.

From the stress-strain curves the static elastic modulus was calculated as a chord modulus between zero stress and one third of the peak stress. For results see Table 1.

Table 2 Evaluation of Edyn (P-wave modulus) for the main building periods

Sample	Building period			
	n	E_{dyn}^1 [N/mm ²]	n ¹ /n	E_{dyn}^1 [N/mm ²]
1.1	8	4,403		
2	2	5,354		Middle ages
3.2	6	5,816	16/3	5,052
3.5	3	10,204		Twentieth century, repair mortar
9.2	5	4,960		
9.3	7	6,358		Nineteenth century
11.1	8	7,519	20/3	6,473
12.3	7	5,772		Baroque
12.1	2	2,883	9/2	5,130

n^1 total number of samples

n^2 number of sampling locations

E_{dyn}^1 average value

2.3 Ultrasonic Tests

Since no direct measurement was possible on mortar from the baroque masonry and only a few samples of medieval mortars could be tested, the elastic modulus was verified by ultrasonic tests. From the ultrasonic pulse velocity v the dynamic modulus, or P-wave modulus, is calculated with the density as:

$$E_{dyn} = \rho \cdot v^2 \quad (1)$$

Table 1 compares moduli obtained by direct testing to those calculated from the pulse velocity. For concrete or cement mortar the dynamic modulus is about 30% higher than the static modulus [4]. Here the difference seems to be larger; 50% were measured in this series but the coefficient of variation is too high to permit a generalisation; however it was shown qualitatively that the baroque mortars behave similar to those of the older part of this building (Table 2, Fig. 9).

Chemical and mineralogical investigations carried out at the Federal Institute for Materials Research and Testing (BAM) in Berlin confirmed that mortars of both medieval and baroque building periods had a very similar composition.

Ultrasonic tests could also be adopted to assess the compressive strength if a reliable correlation between the dynamic modulus and strength was known. In Fig. 10 the elastic modulus is related to the compressive strength measured in direct compression tests on cubes (edge length between 15 and 35 mm) of medieval mortars and on samples from the nineteenth century masonry (see Fig. 6).

This is compared with the empirical relation that was established for new masonry mortars by Schubert [4].

$$E_m = 2100 \cdot f_m^{0.7} \quad (2)$$

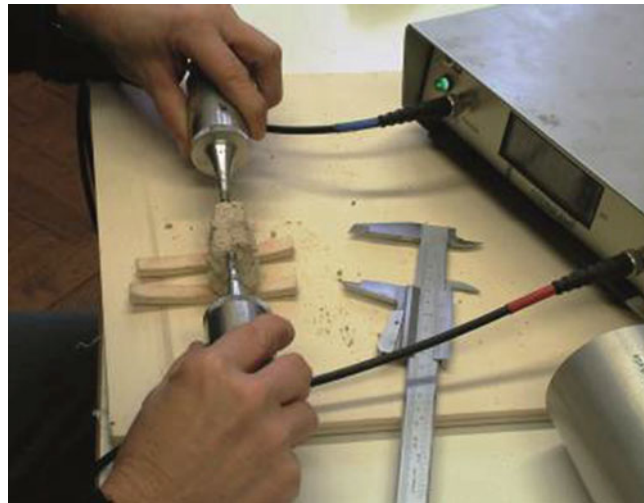


Fig. 9 P-wave velocity measurement on friable mortar prism

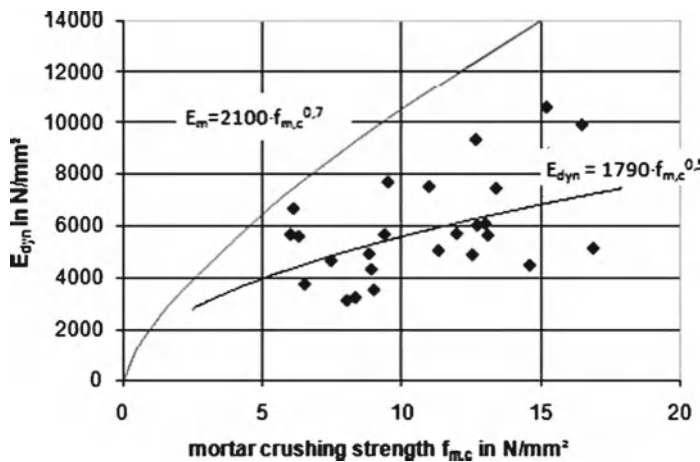


Fig. 10 Relationship of mortar strength and elastic modulus

The measured data would rather be described by the equation

$$E_m = 1790 \cdot f_m^{0.5} \quad (3)$$

still with a very low coefficient of determination ($R^2=0.234$).

It becomes evident that the behaviour of old mortar cannot be determined from property relations found in modern material without adaption. A similar problem has been observed in trying to establish shape factors for compression tests on weak mortars with different lime binders [5]. Test methods need individual calibration.

Fig. 11 Bed joint drill core

2.4 Masonry Assessment

After investigation of the stone properties and the geometric parameters the masonry strength was calculated using the following: the German national standards (DIN 1053 and DIN ENV 1996 (EC6)) and calculations based on the analytical models from Sabha [6]. While allowable stresses according to the design standards would have been between 1.7 N/mm² for the weaker masonry bond and 2.3 N/mm³ for the ashlar masonry, stresses from of 3.1 to 3.9 N/mm² could be allowed according to the results of the analytical approach. Still the limited number of mortar samples and the wide scattering constituted an element of uncertainty. For this reason a third approach was tested, the method of bed joint drill cores (Fig. 11). The advantage of this method is that the influence of mortar strength and stone-mortar-bond is taken directly into account without further preparation of individual mortar samples. This procedure was developed by Berger [2] for brick masonry and has been modified for ashlar masonry by Egermann [7, 8]. It is based on the observation that the ratio between splitting tensile strength of homogeneous drill cores from stone and drill cores containing a mortar bed is similar to the ratio between the compressive strength of stone and masonry strength.

This relation is valid for stone masonry with even bed joints if the thickness of the mortar bed is less than 0.1 of the height of the stone unit. For higher stone-mortar ratio the stress distribution of a bed joint core does not represent the stress distribution within the wall. Masonry strength rises with decreasing relative joint thickness t_m/t_s . According to Egermann, the influence of geometry

Table 3 Calculation of masonry strength from tests on stone and bed joint drill cores

		Middle ages	Baroque	Nineteenth century
Medium splitting tensile strength of bed joint core	$f_{j,st}$ [N/mm ²]	2.24	2.34	1.57
Medium splitting tensile strength of stone	$f_{s,st}$ [N/mm ²]	3.84	3.84	3.84
Compressive strength of stone	$f_{s,c}$ [N/mm ²]	30	30	30
Ratio of splitting tensile strength of stone and bed joint core	$a = f_{j,st}/f_{s,st}$	0.583	0.609	0.409
Joint thickness (average)	t_m [mm]	30	30	30
Diameter of the bed joint drill core	d_j [mm]	93	93	93
Medium height of stone unit	t_s [mm]	150	150	300
Geometric coefficient	k	1.3	1.3	1.6
Masonry compressive strength	$f_{w,0}$ [N/mm ²]	23.1	24.1	19.6
Allowable stresses	f_d [N/mm ²]	4.4	4.5	3.9
Number of tests	n	9	7	22

can be considered by a geometric coefficient derived from experimental data by regression analysis [8, p. 136],

$$k = \frac{1 + 3,24 \cdot \sqrt{\frac{t_m}{d_j - t_m}}}{1 + 3,24 \cdot \sqrt{\frac{t_m}{t_s}}} \quad (4)$$

where t_s is the height of stone and t_m the bed joint thickness. d_j is the diameter of the bed joint core. The medium compressive strength $f_{w,0}$ of a single leaf ashlar or squared stone wall then can be assessed as:

$$f_{w,0} = k \cdot \frac{f_{j,st}}{f_{s,st}} \cdot f_{s,c} \quad (5)$$

The results of the material investigations and the geometric parameters which have been used to calculate the masonry strength are summarized in Table 3.

Again the results of the medieval samples are close to those of the baroque arches. The compressive strength in Table 3 has to be considered as a medium crushing strength. It is converted to the characteristic strength by a reducing factor of 0.85 for the decrease of strength under sustaining load and a factor of 0.7 for the difference between average strength and 5% fractile. Applying a global safety factor of $\gamma=3.0$ the allowed stresses are obtained:

$$f_d = 1/3 \cdot 0.85 \cdot 0.7 \cdot f_{w,0} \quad (6)$$

The values show that the compressive strength calculated from the stone and mortar properties were sufficiently safe.

2.5 Elastic Modulus of Masonry

In masonry design the elastic modulus E_{ma} is evaluated from the design strength f_d as:

$$E_{ma} = 3500 \cdot f_d \quad (7)$$

For the older parts of the bridge this would have given a value of 6,000 and 8,000 N/mm² for the ashlar masonry. Since strength values allowed by the modern masonry standards are on the very safe side for stone masonry Eq. 7 underestimates the true masonry stiffness. Especially the nineteenth century masonry, built with large blocks of limestone and so must be more rigid; however even the modulus of the older parts was underestimated by this approach, in spite of the important amount of mortar in these piers.

Using the elastic models for two phase components proposed by Anzani et al. to describe rubble masonry [9], the elastic modulus can be calculated from the stone and mortar properties with good accuracy as follows:

$$\frac{1}{E_{ma}} = \frac{(1 - V_s)^2}{E_m \cdot V_m} + \frac{V_s}{E_s} \quad (8)$$

The model includes the volumes V of stone and mortar and their actual elastic properties. Thus average values of 15,000 N/mm² for the rubble masonry (medieval and baroque arches) and 23,000 N/mm² for the ashlar bond were obtained.

3 Case Study: Baroque Masonry Pillars

In refurbishing the Historic Museum in Frankfurt, the architects intend to increase the load on the pillars of a three storey baroque facade (Fig. 12). A first rough estimation, according to the German masonry standard, indicated that the existing load already exceeded the allowable stresses at least twice. Nevertheless the pillars showed neither cracks nor crushed joints nor any other signs of overloading. A more precise analysis based on material tests and the recalculation of masonry strength using more accurate material models indicated that the higher loads could be allowed for under the condition that the slots and voids discovered in the piers were repaired to allow the section to act as one material. It was therefore vital that the repair masonry must have the identical deformation properties as the original masonry.

Investigations of the material properties here served to assess masonry strength and stiffness in as accurate a manner as possible and to determine the stone and mortar properties necessary for appropriate materials for repair. Initially the thickness of the joints seemed large enough to allow the removal of mortar prisms with a hammer and chisel. It was then observed that the mortar samples close to the surface showed poor cohesion whereas the bed joints in the inner section showed no decay (Fig. 13). Inside of the building this could not be explained by the effects of weathering.



Fig. 12 Baroque masonry pillars



Fig. 13 Mortar samples—
inner section

On mortar cubes from the inner section of the pillars an average compressive strength of 1.85 N/mm² was measured. The strength, as determined by ultrasonic tests, corresponded very well with this result (1.90 N/mm²). Mineralogical analyses confirmed that the mortars were pure lime mortars without hydraulic additives. From earlier research it is known that these mortars plastify at the outer rims of a masonry section at a rather low stress level, up to a depth of some centimetres [10]. The sections of the masonry pillars in this case are large in relation to the plastification zone. Masonry stiffness is therefore not influenced but mortar should be sampled by core drilling in order to obtain sound material.

The stone and masonry bond differed throughout the different pillars; tests on stone and mortar lead to an estimation of the masonry strength between 1.1 and 2.3 N/mm², depending on the bond. The elastic modulus calculated from stone and mortar properties and the geometric relations again exceeded the first estimations with values between 8,000 and 9,500 N/mm² being determined.

4 Conclusions

When assessing the elastic behaviour of old lime mortar masonry the correlations determined empirically on modern material should be handled with care.

- Strength of existing masonry is usually underestimated for reasons of safety. Evaluating the elastic modulus from this value leads to an underestimation of stiffness.
- The more the detailed properties of stone and mortar are investigated, the more accurate the assessment of the load bearing behaviour of old masonry is. Combining direct tests on stone and mortar prisms or on bed joint drill cores allow the calibration of ultrasonic measurements. Masonry properties can then be calculated from analytical models.
- Stress distribution in masonry with very strong stone units and weak joints is not uniform. The quality of mortar is influenced by the position of the sampled mortar in the section. This observation is not to be neglected when choosing representative sampling points.
- In calculating the modulus of thin masonry sections from the elastic properties of stone and mortar under uniaxial compression, the plastification of mortar has to be taken into account.
- Due to weathering, salts, inappropriate repointing or dense renderings bed joint mortars frequently show signs of deterioration. The depth of deterioration influences the masonry's strength and elastic properties. Careful visual investigations in some cases are even more important for a correct assessment of the mechanical behaviour of masonry than sophisticated material models.

References

1. Binda, L., et al.: Investigation procedures for the diagnosis of historic masonry. *Construct. Build. Mater.* **14**(4), 199–233 (2000). doi:[10.1016/S0950-0618\(00\)00018-0](https://doi.org/10.1016/S0950-0618(00)00018-0)
2. Berger, F.: Assessment of old masonry by means of partially destructive methods. In: Brebbia C.A. (ed.) *Structural Repair and Maintenance of Historical Buildings*, Proceedings of the 1st International Conference on Structural Repairs and Maintenance of Historical Buildings, pp. 103–117. Florence, Southampton (1989)
3. Hughes, J.J., Callebaut, K.: In-situ visual analysis and practical sampling of historic mortars. *Mater. Struct./Matériaux de Constructions* **35**, 70–75 (2002). doi:[10.1007/BF02482103](https://doi.org/10.1007/BF02482103)
4. Schubert, P.: Eigenschaften von Mauerwerk, Mauersteinen und Mauermörtel. In: Irmschler, H.-J., Schubert, P., Jäger, W. (eds.) *Mauerwerkkalender*, pp. 3–27. Ernst & Sohn, Berlin (2005)
5. Drdácký, M., et al.: Compression tests on non-standard historic mortar specimens http://web.natur.cuni.cz/uwigug/masin/download/DMMS_HMC08.pdf (2008). Accessed 15 Oct 2009
6. Pöschel, G., Sabha, A.: Ein theoretisches Modell zum Tragverhalten von Elbsandsteinmauerwerk. In: Wenzel F. (ed.) *Erhalten historisch bedeutsamer Bauwerke*, pp. 111–118. Jahrbuch 1993 des SFB 315 (1996)
7. Wenzel, F. (ed.): Historisches Mauerwerk, Untersuchen, Bewerten und Instandsetzen. Erhalten historisch bedeutsamer Bauwerke – Empfehlungen für die Praxis. Karlsruhe Sonderforschungsbereich, Karlsruhe (2000)
8. Egermann, R.: Tragverhalten mehrschaliger Mauerwerkkonstruktionen. In: *Aus Forschung und Lehre, Inst. für Tagkonstruktionen*, Heft 29, Karlsruhe, S. 136 (1995)
9. Anzani, A., Binda, L., Fonta, A., Henriques, P.: An experimental investigation on multiple-leaf stone masonry. In: *Proceedings of the 13th International Brick/Block Masonry Conference*, July 4–7, Amsterdam, 10 p. CD-ROM (2004)
10. Neuwald-Burg, C.: Investigations into the stress strain relationship of old brickwork. In: *Proceedings of the 5th International Masonry Conference*, pp. 301–309. London (1998)

Influence of the Mechanical Properties of Lime Mortar on the Strength of Brick Masonry

Adrian Costigan and Sara Pavía

Abstract This paper aims at improving the quality of lime mortar masonry by understanding the mechanics of mortars and masonry and their interaction. It investigates how the mortar's compressive and flexural strengths impact the compressive and bond strength of clay brick masonry bound with calcium lime (CL) and natural hydraulic lime (NHL) mortars. It concludes that the strength of the bond has a greater impact on the compressive strength of masonry than the mortar's strength. The masonry compressive strength increased proportionally to the strength of the bond up to 6 months. A regression analysis, giving a second order equation with coefficient of determination (R^2) of 0.918, demonstrates a strong and predictable relationship between bond strength and masonry compressive strength. It was noted that CL90s mortar masonry reaching a high bond value was stronger than that built with a stronger mortar but displaying a poorer bond. Finally, the mechanics of lime mortars and their masonry are similar. The predominantly elastic behaviour of the mortars of higher hydraulic strength compares well with the elastic and brittle behaviour of their masonry, with either little (NHL2) or non-existent plasticity (NHL3.5 and 5); in contrast, the CL90 mortar and masonry exhibit a plastic behaviour.

1 Introduction

Mortars influence masonry to such a great extent that they can either enhance or adversely affect the durability of masonry. It is widely accepted that, to ensure durability, historic mortars should be replaced with similar, compatible mixes. Research has focused on specifying repair mortars based on the characteristics of the originals.

A. Costigan • S. Pavía (✉)
Department of Civil, Structural & Environmental Engineering,
Trinity College Dublin, Dublin, Ireland
e-mail: costigaf@tcd.ie; pavias@tcd.ie

Rather, this work proposes to understand the mechanical properties of mortar and masonry and their interactions in order to specify mortar repairs. It does not consider the properties of the original mortar but those of the new mortars, building units and resultant masonry. It investigates compressive and bond strength of masonry bound with lime mortars of diverse hydraulic strength (made with non hydraulic as well as feebly, moderately and eminently hydraulic limes) and thus different stiffness and deformability.

There is no agreement on the mechanics of masonry and the reasons for failure; some authors give more importance to the mortar properties and deformation while others believe that it is the masonry units that determine failure. For example, it has been reported that mortar deformations have a greater effect on the behaviour of masonry structures than the strength/stiffness of the units [1], and that the difference in the elastic properties of unit and mortar is the precursor of failure in compression ([2] referring to Hilsdorf 1969 and McNary and Abrams 1985). In contrast, according to other authors [3], the crushing strength of the weakest brick, rather than the interaction between brick and mortar, often determines masonry strength; and this can mask the influence of the mortar's strength on the strength of the masonry. Yet other authors have stated that masonry compressive strength is not sensitive to bond strength variations when the masonry unit is stiffer than the mortar [4].

Uniaxial compression of masonry leads to a state of tri-axial compression in the mortar and of compression/biaxial tension in the unit: during compression, lime mortars expand laterally more than bricks due to their lesser stiffness, however, within masonry, the mortar is laterally confined at the brick-mortar interface. As a result, shear stresses at the interface result in an internal state of stress which consists of triaxial compression in mortar and bilateral tension coupled with uniaxial compression in bricks. This state of stress initiates vertical splitting cracks in bricks that lead to prism failure ([5] referring to Atkinson and Nolan 1983 and Drysdale et al. 1994).

The strength of the bond between mortar and unit is essential, as it determines how the masonry transfers and resists stresses due to various applied loads. Water absorption has a significant influence on bond development and hence flexural strength [6, 7]. Mortars of different compressive strengths but similar bond strength result in similar masonry compressive strength; and both the bond strength and the masonry's compressive strength are not significantly impacted by the strength of the mortar [5, 8]. Current literature indicates that an increase in bond strength, while keeping the mortar strength constant, results in an increase in the compressive strength of the masonry [9]. The rate of brick absorption and the mortar water retention are essential to bond development, as they control moisture transport at the interface allowing for the formation of the hydrates that enable bonding [10]. Results by [11] agree with these, stating that the main mortar parameter that influences bond strength of NHL-mortar masonry is water retention, followed by water content and, finally, the mortar's hydraulic strength. These authors demonstrated that the strength of the bond is not determined by the hydraulic strength of the binder, but it increases with the mortar's water retention.

2 Materials and Methods

2.1 Materials

Mortars were made with CL90-s and three NHLs of hydraulic strengths 2, 3.5 and 5 MPa. A siliceous aggregate (particle size distribution ranging within the standard limits [12]) and moulded, frogged clay bricks (Table 1) were used. A binder: aggregate ratio of 1:3 by weight was kept constant as prescribed by the standards [12, 13]. In all compression and flexural tests the measured values are the arithmetic mean of three specimens; and the mean of five values for the flexural bond strength tests.

2.2 Mixing and Curing. Initial Flow and Workability

Water content is the main contributor to mortar workability and determines initial flow, a measurement that takes into account variables affecting workability, such as porosity, size/shape of aggregate, binder type and aggregate/binder [13]. Based on previous research [14] an initial flow of 165 ± 3 mm was specified for all mortars to ensure adequate workability. Initial flow was measured, and the water content reported as the ratio of water to total mortar by mass in accordance with EN 459 [14]. Mixing, curing and storage were in accordance with EN 459 [14]: at 20°C and 65% RH for CL90s; 7 days at 95% and 21 days at 65% for NHL2 and 3.5; and 95% RH for NHL5. Wallettes were constructed in accordance with EN 1052 for compressive, flexural and bond strength respectively [15–17] and cured and stored in exactly the same conditions as the corresponding mortar.

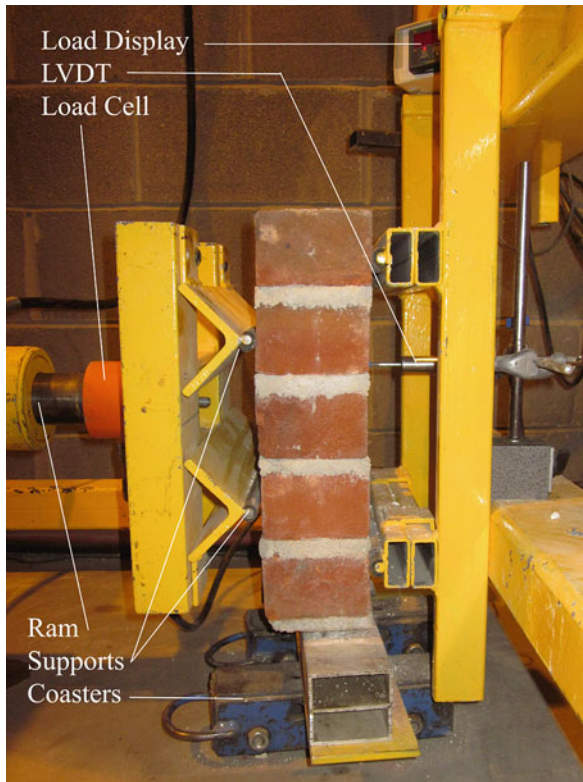
2.3 Mechanical Properties of Mortar

During the compression and flexural mortar tests, the force-strain curves were recorded in order to study the mechanical behavior of the mortars under load application.

Table 1 Brick characteristics

Property	(Testing standard: EN 771-1 :2003)
Compressive strength (N/mm ²)	≥12
Water absorption (%)	Max 15
Unit size (mm)/size tolerance	215×102.5×65/T2 – R1
Gross/net density (kg/m ³)	1,630/1,920
Initial rate of absorption (kg/m ² /min)	1.0

Fig. 1 Flexural strength masonry test set up



Compressive (R_c) and flexural (R_f) strength were determined on prisms as specified in the standards using Eqs. 1 and 2 [12, 13]. Where: F_c is the max load at fracture (N); 6,400-area of the face (mm^2); F_f -load at fracture (N); b -prism section (mm^2); l -distance between supports (mm).

$$R_c = \frac{F_c}{6400} \quad (\text{N / mm}^2) \quad (1)$$

$$R_f = \frac{1.5 \times F_f \times l}{b^3} \quad (\text{N / mm}^2) \quad (2)$$

2.4 Compressive, Flexural and Bond Strength of Masonry

The compressive and flexural strengths were tested according to EN 1052 parts 1 and 2 respectively [15, 16] on masonry wallets built according to the aforementioned standard (Fig. 1). During the compression and flexural masonry tests, force-strain



Fig. 2 Bond strength test set up

curves were recorded with the strain values provided by lateral variable displacement transducers continuously monitoring the change in length on application of the load. Equations 3 and 4 were used to determine the compressive (f_i) and characteristic compressive strength. Where: $F_{i,\max}$ -max load (N); A -loaded cross-section (mm^2). The flexural bond strength was determined with the bond wrench test according to EN 1052, using five-brick-high bonded prism stacks (Fig. 2) [13, 17].

$$f_i = \frac{F_{i,\max}}{A_i} \quad (\text{N / mm}^2) \quad (3)$$

$$f_k = \frac{f}{1.2} \quad \text{or} \quad f_k = f_{i,\min} \quad (\text{N / mm}^2) \quad \text{whichever is smaller} \quad (4)$$

3 Results and Discussion

3.1 Properties of Lime Mortars

As expected (Figs. 3 and 4), most hydraulic limes build strength faster and reach a higher ultimate strength. The NHL3.5 and 5 mortars gain compressive strength at similar rates throughout curing while the NHL2 mortar increases compressive

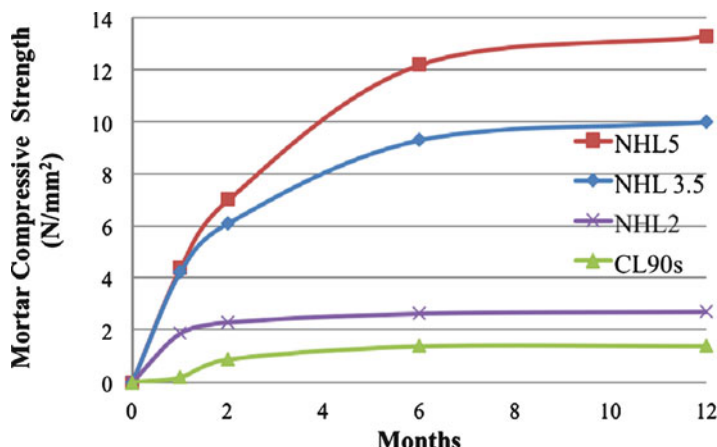


Fig. 3 Compressive strength of mortars

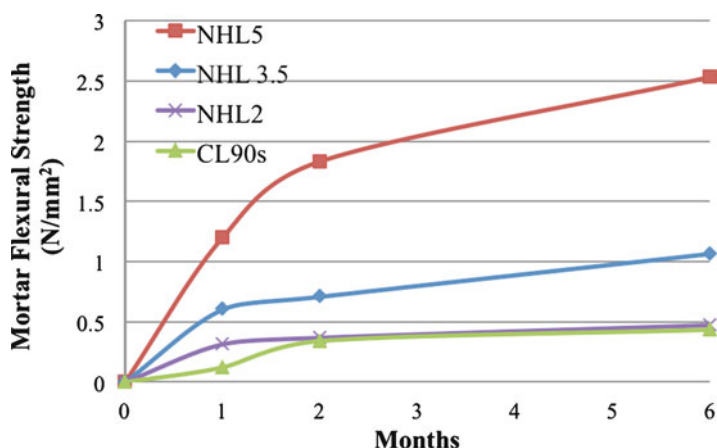


Fig. 4 Flexural strength of mortars

strength by only 18% between 1 and 2 months. The flexural strength of the CL90 mortar increases by 64% between 1 and 2 months and by a factor of 4 between 2 and 6. The flexural strength of NHL3.5 mortar also increases substantially between 2 and 6 months (by a factor of 3) while the NHL5 mortar increases by 35% between 1 and 2 months and again by 35% between 2 and 6 months.

The stress-strain results revealed that, under compression, the mortars of higher hydraulic strength exhibit a predominantly elastic behaviour whereas the NHL2 and CL90 mortars behave in a more plastic manner (Fig. 5). According to Fig. 5, under compression, the NHL5 mortar displays the greatest elastic region while the NHL2 and CL90 mortars show the smallest elastic regions and the greatest plasticity.

Fig. 5 Deformability of mortars under compression after 56 days of curing

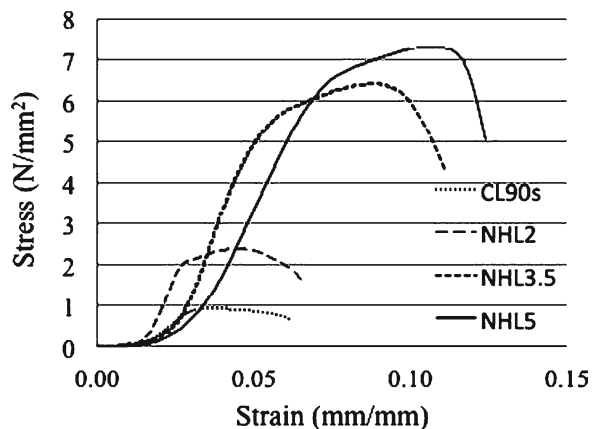
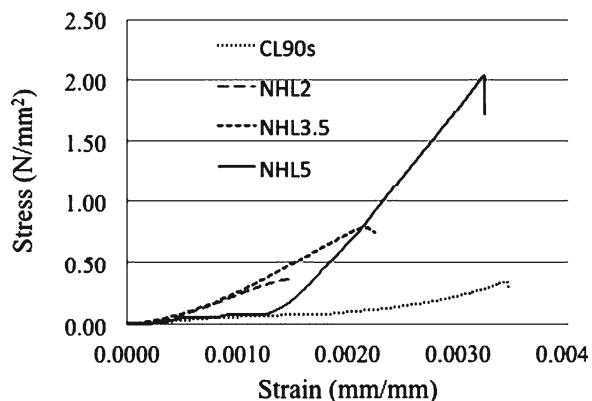


Fig. 6 Deformability of mortars under flexion after 56 days of curing



Therefore, extent of the elastic region increases while the plastic region tends to decrease as the mortar's compressive strength increases.

In flexion, the extent of the elastic region increases with the mortar's flexural strength (Fig. 6); and most mortars do not show a plastic region but strain linearly on stress application until failure occurs, and failure appears suddenly with no plastic deformation. In flexion, the CL90-s mortar strains significantly before failing at a relatively low strength when compared to the other mortars.

3.2 Properties of Masonry

The compressive strength development of NHL5 and 3.5 mortar masonry is similar (Fig. 7). Initially, they gain strength at the same rate; however after 28 days the NHL3.5 masonry gain is faster, becoming 6% stronger than the NHL5 masonry at 6 months and 5% at 1 year. This is due to the higher water demand of the NHL5

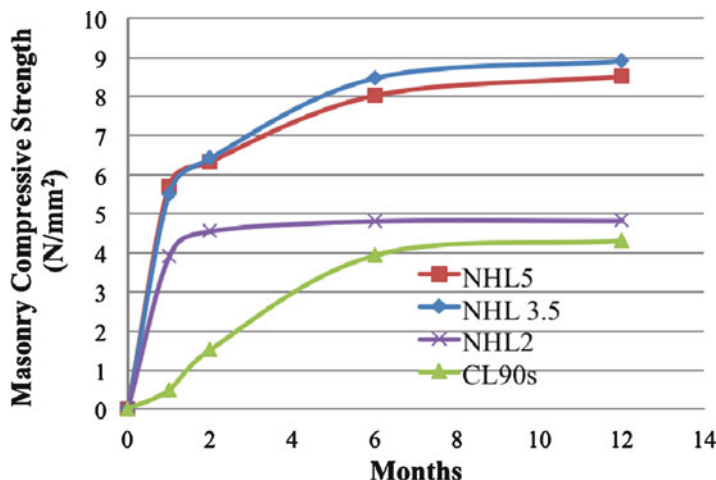


Fig. 7 Compressive strength of masonry

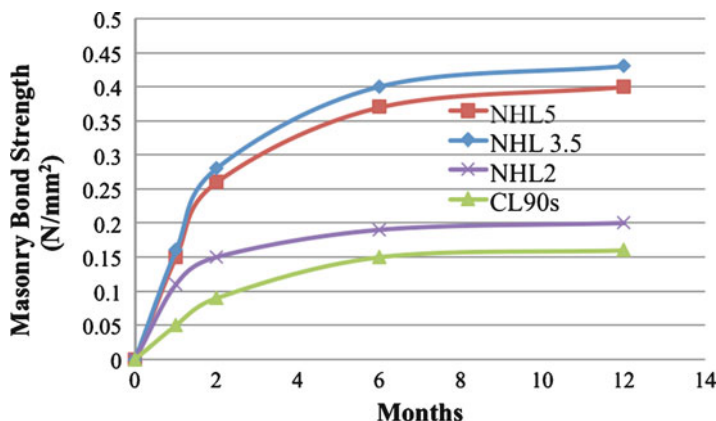


Fig. 8 Bond strength development over time

so that, at equal flows, the NHL3.5 mortar has more water available to develop a stronger bond.

The NHL5 and 3.5 masonry gain strength quickly; at 56 days both have reached over 70% of their 1-year strength. NHL2 shows a similar trend as significant gains occur in the first 28 days. In contrast, the largest gain of the CL90 masonry occurs between 2 and 6 months (at 150%), having gained over 90% of its 1 year strength at 6 months.

According to the bond strength results, 60–90% of the ultimate bond strength is achieved after 56 days (Fig. 8): at 2 months the CL90 masonry has reached 36% of its total 1 year bond strength, while NHL5 and 3.5 have reached 65%; the CL90 masonry bond strength at 6 months equals that of the NHL2 masonry at 2 months. However, the bond strength of the NHL3.5 masonry is greater than that of the NHL5 masonry (8% greater at 6 months).

Fig. 9 Deformability of CL90s, NHL2, NHL3.5 and NHL5 masonry under compression at 56 days

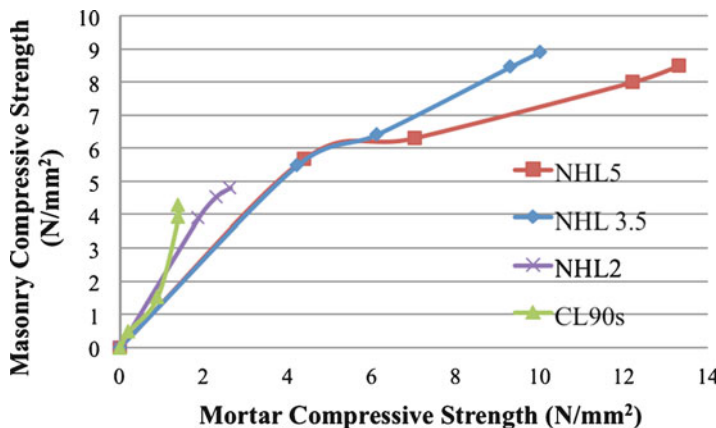
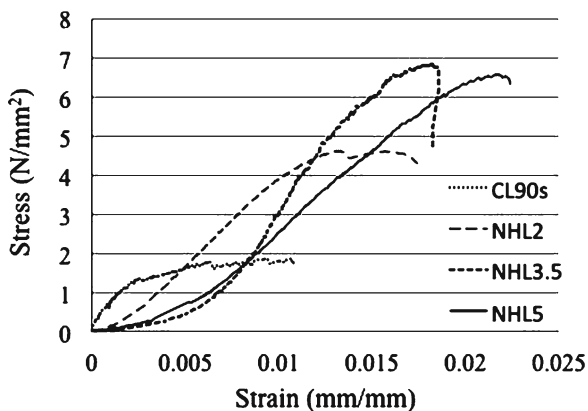


Fig. 10 Influence of mortar compressive strength on masonry compressive strength

As for the mortars (Figs. 5 and 6), the stress-strain curves of masonry in Fig. 9 evidenced the plastic behaviour of the CL90s masonry, supporting small stress increases while progressively deforming and displaying a short elastic region. In contrast, all the NHL mortar masonry displays large elastic regions and either little (NHL2) or no plasticity (NHL3.5 and 5). The results also showed that the NHL3.5 is stiffer than the NHL5 masonry and deflects less under the same applied stress.

3.3 *Influence of Mortar Properties on Masonry Strength*

The results evidenced that large increases in mortar compressive strength do not lead to significant increases in masonry compressive strength (Fig. 10). This agrees with previous authors [3, 6] stating that masonry compressive strength is not significantly impacted by mortar strength. As can be seen from the results, between

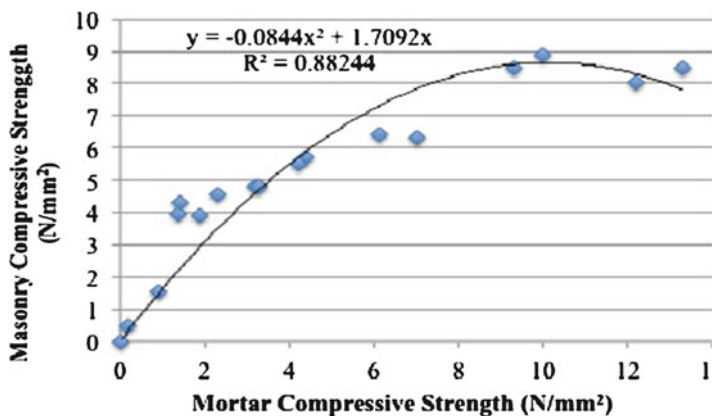


Fig. 11 Regression analysis of data in Fig. 10

28 and 56 days, the compressive strength of NHL5 mortar increases by 60% however, the corresponding masonry only increases by 11%. The same relationship is maintained between 2 and 6 months, where the mortar strength increases by 75% and the masonry's only by 30%. The regression analysis evidences that the values fit well with a polynomial line (R^2 value of 0.88), Fig. 11. This indicates a strong, non-linear relationship between mortar and masonry strength, with a maximum masonry strength of 8.9 N/mm^2 for this particular brick.

According to the results in Fig. 10, the mortars of higher hydraulic strengths (NHL5 and 3.5) are stronger than their corresponding masonry: after a year, the NHL5 mortar is stronger in compression (12.21 N/mm^2) than its masonry (8.01 N/mm^2); and NHL3.5 mortars follow the same trend (a 10 N/mm^2 mortar vs. a 8.9 N/mm^2 masonry). In contrast, NHL2 and CL90s show the opposite trend: the mortars have a mean 56 day compressive strength of 2.29 and 1.39 N/mm^2 respectively while their corresponding masonry strengths are much higher, at 4.54 and 4.3 N/mm^2 respectively.

In addition, the hydraulic strength of the lime (thus mortar strength) and the bond strength of the resultant masonry tend to display an inverse relationship (Fig. 12). As it can be seen from this figure, the lower the hydraulic strength of the lime (CL90s and NHL2 mortars) the faster the rate of bond strength increase therefore the bond develops faster in the mortars of lower hydraulic strength.

In relation to the impact of the mortar's flexural strength on the compressive and bond strength of masonry (Figs. 13 and 14 respectively). In general, the lower the hydraulic strength of the lime, the stronger the impact of the flexural strength of the mortar on the compressive and bond strength of the masonry.

As it can be seen from the results, bond strength has a much stronger relationship with the masonry compressive strength than mortar strength (Figs. 10, 15, 16 and 17). Statistical analysis (Fig. 16) shows a non-linear relationship and a R^2 value of 0.92 at 5% CI. This indicates that these two properties (masonry bond and compressive strength) are very closely related to each other. In addition, when

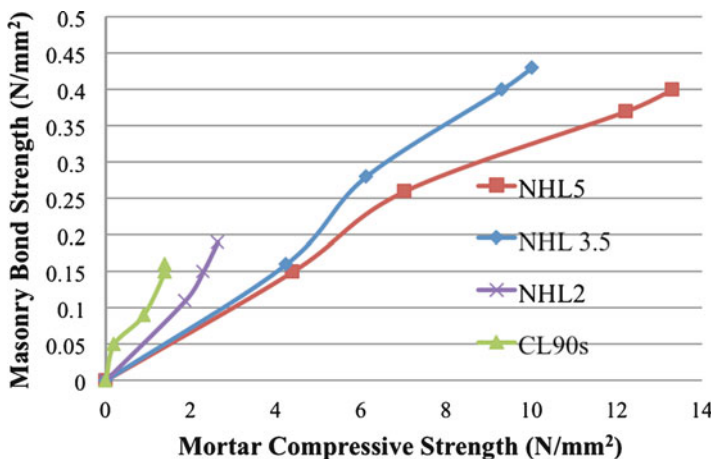


Fig. 12 Influence of mortar compressive strength on masonry bond strength

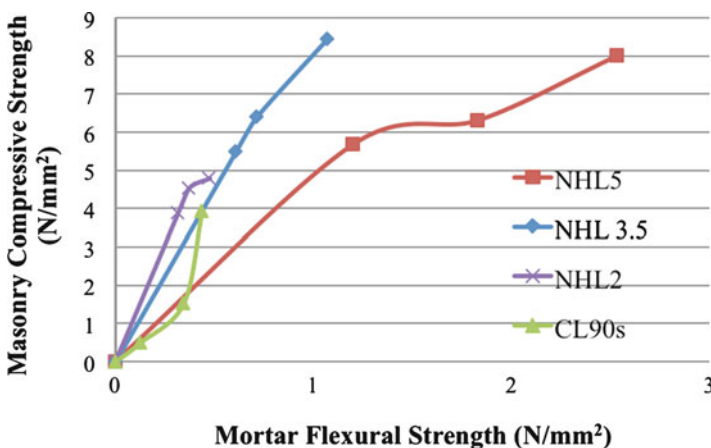


Fig. 13 Influence of mortar flexural strength on masonry compressive strength

only the NHL mortar masonry is considered, the best fit becomes linear (Fig. 17) with an R^2 value of 0.94; when bond strength ranges between 0.1 and 0.4 N/mm², there is a clear linear relationship between the bond and the compressive strength of the masonry. This evidences that the bond strength of higher strength mortars has a greater impact on the masonry compressive strength. The results also revealed that a low-strength mortar (CL90) with a good bond (Fig. 15) performs better than a strong mortar with a poorer bond: CL90 masonry with good bond (0.15 N/mm²) reaches 4 N/mm² compressive strength, whereas hydraulic mortar masonry with a poorer bond (0.1 N/mm² or under) does not reach this value. The above evidences that bond strength strongly impacts the compressive strength of masonry, agreeing with previous authors [7].

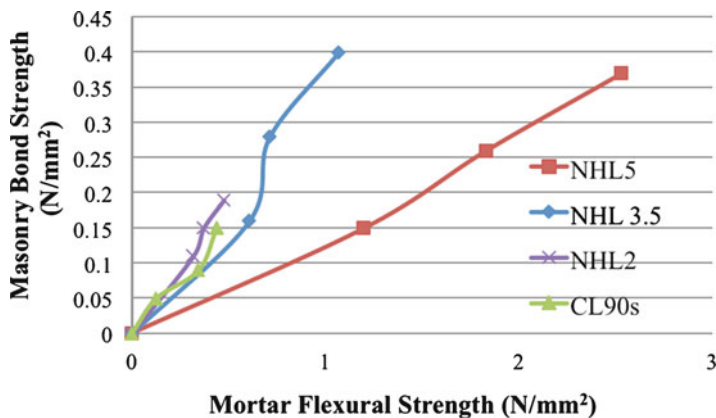


Fig. 14 Influence of mortar flexural strength on masonry bond strength

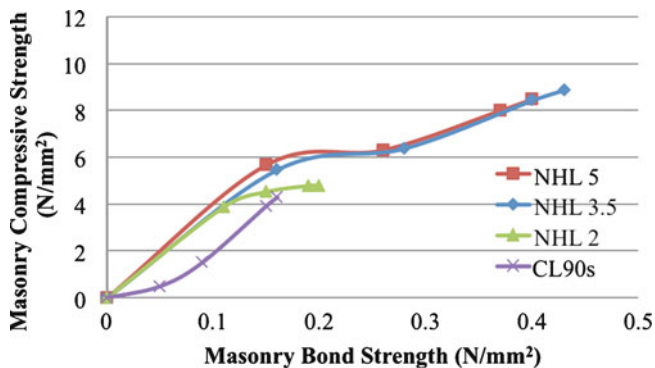


Fig. 15 Influence of bond strength on masonry compressive strength

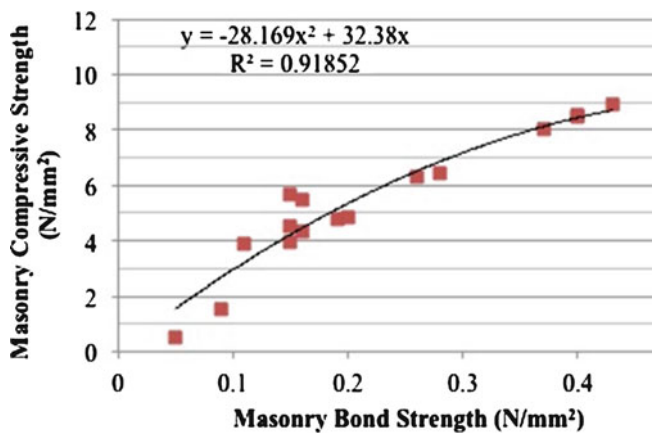


Fig. 16 Nonlinear regression analysis of data in Fig. 15 including all mortars

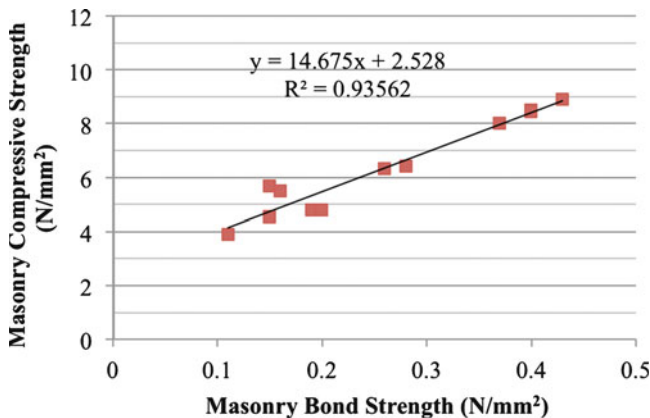


Fig. 17 Linear regression analysis of data in Fig. 15 including NHL mortars only

4 Conclusion

The mechanics of lime mortar and lime mortar masonry are similar in compression: the mortars of higher hydraulic strength exhibit a predominantly elastic behaviour whereas the NHL2 and CL90 mortars behave in a more plastic manner. Similarly, the results evidenced the plastic behaviour of the CL90 masonry (with a short elastic region) against the elastic and brittle behaviour of the NHL masonry, with either little (NHL2) or non-existent plasticity (NHL3.5/5).

This paper concludes that masonry compressive strength is more determined by the strength of the bond rather than by the mortar's compressive strength. This is supported by the following conclusions:

- Increasing mortar strength does not significantly increase masonry strength:
 - The compressive strength of NHL5 mortar increases by 60% (between 1 and 2 months) and 75% (between 2 and 6) while the corresponding masonry only increases strength by 30% and 11% respectively.
 - A mortar of lower hydraulic strength can deliver stronger masonry than an eminently hydraulic mortar: the compressive and bond strengths of NHL3.5 masonry are greater than those of NHL5 masonry, while the NHL3.5 mortar strengths are lower than those of the NHL5 mortar.
- A low-strength mortar (CL90) which has developed a good bond delivers stronger masonry than a stronger mortar with a poorer bond.

Acknowledgements The authors thank Paul McMahon, Architectural Heritage Division, Office of Public Works, for supporting this project. All testing was carried out in the Dept. of Civil Engineering, Trinity College Dublin. The authors thank Chris O'Donovan, Dr. Kevin Ryan and Dave McAuley for their assistance with testing; and The Traditional Lime Company, St Astier/CESA Limes, Clogrenanne Lime Ltd and Kingscourt brick for donating materials.

References

1. Boothby, T.E.: Analysis of masonry arches and vaults. *Prog. Struct. Eng. Mater.* **3**, 246–256 (2001)
2. Zucchini, A., Lourenzo, P.B.: Mechanics of masonry in compression: results from a homogenisation approach. *Comput. Struct.* **85**, 193–204 (2006)
3. Gumeste, K.S., Venkatarama Reddy, B.V.: Strength and elasticity of brick masonry prisms and wallettes under compression. *Mater. Struct.* **29**, 241–253 (2007)
4. Venkatarama Reddy, B.V., Vyas Uday, C.V.: Influence of shear bond strength on compressive strength and stress-strain of masonry. *Mater. Struct.* **41**, 1697–1712 (2008)
5. Kaushik, H.B., Rai, D.C., Jain, S.K.: Stress-strain characteristics of clay brick masonry under uniaxial compression. *J. Mater. Civil Eng. (ASCE)* **19**(9), 728–739 (2007)
6. Hedstrom, E.G., Tarhini, K.M., Thomas, R.D., et al.: Flexural bond strength of concrete masonry prisms using PC and hydrated lime mortars. *Mason. Soc. J.* **9**(2), 8–23 (1991)
7. Portland Cement Association (PCA): Bond strength testing of masonry. *Masonry Information*, Skokie (1994)
8. Venumadhava Rao, K., Venkatarama Reddy, B.V., Jagadish, K.S.: Influence of flexural bond strength on the compressive strength of masonry. In: Proceedings of the National Conference on Civil Engineering Materials and Structures, pp. 103–108. Osmania University, Hyderabad, India (1995)
9. Sarangapani, G., Venkatarama Reddy, B.V., Jagadish, K.S.: Brick–mortar bond and masonry compressive strength. *J. Mater. Civil Eng. (ASCE)* **17**(2), 229–237 (2005)
10. Groot, C.J.W.S.: Effects of water on mortar brick bond. PhD thesis, University of Delft, Delft, The Netherlands (1993)
11. Pavía, S., Hanley, R.: Flexural bond strength of natural hydraulic lime mortar and clay brick. *Mater. Struct.* **43**(7), 913–922 (2010). doi:[10.1617/s11527-009-9555-2](https://doi.org/10.1617/s11527-009-9555-2)
12. CEN: Method of testing cement. Determination of strength, EN 196-1 (2005)
13. CEN: Building lime. Part 2. Test methods, EN 459-2 (2001)
14. Hanley, R., Pavía, S.: A study of the workability of natural hydraulic lime mortars and its influence on strength. *Mater. Struct.* **41**(2), 373–381 (2008). doi:[10.1617/s11527-007-9250-0](https://doi.org/10.1617/s11527-007-9250-0)
15. CEN: Method of test masonry: determination of compressive strength, EN 1052-1 (1999)
16. CEN: Method of test masonry: determination of flexural strength, EN 1052-2 (1999)
17. CEN: Method of test masonry: determination of bond strength, EN 1052-5 (2005)

Influence of Interfacial Material Pore Structure on the Strength of the Brick/Lime Mortar Bond

Mike Lawrence, Pete Walker, and Zhaoxia Zhou

Abstract This paper builds on previous work investigating the flexural bond strength, initial shear strength and compressive strength of fired clay brickwork built using hydraulic lime mortars. It has been shown that whilst flexural bond strength and initial shear strength of the brickwork generally increased with mortar strength, flexural bond strength was significantly impaired by both low and high brick water absorption. This paper describes a study of the pore size distribution of the surfaces of brick and mortar at the brick/mortar interface using Mercury Intrusion Porosimetry. The paper identifies critical pore sizes at the brick surface which would appear to govern resultant bond strength.

1 Introduction

Lime has been used as a binder in construction for thousands of years. Examples of its use have been found in Palestine and Turkey dating from 12000 B.C. [1]. Lime mortars were widely used by the Romans, and techniques for its manufacture and the design of mortars to different performance criteria were well understood. Vitruvius [2] in 30 B.C. described the manufacture of lime mortars and the key criteria to be considered in order to manufacture a good quality mortar. In 1837 an English translation of Vicat's 1828 publication gave a comprehensive analysis of the state of the art [3]. Practical formulations and application techniques were given in the form of a textbook for students of Building Materials published by Rivington's in 1875 [4], and detailed specifications were published by the Building

M. Lawrence (✉) • P. Walker • Z. Zhou
BRE Centre for Innovative Construction Materials, University of Bath, Bath, UK
e-mail: M.Lawrence@bath.ac.uk

Research Establishment in 1927 [5]. Since the end of the 2nd World War, lime has displaced by the faster acting, stronger, cement based mortars. Much expertise and understanding of lime based mortars has been lost, and there is very little guidance and performance data available to support structural design codes.

In recent years some research has been completed investigating the properties of hydraulic lime mortars [6, 7], but there is a general scarcity of data on the mechanical properties of lime mortared masonry.

Previous work [8] has investigated flexural bond strengths of a range of brick types constructed with different hydraulic lime mortars varying from NHL2 to NHL5 at varying concentrations. It was found that brick water absorption characteristics had a significant influence on bond development of brickwork. Both high and low absorption bricks developed lower bond strengths than medium absorption bricks.

The results presented herein are a re-analysis of these data taking into account the pore size distribution of the surface of the bricks in an attempt to identify critical pore sizes involved in the mortar:brick bond.

2 Experimental Programme

The hypothesis of this investigation is that the pore size distribution of the brick at the mortar:brick interface is modified by mortar products penetrating into its pore structure. The experimental programme investigated the relationship between the pore size distribution of a ~2 mm thick section of the top surface of a fresh brick, the pore size distribution of a ~2 mm thick section of the top surface of a mortared brick from which the mortar has been removed, and the bond strength characteristics of the brick : mortar combination.

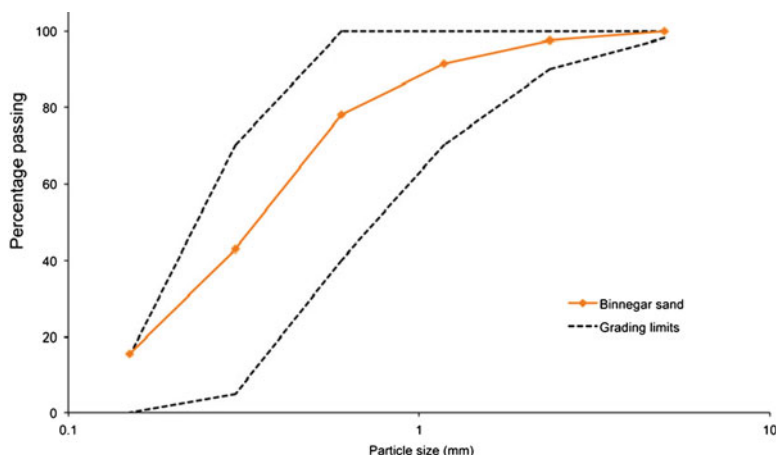
2.1 Materials

Seven types of standard size (nominal dimensions $15 \times 102.5 \times 65$ mm) wire cut, extruded fired clay bricks were selected for this study, chosen out of the 30 bricks in the earlier study. The bricks were selected to be broadly representative of a typical range of water absorption characteristics in the UK. Brick properties, including 24 h immersion water absorption and initial rate of water absorption described elsewhere [8] are summarised in Table 1.

Castle Cement Ltd NHL was used with a well-graded blended mortar sand (Binnegar sand) for the mortar mix. The sand grading curve is shown in Fig. 1. The mortar used was 1 part NHL3.5–2.25 parts Binnegar sand by volume; equivalent to 1 part NHL3.5–6.62 parts sand by mass. The water/lime ratio was 1.40 and the flow value was 160 mm.

Table 1 Brick characteristics

Brick no. and name	Initial rate of absorption (kg.m ⁻² .min ⁻¹)		24 h water absorption (%)		Sorptivity (mm.min ⁻¹)	
	Average	CV (%)	Average	CV (%)	Average	CV (%)
15. Cheddar Brown	0.5	14.4	4.5	13.5	0.17	30.6
7. Surrey Orange	0.6	27.1	7.2	16.2	0.42	28.9
2. Ruskin Red 73	0.7	6.3	6.1	4.4	0.48	15.4
4. Tradesman Antique	0.9	6.7	6.7	2.5	0.37	12.6
1. Red Multi	1.7	15.7	8.0	10.1	1.12	20.0
29. West Hoathly	1.9	25.6	7.4	6.3	0.45	36.4
12. Dorset Red Stock	2.1	4.6	12.7	1.2	1.31	11.1

**Fig. 1** Sand grading

2.2 Manufacture, Curing and Testing of Specimens

All bricks were dried under controlled (20°C, 65% relative humidity) laboratory conditions prior to construction. Dry binder and sand were initially thoroughly mixed in a drum mixer and thereafter water was added gradually and mixing continued for 10 min in total. The mortar was left to stand (under cover to prevent evaporative moisture loss) for 50 min before briefly re-mixing and use. This stand time, following common site practice, is believed to improve workability. In order to control materials the bricks were not wetted by the bricklayer during construction to adjust suction.

All masonry specimens and mortar specimens were covered with plastic after fabrication for 1 week, to prevent initial rapid drying in laboratory conditions, and afterwards uncovered and stored in a climate room, maintained at 20°C ± 2°C and relative humidity 65% ± 5% with ambient CO₂ levels, until testing. Masonry and mortar were tested at 91 days. Full details of the flexural strength tests are reported elsewhere [8].

Bond strength data are shown in Table 2. The flexural strength of the mortar at 91 days was 0.45 N.mm^{-2} with a coefficient of variation (CV) of 27%; the compressive strength at 91 days was 1.0 N.mm^{-2} with a CV of 12%.

After testing, bricks with one mortared face were sampled for porosimetry testing. For each brick the mortared face was gently scraped clean of mortar, taking care not to abrade the surface of the brick. A $2\text{--}3 \text{ mm}$ slice was cut from opposite faces of the brick producing specimens of $\sim 10 \times 20 \times 2 \text{ mm}$ as shown in Fig. 2.

Specimens were tested using Mercury Intrusion Porosimetry (MIP) using a Micromeritics Autopore III. Approximately 1 g of material was tested in each case and intrusion pressures were increased in steps up to 400 MPa, which allowed intrusions into pores as small as 40 nm. The pore size distribution of the clean face of the surface of each brick was established and mapped against the bond strength. In addition, the pore size distribution of an un-mortared face was subtracted from the pore size distribution of a mortared face in order to identify changes in pore size distribution induced by the mortar. These changes were also mapped against bond strength.

It should be noted that MIP produces a pore size distribution of pores that are accessible to intrusion (open pores), typically in a range of 4 nm to $250 \mu\text{m}$. Closed pores will only be accessed when pore walls collapse under external pressure, which will only occur at high pressures, and small apparent pore sizes. Figure 3 shows a small peak at $\sim 0.01 \mu\text{m}$ which is likely to have been produced by this collapse of pore walls. These closed pores would not be accessible to mortar products and therefore would not be involved in mortar bonding. In addition, the volume of pores smaller than $0.01 \mu\text{m}$ (which would include all closed pores) is less than 7.5% of total pore volume in all cases, and therefore would not affect the conclusions drawn here.

3 Porosimetry Analysis

Figure 3 shows the relative pore size distribution of the surface of the individual bricks.

It can be seen that the majority of pore sizes in all bricks can be found between 10 and $0.1 \mu\text{m}$, and in most cases the peak concentration of pores is around $1 \mu\text{m}$.

Some bricks have large pores, between 50 and $250 \mu\text{m}$, and there is also a small peak of pores at around $0.01 \mu\text{m}$, which includes the volume of larger closed pores as explained above.

In general, once mortared, there is a reduction in pores between 100 and $10 \mu\text{m}$ towards pores between 1 and $0.1 \mu\text{m}$. This trend can be seen in Fig. 4 which shows a subtraction of pore size distribution between clean surfaces and mortared surfaces. With the exception of Specimen #29 where there is no reduction in large pore sizes, all specimens show the same trend. This is likely to be due to the fact that this brick has a high percentage of pores greater than $100 \mu\text{m}$ compared with the pore size distribution between 100 and $10 \mu\text{m}$. These larger pores would not be blocked by

Table 2 Bond strength data compared with pore size distribution

Brick no. and name	Type and texture	Mean bond strength (N.mm ⁻²)	Characteristic bond strength (N.mm ⁻²)	Initial rate of absorption (kg.m ⁻² .min ⁻¹)	% pores between 0.1 and 1 µm
29. West Hoathly	Handmade	0.28	0.18	1.9	22.75
1. Red Multi	Wire	0.29	0.08	1.7	15.38
12. Dorset Red Stock	Stock	0.34	0.21	2.1	19.05
7. Surrey Orange	Wire-rolled	0.40	0.23	0.6	37.37
4. Tradesman Antique	Wire-rolled	0.46	0.32	0.9	51.33
2. Ruskin Red 73	Wire-smooth	0.52	0.35	0.7	40.58
15. Cheddar Brown	Wire-rolled	0.53	0.26	0.5	44.12

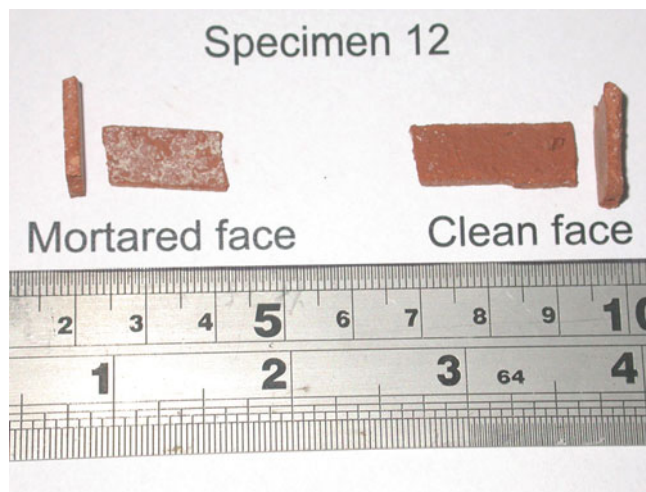


Fig. 2 Specimens for porosimetry testing

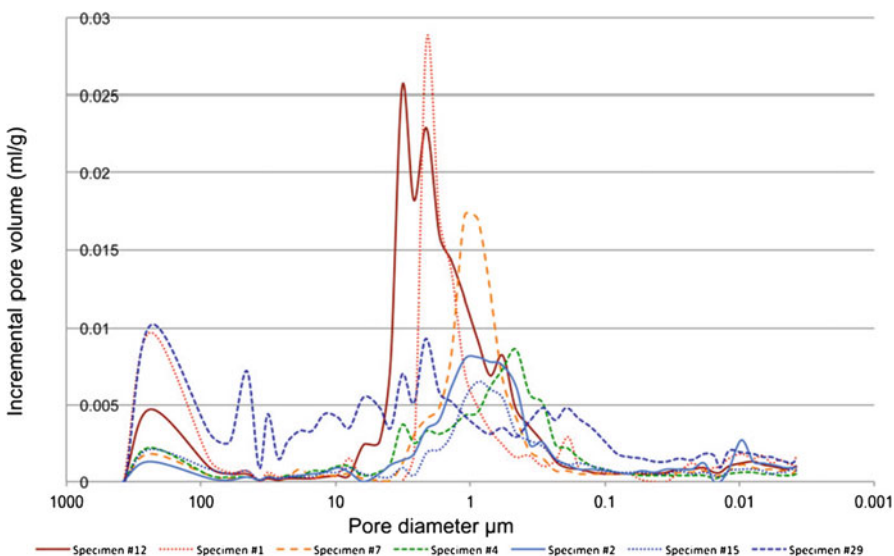


Fig. 3 Pore size distribution of clean brick surface

mortar. An examination of the cumulative intrusion curves shown in Fig. 5 shows a group of four specimens where the percentage of pores intruded increases rapidly as pore size reduces to below 1 μm . These were specimens 12, 7, 1 and 29, where the bond strengths were all below 0.4 N.mm^{-2} .

The other three specimens, numbers 4, 12, and 15 have similar cumulative pore size distributions, and their bond strengths are also similar and in excess of 0.46 N.

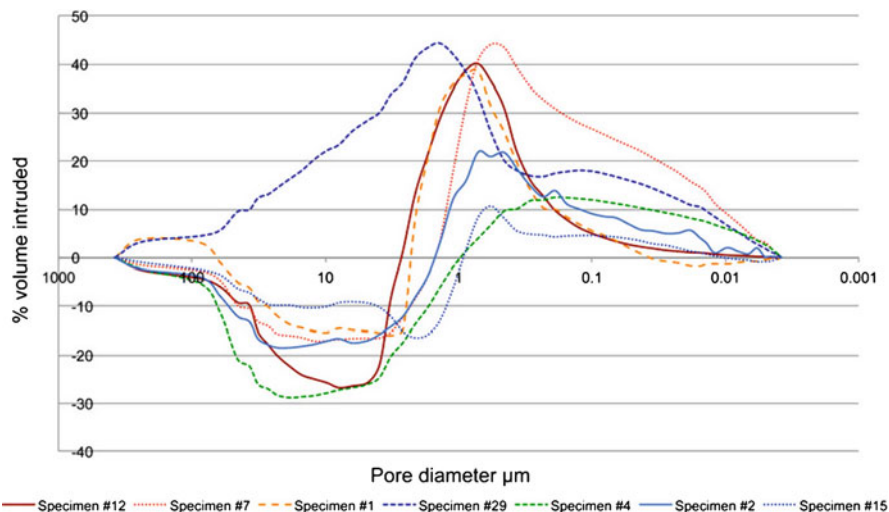


Fig. 4 Pore size distribution comparison of clean and mortared brick surfaces

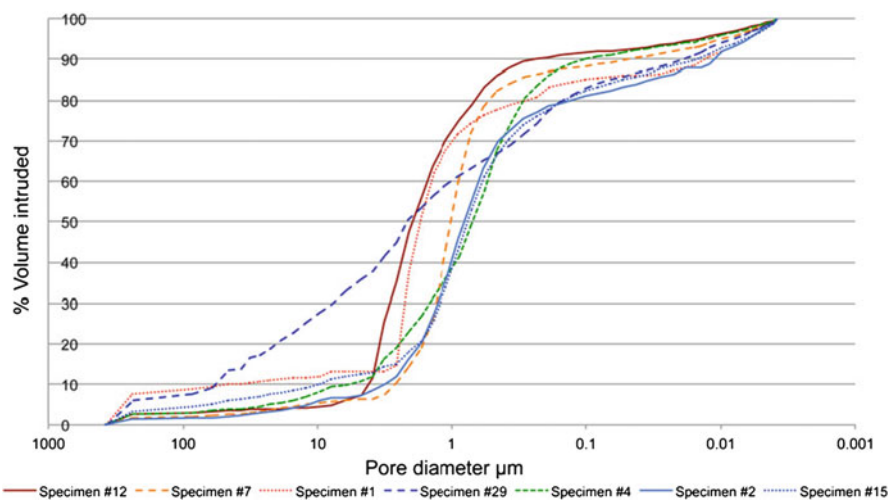


Fig. 5 Cumulative pore size distribution for brick surfaces

mm^{-2} . Figure 6 maps the bond strengths against the proportion of pore volume on the surface of the brick which is taken up by pores that are between 1 and 0.1 μm . There appears to be a linear relationship, with bond strength increasing as the proportion of pore volume that is below 1 μm increases. The linear regression was determined on a statistically low number of points, and additional data would add to the confidence level of the linearity of the relationship. The rationale for a proportional relationship is, however, supported by the discussion and conclusions which follow.

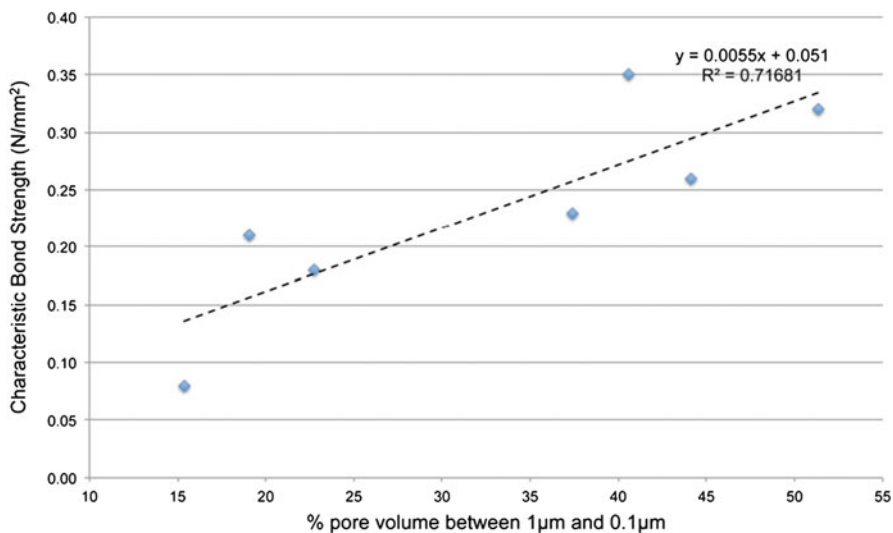


Fig. 6 Relationship between mean bond strength and the proportion of pore volume $> 1 \mu\text{m}$

4 Discussion and Conclusions

Portlandite (calcium hydroxide) crystals range in size between 1 and 10 μm , and calcite (carbonated Portlandite) crystals range between 0.1 and 1 μm [9]. The shift in pore size distribution seen in Fig. 4 suggest that the pore sizes of the brick surface between 1 and 10 μm allow Portlandite to penetrate the pores and crystallise within them, thereby reducing the size of those pores. Calcium silicate hydrates have smaller crystals which range from 0.1 to 0.001 μm in size [10]. Since these hydraulic elements form a stronger bond than the Portlandite, and they are able to penetrate smaller pores, this would tend to explain the better bond strengths seen in bricks where a greater proportion of the pore volume is below 1 μm .

The general trend, therefore, is that the greater the percentage of pore volume on the surface of the brick that is represented by pores with sizes below 1 μm , the better the bond strength with hydraulic lime mortars. Where bricks are known to have a higher than normal percentage of pore volume represented by pores larger than 1 μm , designers might want to consider increasing the strength of the mortar in order to achieve a satisfactory bond strength. This could be done either by increasing the proportion of lime in the mortar, or changing from NHL3.5 to NHL5.

References

1. Von Landsberg, D.: The history of lime production and use from early times to the industrial revolution. *Zement-Kalk-Gips* **45**, 199–203 (1992)
2. Vitruvius: Ten books on architecture. Translated from the Latin by I.D. Rowland, Ed. T.N. Howe. 30–20 BC. Cambridge University Press, Cambridge (1999)

3. Vicat, L.J.: Mortars and cements. Translated by J T Smith. Donhead, Shaftesbury (1997)
4. Smith, P.: Rivington's Building Construction. Donhead, Shaftesbury (2004)
5. Cowper, A.D.: Lime and Lime Mortars. Donhead, Shaftesbury (1998)
6. Allen, G., Allen, J., Elton, N., Farey, M., Holmes, S., Livesey, P., Radonjic, M.: Hydraulic Lime Mortar for Stone, Brick and Masonry. Donhead, Shaftesbury (2003)
7. Lanas, J., Pérez Bernal, J.L., Bello, M.A., Alvarez Galindo, J.I.: Mechanical properties of natural hydraulic lime-based mortars. *Cem. Concr. Res.* **34**, 2191–2201 (2004)
8. Zhou, Z., Walker, P., D'Ayala, D.: Strength characteristics of hydraulic lime mortared brick-work. *Proc. Inst. Civ. Eng. Constr. Mater.* **161**, 139–146 (2008)
9. Rodriguez-Navarro, C., Ruiz-Agudo, E., Ortega-Huertas, M., Hansen, E.: Nanostructure and irreversible colloidal behaviour of Ca(OH)₂: implications in cultural heritage conservation. *Langmuir* **21**, 10948–10957 (2005)
10. Jennings, H.M.: A model for the microstructure of calcium silicate hydrate in cement paste. *Cem. Concr. Res.* **30**, 101–111 (2000)

Grouts for Injection of Historical Masonries: Influence of the Binding System and Other Additions on the Properties of the Matrix

Ioanna Papayianni, Maria Stefanidou, and Vasiliki Pachta

Abstract Grouting of historical masonries has been a widely used technique for regaining their integrity or strengthening them. Since cement-based grouts proved very strong, and in some cases destructive for these old masonries, grouts based on a lime-pozzolan binding system have been developed by researchers as an alternative, meeting compatibility issues required for repair interventions. In this paper, a number of grout compositions based on lime and other traditional binders are studied, with and without additions of limestone filler and nanoparticles of silica. In some, a small quantity of white cement (15 wt.%) was incorporated into the system. Apart from the different constituents of the binding system, the addition of admixtures was used for improving the properties of grouts. Rheological properties, such as fluidity, volume stability and penetrability of the grouts, were measured in the fresh state. Mechanical properties of dried grouts and grouted sand were checked. Volume changes due to drying shrinkage of grouts were recorded after demoulding and up to 28 days. The microstructure of the dried grouts of the control mixture and of that with silica nanoparticles was examined by stereoscope, image analysis, and DTA-TG methodology.

1 Introduction

Injecting grouts into masonry is a widely used repair technique for consolidating and strengthening old structures. It has a long history, but the first systematic work started in the 1980s [1–6]. Since then the technique of grout manufacture has been improved by introducing high speed or ultrasonic wave mixers and establishing

I. Papayianni (✉) • M. Stefanidou • V. Pachta
Civil Engineering Department, AUTH, Thessaloniki, Greece
e-mail: papayan@civil.auth.gr; stefan@civil.auth.gr; vpachta@civil.auth.gr

criteria for designing a suitable grout for each case study grout. The first applied grouts were rather cement-based, modified with organic or inorganic additives. As experience has accumulated and compatibility issues in the repair of monumental or historical structures have gained acceptance by the scientific community, many efforts have been made to develop softer grouts. In these experiments, cement was partly replaced with lime and pozzolanic materials, since the cement-based mixtures were very strong and changed the behaviour of the old structure. By testing not only the grout mixtures but also the response of grout-repaired masonry to different types of loadings, ternary binding systems of grouts are proposed and experimentally justified [7].

The need for relatively early strength development of high water/binder grout mixtures does not allow a large percentage of cement to be substituted by softer binders. However, modern advanced admixtures, in which the water/binder ratio can be substantially reduced for the benefit of strength in combination with higher reactivity of fine-grained traditional binders, have created new opportunities for designing a compatible and effective grout.

Nanotechnology tools and nanoscale materials are very promising items with which the properties of microstructure can be steadily modified. According to the literature, nanosilica particles decrease the Ca/Si of C-S-H compounds and increase the mean silicate chain length, leading very possibly to a C-S-H matrix of long-term stability [8–10]. In general, nanoparticles of Si are believed to possibly reduce portlandite leaching and increase strength and durability by enhancing the matrix-aggregate interface and C-S-H gel formation.

Since the grain size of the solid constituents of grout is of paramount importance for its penetrability, very fine limestone filler and nanosilica particles were chosen as additions for improving the strength, capacity and performance of lime-pozzolan grouts. Therefore, the scope of the research is to find the potential of lime-pozzolan mixtures for well-defined pozzolans and additions.

2 Experimental

The intent of this experimental work was to study lime and pozzolan-based soft grouts and to attempt to improve their properties by adding fine limestone filler and nanoparticles of silica fume. This lime-pozzolan binding system was selected because it has been found in the majority of old mortars of the Roman and Byzantine period. Two natural pozzolanic materials were used after milling to increase their fineness, including a volcanic material from the island of Milos and a diatomite. Brick dust from modern fired bricks was also added as pozzolanic or inert material. Its particle size was smaller than 0.2 mm. In one group of mixtures 15% of white cement was added to replace pozzolan. Some of the characteristics of the binders and additions used are shown in Table 1. The proportions of the grout mixtures are given in Table 2.

Table 1 Characteristics of the constituents of the grouts

Constituents	App. specific density	Specific surface area (m ² /g)	Pozzolanicity index ASTM C311:77 (MPa)	Particle size analysis maximum diameter of grains (μm)
Lime powder	2.471	2.250	—	10.8
Milos pozzolan	2.403	1.820	10.5	11.6
Diatomite	2.425	1.070	9.0	59.8
Cement	3.100	1.030	—	57.9
Brick dust	2.851	0.225	2.5	454.4
Limestone filler	2.846	0.408	—	152.9
Silica fume	2.20	200.0	—	150 nm
Hydrophilic nanosilica	2.20	170–230	—	14 nm

The quantity of water was adjusted to keep flow time measured by Marsh cone (ASTM C939-87) 9–11 s, which was previously defined as adequate based on *in-situ* experiments in old masonry. The flow time was measured immediately and 1 h after mixing. Special attention was given to make high performance grout mixtures of acceptable fluidity, penetrability, and stability. Therefore, a mix of superplasticizer on polycarboxylic basis and retarder 1.5% by mass of binders was added to all grout mixtures. A high speed mixer (up to 8,000 rpm) was used. The admixtures were added into a small quantity of water, which was part of the total added quantity.

Nanoparticles of SiO₂ were also pre-mixed with water before their addition to the mixture. The mixing started with low speed and was gradually increased up to 8,000 rpm. The total mixing time was 5 min for grout mixtures without nanoparticles and around 8 min for those with nanoparticles. Penetrability of the fresh mixtures measured by using sand-column test (NORM NFP 18–891, 1986) filled with sand 2–4 mm. The grouted sand of the column of each test was immediately cast into 4 cm × 4 cm × 4 cm steel moulds for testing the compressive strength.

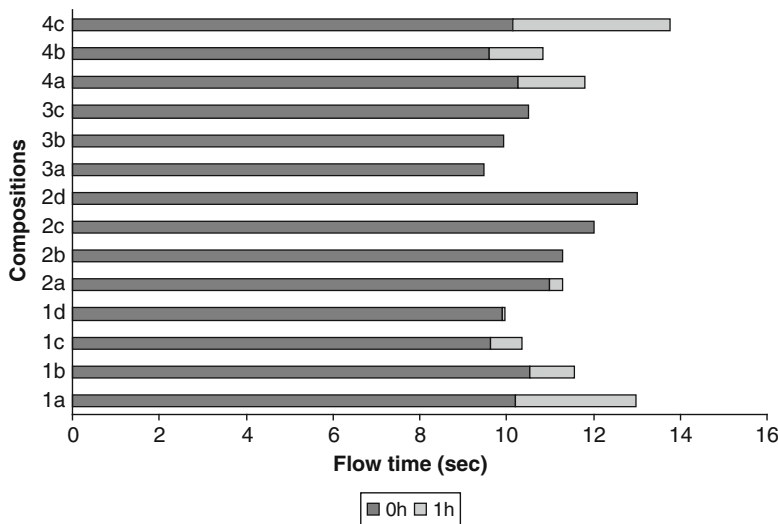
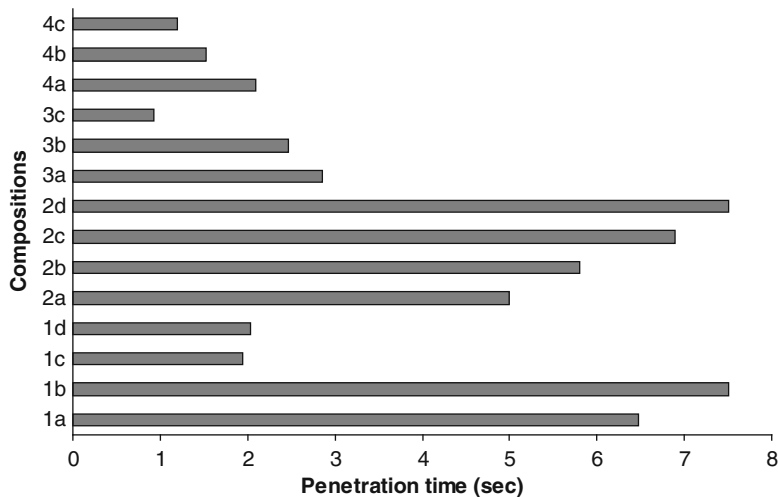
Volume stability of grouts was measured after 24 h from mixing by using cylindrical containers, according to DIN 4227 Teil 5 standards. The test results concerning fluidity, penetrability, and 24 h bleeding are shown in Figs. 1, 2, and 3. Three triplets of 4 cm × 4 cm × 16 cm steel moulds were sealed and filled with fresh grouts and cured at climatic chamber of 90% RH and 20°C up to testing date.

3 Results and Discussion

The tests of fresh grouts showed that the water/binder ratio decreases in the grout mixtures to which extra limestone filler is added, while volume loss after 24 h seems to increase. On the contrary, the extra addition of nanosilica particles 1% by mass of binders, without changing the percentage of the admixtures, clearly increases the water/binder ratio to keep the flow time limits. Furthermore, penetrability is significantly

Table 2 Composition of the grout mixtures

Code Nr	Parts by weight					Nanoparticles (% by mass of the binder)			w/b ratio
	Lime powder	Milos Pozzolan	Diatomite	Brick dust	White cement	Limestone filler	Nano-silica	Silica fume	
1a	1	1	-	-	-	-	-	-	1.09
1b	1	1	-	-	-	-	-	-	0.86
1c	1	1	-	-	-	-	1	-	1.18
1d	1	1	-	-	-	-	-	-	1.43
2a	1	0.6	-	0.4	-	-	-	-	0.90
2b	1	0.4	-	0.6	-	-	-	-	0.95
2c	1	0.2	-	0.8	-	-	-	-	0.90
2d	1	-	-	1	-	-	-	-	0.85
3a	1	-	1	-	-	-	-	-	0.86
3b	1	-	1	-	-	0.5	-	-	0.71
3c	1	-	1	-	-	-	1	-	1.03
4a	1	0.7	-	-	0.3	-	-	-	0.97
4b	1	0.7	-	-	0.3	-	-	-	0.83
4c	1	0.7	-	-	0.3	-	1	-	1.04

**Fig. 1** Flow time of lime-based grouts**Fig. 2** Penetrability of lime-based grouts

improved by reducing the required time for penetrating the sand column. The volume loss of nanosilica modified grouts is also considerably reduced, except in the case of nanosilica fume added-grout for which the water/binder was very high in comparison to the control grout. Considering only the basic properties of the fresh grouts, it seems that the nanosilica addition influences them positively. That is very important for the good performance of grouts. The addition of brick dust, which reacts both as pozzolanic agent and inert filler, seems to decrease the water/binder ratio, but flow and

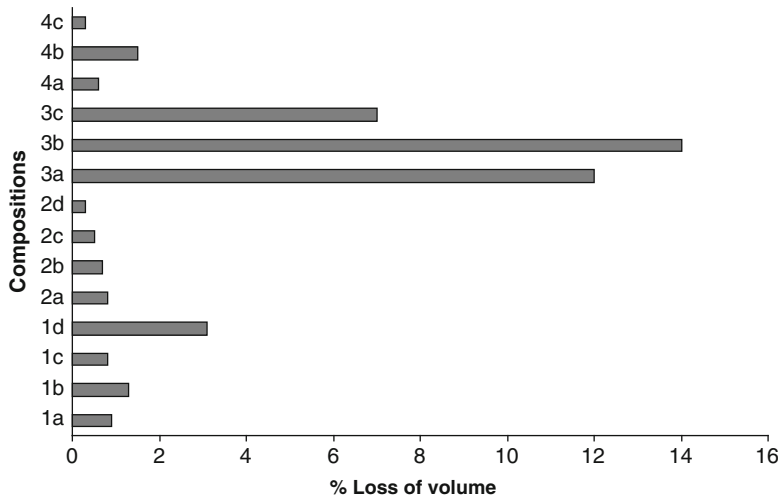


Fig. 3 Bleeding water volume after 1 h of lime-based grouts

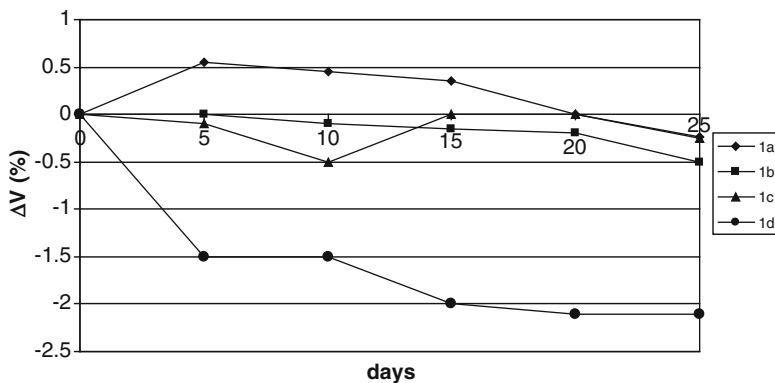


Fig. 4 Volume changes with time after demoulding of grout mixture with code Nr1

penetrability time are unacceptably increased, while the volume stability is improved. The volume loss of lime-diatomite mixtures is also very high, a negative point for this combination of binders. After demoulding (1–2 days after casting), the prismatic specimens were placed in a room of relative humidity below 60% and temperature around 20°C, and deformation as volume change percentage were recorded for 25 days. Volume changes were measured, instead of length changes as mentioned in DIN 52450:1985 standard, as it is considered more representative for drying shrinkage deformation in lime-based mortars. In Figs. 4 and 5, the measurements are given for the best two compositions 1a, b, c, d and 4a, b, c. It is obvious that drying shrinkage deformations are higher when nanosilica is added, while the extra addition of limestone filler does not differentiate them so much.

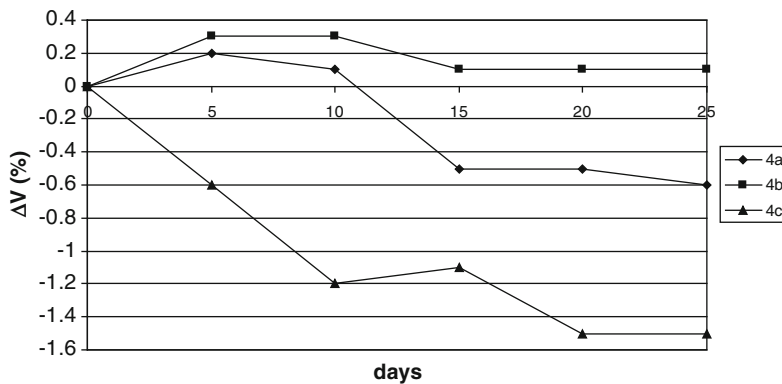


Fig. 5 Volume changes with time after demoulding of grout mixtures with code Nr4

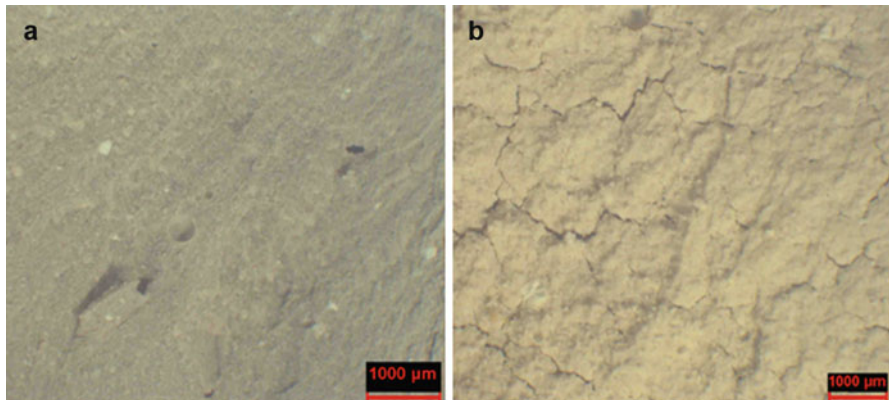


Fig. 6 (a) Stereoscopic images of hardened grout without nanoparticles. Composition 1a. (b) Stereoscopic images of hardened grout with nanoparticles. Composition 1d

The stereoscopic examination (magnification 10×) of the sections of these specimens with nanosilica showed the characteristic pattern of very intensive cracks, as indicated in Figs. 6a, b and 7a, b.

The compressive and flexural strength of prismatic specimens and the crushing value of grouted sand cubes were tested at 28 days age after continuous curing in moist conditions. As mentioned above, the results representing the mean value of three prismatic ($4 \text{ cm} \times 4 \text{ cm} \times 16 \text{ cm}$) and three cubic ($4 \text{ cm} \times 4 \text{ cm} \times 4 \text{ cm}$) specimens are included in Table 3. In addition, the dynamic modulus of elasticity was measured using ultra sonic wave sonometer. The results for the compositions of group code Nr 1 and Nr 4 are depicted in Fig. 8.

Furthermore, the porosity of hardened grout mixtures was measured and listed in Table 3. The values mentioned are the average of four samples.

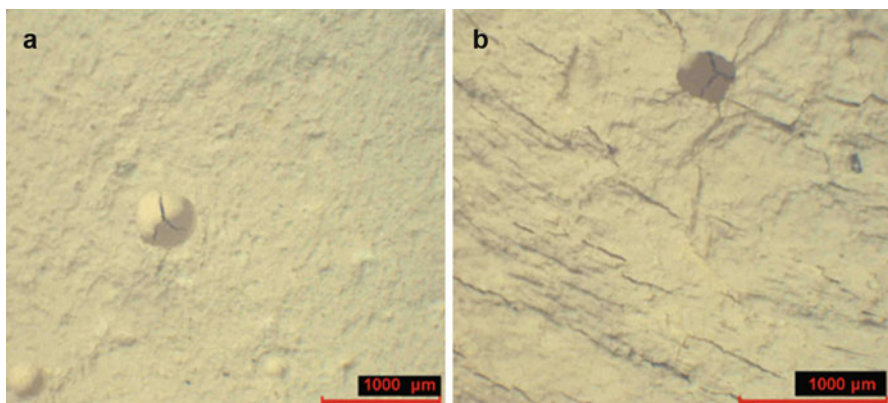


Fig. 7 (a) Stereoscopic images of grout with cement without nanoparticles. Composition 4a. (b) Stereoscopic images of grout with cement with nanoparticles. Composition 4c

Table 3 Strength and porosity of grouts

Code Nr	Compressive strength 28-days MPa specimen:prism	Flexural strength 28-days MPa specimen:prism	Compressive strength 28-days MPa (grout sand) specimen:cubes	Porosity 28-days %
1a	2.24	0.76	1.15	41.07
1b	2.48	1.03	1.37	39.8
1c	1.96	0.74	0.7	42.3
1d	1.40	0.67	0.59	50.53
2a	3.35	1.23	—	—
2b	2.33	0.88	—	—
2c	1.52	0.62	—	—
2d	0.87	0.51	—	—
3a	1.16	0.58	0.90	36.55
3b	0.86	0.46	1.40	39.60
3c	0.72	0.51	0.68	43.99
4a	2.63	1.09	1.64	39.3
4b	2.33	0.97	1.48	31.5
4c	1.45	0.70	0.99	42.68

Results indicate that limestone filler contributes to higher strength development of lime-pozzolan grout, while there is either no such increase in lime-diatomite and lime-pozzolan-cement or the strength is almost of the same level. When brick dust replaces pozzolan the 28 days strength is considerably lower, proving less pozzolanic capacity, although the water/binder ratio was lower than the control mixture 1a. When nanosilica is added, the strength and dynamic modulus of elasticity is decreased significantly. This could be attributed to higher water/binder ratio and higher values of porosity in comparison to the control mixtures, but it needs further investigation because it is a negative, unexpected issue. Additionally, the thermogravimetric analysis

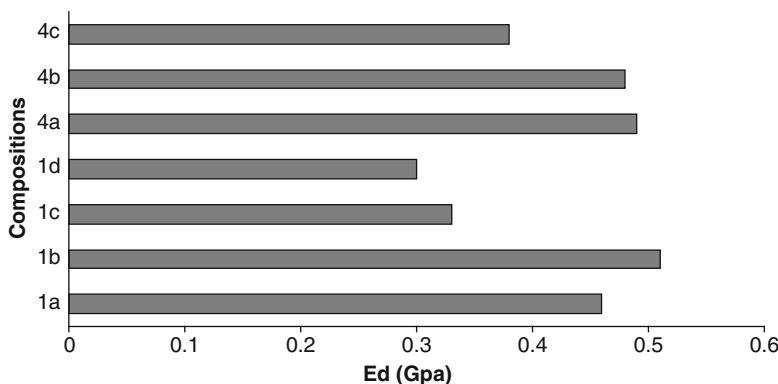


Fig. 8 Dynamic modulus of elasticity of grouts of code Nr1 and 4

Table 4 Content of $\text{Ca}(\text{OH})_2$ and CaCO_3 measured by DTA-TG method at 28-days and 3-months age

Code Nr	$\text{Ca}(\text{OH})_2$ (%)		CaCO_3 (%)	
	28-days	3 months	28-days	3 months
1a	8.37	7.24	30.75	31.11
1c	7.19	6.44	23.59	28.70
1d	6.10	3.44	25.09	31.25

(DTA-TG) of the control 1a and 1c, 1d matrices at 28 days and 3 months showed there was a reduction in $\text{Ca}(\text{OH})_2$ and an increase of CaCO_3 (Table 4). Significant reduction of $\text{Ca}(\text{OH})_2$ was recorded for 1c (43.6%), and the increase of CaCO_3 for that sample was 24.5%.

4 Conclusions

Net lime-pozzolan grouts of acceptable fluidity, penetrability, and volume stability develop strength 2.3 MPa. Replacing 40% of pozzolan by brick dust, the strength increased (from 2.3 to 3.3 MPa) but fluidity is decreased. If 15% of pozzolan is replaced by cement, the properties of fresh grout are good and the strength is slightly increased (from 2.3 to 2.65 MPa). The limestone filler improves the strength of lime-pozzolan grout but influences negatively the performance of fresh grouts. Diatomite as pozzolanic material does not contribute to the improvement of the grout properties in the fresh and hardened states. The addition of nanosilica particles (hydrophilic and silica fume) under the defined terms, without using higher percentages of admixtures to manage the extra water demand, proved very positive for the fluidity, penetrability, and volume stability of grouts. However, it was clearly detrimental to strength development, resulting in a drop in strength from 2.24 to 1.96 MPa for Nr 1 series and from 2.64 to 1.46 MPa for Nr 4 series. Further investigation is necessary.

Acknowledgements The authors would like to thank students Lemonia Apostolaki and Anna Gontia for their assistance in the laboratory work.

References

1. Ferragni, D., Forti, M., Malliet, J., Teutonico, J.M., Torraca, G.: In situ consolidation of wall and floor mosaics by means of injection grouting techniques. In: Conservation in Situ Mosaics, vol. 3, pp. 83–101. ICCROM Edition, Rome (1985)
2. Penelis, G., Karaveziroglou, M., Papayianni, I.: Grouts for repairing and strengthening old masonry structures. In: Brebbia, C. (ed.) International Conference on Structural Repair and Maintenance of Historic Buildings STREMAH, pp. 179–188. Florence (1988)
3. Miltiadou, A.: Contribution à l'étude des coulis hydraulique pour la réparation et le renforcement des structures et des monuments historiques en maçonnerie. Ph.D. thesis, ENPC, Paris (1990)
4. Binda, L., Modena, C., Baronio, G.: Strengthening of masonry by injection technique. In: Proceedings of the 6th NAMC, pp. 1–14. Philadelphia (1993)
5. Miltiadou-Fezans.: Criteria for the design of hydraulic grouts injectable into fine cracks and evaluation of their efficiency. In: Biscotin, G., Moropoulou, A., Erdik, M., Rodrigues J. (eds.) Proceedings of International Conference PACT 56, pp. 149–164. Athens (1998)
6. Binda, L., Modena, C., Baronio, G., Gelmi, A.: Experimental qualification of injection admixtures used for repair and strengthening of stone masonry walls. In: Proceedings of the 10th International Brick and Block Masonry Conference, pp. 539–548. Calgary (1994)
7. Toubakari, E.: Lime-Pozzolan –cement grouts and their structural effects on composite masonry walls. Ph.D. thesis, Katholieke Universiteit, Leuven, pp. 1–95 (2002)
8. Layerblod, B., Jennings, H.M., Chen, J.J.: Modification of cement paste with silica fume: a NMR study. In: Bartos, P.J.M., Hughes, J.J., Tritik, P., Zhu, W. (eds.) Nanotechnology in Construction, pp. 123–131. Royal Society of Chemistry, Cambridge (2004)
9. Gaitero, J.J., Campillo, J., Guerrero, A.: Reduction of the calcium leaching rate of cement paste by addition of silica nanoparticles. *Cem. Concr. Res.* **28**, 1112–1118 (2008)
10. Li, H., Hui-gang, X., Jie, Y., Jinping, O.: Microstructure of cement mortar with nanoparticles. *Compos. Part B* **35**, 185–189 (2004)

Lime Based Grouts for Strengthening of Historical Masonry Buildings in Slovenia

Mojmir Uranjek, Vlatko Bosiljkov, Roko Žarnić,
and Violeta Bokan Bosiljkov

Abstract Most of the historical masonry buildings in Slovenia were built out of local stone or stone and brick with lime-based mortars. An efficient technique for improving the mechanical properties of stone or stone-brick walls is grout injection. In order to evaluate the quality and compatibility of commercially available injection grouts with materials present in historical masonry buildings, several types of hydraulic lime-pozzolana, lime-cement and cement grouts were tested. Chemical, physical and mechanical criteria to select optimal grout mixture for strengthening of historical masonry buildings were proposed, by which tested grouts were classified in three quality classes A, B and C. Only two commercial lime-cement grouts and one cement grout were able to meet the set requirements and were qualified in class B as medium quality grout (one lime-cement grout) or in class C as low quality grouts. Therefore, the design of hydrated lime-based grouts was carried out in continuation of our study, in order to obtain a grout that is highly compatible with the historical masonry in Slovenia. Among available limes, hydrated lime in powdered state and lime putty were used. Ground granulated blast furnace slag (GGBS), volcanic tuff, and limestone powder were used as mineral additives. It was found that the added combination of limestone powder and supplementary cementitious material (GGBS or tuff) has a beneficial influence on the properties of designed grout compositions.

M. Uranjek (✉)

Building and Civil Engineering Institute ZRMK, Ljubljana, Slovenia
e-mail: mojmir.uranjek@gi-zrmk.si

V. Bosiljkov • R. Žarnić • V.B. Bosiljkov

Faculty of Civil and Geodetic Engineering, University of Ljubljana,
Ljubljana, Slovenia

e-mail: vlatko.bosiljkov@fgg.uni-lj.si; roko.zarnic@fgg.uni-lj.si; vbokan@fgg.uni-lj.si

1 Introduction

Stone masonry is the most frequent type of historical building in rural areas of Slovenia, both in case of residential as well as more important buildings. In urban areas, however, brick masonry prevails, although monumental historical masonry buildings, such as castles and churches, were still mainly built out of stone or mixture of stones and brick. In the case of stone masonry, stone types such as limestone, sandstone and slate were used and in some cases brick inclusions were found to be included in structures. Thicker walls were mainly constructed in three layers (two outer layers of partly cut stones with an inner core built from leftovers and smaller stones), while thinner walls tended to have only two layers. In general low strength lime mortars with the lime:sand volume proportion of 1:3 were used to bind the stone masonry units. Characterisation of historical mortars in Slovenia, performed as part of archaeological post-excavation analyses, revealed that hydrated lime or in some cases hydrated lime with pozzolanic additives such as volcanic tuff and crushed bricks were used when preparing such mortars [1, 2]. Rural stone masonry walls are often characterised also by inadequate connections between the separate stones and by voids. Consequently, their seismic resistance is usually insufficient and in most cases more critical than seismic resistance of brick masonry. Mechanical properties of such walls can be efficiently improved by grout injection.

There are several types of commercial injection grouts available on the Slovenian market, containing hydraulic lime and pozzolana, lime and cement or only cement as a binder. Regarding chemical, mechanical and physical compatibility with existing materials in the walls of historical buildings, the use of lime-based materials is the most appropriate for the application of strengthening procedures. Therefore the main objective of our experimental work was to evaluate the lime-based injection grouts available in Slovenian market. For this purpose chemical, physical and mechanical criteria for selecting optimal commercial grout mixture for strengthening of historical buildings were proposed first, based on available literature data and demands of conservators of Restoration Centre, Institute for the Protection of Cultural Heritage of Slovenia (RC ZVKDS). According to the adopted criteria, the grouts were classified in three groups. In continuation of our study, several hydrated lime-based compositions of injection grouts (intended for grout injection of stone or stone-brick walls with voids) were designed and their suitability for strengthening of historical buildings was evaluated. Among available limes, hydrated lime in powdered state and lime putty were used. Ground granulated blast furnace slag (GGBS), volcanic tuff and limestone powder were used as mineral additives.

2 Grout Injection – Application and Frequent Errors

Grout injection is a technique where grout is injected into a wall under moderate pressure (2–3 bars) to achieve a better bond between stones and layers and to improve the mechanical properties of the injected wall. Basic steps for the application of grout injection technique are shown in Fig. 1.

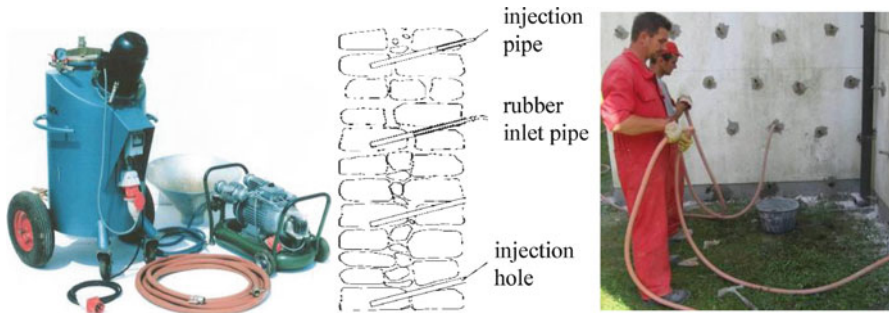


Fig. 1 The image to the *left* shows the apparatus for grouting, setting up of the injection holes in the *middle*, and the image to the *right* the application of grout injection

Unfortunately, because of a lack of knowledge about the morphology and type of walls, incompatibility of existent and applied materials, errors during application, mistakes and even damage may occur by the application of grout injection. Some of the most common reasons for errors that can lead to inadequate quality of grout injection or even damage of stone masonry walls can be summarised as:

2.1 *Lack of Knowledge About the Morphology of the Walls*

Lack of knowledge about the morphology can be the reason for selecting an ineffective strengthening method. Grout injection is not effective in the case of non-injectable walls with less than 4% voids [3]. In such cases more appropriate strengthening methods should be applied.

2.2 *Incompatibility Between Existing and Applied Materials*

Because of chemical and mechanical-physical incompatibility between existing and applied materials, degradation and damage of the existing materials can occur. Reasons for such degradation were described in detail by Collepardi [4].

2.3 *Lack of Knowledge About Moisture Content in Walls*

Excessive moisture content in a wall is a problem that has to be addressed before strengthening by means of grout injection. The application of the grout injection procedure without the elimination of the causes and consequences of excessive moisture content may lead to accelerated degradation of the masonry.

2.4 Errors During Application of Grout Injection

During the supervision of strengthening procedures conducted as part of reconstruction works undertaken after strong earthquakes between 1998 and 2004 in the seismic prone area of Posočje, Slovenia, it was found that some errors occur frequently [5]:

- Preparation of the grout with uncontrolled water/binder ratios which can lead to segregation and extensive bleeding of the grout;
- Interruptions to the working process that can cause lower workability and fluidity because of setting of the grout;
- Inadequate preparation of the wall before injection: proper arrangement of the injection holes, angle of drilling, depth of holes and the amount of water used to wet the wall are all factors that influence the quality of grout injection;
- Inadequate pressure: higher injection pressure enables better penetration of the grout into cracks and voids inside the wall; however, at the same time it can also provoke further damage to the plaster or even the outer layers of the wall;
- Inadequate sequence of the working procedure: grout injection must always be applied gradually from the lower to the upper parts of the wall; a reverse procedure will cause the closing of voids due to the hardening of the grout which will consequently prevent the penetration of the grout to the lower parts of the wall;
- Damage that occurred in buildings exposed to seismic loads after strengthening by means of grout injection shows that the injecting of selective parts of walls or building intersections and corners is not a good solution.

3 Criteria for Grout Classification

As stated earlier, chemical, physical and mechanical criteria for the selection of grout for strengthening of historical buildings were determined through a literature survey and in collaboration with conservators. The criteria were classified in three quality classes A, B and C, where class A stands for a high quality grout (used for important historical monuments with architectural and cultural assets), B for a medium quality grout and C for a low quality grout (for common historical buildings). In continuation a more detailed explanation about the backgrounds for the selection of criteria belonging to the particular quality class is presented.

3.1 Content of Potentially Harmful Substances in Dry Grout

Standard EN 447 [6] which deals with grouts for pre-stressing tendons sets the limit value of chlorides to 0.1% by mass. Sulphates can in some circumstances [4] have a negative influence, because sulphate salt reactions can cause the formation of

ettringite and/or thaumasite. High alkali content may be dangerous because of the efflorescence phenomena and the possibility of alkali-silica or alkali-carbonate reactions. Van Rickstal [7] recommends that for preparing grouts, cements with alkali content lower than 0.1% by mass should be used. When using reactive aggregates to prepare concrete, the alkali content should not exceed 0.6% by mass [8]. Based on the above given data and demands of RC ZVKDS, criteria regarding the allowed content of potentially harmful substances in dry grout was set for the particular class as follows: in the case of chlorides at $A \leq 0.01\%$, $B \leq 0.02\%$ and $C \leq 0.05\%$; in case of sulphates at $A \leq 0.1\%$, $B \leq 0.5\%$ and $C \leq 3.0\%$; and in case of alkalis (Na_2O equivalent) at $A \leq 0.1\%$, $B \leq 0.5\%$ and $C \leq 1.0\%$.

3.2 Fresh Grout

Decisive properties of fresh grout, based on which grouts were classified, were w/b (water/binder) ratio, fluidity and bleeding. For the w/b ratio the criterion of a maximum value of 0.60 was used by Valuzzi et al. [9] to avoid the unfavourable effect of high water content on the mechanical properties of a hardened grout. We also set the maximum value to 0.60, with a tolerance of +10%, for classes A, B and C. In the research performed by Valuzzi et al. [9], time of fluidity for injection grouts was limited to 25–30 s. In our criterion, maximum time of fluidity for grouts of class A was set to 25 s, with the difference between fluidity measured immediately after mixing and after 30 min limited to 10%. For grouts of class B the measured time of fluidity should not exceed 25 or 30 s with the maximum of a 20% or 10% difference between the measurements immediately after mixing and after 30 min, respectively. For class C, however, the measured time of fluidity should not exceed 30 s with not more than 20% difference between the measurements immediately after mixing and after 30 min. Bleeding of grout after 3 h, as defined in standard EN 447 [6], should not exceed 2.0% of the initial volume of the grout; this was also set as a limit value for all classes of grout in our criteria (with tolerance of +10%).

3.3 Hardened Grout

Admissible volume change according to standard EN 447 [6] lays in the interval of $-1.0\% \leq \Delta V \leq 5.0\%$. For our criteria the volume change limits were set to $-0.3\% \leq A \leq 0.3\%$ for class A, $-0.6\% \leq B \leq 0.6\%$ for class B, and $-1.0\% \leq C \leq 1.0\%$ for class C. For the flexural and compressive strength of grouts the same criterion as proposed by Miltiadou et al. [10] was adopted. For all quality classes flexural strength should be greater than $f_{fg} \geq 2.0 \text{ MPa}$ and compressive strength greater than $f_{cg} \geq 6.0 \text{ MPa}$. For tensile splitting strength the criterion of $f_{tg} \geq 0.80 \text{ MPa}$ was considered for all classes of grouts.

Table 1 Summary of proposed criteria for grouts in dry, fresh and hardened state

Dry grout	Fresh grout	Hardened grout
Chloride content A≤0.01%, B≤0.02%, C≤0.05%	w/b ratio A,B,C≤0.60	Volume change A: ±0.3%, B: ±0.6%, C: ±1.0%
Alkali content A≤0.1%, B≤0.5%, C≤1.0%	(Tolerance of +10%)	Flexural strength A,B,C≥2.0 MPa
Sulphate content A≤0.1%, B≤0.5%, C≤3.0%	Fluidity A≤25 s ($\Delta t \leq 10\%$) ^a B≤30 s ($\Delta t \leq 10\%$) ^a or ≤25 s ($\Delta t \leq 20\%$) ^a C≤30 s ($\Delta t \leq 20\%$) ^a	Compressive strength f A,B,C≥6.0 MPa Tensile splitting strength A,B,C≥0.80 MPa
	Bleeding A,B,C≤2.0% (Tolerance of +10%)	

^aRefers to the difference between fluidity immediately after mixing and after 30 min

3.4 Summary of Proposed Criteria

In Table 1 the summary of proposed criteria for grouts in dry, fresh and hardened state for each quality class (A, B, C) is presented.

4 Laboratory Tests of Commercial Injection Grouts

Nine types of commercial injection grouts containing hydraulic lime and pozzolana (LP1, LP2, LP3 and LP4), lime-cement grouts (LC1, LC2 and LC3), and cement grouts (C1 and C2), available in Slovenia, were subjected to laboratory tests. Cement grouts were selected as comparable mixtures that are frequently used for strengthening of stone masonry buildings in Slovenia. The laboratory tests were divided into four parts. In the first part the content of potentially harmful substances for nine different injection grouts were analysed. In the second and third parts, properties of fresh and hardened grouts were determined. In the fourth part, cylindrical specimens that represented the internal core of an injected wall were tested and their mechanical parameters were evaluated. For the assessment of the supplied grouts existing standards for concrete and mortar and also standards for grouts for pre-stressing tendons EN 445-447:1996 [6, 11–12] were used, with modifications where needed.

4.1 Tests and Classification of Grouts

First the content of potentially harmful substances in dry grout that could, in conjunction with other factors, cause damage to the final layers and paint applied to a wall was analysed. Contents of chlorides, sulphates and alkalis were determined in accordance with SIST EN 196-2 [13].

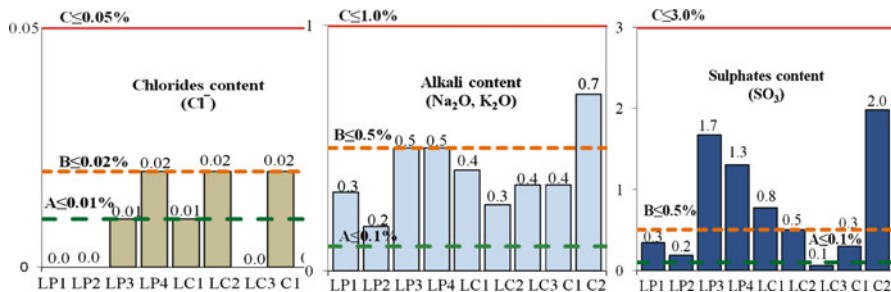


Fig. 2 Contents of water soluble chlorides, alkalis and sulphates in analyzed grouts in % by mass

The obtained contents of potentially harmful substances and set limitations for each quality class are presented in Fig. 2. All grouts met the criteria set for class C, grouts LP1, LP2, LC2, LC3 and C1 met the criteria set for class B, but none of the grouts fulfilled the criteria set for class A.

Fresh grouts were prepared according to the specifications of the manufacturers. Properties which influence workability, injectability and consequently the quality of grout injection were analysed. Bulk density was determined in accordance with standard SIST EN 1015-6 [14] and fluidity and bleeding according to standard EN 445 [11]. The fluidity of the grout was measured by the time necessary for a volume of 1.7 l of grout to pass through the orifice of the standardised cone. Bleeding of the grout was measured by using transparent 100 ml cylinders, 25 mm in diameter and 250 mm in height and graduated in mm. The test consisted of measuring the quantity of water remaining on the surface of the grout, allowed to stand protected from evaporation for 3 h. The obtained results are given in Table 2.

On the basis of the set criteria for fresh grout, grouts LP1, LP2 and LC1 were placed in class A, and grouts LP4, LC2 and C1 in class B. Grouts LP3, LC3 and C2 did not fulfil the criteria summarised in Table 1.

Volume change, bulk density and flexural, compressive, and tensile splitting strength were analysed through the test results of hardened grout. The volume change of grout was measured according to the test method described in standard EN 445 [11], bulk density according to SIST EN 1015-10 [15], flexural and compressive strength in agreement with SIST EN 1015-11 [16] and the tensile splitting test following the procedure described in SIST EN 12390-6 [17]. The obtained results are given in Table 3.

Based on the set criteria for hardened grout (Table 1), grouts LC3 and C2 were classified as class A, grout LC2 as class B and grouts LC1 and C1 as class C, while other grouts did not fulfil the requirements.

Considering that each property of dry, fresh and hardened grout used for classification had the same constraint, only lime-cement grouts LC1 and LC2 and cement grout C1 were able to meet the requirements. Grout LC2 was qualified in class B as medium quality grout and grouts LC1 and C1 were qualified in class C as low quality grouts.

Table 2 Properties of fresh commercial grout

	LP1	LP2	LP3	LP4	LC1	LC2	LC3	C1	C2
w/b ratio	0.45	0.45	0.55	0.38	0.50	0.62	0.50	0.40	0.43
Bulk density (kg/m ³)	1,599	1,778	1,563	1,821	1,673	1,659	1,712	1,895	1,856
Fluidity (s) ^a	19.8/20.0	14.4/14.4	35.9/36.6	28.3/28.5	13.5/13.4	13.6/16.3	17.4/45.0	13.8/15.5	27.2/44.5
Bleeding (%)	0.0	2.1	0.0	2.1	0.2	0.5	0.0	0.5	1.0

^aMeasured immediately after mixing and after 30 min

Table 3 Properties of hardened commercial grout at the age of 90 days

	LP1	LP2	LP3	LP4	LC1	LC2	LC3	C1	C2
Volume change (%)	12.8	3.7	1.2	5.2	0.9	0.6	0.0	1.0	0.0
Bulk density (kg/m ³)	1,373	1,400	1,356	1,620	1,467	1,361	1,518	1,815	1,683
Flexural strength (MPa)	1.3	2.0	0.4	0.6	6.3	2.8	3.1	4.4	4.4
Compressive strength (MPa)	11.2	2.0	12.4	12.5	23.7	21.7	26.9	52.3	47.0
Tensile strength (MPa)	–	0.3	0.7	0.9	0.9	1.4	1.3	1.4	1.6

**Fig. 3** From left: Injection of cylinder, compression strength test, tensile splitting test

4.2 Tests on Cylinders

Cylinders with a diameter of 15 cm and a height of 30 cm were prepared as a simulation of the inner core of a multiple layer stone masonry wall. Cylinders were gradually filled with limestone and sandstone, i.e. 37 wt.% of fraction 45/63 mm and fraction 32/45 mm, 25 wt.% of fraction 16/32 mm and 1 wt.% of fraction 8/16 mm. Specimens were injected with grouts LC1, LC2 and C1, which fulfilled the adopted criteria, and also with grouts C2 and LP3 that did not meet some of the criteria. Grout C2 did not meet the criterion regarding the fluidity retention after 30 min after mixing and grout LP3 did not meet the criterion regarding the fluidity immediately after mixing, as well as criteria regarding volume change and flexural and tensile strengths. However, properties of the hardened grout LP3 are close to the set criteria for the volume change and tensile strength given in Table 1. Thus, overall properties of grout LP3 were most optimal between the hydraulic lime-pozzolana grouts, which was the reason for its selection.

For each grout six specimens were prepared; three for compressive and three for tensile splitting tests. At the age of 90 days cylinders were subjected to compressive tests according to SIST EN 12390-3 [18] and tensile splitting strength tests according to SIST EN 12390-6 [17]. Preparation of specimens, execution of compressive and tensile splitting strength tests and the results are presented in Figs. 3 and 4.

On average, the area of stone represented about 68% and the area of grout 32% of the entire cross-section. For each grout type the percentage of failure across the

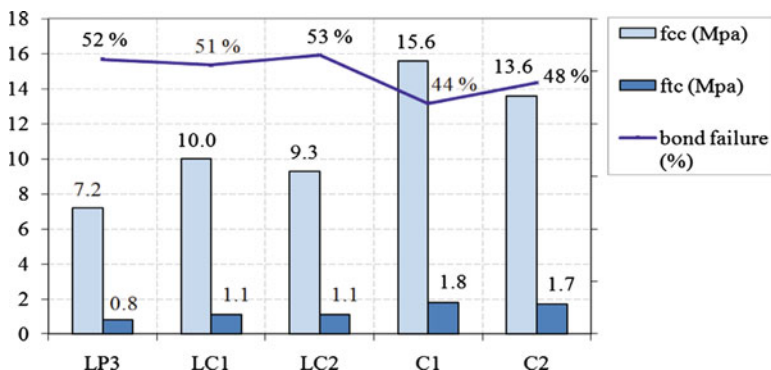


Fig. 4 The average compressive and tensile splitting strengths of cylinders

bond between binder and aggregate was also determined. The results presented in Fig. 4 show that the prevailing mode of failure in the tensile splitting test was that of the bond between the stones and the grout, regardless of the type of used grout, and that slightly better bonding was achieved in the case of cement grouts. Namely, the percentage of failure across bond between binder and aggregate was 51–53% in case of cement-lime grouts and hydraulic lime and pozzolana grout, and 44–48% in the case of cement grouts. As expected, both compressive and tensile splitting strengths were greater in the case of the cement grouted cylinders compared to the cement-lime and hydraulic lime and pozzolana specimens.

5 Laboratory Tests of Designed Injection Grouts

5.1 Constitutive Materials for Grouts

Several compositions of injection grouts using hydrated lime in powdered state or as lime putty and limestone powder, GGBS and tuff as mineral additives were designed and subjected to testing in fresh and hardened state. GGBS and tuff are active mineral additives, often designated as supplementary cementitious materials (SCM). Hydrated lime in powdered state (hereinafter hydrated lime) was supplied by the Slovenian company SIA and limestone powder by the Slovenian company Calcit. The lime putty was burned and slaked in the traditional way and was aged for more than 4 years. Water part in the putty mass is about 55%. Used GGBS is a by-product of a steel plant in Trieste, Italy. It was ground to obtain approximately the same grain size distribution as volcanic tuff, which was supplied by the Slovenian company Sanning. Adequate fluidity of grouts was attained with the help of naphthalensulphonate based superplasticizer (SP) produced by the Slovenian company TKK Srpenica.

5.2 *Laboratory Tests of Constitutive Materials*

5.2.1 Chemical Composition

Chemical compositions of constitutive materials are presented in Table 4 and were determined by chemical analysis according to SIST EN 196-2:2005 [13].

5.2.2 Mineralogical Analysis

Two SCMs used in grout compositions: GGBS and tuff were analysed by x-ray diffraction and observed in SEM.

Tuff sample was composed of 45% clinoptilolite/heulandite, 35% quartz, 11% feldspars, 7% illite/muscovite and 2% montmorillonite (Fig. 5). The composition was found to be poly-mineral with round and sharp edged grains with the size up to 200 µm (Fig. 7). The x-ray analysis of GGBS showed 100% amorphous phase (Fig. 6). The analysed sample was composed of angular grains of different sizes (Fig. 7).

5.2.3 Physical Properties

Density and surface area of constitutive materials are given in Table 5. Density was determined by using the pycnometer method and surface area by using Blain apparatus according to SIST EN 196-6:2010 [19].

5.2.4 Pozzolanic and Hydraulic Activity of SCMs

Pozzolanic activity of volcanic tuff and hydraulic activity of GGBS were estimated by strength characteristics of mortar prepared from hydrated lime, volcanic tuff or GGBS, standard sand, and water in ratio 1:2.9:1.8 by mass. The test was carried out according to former Yugoslav standard JUS B.C1.018 [20]. Mortar was cast in a mould and hermetically closed in a metal box. For the first 24 h the metal box was kept at a temperature of 20°C, then for 5 days at a temperature of 55°C and finally, until the age of 7 days, in the laboratory at a temperature of 20°C. For each additive, three specimens (a, b, c) were tested for flexural strength and six specimens for compressive strength. The results given in Table 6 show that hydraulic activity of GGBS, characterized by flexural and compressive strength development, is greater compared to pozzolanic activity of tuff.

5.3 *Laboratory Tests on Designed Injection Grouts*

In the case of designed grouts, hydrated lime and GGBS were combined to obtain “modern” or industrially produced materials, and lime putty and volcanic tuff were

Table 4 Chemical composition of constitutive materials in % by mass

	SiO ₂	Al ₂ O ₃	Fe ₂ O ₃	CaO	CaCO ₃	MgO	MgCO ₃	MnO	SO ₃	CO ₂	K ₂ O	Na ₂ O	I.o.i.
Tuff	62.96	13.3	3.7	3.76	—	1.94	—	—	0.07	—	3.34	3.07	7.41
GGBS	38.1	9.8	1.1	38.5	—	9.5	—	0.6	2.3	—	—	—	—
Limestone powder	0.07	0.17	0.05	—	97.6	—	1.72	—	—	—	—	—	—
Hydrated lime	0.4	—	0.18	72.0	—	0.83	—	—	0.1	2.56	—	—	25.10
Lime putty	—	—	—	85.99	—	11.5	—	—	0.04	1.46	—	—	—

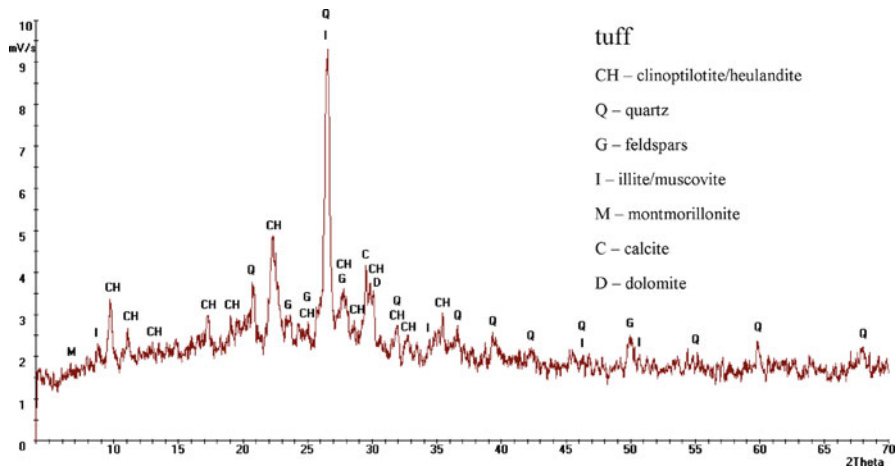


Fig. 5 X-ray diffraction diagram of volcanic tuff

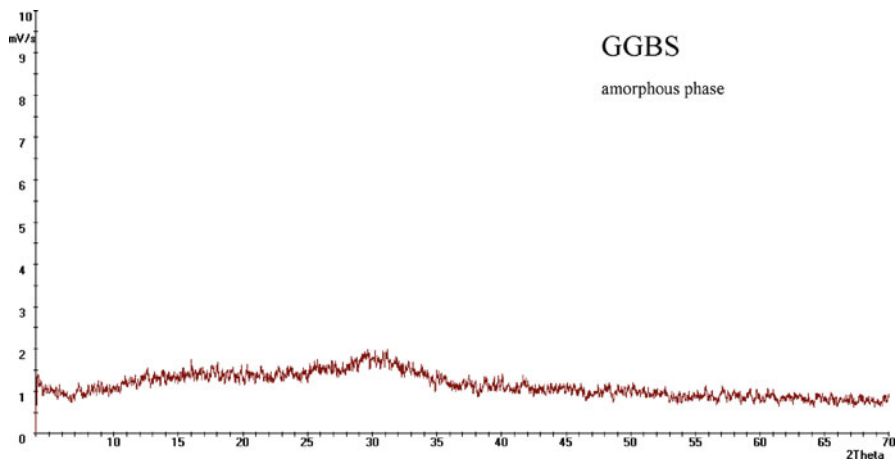


Fig. 6 X-ray diffraction diagram of GGBS

combined to obtain “traditional” materials. Limestone powder and superplasticizer were also added to the grouts.

5.3.1 Composition and Properties of Injection Grouts

In the study four different “modern” grouts (G1 to G4) and four different “traditional” grouts (G5 to G8) were used (Table 7).

Limestone powder, in the amount of 20% was added to grouts G3, G4, G7, and G8. The fluidity tests with grouts containing lime putty (G5-G8) were started without

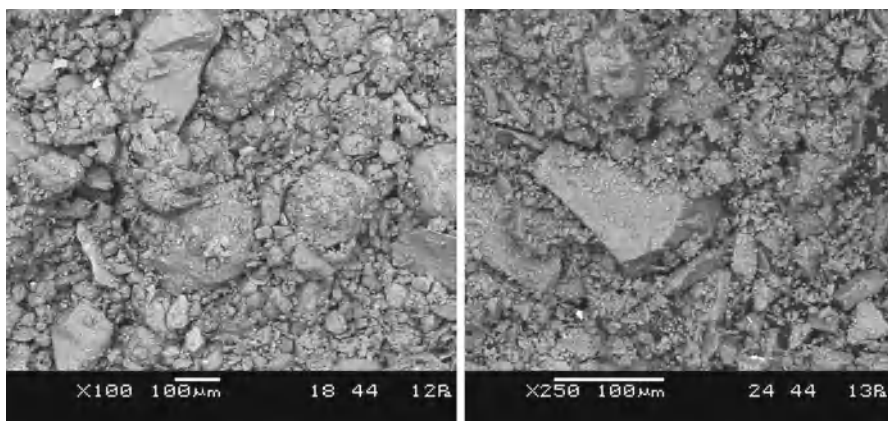


Fig. 7 SEM images of volcanic tuff (*left*) and GGBS (*right*)

Table 5 Physical properties of constitutive materials

	Density (g/cm ³)	Surface area (cm ² /g)
Volcanic tuff	2.41	2,910
GGBS	2.85	2,930
Limestone powder	2.75	3,300
Hydrated lime	2.28	14,920

Table 6 Flexural and compressive strength of mortar with volcanic tuff and GGBS at the age of 7 days

Volcanic tuff	a	b	c	Average
Flexural strength (MPa)	1.5	1.6	1.6	1.6
Compressive strength (MPa)	4.1/4.2	4.5/4.4	4.3/4.5	4.3
GGBS	a	b	c	Average
Flexural strength (MPa)	2.6	2.5	2.4	2.5
Compressive strength (MPa)	5.1/5.2	5.2/5.2	4.9/5.0	5.1

additional water. The addition of SP was optimised in the grouts containing hydrated lime and in the grouts containing lime putty. The influence of added SP was analysed for two mixtures, G1 (basic hydrated lime mixture) and G5 (basic lime putty mixture), by considering two criteria: adequate fluidity (around 20 s) and moderate bleeding ($\leq 2.0\%$). The amount of added SP was optimized by gradually increasing its proportion from 0.5% to 2.5% by mass of binder (lime and SCM) and by simultaneously analysing its effect on fluidity and bleeding. After the comparison of the results, the addition of 1.5% of SP was chosen for mixtures G1-G4 and the addition of 1.0% of SP for mixtures G5-G8. Water content and thus water-binder ratio was adjusted for single grout mix in order to obtain adequate fluidity. Composition of designed injection grouts is given in Table 7.

Density [21], fluidity, volume change and bleeding [11] and compressive and flexural strengths [16] of grouts were determined (Table 8).

Table 7 Composition of dry part of designed injection grouts in %

	Lime (%)		Filler (%)		SCM (%)		w/b ratio
	Hydrated lime	Lime putty ^a	Limestone powder	GGBS	Tuff	SP (%)	
G1	80	0	0	20	0	1.5	0.95
G2	60	0	0	40	0	1.5	0.70
G3	60	0	20	20	0	1.5	0.90
G4	40	0	20	40	0	1.5	0.65
G5	0	80	0	0	20	1.0	0.95
G6	0	60	0	0	40	1.0	0.71
G7	0	60	20	0	20	1.0	0.97
G8	0	40	20	0	40	1.0	0.68

^aOnly lime in the lime putty

Table 8 Properties of designed injection grouts in fresh and hardened state at the age of 28 days

	Density (kg/m ³)	Fluidity ^a (s)	Volume change (%)	Bleeding (%)	Compressive strength (MPa)	Flexural strength (MPa)
G1	1,400	16.2/15.6	4.7	2.6	0.8	—
G2	1,510	20.3/18.2	3.9	3.2	1.9	—
G3	1,460	16.6/16.1	4.3	2.8	1.1	—
G4	1,560	17.4/17.0	2.4	1.6	3.6	—
G5	1,435	12.6/13.9	11.1	1.3	2.5	0.9
G6	1,516	17.6/18.1	6.2	0.8	2.8	0.9
G7	1,488	13.1/13.3	9.6	1.0	2.8	0.8
G8	1,616	11.8/12.0	5.3	1.6	2.9	1.1

^aMeasured immediately after mixing and after 30 min

Although properties of the designed injection grouts in hardened state were determined already after 28 days and not after 90 days, as for the commercial grouts, the obtained results indicate that after 90 days some of the designed grouts could fulfil the preset criteria (Table 1). The most promising results were achieved with grouts G4 and G8, with the addition of 20% of limestone powder and 40% of GGBS and volcanic tuff. Relatively low fluidity values (17.4/17.0 s in G4 and 11.8/12.0 s in G8), moderate volume change (2.4% for G4 and 5.3% for G8) and bleeding (1.6% for both grouts), as well as relatively high compressive strengths (3.6 MPa for G4 and 2.9 MPa in case of G8), were attained for these two mixtures. In case of “traditional” grout G8 also the highest flexural strength (1.1 MPa) was obtained.

6 Conclusion

Adopted criteria for commercial injection grouts in dry, fresh and hardened state aimed to be universal and should be used when selecting the optimal grout for strengthening of heritage structures with architectural and cultural assets (frescoes, stucco, etc.). However, it seems that criteria regarding strength characteristics of

grouts are too high for lime-based grouts to be selected as adequate material. Tensile splitting tests performed on cylinders injected by commercial grouts pointed out the importance of the bond achieved between the stones and the grout: the prevailing mode of failure was always that of the bond between the stones and the grout, regardless the type of grout used. These results favour the importance of bonding achieved between the two materials rather than their individual mechanical properties. Since, as stated above, bond strength between grout and stones is the governing property that shows the efficiency of hardened grout, values regarding compressive and tensile splitting strength obtained on grout injected cylinders could be more relevant than those obtained solely on hardened injection grouts.

The aim of designing hydrated lime-based injection grouts was to obtain compositions that would be more suitable for the strengthening of historic masonry buildings, due to their compatibility with materials present in the buildings. So far, the most promising results regarding their workability, stability and strength characteristics have been achieved with the lime-based grouts G4 and G8 with the addition of 20% of limestone powder and 40% of SCM (GGBS or pozzolana). The lowest value of volume change was attained with compositions containing 40% of GGBS. However, when applying GGBS in injection grout compositions, one has to be aware of its limitations. Sulphates present in GGBS can be, under some circumstances, damaging for the old masonry to be treated [4].

Acknowledgement The research was financed by the European Union, European Social Fund through Slovenian Technology Agency TIA. Their contribution is gratefully acknowledged.

References

1. Kramar, S., Mirtič, B.: Characterisation of historical mortars as a part of conservation – restoration interventions and archaeological post-excavation analyses. Mater. Geoenviron. **56**(4), 501–519 (2009)
2. Zalar, V.: Mineralogical characterization of Roman age renders from Mošnje and Ljubljana (in Slovenian). Undergraduate thesis, University of Ljubljana. Faculty of Natural Sciences and Engineering, Department of Geology, Ljubljana, 136 p (2009)
3. Penazzi, D., Valluzzi, M.R., Saisi, A., Binda, L., Modena, C.: Repair and strengthening of historic masonry buildings in seismic areas. In: Proceedings of the International Congress on the More than Two Thousand Years in the History of Architecture Safeguarding the Structure of our Architectural Heritage, Bethlehem, Palestine, 2, Sec. 5, Bethlehem, 1–6 (2001)
4. Collepardi, M.: Degradation and restoration of masonry walls of historical buildings. Mater. Struct. **23**, 81–102 (1990)
5. Uranjek, M., Žarnić, R., Bosiljkov, V.: Strengthening of heritage buildings by means of Grout injection-problems and solutions. HMC 2010, Prague, 22–24 September 2010, 769–777 (2010)
6. EN 447.: Grout for prestressing tendons- specification for common grout, 5 p (1996)
7. Van Rickstal, F.: Grout injection of Masonry, scientific approach and modelling. Doctoral Dissertation. Leuven, Katholieke University Leuven, 195 p (2000)
8. Zatler-Zupančič, B., Mladenovič, A.: Alkali reaction in concrete (in Slovenian). Information ZRMK Ljubljana 312, XXXV, 3 – 4 – 5, Ljubljana, 5 p (1994)

9. Valuzzi, M. R., Binda, L., Modena, C.: Experimental and analytical studies for the choice of repair techniques applied to historic buildings. *Mater. and Struct.* June 2002, **35**, 285–292
10. Miltiadou, A., Kalagri, A., Delinikolas, N.: Design of hydraulic grout and application methodology for stone masonry structures bearing mosaics and mural paintings: the case of the katholikon of Dafni Monastery. In: International Symposium: Studies on Historical Heritage, Antalya, Turkey, 17–21 September 2007, p 649–656. Istanbul, Yildiz Technical University, RCPHH, Istanbul (2007)
11. EN 445.: Grout for prestressing tendons – test methods, 12 p (1996)
12. EN 446.: Grout for prestressing tendons- Grouting procedures, 8 p (1996)
13. SIST EN 196-2:2005.: Methods of testing cement: chemical analysis of cement (2005)
14. SIST EN 1015-6: 1999.: Methods of test for mortar for masonry – Part 6: Determination of bulk density of fresh mortar, 9 p (1999)
15. SIST EN 1015-10: 2001.: Methods of test for mortar for masonry – Part 10: Determination of dry bulk density of hardened mortar, 7 p (2001)
16. SIST EN 1015-11: 2001.: Methods of test for mortar for masonry – Part 11: Determination of flexural and compressive strength of hardened mortar, 12 p (2001)
17. SIST EN 12390-6: 2001.: Testing hardened concrete – Part 6: Tensile splitting strength of test specimens, 10 p (2001)
18. SIST EN 12390-3: 2002.: Testing hardened concrete – Part 3: Compressive strength of test specimens, 15 p (2002)
19. SIST EN 196-6:2010.: Methods of testing cement – Part 6: Determination of fineness (2010)
20. JUS B.C1.018.: Pozzolana: Quality and testing methods (in Slovenian) (1959)
21. SIST EN 1015-3:2001.: Methods of test for mortar for masonry – Part 3: Determination of consistence of fresh mortar (2001)

Part IV

Assessment and Testing

Characterisation of Mortars Using Drilling Resistance Measurement System (DRMS): Tests on Field Panels Samples

Dória Costa, Ana Magalhães, and Maria do Rosário Veiga

Abstract Non-destructive or micro-destructive *in situ* tests are very relevant to the physical characterisation of materials used in historical buildings. “*Controlled penetration*,” “*sphere shock*” and “*sonic methods*” can be used to evaluate the mechanical resistance of mortars and renders or to monitor the hardening process after their application. Used to evaluate surface hardness, *micro-drilling* (DRMS) is a very sensitive technique, and its use in this field is expected to contribute to more precise results. However, the diversity of the composition of mortars and the systematic presence of abrasive components are limiting factors for the use of this method in this field. In this study, several mortars with different composition and hardness are compared using drilling resistance as the comparative parameter. The mortars were applied on-site aiming at their use in real situations. Extracted mortar samples were tested in the laboratory using resistance drilling which was complemented by additional methods currently used for *in situ* characterisation of these materials. The results highlight the need for an integrated perspective of laboratory and on-site information.

1 In Situ Testing of Mortars and Renders: General Aspects

The conservation of old renders and mortars requires a full characterisation of the old materials, as well as a very good knowledge of the new ones considered as the most adequate solutions for their replacement. In general, both laboratory and *in*

D. Costa (✉)

National Laboratory for Civil Engineering (LNEC), Lisbon, Portugal
e-mail: drcosta@lnec.pt

A. Magalhães • M. do Rosário Veiga

LNEC, Lisbon, Portugal
e-mail: anacristian@hotmail.com; rveiga@lnec.pt

situ characterisations are considered necessary, and the integration of these two types of information is required for a correct diagnosis and to reach the best solution during conservation or restoration works.

Studies performed in laboratory conditions involving mortars and renders usually consider several parameters and are very well documented in the vast literature published in this domain [1–4]. Although the characterisation of the materials applied on-site is considered necessary, the few techniques available are considered inaccurate. The LNEC team has been using several methods to characterize old mortars *in situ* to evaluate the decay state and the properties of the old materials where they are still well-preserved. In some cases, to complement laboratory studies, experimental panels of new formulations have been prepared in order to predict their behaviour, to allow a better selection for the specific case and to evaluate the compatibility with locally preserved old materials [5–7].

In situ evaluation of a good performance of mortars and renders includes several parameters; “the adhesion to background” and “degree of carbonation” (applicable to control the evolution of new formulations in time), as well as moisture properties, such as “moisture content” and “water permeability under low pressure” are relevant parameters for the purpose. *In situ* techniques can help with controlling the expected behaviour of new formulations or provide more specific information that can explain decay, as the load of salts present. Regarding the mechanical characterisation, some relevant tests can also be done in order to indirectly evaluate the strength of mortars, including: (i) “*sphere impact*” and (ii) “*controlled penetration*,” two tests that are able to evaluate a kind of resistance of material when a physical object hits the surface. A sonic method, namely (iii) “*Pulse wave velocity*,” is a very interesting non-destructive technique; when it is used to characterize a surface, the “*indirect array*” must be used, although, in this case, additional difficulties related to the interpretation of the results are introduced. (iv) “*Schmidt hammer test*” could be also used to evaluate rebound hardness [8] but its use on mortars is limited compared to its use in objects made of concrete. Integration of all information provided by multiple tests is generally accepted as the best practice for improving quality of *in situ* characterisation.

In situ characterisation of materials and its decay state is a universal demand. *Non-destructive* or at least *micro-destructive* techniques and tests have been developed and used in the last years for better characterisation of stone materials used in historical buildings. The “*micro-drilling technique (DRMS)*” was developed for stone characterisation, not only in the laboratory but mainly for *in situ* analysis [9]. When applied to mortars, this technique needs to be properly evaluated, given the nature of these materials, specifically their high quartz content and high heterogeneity. A new instrument has been available and has been successively updated since about 2000 (SINT Technology, Italy) but its use for the characterisation of mortars is still very limited.

2 Materials and Methods

This paper presents the results of drilling tests performed on samples [10] collected from experimental panels prepared with several lime based mortars, applied in a fortress near Lisbon (“Forte dos Oitavos”). The compositions of the mortars were chosen taking into account the original compositions of old lime mortars present and considering compatibility criteria [7].

2.1 Samples

In this study, several compositions of mortars were considered. They include several binders: lime, hydraulic lime, natural pozzolan (from Cabo Verde), silica fume, metakaolin, and white cement. The aggregate nature and grain size distribution was the same for all the panels: quartzitic sand mixed with some clay 0–4 mm for the inner layer and 0–2 mm for the external layer. The panels were prepared according to a specific protocol and the mortars were applied in two layers with different compositions, as it was previously described [7]. The panels’ compositions are described in Table 1. Figure 1 illustrates three zones of those experimental panels on the Fortress walls (a), the macroscopic appearance of the mortars (b) and the drilling equipment used (c).

After *in situ* characterisation (water permeability [7], deformability and mechanical resistance), some samples were removed from the panels for laboratory testing (resistance drilling, ultrasonic and compressive strength tests). These samples are more heterogeneous than conventional laboratory specimens because they are composed of two different layers. Furthermore, they have been exposed to complex conditions, namely, submitted to suction of the substrate in fresh state, variable climatic conditions during the hardening period, and exposure to air over much of the surface. These external conditions produce changes in the microstructure of mortars not expected in laboratory specimens.

2.2 Methods

This study focus on the drilling test (DRMS) results obtained on samples described above. In addition to the DRMS data, ultrasonic and compressive strength results, as well as results from other *in situ* techniques, are used for comparative purposes.

2.2.1 Micro-drilling Technique (DRMS)

The equipment used is from SINT Technology, Italy. The model is a prototype built for the EC project “Development of a new method to determine the superficial hardness of exposed monumental rocks”, updated afterward. The test consists of drilling

Table 1 Composition of mortars tested on the experimental panels

Main constituents	P1 lime/hydraulic lime	P2 lime/white cement	P3 lime/pozzolan	P4 lime/silica fume	P5 lime/metakaolin
Volumetric dosage (air lime: other binder : sand)	1:1.6 (1st) 1:2.9 (2nd)	1:1.6 (1st) 1:2.9 (2nd)	1:0.5:2.5 (1st) 1:0.5:3 (2nd)	1:0.25:2.5 (1st) 1:0.25:3 (2nd)	1:0.5:2.5 (1st) 1:0.5:3 (2nd)

(1st) first (inner) layer, (2nd) second (top) layer

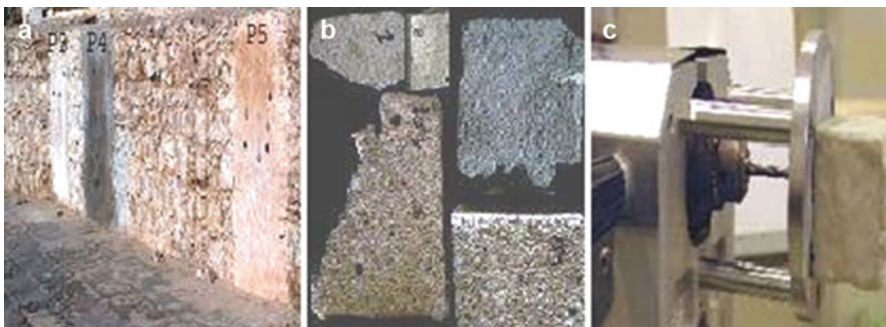


Fig. 1 The experimental panels (a), the macroscopic appearance of the mortars (b), and the DRMS front (c)

a hole and continuously measuring the penetration force with a load cell. During the test, the rotational speed and the penetration rate are kept constant. “Drilling resistance” or “surface hardness determined by drilling” are terms also used to express the value measured.

Several types of drill bits can be used; in this case a 5 j mm of Fischer Extra produced by BOSCH was used. The initial conditions of testing were selected taking into account the expected low resistance of these lime-based materials. The rotation speed of 100 rpm and the penetration rate of 10 mm/min were selected (“100/10”). Moreover, higher values of rotation speed (up to 1,200 rpm) were also used in order to test the harder samples. For comparative purposes, only values obtained with the same drilling conditions can be compared. For this reason, this paper only presents results obtained with “400/10.” In order to have some information on the wear effect of the drill bits, a very soft, non-abrasive and homogeneous limestone (Ancă stone) was also drilled.

The experience gathered by utilizing this method on several rock materials allowed us to take several aspects into account when interpreting the drilling data. The “packing effect” due to difficult removal of cuttings and the “abrasiveness” of the material on the drill bit are two examples of effects that can increase the measured values [11, 12].

2.2.2 Other Techniques

The *Ultrasonic pulse velocity* (UPV) is calculated as the travel time of the longitudinal wave between two points located at a known distance in the material. An electro-acoustical transducer held in contact with the surface produces a pulse of longitudinal vibrations. After traversing the material, the pulse of vibrations is re-converted into an electrical signal by a second transducer placed at a known distance. Electronic timing circuits enable the transit time of the pulse to be measured. The equipment used is the Ultrasonic Tester BP-7, from Steinkamp, Germany.

In laboratory conditions, the UPV was determined following the *direct mode* (transmission), by using exponential transducers of 45 kHz. The *Sphere impact test* consists of impacting a hard body with the energy of 3 J, produced with a steel sphere of 50 mm in diameter [6, 7]. The impact resistance evaluated through the diameter of the concussion made by the sphere, and the type of the damage, make it possible to assess the mortar's deformability.

The *Controlled penetration test* consists of the penetration of a steel nail, guided by a device fixed to Martinet Baronne apparatus to guarantee that the stroke is perpendicular to the surface. Several impacts (typically, three impacts) with constant energy are produced and the respective penetration depths are registered. This test gives information on the mechanical resistance of render, permitting the assessment of their performance [6, 7]. For the *compressive strength* evaluation of the samples an ETIHM-S testing machine with a 200-kN load cell was used; due to the dimensions of these samples, the results should be analyzed in a comparative basis.

3 Results

3.1 Drilling Tests

Drilling tests performed on mortars show very different characteristics in comparison with typical graphs obtained in homogeneous rocks such as Ançã (as it is shown on Fig. 2, blue line in P2, on the left). Mortars are very heterogeneous materials, and the presence of quartz grains justifies the large variations of the registered forces.

Despite being so diverse and heterogeneous, the materials tested are clearly distinct. For instance, sample P4 shows lower values of drilling forces when compared to P3 and P2. P2 is the hardest of the tested materials. In two cases (P2 and P3), the graphs indicate the presence of two zones with different characteristics; the A layer (10–15 mm) is softer than the B, in which the values of forces are higher. This is explained by the application in two layers, with the internal layer designed to be harder than the external one. In the case of P2, the drilling of the “B layer” reaches the maximum limit imposed by the load cell (100N), and even under extreme conditions (1,200 rpm) it was not possible to drill this part of the sample. In this particular case, this is due to the presence of different layers in this sample, but without any information about the characteristics of the material, this effect could be misunderstood or attributed to the well known “packing effect” that results from dust accumulation inside the hole. In P3, the existence of two layers is also identified, but in this case the two zones are much more similar. On the contrary, the results for sample P4 do not differentiate the two layers as established in the preparation protocol.

A certain handicap must be noted when the drilling technique is used to characterize mortars. In very weak materials, the resistance offered by the material is low. Fissures develop and propagate during the process, producing drill holes with irregular borders and increasing the variation of forces measured during the test. The indentation phase, well-recognized on a typical drilling graph, is not evident in the

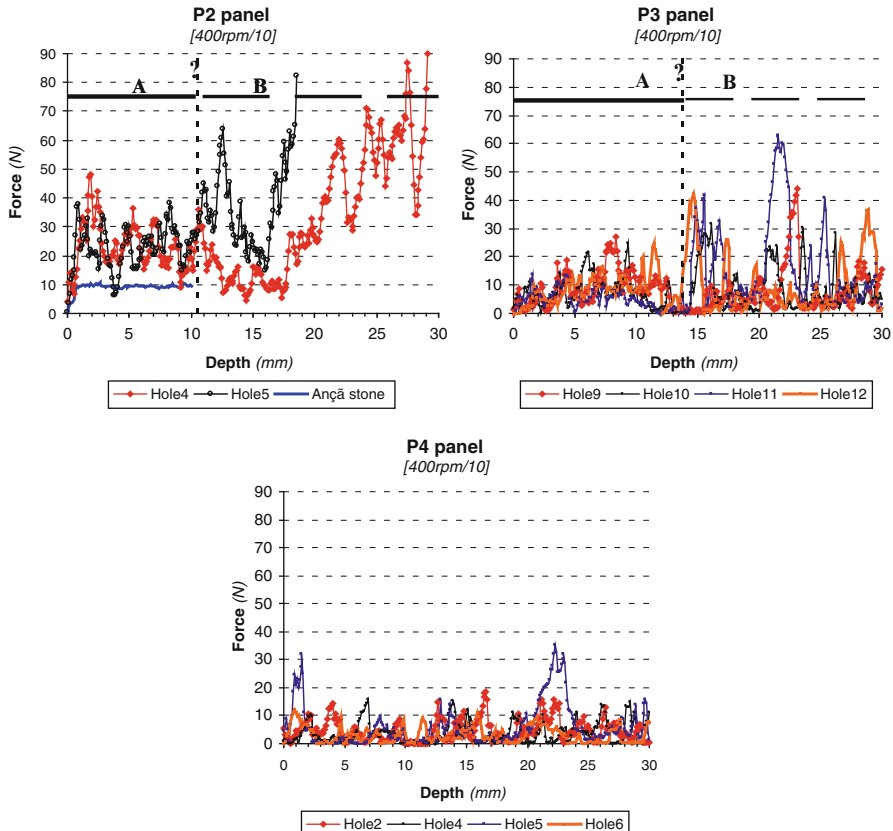


Fig. 2 Drilling graphs of panel samples (**Note: In the panel P2 and P3 two different units are present: “A” is interpreted as the “top layer” in table I, and “B” is interpreted as the “inner layer” in the same table. On the contrary, on P4 these two units are not detected)

graphs obtained on mortars, as clearly seen on the examples. For all these reasons, the distributions of drilling forces obtained on heterogeneous materials have a pronounced range of values; the standard deviation is of the order of magnitude of the average values, and in these circumstances the results and conclusions must be taken with care. Even so, the method can also be used in these particular cases, especially if this information is properly integrated.

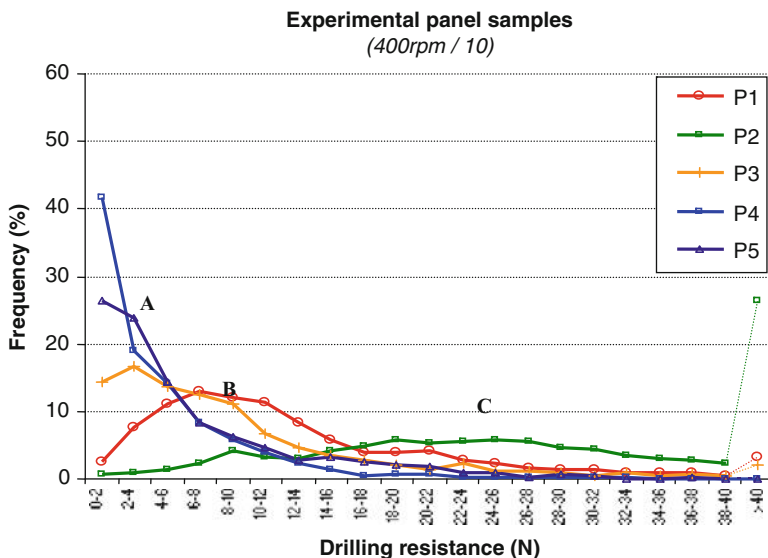
The mortars abrasiveness was taken into account when the drilling tests were planned. The results indicate that all the materials tested were able to wear the drill bit. In this context and for comparative purposes, the raw data without any correction are considered valid.

Table 2 presents the global average results of the drilling tests. These values include both layers, even when drilling tests can discriminate their presence.

Each sample was tested with a different drill bit and about ten holes were drilled. The results are expressed as the mean value of the drilling forces along the total

Table 2 Drilling resistance measurements of mortars (average global values)

Panel samples	P1 lime/ hydraulic lime	P2 lime/ white cement	P3 lime/ pozzolan	P4 lime/ silica fume	P5 lime/ metakaolin
Force (N) [400 rpm/10]	11.9	31.5	9.7	4.4	6.4

**Fig. 3** Frequency distributions of drilling forces on mortar samples

length of the hole. Of special note are effect of the white cement in the resistance increase and effect of addition of natural pozzolan in comparison with metakaolin or silica fume, which produces values similar to those obtained in a mixed formulation with hydraulic lime (P1).

Besides the mean values, the distribution of the values of forces is also meaningful for the comparison of these heterogeneous materials, as evident in the histogram presented in Fig. 3. P4 and P5 are considered “weak” mortars, identified by A in the graph. They are completely distinct from “strong” mortars identified as C, which in this particular case are characterized by a very wide range of values, represented in this group by P2. B group represents intermediate characteristics of hardness and includes P1 and P3.

3.2 Other Measurements

In different phases of the study, several data were obtained on the experimental panels; during the curing process, 14 weeks after application, *sphere impact* and

Table 3 Drilling forces and other resistance measurements

Samples	P1 lime/ hydraulic lime	P2 lime/ white cement	P3 lime/ pozzolan	P4 lime/ silica fume	P5 lime/ metakaolin
DR-Force (N) [400 rpm/10]	11.9	31.5	9.7	4.4	6.4
Ultrasonic velocity (m/s)	1,700	2,900	1,090	950	1,530
Compressive strength (N/mm ²)	1.2	3.8	1.5	0.7	0.8
Sphere impact (φ, mm) ^a	15	12	11	15	11
Controlled penetration (mm) ^{a, b}	11.7	7	6.6	10	9.7

^aDetermined directly on panels after 14 weeks app

^bΣ three penetrations

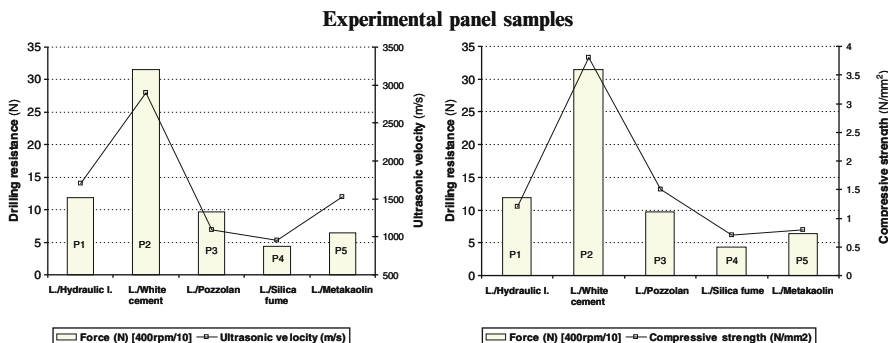


Fig. 4 “Drilling resistance” results versus “Ultrasonic velocity”/“Compressive strength”

controlled penetration tests were performed. Later, samples were extracted and tested in the laboratory in different steps, the last one corresponding to the drilling, and ultrasonic tests. For comparison, all data are presented in Table 3, and the graphs of Fig. 4 represent the most significant correlations.

Measured *in situ*, sphere impact and controlled penetration gave information about the evolution of the resistance in time, and the latter was able to discriminate the different mortar formulations. Nevertheless, as indicators of the final resistance of the surface, the interpretation must be considered with care.

The ultrasonic velocity is in good agreement with drilling results, although expressed by the average values of the distributions with great variations.

For hardness characterisation, the drilling test should be performed on quite homogeneous samples, but these *in situ* samples are much more complex due to the application process by layers. In spite of this fact, the classic correlation of compressive strength to drilling hardness indicates the same behaviour, as is clear from the graphs presented here.

4 Conclusions

In this paper, non-destructive and micro-destructive techniques were used in the laboratory to characterize the mechanical resistance of mortars applied on experimental panels simulating real applications.

The ultrasonic velocity, measured in direct mode, is in good agreement with the drilling results. For hardness characterisation purposes, drilling tests performed on very heterogeneous materials were able to discriminate different formulations of mortars. The correlation of compressive strength to drilling hardness indicates a strong correlation coefficient and must be considered an encouraging finding, but the low number of samples indicates a need for further research in this domain.

Further investigations should be conducted comparing laboratory samples with similar formulations, prepared according to regular procedures used for laboratory testing. *In situ* characterisation of mortars with similar formulations is also needed, not only because the methods must be applied in different conditions (as is the case of the sonic method), but also because the variability of local parameters can influence the final results obtained through *in situ* measurements.

References

1. Elsen, J.: Microscopy of historic mortars – a review. *Cem. Concr. Res.* **36**, 1416–1424 (2006)
2. RILEM TC 203-RHM – repair mortars for historic masonry. Testing of hardened mortars, a process of questioning and interpreting. *Mater. Struct.* vol. 42, No. 7, 2009, pp. 853–865
3. Magalhães, A., Veiga, M.R.: Physical and mechanical characterisation of ancient mortars. Application to the evaluation of the state of conservation. *Mater. Constr.* **59**(295), 61–77 (2009). doi:[10.3989/mc.41907](https://doi.org/10.3989/mc.41907)
4. Veiga, M.R., et al.: Methodologies for characterisation and repair of mortars of ancient buildings. In: International Seminar Historical Constructions 2001. Universidade do Minho, Guimarães, November 2001
5. Magalhães, A.C., Veiga, M.R., Carvalho, F.: Diagnosis of anomalies of wall renderings. Experimental techniques for *in situ* application. In: Proceedings of XXX IAHS World Congress on Housing, Coimbra, Portugal, 9–13 Sept 2002
6. Magalhães, A., Veiga, M.R.: Comparison of *in-situ* mechanical tests on masonry mortars: sphere impact and controlled penetration test. In: International Conference on Heritage, Weathering and Conservation (HWC), Madrid, June 2006
7. Veiga, M.R., Velosa, A.L., Magalhães, A.C.: Experimental applications of mortars with pozzolanic additions. Characterization and performance evaluation. *Construct. Build Mater.* **23**(1), 318–327 (2009)
8. US Department Interior.: Nondestructive method for hardness evaluation of mortars (Project report). Preservation Technology and Training. Publication No 1999–02 (1999)
9. Tiano, P., Filaretto, C., Ponticelli, S., Ferrari, M., Valentini, E.: Drilling force measurement system a new standardisable methodology to determine the stone cohesion: prototype design and validation. *Int. J. Restor. Build. Monum.* **6**(2), 133–150 (2000)
10. EUROPEAN COMMITTEE OF STANDARDIZATION (CEN) – Methods of test for mortar for masonry – Bulk sampling of mortars and preparation of test mortars. CEN EN 1015–2 (1999)

11. Mimoso, J.M., Costa, D.: A new DRMS drilling technique for the laboratory. In: ART'05 – 8th International Conference on Non Destructive Investigations and Microanalysis for the Diagnostics and Conservation of the Cultural and Environmental Heritage, vol. 2, pp. 651–656 (2005)
12. Delgado Rodrigues, J., Costa, D.: A new method for data correction in drill resistance tests for the effect of drill bit wear. Int. J. Restor. **10**(3), 219–236 (2004)

In Situ Techniques for the Characterisation of Rendering Mortars

Ana Paula Ferreira Pinto, Rita Nogueira, and Augusto Gomes

Abstract Compressive strength, porosity and two “*in situ*” techniques (ultrasonic velocity and rebound hardness test) are used for the characterisation of several aerial, hydraulic lime-based and cement-based mortars. Prismatic specimens and mortars applied as a brick render are used for the characterisation. A comparative analysis of the “*in situ*” test results and compressive strength is performed and the relationship between porosity and ultrasound velocity is analysed. A satisfactory relationship between the porosity and ultrasound velocity values is found and this indicates the possibility of estimating porosity from ultrasound velocity. The relationship between ultrasound velocity, rebound values and compressive strength emphasizes the potential of the “*in situ*” test methods for characterisation of mechanical properties of mortars.

1 Introduction

Renders are the most common external wall covering of the world’s built heritage. They are particularly exposed to aggressive physical and mechanical actions and often need conservation operations to prevent further degradation. For the characterisation of renders and the assessment of their degradation forms and processes, several characterisation tests methods need to be used [1]. However, sampling is not always feasible and even if it is, the number of samples that can be taken is often limited and the testing methods that can be used in the laboratory for their characterisation are limited due to their shape and size diversity [2]. The solution is, therefore,

A.P.F. Pinto (✉) • R. Nogueira • A. Gomes

UTL-Instituto Superior Técnico – ICIST, Lisbon, Portugal

e-mail: anapinto@civil.ist.utl.pt; ritanog@civil.ist.utl.pt; augusto@civil.ist.utl.pt

to complement the information that can be achieved with the characterisation of collected samples with the use of “*in situ*” techniques, for assessment of the render’s properties on site [3].

“*In situ*” tests are specially designed to be applied on site and are usually easy to carry out, economical and non-destructive or semi-destructive, and the results are quickly available. However, the interpretation of the results achieved with “*in situ*” test methods is not always straightforward. The long experience of using laboratorial test methods for mortar characterisation and the interest in doing it by means of “*in situ*” tests justify the importance of seeing how possible it is to estimate some of the physical and mechanical properties of rendering mortars through “*in situ*” characterisation test methodologies [3, 4].

The purpose of this paper is to compare results and to establish relations between data provided by current laboratory test methods (compressive strength and porosity) and “*in situ*” test methods (ultrasonic velocity and rebound hardness), so that the long experience and knowledge reached with the first could be transposed to the latter and, hence, make the “*in situ*” tests more trustworthy for dissemination through the scientific and technical community.

2 Mortars and Materials

To achieve the proposed aims, 25 mortar formulations (see Table 1) were tested in order to have a wide range of mechanical and physical properties. This range was obtained with different binders, water/binder ratios, aggregates, curing ages, consistencies and curing conditions. These formulations have been tested within the framework of a research project that addressed the characterisation of rendering mortars, and more detailed information about their characteristics can be found elsewhere [5–12].

Most of the tested mortars have a volumetric binder/aggregate ratio of 1:3. Three different siliceous sands – yellow sand (Y), river sand (R) and fine sand (F) – were used, combined in different proportions or alone, and this provided six different aggregate mixtures with fineness modulus (FM) comprised between 1.5 and 3.0, see Table 1. The maximum aggregate sizes (D) of the sands are: 2.38 mm (Y, R) and 0.59 (F). The fineness modulus was calculated as the sum of the cumulative percentages by mass retained on the sieves (4.76, 2.38, 1.19, 0.59, 0.297 and 0.149 [mm]) divided by 100 [based on prEN13139:1998]. The maximum aggregate size (D) was defined by the size of the smallest sieve opening through which passed 90% or more of the aggregate sample.

Four binders were used: a commercial hydrated lime CL90 [EN459-1:2002]; a lime putty slaked in a laboratory from a CL90 commercial powdered lime; a commercial NHL5 [EN459-1:2002]; and a CEM II/B – L 32.5 N [EN197-1:2000]. The water/binder ratios of the mortars were what was required to achieve a consistency corresponding to the spread of 165 ± 5 mm [13] given by the flow table test [EN1015-3:1999], with the exception of C10 (130 ± 3 mm) and C11 (210 ± 1 mm).

Table 1 Tested mortars

Mortar	Aerial lime (CL90) 1:3			Hydraulic lime (NHL5) 1:3			Cement (CEM II/B-L 32.5 N) 1:3; 1:2.5; 1:3.5		
	Aggregate		w/b ^d	Aggregate		w/b ^d	Mortar		FM
	Comp. ^b	FM ^c		Comp.	FM		Comp.	FM	
A1	½ Y + ½ R	2.8	1.62	H1	½ Y + ½ R	2.8	0.75	C1, C2	½ Y + ½ R
A2 ^a	½ Y + ½ R	2.8	1.73	H2	Y	3.0	0.80	C3	½ Y + ½ R
A3	½ Y + ½ R	2.8	1.55	H3	F	1.5	0.95	C4(1:2.5)	½ Y + ½ R
A4	Y	3.0	1.48	H4	½ Y + ½ F	2.3	0.81	C5(1:3.5)	½ Y + ½ R
A5	R	2.6	1.61	H5	⅔ Y + ⅓ F	2.3	0.80	C6	Y
A6	½ Y + ½ F	2.3	1.48	H6	½ Y + ½ R	2.8	0.82	C7	F
A7	⅔ Y + ⅓ F	2.3	1.44	H7	½ Y + ½ R	2.8	0.77	C8	½ Y + ½ F
								C9	⅔ Y + ⅓ F
								C10(1:2.5)	½ Y + ½ R
								C11(1:3.5)	½ Y + ½ R

Binder, aggregate or aggregate mixture, binder/aggregate ratio and water/binder ratio

^aLime putty

^bComp. Composition of the aggregate mixtures

^cFM Fineness modulus

^dw/b water/binder ratio

The most important factors that influenced the water-binder ratio were: type of binder, aggregate granulometry and binder/aggregate ratio. The flow table value of 165 ± 5 mm was achieved with water/binder ratios ranging from 0.5 to 0.95 for the hydraulic mortars and from 1.44 to 1.73 for the aerial lime based mortars.

Mortar production was based on EN1015-2:1998 recommendations. The mortar characterisation was performed on prismatic specimens ($4 \times 4 \times 16$ cm³) and on mortars applied as brick coat (2 cm thickness) simulating a render. Mortars were cast into prismatic moulds $40 \times 40 \times 160$ [mm] and the specimens were stored in a laboratory room at $20^\circ\text{C} \pm 2^\circ\text{C}$ and $50\% \pm 5\%$ of relative humidity until their characterisation. Hydraulic and lime mortar specimens were removed from the moulds after 2 and 7 days, respectively. The mortars H6, H7, C2 and C3 were cured under wet conditions ($20^\circ\text{C} \pm 2^\circ\text{C}$ and $95\% \pm 5\%$ of relative humidity).

The characterisation of the aerial lime was performed after curing times of 60 and 90 days and the hydraulic mortars with a curing time of 28 days. Some mortars were also tested at younger ages. The mortars A1, A2 and A7 were tested after curing times of 14, 21 and 28 days. The mortars H1, C1, C10 and C11 were tested at some of the following ages: 3, 7, 14, 21, 60 and 90 days.

Considering the influence of curing time on the mortars' physical and mechanical properties [14], the open porosity and ultrasound velocity of all the mortars after 2 years of curing time were also measured. It is expected to find an increase of compressive strength and a decrease of porosity in older mortars, particularly in lime based ones, due to the setting process that is slower in these mortars when compared with hydraulic binder mortars. Lanas et al. [14] found a strong increase in strength of lime mortars between 28 and 365 days of curing.

3 Test Methods

The flexural and compression strength tests performed were based on EN1015-11:1999 and carried out using a Form test – Sneider universal machine, model D-7940. For all the tested mortars and curing times, the flexural strength and the velocity of ultrasound were assessed on three prismatic specimens. The ultrasonic test was performed using PUNDIT equipment (Portable Ultrasonic Non-destructive Digital Indicator Tester), by CNS Electronics, comprising an ultrasonic pulse generating unit and two cylindrical transducers of 5 cm diameter and a frequency of 54 kHz. The measurements of the ultrasound velocity were performed under direct transmission mode on prismatic specimens. Compression strength tests were performed on the fragments of each specimen resulting from the flexural test. The surface hardness of the mortars applied as brick coat was assessed using a Schmidt pendulum hammer type PT [15]. The presented results were obtained from at least six measurements performed on each mortar applied as brick coat.

The porosity accessible to water of all tested mortars was assessed on three prismatic specimens following RILEM I.1 [16] recommendation. Porosity accessible to water is the ratio of the volume of pores accessible to water to the bulk volume of

the specimen, and it is usually expressed as a percentage. After drying the specimens to constant mass (md), they were placed in desiccators under vacuum (20 mm Hg) for 24 h to eliminate the air contained in the pores. Water was slowly introduced into the vessel and the specimens remained immersed under vacuum for 24 h afterwards. Finally, the specimens were left immersed at atmospheric pressure for another 24 h. The hydrostatic weight (mh) and the weight at atmospheric pressure (ms) were determined and the porosity accessible to water (P) was calculated according to the following equation:

$$P = \frac{ms - md}{ms - mh} \times 100 \quad [\%]$$

4 Results and Discussion

Table 2 presents the average and standard deviation values of the porosity, compressive strength, ultrasound velocity and rebound of tested mortars cured under dry conditions, after curing times of 60 days for the aerial lime mortars and 28 days for the hydraulic mortars.

The linear trend-lines between the porosity and velocity of ultrasound values and the correspondent coefficients of determination are presented in Fig. 1 (left and right graphs) for each binder type mortar, with a flow table value of 165 mm and cured under dry conditions.

The coefficient of determination (R^2) gives information about the variability of the dependent variable Y that is explained by the dependent variable X [17]. R^2 is calculated from the correlation coefficient (R). This coefficient (R) can be expressed by the mean of the products of the standard scores of two random variables X and Y according to the following equation:

$$R = \frac{1}{n-1} \sum_{i=1}^n \left(\frac{X_i - \bar{X}}{\sigma_X} \right) \left(\frac{Y_i - \bar{Y}}{\sigma_Y} \right)$$

Where: \bar{X} and \bar{Y} – samples means; σ_X and σ_Y – samples standard deviations.

Table 2 Properties of the tested mortars cured under dry conditions

Mortars (curing ages)	Porosity [vol. - %]	Compressive strength [MPa]	Ultrasound velocity [m/s]	Rebound
Aerial lime (60 days)	29.5 ± 2.0	0.83 ± 0.11	1,500 ± 80	23 ± 2
Hydraulic lime (28 days)	24.2 ± 2.5	2.30 ± 0.49	1,790 ± 270	29 ± 4
Cement (28 days)	21.6 ± 1.9	13.3 ± 3.20	3,140 ± 240	55 ± 6

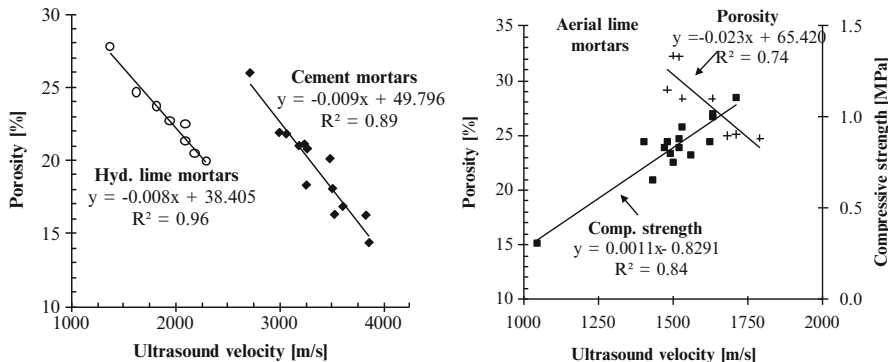


Fig. 1 Hydraulic and aerial lime mortars with a flow table value of 165 mm cured under dry conditions. *Left graph* – Relation between porosity and ultrasound velocity values for hydraulic mortars. *Right graph* – Relation between porosity and ultrasound velocity values, and compressive strength and ultrasound velocity values, for aerial lime mortars

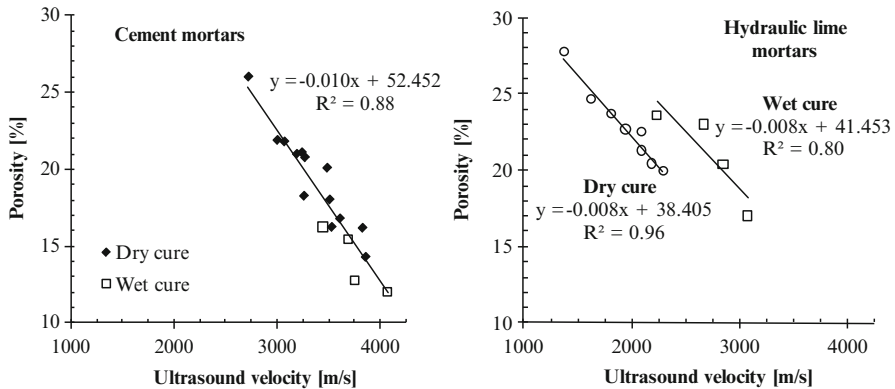


Fig. 2 Hydraulic mortars cured and tested under dry and wet conditions – influence of the curing conditions on the relation between porosity and ultrasound velocity values. *Left graph* – Cement mortars. *Right graph* – Hydraulic lime mortars

The relationship achieved between the porosity and ultrasound velocity confirmed by the coefficients of determination obtained for the aerial (0.74), hydraulic lime (0.96) and cement mortars (0.89) point to the possibility of estimating porosity from ultrasound velocity values.

The influence of the curing conditions on the above relationships was analysed, and is shown in Fig. 2, on hydraulic lime and cement mortars with a flow table value of 165 mm cured under dry and wet conditions. The porosity and ultrasound velocity measured on cement mortars seemed not to be influenced by curing condition (Fig. 2 left graph). However, the values of velocity of ultrasound measured on hydraulic lime mortars cured under wet conditions were higher than the values for mortars cured under dry condition (Fig. 2 right graph). The increase in the ultrasound velocity

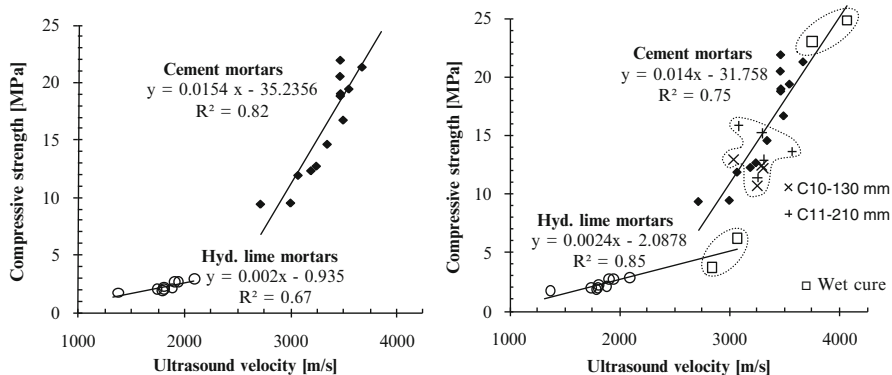


Fig. 3 Hydraulic mortars – relation between compressive strength and ultrasound velocity values. *Left graph* – the results of the mortars with a consistency of 165 mm cured under dry conditions. *Right graph* – the results of all hydraulic mortars tested (different consistencies and curing conditions)

values in this case was not followed by porosity (Fig. 2 right graph). These results indicate that similar mortars cured under different conditions might have similar values of open porosity, although differences in their pore structure may influence the velocity values.

Figures 1 (right graph) and 3 (left graph) present the relation between the compressive strength and the ultrasound velocity values determined on prismatic specimens. Coefficients of determination were obtained for the different tested binder mortars formulated with the same consistency and cured under dry conditions ($R^2=0.84$ – aerial lime mortars, Fig. 1 (right graph); $R^2=0.67$ – hydraulic lime mortars and $R^2=0.82$ – cement mortars, Fig. 3 (left graph)).

The linear trend-lines presented on Fig. 3 (right graph) considered all the tested hydraulic mortars, even those with different flow table values (C10 and C11 – flow table values of 130 and 210 mm, respectively) and wet curing conditions (H6, H7, C2 and C3). For both hydraulic mortars, the relation between ultrasound velocity and compressive strength was not significantly modified, due to the inclusion of some values determined on mortars with different consistencies and both tested curing conditions (Fig. 3 right graph), although coefficients of determination were different ($R^2=0.85$ on hydraulic lime mortars and $R^2=0.75$ on cement mortars). Analysis of the two factors taken separately – curing conditions and consistencies – led to the following conclusions: (i) R^2 became higher when considering only the results of the mortars with a flow table value of 165 mm cured under both conditions ($R^2=0.85$ – hydraulic lime mortars, Fig. 3 (right graph) and $R^2=0.86$ – cement mortars, not shown separately in a graph) than those achieved when only dry conditions are considered ($R^2=0.67$ – hydraulic lime mortars and $R^2=0.82$ – cement mortar, Fig. 3 (left graph)); (ii) R^2 became lower when considering the cement mortars with consistencies corresponding to the three several flow table values tested that were cured under dry condition ($R^2=0.64$ on cement mortars, not shown separately in a graph; no different consistency hydraulic mortars were tested). The increase of the dispersion

Fig. 4 Aerial, hydraulic lime and cement mortars – relations between compressive strength and rebound values considering all tested consistencies and curing conditions

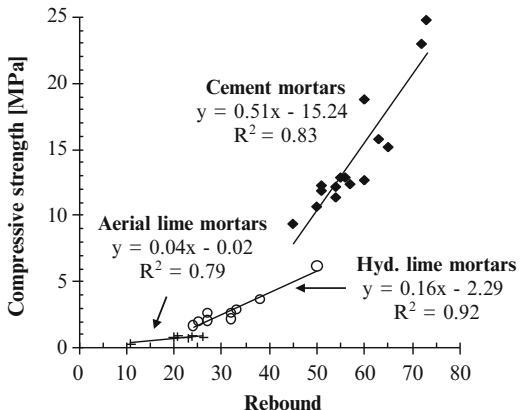
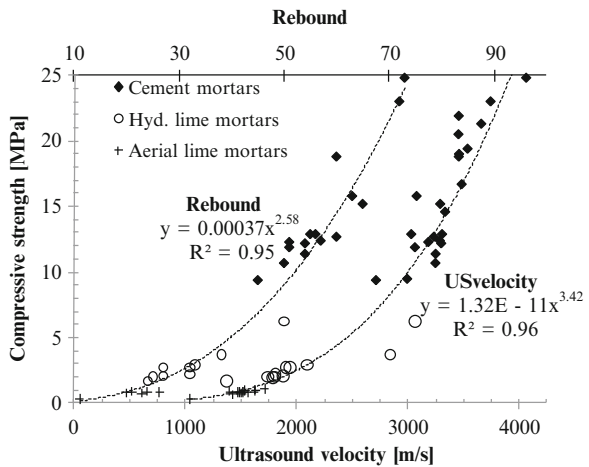


Fig. 5 All tested mortars – relation between compressive strength and ultrasound velocity and rebound values considering all tested consistencies and curing conditions



of the results when considering different consistency mortars points towards a need to develop further research on this issue.

As can be observed in Fig. 4, good relations between the compressive strength and rebound values (R^2 ranging from 0.79 to 0.92) were obtained for all the type of mortars (aerial, hydraulic lime and cement mortars) considering all tested consistencies and curing conditions. The influence of the consistency and curing conditions were also assessed for the rebound values and led to the conclusion that the relation between compressive strength and rebound values was not significantly altered.

Figure 5 presents the power functions between compressive strength and ultrasound velocity values, and compressive strength and rebound values, when all the tested formulations are considered, even those with different consistencies and curing conditions. In both cases good relations were achieved ($R^2=0.95$ – rebound and $R^2=0.96$ – ultrasound velocity), a fact which points to the potential of the studied “*in situ*” techniques for estimating the compressive strength of mortars.

5 Conclusions

Tests were undertaken on several mortars with quite diverse physical and mechanical properties (porosity: 10–30%, compressive strength: 0.6–25 MPa), with the objective of assessing the possibility of estimating compressive strength and porosity through ultrasound velocity and rebound hardness measurements. Different binder types, water/binder ratios, aggregates and consistencies were used for the formulation of the tested mortars, and the assessment of their properties with different curing periods and conditions was also tested.

A relationship between the porosity and ultrasound velocity values was achieved, which points to the possibility of estimating porosity from ultrasound velocity. The results also demonstrate the potential of both “*in situ*” test techniques to estimate the compressive strength of mortars with unknown formulation or when destructive tests are not possible. Among the interesting findings is the value of using the rebound test for on-site characterisation of rendering mortars.

The good relationship between compressive strength and ultrasound velocity assessed on prismatic specimens enhances the interest in developing future research, already in progress, to study the behaviour of this feature when measured under indirect transmission mode over mortars simulating rendering coats.

Acknowledgements The authors would like to thank the Foundation for Science and Technology through the funding allocated to ICIST, Institute of Structural Engineering, Planning and Construction. They are also grateful to C. Agostinho, I. Santos, A. Fernandes, B. Mendonça, A. Martins, N. Cruz and P. Lima for their collaboration in the experimental work within the scope of their MSc dissertations.

References

- Binda, L., Saisi, A., Tiraboschi, C.: Investigation procedures for the diagnosis of historic masonries. *Construct. Build Mater.* **14**, 199–233 (2000)
- Veiga, M.R., Magalhães, A., Bokan-Bosilikov, V.: Capillarity tests on historic mortar samples extracted from site. Methodology and compared results. In: Proceedings of the 13th International Brick and Block Masonry Conference, Amsterdam, 4–7 July 2004
- Veiga, M.R., Velosa, A., Magalhães, A.: Experimental applications of mortars with pozzolanic additions: characterization and performance evaluation. *Construct. Build Mater.* **23**, 318–327 (2009)
- Lafhaj, Z., Goueygou, M.: Experimental study on sound and damaged mortar: variation of ultrasonic parameters with porosity. *Construct. Build Mater.* **23**, 953–958 (2009)
- Agostinho, C.: Study of the evolution of lime mortars behaviour along time. Dissertation (Integrated Master in Civil Engineering), UTL, Instituto Superior Técnico, Lisbon (in Portuguese) (2008)
- Santos, M.I.: Rendering mortars with incorporation of pozzolanic admixtures for ancient building. Dissertation (Integrated Master in Civil Engineering), UTL, Instituto Superior Técnico, Lisbon (in Portuguese) (2009)
- Fernandes, M.: Study of the influence of sand grain size distribution in the performance of ancient building renders. Dissertation (Integrated Master in Civil Engineering), UTL, Instituto Superior Técnico, Lisbon (in Portuguese) (2009)

8. Mendonça, B.: Study of the behaviour of hydraulic mortars. Dissertation (Integrated Master in Civil Engineering), UTL, Instituto Superior Técnico, Lisbon (in Portuguese) (2007)
9. Martins, A.: The influence of the cement dosage on the performance of rendering mortars. Dissertation (Integrated Master in Civil Engineering), UTL, Instituto Superior Técnico, Lisbon (in Portuguese) (2008)
10. Cruz, N.: The influence of sand grain size distribution in the performance of hydraulic binder renders. Dissertation (Integrated Master in Civil Engineering), UTL, Instituto Superior Técnico, Lisbon (in Portuguese) (2008)
11. Lima, P.: Study of the influence of the binding mixture in the behaviour of hydraulic renderings. Dissertation (Integrated Master in Civil Engineering), UTL, Instituto Superior Técnico, Lisbon (in Portuguese) (2009)
12. Ferreira Pinto, A.P., Gomes, A., Nogueira, R.: Mechanical characterization in situ techniques for rendering mortars. In: Proceedings of the 3rd Portuguese Congress of Building Mortars, APFAC, Lisbon (in Portuguese) (2010)
13. Lanas, J., Sirera, R., Alvarez, J.I.: Compositional changes in lime-based mortars exposed to different environments. *Thermochim. Acta* **429**, 219–226 (2005)
14. Lanas, J., Alvarez-Galindo, J.I.: Masonry repair lime-based mortars: factors affecting the mechanical behavior. *Cem. Concr. Res.* **33**, 1867–1876 (2003)
15. Pendulum hammer type PT <http://www.proceq.com>. Accessed 4 Apr 2010
16. RILEM.: Tests defining the structure. Porosity accessible to water, Test N°I.1, Recommendations provisoires, Paris (1980)
17. Cox, D.R., Hinkley, D.V.: Theoretical Statistics. Chapman & Hall, London (1974)

Application of ^1H NMR to the Hydration Monitoring of Lime-Pozzolan Mortars

Maria Tziotziou, Eleni Karakosta, Ioannis Karatasios, Michalis Fardis, Pagona Maravelaki-Kalaitzaki, Georgios Papavassiliou, and Vassilis Kilikoglou

Abstract The micro-structural evolution of a lime-pozzolan system, during hydration, was studied by ^1H Nuclear Magnetic Resonance (NMR). The hydration process was monitored for a period of 1 year by ^1H NMR spin-lattice relaxation measurements, performed in a portable magnet. The development of the hydration was also examined by scanning electron microscopy (SEM), X-ray diffraction (XRD), mercury intrusion porosimetry (MIP), infrared spectroscopy (FT-IR) and thermal analysis (DTA/TG) and compared with the NMR results. The results indicated that ^1H NMR provides valuable information on the hydration process of lime-pozzolan mortars in a non-invasive way, as it was possible to monitor the development of the hydration phases through the resulted microstructure, in real-time.

M. Tziotziou (✉)

Institute of Materials Science, National Centre of Scientific Research “Demokritos”, Athens, Greece

Analytical and Environmental Chemistry Lab, Technical University of Crete, Chania, Greece
e-mail: mtzio@ims.demokritos.gr

E. Karakosta • I. Karatasios • M. Fardis • G. Papavassiliou • V. Kilikoglou
Institute of Materials Science, National Centre of Scientific Research “Demokritos”, Athens, Greece
e-mail: elkarako@ims.demokritos.gr; ikarat@ims.demokritos.gr;
mfardis@ims.demokritos.gr; gpapav@ims.demokritos.gr; kilikog@ims.demokritos.gr

P. Maravelaki-Kalaitzaki
Analytical and Environmental Chemistry Lab, Technical University of Crete, Chania, Greece
e-mail: pmaravel@elci.tuc.gr

1 Introduction

Lime-pozzolan mortars face, nowadays, an increased preference in the restoration of architectural monuments and also in the construction of buildings. This is mainly due to their enhanced chemical, physical and structural/mechanical compatibility with both archaeological and historical building materials (stones, bricks and mortars). On the contrary, the application of cement mixtures as restoration materials have proved to be problematic, due to disadvantages related to incompatibility matters, high salt content, limited elasticity etc. [1]. Moreover, lime-pozzolan mortars are more environmentally friendly materials, compared to cement mortars, when issues such as reduced energy consumption [2, 3], reduced CO₂ and particulate matter emissions are considered [4].

The study of the hydration process of lime-pozzolan mortars, through the monitoring of the C-S-H and C-A-H formation and the consequent changes of micro-structure [5], is essential in order to evaluate the performance characteristics of the mortar, in terms of physical and mechanical properties, which are also interrelated with the longevity of the mortar.

In this context, the aim of this work was to study the micro-structural evolution of lime-pozzolan systems, during hydration, by ¹H Nuclear Magnetic Resonance (NMR), using NMR spin-lattice relaxation measurements [6–10]. ¹H NMR is a fast, powerful experimental technique that can be used to monitor in a non-invasive way the micro-structural evolution of the paste continuously and in real time, providing information on both the development of the hydration phases and the resulted microstructure changes of the binary paste. Contrary to conventional methods, such as XRD, DTA/TG, FT-IR and MIP, NMR does not require a drying process before the analysis. The hydration process is monitored by measuring the proton spin-lattice relaxation time T_1 , where the relationship between the T_1 and the pore size is based on the fast-exchange relaxation theory [11].

In principle, the T_1 of a fluid (typically water) confined within a pore can be used to determine the pore diameter (actually, the ratio of pore volume to surface area). The presence of the pore wall increases the relaxation rate and thus, for a given material, T_1 will decrease as the pore size decreases [7, 12]. As a consequence, in complex porous materials such as lime-pozzolan systems, with pore sizes extending from nanometres to micrometers, T_1 spreads over a wide distribution of relaxation times, which directly reflects the complicated pore microstructure and the interaction strength between the adsorbed water molecules and the pore surface [13]. Specifically, during the mortar hydration the nuclear magnetization in a saturation recovery experiment can be expressed as [13]:

$$R(t) = \frac{M_0 - M(t)}{M_0} = \int_0^\infty g(T_1) \exp(-t/T_1) dT_1 \quad (1)$$

where, $R(t)$ is the proton magnetization recovery function, M_0 is the magnitude of the magnetization at equilibrium, $M(t)$ is the observed magnetization as a function

of time t and $g(T_1)$ is the spin-lattice relaxation time T_1 distribution function, which can be resolved by means of an inverse Laplace transform, [14] unveiling important information about the porous microstructure in the hardened material.

In this work, we present a detailed study of ^1H NMR T_1 distribution profiles, attributed to mobile water molecules in a lime-pozzolan paste, as a function of hydration time, by excluding the undesirable NMR signal components (spin grouping method) [15] and keeping only those corresponding to pore (free) water. The T_1 distribution profiles clearly demonstrated the evolution of porosity and particularly the formation of two distinct pore reservoirs. In addition, the hydration process was also examined by scanning electron microscopy (SEM), X-ray diffraction (XRD), infra-red spectroscopy (FT-IR), thermal analysis (DTA/TG) and mercury intrusion porosimetry (MIP).

2 Experimental

The hydration process was monitored for a period of 1 year, (under standard humidity conditions), on a lime-pozzolan mixture. The mixture consisted of equal parts of lime powder ($\text{Ca}(\text{OH})_2$) (Merck, Germany) and a natural pozzolan powder of volcanic origin, a commercial, finely ground product with particle size below 75 μm , namely Lava Antica (LA), supplied by AGET, Greece.

The water to binder ratio was set to 0.7 and satisfied the requirement for optimum flow characteristics [16], while the mixture presented a flow value of 190 mm. The paste was prepared according to the procedure described in the EN 196-1 [17] standard. After mixing, the sample was sealed into NMR glass tube using Parafilm® membrane to avoid moisture loss and drying and then, immediately placed into the spectrometer. The sample dimensions were 9 mm in diameter and 30 mm in height. An additional amount of the above mixture was moulded in prismatic moulds, with dimension of $20 \times 20 \times 80$ mm, and then placed in a curing chamber for setting, at $\text{RH}=95\% \pm 3\%$ and $\text{T}=20^\circ\text{C} \pm 2^\circ\text{C}$.

^1H NMR spin-lattice T_1 relaxation experiments were conducted using a circular Halbach array magnet, capable of low-field NMR measurements [18]. The field at the magnet centre was 0.29 T, corresponding to a proton resonance frequency of 12.1718 MHz, and a magnetic field gradient (G) equal to 1.03 T m^{-1} . The spin-lattice relaxation time, T_1 was measured using a standard saturation recovery technique $[(\pi/2) - t - (\pi/2) - \tau - (\pi)]$. This sequence is applied to a sample in the equilibrium state (i.e., where there is a net magnetization aligned with the external magnetic field, which commonly defines the Z axis). The first pulse tips this magnetization to an axis orthogonal to the applied field, and then during a variable time τ , the magnetization regrows along the Z axis. The magnetization which has then been established is again tipped to the orthogonal plane, where it can be measured as function of τ . The characteristic recovery of the magnetization (along the Z axis) is the spin-lattice relaxation time T_1 [10]. In these experiments the interpulse delay, t ,

was ranging from 100 µs to 6 s, using 30 data points in a logarithmic scale. The signal was detected by the common Hahn echo pulse sequence. The experiment was performed at room temperature and the hydration process was monitored on the same sample for up to 12 months. The time intervals between successive experiments ranged from minutes to several hours, without requirement for prior hydration stop.

The setting process of the paste was interrupted at preset time periods, of 7, 21, 28, 60, 120, 180, 270 and 360 days (except MIP measurements that were carried out on specimens cured for 7, 28 and 60 days) according to a hydration stop procedure, which involved the immersion of the sample in two stop-bath solutions (acetone and diethyl-ether) for 60 min each, and then drying at 70°C for 22 h.

The setting mechanism was then studied, using the following analytical setup: X-ray diffraction analysis was performed in powder samples with a Siemens D-500 diffractometer (40 KV/35 mA). The spectra were collected between 5° and 60° 2θ scale, with a step of 0.03°/5 s. SEM examination was carried out in fractured surfaces, using a FEI Quanta Inspect scanning electron microscope. DTA/TG was operated with a Perkin-Elmer Pyris 3000 Thermal Analyser; in static air atmosphere up to 1,000°C at a rate of 10°C/min. FT-IR analysis was operated in a Bruker, Equinox 55/S spectrometer. Transmittance spectra were collected in the region of 4,000–400 cm⁻¹, with 4 cm⁻¹ resolution. The samples were mixed with KBr and scanned 30 times, in order to reduce the signal to noise ratio. MIP measurements were recorded using a Quantachrome Autoscan 60 porosimeter, in the range of 2–4.000 nm.

3 Results and Discussion

Although the pozzolan presented an amorphous matrix, some faint peaks of kaolinite, albite, anorthite and quartz were identified in diffraction patterns. During hydration, the pozzolan particles are corroded, resulting in the leaching of sodium and potassium alkalis in the pore solution. Consequently, Ca²⁺ ions take their place on the pozzolan surface and react with the free OH-, Si-O- and Al-O- radicals. This dissolution-precipitation mechanism inside pores, leads to the formation of calcium-aluminum and calcium-silicon hydrates (C-A-H, C-S-H), depicted on the XRD patterns (Fig. 1a). Moreover, FT-IR spectra (Fig. 1b) and DTA-TG analysis (Fig. 2a) provide a qualitative and quantitative respectively identification of the hydrates formation.

On the FT-IR spectra (Fig. 1b) it is evident that the transmittance peak at 970 cm⁻¹, attributed to C-S-H, makes its appearance around the 28th day of hydration and increases as the hydration proceeds. The peaks at 1,185–1,200 and 1,022–1,140 cm⁻¹ attributed to amorphous Si-O-(Al)-O polymerized bonds are present on both the spectra of the pozzolan and the paste, and decrease as the hydration proceeds [19, 20]. The thermogravimetric analysis, has detected the increasing formation of C-A-H and C-S-H content over the hydration process, by measuring the weight loss in the temperature range of about 90–260°C [21].

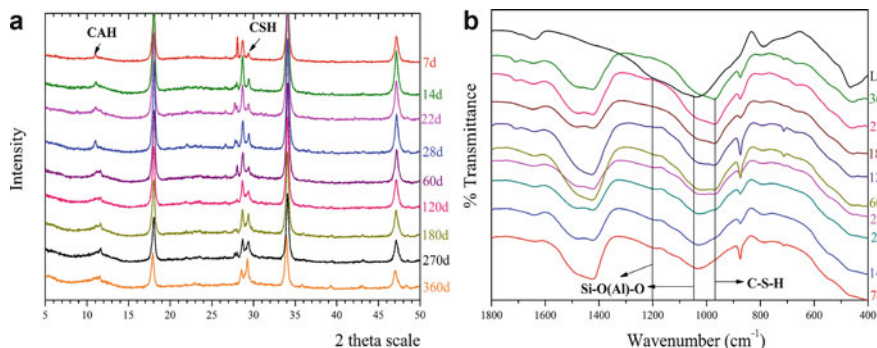


Fig. 1 (a) X-Ray diffraction patterns exhibit the formation of C-A-H and C-S-H phases as hydration proceeds (b) FT-IR spectra of the lime-pozzolan mortar at different hydration ages and of the raw pozzolan (LA)

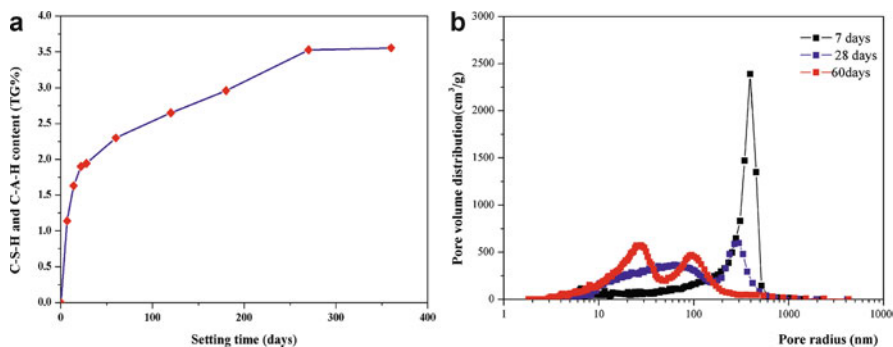


Fig. 2 (a) The C-S-H and C-A-H content vs. hydration time, measured by thermal analysis (b) MIP pore distributions vs. pore radius at 7, 28 and 60 days of hydration

On the T_1 contour plot and T_1 distribution profiles (Fig. 3), resulted from the ^1H NMR relaxometry, we can see that during the early hours of hydration, the T_1 is slightly decreasing, which can be attributed to the initiation of the hydration process and the formation of small amounts of hydrated phases. At this stage, all proton magnetization relaxes with common T_1 , due to the fast exchange between water spins in the various environments [22].

Up to 28 days of hydration, when the initial hydration products are formed (Fig. 4, 7 and 28 days), the T_1 relaxometry data are characterized by a single relaxation time. The hydrates content formed up to this period (28th day) corresponds to the 50% of the total hydrates content formed over a year, according to DTA-TG plot (Fig. 2a). After a hydration period of 28 days the T_1 relaxation mechanism deviates from a single exponential function and a multi-exponential behaviour is observed, which is resolved by means of an inverse Laplace transform, using a modified CONTIN algorithm [23]. In this period, there is a massive growth of the hydrated phases (Fig. 4, 28 and 60 days), and the formation of a second pore population with smaller pore radius, around 50 nm, as detected at 28 days by MIP (Fig. 2b). At this

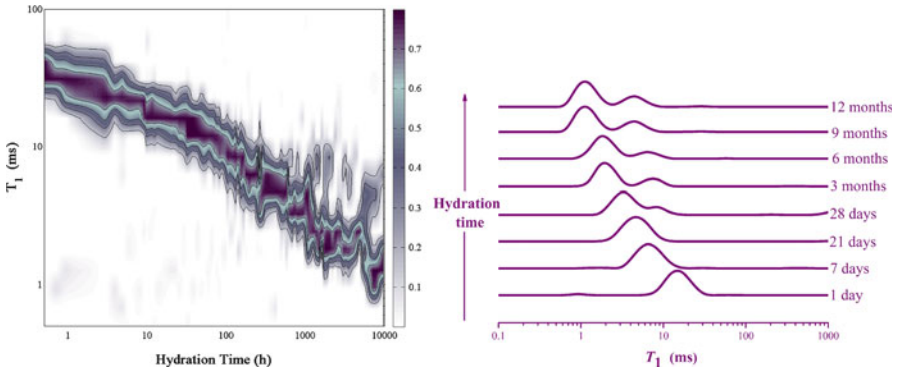


Fig. 3 T_1 contour plot (left) and T_1 distribution profiles (right) vs. hydration time

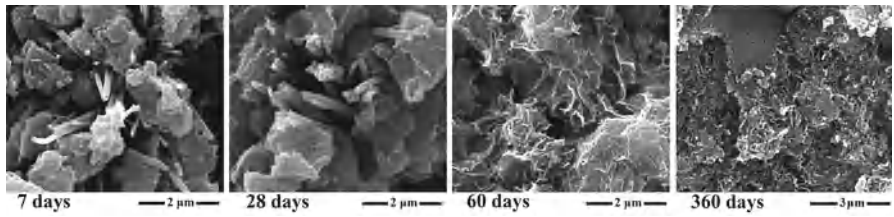


Fig. 4 SEM photomicrographs exhibit the development of hydrated phases; C-A-H and C-S-H are depicted in the form of needle – like fibres (7 days) and as a hydrous amorphous gel respectively; C-S-H gel is appearing denser as the setting time increases, resulting in the filling of micro and macro pores of the paste (360 days)

point the T_1 distribution profiles (Fig. 3) splits in two components similarly to MIP plots (Fig. 2b), which remain almost invariant with hydration time. The rise of the second peak, corresponding to the smaller pores, is indicative of the microstructure evolution of the paste as the setting time increases. The further reduction of T_1 can be explained by the growing dense network of amorphous hydrated phases that fill the majority of pore spaces (Fig. 4, 60 days). The two peaks clearly demonstrate the presence of two distinct pore reservoirs in the paste: one, with short $T_1 \approx 4.5$ ms attributed to small pore sizes and assigned to small capillary pores; and a second, with longer $T_1 \approx 11$ ms, corresponding to bigger pores and assigned to medium capillary pores in the paste (Fig. 4, 360 days).

4 Conclusions

The hydration process of lime-pozzolan paste was successfully monitored by measuring the proton spin-lattice relaxation time T_1 using a portable magnet. The method proved to be a sensitive tool to probe the development of capillary pores, formed

during hydration of lime-pozzolan mixtures. It was therefore possible to assess in real-time the resulted microstructural changes in a consistent way, and to provide information that was in accordance with the results of the XRD, FT-IR, SEM, DTA-TG and MIP techniques.

Specifically, T_1 distribution profiles clearly demonstrated the evolution of porosity and particularly the formation of two distinct pore reservoirs assigned to small and medium capillary pores.

The use of a portable magnet shows the great potential of ^1H NMR for studying both at the laboratory and in field the hydration process of lime-pozzolan mortars. The ability of the method to continuously monitor the setting process and the evolution of the microstructure provides a promising tool for people involved in conservation of architectural heritage to accurately evaluate in field the durability and service life of lime-pozzolan mortars.

References

1. Holmstrom, I.: Mortars. In: Proceedings of the ICCROM Symposium Mortars, Cements and Grouts Used in the Conservation of Historic Buildings, ICCROM, Rome (1981)
2. Cerny, R., Kunca, A., Tydlitat, V., et al.: Effect of pozzolanic admixtures on mechanical, thermal and hygric properties of lime plasters. *Constr. Build Mater.* **20**, 849–857 (2006)
3. Velosa, A., Cachim, P.: Eco-concrete: preliminary studies for concretes based on hydraulic lime. In: SB07 Lisbon – Sustainable Construction, Materials and Practices: Challenge of the Industry for the New Millennium. <http://www.irbnet.de/daten/iconda/CIB11778.pdf> (2008). Accessed 1 Mar 2010
4. Rehan, R., Nehdi, M.: Carbon dioxide emissions and climate change: policy implications for the cement industry. *Environ. Sci. Policy* **8**, 105–114 (2005)
5. Massazza, F.: Pozzolana and pozzolanic cements. In: Hewlett, P.C. (ed.) Lea's Chemistry of Cement and Concrete, 4th edn. Elsevier Butterworth-Heinemann, Oxford (2004)
6. Blinc, R., Lahajnar, G., Zumer, S., et al.: NMR study of the time evolution of the fractal geometry of cement gels. *Phys. Rev. B* **38**, 2873–2875 (1988)
7. Schreiner, L.J., Mactavish, J.C., Miljkovic, L., et al.: NMR line shape-spin-lattice relaxation correlation study of Portland cement hydration. *J. Am. Ceram. Soc.* **68**, 10–16 (1985)
8. Plassais, A., Pomies, M.-P., Lequeux, N., et al.: Micropore size analysis by NMR in hydrated cement. *Magn. Reson. Imaging* **21**, 369–371 (2003)
9. Papavassiliou, G., Fardis, M., Laganas, E., et al.: Role of the surface morphology in cement gel growth dynamics: a combined nuclear magnetic resonance and atomic force microscopy study. *J. Appl. Phys.* **82**, 449–452 (1997)
10. Fardis, M., Papavassiliou, G., Abulnasr, L., et al.: Effect of clay minerals on the hydration of cement. An NMR study. *Adv. Cem. Based Mater.* **1**, 243–247 (1994)
11. Blinc, R., Dolinsek, J., Lahajnar, G., et al.: Spin-lattice relaxation of water in cement gels. *Z. Naturforsch.* **43a**, 1026–1038 (1988)
12. Holly, R., Reardon, E.J., Hansson, C.M., et al.: Proton spin-spin relaxation study of the effect of temperature on white cement hydration. *J. Am. Ceram. Soc.* **90**, 570–578 (2007)
13. Laganas, E., Papavassiliou, G., Fardis, M., et al.: Analysis of complex ^1H nuclear magnetic resonance relaxation measurements in developing porous structures: a study in hydrating cement. *J. Appl. Phys.* **77**, 3343–3348 (1995)
14. Blumich, B., Perlo, J., Casanova, F.: Mobile single-sided NMR. *Prog. Nucl. Magn. Reson. Spectrosc.* **52**, 197–269 (2008)

15. Lasic, D.D., Corbett, J.M., Jiant, J., et al.: NMR spin grouping in hydrating cement at 200 MHz. *Cem. Concr. Res.* **18**, 649–653 (1988)
16. EN 1015–3: Methods of test for mortar for masonry – Part 3: Determination of consistence of fresh mortar (by flow table). European Committee for Standardization (1999)
17. EN 196–1: Methods of testing cement – Part 1: Determination of strength. European Committee for Standardization (1994)
18. Karakosta, E., Diamantopoulos, G., Katsiotis, M.S., et al.: In situ monitoring of cement gel growth dynamics. Use of a miniaturized permanent Halbach magnet for precise ^1H NMR studies. *Ind. Eng. Chem. Res.* **49**, 613–622 (2010)
19. Payá, J., Monzó, J., Borrachero, M.V., et al.: Determination of the pozzolanic activity of fluid catalytic cracking residue. Thermogravimetric analysis studies on FC3R–lime pastes. *Cem. Concr. Res.* **33**, 1085–1091 (2003)
20. Budak, M., Maravelaki-Kalaitzaki, P., Kallithrakas-Kontos, N.: Chemical characterization of Cretan clays for the design of restoration mortars. *Microchim. Acta* **162**, 325–331 (2008)
21. Ubbriaco, P., Traini, A., Manigrassi, D.: Characterization of FDR fly ash and brick/lime mixtures. *J. Therm. Anal. Calorim.* **92**, 301–305 (2008)
22. Nestle, N.A.: Simple semiempiric model for NMR relaxometry data of hydrating cement pastes. *Cem. Concr. Res.* **34**, 447–454 (2004)
23. Provencher, S.W.: A constrained regularization method for inverting data represented by linear algebraic or integral equations. *Comput. Phys. Commun.* **27**, 213–222 (1982)

Non-standard Testing in Characterisation and Consolidation Assessment of Historic Mortars

Miloš Drdácký

Abstract Non-standard tests are carried out on specimens made of materials extracted from historical objects, and they typically have non-standard dimensions. Assessments of strengthening effects are also usually studied on non-standard specimens purposely designed and made of materials modelled on the historic materials. The tests themselves are destructive, as engineers prefer destructive tests on a real material for a better understanding of the real material's behaviour. Destructive tests provide a better opportunity to acquire data for numerical modelling and for following the gradients of qualities, namely after consolidation interventions. The tests include compression tests, bending tests, shear tests, and a series of tests on specific specimens designed for studies of consolidation effects.

1 Introduction

Conservation policy requirements and a wide range of problems in the field of preservation and protection of historic materials and monuments call for the development and application of testing methods and procedures that are tailored for specific tasks and have not been standardised. Although a certain degree of creativity is indispensable here, the techniques, procedures and protocols that are adopted should be verified, and must reliably provide reproducible results or data. The most severe limitation stems from the fact that material samples can typically be extracted only in small amounts and with limited dimensions. It was therefore necessary to develop methods that enable tests on specimens of non-standard shapes and dimensions, and

M. Drdácký (✉)

Institute of Theoretical and Applied Mechanics of the Academy of Sciences
of the Czech Republic, Prague, Czech Republic
e-mail: drdacky@itam.cas.cz

methods for evaluating the measured data and for assessing its probable relation to equivalent standard values.

This paper discusses direct non-standard methods for measuring mechanical characteristics. Only sampling tests that are destructive in a minor and considerate manner – in terms of conserving the object – are presented here. They are carried out on specimens made of materials extracted from historical objects, and their dimensions are typically non-standard, because it is usually possible to extract pieces of joint mortar or plaster only about 20 mm in thickness. Strengthening effects are typically tested on specially-designed non-standard specimens made of materials that model historic materials. All reported tests are destructive, but the acquired data must be appropriately interpreted in relation to existing standard test results.

2 Non-standard Testing of Historic Mortars

Although quite reliable methods for testing historic mortars have been developed and verified, the problem of the representativeness of the real material samples remains, since it is not possible in practice to extract quantities of original material that are sufficient for statistically significant series' of specimens. For this reason, the tests described below must be understood as study tests providing only indicative characteristics or data. Nevertheless, such data is valuable for designing compatible repair mortars and/or for assessing the safety and reliability of historic masonry structures, or for retrofitting them.

2.1 Compression Tests

The size and shape of specimens for use in determining the compressive strength of materials have been studied for more than a century. It has been known since the nineteenth century that the size of a testing specimen has a significant influence on the measured strength, and numerous forms have been proposed for transferring the attained characteristics of concrete and cement mortars to standard values. The correction functions depend mainly on the length of the specimen base edge, on the slenderness or the height-to-base edge length ratio, and on the quality (compression strength) of the mortar. Tests on small specimens are further influenced by other factors. Manufacturing the specimen for a compression test (cutting a cube) has a significant influence on the properties of the sample, as it basically disturbs the surface strata and reduces the strength. In most cases, the compressed surfaces need to be supplemented by a leveling layer. For this reason, specimens in the shape of irregular mortar “cakes” from the masonry joint have also been suggested or applied for compression tests in recent times, e.g. [1].

The strength attained on non-standard samples is always higher than the strength measured on standard specimens. A review of results of tests on cement mortars,

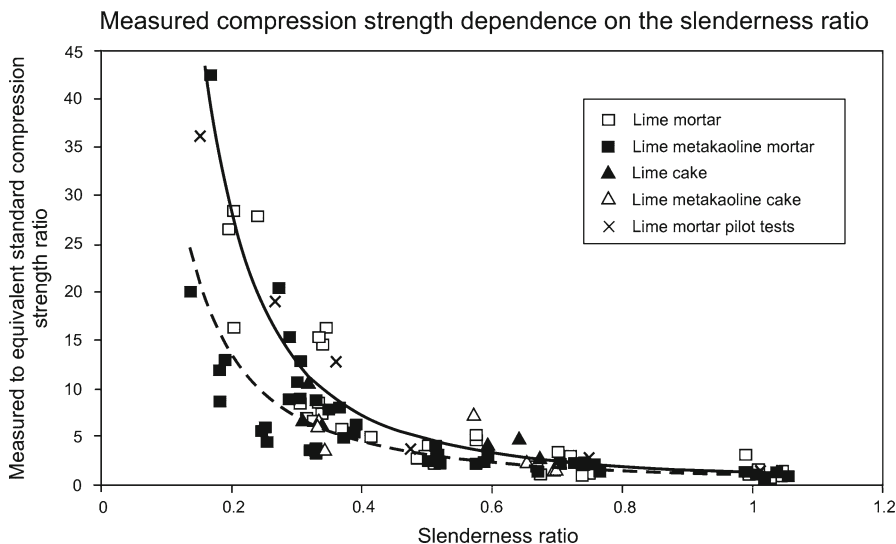


Fig. 1 Results of compression tests on specimens of various mixture and base side dimension (squares of 20, 40, 60 mm and discs 60 mm in diameter). The *full line* corresponds to Eq. 1, the *dashed line* represents a trend line for lime metakaoline mortars

based on a literature survey supplemented by a series of tests on a cement mortar [2], was published in [3], where the author presents correction coefficients applicable for assessing the equivalent standard compression strength from tests on non-standard specimens.

For lime mortars of very low standard strength of about 0.365 MPa, corresponding to degraded historic mortars, the experimentally measured strength of specimens with low slenderness can be corrected with the use of Eq. 1

$$f_c = f_e / (h/a)^{-1.9} \quad (1)$$

where f_c denotes the computed equivalent standard compression strength, f_e is the experimentally attained compression strength, and h/a is the slenderness of the specimen. The formula is valid for specimens with length a of the base side of about 40 mm and with low strength (the lime : sand mixture was only 1:9 (vol.)).

Further series' of tests showed that the experimentally attained differences in the exponent in Eq. 1 are not very severe for lime mortars of various strengths, even if they are modified with pozzolana additives [4]. Form (1) is therefore recommended for an approximate assessment of the standard equivalent historic lime mortar qualities (compressive strength) applicable in standard redesign processes, Fig. 1.

The circular plates with diameter larger than the punching steel plates, Fig. 2, exhibit approximately the same average strength as the square regular shapes, see Fig. 1. Therefore the same reduction corrections are applicable.

Recent research has confirmed that the behaviour of non-standard mortar specimens can be predicted numerically with reasonable accuracy, making use of a



Fig. 2 Compression test on circular discs

description of the material behaviour by an elasto-plastic Mohr-Coulomb constitutive model [4].

For material models the deformation characteristics are needed. They can be acquired iteratively by approximation of the known load-deformation diagrams, as applied in the above-mentioned Mohr-Coulomb constitutive modelling. Strains can be measured directly on the surface of small specimens, using optical methods, namely the digital image correlation. Here the sand grains on the surface create a sufficiently characteristic pattern, which may be used to follow up the deformation path in the course of loading [5]. However, the attained strain distribution field reflects the overall 3D deformation (substantially constrained on the contacts between the loading plates and the specimen) of the tested specimen, and the assessment of the modulus of elasticity must take this fact into account. For deformation measurements, the most satisfactory results are still obtained from bending tests.

2.2 *Bending Tests*

The extracted sample size of mortars is usually too small for flexural tests. The author therefore devised and has been using a sample extension with another material in the form of so-called “prostheses”. The method was developed at ITAM in 1998 and has been used, among other things, for analysing various types of historic mortars [2], and also lime mortars reinforced with organic fibres [6]. In the course of “prosthe-sization”, the sample of material taken from the structure is supplemented symmetrically on both ends to the required length, with two “prostheses”, in order to satisfy

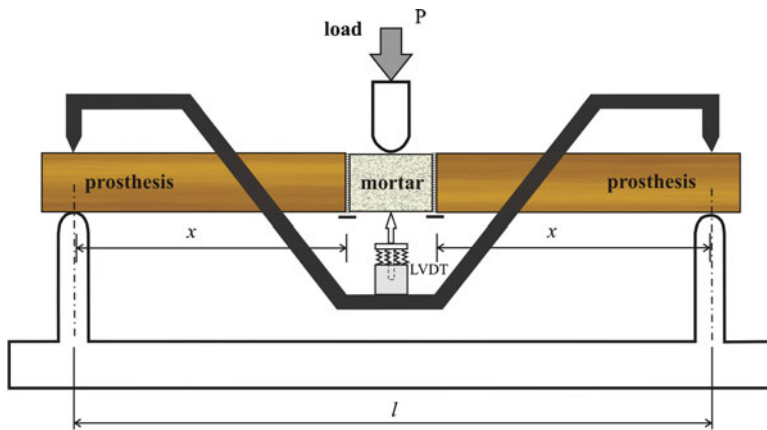


Fig. 3 Bending test rig with a prosthesisized mortar specimen

Navier's assumption of linear stress distribution along the cross section in flexure. Wood has been found to be a suitable material for mortar prosthesisization. The tested material is placed at the centre of the test specimen, Fig. 3.

According to the results of tests comparing the flexural strength of pure mortar beams with the strength ascertained on prosthesisized identical material, the influence of prosthesisization is negligible. The values for the ratio of the strength of the prosthesisized sample to that of "standard" all-mortar specimens were between 0.98 and 1.02 if the specimen broke in its central part (undisturbed mortar). The effect of size on bending strength was also evaluated from these tests. Again, higher strengths than the standard values are measured on the small size specimens, and the necessary reduction tendency can be assessed by an approximate Eq. 2

$$f_b = f_e / \left(1 + C_{ssb} - C_{ssb} h / h_s \right) \quad (2)$$

where f_b denotes the computed standard flexural strength, f_e the experimentally-attained flexural strength, h/h_s the cross-sectional height of the specimen to the standard $h_s = 40 \text{ mm}$ ratio, and the small size bending correction coefficient C_{ssb} varies on an average around 0.47 for lime mortar specimens between 20 and 40 mm in height, (the measured C_{ssb} varied from 0.36 to 0.58 and apparently depends on the technological parameters, e.g. compacting and treatment).

The modulus of elasticity can be estimated from the measured deflection of the beam during the course of loading. To calculate the modulus of elasticity in the case of three-point bending we exploit formula (3), developed with the use of Mohr's methodology for calculating the deflection as a moment on the so-called dual beam loaded by a reduced moment diagram. This gives the following form for the Young's modulus of mortar E

$$E = P (1-x) E J ((1-x)^2 + 6(1-x)x + 12x^2) / 8 (6y J E_1 J_1 - P J x^3) \quad (3)$$

where P denotes the acting force, l the span of the composite beam, E_l , J_l the modulus of elasticity and the cross-sectional moment of inertia of the prosthesis material (usually wood), $J = b h^3/12$ (b being the width of the mortar beam and h its height), y the measured central deflection, and x denotes the length of the prosthesis on the beam between the supports, which is equal to 0.5 (*span l – length of the mortar specimen*).

2.3 Shear Tests

The broken parts from the bending tests can be advantageously re-used in shear tests derived from the methodology for shear testing of soils. For tests of this type, a specimen of any convex shape is embedded into a block of stiff material, e.g., epoxy resin divided into halves. The dividing plane is provided with a separation and a sliding layer. Then the block is tested in a simple shear box and the measured normal and shear stress is evaluated using the standard soil mechanics methodology.

3 Non-standard Testing of the Effects of Consolidation on Model Mortars

Difficulties connected with the on-site extracting of real degraded mortar samples from existing buildings or structures, on the one hand and, in some cases, a need to measure very subtle strengthening effects, on the other, call for the development and application of test procedures which use model materials and specifically shaped testing specimens. Compacted crushed old mortars or sand are used for modelling the disintegrated mortars and lean mortars that typically substitute degraded mortars. As concerns the mode of testing and the shape of the tested specimens, creative approaches according to the problem under study give the most satisfactory results. Examples developed for testing the effects of lime water treatment on mortars are presented below.

3.1 Test Specimens

The specimens were designed on the basis of a thorough literature survey, which indicated very slight effects, with regards to both penetration and strengthening, of repeatedly wetting historic mortars or stone with lime water. Specific test specimens in the form of short and rather thin-walled tubes for compression tests and plates for tension tests were therefore applied, Fig. 4. The specimens were fabricated

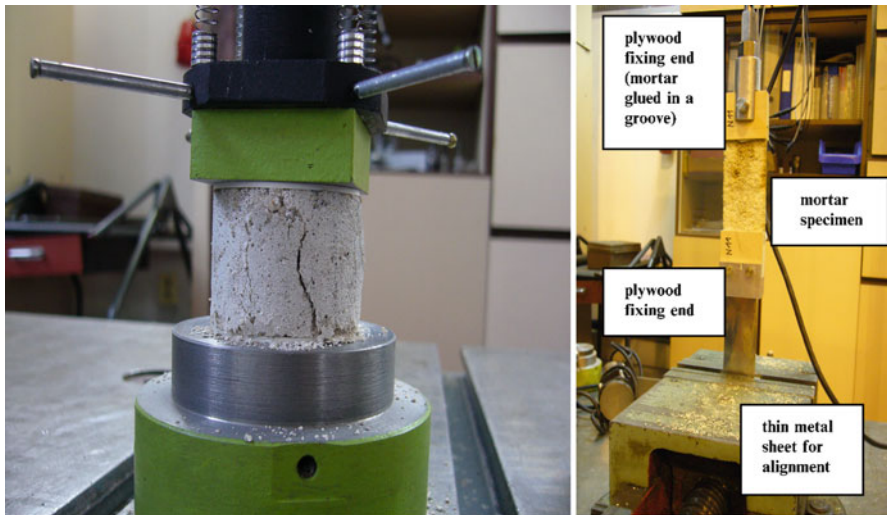


Fig. 4 Arrangement of compression tests of thin-walled mortar tubes and tension tests of thin mortar plates

from a very weak lime mixture, cast in stainless formwork, with no separation and well compacted, which enabled them to be pushed out from the formwork immediately after casting, and prevented the origination of shrinkage cracks. The thin-wall forms increased the surface-to-cross-section area ratio and intensified the measurable strengthening effect. It also improved the agent penetration and the maturing conditions.

The plates for the tension tests were provided with wooden (plywood) heads to enable them to be fixed into the special flexible loading grips, ensuring the correct alignment without disturbing bending and without eccentricity, Fig. 4. This mode was more effective than the use of special tension grips, which were also developed. It is beyond the scope of this paper to go into a more profound discussion. The reader may find details e.g. in [7].

3.2 In-Situ Testing of Consolidation or Strengthening Effects

It is very difficult to make *in-situ* tests for subtle changes in the surface characteristics of consolidated mortars. One method relies on peeling off the surface material by sticking some scotch tape on and then rapidly removing it. Though the results do not fully correlate with the mechanical characteristics of the material, this test can be used for a very rough check on the consolidation effect. It is only necessary to keep to the recommended procedure, which consists of repeating the test on the same surface area several times (a minimum of 5 times) before applying the treatment,

and doing the same again after the treatment. Then the results give reasonably objective data for a relative or comparative assessment of the consolidation or strengthening efficiency. More detailed information is given in [7] or on the website of the EC 7th FP project STONECORE www.stonecore-europe.eu

4 Conclusion

Our non-standard methodology for testing historic mortars provides engineers with a reliable tool for assessing the realistic material characteristics of historic masonry. It further enables a study of various correlations among different characteristics of historic mortars, providing interesting results and a new insight into the composition of the mortar and the historic mixture preparation technology.

The methodology of prosthesisization also plays an important role in the development of new mortars. Here, usual standard mortar test specimens with dimensions 40×40×160 mm are tested in bending, and their broken halves after the tests can be used for compression tests and fracture bending tests on prosthesisized beams with an artificial notch. In this way, we obtain data on several basic material characteristics acquired on identical specimens by means of destructive tests. This is an additional and substantial advantage of our technique.

Acknowledgements The author gratefully acknowledges support from national research plan grant AV0Z20710524 and from Czech Grant Agency project 103/09/2067.

References

- Binda, L., Papaianni, I., Toumbakari, E., Van Hees, R.: Mechanical tests on mortars and assemblages. In: Groot, C., Ashall, G., Hughes, J. (eds.) Characterisation of Old Mortars with Respect to Their Repair. Final Report of RILEM TC 167-COM (2004)
- Drdácký, M., Slížková, Z.: Mechanical characteristics of historical mortars from tests on small-sample non-standard specimens. Mater. Sci. Appl. Chem. (Materiālzin tne un lietišķā ķīmija), Sērija 1, Sējums 17, 21–29 (2008)
- Drdácký, M.: Experimental approach to the analysis of historic timber and masonry structures. In: Lourenço, P.B., Roca, P., Modena, C., Agrawal, S. (eds.) Structural Analysis of Historical Constructions, vol. 1, pp. 25–40. Macmillan India, New Delhi (2007)
- Drdácký, M., Mašín, D., Mekonone, M.D., Slížková, Z.: Compression tests on non-standard historic mortar specimens. In: Book of Abstracts “HMC08 1st Historical Mortars Conference”, LNEC, Lisbon, p. 53 (+ CD ROM full paper) (2008)
- Drdácký, M., Jiroušek, O., Slížková, Z., Valach, J., Vavřík, D.: Hybrid testing of historic materials. In: Gdoutos, E. (ed.) Experimental Analysis of Nano and Engineering Materials and Structures. Alexandroupolis, Greece, pp. 275–276 (+ CD ROM full paper) (2007)
- Drdácký, M., Michoinová, D.: Lime mortars with natural fibres. In: Brandt, A.M., Li, V.C., Marshall, I.H. (eds.) Brittle Matrix Composites, vol. 7, pp. 523–532. Woodhead Publishing Ltd./Zturek Research Sci. Inst, Cambridge/Warsaw (2003)
- Drdácký, M., Slížková, Z.: Calcium hydroxide based consolidation of lime mortars and stone. In: Delgado-Rodrigues, J., Mimoso, J.M. (eds.) Proceedings of the International Symposium on Stone Consolidation in Cultural Heritage, pp. 299–308. LNEC, Lisbon (2008)

RILEM Publications

The following list is presenting our global offer, sorted by series.

RILEM Proceedings

PRO 1: Durability of High Performance Concrete (1994) 266 pp., ISBN: 2-91214-303-9; e-ISBN: 2-35158-012-5; *Ed. H. Sommer*

PRO 2: Chloride Penetration into Concrete (1995) 496 pp., ISBN: 2-912143-00-4; e-ISBN: 2-912143-45-4; *Eds. L.-O. Nilsson and J.-P. Ollivier*

PRO 3: Evaluation and Strengthening of Existing Masonry Structures (1995) 234 pp., ISBN: 2-912143-02-0; e-ISBN: 2-351580-14-1; *Eds. L. Bindu and C. Modena*

PRO 4: Concrete: From Material to Structure (1996) 360 pp., ISBN: 2-912143-04-7; e-ISBN: 2-35158-020-6; *Eds. J.-P. Bournazel and Y. Malier*

PRO 5: The Role of Admixtures in High Performance Concrete (1999) 520 pp., ISBN: 2-912143-05-5; e-ISBN: 2-35158-021-4; *Eds. J. G. Cabrera and R. Rivera-Villarreal*

PRO 6: High Performance Fiber Reinforced Cement Composites (HPFRCC 3) (1999) 686 pp., ISBN: 2-912143-06-3; e-ISBN: 2-35158-022-2; *Eds. H. W. Reinhardt and A. E. Naaman*

PRO 7: 1st International RILEM Symposium on Self-Compacting Concrete (1999) 804 pp., ISBN: 2-912143-09-8; e-ISBN: 2-912143-72-1; *Eds. Å. Skarendahl and Ö. Petersson*

PRO 8: International RILEM Symposium on Timber Engineering (1999) 860 pp., ISBN: 2-912143-10-1; e-ISBN: 2-35158-023-0; *Ed. L. Boström*

PRO 9: 2nd International RILEM Symposium on Adhesion Between Polymers and Concrete ISAP '99 (1999) 600 pp., ISBN: 2-912143-11-X; e-ISBN: 2-35158-024-9; *Eds. Y. Ohama and M. Puterman*

PRO 10: 3rd International RILEM Symposium on Durability of Building and Construction Sealants (2000) 360 pp., ISBN: 2-912143-13-6; e-ISBN: 2-351580-25-7; *Eds. A. T. Wolf*

PRO 11: 4th International RILEM Conference on Reflective Cracking in Pavements (2000) 549 pp., ISBN: 2-912143-14-4; e-ISBN: 2-351580-026-5; *Eds. A. O. Abd El Halim, D. A. Taylor and El H. H. Mohamed*

PRO 12: International RILEM Workshop on Historic Mortars: Characteristics and Tests (1999) 460 pp., ISBN: 2-912143-15-2; e-ISBN: 2-351580-27-3; *Eds. P. Bartos, C. Groot and J. J. Hughes*

PRO 13: 2nd International RILEM Symposium on Hydration and Setting (1997) 438 pp., ISBN: 2-912143-16-0; e-ISBN: 2-351580-028-1; *Ed. A. Nonat*

PRO 14: Integrated Life-Cycle Design of Materials and Structures (ILCDES 2000) (2000) 550 pp., ISBN: 951-758-408-3; e-ISBN: 2-351580-29-X, ISSN: 0356-9403; *Ed. S. Sarja*

PRO 15: Fifth RILEM Symposium on Fibre-Reinforced Concretes (FRC) – BEFIB'2000 (2000) 810 pp., ISBN: 2-912143-18-7; e-ISBN: 2-912143-73-X; *Eds. P. Rossi and G. Chanvillard*

PRO 16: Life Prediction and Management of Concrete Structures (2000) 242 pp., ISBN: 2-912143-19-5; e-ISBN: 2-351580-30-3; *Ed. D. Naus*

PRO 17: Shrinkage of Concrete – Shrinkage 2000 (2000) 586 pp., ISBN: 2-912143-20-9; e-ISBN: 2-351580-31-1; *Eds. V. Baroghel-Bouny and P.-C. Aïtcin*

PRO 18: Measurement and Interpretation of the On-Site Corrosion Rate (1999) 238 pp., ISBN: 2-912143-21-7; e-ISBN: 2-351580-32-X; *Eds. C. Andrade, C. Alonso, J. Fullea, J. Polimon and J. Rodriguez*

PRO 19: Testing and Modelling the Chloride Ingress into Concrete (2000) 516 pp., ISBN: 2-912143-22-5; e-ISBN: 2-351580-33-8, Soft cover; *Eds. C. Andrade and J. Kropff*

PRO 20: 1st International RILEM Workshop on Microbial Impacts on Building Materials (2000) 74 pp., e-ISBN: 2-351580-013-3; *Ed. M. Ribas Silva (CD 02)*

PRO 21: International RILEM Symposium on Connections Between Steel and Concrete (2001) 1448 pp., ISBN: 2-912143-25-X; e-ISBN: 2-351580-34-6; *Ed. R. Elieghausen*

PRO 22: International RILEM Symposium on Joints in Timber Structures (2001) 672 pp., ISBN: 2-912143-28-4; e-ISBN: 2-351580-35-4; *Eds. S. Aicher and H.-W. Reinhardt*

PRO 23: International RILEM Conference on Early Age Cracking in Cementitious Systems (2003) 398 pp., ISBN: 2-912143-29-2; e-ISBN: 2-351580-36-2; *Eds. K. Kovler and A. Bentur*

PRO 24: 2nd International RILEM Workshop on Frost Resistance of Concrete (2002) 400 pp., ISBN: 2-912143-30-6; e-ISBN: 2-351580-37-0, Hard back; *Eds. M. J. Setzer, R. Auberg and H.-J. Keck*

PRO 25: International RILEM Workshop on Frost Damage in Concrete (1999) 312 pp., ISBN: 2-912143-31-4; e-ISBN: 2-351580-38-9, Soft cover; *Eds. D. J. Janssen, M. J. Setzer and M. B. Snyder*

PRO 26: International RILEM Workshop on On-Site Control and Evaluation of Masonry Structures (2003) 386 pp., ISBN: 2-912143-34-9; e-ISBN: 2-351580-14-1, Soft cover; *Eds. L. Bindu and R. C. de Vekey*

PRO 27: International RILEM Symposium on Building Joint Sealants (1988) 240 pp., e-ISBN: 2-351580-15-X; *Ed. A. T. Wolf, (CD03)*

PRO 28: 6th International RILEM Symposium on Performance Testing and Evaluation of Bituminous Materials, PTEBM'03, Zurich, Switzerland (2003) 652 pp., ISBN: 2-912143-35-7; e-ISBN: 2-912143-77-2, Soft cover; *Ed. M. N. Partl (CD06)*

PRO 29: 2nd International RILEM Workshop on Life Prediction and Ageing Management of Concrete Structures, Paris, France (2003) 402 pp., ISBN: 2-912143-36-5; e-ISBN: 2-912143-78-0, Soft cover; *Ed. D. J. Naus*

PRO 30: 4th International RILEM Workshop on High Performance Fiber Reinforced Cement Composites – HPFRCC 4, University of Michigan, Ann Arbor, USA (2003) 562 pp., ISBN: 2-912143-37-3; e-ISBN: 2-912143-79-9, Hard back; *Eds. A. E. Naaman and H. W. Reinhardt*

PRO 31: International RILEM Workshop on Test and Design Methods for Steel Fibre Reinforced Concrete: Background and Experiences (2003) 230 pp., ISBN: 2-912143-38-1; e-ISBN: 2-351580-16-8, Soft cover; *Eds. B. Schnütgen and L. Vandewalle*

PRO 32: International Conference on Advances in Concrete and Structures, 2 volumes (2003) 1592 pp., ISBN (set): 2-912143-41-1; e-ISBN: 2-351580-17-6, Soft cover; *Eds. Ying-shu Yuan, Surendra P. Shah and Heng-lin Lü*

PRO 33: 3rd International Symposium on Self-Compacting Concrete (2003) 1048 pp., ISBN: 2-912143-42-X; e-ISBN: 2-912143-71-3, Soft cover; *Eds. Ö. Wallevik and I. Nielsson*

PRO 34: International RILEM Conference on Microbial Impact on Building Materials (2003) 108 pp., ISBN: 2-912143-43-8; e-ISBN: 2-351580-18-4; *Ed. M. Ribas Silva*

PRO 35: International RILEM TC 186-ISA on Internal Sulfate Attack and Delayed Ettringite Formation (2002) 316 pp., ISBN: 2-912143-44-6; e-ISBN: 2-912143-80-2, Soft cover; *Eds. K. Scrivener and J. Skalny*

PRO 36: International RILEM Symposium on Concrete Science and Engineering – A Tribute to Arnon Bentur (2004) 264 pp., ISBN: 2-912143-46-2; e-ISBN: 2-912143-58-6, Hard back; *Eds. K. Kovler, J. Marchand, S. Mindess and J. Weiss*

PRO 37: 5th International RILEM Conference on Cracking in Pavements – Mitigation, Risk Assessment and Prevention (2004) 740 pp., ISBN: 2-912143-47-0; e-ISBN: 2-912143-76-4, Hard back; *Eds. C. Petit, I. Al-Qadi and A. Millien*

PRO 38: 3rd International RILEM Workshop on Testing and Modelling the Chloride Ingress into Concrete (2002) 462 pp., ISBN: 2-912143-48-9; e-ISBN: 2-912143-57-8, Soft cover; *Eds. C. Andrade and J. Kropf*

PRO 39: 6th International RILEM Symposium on Fibre-Reinforced Concretes (BEFIB 2004), 2 volumes (2004) 1536 pp., ISBN: 2-912143-51-9 (set); e-ISBN: 2-912143-74-8, Hard back; *Eds. M. Di Prisco, R. Felicetti and G. A. Plizzari*

PRO 40: International RILEM Conference on the Use of Recycled Materials in Buildings and Structures (2004) 1154 pp., ISBN: 2-912143-52-7 (set); e-ISBN: 2-912143-75-6, Soft cover; *Eds. E. Vázquez, Ch. F. Hendriks and G. M. T. Janssen*

PRO 41: RILEM International Symposium on Environment-Conscious Materials and Systems for Sustainable Development (2005) 450 pp., ISBN: 2-912143-55-1; e-ISBN: 2-912143-64-0, Soft cover; *Eds. N. Kashino and Y. Ohama*

PRO 42: SCC'2005 – China: 1st International Symposium on Design, Performance and Use of Self-Consolidating Concrete (2005) 726 pp., ISBN: 2-912143-61-6; e-ISBN: 2-912143-62-4, Hard back; *Eds. Zhiwu Yu, Caijun Shi, Kamal Henri Khayat and Youjun Xie*

PRO 43: International RILEM Workshop on Bonded Concrete Overlays (2004) 114 pp., e-ISBN: 2-912143-83-7; *Eds. J. L. Granju and J. Silfwerbrand*

PRO 44: 2nd International RILEM Workshop on Microbial Impacts on Building Materials (Brazil 2004) (CD11) 90 pp., e-ISBN: 2-912143-84-5; *Ed. M. Ribas Silva*

PRO 45: 2nd International Symposium on Nanotechnology in Construction, Bilbao, Spain (2005) 414 pp., ISBN: 2-912143-87-X; e-ISBN: 2-912143-88-8, Soft cover; *Eds. Peter J. M. Bartos, Yolanda de Miguel and Antonio Porro*

PRO 46: ConcreteLife'06 – International RILEM-JCI Seminar on Concrete Durability and Service Life Planning: Curing, Crack Control, Performance in Harsh Environments (2006) 526 pp., ISBN: 2-912143-89-6; e-ISBN: 2-912143-90-X, Hard back; *Ed. K. Kovler*

PRO 47: International RILEM Workshop on Performance Based Evaluation and Indicators for Concrete Durability (2007) 385 pp., ISBN: 978-2-912143-95-2; e-ISBN: 978-2-912143-96-9, Soft cover; *Eds. V. Baroghel-Bouny, C. Andrade, R. Torrent and K. Scrivener*

PRO 48: 1st International RILEM Symposium on Advances in Concrete Through Science and Engineering (2004) 1616 pp., e-ISBN: 2-912143-92-6; *Eds. J. Weiss, K. Kovler, J. Marchand and S. Mindess*

PRO 49: International RILEM Workshop on High Performance Fiber Reinforced Cementitious Composites in Structural Applications (2006) 598 pp., ISBN: 2-912143-93-4; e-ISBN: 2-912143-94-2, Soft cover; *Eds. G. Fischer and V. C. Li*

PRO 50: 1st International RILEM Symposium on Textile Reinforced Concrete (2006) 418 pp., ISBN: 2-912143-97-7; e-ISBN: 2-351580-08-7, Soft cover; *Eds. Josef Hegger, Wolfgang Bramshuber and Norbert Will*

PRO 51: 2nd International Symposium on Advances in Concrete through Science and Engineering (2006) 462 pp., ISBN: 2-35158-003-6; e-ISBN: 2-35158-002-8, Hard back; *Eds. J. Marchand, B. Bissonnette, R. Gagné, M. Jolin and F. Paradis*

PRO 52: Volume Changes of Hardening Concrete: Testing and Mitigation (2006) 428 pp., ISBN: 2-35158-004-4; e-ISBN: 2-35158-005-2, Soft cover; *Eds. O. M. Jensen, P. Lura and K. Kovler*

PRO 53: High Performance Fiber Reinforced Cement Composites HPFRCC5 (2007) 542 pp., ISBN: 978-2-35158-046-2; e-ISBN: 978-2-35158-089-9, Hard back; *Eds. H. W. Reinhardt and A. E. Naaman*

PRO 54: 5th International RILEM Symposium on Self-Compacting Concrete, 3 Volumes (2007) 1198 pp., ISBN: 978-2-35158-047-9; e-ISBN: 978-2-35158-088-2, Soft cover; *Eds. G. De Schutter and V. Boel*

PRO 55: International RILEM Symposium Photocatalysis, Environment and Construction Materials (2007) 350 pp., ISBN: 978-2-35158-056-1; e-ISBN: 978-2-35158-057-8, Soft cover; *Eds. P. Baglioni and L. Cassar*

PRO 56: International RILEM Workshop on Integral Service Life Modelling of Concrete Structures (2007) 458 pp., ISBN 978-2-35158-058-5; e-ISBN: 978-2-35158-090-5, Hard back; *Eds. R. M. Ferreira, J. Gulikers and C. Andrade*

PRO 57: RILEM Workshop on Performance of Cement-Based Materials in Aggressive Aqueous Environments (2008) 132 pp., e-ISBN: 978-2-35158-059-2; *Ed. N. De Belie*

PRO 58: International RILEM Symposium on Concrete Modelling CONMOD'08 (2008) 847 pp., ISBN: 978-2-35158-060-8; e-ISBN: 978-2-35158-076-9, Soft cover; *Eds. E. Schlangen and G. De Schutter*

PRO 59: International RILEM Conference on On Site Assessment of Concrete, Masonry and Timber Structures SACoMaTiS 2008, 2 volumes (2008) 1232 pp., ISBN: 978-2-35158-061-5 (set); e-ISBN: 978-2-35158-075-2, Hard back; *Eds. L. Bindu, M. di Prisco and R. Felicetti*

PRO 60: Seventh RILEM International Symposium (BEFIB 2008) on Fibre Reinforced Concrete: Design and Applications (2008) 1181 pp., ISBN: 978-2-35158-064-6; e-ISBN: 978-2-35158-086-8, Hard back; *Ed. R. Gettu*

PRO 61: 1st International Conference on Microstructure Related Durability of Cementitious Composites (Nanjing), 2 volumes (2008) 1524 pp., ISBN: 978-2-35158-065-3; e-ISBN: 978-2-35158-084-4; *Eds. W. Sun, K. van Breugel, C. Miao, G. Ye and H. Chen*

PRO 62: NSF/ RILEM Workshop: In-Situ Evaluation of Historic Wood and Masonry Structures (2008) 130 pp., e-ISBN: 978-2-35158-068-4; *Eds. B. Kasal, R. Anthony and M. Drdácký*

PRO 63: Concrete in Aggressive Aqueous Environments: Performance, Testing and Modelling, 2 volumes (2009) 631 pp., ISBN: 978-2-35158-071-4; e-ISBN: 978-2-35158-082-0, Soft cover; *Eds. M. G. Alexander and A. Bertron*

PRO 64: Long Term Performance of Cementitious Barriers and Reinforced Concrete in Nuclear Power Plants and Waste Management – NUCPERF 2009 (2009) 359 pp., ISBN: 978-2-35158-072-1; e-ISBN: 978-2-35158-087-5; *Eds. V. L'Hostis, R. Gens and C. Gallé*

PRO 65: Design Performance and Use of Self-Consolidating Concrete, SCC'2009 (2009) 913 pp., ISBN: 978-2-35158-073-8; e-ISBN: 978-2-35158-093-6; *Eds. C. Shi, Z. Yu, K. H. Khayat and P. Yan*

PRO 66: Concrete Durability and Service Life Planning, 2nd International RILEM Workshop, ConcreteLife'09 (2009) 626 pp., ISBN: 978-2-35158-074-5; e-ISBN: 978-2-35158-085-1; *Ed. K. Kovler*

PRO 67: Repairs Mortars for Historic Masonry (2009) 397 pp., e-ISBN: 978-2-35158-083-7; *Ed. C. Groot*

PRO 68: Proceedings of the 3rd International RILEM Symposium on 'Rheology of Cement Suspensions such as Fresh Concrete' (2009) 372 pp., ISBN: 978-2-35158-091-2; e-ISBN: 978-2-35158-092-9; *Eds. O. H. Wallevik, S. Kubens and S. Oesterheld*

PRO 69: 3rd International PhD Student Workshop on 'Modelling the Durability of Reinforced Concrete' (2009) 122 pp., ISBN: 978-2-35158-095-0; e-ISBN: 978-2-35158-094-3; *Eds. R. M. Ferreira, J. Gulikers and C. Andrade*

PRO 71: Advances in Civil Engineering Materials, Proceedings of the 'The 50-year Teaching Anniversary of Prof. Sun Wei' (2010) 307 pp., ISBN: 978-2-35158-098-1; e-ISBN: 978-2-35158-099-8; *Eds. C. Miao, G. Ye and H. Chen*

PRO 74: International RILEM Conference on 'Use of Superabsorbent Polymers and Other New Additives in Concrete' (2010) 374 pp., ISBN: 978-2-35158-104-9; e-ISBN: 978-2-35158-105-6; *Eds. O. M. Jensen, M. T. Hasholt and S. Laustsen*

PRO 75: International Conference on 'Material Science - 2nd ICTRC - Textile Reinforced Concrete - Theme 1' (2010) 436 pp., ISBN: 978-2-35158-106-3; e-ISBN: 978-2-35158-107-0; *Ed. W. Brameshuber*

PRO 76: International Conference on ‘Material Science – HetMat – Modelling of Heterogeneous Materials - Theme 2’ (2010) 255 pp., ISBN: 978-2-35158-108-7; e-ISBN: 978-2-35158-109-4; *Ed. W. Brameshuber*

PRO 77: International Conference on ‘Material Science – AdIPoC – Additions Improving Properties of Concrete - Theme 3’ (2010) 459 pp., ISBN: 978-2-35158-110-0; e-ISBN: 978-2-35158-111-7; *Ed. W. Brameshuber*

PRO 78: 2nd Historic Mortars Conference and RILEM TC 203-RHM Final Workshop – HMC2010 (2010) 1416 pp., e-ISBN: 978-2-35158-112-4; *Eds J. Válek, C. Groot and J. J. Hughes*

PRO 79: International RILEM Conference on Advances in Construction Materials Through Science and Engineering (2011) 213 pp., e-ISBN: 978-2-35158-117-9; *Eds Christopher Leung and K. T. Wan*

PRO 80: 2nd International RILEM Conference on Concrete Spalling due to Fire Exposure (2011) 453 pp., ISBN: 978-2-35158-118-6; e-ISBN: 978-2-35158-119-3; *Eds E. A. B. Koenders and F. Dehn*

PRO 81: 2nd International RILEM Conference on Strain Hardening Cementitious Composites (SHCC2-Rio) (2011) 451 pp., ISBN: 978-2-35158-120-9; e-ISBN: 978-2-35158-121-6; *Eds R. D. Toledo Filho, F. A. Silva, E. A. B. Koenders and E. M. R. Fairbairn*

PRO 82: 2nd International RILEM Conference on Progress of Recycling in the Built Environment (2011) 507 pp., e-ISBN: 978-2-35158-122-3; *Eds V. M. John, E. Vazquez, S. C. Angulo and C. Ulsen*

PRO 85: RILEM-JCI International Workshop on Crack Control of Mass Concrete and Related Issues concerning Early-Age of Concrete Structures – ConCrack 3 (2012) 237 pp., ISBN: 978-2-35158-125-4; e-ISBN: 978-2-35158-126-1; *Eds F. Toutlemonde and J. M. Torrenti*

RILEM Reports

Report 19: Considerations for Use in Managing the Aging of Nuclear Power Plant Concrete Structures (1999) 224 pp., ISBN: 2-912143-07-1; e-ISBN: 2-35158-039-7; *Ed. D. J. Naus*

Report 20: Engineering and Transport Properties of the Interfacial Transition Zone in Cementitious Composites (1999) 396 pp., ISBN: 2-912143-08-X; e-ISBN: 2-35158-040-0; *Eds. M. G. Alexander, G. Arligue, G. Ballivy, A. Bentur and J. Marchand*

Report 21: Durability of Building Sealants (1999) 450 pp., ISBN: 2-912143-12-8; e-ISBN: 2-35158-041-9; *Ed. A. T. Wolf*

Report 22: Sustainable Raw Materials – Construction and Demolition Waste (2000) 202 pp., ISBN: 2-912143-17-9; e-ISBN: 2-35158-042-7; *Eds. C. F. Hendriks and H. S. Petersen*

Report 23: Self-Compacting Concrete State-of-the-Art Report (2001) 166 pp., ISBN: 2-912143-23-3; e-ISBN: 2-912143-59-4, Soft cover; *Eds. Å. Skarendahl and Ö. Petersson*

Report 24: Workability and Rheology of Fresh Concrete: Compendium of Tests (2002) 154 pp., ISBN: 2-912143-32-2; e-ISBN: 2-35158-043-5, Soft cover; *Eds. P. J. M. Bartos, M. Sonebi and A. K. Tamimi*

Report 25: Early Age Cracking in Cementitious Systems (2003) 350 pp., ISBN: 2-912143-33-0; e-ISBN: 2-912143-63-2, Soft cover; *Ed. A. Bentur*

Report 26: Towards Sustainable Roofing (Joint Committee CIB/RILEM) (CD 07), (2001) 28 pp., e-ISBN: 2-912143-65-9; *Eds. Thomas W. Hutchinson and Keith Roberts*

Report 27: Condition Assessment of Roofs (Joint Committee CIB/RILEM) (CD 08) (2003) 12 pp., e-ISBN: 2-912143-66-7

Report 28: Final report of RILEM TC 167-COM ‘Characterisation of Old Mortars with Respect to Their Repair’ (2007) 192 pp., ISBN: 978-2-912143-56-3; e-ISBN: 978-2-912143-67-9, Soft cover; *Eds. C. Groot, G. Ashall and J. Hughes*

Report 29: Pavement Performance Prediction and Evaluation (PPPE): Interlaboratory Tests (2005) 194 pp., e-ISBN: 2-912143-68-3; *Eds. M. Partl and H. Piber*

Report 30: Final Report of RILEM TC 198-URM ‘Use of Recycled Materials’ (2005) 74 pp., ISBN: 2-912143-82-9; e-ISBN: 2-912143-69-1, Soft cover; *Eds. Ch. F. Hendriks, G. M. T. Janssen and E. Vázquez*

Report 31: Final Report of RILEM TC 185-ATC ‘Advanced Testing of Cement-Based Materials During Setting and Hardening’ (2005) 362 pp., ISBN: 2-912143-81-0; e-ISBN: 2-912143-70-5, Soft cover; *Eds. H. W. Reinhardt and C. U. Grosse*

Report 32: Probabilistic Assessment of Existing Structures. A JCSS publication (2001) 176 pp., ISBN 2-912143-24-1; e-ISBN: 2-912143-60-8, Hard back; *Ed. D. Diamantidis*

Report 33: State-of-the-Art Report of RILEM Technical Committee TC 184-IFE ‘Industrial Floors’ (2006) 158 pp., ISBN 2-35158-006-0; e-ISBN: 2-35158-007-9, Soft cover; *Ed. P. Seidler*

Report 34: Report of RILEM Technical Committee TC 147-FMB ‘Fracture Mechanics Applications to Anchorage and Bond’ Tension of Reinforced Concrete Prisms – Round Robin Analysis and Tests on Bond (2001) 248 pp., e-ISBN 2-912143-91-8; *Eds. L. Elfgrén and K. Noghabai*

Report 35: Final Report of RILEM Technical Committee TC 188-CSC ‘Casting of Self Compacting Concrete’ (2006) 40 pp., ISBN 2-35158-001-X; e-ISBN: 2-912143-98-5, Soft cover; *Eds. Å. Skarendahl and P. Billberg*

Report 36: State-of-the-Art Report of RILEM Technical Committee TC 201-TRC ‘Textile Reinforced Concrete’ (2006) 292 pp., ISBN 2-912143-99-3; e-ISBN: 2-35158-000-1, Soft cover; *Ed. W. Brameshuber*

Report 37: State-of-the-Art Report of RILEM Technical Committee TC 192-ECM ‘Environment-Conscious Construction Materials and Systems’ (2007) 88 pp., ISBN: 978-2-35158-053-0; e-ISBN: 2-35158-079-0, Soft cover; *Eds. N. Kashino, D. Van Gemert and K. Imamoto*

Report 38: State-of-the-Art Report of RILEM Technical Committee TC 205-DSC ‘Durability of Self-Compacting Concrete’ (2007) 204 pp., ISBN: 978-2-35158-048-6; e-ISBN: 2-35158-077-6, Soft cover; *Eds. G. De Schutter and K. Audenaert*

Report 39: Final Report of RILEM Technical Committee TC 187-SOC ‘Experimental Determination of the Stress-Crack Opening Curve for Concrete in Tension’ (2007) 54 pp., ISBN 978-2-35158-049-3; e-ISBN: 978-2-35158-078-3, Soft cover; *Ed. J. Planas*

Report 40: State-of-the-Art Report of RILEM Technical Committee TC 189-NEC ‘Non-Destructive Evaluation of the Penetrability and Thickness of the Concrete Cover’ (2007) 246 pp., ISBN 978-2-35158-054-7; e-ISBN: 978-2-35158-080-6, Soft cover; *Eds. R. Torrent and L. Fernández Luco*

Report 41: State-of-the-Art Report of RILEM Technical Committee TC 196-ICC ‘Internal Curing of Concrete’ (2007) 164 pp., ISBN: 978-2-35158-009-7; e-ISBN: 978-2-35158-082-0, Soft cover; *Eds. K. Kovler and O. M. Jensen*

Report 42: ‘Acoustic Emission and Related Non-destructive Evaluation Techniques for Crack Detection and Damage Evaluation in Concrete’ – Final Report of RILEM Technical Committee 212-ACD (2010) 12 pp., e-ISBN: 978-2-35158-100-1; *Ed. M. Ohtsu*

RILEM Publications Published by Springer

RILEM Bookseries (Proceedings)

VOL. 1: Design, Production and Placement of Self-Consolidating Concrete (2010) 466 pp., ISBN: 978-90-481-9663-0; e-ISBN: 978-90-481-9664-7, Hardcover; *Eds. K. Khayat and D. Feyes*

VOL. 2: High Performance Fiber Reinforced Cement Composites 6 – HPFRCC6 (2011) 584 pp., ISBN: 978-94-007-2435-8; e-ISBN: 978-94-007-2436-5, Hardcover; *Eds. G. J. Parra-Montesinos, H. W. Reinhardt and A. E. Naaman*

VOL. 3: Advances in Modeling Concrete Service Life – Proceedings of 4th International RILEM PhD Workshop held in Madrid, Spain, November 19, 2010 (2012) 170 pp., ISBN: 978-94-007-2702-1; e-ISBN: 978-94-007-2703-8, Hardcover; *Eds. C. Andrade and Joost Gulikers*

VOL. 5: Joint fib-RILEM Workshop on Modelling of Corroding Concrete Structures (2011) 290 pp., ISBN: 978-94-007-0676-7; e-ISBN: 978-94-007-0677-4, Hardcover; *Eds. C. Andrade and G. Mancini*

For the latest publications in the RILEM Bookseries, please visit <http://www.springer.com/series/8781>

RILEM State-of-the-Art Reports

VOL. 1: State-of-the-Art Report of RILEM Technical Committee TC 207-INR ‘Non-Destructive Assessment of Concrete Structures: Reliability and Limits of Single and Combined Techniques’ (2012) 390 pp., ISBN: 978-94-007-2735-9; e-ISBN: 978-94-007-2736-6, Hardcover; *Ed. D. Breysse*

VOL. 2: State-of-the-Art Report of RILEM Technical Committee TC 225-SAP ‘Application of Super Absorbent Polymers (SAP) in Concrete Construction’ (2012)

165 pp., ISBN: 978-94-007-2732-8; e-ISBN: 978-94-007-2733-5, Hardcover; *Eds. V. Mechtcherine and H.-W. Reinhardt*

VOL. 3: State-of-the-Art Report of RILEM Technical Committee TC 193-RLS ‘Bonded Cement-Based Material Overlays for the Repair, the Lining or the Strengthening of Slabs or Pavements’ (2011) 198 pp., ISBN: 978-94-007-1238-6; e-ISBN: 978-94-007-1239-3, Hardcover; *Eds. B. Bissonnette, L. Courard, D. W. Fowler and J.-L. Granju*

VOL. 4: State-of-the-Art Report Prepared by Subcommittee 2 of RILEM Technical Committee TC 208-HFC ‘Durability of Strain-Hardening Fibre-Reinforced Cement-Based Composites’ (SHCC) (2011) 151 pp., ISBN: 978-94-007-0337-7; e-ISBN: 978-94-007-0338-4, Hardcover; *Eds. G. P. A. G. van Zijl and F. H. Wittmann*

VOL. 5: State-of-the-Art Report of RILEM Technical Committee TC 194-TDP ‘Application of Titanium Dioxide Photocatalysis to Construction Materials’ (2011) 60 pp., ISBN: 978-94-007-1296-6; e-ISBN: 978-94-007-1297-3, Hardcover; *Eds. Yoshihiko Ohama and Dionys Van Gemert*

VOL. 7: State-of-the-Art Report of RILEM Technical Committee TC 215-AST ‘In Situ Assessment of Structural Timber’ (2010) 152 pp., ISBN: 978-94-007-0559-3; e-ISBN: 978-94-007-0560-9, Hardcover; *Eds. B. Kasal and T. Tannert*

For the latest publications in the RILEM State-of-the-Art Reports, please visit <http://www.springer.com/series/8780>

Author Index

A

Amenta, M., 309

B

Barreiros, B., 175

Bayer, K., 89

Binda, L., 153

Bläuer, C., 239

Borsoi, G., 175

Bosiljkov, V.B., 393

Bouichou, M., 247

Brandon, C., 49

C

Cailleux, E., 247

Carran, D., 283

Cavallo, G., 227

Condoleo, P., 153

Corredig, G., 227

Costa, D., 413

Costigan, A., 359

D

de Brito, J., 141

Diekamp, A., 105

Drdácký, M., 165, 443

E

Elsen, J., 125

F

Fardis, M., 435

Feldman, S.B., 297

Feneuille, S., 37

Forster, A.M., 197

Fragata, A., 175

Frankeová, D., 165

Freire, T., 141

G

Gomes, A., 425

Gosselin, C., 297

Groot, C.J.W.P., 1, 257

Gunneweg, J., 257

H

Haas, S., 319

Häberli, H., 239

Hendrickx, R., 329

Hohlfelder, R.L., 49

Hughes, J.J., 1, 283

J

Jackson, M.D., 49

Johansson, S., 77

Jornet, A., 227

K

Karakosta, E., 435

Karatasis, I., 309, 435

Kennedy, C., 283

Kilikoglou, V.,
309, 435

Klein, D., 319

Konzett, J., 105

L

- Lawrence, M., 373
 Leslie, A., 283
 Letourneau, J.-P., 37
 Lindqvist, J.E., 77
 Llera, F., 175
 Löffel, A., 239

M

- Magalhães, A., 413
 Maravelaki-Kalaitzaki, P., 435
 Marie-Victoire, E., 247
 Marinowitz, C., 15
 Matas, T., 269
 Mertens, G., 125
 Michalski, S., 115
 Middendorf, B., 319
 Mirwald, P.W., 105
 Mosca, C., 227

N

- Neuwald-Burg, C., 15, 343
 Nogueira, R., 425

O

- Oleson, J.P., 49

P

- Pachta, V., 383
 Papavassiliou, G., 435
 Papayianni, I., 383
 Pavía, S., 359
 Pfeifer, M., 15, 343
 Philokyprou, M., 25
 Pintér, F., 89
 Pinto, A.P.F., 425

R

- Roels, S., 329
 Rousset, B., 239

S

- Scheetz, B.E., 49
 Schmidt, S.-O., 319
 Schwarz, W., 297
 Scrivener, K.L., 297
 Siedel, H., 115
 Silva, A.S.,
 141, 175

- Slížková, Z., 165
 Sommain, D., 247
 Stalder, R., 105
 Stefanidou, M., 383

T

- Tavares, M., 175
 Tedeschi, C., 153
 Teixeira, T., 175
 Tziotziou, M.,
 309, 435

U

- Ullrich, B., 115
 Uranjek, M., 393

V

- Válek, J., 1, 269
 Van Balen, K.,
 125, 329
 Veiga, M.d.R., 141, 175,
 207, 413
 Vola, G., 49
 Všianský, D., 49

W

- Walker, P., 373
 Weber, J., 89

Z

- Žarnić, R., 393
 Zhou, Z., 373